ACS SYMPOSIUM SERIES 1024

# Controlled/Living Radical Polymerization:
## Progress in RAFT, DT, NMP & OMRP

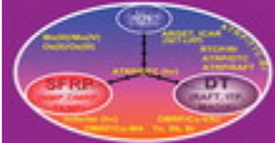
ARGET, ICAR
SFRP
DT

EDITED BY
Krzysztof Matyjaszewski

Downloaded by 89.163.34.136 on June 25, 2012 | http://pubs.acs.org
Publication Date: August 13, 2009 | doi: 10.1021/bk-2009-1024.fw001

# Controlled/Living Radical Polymerization: Progress in RAFT, DT, NMP & OMRP

Downloaded by 89.163.34.136 on June 25, 2012 | http://pubs.acs.org
Publication Date: August 13, 2009 | doi: 10.1021/bk-2009-1024.fw001

ACS SYMPOSIUM SERIES **1024**

# Controlled/Living Radical Polymerization: Progress in RAFT, DT, NMP & OMRP

**Krzysztof Matyjaszewski,** Editor
*Carnegie Mellon University*

Downloaded by 89.163.34.136 on June 25, 2012 | http://pubs.acs.org
Publication Date: August 13, 2009 | doi: 10.1021/bk-2009-1024.fw001

**Sponsored by the**
**ACS Division of Polymer Chemistry, Inc.**
**ACS Petroleum Research Foundation**
**Arkena, Bayer, Boston Scientific, Ciba, CIP, Dionex, DSM,**
**Elsevier, Evonik, General Electric, JSR, Lion,**
**Mitsui Chemicals, National Starch, PPG and Sumitomo**

American Chemical Society, Washington DC

Downloaded by 89.163.34.136 on June 25, 2012 | http://pubs.acs.org
Publication Date: August 13, 2009 | doi: 10.1021/bk-2009-1024.fw001

Library of Congress Cataloging-in-Publication Data

Controlled/living radical polymerization : progress in RAFT, DT, NMP & OMRP / Krzysztof Matyjaszewski, editor.
p. cm.
Includes bibliographical references and index.
ISBN 978-0-8412-6996-5
1. Polymerization--Congresses. 2. Free radical reactions--Congresses. I. Matyjaszewski, K. (Krzysztof)
QD281.P6C6557 2009
547'.28--dc22
2009020533

The paper used in this publication meets the minimum requirements of American National Standard for Information Sciences—Permanence of Paper for Printed Library Materials, ANSI Z39.48−1984.

Copyright © 2009 American Chemical Society

Distributed by Oxford University Press

All Rights Reserved. Reprographic copying beyond that permitted by Sections 107 or 108 of the U.S. Copyright Act is allowed for internal use only, provided that a per-chapter fee of $40.25 plus $0.75 per page is paid to the Copyright Clearance Center, Inc., 222 Rosewood Drive, Danvers, MA 01923, USA. Republication or reproduction for sale of pages in this book is permitted only under license from ACS. Direct these and other permission requests to ACS Copyright Office, Publications Division, 1155 16th Street, N.W., Washington, DC 20036.

The citation of trade names and/or names of manufacturers in this publication is not to be construed as an endorsement or as approval by ACS of the commercial products or services referenced herein; nor should the mere reference herein to any drawing, specification, chemical process, or other data be regarded as a license or as a conveyance of any right or permission to the holder, reader, or any other person or corporation, to manufacture, reproduce, use, or sell any patented invention or copyrighted work that may in any way be related thereto. Registered names, trademarks, etc., used in this publication, even without specific indication thereof, are not to be considered unprotected by law.

PRINTED IN THE UNITED STATES OF AMERICA

Downloaded by 89.163.34.136 on June 25, 2012 | http://pubs.acs.org
Publication Date: August 13, 2009 | doi: 10.1021/bk-2009-1024.fw001

# Foreword

The ACS Symposium Series was first published in 1974 to provide a mechanism for publishing symposia quickly in book form. The purpose of the series is to publish timely, comprehensive books developed from the ACS sponsored symposia based on current scientific research. Occasionally, books are developed from symposia sponsored by other organizations when the topic is of keen interest to the chemistry audience.

Before agreeing to publish a book, the proposed table of contents is reviewed for appropriate and comprehensive coverage and for interest to the audience. Some papers may be excluded to better focus the book; others may be added to provide comprehensiveness. When appropriate, overview or introductory chapters are added. Drafts of chapters are peer-reviewed prior to final acceptance or rejection, and manuscripts are prepared in camera-ready format.

As a rule, only original research papers and original review papers are included in the volumes. Verbatim reproductions of previous published papers are not accepted.

**ACS Books Department**

In Controlled/Living Radical Polymerization: Progress in RAFT, DT, NMP & OMRP; Matyjaszewski, K.;
ACS Symposium Series; American Chemical Society: Washington, DC, 2009.

Downloaded by 89.163.34.136 on June 25, 2012 | http://pubs.acs.org
Publication Date: August 13, 2009 | doi: 10.1021/bk-2009-1024.pr001

# Preface

This book and an accompanying volume are addressed to chemists who are interested in radical processes and especially in controlled/living radical polymerization. They summarize the most recent accomplishments in the field.

The two volumes comprise the topical reviews and specialists' contributions presented at the American Chemical Society Symposium entitled *Controlled/Living Radical Polymerization* that was held in Philadelphia, Pennsylvania, August 17-21, 2008. The Philadelphia Meeting was a sequel to the previous ACS Symposia held in San Francisco, California, in 1997, in New Orleans, Louisiana, in 1999, in Boston, Massachusetts, in 2002 and in Washington, DC, in 2005. They were summarized in the ACS Symposium Series Volume 685, *Controlled Radical Polymerization*, Volume 768, *Controlled/Living Radical Polymerization: Progress in ATRP, NMP and RAFT,* Volume 854 *Advances in Controlled/Living Radical Polymerization* and Volume 944, *Controlled/Living Radical Polymerization: From Synthesis to Materials.* The Philadelphia Meeting was very successful with 90 lectures and 123 posters presented. This illustrates a continuous growth in comparison with the San Francisco Meeting (32 lectures and 35 posters), the New Orleans (50 lectures and 50 posters), the Boston Meeting (80 lectures and 79 posters) and with the Washington Meeting (77 lectures and 119 posters).

The fifty chapters submitted for publication in the ACS Symposium series could not fit into one volume and therefore we decided to split them into two volumes. In order to balance the size of each volume we did not divide the chapters into volumes related to mechanisms and materials but rather to those related to atom transfer radical polymerization (ATRP) and to other controlled/living radical polymerization methods: reversible-addition fragmentation transfer (RAFT) and other degenerative transfer techniques, as well as stable free radical polymerizations (SFRP) including nitroxide mediated polymerization (NMP) and organometallic mediated radical polymerization (OMRP).

In Controlled/Living Radical Polymerization: Progress in RAFT, DT, NMP & OMRP; Matyjaszewski, K.;
ACS Symposium Series; American Chemical Society: Washington, DC, 2009.

This volume contains 10 chapters on mechanisms and kinetics of RAFT, other degenerative transfer processes, NMP and OMRP. They are followed by six chapters devoted to molecular architecture accessible by these techniques. Various materials aspects of the resulting polymers are covered in six chapters. The last two chapters present commercial application of polymers prepared by NMP and RAFT (or MADIX).

The first chapter in the preceding volume provides an overview of the current status of controlled/living radical polymerization (CRP) systems. The following three chapters discuss important issues relevant to all radical polymerization methods. The mechanistic and kinetic topics of ATRP are covered in eight chapters. The macromolecular architecture, various hybrids and bio-related polymers prepared by ATRP are discussed in the next six chapters, Characterization and materials aspects of ATRP polymers are covered in six chapters, whereas the last four chapters discuss industrial applications of ATRP.

Fifty chapters published in two volumes show that CRP has made a significant progress within the last decade. New systems have been discovered; substantial progress has been achieved in understanding the mechanism and kinetics of reactions involved in all CRP systems. Significant progress has been made towards a comprehensive relationship between molecular structure and macroscopic properties. Some commercial applications of CRP were announced at the Philadelphia Meeting and it is anticipated that many new products will be soon on the market.

The financial support for the symposium from the following organizations is acknowledged: ACS Division of Polymer Chemistry, Inc., ACS Petroleum Research Foundation, Arkema, Bayer, Boston Scientific, Ciba, CIP, Dionex, DSM, Elsevier, Evonik, General Electric, JSR, Lion, Mitsui Chemicals, National Starch, PPG and Sumitomo. The excellent editorial assistance from Joyce Von Vreckin is gratefully acknowledged.

**Krzysztof Matyjaszewski**

Department of Chemistry
Carnegie Mellon University
4400 Fifth Avenue
Pittsburgh, PA 15213

Downloaded by 89.163.34.136 on June 25, 2012 | http://pubs.acs.org
Publication Date: August 13, 2009 | doi: 10.1021/bk-2009-1024.pr001

Downloaded by 89.163.34.136 on June 25, 2012 | http://pubs.acs.org
Publication Date: August 13, 2009 | doi: 10.1021/bk-2009-1024.ch001

# Chapter 1

# New Features of the Mechanism of RAFT Polymerization

**Graeme Moad,* Y.K. Chong, Roger Mulder, Ezio Rizzardo, San H. Thang,**

**CSIRO Molecular and Health Technologies, Bag 10, Clayton South, Victoria 3169, Australia**

RAFT polymerizations of styrene with azobis(isobutyronitrile-$\alpha$-$^{13}$C) as initiator and various RAFT agents (cumyl dithiobenzoate (**5**), cyanoisopropyl dithiobenzoate (**6**), benzyl dithiobenzoate-*thiocarbonyl*-$^{13}$C (**7**) or cyanoisopropyl dodecyl trithiocarbonate (**8**)) were followed by real time $^{13}$C NMR. While the rate of AIBN decomposition and the initial fate of the initiator-derived radicals (the initiator efficiency) were not substantially affected by the RAFT agent, the rate of polymerization was strongly dependent on both the type and concentration of RAFT agent. Polymerizations with the more active dithiobenzoate (**5**,**6**) RAFT agents and trithiocarbonate **8** display formation of a single unit styrene chain prior to any substantial formation of higher oligomers. An unexpected finding is the observation of $^{13}$C CIDNP for the ketenimine formed by cage recombination of AIBN-derived cyanoisopropyl radicals. With benzyl dithiobenzoate (**7**), consumption of the initial RAFT agent is slow. By-products from intermediate radical termination are also observed.

In Controlled/Living Radical Polymerization: Progress in RAFT, DT, NMP & OMRP; Matyjaszewski, K.;
ACS Symposium Series; American Chemical Society: Washington, DC, 2009.

# Introduction

The RAFT process is a versatile method for conferring living characteristics on radical polymerizations which provides unprecedented control over molecular weight, molecular weight distribution, composition and architecture.[1-5] It is suitable for most monomers polymerizable by radical polymerization and is robust under a wide range of reaction conditions. RAFT polymerizations of styrene were described in the first communication of RAFT polymerization in 1998[6] and have been the subject of many subsequent papers. The mechanism of the RAFT process is shown in Scheme 1. Ideally, since radicals are neither formed nor destroyed as a consequence of the RAFT equilibria, they should not directly affect the rate of polymerization. RAFT agents can behave as ideal chain transfer agents.[7-9]

*Scheme 1 Mechanism of RAFT polymerization*

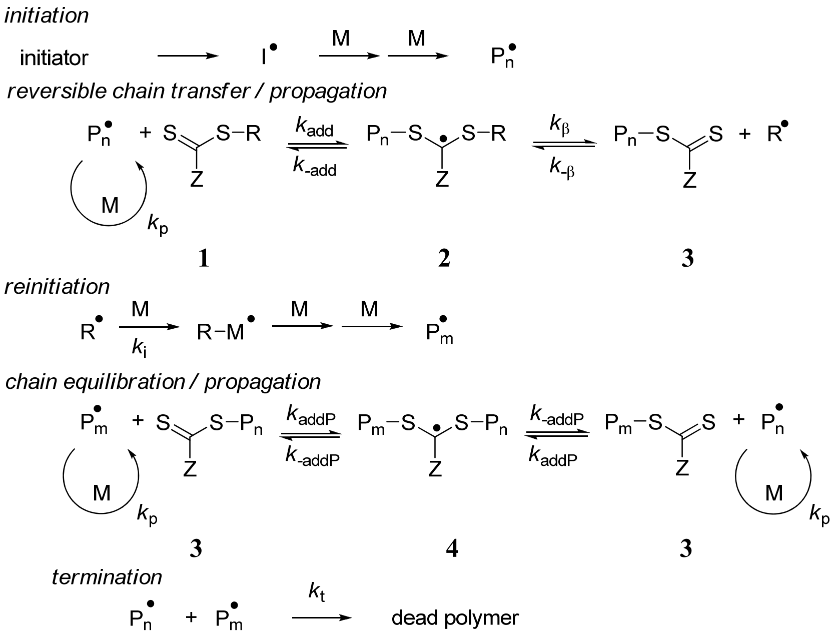
initiation
initiator
I•
M
M
$P_n^\bullet$
reversible chain transfer / propagation
$k_{add}$
$k_{-add}$
$k_\beta$
$k_{-\beta}$
$k_p$
1
2
3
reinitiation
R•
R−M•
$k_i$
$P_m^\bullet$
chain equilibration / propagation
$k_{addP}$
$k_{-addP}$
3
4
3
termination
$k_t$
dead polymer

However, retardation has been observed in some circumstances. In 2000,[1] we reported that RAFT polymerizations of styrene, BA and MMA were subject to retardation when high concentrations of RAFT agent were used and that the extent, mechanism and particular manifestation of retardation were dependent on the specific RAFT agent-monomer combination used. Much has now been published on retardation in RAFT polymerization and the possible causes of a slower rate of polymerization.[7] The situation with respect to control of radical polymerization with dithiobenzoate RAFT agents has been summarized by an IUPAC task group in a 'dilemma' paper.[10] Factors that may influence the polymerization kinetics include (a) slow fragmentation of the intermediated

Downloaded by 89.163.34.136 on June 25, 2012 | http://pubs.acs.org
Publication Date: August 13, 2009 | doi: 10.1021/bk-2009-1024.ch001

radical,[11-14] (b) intermediate radical termination,[15-17] (c) “missing steps”,[18-20] (d) inefficient reinitiation,[8] (e) a reduced gel or Trommsdorf effect and effects of chain length dependent termination,[9,12] (f) high $C_{\text{-tr}}$ ($=k_{-\beta}/k_{\text{i}}$)[21] (g) impurities in the RAFT agent,[22] (h) impurities such as oxygen in the reaction medium,[2] and (i) various combinations of these effects. High level molecular orbital calculations suggest that, when dithiobenzoate RAFT agents are used, the intermediates formed (**2** and/or **4**) have sufficient stability such that slow fragmentation, by itself, is a potential cause of retardation.[13] ESR studies show that the intermediates (**2** and/or **4**) are present only in very low concentrations and by implication that slow fragmentation, by itself, cannot be the cause of retardation.[23-25] A recent paper by Konkolewicz et al.[26] purports to suggest a possible resolution of these conflicting results. This study suggests that intermediate radical termination occurs, but only involves initiator-derived or oligomeric chains. With many rate constants unknown or uncertain, kinetic modeling, while a useful tool for excluding some possibilities, is not able to unambiguously discriminate the models for retardation. It is possible to fit the evolution of the molecular weight distribution with time using many of the above-mentioned models.

Real-time $^{1}$H NMR has previously been used to study RAFT polymerization of styrene with azobis(isobutyronitrile) (AIBN) initiator and with cumyl[27] or cyanoisopropyl dithiobenzoate[28] as the RAFT agent and more recently polymerizations of methyl acrylate,[29,30] vinyl acetate[31] N-vinyl pyrrolidone[31] and styrene-maleic anhydride[32,33] and styrene-acrylonitrile copolymerization[33] with various RAFT agents. $^{13}$C NMR was also used to study RAFT polymerization of styrene with AIBN initiator and cumyl dithiobenzoate-*thiocarbonyl*-$^{13}$C as the RAFT agent.[34]

For styrene polymerization at 70 or 84 ºC with high concentrations of cumyl or cyanoisopropyl dithiobenzoate, complete conversion of the initial RAFT agent to a single unit ‘chain’ was observed prior to any significant formation of two unit or higher chains.[27,28,34] This phenomenon was called ‘efficient initialization’. This outcome can be predicted by kinetic simulation based on (a) the assumption of slow fragmentation and rate constants estimated by *ab initio* calculations[12,13] or (b) with faster fragmentation (so as not to cause retardation directly) and intermediate radical termination.[35] Our kinetic modeling studies show that the observation of such ‘efficient initialization’ is not dependent on slow fragmentation or the occurrence of intermediate radical fragmentation. It is observed for the more active RAFT agents when the rate constant for the first monomer addition ($k_{\text{i}}$) is rapid with respect to that for subsequent propagation steps (as is usually the case) and the RAFT agent concentration is such that <1 monomer unit is added per activation cycle.

Some time ago we reported on the use of $^{13}$C-labeled initiators to follow the course and efficiency of initiation of radical polymerization of styrene with azobis(isobutyronitrile-$\alpha$-$^{13}$C) (AIBN-$\alpha$-$^{13}$C) as initiator.[36-39] In this paper we report a real time $^{13}$C NMR study of initialization of RAFT polymerization of styrene with cumyl dithiobenzoate (**5**), cyanoisopropyl dithiobenzoate (**6**), benzyl dithiobenzoate-*thiocarbonyl*-$^{13}$C (**7**) or cyanoisopropyl dodecyl trithiocarbonate (**8**) as RAFT agent carried out with the aim of further defining the initiation process under RAFT polymerization conditions. In each case

Downloaded by 89.163.34.136 on June 25, 2012 | http://pubs.acs.org
Publication Date: August 13, 2009 | doi: 10.1021/bk-2009-1024.ch001

AIBN-α-$^{13}$C was used as the initiator. A full analysis of these data has not yet been performed. This will be presented in a forthcoming paper.

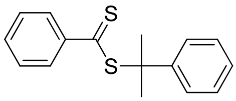

**5**

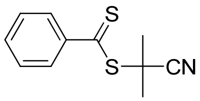

**6**

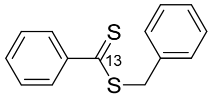

**7**

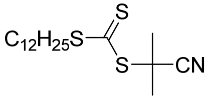

**8**

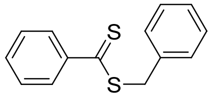

**7a**

## Results and Discussion

The established mechanism for thermal decomposition of AIBN is shown in Scheme 2. AIBN dissociates irreversibly to form two cyanoisopropyl radicals and a molecule of nitrogen. The cyanoisopropyl radicals may undergo self-reaction within the solvent cage by one of three pathways (C-C coupling, C-N coupling, or disproportionation) or escape to form products (e.g. initiate polymerization). Tetramethylsuccinodinitrile (TMSN) and isobutyronitrile (IBN) are inert under polymerization conditions. The ketenimine (K) formed by C-N coupling is itself thermally labile and (in the absence of RAFT agent) decomposes thermally to reform cyanoisopropyl radicals. Methacrylonitrile (MAN) may react by addition of radicals and may be consumed by copolymerization during radical polymerization.[37]

With the temperature of the NMR probe set to 70 °C, the actual reaction temperature was calibrated as ~68.5 ºC by comparing the rate constant for disappearance of AIBN measured in our experiments with that predicted by literature Arrhenius parameters (from the slopes of the lines in Figure 1).[40] There are reports of an effect of magnetic field on the efficiency of initiation of azo-compounds including AIBN.[41] In this work, we found no discernable difference between samples polymerized in the NMR probe and samples polymerized in a conventional thermostatted heating bath.

Downloaded by 89.163.34.136 on June 25, 2012 | http://pubs.acs.org
Publication Date: August 13, 2009 | doi: 10.1021/bk-2009-1024.ch001

*Scheme 2 Mechanism for thermal decomposition of azobisisobutyronitrile*

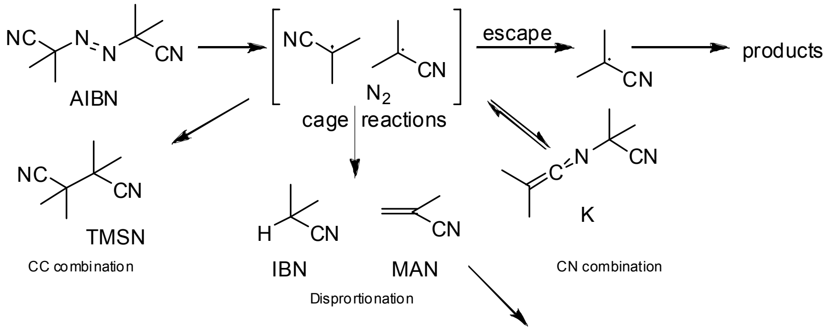

The rate of AIBN decomposition is the same, within experimental error, whether in the presence and absence of RAFT agent (Figure 1) irrespective of the RAFT agent (of **5**-**8**) is used and its concentration (0.1-0.5 M). The initial fate of the cyanoisopropyl radical (relative yields of TMSN, IBN and cyanoisopropyl end groups) is also largely unaffected by presence of the RAFT agent. The initiator efficiency (= the yield of cyanoisopropyl end groups) is therefore also substantially unaffected.

The yield of K could not be directly determined from the real-time NMR spectra. An unexpected finding of the present study is that the resonance attributable to K displays CIDNP (Chemically Induced Dynamic Nuclear Polarization)[42] emission (e.g. Figure 2a) in all experiments with added RAFT agent and that K is wholly or partly converted to a byproduct (designated KB). The intensity of the CIDNP emission and the yield of KB and was dependent on the type of RAFT agent and and was greater for higher RAFT agent concentrations. No CDNIP effect or formation of KB was observed in experiments carried out in the absence of RAFT agent (during conventional AIBN initiated polymerization or styrene or during decomposition of AIBN in benzene). The CDNIP emission ceased immediately when the NMR tube was cooled to ambient temperature. In polymerizations carried out in the presence of a high concentration of RAFT agents **5** or **7** (0.5 M), the conversion to KB was almost quantitative and K was barely detectable in the final product mixture.

Downloaded by 89.163.34.136 on June 25, 2012 | http://pubs.acs.org
Publication Date: August 13, 2009 | doi: 10.1021/bk-2009-1024.ch001

Downloaded by 89.163.34.136 on June 25, 2012 | http://pubs.acs.org
Publication Date: August 13, 2009 | doi: 10.1021/bk-2009-1024.ch001

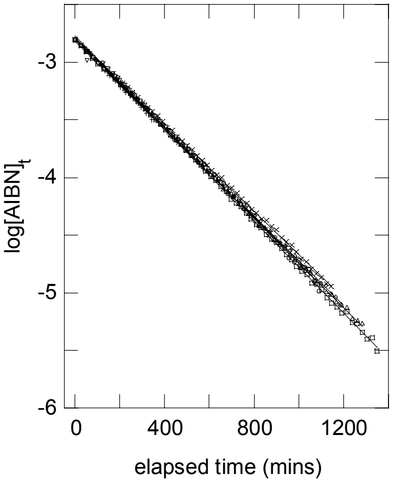

*Figure 1. Kinetic plot showing rate of azobis(isobutyronitrile) consumption with time during polymerization of styrene in benzene-$d_6$ (50% v/v) at 68.5 ºC with no RAFT agent (+), 0.5 M [**5**] (□), 0.1 M [**5**] (∇),0.5 M [**6**] (○), 0.5 M [7] (◊),0.1 M [7] (Δ) , 0.5 M [**8**] (×) RAFT agent and with 0.1 M azobis(isobutyronitrile). Note that all data are sumperimposed.*

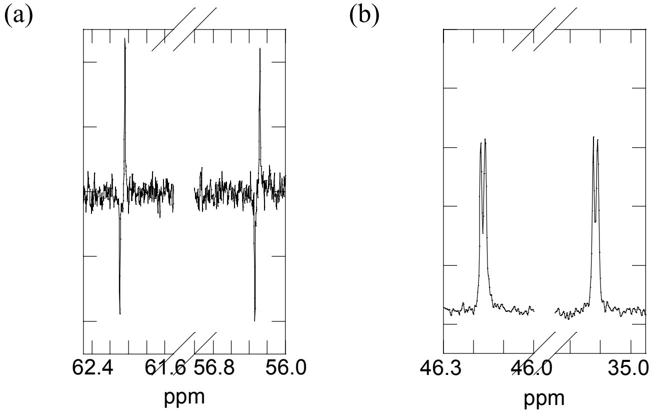

*Figure 2. Portions of the NMR spectrum recorded during polymerization of styrene (4.36 M in benzene-$d_6$) at 68.5 ºC with benzyl dithiobenzoate-thiocarbonyl-$^{13}$C (7, 0.1 M), benzyl dithiobenzoate (7**a**, 0.4M) and azobis(isobutyronitrile)-α-$^{13}$C (0.1 M) after 246 min showing resonances attributable to (a) ketenimine (K) displaying CIDNP emission and (b) byproduct (KB).*

The precise identity of the by-product KB has not yet been firmly established. The NMR spectrum (e.g. Figure 2b) shows coupled ($J_{CC}$=2 Hz) isopropyl δ 35.1 (isopropyl hydrogen appears in $^1$H NMR as a doublet to heptets at δ 1.87, $J_{CH}$=25 Hz, $J_{HH}$=7 Hz, and the methyls as a doublet of doublets at δ 1.02, $J_{CH}$=5 Hz, $J_{HH}$=7 Hz – connectivity proved by 2D HMBC experiment) and quaternary (cyanoisopropyl) carbons δ 46.2 (methyls appear as doublet at δ 1.26, $J_{CH}$=5 Hz). This is consistent with the structural fragment shown in Scheme 3. The byproduct KB appeared inert under polymerization conditions.

*Scheme 3 Formation of byproduct KB from ketenimine K*

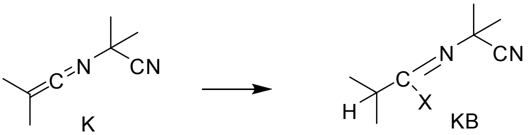

For the experiments with 0.5M RAFT agent the disappearance of RAFT agent could be followed even when unlabeled RAFT agent was used by observation of the thiocarbonyl signals in the $^{13}$C NMR spectra (e.g. Figure 5). For the experiments with lower (0.1 M) RAFT agent concentrations the thiocarbonyl resonances were not observable above noise. In the case of experiments with cumyl dithiobenzoate (**5**) the rate of appearance of total monoadduct corresponded with the appearance of the corresponding cyanoisopropyl initiated chains demonstrating that there was rapid equilibration between the chains with different end groups. For the experiments with cyanoisopropyl RAFT agents (**6** and **8**) the rate of disappearance of the initial RAFT agent was extremely rapid and was essentially complete within 12 minutes. Combination products (TMSN, K, or KB) from encounter reactions which should have a statistical mixture of labeled (from AIBN-α-$^{13}$C) and unlabeled carbons (from the RAFT agent) were not detected. Not surprisingly, therefore, the formation of the cyanoisopropyl RAFT agent was not detected in any of the polymerization experiments. The formation of a small amount (<3%) of what may be cyanoisopropyl benzoate was observed when AIBN was decomposed in the presence of 0.1 M **7** in benzene in the absence of monomer.

Formation of another dithioester characterized by a thiocarbonyl resonance at δ 225.9 was observed in experiments with benzyl dithiobenzoate **7**. This has not been identified but could correspond to a ring substituted benzyl dithiobenzoate (e.g. **17**) formed by a "missing step" process.[18-20]

Downloaded by 89.163.34.136 on June 25, 2012 | http://pubs.acs.org
Publication Date: August 13, 2009 | doi: 10.1021/bk-2009-1024.ch001

Downloaded by 89.163.34.136 on June 25, 2012 | http://pubs.acs.org
Publication Date: August 13, 2009 | doi: 10.1021/bk-2009-1024.ch001

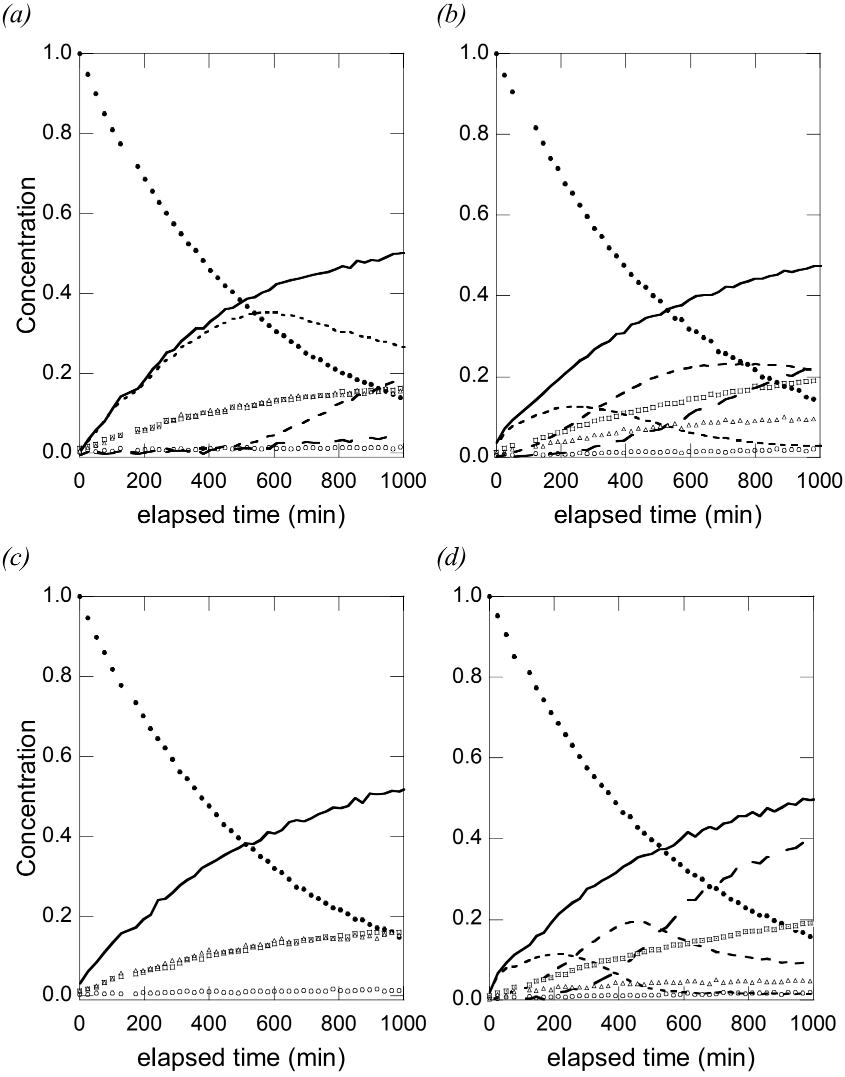

*Figure 3. Signal intensities in $^{13}$C NMR spectra in polymerization of styrene (4.36 M in benzene-$d_6$) at 70 ºC with (a) cumyl dithiobenzoate (**5** , 0.5M), (b) cyanoisopropyl dithiobenzoate (**6**, 0.5 M), (c) benzyl dithiobenzoate (7, 0.1 M; 7**a**, 0.4 M), or (d) cyanoisopropyl dodecyl trithiocarbonate (**8**, 0.5 M) and AIBN-α-$^{13}$C (0.1 M). AIBN (●), TMSN (□), KB (Δ), IBN (○), total cyanoisopropyl end groups (——) and those with n=1 (----), n=2(— —), and >3(—— ——) (individual oligomers were not resolved in experiments with 7, the average chain length was >3 even for small elapsed time).*

Downloaded by 89.163.34.136 on June 25, 2012 | http://pubs.acs.org
Publication Date: August 13, 2009 | doi: 10.1021/bk-2009-1024.ch001

The evolution of the normalized concentration of the various AIBN derived products with time for experiments with 0.5 M RAFT agent is shown in Figure 3. It can be seen that the rate of disappearance of AIBN and formation of TMSN, IBN and total end groups is similar for all experiments. As mentioned above the amount of K could not be directly determined. However, the amount of K formed approximated as 1-(AIBN+TMSN+IBN(×2) + total labeled cyanoisopropyl end groups)+KB is also essentially independent of the RAFT agent and is consistent with the amount of K observed in the polymerization mixture after it had been cooled to ambient temperature. Even though the total labeled cyanoisopropyl end groups is RAFT agent independent, the fractions of oligomers of different chain lengths is strongly dependent on the particular RAFT agent.

In experiments with benzyl dithiobenzoate-*thiocarbonyl*-$^{13}$C (**7**) a group of resonances is seen in the region δ 70-80. These are tentatively attributed to the labeled dithioacetal carbon of "3-arm stars" such as **10**-**12**. Calitz et al. reported products tentatively identified as 3-arm or 4 armed stars in experiments with cumyl dithiobenzoate-α-$^{13}$C at longer reaction times. Kwak et al. observed formation of **9** when phenylethyl radical was generated in the presence of phenylethyl dithiobenzoate.

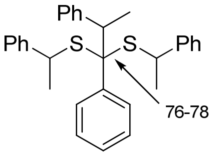

**9**[17]

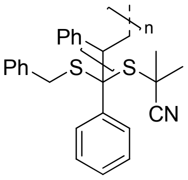

**10**

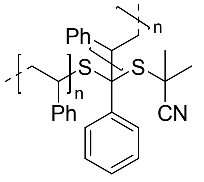

**11**

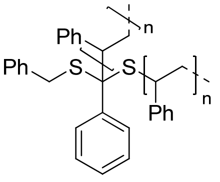

**12**

When AIBN-α$^{13}$C is decomposed in the presence of benzyl dithiobenzoate but in the absence of monomer, signals attributable to the product **14** (Scheme 4) are observed. This product is not observed in polymerization experiments probably because the cyanoisopropyl radical is preferentially consumed by reaction with styrene under those conditions. There is also evidence for the formation of other dithioesters. Such (e.g. **17**) might be formed as shown in Scheme 4. Signals associated with dithioketene acetals (e.g. **15**) have not been identified.

One product observed with benzyl dithiobenzoate is characterized by doublet resonances at δ 74.7 (derived from **7**) and 34.3 (derived from AIBN-α$^{13}$C) with $J_{cc}$ 4.2 Hz (a singlet resonance 34.3 derived from AIBN-α$^{13}$C in experiment with unlabeled RAFT agent **7a**). The analogous product was not observed in experiments with the other RAFT agents as evidenced by the absence of signals at δ 34.3.

*Scheme 4. Some Possible Side Reactions of Benzyl Dithiobenzoate*

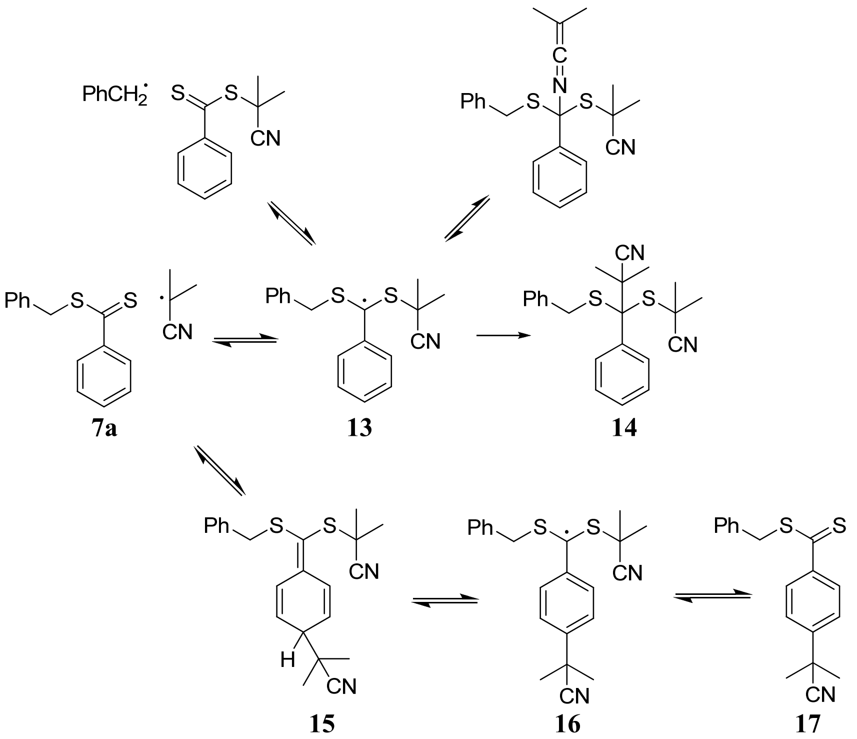

The rate of monomer consumption with time was linear with time in all experiments indicating that a steady state of some form was established (Figure 4). For experiments with 0.5 M RAFT agent, the rate of styrene consumption increased in the series cumyl dithiobenzoate ~ benzyl dithiobenzoate < cyanoisopropyl dithiobenzoate < cyanoisopropyl trithiocarbonate. For both 0.1 M and 0.5 M RAFT agent the rates of styrene consumption were similar with cumyl and benzyl dithiobenzoates even though the rate of consumption of RAFT agent and the molecular weight of polymer formed was very different (vide infra). With both cyanoisopropyl RAFT agents the consumption of styrene is initially rapid with respect to the steady state rate.

Downloaded by 89.163.34.136 on June 25, 2012 | http://pubs.acs.org
Publication Date: August 13, 2009 | doi: 10.1021/bk-2009-1024.ch001

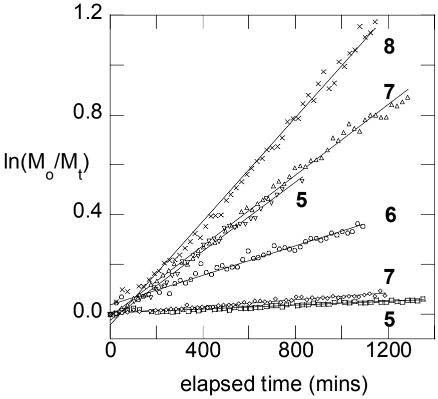

*Figure 4. Kinetic plot showing rate of monomer consumption with time during polymerization of styrene in benzene-d$_6$ (50% v/v) at 68.5 ºC with 0.5 M [**5**] (□), 0.1 M [**5**] (▽), 0.5 M [**6**] (○), 0.5 M [7] (◊), 0.1 M [7] (Δ), 0.5 M [**8**] (×) RAFT agent and with 0.1 M azobis(isobutyronitrile).*

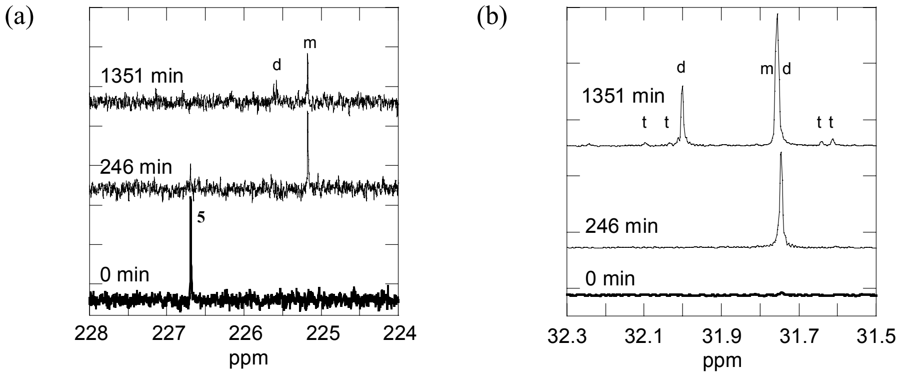

*Figure 5. Portions of $^{13}$C NMR spectra recorded during polymerization of styrene (4.36 M in benzene-d$_6$) at 70 ºC with cumyl dithiobenzoate (**5**, 0.5 M) and AIBN-α-$^{13}$C (0.1 M) showing signals attributed to (a) labeled thiocarbonyl carbons and (b) the labeled cyanoisopropyl end groups of styrene oligomers (m=1 unit chain (e.g. **19**), d=2 unit chain (e.g. **20**), t=3 unit chain (e.g. **21**)). For details of signal assignments see Figure 6.*

Downloaded by 89.163.34.136 on June 25, 2012 | http://pubs.acs.org
Publication Date: August 13, 2009 | doi: 10.1021/bk-2009-1024.ch001

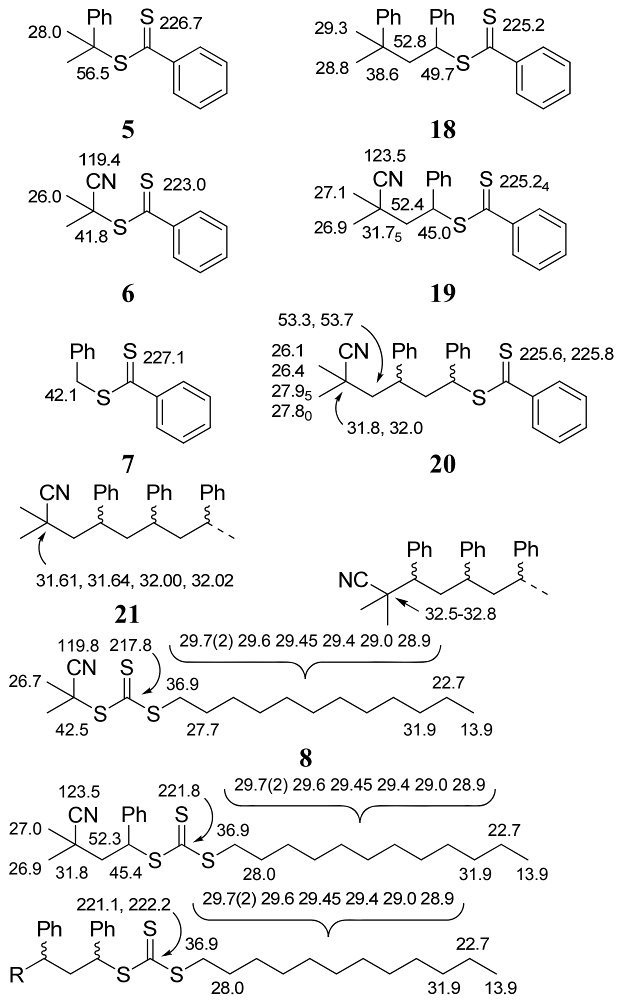
28.0
Ph
S 226.7
56.5
S
5
29.3
Ph
Ph
S 225.2
52.8
28.8
38.6
49.7
S
18
119.4
CN
S 223.0
26.0
41.8
S
6
123.5
CN
Ph
S 225.2₄
27.1
52.4
26.9
31.7₅
45.0
S
19
Ph
S 227.1
42.1
S
7
53.3, 53.7
26.1
26.4
27.9₅
27.8₀
CN
Ph
Ph
S 225.6, 225.8
S
31.8, 32.0
20
CN
Ph
Ph
Ph
31.61, 31.64, 32.00, 32.02
21
Ph
Ph
Ph
NC
32.5-32.8
119.8
217.8
29.7(2) 29.6 29.45 29.4 29.0 28.9
CN
S
26.7
36.9
22.7
42.5
S
S
27.7
31.9
13.9
8
123.5
221.8
29.7(2) 29.6 29.45 29.4 29.0 28.9
CN
Ph
S
27.0
52.3
36.9
22.7
26.9
31.8
45.4
S
S
28.0
31.9
13.9
221.1, 222.2
29.7(2) 29.6 29.45 29.4 29.0 28.9
Ph
Ph
S
36.9
22.7
R
S
S
28.0
31.9
13.9

*Figure 6. $^{13}$C NMR chemical shifts (benzene-d$_6$, 70 ºC) of RAFT agents and macro RAFT agents formed with styrene.*

Conversion of the K to a stable byproduct KB by itself is expected to cause some retardation, since in other circumstances, K would revert to cyanoisopropyl radicals. However, this effect should be of little significance. Nonetheless, there appears to be a correlation (possibly fortuitous) between the rate of styrene consumption and the yield of the ketenimine by-product KB.

Downloaded by 89.163.34.136 on June 25, 2012 | http://pubs.acs.org
Publication Date: August 13, 2009 | doi: 10.1021/bk-2009-1024.ch001

## Conclusions

Real-time NMR has been used to study RAFT polymerizations of styrene with azobis(isobutyronitrile-α-$^{13}$C) as initiator and various RAFT agents. The rate of AIBN decomposition and the initiator efficiency are essentially affected by the presence of RAFT agent even when high concentrations are used. However, the rate of polymerization and the polystyrene chain length distribution is strongly dependent on both the type and concentration of RAFT agent with the rate of styrene consumption increasing in the series cumyl dithiobenzoate ~ benzyl dithiobenzoate < cyanoisopropyl dithiobenzoate < cyanoisopropyl trithiocarbonate.

An unexpected finding is the observation of $^{13}$C CIDNP for K formed by cage recombination of AIBN-derived cyanoisopropyl radicals and the formation of an as yet unidentified by-product (KB) from K. There appears to be a correlation between the yield of KB and the observed rate of polymerization though this may be fortuitous.

With benzyl dithiobenzoate (**7**), consumption of the initial RAFT agent is relatively very slow and various by-products. These byproducts include direct coupling with the RAFT intermediate (intermediate radical termination) and other products possibly include some formed by the "missing step" process proposed by Buback and Vana.

Downloaded by 89.163.34.136 on June 25, 2012 | http://pubs.acs.org
Publication Date: August 13, 2009 | doi: 10.1021/bk-2009-1024.ch001

## Experimental

Nuclear magnetic resonance (NMR) spectra were obtained with a Bruker DRX500 spectrometer operating at 125.8 MHz for $^{13}$C and 500.1 MHz for $^{1}$H. Chemical shifts are reported in ppm from external tetramethylsilane. Quantitative $^{13}$C NMR spectra were obtained using an inverse-gated pulse sequence with a 30° pulse (zgig30) allowing a 20 s relaxation delay between scans and were summed over 64 scans for each data point. The following reagents were used without further purification: Benzoic-*carbonyl*-$^{13}$C acid (Aldrich, 99 atom% $^{13}$C); dicyclohexylcarbodiimide (Aldrich 99%); Lawesson reagent (Aldrich 97%). AIBN (DuPont) was purified by crystallization from chloroform /methanol at -20ºC.

**Benzyl Dithiobenzoate-*thiocarbonyl*-$^{13}$C.** Dicyclohexylcarbodiimide (0.84 g, 4.1 mmol) was added in one portion to a solution of benzoic-*carbonyl*-$^{13}$C acid (0.5 g, 4.06 mmol) and benzyl mercaptan (0.51 g, 4.06 mmol) in dichloromethane (10 mL). The resulting mixture was allowed to stir at room temperature overnight. The by-product, dicyclohexyl urea, was separated by filtration and the filtrate was concentrated to give the product, *S*-benzyl thiobenzoate-*carbonyl*-$^{13}$C (0.41 g, 46.5 %) as a colorless liquid which was used directly in the next step. $^{13}$C NMR ($CDCl_3$) δ191.3 (C=O)

A solution of *S*-benzyl thiobenzoate-carbonyl-$^{13}$C (0.41 g) and Lawesson reagent (0.46 g) in toluene (5 mL) were heated at 110 °C for 45 hours during this time the initially colorless reaction mixture turned dark red. After cooling to room temperature, the reaction mixture was concentrated and chromatographed on a silica-gel with 3% ethyl acetate in *n*-hexane as eluent to yield benzyl dithiobenzoate-*thiocarbonyl*-$^{13}$C (0.35 g, 75.6%). The $^{13}$C NMR showed the product to be contaminated with ca 5% of the unchanged *S*-benzyl thiobenzoate-*carbonyl*-$^{13}$C.

$^{13}$C NMR (benzene-$d_6$ , 70 ºC) δ227.1 (C=S), 145.0 (d, $C_1$, $J_{CC}$=54 Hz), 135.3 (d, benzyl $C_1$, $J_{CC}$=2.3 Hz), 131.9 (d, $C_4$, $J_{CC}$=1.3 Hz), 129.2 (s, 2×benzyl $C_3$), 128.7 (s, benzyl $C_4$), 128.5 (s, 2×benzyl $C_2$) 128.1 (d, 2×$C_3$, $J_{CC}$=4.5 Hz), 126.9 (d, 2×$C_2$, $J_{CC}$=2.6 Hz) , 42.1 (d, $CH_2$, $J_{CC}$=1 Hz).

**AIBN-α-$^{13}$C.** AIBN-α-$^{13}$C was available from our previous study.[36,37] $^{13}$C NMR (benzene-$d_6$, 70 ºC) δ 118.3 (s, C≡N) 67.6 (s, $C_q$), 24.5 (d, $CH_3$, $J_{CC}$=60Hz)

**Polymerizations.** The following experiment is typical. Benzyl dithiobenzoate-*thiocarbonyl*-$^{13}$C (14.7 mg, 0.1 M) and AIBN (9.96 mg, 0.1 M) were weighed in a vial and styrene (0.3 mL, 273 mg, 4.36 M) and benzene-$d_6$ (0.3 mL, 264 mg, 5.63 M) added and the solution was transferred to an NMR tube. The contents of the NMR tube were degassed through three freeze-evacuate-thaw cycles and the NMR tube sealed under nitrogen. The NMR tube was then placed in the preheated probe of the NMR spectrometer and the acquisition of data commenced immediately (first data point after ~7 minutes). Details of reagent concentrations used in other experiments are provided in Table 1.

**Table 1.** Reagents concentrations used in styrene polymerizations[a]

| *[AIBN-α-$^{13}$C] M* | *RAFT agent* | *[RAFT agent] M* | *[Styrene] M* |
|---|---|---|---|
| 0.1 | **5** | 0.1 | 4.36 |
| 0.1 | **5** | 0.5 | 4.36 |
| 0.1 | **6** | 0.5 | 4.36 |
| 0.1 | **7** | 0.1 | 4.36 |
| 0.1 | **7** | 0.1 | 0[b] |
| 0.1 | **7+7a** | 0.1+0.4 | 4.36 |
| 0.1 | **8** | 0.5 | 4.36 |

[a] Concentrations at 22 ºC, solvent is benzene-$d_6$. [b] Control experiment.

Downloaded by 89.163.34.136 on June 25, 2012 | http://pubs.acs.org
Publication Date: August 13, 2009 | doi: 10.1021/bk-2009-1024.ch001

# References

1. Moad, G.; Chiefari, J.; Krstina, J.; Postma, A.; Mayadunne, R. T. A.; Rizzardo, E.; Thang, S. H. *Polym. Int.* **2000,** 49, 993-1001.
2. Moad, G.; Rizzardo, E.; Thang, S. H. *Aust. J. Chem.* **2005,** 58, 379-410.
3. Moad, G.; Rizzardo, E.; Thang, S. H. *Aust. J. Chem.* **2006,** 59, 669-692.
4. Moad, G.; Rizzardo, E.; Thang, S. H. *Polymer* **2008,** 49, 1079-1131.
5. Moad, G.; Rizzardo, E.; Thang, S. H. *Acc. Chem. Res.* **2008,** 41, 1133-1142.
6. Chiefari, J.; Chong, Y. K.; Ercole, F.; Krstina, J.; Jeffery, J.; Le, T. P. T.; Mayadunne, R. T. A.; Meijs, G. F.; Moad, C. L.; Moad, G.; Rizzardo, E.; Thang, S. H. *Macromolecules* **1998,** 31, 5559-62.
7. Moad, G.; Barner-Kowollik, C., The Mechanism and Kinetics of the RAFT Process: Overview, Rates, Stabilities, Side Reactions, Product Spectrum and Outstanding Challenges. In *Handbook of RAFT Polymerization*, Barner-Kowollik, C., Ed. Wiley-VCH, : Weinheim, Germany, 2008; pp 51-104.
8. Moad, G.; Chiefari, J.; Moad, C. L.; Postma, A.; Mayadunne, R. T. A.; Rizzardo, E.; Thang, S. H. *Macromol. Symp.* **2002,** 182, 65-80.
9. Chong, Y. K.; Krstina, J.; Le, T. P. T.; Moad, G.; Postma, A.; Rizzardo, E.; Thang, S. H. *Macromolecules* **2003,** 36, 2256-2272.
10. Barner-Kowollik, C.; Buback, M.; Charleux, B.; Coote, M. L.; Drache, M.; Fukuda, T.; Goto, A.; Klumperman, B.; Lowe, A. B.; Mcleary, J. B.; Moad, G.; Monteiro, M. J.; Sanderson, R. D.; Tonge, M. P.; Vana, P. *J. Polym. Sci., Part A, Polym Chem* **2006,** 44, 5809-5831.
11. Barner-Kowollik, C.; Quinn, J. F.; Morsley, D. R.; Davis, T. P. *J. Polym. Sci., Part A, Polym. Chem.* **2001,** 39, 1353-1365.
12. Izgorodina, E. I.; Coote, M. L. *Macromol. Theory Simul.* **2006,** 15, 394-403.
13. Coote, M. L.; Izgorodina, E. I.; Krenske, E. H.; Busch, M.; Barner-Kowollik, C. *Macromol. Rapid. Commun.* **2006,** 27, 1015-1022.
14. Feldermann, A.; Coote, M. L.; Stenzel, M. H.; Davis, T. P.; Barner-Kowollik, C. *J. Am. Chem. Soc.* **2004,** 126, 15915-15923.
15. Monteiro, M. J.; de Brouwer, H. *Macromolecules* **2001,** 34, 349-352.
16. Kwak, Y.; Goto, A.; Fukuda, T. *Macromolecules* **2004,** 37, 1219-1225.
17. Kwak, Y.; Goto, A.; Komatsu, K.; Sugiura, Y.; Fukuda, T. *Macromolecules* **2004,** 37, 4434-4440.
18. Buback, M.; Vana, P. *Macromol. Rapid. Commun.* **2006,** 27, 1299-1305.
19. Buback, M.; Janssen, O.; Oswald, R.; Schmatz, S.; Vana, P. *Macromol. Symp.* **2007,** 248, 158-167.
20. Vana, P. *Macromol. Symp.* **2007,** 248, 71-81.
21. Drache, M.; Schmidt-Naake, G. *Macromol. Symp.* **2007,** 259, 397-405.
22. Plummer, R.; Goh, Y. K.; Whittaker, A. K.; Monteiro, M. J. *Macromolecules* **2005,** 38, 5352-5355.
23. Hawthorne, D. G.; Moad, G.; Rizzardo, E.; Thang, S. H. *Macromolecules* **1999,** 32, 5457-5459.
24. Calitz, F. M.; Tonge, M. P.; Sanderson, R. D. *Macromolecules* **2003,** 36, 5-8.
25. Alberti, A.; Benaglia, M.; Laus, M.; Macciantelli, D.; Sparnacci, K. *Macromolecules* **2003,** 36, 736-740.

Downloaded by 89.163.34.136 on June 25, 2012 | http://pubs.acs.org
Publication Date: August 13, 2009 | doi: 10.1021/bk-2009-1024.ch001

26. Konkolewicz, D.; Hawkett, B. S.; Gray-Weale, A.; Perrier, S. *Macromolecules* **2008,** 41, 6400-6412.
27. McLeary, J. B.; Calitz, F. M.; McKenzie, J. M.; Tonge, M. P.; Sanderson, R. D.; Klumperman, B. *Macromolecules* **2005,** 38, 3151-3161.
28. McLeary, J. B.; Calitz, F. M.; McKenzie, J. M.; Tonge, M. P.; Sanderson, R. D.; Klumperman, B. *Macromolecules* **2004,** 37, 2383-2394.
29. McLeary, J. B.; McKenzie, J. M.; Tonge, M. P.; Sanderson, R. D.; Klumperman, B. *Chem. Commun.* **2004**, 1950-1951.
30. van den Dungen, E. T. A.; Matahwa, H.; McLeary, J. B.; Sanderson, R. D.; Klumperman, B. *J. Polym. Sci., Part A, Polym. Chem.* **2008,** 46, 2500-2509.
31. Pound, G.; McLeary, J. B.; McKenzie, J. M.; Lange, R. F. M.; Klumperman, B. *Macromolecules* **2006,** 39, 7796-7797.
32. van den Dungen, E. T. A.; Rinquest, J.; Pretorius, N. O.; McKenzie, J. M.; McLeary, J. B.; Sanderson, R. D.; Klumperman, B. *Aust. J. Chem.* **2006,** 59, 742-748.
33. Klumperman, B.; McLeary, J. B.; Van den Dungen, E. T. A.; Soer, W. J.; Bozovic, J. *ACS Symp. Ser.* **2005,** 944, 501-513.
34. Calitz, F. M.; McLeary, J. B.; McKenzie, J. M.; Tonge, M. P.; Klumperman, B.; Sanderson, R. D. *Macromolecules* **2003,** 36, 9687-9690.
35. McLeary, J. B.; Tonge, M. P.; Klumperman, B. *Macromol. Rapid. Commun.* **2006,** 27, 1233-1240.
36. Moad, G.; Rizzardo, E.; Solomon, D. H.; Johns, S. R.; Willing, R. I. *Makromol. Chem., Rapid Commun.* **1984,** 5, 793-8.
37. Moad, G.; Solomon, D. H.; Johns, S. R.; Willing, R. I. *Macromolecules* **1984,** 17, 1094-9.
38. Krstina, J.; Moad, G.; Willing, R. I.; Danek, S. K.; Kelly, D. P.; Jones, S. L.; Solomon, D. H. *Eur. Polym. J.* **1993,** 29, 379-88.
39. Krstina, J.; Moad, G.; Solomon, D. H. *Eur. Polym. J.* **1992,** 28, 275-82.
40. Moad, G.; Solomon, D. H., *The Chemistry of Radical Polymerization*. 2nd ed.; Elsevier: Oxford, 2006.
41. Aurica, P. C. *J Appl Polym Sci* **2005,** 98, 1025-1031.
42. Joachim, B. *Helvetica Chimica Acta* **2006,** 89, 2082-2102.

Downloaded by 89.163.34.136 on June 25, 2012 | http://pubs.acs.org
Publication Date: August 13, 2009 | doi: 10.1021/bk-2009-1024.ch001

Downloaded by UNIV OF GUELPH LIBRARY on June 26, 2012 | http://pubs.acs.org
Publication Date: August 13, 2009 | doi: 10.1021/bk-2009-1024.ch002

## Chapter 2

# Influence of Molecular Weight Distribution (MWD) on $k_t$ and the Onset of the Gel Effect using the RAFT-CLD-T Method

**Geoffrey Johnston-Hall, and Michael J. Monteiro***

Australian Institute of Bioengineering and Nanotechnology (AIBN), University of Queensland, Brisbane QLD 4072, Australia, e-mail: m.monteiro@uq.edu.au

Understanding how the broadening of the molecular weight distribution (MWD) affects the termination rate coefficient, $\langle k_t \rangle$, during free radical polymerization (FRP) is important for developing models capable of accurately predicting rates of polymerization and the resulting MWDs. In this article, we studied the evolution of $\langle k_t \rangle$ for the RAFT-mediated polymerization of styrene at 90 °C. A difunctional RAFT agent was used to control the evolution of PDI with conversion and the RAFT-CLD-T method was used to determine $\langle k_t \rangle$. We found that when concentration ratios of initiator to RAFT agent (i.e. $[I]_0$:$[RAFT]_0$) are greater than 1:1, $\langle k_t \rangle$ increased due to significant amounts of short-long termination in agreement with theoretical predictions. The onset of the gel effect was examined and a surprising result was found. As the PDI increased there was a concomitant decrease in the molecular weight and weight fraction of polymer at which the onset of the gel effect was observed. This seems counterintuitive to all physical theories for the gel effect. However, when broad MWDs are accounted for using chain dynamic statistics, chain overlap (or c*) can once again account for the onset of the gel effect in agreement with previous work for narrow MWDs. These results are important and provide strong evidence for chain overlap as the cause of

In Controlled/Living Radical Polymerization: Progress in RAFT, DT, NMP & OMRP; Matyjaszewski, K.; ACS Symposium Series; American Chemical Society: Washington, DC, 2009.

the onset of the gel effect. The RAFT-CLD-T method has provided valuable insight into the effects of polymer chain shape, interactions and mobility on $k_t$.

Downloaded by UNIV OF GUELPH LIBRARY on June 26, 2012 | http://pubs.acs.org
Publication Date: August 13, 2009 | doi: 10.1021/bk-2009-1024.ch002

## Introduction

Reversible addition-fragmentation chain transfer (RAFT) allows the accurate determination of chain length dependent (CLD) termination rate coefficients, $k_t^{i,i}$'s. The technique known as the RAFT-CLD-T method*(10)* is a simple, robust and model independent way to elucidate the complex mechanisms of diffusion-controlled bimolecular radical termination over a wide range of polymerization conditions, monomers and matrix architectures.*(2)* This method has recently been reviewed by Johnston-Hall and Monteiro.*(2)(3)* The criteria that should be used to elucidate accurate measurements from the RAFT-CLD-T method were determined using kinetic simulations, and provided useful guidelines.*(3)* It was found that high amounts of termination between a 'short' chain radical ($i < 6$) and a 'long' chain radical ($i \geq 6$) was the main cause for loss in accuracy. An ideal way to experimentally verify the effect of short-long termination without high amounts of bimolecular termination products was through the use of a highly reactive difunctional RAFT agent.

Previous work*(4,5)* carried out using simulations and experiments showed that the number-average molecular weight ($M_n$) increased linearly with conversion as expected from theory, and the polydispersity index (PDI) was controlled depending on the ratio of initiator to RAFT agent concentration. Importantly, in a difunctional RAFT-mediated polymerization there is negligible dead polymer, unlike the high amounts found in a monofunctional RAFT system under similar high initiator to RAFT ratios. It has been shown for the difunctional RAFT- mediated polymerization that at greater initiator to RAFT concentrations the greater the corresponding increase in PDI as a function of conversion. This important observation provides a means to study how a linear increase in $M_n$ and a broadening molecular weight distribution (MWD) can affect the evolution of $\langle k_t \rangle$. It is expected that as the initiator concentration is increased there will be much greater short-long termination and thus deviation from accurate $k_t$ *vs* $i$ profiles. The results will also provide valuable insight into how broad MWDs affect the onset of the gel effect.

A number of conflicting opinions concerning what physical mechanism controls bimolecular termination and the point at which the gel effect occurs during FRP have been given.*(6)* However, these opinions have been obtained from $\langle k_t \rangle$ data for polymer with broad MWDs, and it can be difficult to discriminate between theories for the mechanism of diffusion controlled termination due to other competing factors, such as 'short-long' termination.*(3,7)* An understanding of how the MWD affects $\langle k_t \rangle$ and the onset of the gel effect is important for (1) resolving the conflicting information in the literature concerning the mechanism of bimolecular termination and (2) for developing models capable of accurately predicting termination rate coefficients during FRP.

# Experimental

## Chemicals

Styrene (STY, 99 %, Aldrich) was purified by filtration through basic alumina (70-230 mesh) to remove inhibitors prior to use. 1,1- azobis (cyclohexanecarbonitrile) (VAZO88, 99 %, Du Pont) was purified by by two recrystallizations from methanol. All other reagents used in the synthesis of RAFT agents (described below) were obtained from Aldrich (99 % purity or greater) and used as received. 1,3-bis(benzyl-thiocarbonyl-sulfanyl-2-prop-2-yl)benzene (BTBTPB) was synthesized according to the literature and confirmed by $H^1$-NMR and elemental analysis *(4,8)*.

## A Typical Procedure for the RAFT-Mediated Polymerization of STY

Styrene (25 mL, 8.15 M), VAZO88 (1.223 g, 199.98 mM), and BTBTPB (0.305 g, 49.98 mM) were added to a reaction vessel, degassed by four successive freeze-pump-thaw cycles, sealed under vacuum, and polymerized at 90 °C. Conversion was measured gravimetrically by drying the samples in a vacuum oven at ambient temperature until at constant weight. The molecular weight distribution was determined by size exclusion chromatography (SEC).

## A Typical Differential Scanning Calorimetry (DSC) RAFT Polymerization of STY

Polymerizations, monitored by DSC, were all performed in duplicate. 2mL of a stock solution (ie 25mL of styrene, 1.223 g of VAZO88, and 0.305 g of BTBTPB) were transferred to a reaction vessel, degassed by four successive freeze-pump-thaw cycles, and transferred into gas tight DSC pans using a glove bag under nitrogen. The sample weights in the DSC pans ranged between 30 to 65 mg. (The weight in the DSC pans was measured by mass difference between empty and full.) The polymerizations were carried out isothermally at 90 °C, and the heat of polymerization measured by comparing the heat flow from the polymerization pan and an empty pan on a Perkin Elmer DSC 7 with a TAC 7/DX Thermal Analysis Instrument Controller. The DSC instrument was calibrated with a standard Indium sample of known mass, melting point temperature and associated enthalpy change. The rate of polymerization ($R_p$) and monomer conversion ($x$) were calculated using literature values for the heat of polymerization of STY ($\Delta H_p = -73$ kJ mol$^{-1}$)*(9)*.

Downloaded by UNIV OF GUELPH LIBRARY on June 26, 2012 | http://pubs.acs.org
Publication Date: August 13, 2009 | doi: 10.1021/bk-2009-1024.ch002

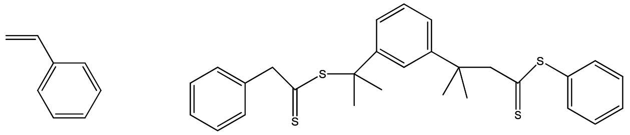

**STY** **BTBTPB**

*Scheme 1. Structures of styrene (STY) and the difunctional RAFT agent 1,3-bis(benzyl-thiocarbonyl-sulfanyl-2-prop-2-yl)benzene (BTBTPB).*

## Size Exclusion Chromatography

Size exclusion chromatography (SEC) measurements of the linear polymer were performed using a Waters Alliance 2690 Separations Module equipped with an autosampler, column heater, differential refractive index detector and a Photo Diode Array (PDA) connected in series. HPLC grade tetrahydrofuran was used as eluent at a flow rate of 1 mL min$^{-1}$. The columns consisted of three 7.8 × 300mm Waters Styragel GPC columns connected in series, comprising 2 linear Ultrastyragel and one Styragel HR3 columns. Polystyrene standards ranging from 2000000 - 517 g mol$^{-1}$ were used for calibration.

## Determination of Termination Rate Coefficients

Termination rate coefficients, $k_t$'s, were determined using the RAFT-CLD-T Method*(7,10-12)*. Due to the moderate reaction temperature (90 ºC) self-initiation of styrene through thermal reactions could not be excluded. An expression for the rate of auto-initiation*(13)*, $R_{th}$, was therefore included in the calculation of the time-dependent termination rate coefficient, $k_t$(t) (eq 1). Elsewhere we have shown this treatment to be accurate(*6*).

$$k_{\mathrm{t}}(t)=\frac{2\cdot f\cdot k_{\mathrm{d}}\cdot[I]_0\cdot e^{-k_{\mathrm{d}}\cdot t}+R_{\mathrm{th}}-\dfrac{d\left(\dfrac{R_{\mathrm{p}}(t)}{k_{\mathrm{p}}\cdot\left([M]_0-\int\limits_0^t R_{\mathrm{p}}(t)\ dt\right)}\right)}{dt}}{2\cdot\left(\dfrac{R_{\mathrm{p}}(t)}{k_{\mathrm{p}}\cdot\left([M]_0-\int\limits_0^t R_{\mathrm{p}}(t)\ dt\right)}\right)^2} \qquad (1)$$

Here $[I]_o$ is the initial initiator concentration, $[M]_o$ is the initial monomer concentration, $k_d$ is the initiator decomposition rate coefficient, $k_p$ is the propagation rate coefficient, and $f$ is the initiator efficiency. Transformation of the time dependent termination rate coefficient, $k_t$(t), in eq 1 to the conversion

Downloaded by UNIV OF GUELPH LIBRARY on June 26, 2012 | http://pubs.acs.org
Publication Date: August 13, 2009 | doi: 10.1021/bk-2009-1024.ch002

and chain-length-dependent termination rate coefficient, $k_t^{i,i}(x)$, proceeds in a simple manner*(14,15)* using the experimentally determined conversion, $x$, and the experimentally observed evolution of chain length, $i$, with $x$.The auto-initiation rate constant, $R_{th}$, used in all calculations was taken from the literature *(14)*(see Table I). This value was used as constant over the full conversion range even though it is generally accepted that this will vary as a function of monomer concentration. Nonetheless, it should be noted that under the experimental conditions used in this work, the $\langle k_t \rangle$(t) values determined were relatively unaffected by $R_{th}$. All other rate coefficients used in eq 1 were taken from reliable literature sources and are listed in Table I.

Downloaded by UNIV OF GUELPH LIBRARY on June 26, 2012 | http://pubs.acs.org
Publication Date: August 13, 2009 | doi: 10.1021/bk-2009-1024.ch002

*Table I. Kinetics parameters used for determination of kt during the RAFT-mediated bulk polymerization of styrene (STY, 8.15 M) initiated with 1,1- azobis (cyclohexanecarbonitrile) (VAZO88) at 90 °C, in the presence of 1,3-bis(benzyl-thiocarbonyl-sulfanyl-2-prop-2-yl)benzene (BTBTPB).*

| *T* (°C) | $k_p$ ($L mol^{-1} s^{-1}$) | $k_d$ ($s^{-1}$) | $R_{th}$ ($mol\ L^{-1} s^{-1}$) | *f* |
|---|---|---|---|---|
| *90* | *900 (16)* | $2.7\times10^{-5}$ *(17)* | $2\times10^{-9}$ *(14)* | *0.70 (10)* |

## Results and Discussion

Based on the kinetic simulations from previous work,*(5)* reaction conditions were chosen to prepare polymers with similar $M_n$ *vs* conversion profiles but with different PDI *vs* conversion profiles. Styrene was polymerized in the presence of a highly reactive difunctional RAFT agent (1,3-bis(benzyl-thiocarbonyl-sulfanyl-2-prop-2-yl)benzene, BTBTPB) at 90 °C under bulk conditions. The ratio of initiator (VAZO88) to BTBTPB concentration (i.e. $[VAZO88]_0$:$[BTBTPB]_0$) was varied from 1:4 to 2:1 while maintaining the BTBTPB concentration constant at 50 mM. The RAFT-CLD-T method was then used to obtain $\langle k_t \rangle$ as a function of conversion and $\langle M_n \rangle$. All reaction conditions used in the polymerizations are listed in Table II.

***Table II. Reaction conditions used for the bulk polymerization of styrene (STY, 8.15 M) initiated with 1,1- azobis (cyclohexanecarbonitrile) (VAZO88) at 90 °C, in the presence of the difunctional RAFT agent 1,3-bis(benzyl-thiocarbonyl-sulfanyl-2-prop-2-yl)benzene (BTBTPB)*.**

| *Expt* | *Agent* | $[RAFT]_0$ (mM) | $[VAZO88]_0$ (mM) | $[RAFT]_0:[VAZO88]_0$ |
|---|---|---|---|---|
| *1* | *BTBTPB* | *49.96* | *25.00* | *2:1* |
| *2* | *BTBTPB* | *49.92* | *49.99* | *1:1* |
| *3* | *BTBTPB* | *50.10* | *99.99* | *1:2* |
| *4* | *BTBTPB* | *50.04* | *149.98* | *1:3* |
| *5* | *BTBTPB* | *49.98* | *199.97* | *1:4* |

Figure 1A shows the conversion *vs* time profiles for Expts 1 to 5 (Table II). When the concentration of initiator (I) was increased from 25 mM (curve a) to 200mM (curve e) the initial rate of polymerization, $R_p$, as determine from the slopes of the curves increased as expected (i.e. $R_p$~$[I]^{0.5}$). The higher initiator concentrations resulted in much faster polymerizations. The effect of these high initiator ratios on the $M_n$ *vs* conversion profiles are given in Figure 1B. All polymerizations with different initiator concentrations showed a linear increase in $M_n$ with conversion. However, only Expts 1 to 3 gave profiles close to theory, whereas Expts 4 and 5 showed deviation due to the large amount of initiator.It is unclear why the $M_n$ *vs* conversion profiles did not show a continuous change and why there are two distinct curves observed.

The effect of initiator was more clearly seen in Figure 1C, which showed the PDI *vs* conversion profiles. As the initiator concentration was increased, the evolution of the PDI with conversion also increased. At low conversions (< 20 %) the PDIs for all polymers were below 1.2, and depending upon the concentration of initiator increased from 1.3 for the lowest [I] to 1.6 for the highest [I] at high conversion. All these trends are in excellent agreement with our theoretical predictions presented previously, indicating high initiator concentrations lead to the formation of a lower molecular weight monofunctional polymeric RAFT species resulting in higher PDI's.*(5)*

The change in MWD as a function of conversion for Expts 1, 3, and 5 are shown in Figure 2, illustrating the influence of initiator concentration. In the presence of low concentrations of initiator (Expt 1, Figure 2A), the MWDs were narrow but with a low molecular weight shoulder at half the molecular weight of the main peak, becoming more predominant especially at high conversions. This is due to the formation of polymer chains with only one RAFT end-group. At higher initiator concentrations (Figure 2B and 2C), the MWDs became broader particular at moderate to high conversions. The low molecular weight shoulder

Downloaded by UNIV OF GUELPH LIBRARY on June 26, 2012 | http://pubs.acs.org
Publication Date: August 13, 2009 | doi: 10.1021/bk-2009-1024.ch002

observed in the SEC traces became even more predominant attributable to a greater rate of formation of the monofunctional polymeric RAFT agent,*(5)* and was particularly pronounced for Expt 5 at high conversions (curve e, Figure 2C).

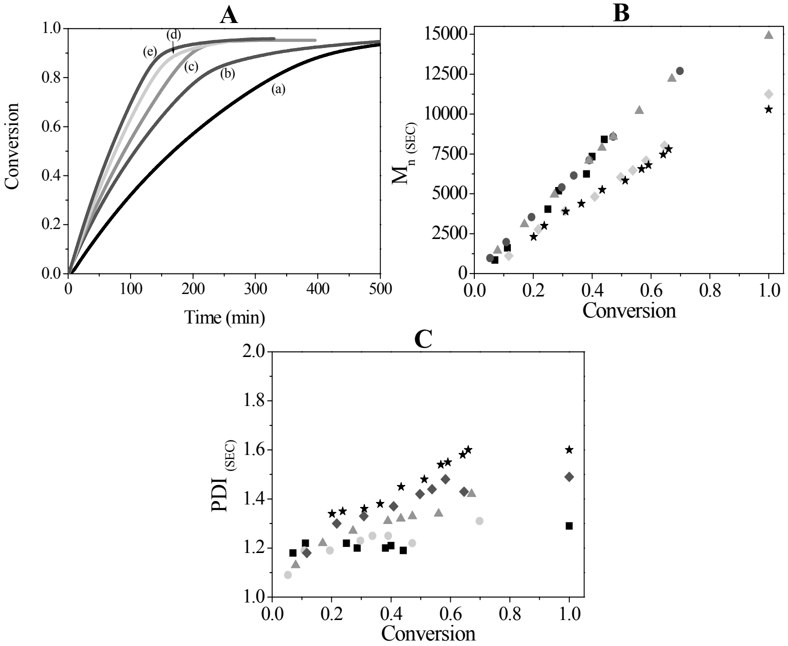

*Figure 1. (A) Conversion-time, (B) Mn vs conversion and (C) PDI vs conversion profiles determined for the difunctional RAFT agent mediated polymerization of styrene (STY, 8.15M) at 90 °C, using 1,3-bis(benzyl-thiocarbonyl-sulfanyl-2-prop-2-yl)benzene (BTBTPB, 50mM) and 1,1- azobis (cyclohexanecarbonitrile) (VAZO88) as initiator. The concentrations of VAZO88 used were (a) 25mM (■), (b) 50mM (●), (c) 100mM (▲), (d) 150mM (◆) and (e) 200mM (★).*

Using the RAFT-CLD-T method (eq. 1), termination rate coefficients were determined for Expts 1 to 5. Figure 3 shows the $k_t$ profiles for all Expts over the full conversion range. In the presence of a low initiator concentration (i.e. curves a and b), the evolution of log $\langle k_t \rangle$ *vs* log *i* follows the composite model description for termination observed previously for MMA, STY and MA.*(2,12,14)* For example, in dilute solution $k_t$ decreased quickly for chains shorter than $i_{SL}$~9, decreased moderately for chains lengths greater than 9 (i.e. termed 'long' chains), and then sharply decreased after the onset of the gel effect ($i_{gel}$) and well into the concentrated solution regime. However, as the ratio of initiator to RAFT agent was increased above 1:1 (curves (c), (d) and (e) in Figure 3), this transition became less well-defined and $\langle k_t \rangle$ was significantly higher especially in the dilute 'long' chain regime. In this regime, log $\langle k_t \rangle$ is approximately equal to 7.85 for Expts 1 and 2, close to the value of 8.0 previously reported for styrene*(14)*. However, as the initiator concentration was increased log $\langle k_t \rangle$ increased to between 8.05 and 8.2 for Expts 3 to 5. This

Downloaded by UNIV OF GUELPH LIBRARY on June 26, 2012 | http://pubs.acs.org
Publication Date: August 13, 2009 | doi: 10.1021/bk-2009-1024.ch002

gradual increase in log $\langle k_t \rangle$ values at low conversion going from Expts 1 to 5 imply that short-long termination becomes increasingly significant. The higher concentrations of ‘short’ (*i.e.* fast terminating) polymeric radicals will therefore terminate preferentially with the slow terminating ‘long’ radicals (generally in high concentration), and is supported with the pronounced low-molecular weight shoulder observed in the MWDs (see Figure 2). Also worth noting is that the slope of the dilute ‘long’ chain regime increased as the initiator was increased.

In a theoretical study using simulations to examine the experimental limitations of the RAFT-CLD-T method, it was found that for concentration ratios of initiator to RAFT agent as high as 1:1, the average termination rate coefficients were equal to the chain-length-dependent termination rate coefficient, $k_t^{i,i}$.*(3)* However, for ratios greater than 1:1, short-long termination could significantly affect the accuracy of the $k_t^{i,i}$ measurements. It was also found that broadening of the MWD (resulting from a poorly controlled RAFT-mediated polymerisation) caused $\langle k_t \rangle$ to increase and composite model behavior to disappear as a result of short-long termination. Thus, the observation that log $\langle k_t \rangle$ *vs* log *i* profiles for Expts 1 and 2 are similar but different from Expts 3 to 5 is in good agreement with these theoretical predictions,*(3)* and a strong indicator that ‘short’ radicals are of importance. These results also support the theoretical predictions that indicated initiator to RAFT agent ratios no greater than 1:1 may be used to determine accurate $k_t^{i,i}$ values via the RAFT-CLD-T method.*(3)*

Downloaded by UNIV OF GUELPH LIBRARY on June 26, 2012 | http://pubs.acs.org
Publication Date: August 13, 2009 | doi: 10.1021/bk-2009-1024.ch002

Downloaded by UNIV OF GUELPH LIBRARY on June 26, 2012 | http://pubs.acs.org
Publication Date: August 13, 2009 | doi: 10.1021/bk-2009-1024.ch002

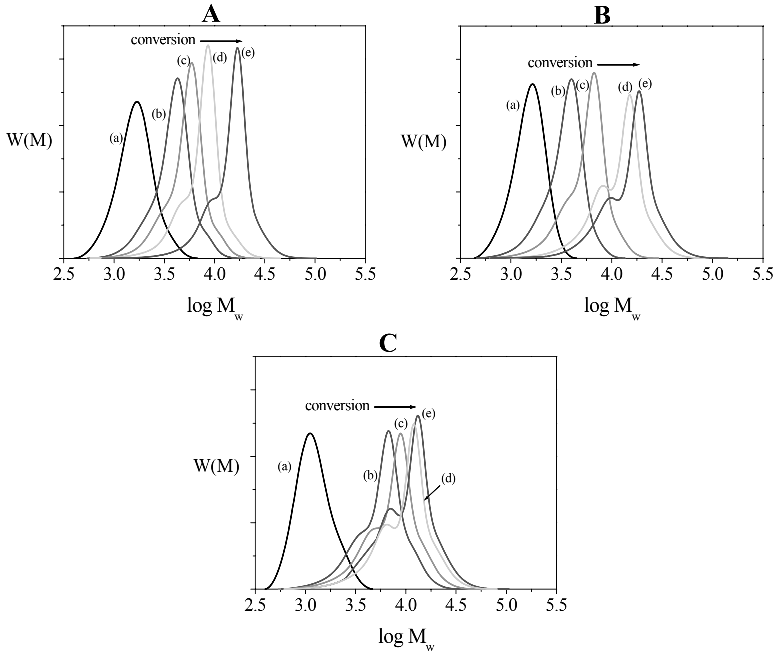

*Figure 2. Experimental MWDs for the polymerization of styrene (STY, 8.15M) at 90℃, using the difunctional RAFT agent 1,3-bis(benzyl-thiocarbonyl-sulfanyl-2-prop-2-yl)benzene (BTBTPB, 50mM) and 1,1- azobis (cyclohexanecarbonitrile) (VAZO88) as initiator. Figures correspond to initiator concentrations of (A) 25 mM, (B) 100mM and (C) 200 mM. In Figure 4A, the MWD traces correspond to (a) 10%, (b) 20%, (c) 29%, (d) 43%, and (e) 96% conversion. In Figure 4B, the MWD traces correspond to (a) 10%, (b) 25%, (c) 30%, (d) 65%, and (e) 96% conversion. In Figure 4C, the MWD traces correspond to (a) 6%, (b) 26%, (c) 33%, (d) 40%, and (e) 96% conversion. Note: at high conversions, a second low molecular weight peak appears corresponding to the formation of the mono-functional RAFT agent species (refer to text).*

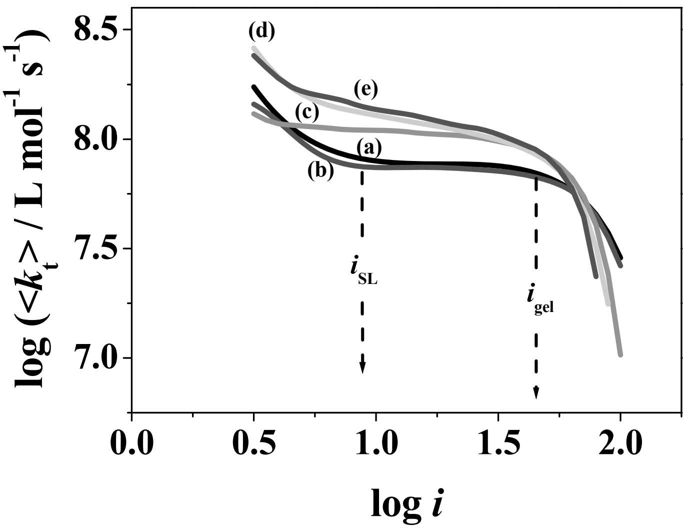

*Figure 3. log ⟨$k_t$⟩ vs. log i profiles determined using the RAFT-CLD-T Method are shown for the difunctional RAFT agent mediated polymerization of styrene (STY, 8.15M) at 90°C, using 1,3-bis(benzyl-thiocarbonyl-sulfanyl-2-prop-2-yl)benzene (BTBTPB, 50mM) and 1,1- azobis (cyclohexanecarbonitrile) (VAZO88) as initiator. The concentrations of VAZO88 used are approximately (a) 25mM, (b) 50mM, (c) 100mM, (d) 150mM, and (e) 200mM.*

Downloaded by UNIV OF GUELPH LIBRARY on June 26, 2012 | http://pubs.acs.org
Publication Date: August 13, 2009 | doi: 10.1021/bk-2009-1024.ch002

Downloaded by UNIV OF GUELPH LIBRARY on June 26, 2012 | http://pubs.acs.org
Publication Date: August 13, 2009 | doi: 10.1021/bk-2009-1024.ch002

*Influence of Increasing PDI on the Onset of the Gel Effect*

In Expts 1 to 5, the onset of the gel effect was observed by a sudden decrease in the log $\langle k_t \rangle$ vs. log $i$ profile at moderate to high conversions. Over the years, a number of theories have been proposed to account for the effects of chain mobility and dimension on $k_t$. However, the evidence collected in the literature is often conflicting, due largely to the broadening of the MWD which in turn greatly affects the evolution of $\langle k_t \rangle$ during a conventional FRP. To examine the influence of MWDs on the gel effect, the molecular weight at onset of the gel effect, $M_{n,gel}$, for Expts 1 to 5 was determined using the method reported previously, from the conversion when an initial change in linearity was observed in a plot of *log* $k_t^{i,i}$ *vs log x. (11)* Subsequently, the corresponding conversion and PDI values at the onset of the get effect ($x_{gel}$ and $PDI_{gel}$, respectively) were also determined (see Figure 3). The values of $x_{gel}$, $M_{n,gel}$, and $PDI_{gel}$ for Expts 1 to 5 are listed in Table III. As the concentration of initiator was increased, $M_{n,gel}$ decreased from 5360 (Expt 1) to 2510 (Expt 5), while $x_{gel}$ also decreased from 0.29 (Expt 1) to 0.21 (Expt 5). On the other hand, $PDI_{gel}$ increased from 1.20 to 1.31.

*Table III. Conversion, molecular weight and polydispersity index at onset of the gel effect ( $x_{gel}$, $M_{n,gel}$ and $PDI_{gel}$, respectively) were determined from the RAFT mediated polymerization of styrene (STY, 8.15M) at 90 ℃, using the difunctional RAFT agent 1,3-bis(benzyl-thiocarbonyl-sulfanyl-2-prop-2-yl)benzene (BTBTPB, 50mM) and 1,1- azobis (cyclohexanecarbonitrile) (VAZO88) as initiator. The concentrations of initiator used were: $[I]_0$= (1) 25 mM, (2) 50 mM, (3) 100 mM, (4) 150 mM, and (5) 200 mM.*

| *Rxn* | $[I]_0:[RAFT]_0$ | $x_{gel}$ | $M_{n,gel}$ | $PDI_{gel}$ |
|---|---|---|---|---|
| *1* | *1:2* | *0.29* | *5360* | *1.20* |
| *2* | *1:1* | *0.285* | *5300* | *1.23* |
| *3* | *2:1* | *0.25* | *3840* | *1.27* |
| *4* | *3:1* | *0.23* | *3000* | *1.31* |
| *5* | *4:1* | *0.21* | *2510* | *1.36* |

A number of physical explanations have been proposed for the cause of the gel effect. It has been suggested, for example, that entanglement formation may provide an explanation for the gel effect onset.*(18,19)* For polystyrene in the melt-state, entanglement molecular weights are estimated at ~ 16600 and increase with dilution (according to $M_{entanglement}$ ~ $c^{-1}$) *.(20)* However, we observed that the $M_{n'gel}$ at onset of the gel effect in Table III were far too small to be entangled. Torkelson et al arrived at the same conclusion after examining the effects of adding high concentrations of initiator and chain transfer agent to the conventional FRP of methyl methacrylate.*(6)* The authors found many of their results could be explained by a critical free volume,*(21)* which is independent of molecular weight. The data from Table III shows a clear molecular weight dependence that is further supported throughout the literature.*(2,6,7,11,12,14,18,22)*

Previously, we observed that for a system with a monodisperse MWD the onset of the gel effect coincided with the concentration at which all the chains in solution overlap (i.e. the overlap concentration, $c$*).*(12,14)* The theoretical overlap concentration for a monodisperse polymer sample, $c^*_{,\mathrm{mono}}$, with a given molecular weight, $M_\mathrm{n}$, and radius of gyration, $R_\mathrm{g}$, can be calculated according to eq 2,*(12,14,23)*

$$c^*_{,mono} = \frac{M_\mathrm{n}}{R_\mathrm{g}{}^3 N_\mathrm{av}} \tag{2}$$

where $N_\mathrm{av}$ is Avogadro's number and the radius of gyration, $R_\mathrm{g}$, is given in terms of the molecular weight of monomer, $mw$, the length between two monomer units, $l$, and the expansion factor, $C^\infty$, via the expression*(24)*

$$R_\mathrm{g} = \sqrt{\frac{\mathrm{C}^\infty M_\mathrm{n} l^2}{mw}} \tag{3}$$

Eqs 2 and 3 predict $c^*_\mathrm{mono}$ scales with an inverse square-root molecular weight dependence ($c^*_{,\mathrm{mono}}$~$M_\mathrm{n}^{-0.5}$). In contrast, the molecular weight dependence for $x_\mathrm{gel}$ with $M_\mathrm{n,gel}$ in Table III increases with a power law exponent of 0.4 (ie $x_\mathrm{gel}$~$M_\mathrm{n}^{+0.4}$). At first glance this appears to contradict the view that molecular overlap is the cause for the gel effect. However, it is important to account for the effect of MWD on molecular overlap since $\mathrm{PDI_{gel}}$ changes with $x_\mathrm{gel}$ for Expts 1 to 5.

For polydisperse samples, the $R_\mathrm{g}$ predicted by eqs 2 and 3 must be corrected for broadening of the MWD.*(25,26)* According to Gaussian chain statistics, the mean square radius of gyration $\langle R_\mathrm{g}{}^2\rangle$ for a polydisperse sample can be estimated from the persistence length, $b$, and contour length, $L$, using eq 4 (where $U = M_\mathrm{w}/M_\mathrm{n}-1$).*(25,26)*

$$\left\langle R_\mathrm{g}{}^2 \right\rangle = \frac{bL(2U+1)}{3(U+1)} \tag{4}$$

Thus, from eqs 2 to 4 the theoretical $c$* for a polydisperse polymer, $c^*_\mathrm{poly}$, compared with a monodisperse polymer, $c^*_\mathrm{mono}$, of equal $M_\mathrm{n}$ is given by eq 5.

Downloaded by UNIV OF GUELPH LIBRARY on June 26, 2012 | http://pubs.acs.org
Publication Date: August 13, 2009 | doi: 10.1021/bk-2009-1024.ch002

$$c^*_{,\,\mathrm{poly}} = \frac{c^*_{,\,\mathrm{mono}}}{\left[(2U+1)/(U+1)\right]^{3/2}} \qquad (5)$$

Importantly, eq 5 predicts that for a polydisperse polymer the overlap concentration will decrease as PDIs increase, in direct correlation with the data found in Table III. Both $M_{\mathrm{n,gel}}$ and $x_{\mathrm{gel}}$ decreased as $\mathrm{PDI}_{\mathrm{gel}}$ increased and was in excellent agreement with eq 5. One can see why there was so much confusion in the literature and how many conclusions were drawn from similar polymerizations.

Figure 4 compares the experimental $\mathrm{M}_{\mathrm{n,gel}}$ vs. $x_{\mathrm{gel}}$ data presented in Table III against theoretical profiles for $\mathrm{c}^*_{,\mathrm{poly}}$ determined using eq's 2 to 5. The $\mathrm{M}_{\mathrm{n}}$ vs $\mathrm{c}^*_{,\mathrm{poly}}$ profiles were shown for PDI's of 1.0, 1.1, 1.2, 1.3, 1.4, and 1.5. It was encouraging that c* for a PDI = 1.0 compared favorably with $x_{\mathrm{gel}}$ for the near monodisperse polymer sample (Expt 1, curve a). As the PDI's increased, $\mathrm{c}^*_{,\mathrm{poly}}$ decreased following a similar trend to $x_{\mathrm{gel}}$. While the results in Figure 4 agree qualitatively with eq's 2 to 5, quantitatively the theoretical values predicted for $\mathrm{c}^*_{,\mathrm{poly}}$ differ from the experimentally measured $x_{\mathrm{gel}}$ values. Although the cause for this difference is not clear, there are a number of factors that are likely to contribute to this, including 'short-long' termination. Also, it must be acknowledged that the theoretical $\mathrm{c}^*_{,\mathrm{poly}}$ values determined using eq 4 are derived based on Gaussian chain statistics for a Schulz-Flory distribution, which is unlikely to represent an ideal approximation for the system studied here. Nonetheless, the similarities between eq 5 and experiment are very encouraging, indicating molecular overlap can explain the onset of the gel effect even in polydisperse systems.

This is an important result, especially when one considers that over the years many of the experimental approaches used to investigate the cause of the gel effect have used the introduction of large amounts of initiator or chain transfer agent to manipulate the evolution of $M_{\mathrm{n}}$ with $x$.*(6,28,29)* However, results obtained from such studies must be considered with caution, since these practices can significantly affect the evolution of the MWD (and therefore $c^*$ and short-long termination). For example, Torkelson *et al* used various concentrations of initiator and chain transfer agent to examine the influence of $M_{\mathrm{n}}$ on the onset of the gel effect during the polymerization of MMA.*(6)* However, at only moderate polymer concentrations (i.e. no greater than 30 % weight fraction of polymer) significant scatter was observed in the PDI values: ranging from 2 to 6. Although the PDI's in this work are considerably lower than 6, it is clear from our findings above that one should be extremely cautious in drawing conclusions from data with high PDI's or large scatter in PDI values. The MWD plays a significant role, and affects the onset of molecular overlap as well as the amount of short-long termination. As a result, chain size, the MWD is a principal factor determining $\langle k_{\mathrm{t}} \rangle$ and the onset of the gel effect during FRP.

Downloaded by UNIV OF GUELPH LIBRARY on June 26, 2012 | http://pubs.acs.org
Publication Date: August 13, 2009 | doi: 10.1021/bk-2009-1024.ch002

Downloaded by UNIV OF GUELPH LIBRARY on June 26, 2012 | http://pubs.acs.org
Publication Date: August 13, 2009 | doi: 10.1021/bk-2009-1024.ch002

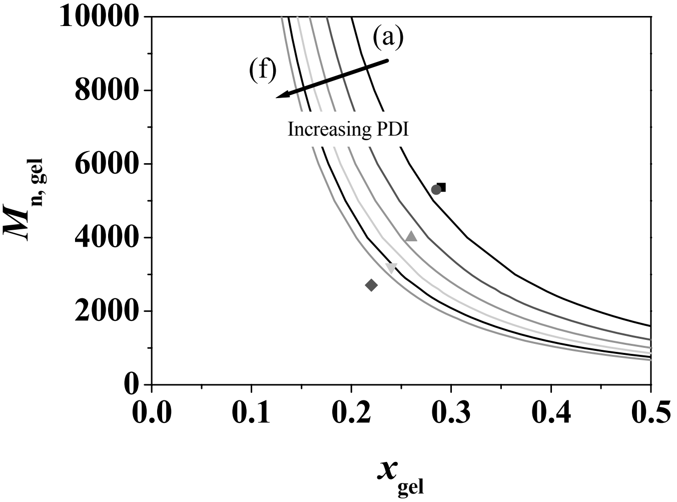

*Figure 4. Molecular weight, $M_{n,\ gel}$, vs. conversion, $x_{gel}$, determined at onset of the gel effect (symbols), are compared against the theoretical overlap concentration, $c^*_{poly}$ (solid lines), for a range of polydisperse polymers. Experimental data were determined using $[BTBTPB]_0$ = 50 mM, and initiator concentrations: $[I]_0$ = (■) 25mM (PDI = 1.2), (●) 50mM (PDI = 1.23), (▲) 100mM (PDI = 1.27), (▼) 150mM (PDI = 1.31), (◆) and 200mM (PDI = 1.36). Theoretical $c^*_{poly}$ profiles shown were calculated for PDI values of (a) PDI = 1, (b) PDI = 1.1, (c) PDI = 1.2, (d) PDI = 1.3, (e) PDI = 1.4, and (f) PDI = 1.5. $c^*_{poly}$ was calculated using eq's 2-4 and mw 104.15 g $mol^{-1}$, $l = 2 \times 1.54$ Å, and $C^{\infty}$ = 9.89(27).*

These findings for 'controlled/living' RAFT polymerization are particularly important in the context of conventional free-radical polymerization (CFRP), where PDI's are consistently high. In CFRP, very broad MWD's are expected to cause the onset of the gel effect at very low conversion, which is consistent with the data in literature.*(12)* However, in CFRP short-long termination events are also expected to play an even greater role in affecting $\langle k_t \rangle$.*(7)* This complex interplay would make the relationship between the observable onset of the gel effect and the theoretical overlap concentration more difficult to ascertain, which is also consistent with the body of information reported in the literature on this subject.*(6)*

# Conclusions

We have experimentally examined how the molecular weight distribution (MWD) influences the evolution of the average observable termination rate coefficient, $\langle k_t \rangle$, during the FRP of styrene at 90 °C. A difunctional RAFT agent was used to prepare polymers with a range of PDIs and a range of $M_n$'s. For the difunctional RAFT-mediated polymerisation, we showed that when ratios of initiator to RAFT agent were higher than 1:1, the termination rate coefficients increased. This was explained by increasing amounts of short-long termination influencing the $k_t$ profiles. For a ratio of initiator to RAFT agent no larger than 1:1 on the other hand, the average termination rate coefficients were unaffected by changing the initiator concentration in agreement with theoretical predictions indicating that short-long termination was negligible.

Upon examination of the relationship between the molecular weight and polymer concentration at the onset of the gel effect, the high ratios of initiator to RAFT agent uncovered a surprising result. As PDIs increased with high concentrations of initiator, the transition to the onset of the gel effect was found to occur at lower polymer concentrations and lower molecular weights. At first glance, this result seems counterintuitive to all physical theories for the gel effect. However, by correcting the theoretical chain overlap concentration for broadening of the MWD it was shown that chain overlap can explain this phenomenon. Importantly, for reactions with very high PDI\s the influence of short-long termination on the gel effect could not be ignored, and influenced the value of the molecular weight at the onset of the gel effect. These results are important and provide strong evidence for chain overlap as the cause of the onset of the gel effect. The RAFT-CLD-T method has provided an excellent technique to study the influence of MWDs on $k_t$.

# Acknowledgments

G.J.-H. acknowledges financial support from the Australian Institute for Nuclear Science and Engineering (AINSE PGRA) and the University of Queensland (UQJRS scholarship). M J M acknowledges financial support from an Australian Research Council (ARC) Discovery grant and receipt of a QEII Fellowship (ARC fellowship).

Downloaded by UNIV OF GUELPH LIBRARY on June 26, 2012 | http://pubs.acs.org
Publication Date: August 13, 2009 | doi: 10.1021/bk-2009-1024.ch002

## References

(1) Theis, A.; Feldermann, A.; Charton, N.; Stenzel, M. H.; Davis, T. P.; Barner-Kowollik, C. *Macromolecules* **2005**, *38*, 2595-2605.

(2) Johnston-Hall, G.; Monteiro, M. J. *J. Polym. Sci., Part A: Polym. Chem.* **2008**, *46*, 3155-3173.

(3) Johnston-Hall, G.; Barner-Kowollik, C.; Monteiro, M. J. *Macromol. Theory. Simul.* (In Press).

(4) Goh, Y.-K.; Monteiro, M. J. *Macromolecules* **2006**, *39*, 4966-4974.

(5) Johnston-Hall, G.; Monteiro, M. J. In *ACS Symposium Series on Controlled/Living Free Radical Polymerization*, **2006**; Vol. 944; pp 421-437.

(6) O'Neil, G. A.; Wisnudel, M. B.; Torkelson, J. M. *Macromolecules* **1996**, *29*, 7477-7490.

(7) Johnston-Hall, G.; Monteiro, M. J. *Macromolecules* **2007**, *40*, 7171-7179.

(8) Charmot, D.; Corpart, P.; Michelet, D.; Zard, S.; Biadatti, T. In *Chemical Abstracts*; Chemie, R., Ed., **1998**; Vol. WO 9858974.

(9) Bywater, D. J.; Worsford, J. *J. Polym. Sci.* **1962**, *58*, 571.

(10) Vana, P.; Davis, T. P.; Barner-Kowollik, C. *Macromol. Rapid Commun.* **2002**, *23*, 952-956.

(11) Johnston-Hall, G.; Theis, A.; Monteiro, M. J.; Davis, T. P.; Stenzel, M. H.; Barner-Kowollik, C. *Macromol Chem. Phys.* **2005**, *206*, 2047-2053.

(12) Johnston-Hall, G.; Stenzel, M. H.; Davis, T. P.; Barner-Kowollik, C.; Monteiro, M. J. *Macromolecules* **2007**, *40*, 2730-2736.

(13) Pryor, W. A.; Lasswell, L. D. *Advances in Free Radical Chemistry*; 1 ed.; Academic Press: New York, **1975**.

(14) Johnston-Hall, G.; Monteiro, M. J. *Macromolecules* **2008**, *41*, 727-736.

(15) Monteiro, M. J. *J. Polym. Sci., Part A: Polym. Chem.* **2005**, *43*, 3189-3204.

(16) Buback, M.; Gilbert, R. G.; Hutchinson, R. A.; Klumpermann, B.; Kutcha, F.-D.; Manders, B. G.; O'Driscoll, K.; Russell, G. T.; Schweer, J. *Macromol Chem. Phys.* **1995**, *196*, 3267-3280.

Downloaded by UNIV OF GUELPH LIBRARY on June 26, 2012 | http://pubs.acs.org
Publication Date: August 13, 2009 | doi: 10.1021/bk-2009-1024.ch002

(17) Brandup, J.; Immergut, E. H.; Grulke, E. A. *Polymer Handbook*; 4th ed.; J. Wiley &Sons: New York, **1999**.

(18) Tulig, T. J.; Tirrell, M. *Macromolecules* **1981**, *14*, 1501-1511.

(19) Tulig, T. J.; Tirrell, M. *Macromolecules* **1982**, *15*, 459-463.

(20) De Gennes, P. G. *Scaling Concepts in Polymer Physics*; Cornell University Press: Ithaca, NY, **1979**.

(21) O'Neil, G. A.; Wisnudel, M. B.; Torkelson, J. M. *Macromolecules* **1998**, *31*, 4537-4545.

(22) Lee, H. B.; Turner, D. T. *Macromolecules* **1977**, *10*, 226-231.

(23) Cotton, J. P.; Nierlich, M.; Boue, F.; Daoud, M.; Farnoux, B.; Jannink, G.; Duplessix, R.; Picot, C. *J. Chem. Phys.* **1976**, *65*, 1101-1108.

(24) Lodge, T. P.; Muthukumar, M. *J. Phys. Chem.* **1996**, *100*, 13275-13292.

(25) Oberthur, R. C. *Makromol. Chemie* **1978**, *179*, 2693-2706.

(26) Ogino, Y.; Fukushima, H.; Matsuba, G.; Takahashi, N.; Nishida, K.; Kanaya, T. *Polymer* **2006**, *47*, 5669-5677.

(27) Bovey, F. A. *Chain Structure and Conformation of Macromolecules*; Academic Press: New York, **1982**.

(28) Trommsdorf, E.; Kohle, H.; Lagally, P. *Makromol. Chem.* **1948**, *1*, 169-198.

(29) Wang, X.; Ruckenstein, E. *J. Appl. Polym. Sci.* **1993**, *49*, 2179-2188.

Downloaded by UNIV OF GUELPH LIBRARY on June 26, 2012 | http://pubs.acs.org
Publication Date: August 13, 2009 | doi: 10.1021/bk-2009-1024.ch002

Downloaded by PENNSYLVANIA STATE UNIV on June 26, 2012 | http://pubs.acs.org
Publication Date: August 13, 2009 | doi: 10.1021/bk-2009-1024.ch003

## Chapter 3

# RAFT Polymerization of Vinyl Acetate, Styrene and Acrylates Using *N*,*N*-Dithiocarbamates

**Vidyasagar Malepu, Christy D. Petruczok, TuTrinh Tran, Tianxi Zhang, Mahesh Thopasridharan and Devon A. Shipp***

**Department of Chemistry and Biomolecular Science, and**
**Center for Advanced Materials Processing**
**Clarkson University, Potsdam, NY 13699-5810, USA**

Homo- and block-copolymers comprised of vinyl acetate, styrene, methyl acrylate and *tert*-butyl acrylate monomers were prepared by reversible addition-fragmentation chain transfer (RAFT) polymerization using *N*,*N*-dithiocarbamates as transfer agents. Of the RAFT agents studied, malonate *N*,*N*-diphenyldithiocarbamate was able to produce poly(vinyl acetate) with number average molecular weights of over 50,000 and polydispersities less than 1.5. This same RAFT agent was also able to produce polystyrene and polyacrylates with reasonable control (i.e. predictable molecular weights and polydispersities less than 1.5). Thus, the one RAFT agent was used to make block copolymers of poly(methyl acrylate) and poly(vinyl acetate). The order of monomer polymerization was found to be vital in determining the success of the block copolymerization.

# Introduction

Vinyl acetate (VAc) is a very important monomer; its co-polymers and polymers find uses as a water-based paints, as adhesives for paper, textiles, and wood (labeling, white glue), and as a sizing or coating compound for paper and textiles. Poly(vinyl acetate) (PVAc) is soluble in aromatic solvents and also in alcohols or esters. In addition to its use in a variety of plastic applications, PVAc is used to produce poly(vinyl alcohol) and poly(vinyl acetal) which cannot be synthesized directly. Because of wide range of applications of PVAc and poly(vinyl alcohol), the synthesis of PVAc with controlled molecular weights and functionality has therefore became an attractive goal.

Several studies in the literature report the controlled/living radical polymerization (CLRP) of VAc. Although VAc can be polymerized through the free radical mechanism, it is typically more difficult to control during radical polymerization compared to the other conjugated monomers such as styrene and (meth)acrylates. Despite the constant improvements in the CLRP techniques, there has been comparatively limited success for the control of VAc polymerization. Recently, a few reports in literature for the CLRP of VAc include MADIX/RAFT,[1-5] iron-catalyzed,[6] degenerative transfer with alkyl iodides,[7,8] cobalt mediated,[9-14] and organo-tellium- and organostilbine-mediated process. Most of these approaches are based on the reversible chain transfer process. Copper-mediated ATRP of VAc has not been successful because of low equilibrium constant[15] of the VAc polymerization and the presence of side reactions, such as decomposition of the dormant species and possibility transformation of growing radicals to carbocations.[16]

Destarac et. al.[2] reported the use of *N*,*N*-dialkydithiocarbamates as efficient RAFT agents for CLRP of VAc, noting that the lone pair of electrons of the nitrogen atom of the dithiocarbamate RAFT agent must be conjugated with carbonyl or aromatic groups for facile transfer. Thus, *N*,*N*-disubstituted and cyclic dithiocarbamates having these structural features showed reasonable control of VAc polymerization. However, they synthesized PVAc of low $M_n$ (< 6,000). The advantages of dithiocarbamates over other mediating agents include ease of synthesis, lower coloration, no metal contamination, and the potential ability to form block copolymers with various monomer types using a single RAFT agent.

The primary objective of this work was to evaluate several *N*,*N*-dialkydithiocarbamates (DTCs) in their role as RAFT agents for the polymerization of VAc, with specific aims of obtaining high molecular weights, narrow molecular weight distributions and PVAc-containing block copolymers.

# Experimental

## Materials

*N*-Methyl aniline (98%), *N*,*N*-diphenyl amine (99%), carbon disulfide (99.9%), diethyl chloromalonate (95%), ethyl bromoacetate (98%), methyl-2-

Downloaded by PENNSYLVANIA STATE UNIV on June 26, 2012 | http://pubs.acs.org
Publication Date: August 13, 2009 | doi: 10.1021/bk-2009-1024.ch003

Downloaded by PENNSYLVANIA STATE UNIV on June 26, 2012 | http://pubs.acs.org
Publication Date: August 13, 2009 | doi: 10.1021/bk-2009-1024.ch003

bromopropionate (98%), sodium hydride (60%, dispersed in mineral oil) were all purchased from Aldrich and used as received. Tetrahydrofuran (THF), dimethyl sulfoxide (DMSO, 99.9%), $MgSO_4$ (anhydrous) and ethyl ether (anhydrous) were purchased from JT Baker and used as received. Azobisisobutyronitrile (AIBN) was purchased from Aldrich and recrystallized from methanol. Vinyl acetate (VAc), styrene, methyl acrylate (MA) and *tert*-butyl acrylate (*t*BA) were purchased from Aldrich and purified by removing inhibitor by passing each monomer through activated basic alumina followed by distillation under a reduced pressure.

## Instrumentation

Gel permeation chromatography (GPC) was carried out in THF (flow rate: 1.0 mL $min^{-1}$) at 30°C with a Waters 515 HPLC pump, 2 columns, a Viscotek LR40 refractive index detector and a Waters 717 autosampler. Polystyrene standards were used for calibration. Monomer conversion was carried out with Hewlett Packard 5890 Series II gas chromatograph (GC) equipped with FID detector, and HP-5 (cross-linked 5% PH ME silicone column) column with 30m × 0.32 mm × 0.25 μm film thickness. Nuclear magnetic resonance (NMR) spectroscopy was carried out on a Bruker Avance DMX 400 MHz spectrometer.

## RAFT Agent Syntheses

Each RAFT agent was synthesized using the same approach: NaH was added to either *N*-methyl aniline or *N*,*N*-diphenyl amine in THF. Addition of $CS_2$ and then the appropriate alkyl halide yielded the desired RAFT agent. A typical synthesis, for malonate *N*,*N*-diphenyl dithiocarbamate (MDP-DTC), is as follows: 1.24 g of NaH (26 mmol., 1.3 equivalents) suspended in 10 ml of THF in round bottom flask placed under $N_2$ gas. 3.38 g of *N*,*N*-diphenylamine (20 mmol., 1 equivalent) dissolved in a mixture of 18 ml of DMSO and 9 ml of THF was added at $0^oC$; the color of the solution turned pale green. After stirring for one hour, 2.84 ml of $CS_2$ (47.2 mmol., 2.36 equivalents) was added and the solution became orange-yellow. After stirring for 30 minutes the solution was cooled to $-20^oC$, and one equivalent of chlorinating agent (20 mmol., 3.2ml) was added. The solution was allowed stir for 2 hours at room temperature. After hydrolysis, it was extracted into ethyl ether and dried over $MgSO_4$ and concentrated under vacuum. The product was isolated as a solid. Yield 52.35%. $^1H$ NMR (400 MHz, $CDCl_3$): δ (ppm) 7.4-7.5 (m, 10H, $(C_6H_5)_2$), 5.74 (s, 1H, CH), 4.23 (q, 4H, $OCH_2$), 1.28 (t, 6H, $CH_3CH_2O$).

NMR data for other RAFT agents: Malonate *N*,*N*-methylphenyl dithiocarbamate (MMP-DTC) – $^1H$ NMR (400 MHz, $CDCl_3$): 7.4 (m, 5H, $C_6H_5$), 5.72 (s, 1H, S-CH), 4.2 (q, 4H, $OCH_2$), 3.79 (s, 3H, N-$CH_3$), 1.25 (q, 6H, $CH_3CH_2O$). Acetate *N*,*N*-methylphenyldithiocarbamate (AMP-DTC) – $^1H$ NMR (400 MHz, $CDCl_3$): δ (ppm) 7.4 (m, 5H, $C_6H_5$), 4.2 (q, 2H, $OCH_2$), 4.0 (s, 2H, S-$CH_2$), 1.28 (t, 3H, $CH_3CH_2O$). Acetate *N*,*N*-diphenyldithiocarbamate (ADP-DTC) – $^1H$ NMR (400 MHz, $CDCl_3$): δ (ppm) 7.4 (m, 10H, $(C_6H_5)_2$), 4.2 (q, 2H,

$OCH_2$), 4.1 (s,2H, S-$CH_2$), 1.28 (t, 3H, $CH_3CH_2O$). Propionate *N,N*-Methylphenyldithiocarbamate (PMP-DTC) – $^1H$ NMR (400 MHz, $CDCl_3$): δ (ppm) 7.4 (m, 5H, $C_6H_5$), 4.65 (q, 1H, CH-$CH_3$), 3.8 (s,3H, O-$CH_3$), 3.78 (s, 3H, N-$CH_3$), 1.45 (d, 3H, CH-$CH_3$). Propionate *N,N*-diphenyldithiocarbamate (PDP-DTC) – $^1H$ NMR (400 MHz, $CDCl_3$): δ (ppm) 7.4 (m, 10H, $(C_6H_5)_2$), 4.7 (q, 1H, S-CH), 4.65 (q, 1H, CH-$CH_3$), 3.8 (s, 3H, O-$CH_3$), 1.56 (d, 3H, CH-$CH_3$).

### Typical Procedure for the RAFT Polymerization of Vinyl Acetate & Other Monomers

In typical VAc bulk polymerization reaction, the required amounts of VAc, AIBN, RAFT and anisole were combined in 25 ml Schlenk flask equipped with magnetic stirrer bar and capped with rubber septum. The resulting mixture was stirred at room temperature for 10 minutes. A small amount anisole (0.2 ml) was used as internal standard for calculation of % monomer conversion by GC. The monomer and anisole were purged with $N_2$ for 30 minutes before adding to the flask. The flask was evacuated by 4 freeze-pump–thaw cycles and back filled with $N_2$. The utmost care is taken to make sure air is not introduced into the reactor when adding reagents or removing samples via syringe and needles. After taking the initial sample, the reaction was started by heating the mixture to 60°C. Samples were taken via a syringe periodically to follow the kinetics of the polymerization. The samples were diluted with toluene and injected into the GC to estimate % monomer conversion. After the GC measurement, samples were diluted with THF and passed through a 0.2μm PTFE filter for gel permeation chromatography (GPC) analysis.

Downloaded by PENNSYLVANIA STATE UNIV on June 26, 2012 | http://pubs.acs.org
Publication Date: August 13, 2009 | doi: 10.1021/bk-2009-1024.ch003

## Results and Discussion

The initial *N,N*-dialkyldithiocarbamate RAFT agent synthesized and used for RAFT polymerization of VAc was malonate *N,N*,-diphenyldithiocarbamate (MDP-DTC). Mole ratios of monomer, RAFT agent and AIBN (VAc:RAFT agent:AIBN = 1250:1:0.5) were chosen to give number average molecular weight ($M_n$) values of at least several tens-of-thousands if the RAFT polymerizations were successful. As a reference, a polymerization using these ratios of AIBN and VAc but no added RAFT agent yielded fairly high $M_n$ and polydispersity (PD) values ($M_n$=197,000 and PD=2.21 after 2.5 hours, 55% conversion; $M_n$=96,000 and PD=4.84 after 4 hours, 85% conversion). Molecular weight distribution data shown in Figure 1 (open and closed circles) indicate that the MDP-DTC RAFT agent does indeed seem to have reasonable control of the VAc polymerization, at least up until approximately 60% conversion, after which both the $M_n$ and PD increase, probably due to chain transfer to monomer and polymer which are unavoidable even during RAFT polymerization.[17]

Another four dithiocarbamate RAFT agents (Scheme 1) were also synthesized and evaluated for their ability to control the RAFT polymerization of VAc. The $M_n$ and PD vs. conversion data are shown in Figures 1 and 2. It should be possible to correlate the performance of these RAFT agents with their structure, in particular the degree of conjugation of the lone pair of electrons on the N atom (diphenyl vs. methyl phenyl), and the stability of the leaving “R” group radical (acetate vs. propionate). In terms of the *N*-substituents (diphenyl vs. methyl phenyl), both the methyl phenyl derivatives (PMP-DTC and AMP-DTC) give higher PD values compared with their diphenyl analogues (PDP-DTC and ADP-DTC, respectively). This is due to greater delocalization of the lone pair of electrons on the N atom in the methyl phenyl derivatives (cf. the diphenyl analogues) which reduces the rate of addition to the thiocarbonyl group, and hence results in slower transfer and exchange dynamics of the methyl phenyl-based RAFT agents.[2,18]

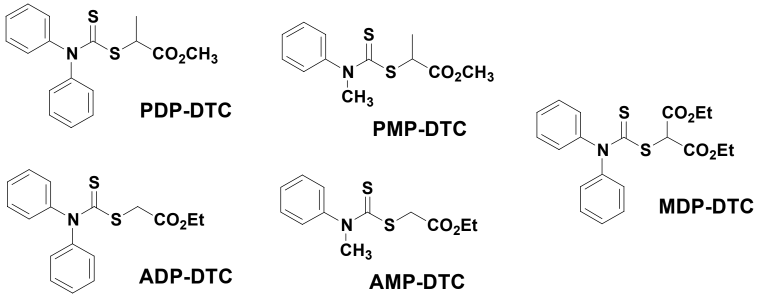

*Scheme 1*

A comparison of the acetate vs. propionate “R” groups (PMP-DTC vs. AMP-DTC, PDP-DTC vs. ADP-DTC), and the malonate group (for the diphenyl compounds) indicates no major differences in their ability to control $M_n$ or PD. The “R” group can have significant effects on the overall control and needs to be chosen carefully. If the “R” group provides too much stabilization then the resulting slow initiation may yield high polydispersities. If the “R” group does not provide enough stabilize then fragmentation may not occur, resulting in no control of $M_n$ or PD. It has been shown that radical stabilizing “R” groups can potentially provide what Klumperman et al.[19] refer to as “selective initialization”, which provide lower PDs, albeit with some inhibition of the early stages of the polymerization. In the case of MDP-DTC, there was a 2-3 hour induction period for each polymerization, and so MDP-DTC may be providing selective initialization. The result is reasonably low PD values and a linear increase $M_n$. Since the MDP-DTC RAFT agent provided the best overall results we therefore concentrated on using the MDP-DTC for other monomers such as styrene and acrylates.

Downloaded by PENNSYLVANIA STATE UNIV on June 26, 2012 | http://pubs.acs.org
Publication Date: August 13, 2009 | doi: 10.1021/bk-2009-1024.ch003

Downloaded by PENNSYLVANIA STATE UNIV on June 26, 2012 | http://pubs.acs.org
Publication Date: August 13, 2009 | doi: 10.1021/bk-2009-1024.ch003

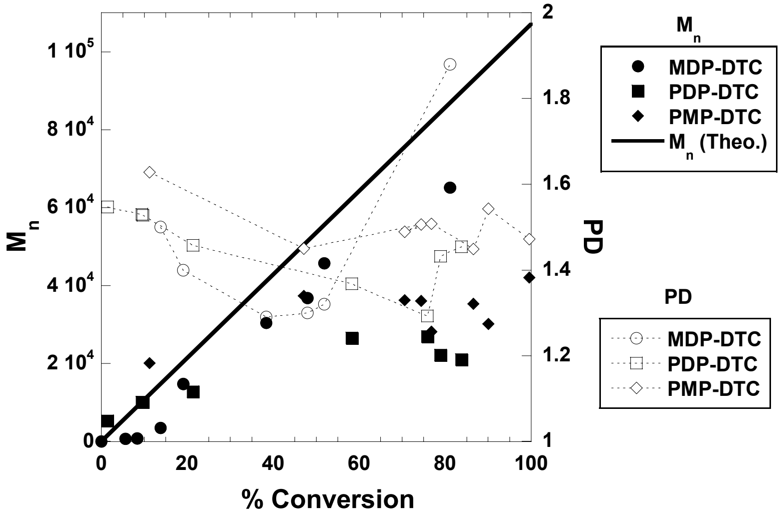

*Figure 1. Variation of $M_n$ & PD as a function of VAc conversion using various DTCs as RAFT agents (mole ratios: VAc:RAFT agent:AIBN = 1250:1:0.5).*

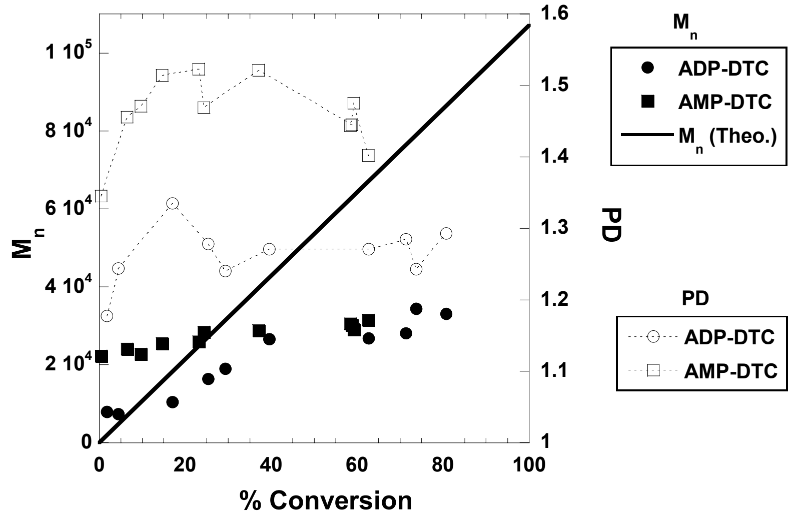

*Figure 2. Variation of $M_n$ & PD as a function of VAc conversion using various DTCs as RAFT agents (mole ratios: VAc:RAFT agent:AIBN = 1250:1:0.5).*

The MDP-DTC RAFT agent was used to polymerization styrene and two acrylate monomers. Table 1 shows the outcomes of the polymerization of styrene, methyl acrylate (MA) and *tert*-butyl acrylate (*t*BA) using MDP-DTC. In the *t*BA case the $M_n$ data is a little lower than the predicted value, and while the PD values for both MA and *t*BA polymers are not as low as can be achieved using other RAFT agents (or other LRP methods), they are below 1.5. Furthermore, the MA appears to be better controlled than either the *t*BA or the styrene polymerizations. The degree of control during the styrene polymerizations appears to depend on the starting monomer:RAFT agent ratio. At the higher monomer:RAFT agent ratio, the $M_n$ agrees better with the calculated $M_n$, but the PD is higher than compared with lower monomer:RAFT agent ratio.

**Table 1. Data from the RAFT Polymerization of Styrene, MA and *t*BA using MDP-DTC as the RAFT Agent**

| *Monomer* | *Mole Ratios*[a] | *Time (hr)* | *Temp. (°C)* | *% Conv.* | *Mn* | *PD* |
|---|---|---|---|---|---|---|
| Styrene | 27:1:0 | 32.5 | 110 | 90 | 3,780 | 1.42 |
| Styrene | 440:1:0 | 9 | 110 | 93 | 44,700 | 1.66 |
| MA | 200:1:0.2 | 8 | 60 | [b] | 16,000 | 1.22 |
| *t*BA | 200:1:0.2 | 22 | 60 | 90 | 19,600 | 1.36 |

a. Mole ratios of monomer:MDP-DTC:AIBN

b. Not measured

Since the MDP-DTC RAFT agent was successful in gaining moderate control of the homopolymerizations of VAc, styrene and acrylate monomers, we then pursued the synthesis of block copolymers of these monomers using the single RAFT agent. Initially we used a sample of PVAc as a macroinitiator for MA and styrene (Scheme 2). GPC results from these polymerizations are shown in Figures 3 and 4. These clearly show that the chain extension of the PVAc with either MA or styrene failed. Further analysis of the PVAc-styrene attempt by soxhlet extraction with methanol showed that it was a mixture of PVAc and polystyrene homopolymers (see Figure 4). These results were confirmed by $^1$H NMR.

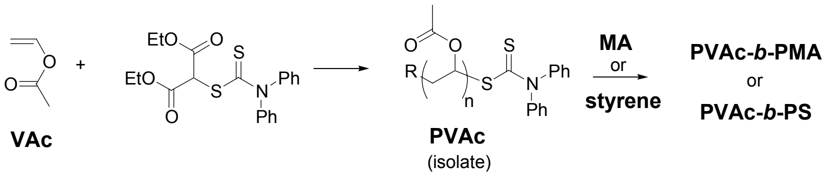

*Scheme 2. Outline of block copolymer synthesis starting with PVAc as macroinitiator (R = malonate group).*

Downloaded by PENNSYLVANIA STATE UNIV on June 26, 2012 | http://pubs.acs.org
Publication Date: August 13, 2009 | doi: 10.1021/bk-2009-1024.ch003

Downloaded by PENNSYLVANIA STATE UNIV on June 26, 2012 | http://pubs.acs.org
Publication Date: August 13, 2009 | doi: 10.1021/bk-2009-1024.ch003

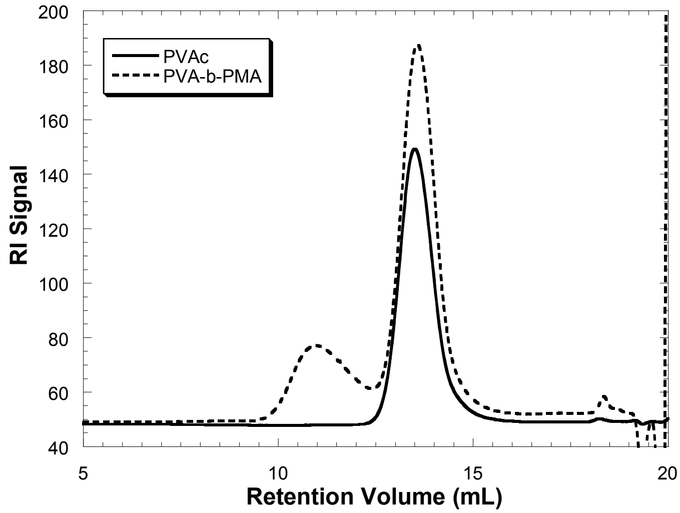

*Figure 3. GPC chromatograms of the attempted RAFT polymerization using PVAc as macroinitiator and MA as monomer.*

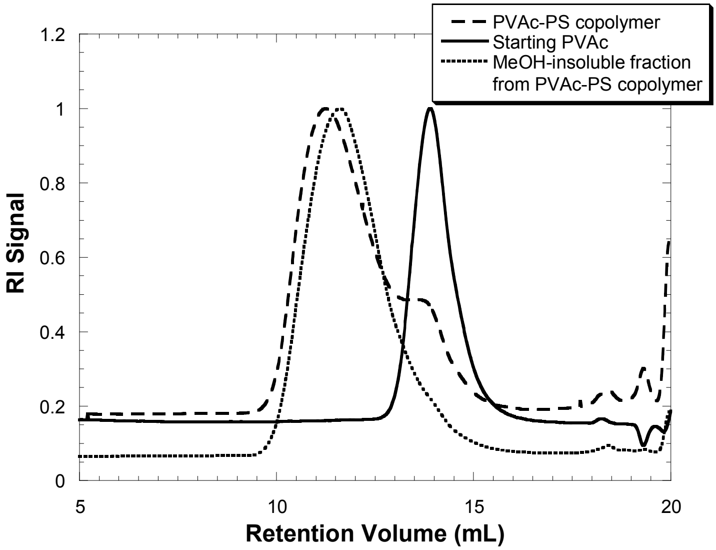

*Figure 4. GPC chromatograms of the attempted RAFT polymerization using PVAc as macroinitiator and styrene as monomer.*

A second attempt of making the PVAc-*block*-PMA copolymer was then undertaken, this time with the order of monomer polymerization reversed (Scheme 3). The PMA was made using the MDP-DTC RAFT agent, isolated and then used as the macroinitiator ($M_n$ = 16,000, PD = 1.22) for the VAc polymerization. In this case, as can be seen in Figure 5, the molecular weight distribution moved cleanly to higher molecular weights and showed no sign of unreacted PMA or slow re-initiation of the PMA. The final block copolymer had a $M_n$ of 32,000 and PD of 1.37. The $^1$H NMR spectrum shown in Figure 6 confirms the incorporation of the PVAc onto the PMA chains. This shows that the order of which the monomers are polymerized to make the block copolymer is vitally important. In this particular case, the PMA must be polymerized first, then followed by the VAc. The importance of polymerization order has also been shown for other monomer pairs.[20] Attempts to make an analogous PS-*block*-PVAc using the MDP-DTC RAFT agent failed, presumably because the inability of the styryl radical to add to the VAc monomer.

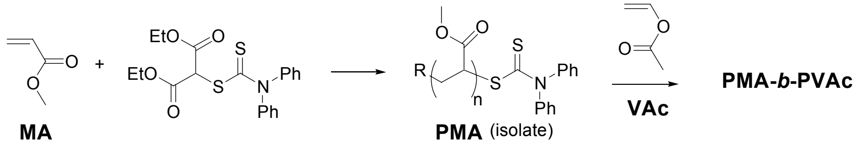

*Scheme 3. Outline of block copolymer synthesis starting with PMA as macroinitiator (R = malonate group).*

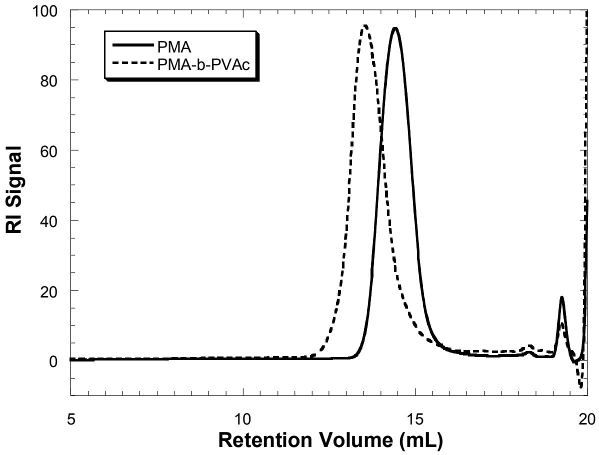

*Figure 5. GPC chromatograms of the RAFT polymerization of VAc using PMA as a macroinitiator.*

Downloaded by PENNSYLVANIA STATE UNIV on June 26, 2012 | http://pubs.acs.org
Publication Date: August 13, 2009 | doi: 10.1021/bk-2009-1024.ch003

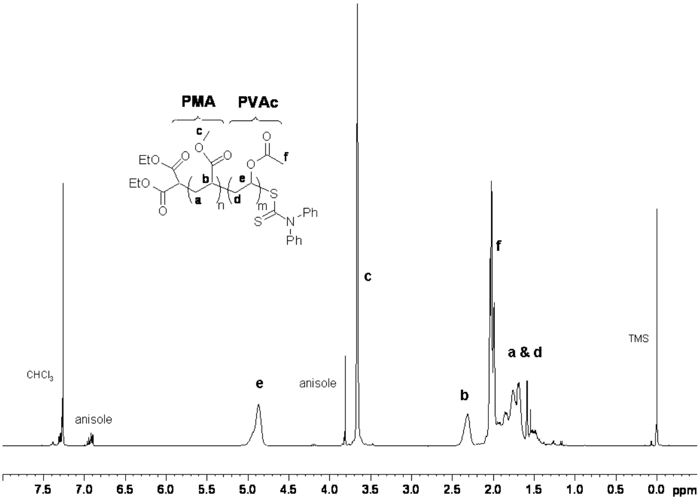

*Figure 6. $^1$H NMR spectrum of PMA-block-PVAc made by the polymerization of VAc using PMA as macroinitiator.*

## Conclusions

The ability to control VAc radical polymerization using several dithiocarbamate RAFT agents was studied. Among these dithiocarbamate RAFT agents, only one RAFT agent, MDP-DTC, showed consistently good control over the polymerization of VAc, yielding a polymer of $M_n$=50,000 and polydispersity of 1.3-1.5. This same RAFT agent was also able to gain some control over the polymerization of styrene, methyl acrylate and *tert*-butyl acrylate. Thus, the one RAFT agent was able to make block copolymers containing VAc and MA. The polymerization order was found to be important in obtaining good block copolymers; the MA must be polymerized first, and the resulting PMA used as macroinitiator for the subsequent VAc polymerization.

### Acknowledgements

We thank Kuraray America Inc. for financial support. We also thank the Honors (to CDP) and McNair Scholars (to TTT) programs, and the Center for Advanced Materials Processing (CAMP) at Clarkson University, a New York State Center for Advanced Technology for support.

Downloaded by PENNSYLVANIA STATE UNIV on June 26, 2012 | http://pubs.acs.org
Publication Date: August 13, 2009 | doi: 10.1021/bk-2009-1024.ch003

# References

1. Boschmann, D.; Vana, P. *Polym. Bull.* **2005**, *53*, 231-242.
2. Destarac, M.; Charmot, D.; Franck, X.; Zard, S. Z. *Macromol. Rapid Commun.* **2000**, *21*, 1035-1039.
3. Favier, A.; Barner-Kowollik, C.; Davis, T. P.; Stenzel, M. H. *Macromol. Chem. Phys.* **2004**, *2005*, 925-936.
4. Rizzardo, E.; Chiefari, J.; Mayadunne, R. T. A.; Moad, G.; Thang, S. H. *ACS Symp. Ser.* **2000**, *786*, 278-296.
5. Russman, J. P.; Barbre, N. D.; Jones, C. W.; Schork, F. J. *J. Polym. Sci. Part A: Polym. Chem.* **2005**, *43*, 2188-2193.
6. Wakioka, M.; Baek, K.-Y.; Ando, T.; Kamigaito, M.; Sawamoto, M. *Macromolecules* **2002**, *35*, 330-333.
7. Borkar, S.; Sen, A. *J. Polym. Sci. Part A: Polym. Chem.* **2005**, *43*, 3728-3736.
8. Iovu, M. C.; Matyjaszewski, K. *Macromolecules* **2003**, *36*, 9346-9354.
9. Bryaskova, R.; Willet, N.; Debuigne, A.; Jérôme, R.; Detrembleur, C. *J. Polym. Sci. Part A: Polym. Chem.* **2007**, *45*, 81-89.
10. Debuigne, A.; Caille, J.-R.; Detrembleur, C.; Jérôme, R. *Angew. Chem., Int. Ed.* **2005**, *44*, 3439-3442.
11. Debuigne, A.; Caille, J.-R.; Willet, N.; Jérôme, R. *Macromolecules* **2005**, *38*, 9488-9496.
12. Debuigne, A.; Warnant, J.; Jérôme, R.; Voets, I.; de Keizer, A.; Cohen Stuart, M. A.; Detrembleur, C. *Macromolecules* **2008**, *41*, 2353-2360.
13. Detrembleur, C.; Debuigne, A.; Bryaskova, R.; Charleux, B.; Jérôme, R. *Macromol. Rapid Commun.* **2006**, *27*, 37-41.
14. Scainnamea, V.; Debuigne, A.; Piette, Y.; Jerome, R.; Detrembleur, C. *Chem. Comm.* **2006**, 4180-4182.
15. Gillies, M. B.; Matyjaszewski, K.; Norrby, P. O.; Pintauer, T.; Poli, R.; Richard, P. *Macromolecules* **2003**, *36*, 8551-8559.
16. Paik, H.-J.; Teodorescu, M.; Xia, J.; Matyjaszewski, K. *Macromolecules* **1999**, *32*, 7023-7031.
17. Moad, G.; Rizzardo, E.; Thang, S. H. *Acc. Chem. Res.* **2008**, *41*, 1133-1142.
18. Coote, M. L.; Henry, D. J. *Macromolecules* **2005**, *38*, 1415-1433.
19. Pound, G.; McLeary, J. B.; McKenzie, J. M.; Lange, R. F. M.; Klumperman, B. *Macromolecules* **2006**, *39*, 7796-7797.
20. Chong, Y. K.; Le, T. P. T.; Moad, G.; Rizzardo, E.; Thang, S. H. *Macromolecules* **1999**, *32*, 2071-2074.

Downloaded by PENNSYLVANIA STATE UNIV on June 26, 2012 | http://pubs.acs.org
Publication Date: August 13, 2009 | doi: 10.1021/bk-2009-1024.ch003

Downloaded by CORNELL UNIV on June 26, 2012 | http://pubs.acs.org
Publication Date: August 13, 2009 | doi: 10.1021/bk-2009-1024.ch004

## Chapter 4

# Thiourea-Mediated Stereospecific Radical Polymerization of Acrylamides and Combination with RAFT for Simultaneous Control of Molecular Weight and Tacticity

**Harumi Murayama, Kotaro Satoh, and Masami Kamigaito**

**Department of Applied Chemistry, Graduate School o f Engineering, Nagoya University, Nagoya 464-8603, Japan**

Thiourea derivatives were examined for the stereospecific radical polymerization of acrylamides via hydrogen-bonding interactions between the additives and the monomers and/or the growing polymer terminals. Among the various thioureas, moderately bulky monothioureas possessing one or two 3,5-bis(trifluoromethyl)phenyl substituents proved effective for the isospecific radical polymerization of *N*,*N*-dimethylacrylamide (DMAM) ($m$ = 74%) and *N*-isopropylacrylamide ($m$ = 68%) in $CH_2Cl_2$ at –78 °C. The $^1H$ NMR analysis of mixtures of the thioureas with DMAM or its dimer both indicated 1:1 interactions, accounting for the isospecific radical polymerization via the hydrogen-bonding interactions. A combination with the thioureas and RAFT agents, especially with a trithiocarbonate structure, gave the isotactic-rich polymers with controlled molecular weights and thus proved effective for the metal-free isospecific living radical polymerization of acrylamides.

In Controlled/Living Radical Polymerization: Progress in RAFT, DT, NMP & OMRP; Matyjaszewski, K.;
ACS Symposium Series; American Chemical Society: Washington, DC, 2009.

# Introduction

Since the discoveries of novel systems for living radical polymerizations in the mid 1990s (*1–9*), control of the molecular weights in radical polymerizations has extensively progressed and reached a fairly good level, which can be quite applicable for the synthesis of a variety of controlled polymers, such as block, graft, and star polymers, etc., from various vinyl monomers (*10–17*). In contrast to such explosive developments in the molecular weight control, stereochemical control in radical polymerization has evolved using polar solvents or Lewis acid additives since the late 1990s (*18–21*). These findings changed the view that the stereochemistry in radical polymerization is hardly affected by the reaction media or reagents. For example, a bulky and acidic fluoroalcohol increases the syndiospecificity in the radical polymerization of vinyl acetate and methyl methacrylate via the steric repulsion caused by the hydrogen-bonding interaction of the fluoroalcohol to their carbonyl groups, while rare-earth metal triflates are effective for the isospecific radical polymerization of acrylamides and methyl methacrylate via the multisite coordination of the Lewis acid to the carbonyl groups around the chain end as well as the monomer. Other organic solvents and compounds also proved effective for the stereospecific radical polymerizations via a hydrogen-bonding interaction (*22–24*). However, the stereochemical control in radical polymerization requires further developments for practical application in contrast to that in coordination polymerizations. The tacticity control is thus still one of the most challenging research topics in radical polymerizations.

Another and higher target for controlling the radical polymerization is the simultaneous regulation of the molecular weight and steric structure, which will lead to a more precise and flexible modulation of the polymer properties. One of the more accessible methods for this purpose is to combine the living radical polymerizations with the stereospecific radical polymerizations so that one of the controlling agents should not disturb the other control (*25*). We have already found some effective combinations of various monomers, such as methacrylates, acrylamides, vinyl esters, and vinyl amides, and further utilized these systems for the synthesis of rather novel types of stereocontrolled polymers like stereoblock and stereogradient polymers.

In this study, we employed thiourea derivatives, which may form hydrogen bonds with the carbonyl groups of polar vinyl monomers, for possible effective stereocontrol in the radical polymerizations. The urea and thiourea derivatives have been utilized as host molecules for molecular recognition (*26*) as well as organocatalysts for organic reactions (*27,28*). These compounds possess relatively strong proton-donating abilities and can be relatively easily prepared from thioisocyanates and amines, in which their electronic and steric properties can be modified by their substituents. In organic reactions, there have now been reported various stereoselective reactions mediated by specifically designed urea and thiourea catalysts (*28*). We thus synthesized a series of thiourea derivatives with various substituents and employed them for the possible stereospecific radical polymerization of *N*,*N*-dimethylacrylamide (DMAM) and *N*-isopropylacrylamide (NIPAM) (Scheme 1). Furthermore, the simultaneous control of the molecular weights and tacticity was investigated by combination

Downloaded by CORNELL UNIV on June 26, 2012 | http://pubs.acs.org
Publication Date: August 13, 2009 | doi: 10.1021/bk-2009-1024.ch004

with reversible addition fragmentation chain-transfer (RAFT) polymerizations, in which both the stereo- and molecular-weight-controlling agents are thiocarbonyl compounds and thus free from metal components.

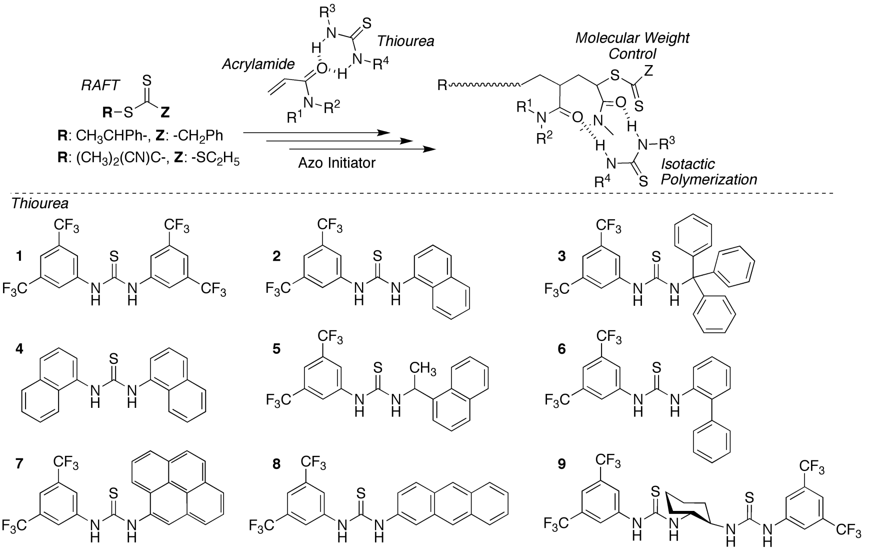

*Scheme 1. Thiourea-mediated stereospecific radical polymerization of acrylamides and combination with RAFT polymerization*

## Results and Discussion

### Stereospecific Radical Polymerization of DMAM and NIPAM in the Presence of Thiourea Derivatives

A series of thiourea derivatives (**1**–**4**) was used for the conventional radical polymerizations of DMAM in several solvents ($CHCl_3$, $CH_2Cl_2$, $CH_3OH$, THF) at various temperatures (60, 20, –78 °C) and amounts ($[\text{thiourea}]_0/[\text{M}]_0 = 0–1.5$) to determine the effects of the additives (Table I). Among these thiourea derivatives, **1** is the strongest proton donor due to the presence of two electron-withdrawing 3,5-bis(trifluoromethyl)phenyl substituents. The unsymmetrical thioureas, **2** and **3**, are designed to have one electron-withdrawing 3,5-bis(trifluoromethyl)phenyl group for delivering a high proton-donating ability while the other group is a relatively bulky substituent, such as the naphtyl and triphenylmethyl group. In contrast, **4** lacks the electron-withdrawing substituent and is the weakest in its hydrogen-bonding activity among these, although it is bulkier due to the two naphtyl substituents.

At 60 °C in $CHCl_3$, there were almost no effects of the thiourea additives on the tacticity. However, at 20 °C in $CH_2Cl_2$, **1** and **2** gave more or less higher isospecificities ($m$ ~ 60%). Upon further decreasing the temperature to –78 °C in $CH_2Cl_2$, the $m$ contents of poly(DMAM) obtained with **1** and **2** further

Downloaded by CORNELL UNIV on June 26, 2012 | http://pubs.acs.org
Publication Date: August 13, 2009 | doi: 10.1021/bk-2009-1024.ch004

increased to 72 and 74%, respectively (Figure 1). In contrast, **3** and **4** were not effective for changing the tacticity even at –78 °C. The choice of solvents was also important because almost no effects due to **2** were observed in $CH_3OH$ and THF, which may disturb the effective hydrogen-bonding interactions. Thus, thioureas **1** and **2** proved effective for the isospecific radical polymerization of DMAM at a low temperature in polar chlorinated hydrocarbon solvents, which are generally good for similar hydrogen-bonding interactions (*26*).

**Table I. Radical Polymerization of DMAM in the Presence of 1–4**[a]

| *Temp. (°C)* | *Solvent* | *Additive* | *$[Add]_0/[M]_0$* | *Conv. (%)* | *$M_n$* | *$M_w/M_n$* | *m/r* |
|---|---|---|---|---|---|---|---|
| 60[b] | $CHCl_3$ | None | 0 | 80 | 11000 | 2.01 | 53.0/47.0 |
| 60[b] | $CHCl_3$ | **1** | 0.40[e] | 86 | 15000 | 2.46 | 55.1/44.9 |
| 60[b] | $CHCl_3$ | **2** | 0.50 | 74 | 12000 | 1.93 | 54.2/45.8 |
| 60[b] | $CHCl_3$ | **3** | 0.50 | 52 | 15000 | 2.17 | 50.0/50.0 |
| 20[c] | $CH_2Cl_2$ | None | 0 | 58 | 27000 | 2.11 | 50.4/49.6 |
| 20[c] | $CH_2Cl_2$ | **1** | 0.75 | 18 | 18000 | 2.13 | 60.3/39.7 |
| 20[c] | $CH_2Cl_2$ | **2** | 0.75 | 36 | 20000 | 2.08 | 62.8/37.2 |
| –78[d] | $CH_2Cl_2$ | None | 0 | 73 | 71000 | 2.67 | 54.8/45.2 |
| –78[d] | $CH_2Cl_2$ | **1** | 1.0 | 79 | 35000 | 2.45 | 72.1/27.9 |
| –78[d] | $CH_2Cl_2$ | **2** | 1.0 | 50 | 73000 | 2.58 | 74.1/25.9 |
| –78[d] | $CH_2Cl_2$ | **3** | 1.0 | 87 | 68000 | 2.13 | 53.5/46.5 |
| –78[d] | $CH_2Cl_2$ | **4** | 1.0 | 57 | 72000 | 2.28 | 55.9/44.1 |
| –78[d] | MeOH | None | 0 | 97 | 46000 | 2.81 | 54.1/45.9 |
| –78[d] | MeOH | **2** | 0.50 | 68 | 37000 | 2.00 | 55.6/44.4 |
| –78[d] | THF | None | 0 | 86 | 24000 | 2.13 | 65.3/34.7 |
| –78[d] | THF | **2** | 1.0 | 58 | 31000 | 2.43 | 69.2/30.8 |

[a] $[DMAM]_0$ = 0.50 M. [b] $[DMAM]_0/[AIBN]_0$ = 200, 24 h. [c] $[DMAM]_0/[V\text{-}70]_0$ = 200, 48 h. [d] $[DMAM]_0/[n\text{-}Bu_3B]_0$ = 10, with $O_2$, 144 h. [e] $[DMAM]_0$ = 1.0 M.

Figure 1 plots the dependence of the isotactic contents (*m*) on the amounts of the additives (**1**–**3**) in $CH_2Cl_2$ at –78 °C. Upon increasing the initial concentrations of **1** and **2**, the *m* values increased from 55% to about 75% although the dependences were slightly different. In contrast, there were almost no changes due to **3**.

Downloaded by CORNELL UNIV on June 26, 2012 | http://pubs.acs.org
Publication Date: August 13, 2009 | doi: 10.1021/bk-2009-1024.ch004

Downloaded by CORNELL UNIV on June 26, 2012 | http://pubs.acs.org
Publication Date: August 13, 2009 | doi: 10.1021/bk-2009-1024.ch004

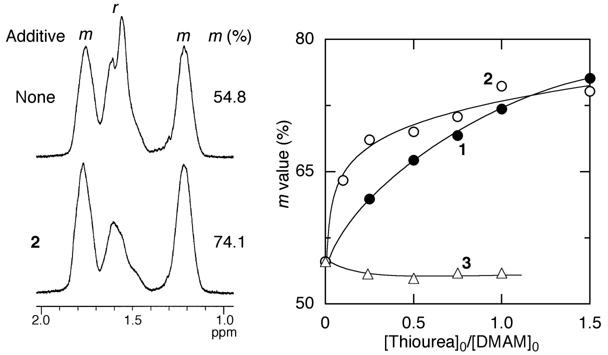

*Figure 1.* $^1$*H NMR spectra (in DMSO-*$d_6$ *at 170 °C) of) of –*$CH_2$*- resonance in poly(DMAM) ([**2**]*$_0$*/[M]*$_0$*= 1.0) and dependence of m contents on [thiourea]*$_0$*/[M]*$_0$ *in radical polymerization of DMAM in* $CH_2Cl_2$ *at –78 °C: [M]*$_0$*/[thiourea]*$_0$*/[n-*$Bu_3B$*]*$_0$ *= 500/0-750/50 mM, with* $O_2$*.*

Thus, thioureas having one or two electron-withdrawing 3,5-bis(trifluoromethyl)phenyl groups proved effective for the isospecific radical polymerization of DMAM. However, the use of an extremely bulky triphenylmethyl group as one of the substituents led to the loss of the effects. Furthermore, thiourea **4** without the electron-withdrawing substituent had no effects on the tacticity. These results suggest that both the electronic and steric factors are important in designing the effective thioureas for the stereospecific radical polymerization of DMAM.

To further search for effective additives, a series of thioureas having one 3,5-bis(trifluoromethyl)phenyl group and other aromatic substituents (**5**–**8**) were prepared and added to the radical polymerization of DMAM in $CH_2Cl_2$ at –78 °C (Table II). Similar increases in the isotacticity were observed with the thioureas possessing the moderately bulky substituents (**5** and **6**). In contrast, a bulkier and planar pyrenyl substituent (**7**) did not affect the tacticity. Unexpectedly, no polymerization occurred with an anthracene derivative (**8**). We also examined a bisthiourea additive (**9**), which slightly increased the isotacticity but the effects were lower than those of the effective monothioureas.

### Table II. Radical Polymerization of DMAM in the Presence of Various Thioureas in $CH_2Cl_2$ at –78 °C[a]

| *Additive* | *Conv. (%)* | *$M_n$* | *$M_w/M_n$* | *m/r* |
|---|---|---|---|---|
| None | 73 | 71000 | 2.67 | 54.8/45.2 |
| **1** | 67 | 31000 | 3.34 | 66.3/33.7 |
| **2** | 82 | 49000 | 2.74 | 69.5/30.5 |
| **3** | 60 | 39000 | 2.03 | 52.9/47.1 |
| **5** | 59 | 70000 | 2.81 | 64.5/35.5 |
| **6** | 95 | 86000 | 3.53 | 68.0/32.0 |
| **7** | 16 | 5000 | 1.85 | 52.6/47.4 |
| **8** | 0 | – | – | – |
| **9** | 79 | 77000 | 3.74 | 60.8/39.2 |

[a] $[DMAM]_0/[n\text{-}Bu_3B]_0/[Additive]_0$ = 500/250/50 mM, with $O_2$, 144 h.

### Table III. Radical Polymerization of NIPAM in the Presence of Various Thioureas[a]

| *Temp. (°C)* | *Solvent* | *Additive* | *$[Add]_0/[M]_0$* | *Conv. (%)* | *$M_n$* | *$M_w/M_n$* | *m/r* |
|---|---|---|---|---|---|---|---|
| 60[b] | $CHCl_3$ | None | 0[d] | 96 | 28000 | 2.29 | 50.8/49.2 |
| 60[b] | $CHCl_3$ | **1** | 1.0 | 49 | 13000 | 1.51 | 56.8/43.2 |
| 60[b] | $CHCl_3$ | **2** | 0.75 | 35 | 19000 | 1.93 | 51.8/48.2 |
| –78[c] | $CH_2Cl_2$ | None | 0 | 63 | 53000 | 4.46 | 47.7/52.3 |
| –78[c] | $CH_2Cl_2$ | **1** | 1.0 | 93 | 45000 | 2.24 | 67.8/32.1 |
| –78[c] | $CH_2Cl_2$ | **2** | 0.75 | 46 | 27000 | 1.66 | 66.0/34.0 |
| –78[c] | $CH_2Cl_2$ | **3** | 1.0 | 74 | 37000 | 1.92 | 53.6/46.4 |
| –78[c] | $CH_2Cl_2$ | **4** | 1.0 | 64 | 35000 | 3.03 | 51.4/48.6 |
| –78[c] | $CH_2Cl_2$ | **5** | 0.50 | 39 | 37000 | 2.11 | 57.2/42.8 |
| –78[c] | $CH_2Cl_2$ | **6** | 0.50 | 76 | 66000 | 2.99 | 55.5/44.5 |
| –78[c] | $CH_2Cl_2$ | **7** | 0.50 | 20 | 8000 | 1.77 | 56.8/43.2 |
| –78[c] | $CH_2Cl_2$ | **8** | 0.50 | 0 | – | – | – |
| –78[c] | $CH_2Cl_2$ | **9** | 0.50 | 53 | 30000 | 1.84 | 56.5/43.5 |

[a] $[NIPAM]_0$ = 0.50 M. [b] $[NIPAM]_0/[AIBN]_0$ = 200, 24 h. [c] $[NIPAM]_0/[n\text{-}Bu_3B]_0$ = 10, with $O_2$, 144 h. [d] $[NIPAM]_0$ = 1.0 M.

A similar series of experiments were examined for NIPAM (Table III). Thioureas **1** and **2** similarly increased the isotacticity of the poly(NIPAM) to 66–68% in $CH_2Cl_2$ at –78 °C although the effects were lower than for DMAM. These additives were not effective at a higher temperature (60 °C) as for the polymerization of DMAM. Other thioureas **3**–**7** and **9** gave slightly higher *m* values (54–57%) than in their absence (*m* = 48%). The anthracene derivative (**8**) also inhibited the radical polymerization. All these effects for NIPMA showed similar tendencies to those for DMAM although the changes were slightly lower. The effects of the amounts of **1**–**3** were also investigated for NIPAM in $CH_2Cl_2$ at –78 °C (Figure 2). Upon increasing the amounts, the *m* value gradually increased and reached an almost constant value. The further addition of **1** and **2** over 0.5 equivalent to NIPAM was not effective for increasing the tacticity.

Downloaded by CORNELL UNIV on June 26, 2012 | http://pubs.acs.org
Publication Date: August 13, 2009 | doi: 10.1021/bk-2009-1024.ch004

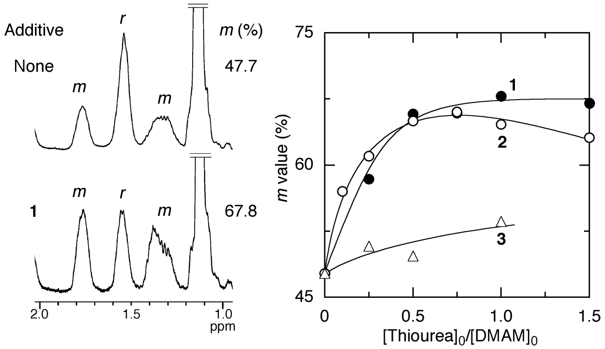

*Figure 2. $^1$H NMR spectra (in DMSO-$d_6$ at 170 °C) of –$CH_2$- resonance in poly(NIPAM) ([**1**]$_0$/[M]$_0$ = 1.0) and dependence of m contents on [thiourea]$_0$/[M]$_0$ in radical polymerization of NIPAM in $CH_2Cl_2$ at –78 °C: [M]$_0$/[thiourea]$_0$/[n-$Bu_3B$]$_0$ = 500/0-750/50 mM, with $O_2$.*

The isospecificities in these polymerizations were lower than the reported ones mediated by metal triflates (*20b*). However, among the organocompound-mediated isospecific radical polymerizations of DMAM and NIPAM, their isotacticities are the highest ones, i.e.; the *m* value for DMAM is the highest (*m* = 74%) and that for NIPAM is almost the same (*m* = 68%) with the reported highest value for the substituted *N*-oxide derivatives in $CHCl_3$ at –60 °C (*24e*). Thus, thioureas proved to be effective organic compounds for the isospecific radical polymerizations of acrylamides.

## Interaction of Thioureas with DMAM Monomer and Dimer

To confirm the hydrogen-bonding interaction between the thioureas and the amide monomers or polymers, the mixtures of DMAM and **1** or **2** was first analyzed by $^1$H NMR spectroscopy in $CD_2Cl_2$ at 30 °C. Upon the addition of DMAM into the solution of **1**, the thiourea protons (*c*) shifted downfield (Figure 3A). A similar downfield shift was observed with **2** although the shifts were lower for **1** (Figure 3B). These results suggest that some interactions occurred between the monomer and the thiourea additives.

Downloaded by CORNELL UNIV on June 26, 2012 | http://pubs.acs.org
Publication Date: August 13, 2009 | doi: 10.1021/bk-2009-1024.ch004

Downloaded by CORNELL UNIV on June 26, 2012 | http://pubs.acs.org
Publication Date: August 13, 2009 | doi: 10.1021/bk-2009-1024.ch004

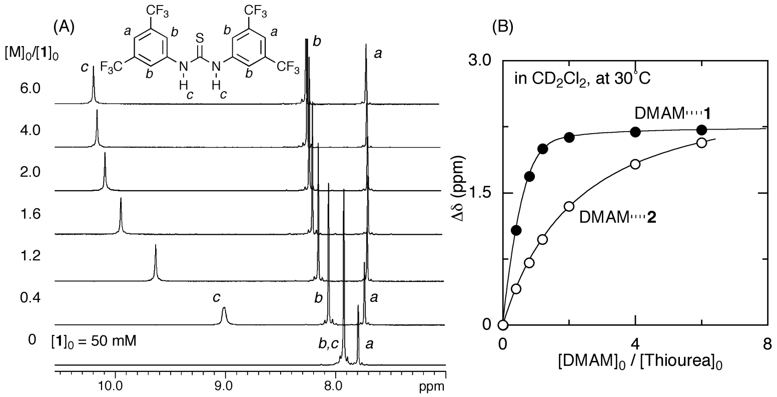

*Figure 3. $^1$H NMR spectra of the mixture of **1** and DMAM by varying the concentration of DMAM in $CD_2Cl_2$ at 30 °C (A) and changes in the thiourea proton chemical shifts of **1** and **2** in the presence of DMAM (B): $[DMAM]_0/[thiourea]_0$ = 0–300/50 mM.*

The stoichiometry of the interactions was then evaluated by Job's method by varying the concentrations of both components while keeping the total concentrations at 100 mM (Figure 4A). The fitted curve showed the maximum values when they were mixed in equimolar amounts, suggesting a 1:1 interaction between the monomer and the thioureas.

The association constants (*K*) were then calculated from the data in Figure 3B based on the assumption that they favorably interact at the 1:1 molar ratio. The *K* for **1** showed a higher value (20.9 $M^{-1}$) than for **2** (15.0 $M^{-1}$), indicating that the interaction is stronger for a better proton donor thiourea with a larger number of electron-withdrawing substituents. Although the former is higher than the latter, the effects on the tacticity were almost the same. This again indicates that both the electronic and steric factors of the thioureas are important for the stereochemistry in radical polymerization.

Furthermore, the interaction of the thioureas with a DMAM dimer, which can be regarded as one of the simplest models of the polymer terminals, was then investigated by Job's method (Figure 4B). These curves also indicated that the thioureas interact with the dimer at a 1:1 molar ratio, indicating a bidendate or bridging interaction of the monothiourea with two carbonyl groups of the dimer. This suggests a chelating interaction of the thiourea around the polymer terminal, leading to a meso conformation in a way similar to that by the lanthanide triflate (*19,20*). The interaction was also evaluated by $^1$H NMR titration by measuring the downfield shifts of the thiourea protons (*c*) upon the addition of the dimer. The *K* values between the dimer and **1** (117.9 $M^{-1}$) was one-order of magnitude higher than that between the monomer and **1**. This suggests the predominant meso sequence upon the addition of the thiourea compounds.

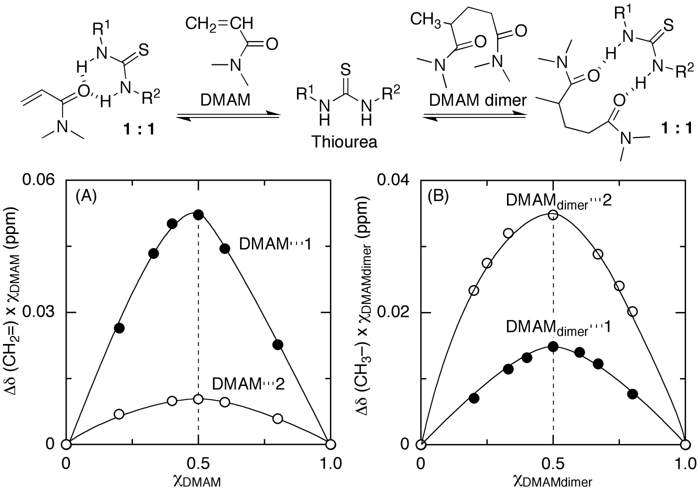

*Figure 4. Job plots for the association of* ***1*** *or* ***2*** *with DMAM monomer (A) or dimer (B) from the changes in chemical shifts of the thiourea proton of* ***1*** *or* ***2*** *($[Additive]_0$ + $[DMAM\ monomer\ or\ dimer]_0$ = 100 mM) in $CD_2Cl_2$ at 30 °C.*

## RAFT Polymerization of DMAM in the Presence of Thiourea Additives

For the simultaneous control of the molecular weight and tacticity in radical polymerization of DMAM, the RAFT agents were employed in the presence of the thiourea additives. The polymerization was first carried out with a dithio-compound (PEPD) (*14*) and V-70 as a radical initiator in the presence and absence of the thiourea additive (**2**) in $CH_2Cl_2$ at 20 °C (Figure 5). The RAFT polymerization of DMAM without thiourea additives was slow and resulted in relatively broad molecular weight distributions (MWDs; $M_w/M_n$ = 1.3–1.5). However, upon the addition of **2**, the polymerization reached slightly higher conversions. In addition, the polymers obtained in the presence of **2** showed narrower MWDs ($M_w/M_n$ = 1.3) throughout the polymerizations than in its absence. The number-average molecular weights ($M_n$) increased in direct proportion to the monomer conversion and agreed with the calculated values assuming that one molecule of PEPD generates one polymer chain. These results indicate that the molecular weight control was achievable and rather better in the absence of the thiourea additive.

Downloaded by CORNELL UNIV on June 26, 2012 | http://pubs.acs.org
Publication Date: August 13, 2009 | doi: 10.1021/bk-2009-1024.ch004

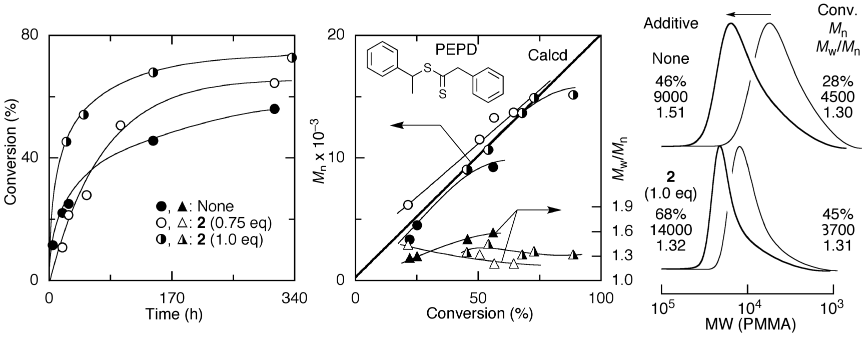

*Figure 5. RAFT polymerization of DMAM in the presence of **2** in $CH_2Cl_2$ at 20 °C: $[M]_0/[PEPD]_0/[V\text{-}70]_0/[\mathbf{2}]_0$ = 1000/5.0/2.5/0–1000 mM.*

A trithiocarbonate-type RAFT agent (CPETC) (*29*) was also used for the DMAM polymerization in conjunction with V-70 in $CH_2Cl_2$ at 20 °C in the absence and presence of **2**. The RAFT polymerization of DMAM with CPETC in the absence of the thiourea additives gave narrower MWDs ($M_w/M_n$ = 1.2) than with PEPD under similar conditions. Thus, CPETC proved a better RAFT agent for controlling the molecular weights of poly(DMAM). The addition of **2** was also examined for the RAFT polymerization with CPETC. Although the conversions were slightly decreased, the obtained polymers showed narrower MWDs ($M_w/M_n$ < 1.2). Thus, the molecular weight control with CPETC was attained or enhanced by the addition of **2**.

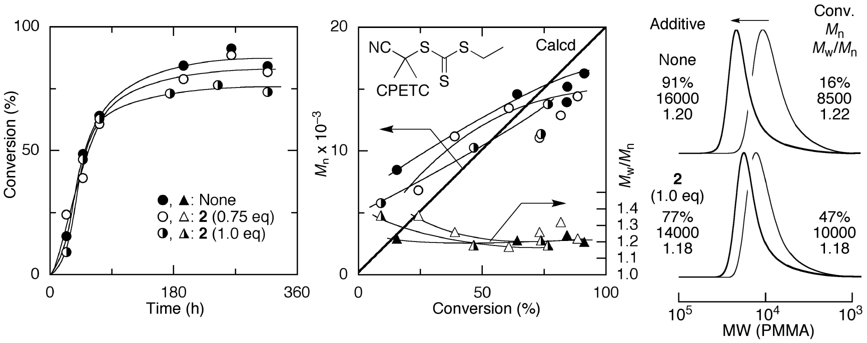

*Figure 6. RAFT polymerization of DMAM in the presence of **2** in $CH_2Cl_2$ at 20 °C: $[M]_0/[CPETC]_0/[V\text{-}70]_0/[\mathbf{2}]_0$ = 1000/5.0/2.5/0–1000 mM.*

The tacticity control was then evaluated by $^1H$ NMR analysis of the obtained polymers (Table IV). The PEPD- or CPETC-mediated RAFT polymerization without thioureas generated almost atactic polymers (*m*/*r* = 51/49) similar to the free radical polymerizations without the RAFT agents. However, upon the addition of an equimolar amount of **2** to DMAM in these RAFT polymerizations, the *m* content increased to 64%, which was almost comparable to that (*m* = 62%) obtained for the radical polymerization without RAFT agents in the presence of **2**. These results indicate that the thiourea

Downloaded by CORNELL UNIV on June 26, 2012 | http://pubs.acs.org
Publication Date: August 13, 2009 | doi: 10.1021/bk-2009-1024.ch004

additives are also effective for controlling the stereochemistry even during the RAFT polymerizations.

**Table IV. RAFT Polymerization of DMAM in the Presence of Thiourea Additives in $CH_2Cl_2$ at 20 °C[a]**

| *RAFT Agent* | *Additive* | *$[Add]_0/[M]_0$* | *Conv. (%)* | *$M_n$* | *$M_w/M_n$* | *m/r* |
|---|---|---|---|---|---|---|
| PEPD | None | 0 | 50 | 7000 | 1.62 | 50.9/49.1 |
| PEPD | **2** | 0.75 | 51 | 8400 | 1.39 | 56.4/43.6 |
| PEPD | **2** | 1.0 | 89 | 14000 | 1.34 | 63.5/36.5 |
| CPETC | None | 0 | 91 | 16000 | 1.20 | 51.4/48.6 |
| CPETC | **2** | 0.75 | 89 | 14000 | 1.22 | 62.0/38.0 |
| CPETC | **2** | 1.0 | 77 | 14000 | 1.18 | 63.8/36.2 |
| None | None | 0 | 69 | 35000 | 1.76 | 51.5/48.5 |
| None | **2** | 0.75 | 69 | 29000 | 1.57 | 62.3/37.7 |

[a] $[DMAM]_0/[RAFT\ Agent]_0/[V\text{-}70]_0$ = 1000/5.0/2.5 mM.

Downloaded by CORNELL UNIV on June 26, 2012 | http://pubs.acs.org
Publication Date: August 13, 2009 | doi: 10.1021/bk-2009-1024.ch004

## Conclusions

In conclusion, thiourea additives induced the isospecific radical polymerization of acrylamides most probably via a hydrogen-bonding interaction with the monomers and the growing polymer terminals. The tacticity significantly depended on the substituents of the thioureas, for which both electron-withdrawing and moderately bulky groups were effective. A combination of the thioureas with trithiocarbonate-type RAFT agents enabled the simultaneous control of the tacticity and molecular weight without any losses of each control. This combination is free from metal compounds, such as transition metal catalysts and Lewis acids (*30–32*), and thus would be beneficial in preparing metal-free polyacrylamides with controlled molecular weight and tacticity from the viewpoint of biomedical applications.

## Experimental

### Materials

*N*,*N*-Dimethylacrylamide (Wako Chemicals; > 98%) was distilled over calcium hydride under reduced pressure before use. *N*-Isopropylacrylamide (Wako Chemicals; > 98%) was purified by recrylstallization from *n*-hexane and dried under reduced pressure before use. α,α-Azobisisobutyronitrile (AIBN) (Kishida, >99%) was purified by recrylstallization from methanol. 2,2'-Azo-bis(4-methoxy-2,4-dimethyl valeronitrile) (V-70) (Wako, >95%) and *n*-$Bu_3B$ (1.0 M in THF) (Aldrich) were used as received. 1-Phenylethyl phenyldithioacetate (PEPD) was synthesized according to the literature.[33] The synthesis of *S*-2-cyano-2-propyl *S*'-ethyl trithiocarbonate (CPETC) was conducted similar to that of the *S'*-methyl or *S'*-dodecyl analogues reported by Rizzardo et al.[34] All other reagents were purified by usual methods.

## Synthesis of DMAM Dimer

DMAM dimer (*N*,*N*,*N'*,*N'*,2-pentamethylglutaryl amide) was prepared as follows: in a 500 ml flask, triphenylphosphine (26.2 g, 0.10 mol) and $CCl_4$ (100 ml, 1.0 mol) were mixed in dry THF (200 ml) under dry nitrogen atmosphere. The mixture was refluxed at 85 °C for 30 min, and then cooled to 5 °C. Into the mixture, 2-methylglutaric acid (7.31 g, 0.05 mol) and dimethylamine (100 ml, 2.0 M solution in THF) were added dropwise and sequentially in this order. The reaction was allowed to proceed at r.t. for 16 h. After filtration and evaporation, the crude product was purified by column chromatography on silica gel with *n*-hexane/ethyl acetate/ethanol (1/1/1) as an eluent. The product was obtained as a white solid (2.46 g, 25% yield).

## Synthesis of Thioureas

The syntheses of thioureas were conducted according to the literature.[35] For a typical example, 1-[3,5-bis(trifluoromethyl)phenyl]-3-(1-naphthalenyl) thiourea (**2**) was prepared as follows: under dry nitrogen atmosphere, 3,5-bis(trifluoromethyl)phenyl isothiocyanate (8.93 ml, 48.9 mmol) was added dropwise into the solution of 1-naphthylamine (7.0 g, 48.9 mmol) in dry THF (100 ml) at 0 °C. To avoid side reactions with adventitious water in the reaction medium, the amine was purified by azeotropic drying with toluene three times just before use. The reaction mixture was stirred at r.t. for 72 h and the reaction mixture was concentrated in vacuo. The crude product was purified by precipitation into *n*-hexane twice to afford **2** (17.9 g, 90 %) as colorless amorphous solid.

## Conventional Radical Polymerization

The polymerizations with *n*-$Bu_3B$ at –78 °C were carried out by syringe technique under dry argon in glass tubes equipped with a three-way stopcock. A typical example for DMAM polymerization is given below. Into a mixture of DMAM (0.15 ml, 1.5 mmol), **2** (0.93 g, 2.25 mmol) in $CH_2Cl_2$ (1.77 ml) was added sequentially a solution of *n*-$Bu_3B$ (0.015 mmol; 0.15 mL of 1.0 M in THF) and 0.60 ml of air. The total volume of the reaction mixture was thus 3.0 mL. After the desired time, the monomer conversion was determined from its residual concentration by $^1H$ NMR (for 144 h, 81% conv.). The solution was added dropwise into a large amount of *n*-hexane and the product was collected by centrifugation, purified by dialysis in methanol, and finally dried under vacuum at r.t. for over night ($M_n = 28700$, $M_w/M_n = 2.41$).

Downloaded by CORNELL UNIV on June 26, 2012 | http://pubs.acs.org
Publication Date: August 13, 2009 | doi: 10.1021/bk-2009-1024.ch004

### RAFT Polymerization

A typical example for the RAFT polymerization of DMAM is given below. In a 50 mL round-bottomed flask were placed $CH_2Cl_2$ (2.50 ml), DMAM (0.72 ml, 7.0 mmol), **2** (2.9 g, 7.0 mmol), 1,2,3,4-tetrahydronaphthalene (0.35 ml) as an internal standard, and $CH_2Cl_2$ solutions of V-70 (0.35 ml, 0.018 mmol) and CPETC (0.18 ml, 0.036 mmol) at 0 °C. The total volume of the reaction mixture was 7.0 ml. Immediately after mixing, the solution was degassed by three cycles of freeze-vacuum-thaw at –78°C and then evenly charged in 7 glass tubes. The tubes were sealed by flame under nitrogen atmosphere and immersed in thermostatic water bath at 20 °C. In predetermined intervals, the polymerization was terminated by the cooling of the reaction mixtures to –78 °C. Monomer conversion was determined from the concentration of residual monomer measured by gas chromatography with 1,2,3,4-tetrahydronaphthalene as an internal standard (for 240 h, 77% conv.). The product was collected and purified as described in the conventional radical polymerization ($M_n$ = 13800, $M_w/M_n$ = 1.18).

Downloaded by CORNELL UNIV on June 26, 2012 | http://pubs.acs.org
Publication Date: August 13, 2009 | doi: 10.1021/bk-2009-1024.ch004

### Measurements

The $^1H$ NMR spectra were recorded on a Varian Gemini 2000 spectrometer operating at 400 MHz. The dyad tacticity of the polymer was determined on the area of the methylene protons of the backbone, and the measurement was carried out at 170 °C in DMSO-$d_6$. The number-average molecular weight ($M_n$) and polydispersity index ($M_w/M_n$) of the polymers were determined by size-exclusion chromatography (SEC) in DMF containing 100 mM LiCl at 40 °C on two polystyrene gel columns [Shodex K-805L (pore size: 20–1000 Å; 8.0 mm i.d. × 30 cm) × 2; flow rate 1.0 mL/min] connected to Jasco PU-980 precision pump and a Jasco 930-RI detector. The columns were calibrated against 7 standard poly(MMA) samples (Shodex; $M_p$ = 1990–1950000; $M_w/M_n$ = 1.02–1.09).

## Acknowledgment

This work was supported in part by a Grant-in-Aid for Young Scientists (S) (No. 19675003) by the Japan Society for the Promotion of Science, a Grant-in-Aid for Scientific Research on Priority Areas "Advanced Molecular Transformation of Carbon Resources" (No. 17065008) from the Ministry of Education, Culture, Sports, Science and Technology, Japan, and the Global COE Program "Elucidation and Design of Materials and Molecular Functions."

## References

1. Georges, M. K.; Veregin, R. P. N.; Kazmaier, P. M.; Hamer, G. K. *Macromolecules* **1993**, *26*, 2987–2988.
2. Hawker, C. J. *J. Am. Chem. Soc.* **1994**, *116*, 11185–11186.
3. Wayland, B. B.; Poszmik, G.; Mukerjee, S. L.; Fryd, M. *J. Am. Chem. Soc.* **1994**, *116*, 7943–7944.
4. Kato, M.; Kamigaito, M.; Sawamoto, M.; Higashimura, T. *Macromolecules* **1995**, *28*, 1721–1723.
5. Wang, J.-S.; Matyjaszewski, K. *J. Am. Chem. Soc.* **1995**, *117*, 5614–5615.
6. Percec, V.; Barboiu, B. *Macromolecules* **1995**, *28*, 7970–7972.
7. Granel, C.; Dubois, P.; Jérôme, R.; Teyssié, P. *Macromolecules* **1996**, *29*, 8576–8582.
8. Haddleton, D. M.; Jasieczek, C. B.; Hannon, M. J.; Shooter, A. J. *Macromolecules* **1997**, *30*, 2190–2193.
9. Chiefari, J.; Chong, Y. K.; Ercole, F.; Krstina, J. Jeffery, K.; Tam, P. T. Le.; Mayadunne, R. T. A.; Meijs, G. F.; Moad, C. L.; Moad, G.; Rizzardo, E.; Thang, S. H. *Macromolecules* **1998**, *31*, 5559–5562.
10. Hawker, C. J.; Bosman, A. W.; Harth, E. *Chem. Rev.* **2001**, *101*, 3661–3688.
11. Studer, A.; Schulte, T. *Chem. Rec.* **2005**, *5*, 27–35.
12. (a) Kamigaito, M.; Ando, T.; Sawamoto, M. *Chem. Rev.* **2001**, *101*, 3689–3745. (b) Kamigaito, M.; Ando, T.; Sawamoto, M. *Chem. Rec.* **2004**, *4*, 159–175. (c) Ouchi, M.; Terashima, T.; Sawamoto, M. *Acc. Chem. Res.* **2008**, *41*, 1120–1132.
13. (a) Matyjaszewski, K.; Xia, J. *Chem. Rev.* **2001**, *101*, 2921–2990. (b) Tsarevsky, N. V.; Matyjaszewski, K. *Chem. Rev.* **2007**, *107*, 2270–2299. (c) Braunecker, W. A.; Matyjaszewski, K. *Prog. Polym. Sci.* **2007**, *32*, 93–146.
14. (a) Moad, G.; Rizzardo, E.; Thang, S. H. *Aust. J. Chem.* **2005**, *58*, 379–410. (b) Moad, G.; Rizzardo, E.; Thang, S. H. *Polymer* **2008**, *49*, 1079–1131. (c) Moad, G.; Rizzardo, E.; Thang, S. H. *Acc. Chem. Res.* **2008**, *41*, 1133–1142.
15. David, G.; Boyer, C.; Tonnar, J.; Ameduri, B.; Lacroix-Desmazes, P.; Boutevin, B. *Chem. Rev.* **2006**, *106*, 3936–3962.
16. Yamago, S. *J. Polym. Sci.: Part A: Polym. Chem.* **2006**, *44*, 1–12.
17. Poli, R.; *Angew. Chem. Int. Ed.* **2006**, *45*, 5058–5070.
18. (a) Yamada, K.; Nakano, T.; Okamoto, Y. *Macromolecules* **1998**, *31*, 7598–7605. (b) Isobe, Y.; Yamada, K.; Nakano, T. Okamoto, Y. *Macromolecules* **1999**, *32*, 5979–5981.
19. Matsumoto, A.; Nakamura, S. *J. Appl. Polym. Sci.* **1999**, *74*, 290–296.
20. (a) Suito, Y.; Isobe, Y.; Habaue, S.; Okamoto, Y. *J. Polym. Sci., Part A: Polym. Chem.* **2002**, *40*, 2496–2500. (b) Isobe, Y.; Fujioka, D.; Habaue, S.; Okamoto, Y. *J. Am. Chem. Soc.* **2001**, *123*, 7180–7181.
21. Habaue, S.; Okamoto, Y.; *Chem. Rec.* **2001**, *1*, 46–52.
22. (a) Shibata, T.; Satoh, K.; Kamigaito, M.; Okamoto, Y. *J. Polym. Sci., Part A: Polym. Chem.* **2006**, *44*, 3609–3615. (b) Miura, Y.; Shibata, T.; Satoh,

Downloaded by CORNELL UNIV on June 26, 2012 | http://pubs.acs.org
Publication Date: August 13, 2009 | doi: 10.1021/bk-2009-1024.ch004

K.; Kamigaito, M.; Okamoto, Y. *J. Am. Chem. Soc.* **2006**, *128*, 16026–16027.

23. Wan, D.; Satoh, K.; Kamigaito, M. *Macromolecules* **2006**, *39*, 6882–6886.
24. (a) Hirano, T.; Miki, H.; Seno, M.; Sato, T. *J. Polym. Sci., Part A: Polym. Chem.* **2004**, *42*, 4404–4408. (b) Hirano, T.; Miki, H.; Seno, M.; Sato, T. *Polymer* **2005**, *46*, 3693–3699. (c) Hirano, T.; Okumura, Y.; Kitajima, H.; Seno, M.; Sato, T. *J. Polym. Sci., Part A: Polym. Chem.* **2006**, *44*, 4450–4460. (d) Hirano, T.; Ishizu, H.; Seno, M.; Sato, T. *Polymer* **2005**, *46*, 10607–10610. (e) Hirano, T.; Ishizu, H.; Sato, T. *Polymer* **2008**, *49*, 438–445.
25. (a) Kamigaito, M. Satoh, K.; Wan. D.; Sugiyama, Y.; Koumura, K.; Shibata, T.; Okamoto, Y. *ACS Symp. Ser.* **2006**, *944*, 26–39. (b) Kamigaito, M.; Satoh, K. *J. Polym. Sci., Part A: Polym. Chem.* **2006**, *44*, 6147–6158. (c) Kamigaito, M.; Satoh, K. *Macromolecules* **2008**, *41*, 6147–6158.
26. (a) Kelly, T. R.; Kim. M. K, *J. Am. Chem. Soc.* **1994**, *116*, 7072–7080. (b) Schmidtchen, F. P.; Berger, M. *Chem. Rev.* **1997**, *97*, 1609–1646. (c) Linton, B. R.; Goodman, M. S.; Hamilton, A. D. *Chem. Eur. J.* **2000**, *6*, 2449–2455.
27. (a) Curran, D. P.; Kuo, L. H. *J. Org. Chem.* **1994**, *59*, 3259–3261. (b) Curran, D. P.; Kuo, L. H. *Tetrahedron Lett.* **1995**, *36*, 6647–6650.
28. (a) Takemoto, Y. *Org. Biomol. Chem.* **2005**, *3*, 4299–4306. (b) Taylor, M. S.; Jacobsen, E. N. *Angew. Chem. Int. Ed.* **2006**, *45*, 1520–1543.
29. Thang, S. H.; Chong, Y. K.; Mayadunne, R. T. A.; Moad, G.; Rizzardo, E. *Tetrahedron Lett.* **1999**, *40*, 2435–2438.
30. (a) Ray, B.; Isobe, Y.; Morioka, K.; Habaue, S.; Okamoto, Y.; Kamigaito, M.; Sawamoto, M. *Macromolecules* **2003**, *36*, 543–545. (b) Ray, B.; Isobe, Y.; Matsumoto, K.; Habaue, S.; Okamoto, Y.; Kamigaito, M.; Sawamoto, M. *Macromolecules* **2004**, *37*, 1702–1710. (c) Ray, B.; Okamoto, Y.; Kamigaito, M.; Sawamoto, M.; Seno, M.; Kanaoka, S.; Aoshima, S. *Polym. J.* **2005**, *37*, 234–237.
31. Sugiyama, Y.; Satoh, K.; Kamigaito, M.; Okamoto, Y. *J. Polym. Sci., Part A: Polym. Chem.* **2006**, *44*, 2086–2098.
32. Lutz, J.-F.; Neugebauer, D.; Matyjaszewski, K. *J. Am. Chem. Soc.* **2003**, *125*, 6986–6993.
33. Quinn, J. F.; Rizzardo, E.; Davis, T. P. *Chem. Commun.* **2001**, 1044–1045.
34. Chiefari, J.; Mayadunne, R. T. A.; Moad, C. L.; Moad, G.; Rizzardo, E.; Postma, A.; Skidmore, M. A.; Thang, S. H. *Macromolecules* **2003**, *36*, 2273–2283.
35. (a) Wilcox, C. S.; Kim, E.-I.; Romano, D.; Kuo, L. H.; Burt, A. L.; Curran, D. P. *Tetrahedron* **1995**, *51*, 621–634. (b) Okino, T.; Yasutaka, H.; Furukawa, T.; Xu, X.; Y. Takemoto *J. Am. Chem. Soc* **2005**, *127*, 119–125.

Downloaded by CORNELL UNIV on June 26, 2012 | http://pubs.acs.org
Publication Date: August 13, 2009 | doi: 10.1021/bk-2009-1024.ch004

Downloaded by UNIV OF DELAWARE MORRIS LIB on June 26, 2012 | http://pubs.acs.org
Publication Date: August 13, 2009 | doi: 10.1021/bk-2009-1024.ch005

## Chapter 5

# Controlled Radical Polymerization of Butyl Acrylate and Methyl Methacrylate by Reverse Iodine Transfer Polymerization (RITP) in Miniemulsion: Use of Hydrogen Peroxide as Oxidant

**Jeff Tonnar and Patrick Lacroix-Desmazes***

**Institut Charles Gerhardt - UMR5253 CNRS/UM2/ENSCM/UM1 - Ingénierie et Architectures Macromoléculaires, Ecole Nationale Supérieure de Chimie de Montpellier, 8 rue de l'Ecole Normale, 34296 Montpellier Cedex 5, France.**

The controlled radical polymerization of methyl methacrylate and butyl acrylate by reverse iodine transfer polymerization in aqueous miniemulsion was achieved. The polymerization was initiated by bis(4-tert-butylcyclohexyl)peroxydicarbonate at T=64°C for methyl methacrylate and by AIBN at T=85°C for butyl acrylate with dodecyl sulfate sodium salt as surfactant, yielding stable latexes. The hydrolytic disproportionation of iodine was counterbalanced by a continuous addition of hydrogen peroxide to regenerate the hydrolyzed iodine, leading to a good correlation between theoretical and experimental molecular weights.

In Controlled/Living Radical Polymerization: Progress in RAFT, DT, NMP & OMRP; Matyjaszewski, K.;
ACS Symposium Series; American Chemical Society: Washington, DC, 2009.

# Introduction

In recent years, controlled radical polymerization (CRP)(*1,2*) has emerged as a unique technique to synthesize polymers with controlled architectures, like block, graft or star copolymers. Several techniques have been developed among which nitroxide–mediated polymerization (NMP),(*3*) metal-catalyzed radical polymerization,(*4*) iodine transfer polymerization (ITP),(*5*) and reversible addition-fragmentation chain transfer polymerization (RAFT)(*6*) are the most widespread. Several groups tried to implement CRP in aqueous medium(*7,8*) but they encountered lots of problems. However some very recent works have shown many improvements.(*9-11*)

A large number of studies have been carried out in miniemulsion because it is a heterogeneous polymerization process where the nucleation step is bypassed and where the transportation across the aqueous phase is not necessary. In miniemulsion polymerization, the monomer droplets are formed by ultrasonication of the initial monomer-in-water emulsion. To increase the stability of these monomer droplets and to avoid Ostwald ripening, a hydrophobic agent such as hexadecane is usually added.(*12*) However, the first CRP miniemulsion polymerizations presented lots of problems such as low polymerization rates, broad molecular weight and particle size distributions and colloidal instability.(*13-15*)

Luo et al.(*16,17*) proposed that the super-swelling occurring in the first stage of CRP in miniemulsion is the cause of the encountered problems. Super-swelling occurs because the oligomer molecules that form in the beginning stages of CRP dramatically reduce the monomer chemical potential in the first nucleated particles. As a consequence, monomer will diffuse from the monomer droplets to these particles. When the particles reach a certain size, they become very sensitive to the shear force and the system is apt to loose stability.(*18*) The superswelling can be limited by increasing the surfactant and hydrophobe concentrations in the reaction medium.(*17*) Moreover, the use of a non ionic polymeric surfactant increases the control over the polymerization, due to the slower monomer transfer in this system.(*19*)

The major issue with traditional miniemulsion polymerization are the high levels of surfactant and hydrophobe used. To avoid these problems, it seems sensible to use compounds that are incorporated into the latex. In RAFT polymerization, the most successful means of overcoming the encountered problems is to use an amphiphilic diblock copolymer as RAFT agent. These amphipathic RAFT agents are used to emulsify the dispersed phase, stabilize the particles, and control the molecular weight of the polymer chains, giving polymer latexes which do not contain free surfactant or co-stabilizer.(*20,21*)

Like in RAFT polymerization, amphiphilic diblock copolymers proved to be very efficient stabilizers for NMP polymerization of styrene.(*21,22*) In nitroxide-mediated polymerization, the TEMPO-mediated acrylate polymerization or the polymerization of styrene at low temperatures showed a slow polymerization rate due to the accumulation of free nitroxide (persistent radical effect).(*23*) Ascorbic acid, a strong reductor for nitroxide was used to eliminate the excess nitroxide in the reaction medium and allowed the polymerization to proceed at a higher rate.(*24-26*) By using the acyclic

Downloaded by UNIV OF DELAWARE MORRIS LIB on June 26, 2012 | http://pubs.acs.org
Publication Date: August 13, 2009 | doi: 10.1021/bk-2009-1024.ch005

phosphonylated SG1 nitroxide, Farcet et al.(*27*) have polymerized butyl acrylate in a controlled manner in miniemulsion without any coagulation or destabilization.

ATRP is even more complicated to implement in miniemulsion polymerization. In fact the ATRP agents are partitioned between the different phases, leading to some hydrolysis in the aqueous phase and a loss over the molecular weight control. Matyjaszewski et al.(*2,28*) have recently developed a new initiating/catalytic system known as activators generated by electron transfer (AGET ATRP). In this system, the activator is generated *in situ* from the $Cu^{II}$ catalyst and a reducing agent like ascorbic acid(*28*) or triethylamine.(*29*) This system was successfully applied in miniemulsion(*30*) and inverse miniemulsion.(*31*) A series of forced gradient copolymers with different monomer distributions along the copolymer backbone were successfully prepared by ATRP in miniemulsion. AGET ATRP was beneficial for forced gradient copolymers preparation because all polymer chains were initiated within the miniemulsion droplets and the miniemulsion remained stable throughout the entire polymerization.(*30*) Finally, PEO-based polymers were successfully used as reactive surfactants in AGET ATRP of butyl acrylate in miniemulsion.(*32*)

Considering iodine transfer polymerization (ITP), good results were obtained in miniemulsion polymerization of styrene.(*33-36*) Pouget et al.(*36*) used ITP in miniemulsion polymerization of styrene to synthesize well-defined poly(styrene)-b-poly(dimethylsiloxane)-b-polystyrene triblock copolymers. In miniemulsion ITP, no loss of colloidal stability due to superswelling was observed. This is probably due to the lower chain transfer constant in iodine mediated polymerization (in contrast to ATRP, RAFT or NMP). Therefore, the polymer chains formed in the beginning stages of the polymerization have a higher molecular weight than for the other CRP methods, limiting the superswelling (presence of several big polymer chains instead of a high amount of low molecular weight oligomers in the beginning stages of the polymerization).

During the past several years a new CRP method named reverse iodine transfer polymerization (RITP), which relies on the use of molecular iodine as control agent, was invented by our group(*37-39*) and patented.(*40-44*) The general mechanism of RITP is given in Scheme 1. The radicals coming from the decomposed initiator react preferably with iodine to form the A-I adduct or add several monomer units before reacting with iodine to form $A\text{-}M_n\text{-}I$ transfer agents *in situ*. Once the whole iodine has been consumed by the decomposed initiator, the core equilibrium of degenerative transfer establishes itself. The targeted molecular weight of the polymer chains $M_{n,target}$ is given by:

Downloaded by UNIV OF DELAWARE MORRIS LIB on June 26, 2012 | http://pubs.acs.org
Publication Date: August 13, 2009 | doi: 10.1021/bk-2009-1024.ch005

**$M_{n,target}$=(*mass of monomer*)/(2×$n_{I2,initial}$) + $M_{A-I}$.**

**With $M_{A-I}$ being the molecular weight of the A-I adduct.**

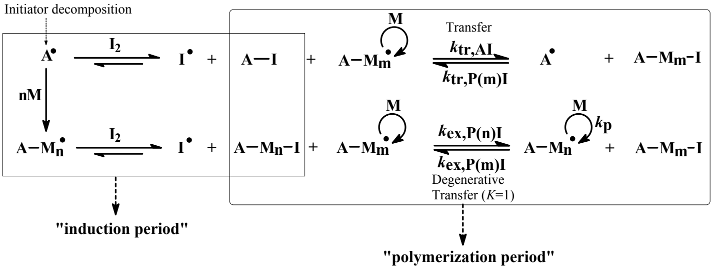

*Scheme 1. Simplified mechanism of reverse iodine transfer polymerization in solution ($A^{\bullet}$: radical from the initiator; $I_2$: molecular iodine; M: monomer unit; n: mean number degree of polymerization).*

Our group polymerized butyl acrylate by RITP in ab initio emulsion polymerization.(*45*) The molecular weight could be modulated by changing the concentration of iodine and a block copolymerization reaction proved the living character of the poly(butyl acrylate) latex. In dispersed aqueous medium, a partitioning of all the species between the different phases occurs. One important reaction to consider in the aqueous phase, is the hydrolytic disproportionation of iodine.(*46*) Iodine hydrolysis (Scheme 2, Equilibrium 1) leads to the formation of hypoiodous acid (HOI) (pKa $_{HOI/IO^-}$ = 11),(*47*) iodide ($I^-$) (pKa $_{HI/I^-}$ = -10)(*48*) and iodate ($IO_3^-$) (pKa $_{HIO3/IO3^-}$= 0.8).(*47*) It also forms protons and thus it tends to lower the pH. This iodine hydrolysis was responsible for an upward deviation of the experimental molecular weight from the targeted molecular weight. The amount of effective iodine was successfully correlated to the observed experimental molecular weight.(*49*)

$$3\,I_{2,aq} + 3H_2O \rightleftharpoons IO_3^- + 5\,I^- + 6\,H^+ \qquad (1)$$

$$H_2O_2 + 2\,H^+ + 2\,I^- \rightleftharpoons I_2 + 2\,H_2O \qquad (2)$$

*Scheme 2: (1) Iodine disproportionation in the aqueous phase; (2) Iodine regeneration by oxidation of iodide by hydrogen peroxide.*

Recently the problem of iodine hydrolysis was overcome in miniemulsion RITP of styrene.(*50*) Hydrogen peroxide was used to regenerate the hydrolysed iodine (Scheme 2, Equilibrium 2), leading to the expected molecular weights. Moreover, the use of an oxidant was further applied to allow the controlled polymerization of butyl acrylate in *ab initio* emulsion polymerization.(*43,51-53*)

Herein, we report the first successful miniemulsion RITP of butyl acrylate and methyl methacrylates by regenerating the hydrolyzed iodine by the addition of hydrogen peroxide in acidic media.

Downloaded by UNIV OF DELAWARE MORRIS LIB on June 26, 2012 | http://pubs.acs.org
Publication Date: August 13, 2009 | doi: 10.1021/bk-2009-1024.ch005

# Experimental

## Materials

Butyl acrylate (BuA, Acros, 99%), methyl methacrylate (MMA, Aldrich) and styrene (Acros, 99%) were purified by vacuum distillation before use. Dodecyl sulfate sodium salt (SDS, Aldrich, 98%, critical micelle concentration CMC = 2.6 $g.L^{-1}$), bis(4-tert-butylcyclohexyl)peroxydicarbonate (Perkadox 16S, Akzo Nobel, 95%), hydrogen peroxide (Acros, 30 wt % solution in water), n-hexadecane (Acros, 99%) and iodine (Aldrich, 99.8%) were used as received. α,α'-Azobisisobutyronitrile (AIBN, Fluka, 98%) was purified by recrystallization in methanol. Water was de-ionized by passing through columns packed with ion exchange resins.

Downloaded by UNIV OF DELAWARE MORRIS LIB on June 26, 2012 | http://pubs.acs.org
Publication Date: August 13, 2009 | doi: 10.1021/bk-2009-1024.ch005

## General procedure for miniemulsion polymerization of methyl methacrylate.

[MMA]/[Perkadox]/[$I_2$] = 200/3.53/1 ($M_{n,targeted}$ = 10 300 $g.mol^{-1}$). Typically, 140 g of water were placed in a 250 ml glass reactor and thoroughly purged with argon for 30 minutes. The reaction medium was acidified by addition of 1 ml of chlorhydric acid HCl 0.1 N. A solution of SDS (400 mg, $M$ = 288.28 $g.mol^{-1}$, 1.39 mmol) in water (10 g) was added in the reactor under argon flow, followed by a solution of Perkadox 16S (1.06 g, $M$ = 398.5 $g.mol^{-1}$, 2.66 mmol), iodine (0.1906 g, $M$ = 253.81 $g.mol^{-1}$, 0.75 mmol) and n-hexadecane (0.45 g, $M$ = 226.45 $g.mol^{-1}$, 1.99 mmol ) in methyl methacrylate (15g, $M$ = 100 $g.mol^{-1}$, 150 mmol). The reaction medium was purged for 15 min with argon. Then the solution was miniemulsified by ultrasonication (Bioblock Scientific Vibra Cell 75043, 1.5 min, 8 KHz) under argon flow. No further argon purging was executed in order to avoid important monomer stripping. The reactor was thermostated at 64°C and the reaction proceeded for 16 hours in the dark under argon atmosphere and magnetic stirring. In the experiments where iodine was regenerated by hydrogen peroxide, an aqueous solution of hydrogen peroxide (0.62 g $H_2O_2$ 30% wt. solution in water, $M$ = 34 $g.mol^{-1}$, 5.47 mmol) in 15 g of water is immediately injected during 3 hours with a Braun Perfusor compact injection pump and a Terumo 20 ml syringe. Monomer conversion was determined by gravimetric analysis. Results are given in Table 1, run 2a.

## General procedure for miniemulsion polymerization of butyl acrylate

[BuA]/[AIBN]/[$I_2$] = 155/3.44/1. Typically, 140 g of water were placed in a 250 ml glass reactor and thoroughly purged with argon for 30 minutes. The reaction medium was acidified by addition of 1 ml of chlorhydric acid HCl 0.1 N. A solution of SDS (400 mg, $M$ = 288.28 $g.mol^{-1}$, 1.39 mmol) in water (10 g) was added in the reactor under argon flow, followed by a solution of AIBN (427 mg, $M$ = 164 $g.mol^{-1}$, 2.6 mmol), iodine (0.1922 g, $M$ = 253.81

g.mol$^{-1}$, 0.76 mmol) and n-hexadecane (0.45 g, $M$ = 226.45 g.mol$^{-1}$, 1.99 mmol) in butyl acrylate (15.04 g, $M$ = 128 g.mol$^{-1}$, 117.5 mmol). The reaction medium was purged for 15 min with argon. Then the solution was miniemulsified by ultrasonication (Bioblock Scientific Vibra Cell 75043, 1.5 min, 8 KHz) under argon flow and the miniemulsion was purged for another 15 minutes with argon. The reactor was thermostated at 85°C and the reaction proceeded for 16 hours in the dark under argon atmosphere and magnetic stirring. In the experiments where iodine was regenerated by hydrogen peroxide an aqueous solution of hydrogen peroxide (0.53 g $H_2O_2$ 30% wt. solution in water, $M$ = 34 g.mol$^{-1}$, 4.72 mmol) in 10 g of water is injected during 2 hours once the reaction medium began to decolour, indicating that there was not a lot of residual free iodine, with a Braun Perfusor compact injection pump and a Terumo 20 ml syringe. Monomer conversion was determined by gravimetric analysis. Results are given in Table 2, run 2a.

## Chain extension

The seed latex was prepared as above: [BuA]/[AIBN]/[$I_2$] = 155/3.44/1 (85% monomer conversion) and continuous addition of hydrogen peroxide (0.53 g $H_2O_2$ 30% wt. solution in water, $M$ = 34 g.mol$^{-1}$, 4.72 mmol) in 10 g of water during 2 hours near the end of the inhibition period. This seed latex ($M_{n,SEC}$ = 9 300 g.mol$^{-1}$, PDI = 2.11) was used to execute a block copolymerization. The seed latex (40.75 g, $M_n$ = 9 300 g.mol$^{-1}$, 0.315 mmol) and a solution of AIBN (0.02 g, $M$ = 164 g.mol$^{-1}$, 0.122 mmol) in styrene (5.14 g, $M$ = 104 g.mol$^{-1}$, 49.4 mmol) were introduced in a 100 mL glass reactor and purged by argon bubbling during 15 minutes. The reaction proceeded in the dark under argon atmosphere with magnetic stirring during 20 hours at T = 80°C. Results are given in Table 3, run 2.

## Characterizations

Size Exclusion Chromatography (SEC) was performed on dried samples dissolved in tetrahydrofuran, with a Spectra Physics Instruments SP8810 pump equipped with two 300 mm columns thermostated at 30°C (columns mixed-C PL-gel 5 µm from Polymer Laboratories : $2\times10^2$ - $2\times10^6$ g.mol$^{-1}$ molecular weight range), a Shodex RIse-61 refractometer detector, and a Milton Roy Ultra-Violet spectrometer detector. Tetrahydrofuran was used as eluent at a flow rate of 1.0 mL.min$^{-1}$. Calibration was performed with polystyrene standards from Polymer Laboratories.

$^1$H NMR analyses were performed on a Bruker Avance 250 MHz in $CDCl_3$. Particle size of the latex was determined with a Nanotrac 250 particle analyzer (Microtrac Inc.). pH measurements were performed with a Consort P500 apparatus from Bioblock Scientific. Iodide concentrations [$I^-$] were measured with a PHM 210 Standard pH Meter from Radiometer Analytical with an iodide

Downloaded by UNIV OF DELAWARE MORRIS LIB on June 26, 2012 | http://pubs.acs.org
Publication Date: August 13, 2009 | doi: 10.1021/bk-2009-1024.ch005

selective electrode ISE25I-9 and a reference electrode REF201 from Radiometer Analytical.

# Results and Discussion

## Reverse Iodine Transfer Polymerization of Methyl Methacrylate in Miniemulsion

In RITP in aqueous medium, iodine hydrolysis is responsible for an upward deviation of the molecular weights.(*49*) This side reaction was counterbalanced by continuously adding a solution of hydrogen peroxide, to regenerate the hydrolysed iodine, during the whole inhibition period (Scheme 2, Equilibrium 2). When adding hydrogen peroxide, the final iodide concentration is very low (around $10^{-7}$ mol.L$^{-1}$).

## Kinetics

The kinetics of MMA miniemulsion RITP was followed in order to gain a better understanding of the reaction mechanism. As it can be seen in figure 1, an inhibition period is clearly observed, where the monomer consumption is very low and the formed radicals are preferably consumed by iodine (due to the strong radical scavenging activity of iodine).(*54*) Once the whole free iodine present in the reaction medium has reacted with radicals to form A-I and A-M$_n$-I transfer agents *in situ*,(*38*) the core equilibrium of degenerative transfer establishes itself and the polymerization proceeds up to high conversions.

A near linear evolution of molecular weight (polystyrene-equivalent) with conversion is observed and a very good polydispersity index around 1.25 is obtained (Figure 2a). Moreover, the whole molecular weight distribution is shifted towards higher molecular weights as the conversion proceeds (Figure 2b). The slight tailing at low molecular weights might be attributed to a small fraction of dead chains due to the relatively unstable tertiary PMMA-I chain-ends. Indeed if the reaction is conducted longer than necessary, the chain-ends rapidly undergo degradation with HI elimination leading to lower chain-end functionality. In addition, the liberated HI can be oxidized by hydrogen peroxide to iodine $I_2$, which can control new small molecular weight polymer chains, which are responsible for a slight tailing on the low molar mass side of the SEC peaks.

Downloaded by UNIV OF DELAWARE MORRIS LIB on June 26, 2012 | http://pubs.acs.org
Publication Date: August 13, 2009 | doi: 10.1021/bk-2009-1024.ch005

Downloaded by UNIV OF DELAWARE MORRIS LIB on June 26, 2012 | http://pubs.acs.org
Publication Date: August 13, 2009 | doi: 10.1021/bk-2009-1024.ch005

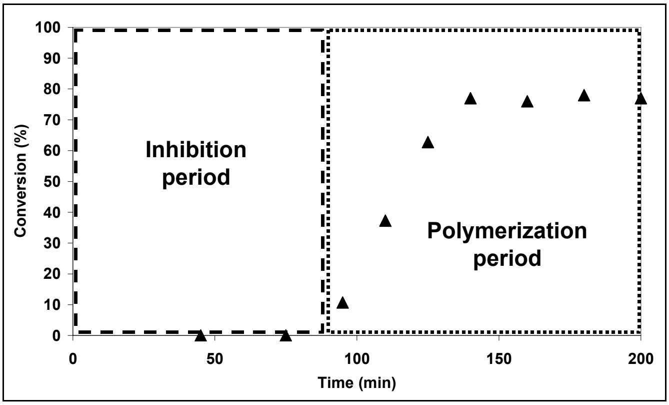

*Figure 1. Evolution of monomer conversion versus time for reverse iodine transfer polymerization of methyl methacrylate in miniemulsion with iodine regeneration by hydrogen peroxide at T=64°C ([Perkadox 16S]/[$I_2$] = 3.53, [Dodecyl sulfate sodium salt] = 2.6 g.$L^{-1}$, $M_{n,targeted}$ = 10 100 g.$mol^{-1}$).*

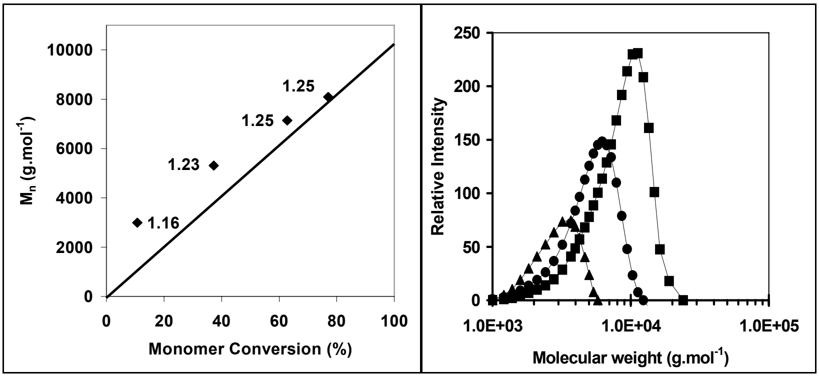

*Figure 2. (2a) : Evolution of the molecular weight, $M_n$ versus monomer conversion for reverse iodine transfer polymerization miniemulsion of methyl methacrylate at T = 64°C when iodine is regenerated by hydrogen peroxide, ([Perkadox 16S]/[$I_2$] = 3.53, [Dodecyl sulfate sodium salt] = 2.6 g.$L^{-1}$, $M_{n,targeted}$ = 10 100 g.$mol^{-1}$) : Molecular weight (◆), polydispersity index (labels), theoretical molecular weight evolution (straight line) ;*
*(2b) Evolution of the molecular weight distribution: (▲) conversion 11%; (●) conversion 38%; (■) conversion 77%.*

## Effect of the iodine concentration

In order to show the controlled character of the polymerization, different molecular weights were targeted by changing the concentration of iodine (Table 1, runs 1-3). Stable monomodal latexes with high monomer conversions around

80% were obtained. After several hours a recolouration due to some iodine regeneration (from the iodide providing from the degraded chain–ends) was observed. A good correlation between experimental and theoretical molecular weights was obtained and the whole molecular weight distribution was shifted towards higher molecular weights if the concentration of iodine was diminished (Figure 3). Polydispersity indexes between 1.25 and 1.37 were obtained which is very good for degenerative transfer by iodine-mediated polymerization in aqueous medium.

**Table 1. Effect of iodine concentration**[a]

| *Run* | *[Perkadox]/ $[I_2]$* | *$M_{n,targeted}$ ($g.mol^{-1}$)* | *Time (h)* | *Conv. (%)*[b] | *$M_{n,th}$ ($g.mol^{-1}$)*[c] | *$M_{n,exp}$ ($g.mol^{-1}$)* | *PDI* | *$d_p$ (nm)*[d] |
|---|---|---|---|---|---|---|---|---|
| 1 | 3.52 | 5 300 | 16 | 72 | 3 900 | 4 900 | 1.25 | 318 |
| 2a | 3.53 | 10 300 | 16 | 86 | 8 900 | 8 800 | 1.26 | 293 |
| 2b | No iodine | n.a. | 5 | 93 | n.a. | 126 500 | 6.15 | 267 |
| 3 | 3.42 | 19 800 | 16 | 80 | 15 900 | 17 000 | 1.37 | 324 |

[a]Polymerization of methyl methacrylate by reverse iodine transfer polymerization in miniemulsion at *T*=64°C in the presence of Perkadox 16S as initiator and hydrogen peroxide as oxidant; [b]Conversion determined by gravimetry; [c]$M_{n,th}$ = (mass of monomer)×(monomer conversion)/($2n_{I2}$) + $M_{AI}$ in which $M_{AI}$ = 282 $g.mol^{-1}$; [d] $d_p$ : particle diameter; n.a.: non applicable.

When comparing the RITP experiment (Table 1, run 2a) with the corresponding reference experiment without iodine but with the same amount of initiator (Table 1, run 2b), one can observe that the RITP experiment leads to a much lower molecular weight and polydispersity index than the corresponding reference experiment (polystyrene equivalent). The slightly lower monomer conversion in the RITP experiments might be explained by the fact that in RITP a part of the initiator is used to synthesize the iodinated transfer agents *in situ*, thus leading to a lower amount of initiator present to initiate the polymerization than in the corresponding reference experiment.

Downloaded by UNIV OF DELAWARE MORRIS LIB on June 26, 2012 | http://pubs.acs.org
Publication Date: August 13, 2009 | doi: 10.1021/bk-2009-1024.ch005

Downloaded by UNIV OF DELAWARE MORRIS LIB on June 26, 2012 | http://pubs.acs.org
Publication Date: August 13, 2009 | doi: 10.1021/bk-2009-1024.ch005

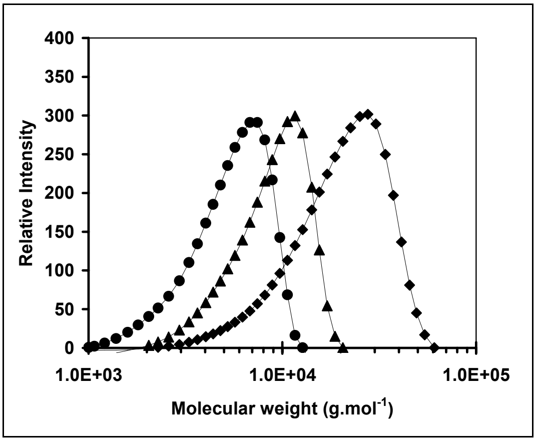

*Figure 3. Molecular weight distributions of poly(methyl methacrylate) samples prepared by reverse iodine transfer polymerization in miniemulsion at T = 64°C ([Perkadox 16S]/[$I_2$] ≈ 3.5, [Dodecyl sulfate sodium salt] = 2.6 g.L$^{-1}$). Targeted molecular weight: (●) 5 300 g.mol$^{-1}$, (▲) 10 300 g.mol$^{-1}$, (◆) 19 800 g.mol$^{-1}$.*

## Reverse Iodine Transfer Polymerization of Butyl Acrylate in Miniemulsion

Butyl acrylate was polymerized by RITP in miniemulsion using α,α'-azobisisobutyronitrile (AIBN) as initiator at 85°C. The reaction was conducted at a higher temperature to enable a fast decomposition of the AIBN initiator (thus avoiding a long inhibition period). At this temperature iodine hydrolysis (Scheme 2, Equilibrium 1) is much faster than at 64°C. Iodine hydrolysis forms iodide $I^-$ but also a small amount of iodate $IO_3^-$ (Scheme 2, Equilibrium 1) (which can not be regenerated to iodine $I_2$ by hydrogen peroxide). For this reason, the iodine $I_2$ regeneration has to be as slow as possible (preferably regenerating just enough iodine $I_2$ to trap the formed radicals). If more iodine $I_2$ is regenerated, it will be hydrolysed another time leading to a more important amount of iodate $IO_3^-$ (diminishing the effective amount of iodine $I_2$). Therefore, the continuous addition of hydrogen peroxide is only started near the end of the inhibition period (determined by the fading of the red colour of iodine $I_2$ in the reaction medium).

### Influence of the concentration of iodine

In order to show the controlled character of the polymerization, different molecular weights were targeted (Table 2, runs 1-3) by changing the concentration of iodine. Correct monomer conversions of about 80% with a relatively good correlation between experimental and theoretical molecular weights were obtained. Experimental molecular weights were slightly higher than the theoretical molecular weights presumably because of a small amount of iodate $IO_3^-$ formed during the process (impossible to regenerate iodine $I_2$) (strict comparison of the experimental/theoretical values must be considered with caution because all experimental molecular weights are polystyrene-equivalent). Moreover, the polydispersity indexes were in an acceptable range for butyl acrylate polymerization by RITP in dispersed aqueous medium.(*45*) The reference experiment (same amount of initiator but without iodine) (Table 2, run 2b) has a much higher and broader molecular weight distribution than the corresponding RITP experiment (Table 2, run 2a). Lastly, the whole molecular weight distribution is shifted towards higher molecular weights if the concentration of iodine is decreased (Figure 4).

**Table 2. Effect of iodine concentration**[a]

| *Run* | *[AIBN]/ $[I_2]$* | *$M_{n,targeted}$ $(g.mol^{-1})$* | *Time (h)* | *Conv. (%)*[b] | *$M_{n,th}$ $(g.mol^{-1})$*[c] | *$M_{n,exp}$ $(g.mol^{-1})$* | *PDI* | *$d_p$ (nm)*[d] |
|---|---|---|---|---|---|---|---|---|
| 1 | 3.61 | 5 100 | 6 | 72 | 3 700 | 4 800 | 1.99 | 338 |
| 2a | 3.44 | 10 100 | 16 | 85 | 8 600 | 9 300 | 2.11 | 336 |
| 2b | No iodine | n.a. | 6 | 92 | n.a. | 513 700 | 3.01 | 236 |
| 3 | 3.64 | 20 200 | 16 | 81 | 16 400 | 21 600 | 2.28 | 359 |

[a]Polymerization of butyl acrylate by reverse iodine transfer polymerization in miniemulsion at *T*=85°C in the presence of α,α'-azobisisobutyronitrile as initiator and hydrogen peroxide as initiator; [b]Conversion determined by gravimetry; [c]Mn,th = (mass of monomer)×(monomer conversion)/($2n_{I2}$) + $M_{AI}$ in which $M_{AI}$ = 195 g.mol$^{-1}$; [d] $d_p$ : particle diameter; n.a.: non applicable.

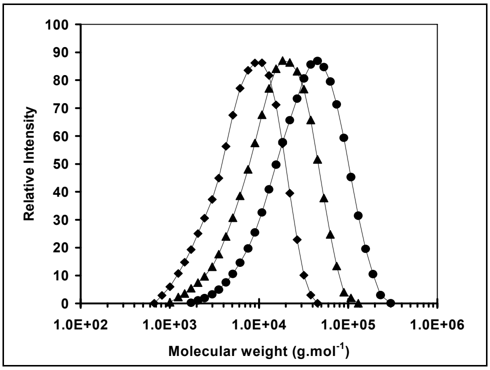

*Figure 4. Molecular weight distributions of poly(butyl acrylate) samples prepared by reverse iodine transfer polymerization in miniemulsion at T=85°C ($[AIBN]/[I_2]$ ≈ 3.5, [SDS] = 2.6 g.L$^{-1}$). Targeted molecular weight: (◆) 5 100 g.mol$^{-1}$, (▲) 10 100 g.mol$^{-1}$, (●) 20 200 g.mol$^{-1}$.*

Downloaded by UNIV OF DELAWARE MORRIS LIB on June 26, 2012 | http://pubs.acs.org
Publication Date: August 13, 2009 | doi: 10.1021/bk-2009-1024.ch005

Downloaded by UNIV OF DELAWARE MORRIS LIB on June 26, 2012 | http://pubs.acs.org
Publication Date: August 13, 2009 | doi: 10.1021/bk-2009-1024.ch005

## Block copolymerization

In order to show the living character of the final poly(butyl acrylate) latex, a block copolymer was synthesized. A poly(butyl acrylate) latex was further used as a seed in seeded emulsion polymerization of styrene. The seed latex (Table 3, run 1) had a high monomer conversion of 85%. The resulting copolymer latex (Table 3, run 2) has an experimental molecular weight of 19 400 g.mol$^{-1}$ while the theoretical molecular weight (Equation 2) at 60% conversion was 20 100 g.mol$^{-1}$. The polydispersity index decreases from 2.11 to 1.77. This is consistent with the formation of a block copolymer.

$$M_{n,th} = M_{n,first\ block} + (mass\ of\ monomers) \times conversion/(moles\ of\ first\ block) \quad \text{Eq.2}$$

**Table 3. Block copolymerization**[a]

| *Run* | *Type* | *Time (h)* | *Conv. (%)* | $M_{n,th,}$ *(g.mol$^{-1}$)* | $M_{n,SEC}$ *(g.mol$^{-1}$)* | *PDI* | $d_p$ *(nm)* |
|---|---|---|---|---|---|---|---|
| 1 | Seed PBuA latex | 16 | 85 | 8 600 | 9 300 | 2.11 | 336 |
| 2 | Block copolymer latex | 20 | 60 | 20 100 | 19 400 | 1.77 | 434 |

[a] Block copolymerization of the poly(butyl acrylate) latex in seeded emulsion polymerization at 80°C: seed PBuA-I latex (40.7 g, $M_n$ = 9 300 g.mol$^{-1}$, 0.315 mmol), α,α'-azobisisobutyronitrile (20 mg, 0.122 mmol), styrene (5.14 g, 49.4 mmol).

The number of polymer particles remains constant during the copolymerization step ($4.25\times10^{12}$ to $4.38\times10^{12}$ particles/cm$^3$). This indicates that neither renucleation nor particle coagulation has occurred during this second step. Figure 5 shows that the whole molecular weight distribution is shifted towards higher molecular weights after the copolymerization. Moreover, the refractive index and UV signals superpose nicely. This proves that all polymer chains contain styrene units and that a block copolymer was successfully synthesized.

# Conclusion

The implementation of controlled radical polymerization in dispersed aqueous media has revealed a lot of problems. Herein the implementation of reverse iodine transfer polymerization (RITP) of methyl methacrylate and butyl acrylate in aqueous miniemulsion is reported. The hydrolytic disproportionation of iodine responsible for an upward deviation of the molecular weights was successfully counterbalanced by continuously adding an aqueous solution of hydrogen peroxide to regenerate the hydrolyzed iodine, leading to a good control of the molecular weights. The controlled character of the polymerization was proved by targeting different molecular weights and the living character of the PBuA latex was demonstrated by synthesizing a block copolymer. This shows that RITP is a very robust method which allows the successful synthesis of block copolymer latexes in miniemulsion polymerization.

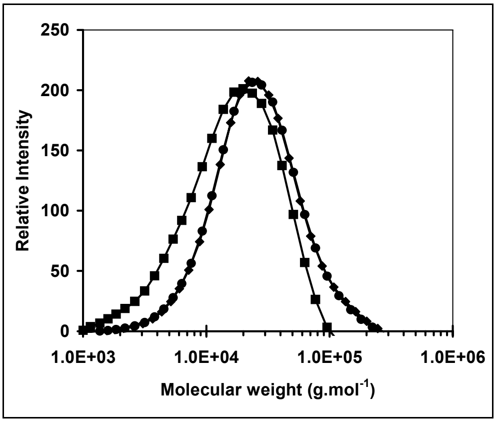

*Figure 5. Overlay of the SEC chromatograms of the seed ([BuA]/[AIBN]/[$I_2$] = 155/3.44/1 ($M_{n,targeted}$ = 10 100 g.mol$^{-1}$)) (■) and the final copolymer latex (prepared by seeded emulsion polymerization of styrene) with refractive index detector (◆) and UV detector (•).*

## References

1. Lacroix-Desmazes, P.; Ameduri, B.; Boutevin, B. *Collect. Czech. Chem. Commun.* **2002**, *67*, 1383-1415.
2. Braunecker, W. A.; Matyjaszewski, K. *Prog. Polym. Sci.* **2007**, *32*, 93-146.
3. Hawker, C. J.; Bosman, A. W.; Harth, E. *Chem. Rev.* **2001**, *101*, 3661-3688.
4. Matyjaszewski, K.; Xia, J. *Chem. Rev.* **2001**, *101*, 2921-2990.
5. David, G.; Boyer, C.; Tonnar, J.; Ameduri, B.; Lacroix-Desmazes, P.; Boutevin, B. *Chem. Rev.* **2006**, *106*, 3936-3962.
6. Moad, G.; Rizzardo, E.; Thang, S. H. *Aust. J. Chem.* **2006**, *59*, 669-692.
7. Save, M.; Guillaneuf, Y.; Gilbert, R. G. *Aust. J. Chem.* **2006**, *59*, 693-711.
8. Cunningham, M. F. *Prog. Polym. Sci.* **2008**, *33*, 365-398.
9. Ferguson, C. J.; Hughes, R. J.; Nguyen, D.; Pham, B. T. T.; Gilbert, R. G.; Serelis, A. K.; Such, C. H.; Hawkett, B. S. *Macromolecules* **2005**, *38*, 2191-2204.
10. Stoffelbach, F.; Tibiletti, L.; Rieger, J.; Charleux, B. *Macromolecules* **2008**, *41*, 7850-7856.
11. Rieger, J.; Stoffelbach, F.; Bui, C.; Alaimo, D.; Jerome, C.; Charleux, B. *Macromolecules* **2008**, *41*, 4065-4068.
12. Asua, J. M. *Prog. Polym. Sci.* **2002**, *27*, 1283-1346.
13. de Brouwer, H.; Tsavalas, J. G.; Schork, F. J.; Monteiro, M. J. *Macromolecules* **2000**, *33*, 9239-9246.

Downloaded by UNIV OF DELAWARE MORRIS LIB on June 26, 2012 | http://pubs.acs.org
Publication Date: August 13, 2009 | doi: 10.1021/bk-2009-1024.ch005

14. Tsavalas, J. G.; Schork, F. J.; de Brouwer, H.; Monteiro, M. J. *Macromolecules* **2001**, *34*, 3938-3946.
15. Lansalot, M.; Davis, T. P.; Heuts, J. P. A. *Macromolecules* **2002**, *35*, 7582-7591.
16. Luo, Y.; Tsavalas, J.; Schork, F. J. *Macromolecules* **2001**, *34*, 5501-5507.
17. Yang, L.; Luo, Y.; Li, B. *Polymer* **2006**, *47*, 751-762.
18. Huang, X.; Sudol, E. D.; Dimonie, V. L.; Anderson, C. D.; El-Aasser, M. S. *Macromolecules* **2006**, *39*, 6944-6950.
19. Urbani, C. N.; Nguyen, H. N.; Monteiro, M. J. *Aust. J. Chem.* **2006**, *59*, 728-732.
20. Pham, B. T. T.; Nguyen, D.; Ferguson, C. J.; Hawkett, B. S.; Serelis, A. K.; Such, C. H. *Macromolecules* **2003**, *36*, 8907-8909.
21. Manguian, M.; Save, M.; Chassenieux, C.; Charleux, B. *Colloid Polym. Sci.* **2005**, *284*, 142-150.
22. Lefay, C.; Save, M.; Charleux, B.; Magnet, S. *Aust. J. Chem.* **2006**, *59*, 544-548.
23. Lutz, J.-F.; Lacroix-Desmazes, P.; Boutevin, B. *Macromol. Rapid Commun.* **2001**, *22*, 189-193.
24. Georges, M. K.; Lukkarila, J. L.; Szkurhan, A. R. *Macromolecules* **2004**, *37*, 1297-1303.
25. Cunningham, M. F.; Ng, D. C. T.; Milton, S. G.; Keoshkerian, B. *J. Polym. Sci., Part A: Polym. Chem.* **2005**, *44*, 232-242.
26. Cunningham, M.; Lin, M.; Buragina, C.; Milton, S.; Ng, D.; Hsu, C. C.; Keoshkerian, B. *Polymer* **2005**, *46*, 1025-1032.
27. Farcet, C.; Belleney, J.; Charleux, B.; Pirri, R. *Macromolecules* **2002**, *35*, 4912-4918.
28. Oh, J. K.; Min, K.; Matyjaszewski, K. *Macromolecules* **2006**, *39*, 3161-3167.
29. Tang, H.; Radosz, M.; Shen, Y. *Macromol. Rapid Commun.* **2006**, *27*, 1127-1131.
30. Min, K.; Oh, J. K.; Matyjaszewski, K. *J. Polym. Sci., Part A: Polym. Chem.* **2007**, *45*, 1413-1423.
31. Oh, J. K.; Perineau, F.; Matyjaszewski, K. *Macromolecules* **2006**, *39*, 8003-8010.
32. Li, W.; Min, K.; Matyjaszewski, K.; Stoffelbach, F.; Charleux, B. *Macromolecules* **2008**, *41*, 6387-6392.
33. Lansalot, M.; Farcet, C.; Charleux, B.; Vairon, J.-P.; Pirri, R. *Macromolecules* **1999**, *32*, 7354-7360.
34. Butte, A.; Storti, G.; Morbidelli, M. *Macromolecules* **2000**, *33*, 3485-3487.
35. Farcet, C.; Lansalot, M.; Pirri, R.; Vairon, J. P.; Charleux, B. *Macromol. Rapid Commun.* **2000**, *21*, 921-926.
36. Pouget, E.; Tonnar, J.; Eloy, C.; Lacroix-Desmazes, P.; Boutevin, B. *Macromolecules* **2006**, *39*, 6009-6016.
37. Lacroix-Desmazes, P.; Severac, R.; Otazaghine, B.; Boutevin, B. *Polym. Prepr. (Am. Chem. Soc., Div. Polym. Chem.)* **2003**, *44*, 683-684.
38. Lacroix-Desmazes, P.; Severac, R.; Boutevin, B. *Macromolecules* **2005**, *38*, 6299-6309.

Downloaded by UNIV OF DELAWARE MORRIS LIB on June 26, 2012 | http://pubs.acs.org
Publication Date: August 13, 2009 | doi: 10.1021/bk-2009-1024.ch005

39. Boyer, C.; Lacroix-Desmazes, P.; Robin, J.-J.; Boutevin, B. *Macromolecules* **2006**, *39*, 4044-4053.
40. Lacroix-Desmazes, P.; Severac, R.; Boutevin, B.; Bodard, V.; Kurowsky, V., WO 03097704, **2003**.
41. Boutevin, B.; Otazaghine, B.; Lacroix-Desmazes, P.; Dubreuil, M.; Bodart, V., Fr 2839725, **2003**.
42. Lacroix-Desmazes, P.; Severac, R.; Boutevin, B.; Bodart, V.; Kurowski, V., WO 2004094356, **2004**.
43. Lacroix-Desmazes, P.; Tonnar, J., WO 2008003729, **2008**.
44. Fringant, C.; Vanderveken, Y.; Lacroix-Desmazes, P.; Tonnar, J., WO 2008003728, **2008**.
45. Tonnar, J.; Lacroix-Desmazes, P.; Boutevin, B. *ACS Symp. Ser.* **2006**, *944 Chapter 41*, 604.
46. Nagy, K.; Koertvelyesi, T.; Nagypal, I. *J. Solution Chem.* **2003**, *32*, 385-393.
47. Kolthoff, I. M. In *Treatise Anal. Chem. (I. M. Kolthoff and Philip J. Elving, editors. Interscience Publishers)*: New York, 1959; Vol. 1, pp 405-420.
48. Brownstein, S.; Stillman, A. E. *J. Phys. Chem.* **1959**, *63*, 2061-2062.
49. Tonnar, J.; Lacroix-Desmazes, P.; Boutevin, B. *Macromol. Rapid Commun.* **2006**, *27*, 1733-1738.
50. Tonnar, J.; Lacroix-Desmazes, P.; Boutevin, B. *Macromolecules* **2007**, *40*, 186-190.
51. Tonnar, J.; Lacroix-Desmazes, P.; Boutevin, B. *Macromolecules* **2007**, *40*, 6076-6081.
52. Tonnar, J.; Lacroix-Desmazes, P. *Angew. Chem.* **2008**, *47*, 1294-1297.
53. Tonnar, J.; Lacroix-Desmazes, P. *Soft Matter* **2008**, *4*, 1255-1260.
54. Foldiak, G.; Schuler, R. H. *J. Phys. Chem.* **1978**, *82*, 2756-2757.

Downloaded by UNIV OF DELAWARE MORRIS LIB on June 26, 2012 | http://pubs.acs.org
Publication Date: August 13, 2009 | doi: 10.1021/bk-2009-1024.ch005

Downloaded by CORNELL UNIV on June 26, 2012 | http://pubs.acs.org
Publication Date: August 13, 2009 | doi: 10.1021/bk-2009-1024.ch006

## Chapter 6

# Current Methods for *N*-Alkoxyamine Synthesis

**Anna C. Greene[1] and Robert B. Grubbs[1,*]**

**[1]Department of Chemistry, Dartmouth College, 6128 Burke Laboratories, Hanover, NH 03755**

The advancement of nitroxide-mediated radical polymerization (NMRP) depends on the development of routes to alkoxyamine initiators that are straightforward and cost-effective. This review examines current methods for initiator synthesis and also includes recent developments from this laboratory for the one-step synthesis of alkoxyamines which generally operate well under NMRP conditions.

In Controlled/Living Radical Polymerization: Progress in RAFT, DT, NMP & OMRP; Matyjaszewski, K.;
ACS Symposium Series; American Chemical Society: Washington, DC, 2009.

# Introduction

Free radical polymerization has been transformed by the advent of controlled methods, such as nitroxide-mediated radical polymerization (NMRP)*(1)*, atom transfer radical polymerization (ATRP)*(2)*, and reversible addition fragmentation transfer (RAFT)*(3)*. These methods rely on a dynamic equilibrium between propagating and dormant polymer chains, and in turn, have allowed the synthesis of well-defined materials with a variety of architectures.

NMRP has proven to be a successful protocol for synthesizing polymers with well-defined molecular weights, narrow molecular weight distributions, and living chain ends. It relies on a reversible equilibrium between propagating and dormant states by which nitroxide radicals trap the propagating radical to form the dormant species. NMRP is governed by the persistent radical effect which allows growing radicals to predominantly cross-couple with the nitroxide instead of terminating with themselves *(4)*. This method has gained considerable attention for its facile implementation given that only monomer and initiator are needed to conduct polymerization. However, advancement of NMRP has been hampered due to difficult initiator syntheses and limitations on polymerizable monomers especially classes of methacrylates. These issues may be addressed by the development of new initiators that can be prepared by straightforward synthetic methods and screened for their efficacy.

Alkoxyamines are the typical class of initiator used for NMRP and have also been recently used in radical crossover reactions for the synthesis of dynamic, covalent polymers *(5, 6)*. These compounds are O-alkylated nitroxide derivatives and are preferred over bimolecular initiating systems (e.g. TEMPO and benzoyl peroxide (BPO)) because of the known 1:1 stoichiometry of initiating to mediating (nitroxide) radical found in the unimolecular (e.g. alkoxyamine) system *(7)*. They possess a labile C-O bond which homolyzes at higher temperatures (generally >120 °C) to release the initiating radical and mediating nitroxide radical.

While there are numerous approaches to alkoxyamine synthesis, the most ubiquitous approach involves the generation of carbon-centered radicals followed by coupling with a nitroxide *(8)*. Methods to generate C-centered radicals include catalytic epoxidation, alkyl halide abstraction, enolate oxidation, and hydrocarbon oxidation, amongst others. This review discusses routes to alkoxyamine synthesis and also highlights the contribution of several laboratories, including our own, to this area through methods involving the double addition of carbon-centered free radicals to the N=O bond of a nitrosoalkane. Though most of the review focuses on routes involving TEMPO as the nitroxide trap, it should be noted that these methods can be extended for use with α-hydrido nitroxides as well.

Downloaded by CORNELL UNIV on June 26, 2012 | http://pubs.acs.org
Publication Date: August 13, 2009 | doi: 10.1021/bk-2009-1024.ch006

# Generation of C-Centered Radicals with Nitroxide *Trapping*

## Mn(III) Based Epoxidation

Manganese(III) epoxidation catalysts are commonly used in the synthesis of alkoxyamines because the reactions are run under mild conditions and a high yield of product is typically obtained. The generally accepted mechanism involves the attack of an alkene moiety of a styrenic compound on the manganese-oxo center to generate a benzylic free radical intermediate which is subsequently trapped by the nitroxide *(9, 10)*. Reduction of this complex with $NaBH_4$ results in the desired alkoxyamine (Scheme 1). Dao et al. introduced and utilized this procedure to produce functionalized initiators containing chloromethyl, alcohol, ester, methoxy, alkene, and other functionality in moderate to high yields *(10)*. These initiators were capable of effecting controlled polymerization of styrene with > 90% retention of the functionalized chain end.

Downloaded by CORNELL UNIV on June 26, 2012 | http://pubs.acs.org
Publication Date: August 13, 2009 | doi: 10.1021/bk-2009-1024.ch006

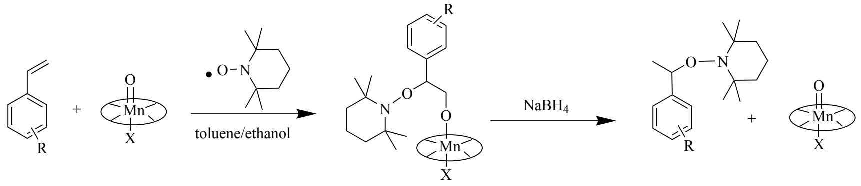

*Scheme 1. Alkoxyamine synthesis with manganese based catalyst.*

This protocol was revised by Bothe and Schmidt-Naake who noted the cost of Jacobsen's catalyst employed originally by Dao et al *(10, 11)*. They prepared a simplified version of Jacobsen's catalyst denoted as Mn(salen)Cl which was synthesized in high yield (89%) by a simple protocol and at low cost *(11)*. This catalyst worked well at synthesizing initiators in moderate to high yield bearing no functionality or functional groups such as chloromethyl and alcohol and additionally bis-nitroxide adducts of a divinyl compound 1,2-bis(4-vinylphenyl)ethane, BVPE. These alkoxyamines were successfully utilized for the NMRP of styrene and *n*-butyl acrylate.

$Mn(OAc)_3$ has also been employed in the synthesis of alkoxyamines. It is commercially available and has a low cost, but must be used in stoichiometric excess to achieve high yields of the desired initiators (e.g. 5 fold excess of catalyst compared to TEMPO for the synthesis of the 1-phenylethoxy derivative in 82% yield) *(12)*. A 5 fold excess of styrene was additionally necessary for the reaction to proceed in high yield. Thiessen and Wolff also utilized $Mn(OAc)_3$ with ultrasound as a method of homogenizing the reaction mixture *(13)*. They employed excesses of vinyl compound (1.1-5.0 equivalents relative to TEMPO) and 5-10 equivalents of manganese compound to achieve high yield. Neither of these methods using $Mn(OAc)_3$ can be considered catalytic with regard to manganese complex due to the large excess necessary for high yield of alkoxyamine. This is in contrast to the methods by Dao et al. or Bothe et al. where only stoichiometric reagents are necessary, and the manganese complex is used in catalytic amounts (typically 0.15 equivalents).

## Radicals Derived from Organic Halides

Another common method of carbon-based radical formation is the atom-transfer radical addition (ATRA) approach utilized by Matyjaszewski et al. (Scheme 2; Route 1) *(14)*. Cu(I) induced transfer of a halogen from an alkyl or benzylic halide produces the necessary radical which is then coupled with a nitroxide. Matyjaszewski et al. were able to synthesize alkoxyamines bearing initiating fragments based on styrene, methacrylates, acrylates, and acrylonitrile coupled with TEMPO in high yield. The structure of the initiating fragment proved important since benzyl and methyl acrylate fragments resulted in polystyrene with broad molecular weight distributions ($M_w/M_n$ = 2.45-2.85), while the other initiating moieties (ethylbenzene, ethyl methacrylate, ethyl cyanide) produced polystyrene with narrow molecular weight distributions ($M_w/M_n < 1.3$).

Another approach which utilizes alkyl halides was developed by Braslau et al. whereby an alkyl or benzyl bromide is displaced by neat hydrazine followed by creation of the carbon radical with lead dioxide and immediate trapping by TEMPO at low temperatures (-78 °C) (Scheme 2; Route 2) *(15)*. The coupling of TEMPO with (1-bromoethyl)benzene yielded the corresponding alkoxyamine in 78% yield. Braslau et al. also reported an additional method of alkoxyamine formation from (1-bromoethyl)benzene. The benzyl halide and cyclopentadienyliron dicarbonyl dimer were photolyzed to yield an intermediate benzylic organoiron species followed by additional irradiation to release the free radical which could be trapped with TEMPO (Scheme 2; Route 3) *(15)*. This method produced the initiator in good yield, although purification of the product was difficult because of iron side products.

An additional method from Braslau et al. involves the use of a thermal initiator, *tert*-butyl hyponitrite, along with tris(trimethyl)silane, an alkyl halide, and a nitroxide (Scheme 2; Route 4) *(16)*. The thermal initiator undergoes homolytic bond cleavage to release two equivalents of *tert*-butoxy radical which then generate silyl radicals after hydrogen abstraction from tris(trimethyl)silane. The silyl radical abstracts the halogen from the alkyl halide to produce the desired carbon-based radical which can then be coupled with a nitroxide. This method yielded initiators in good yield with alkyl and functional group incorporation *(16)*.

Cobalt-mediated radical generation with vitamin $B_{12}$ can also be used to generate carbon-centered radicals and affords the 1-phenylethoxy TEMPO derivative in 80% yield *(13)*. Samarium(II) iodide can be used similarly in catalytic fashion to yield the 1-phenylethoxy TEMPO derivative in 98% yield *(13)*.

Downloaded by CORNELL UNIV on June 26, 2012 | http://pubs.acs.org
Publication Date: August 13, 2009 | doi: 10.1021/bk-2009-1024.ch006

Downloaded by CORNELL UNIV on June 26, 2012 | http://pubs.acs.org
Publication Date: August 13, 2009 | doi: 10.1021/bk-2009-1024.ch006

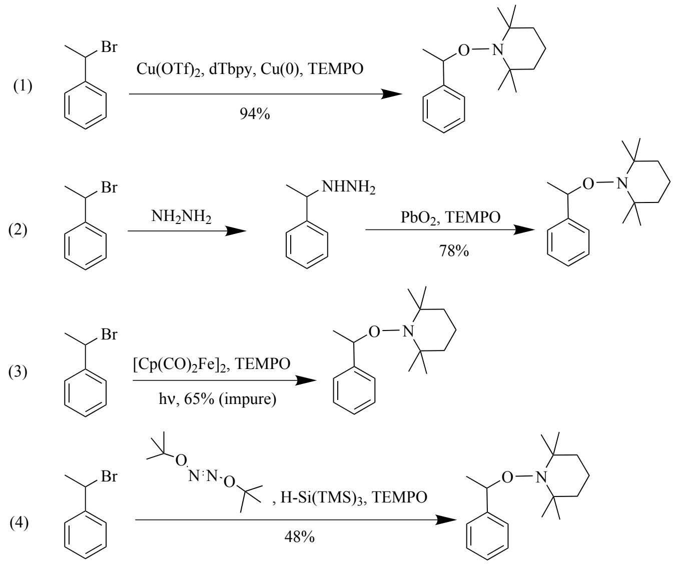

*Scheme 2. Benzylic halide abstraction for alkoxyamine synthesis.*

## Enolate Oxidation

Enolate oxidation is another pathway to carbon-based radicals, though it is limited to compounds which contain enolizable ketones and requires that stringent reaction procedures (e.g. low temperatures and exclusion of water) be followed to ensure good yield of product.

Braslau et al. generated carbanions of tert-butyl propionate and methyl isobutyrate with LDA followed by lithium enolate oxidation with Cu(II)$Cl_2$ in the presence of TEMPO (Scheme 3; Route 1) *(15)*. The initiators were isolated in 52% and 46% yield respectively.

Jahn utilized SET oxidation with ferrocenium hexafluorophosphate of ester enolates to generate radicals which were later trapped with TEMPO (Scheme 3; Route 2) *(17)*. For instance, the ethyl phenylacetate radical was trapped with TEMPO and isolated in 94% yield. Interestingly, this alkoxyamine was chemoselectively reduced with $LiAlH_4$ in 84% yield which provides an initiator with pendant alcohol functionality. This alcohol functional initiator was initially synthesized by Hawker and Hedrick and shown to be an efficient initiator for the polymerization of styrene, but was synthesized in lower overall yield than the method presented by Jahn *(18, 19)*.

Ahn and Kim employed (diacetoxyiodo)benzene as a lithium enolate oxidant (Scheme 3; Route 3) *(20)*. The TEMPO adduct of ethyl phenylacetate was synthesized in 97% yield and was found to effect controlled polymerization of styrene. The oxoammonium salt of TEMPO was also found to be a facile, metal-free method of enolate oxidation though the polymerization of styrene with the TEMPO adduct of diethyl malonate exhibited uncontrolled behavior (Scheme 3; Route 4) *(21)*.

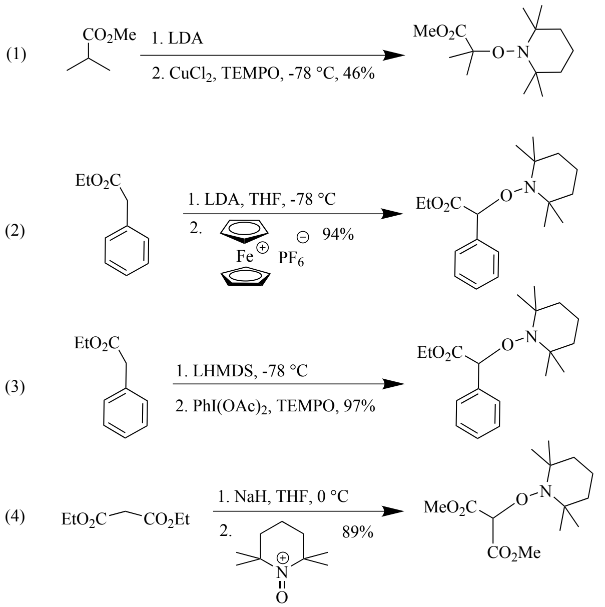

*Scheme 3. Generation of carbon-centered radicals via enolate oxidation and trapping with nitroxide.*

Downloaded by CORNELL UNIV on June 26, 2012 | http://pubs.acs.org
Publication Date: August 13, 2009 | doi: 10.1021/bk-2009-1024.ch006

## Radical Abstraction from Hydrocarbons

Radical abstraction from hydrocarbons is another technique for synthesizing alkoxyamines though the radical initiators employed can be dangerous and require high temperatures or catalysts to activate them. Large excesses of hydrocarbon are often necessary for high yield.

Following a method by Priddy and Howell, Hawker et al. developed TEMPO based alkoxyamines from alkylbenzenes after hydrogen abstraction with di-*tert*-butyl peroxide (Scheme 4; Route 1) *(7, 22)*. High temperatures were used to facilitate the decomposition of radical initiator (125 °C) which is problematic due to the labile C-O bond found in these initiators and allows for thermal decomposition of product. The initiators were retrieved in low yields (27-34%), and the reaction failed with certain ethylbenzene derivatives which was attributed to thermal decomposition of the initiators.

Connolly et al. generated C-centered radicals via irradiation of a radical precursor, di-*tert*-butyl peroxide, which abstracts a benzylic proton from toluene, ethylbenzene, propylbenzene, or cumene, and the resulting radical is then trapped with TEMPO (Scheme 4; Route 2) *(23)*. The photoinduced homolytic cleavage of the C-Br bond of phenacyl bromides was also employed to form the corresponding TEMPO adducts *(23)*. This route has the advantage of being performed at room temperature so that thermal degradation of the product is negligible.

Miura et al. employed di-*tert*-butylperoxyoxalate with mild heating at 35 °C to generate alkoxyamines from ethylbenzene derivatives and various nitroxides

(Scheme 4; Route 3) *(24)*. They also synthesized initiators bearing functionality (4-bromo, 4-ethoxycarbonyl, and 4-methoxy) *(25)*. However, they had to employ an 8 equivalent excess of ethylbenzene derivative to effect a high yield of the initiators which can be expensive and higher boiling point ethylbenzenes can be difficult to remove at room temperature under reduced pressure. Di-*tert*-butylperoxyoxalate can also explode upon pounding or scraping which makes this an undesirable radical initiator *(26)*.

Sugimoto et al. utilized *tert*-butyl hydroperoxide (tert-BuOOH) and a transition metal catalyst ($Co(OAc)_2{\bullet}4H_2O$) to abstract hydrogen from ethylbenzene derivatives which were then trapped with TEMPO at room temperature (Scheme 4; Route 4) *(27)*. The use of *tert*-BuOOH is a pragmatic choice since it is commercially available and shelf-stable.

Kirner et al. reported the catalytic oxidation of hydrocarbons by t-BuOOH and catalytic onium iodide or t-BuOOH and catalytic Cu(II) salt at 60 °C *(28)*. This method also requires large excesses of hydrocarbon (10-12 equivalents relative to TEMPO) to achieve high yield.

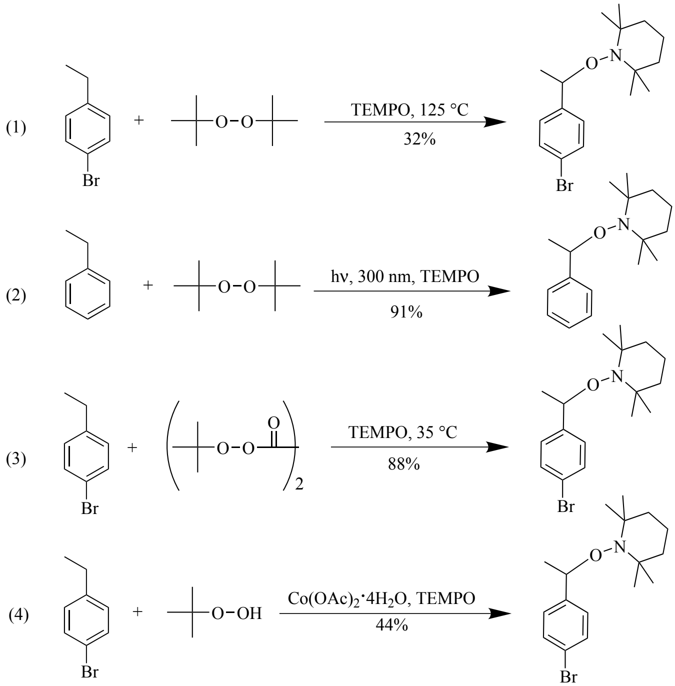

*Scheme 4. Hydrocarbon oxidation synthetic protocols.*

Downloaded by CORNELL UNIV on June 26, 2012 | http://pubs.acs.org
Publication Date: August 13, 2009 | doi: 10.1021/bk-2009-1024.ch006

## Additional Strategies

Other interesting strategies for carbon-based radical generation include the development of 1,3-dithiane based initiators. Herrera and Studer prepared a TEMPO based dithiane initiator from lithiation of 1,3-dithiane and oxidation using TEMPO, which acts as both an oxidant and a radical trap (Scheme 5; Route 1) *(29)*. The resulting alkoxyamine was isolated in 80% yield and was able to control the polymerization of styrene with good agreement between the theoretical and calculated molecular weight and a narrow molecular weight distribution ($M_w/M_n$ = 1.12). An interesting feature of this 1,3-dithiane functionalized polymer is that deprotonation by an alkyl lithium base should yield an anionic initiation site which indicates that this alkoxyamine can also serve dually as an anionic and free radical initiator.

Another facile route to carbon centered-radicals is via photodecomposition of an azo-initiator or dithiocarbamate (Scheme 5; Route 2) with subsequent coupling to SG1 reported by Guillaneuf et al *(30)*. The azo-initiator had to be used in large excess compared to the nitroxide whereas the dithiocarbamate was needed in only a stoichiometric amount which makes this method more industrially relevant. In both cases, the desired alkoxyamines were obtained in high yield.

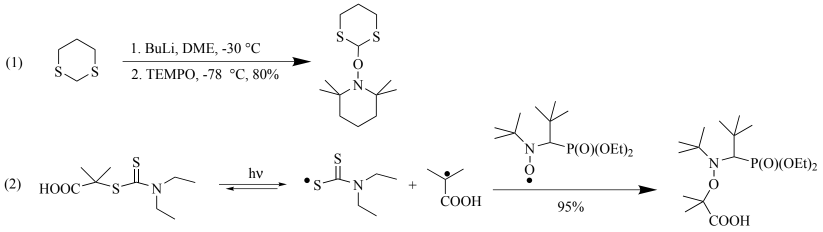

*Scheme 5. Dithiane based initiator synthesis and photodecomposition of dithiocarbamate for alkoxyamine synthesis.*

Moon and Kang utilized sodium or potassium metal to reduce nitroxides, TEMPO or TIPNO, to the corresponding anion *(31)*. The anion was subsequently used to displace the halogen from a benzylic bromide. This method produced the alkoxyamines in high yield due to the lack of radical-radical coupling reactions often found in other procedures. A similar procedure involved the reduction of TEMPO with sodium ascorbate followed by deprotonation with NaH *(32)*. The corresponding anion was used to displace a halide from a halogen containing compound to form the alkoxyamine. Catala et al. also reported halide displacement from (1-bromoethyl)benzene with the sodium salt of di-*tert*-butylnitroxide *(33)*.

Downloaded by CORNELL UNIV on June 26, 2012 | http://pubs.acs.org
Publication Date: August 13, 2009 | doi: 10.1021/bk-2009-1024.ch006

# Trapping of C-Based Radicals with Nitroso Compounds or Nitrones

## Addition of Radicals to Nitroso-*tert*-Octane

One of the most straightforward ways of alkoxyamine synthesis involves the direct addition of two equivalents of radicals to a nitrone or nitroso compound *(34, 35)*. Zink et al. reported the synthesis of an initiator based on the addition of isobutyronitrile radicals derived from the thermal initiator azobisisobutyronitrile (AIBN) to a nitrone, 2,2,5-trimethyl-3,4-dihydro-2*H*-pyrrole-1-oxide, in 21% yield *(36)*. They also reported the addition of cyclohexanecarbonitrile radicals generated from 1,1'-azobis(cyclohexanecarbonitrile), ACCN, across the nitroso bond of nitroso-*tert*-octane to yield the corresponding alkoxyamine in 50% yield (Scheme 6; Route 1). They demonstrated the effective use of both initiators for the polymerization of styrene with polydispersities ranging from 1.15-1.35. The initiators failed to control *n*-butyl acrylate polymerization: large deviations from theoretical molecular weights and high polydispersity indices ($M_w/M_n$ = ~ 2.0-3.0) were observed. Studer et al. followed with a similar report involving the addition of radicals derived from the oxidation of an alkylhydrazine with $PbO_2$ to nitroso-*tert*-octane (Scheme 6; Route 2) *(37)*. This initiator was isolated in 70% yield and was shown to be effective for the polymerization of styrene and *n*-butyl acrylate.

Downloaded by CORNELL UNIV on June 26, 2012 | http://pubs.acs.org
Publication Date: August 13, 2009 | doi: 10.1021/bk-2009-1024.ch006

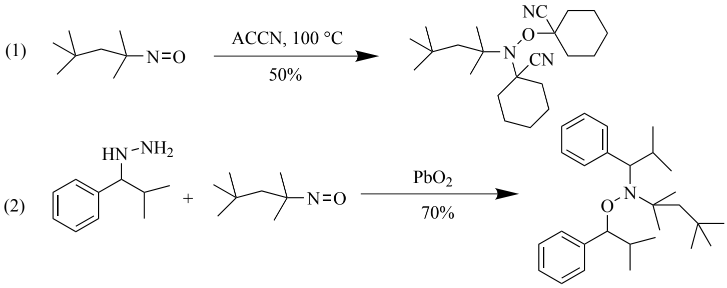

*Scheme 6. Addition of carbon-centered radicals to nitroso-tert-octane.*

## Addition of Radicals to 2-methyl-2-nitrosopropane

Our laboratory has developed a very similar approach using nitroso compounds as radical trapping agents. Our initial report detailed the synthesis of an alkoxyamine from commercially available materials and the use of copper species to promote alkoxyamine formation instead of the use of lead dioxide *(14)*. Two equivalents of 1-phenylethyl radical were added across the nitroso bond of 2-methyl-2-nitrosopropane to form 2,2-dimethyl-3-(1-phenylethoxy)-4-phenyl-3-azapentane (Scheme 7; Route 1) *(38)*. This nitroso compound is commercially available or can be easily synthesized *(39)*. The alkoxyamine was isolated in 68% yield after chromatography and was used to successfully control the polymerization of styrene and isoprene. For example, polymerization of styrene with this initiator for 19 h led to polystyrene with a molecular weight similar to that calculated based upon conversion ($M_{n,SEC} = 17.1$ kg mol$^{-1}$; $M_{n,calc} = 19.1$ kg mol$^{-1}$) with a narrow molecular weight distribution ($M_w/M_n = 1.14$). Polymerization of 200 equivalents of isoprene for 16 hours produced polyisoprene with a narrow molecular weight distribution ($M_w/M_n < 1.3$) and microstructure typical to free radical polymerization.

This initiator is also capable of controlling the polymerization of *n*-butyl acrylate with a preheating step *(40)*. Because of the high rate of propagation for acrylates, a small excess of free nitroxide (0.05%) relative to the theoretical number of chains is generally added to acrylate polymerizations for control to be achieved *(41)*. For cases where the nitroxide is not shelf stable, an alternative strategy has been developed which involves the heating of neat alkoxyamine to generate a low concentration of free nitroxide per the persistent radical effect *(4)*. The preheating protocol proved successful at controlling the polymerization of *n*-butyl acrylate with this initiator. The most notable effect was on the molecular weight distributions of the polyacrylates with and without preheating. Direct polymerization of *n*-butyl acrylate resulted in polydisperse material ($M_w/M_n > 2$), whereas polymerization after a preheating step (30 minutes at 80 °C, 100 °C, or 125 °C) resulted in much greater control with relatively narrow molecular weight distributions ($M_w/M_n = 1.2$-$1.4$) *(40)*.

More recently, a related initiator has been synthesized from the addition of two equivalents of diphenylmethane radical to 2-methyl-2-nitrosopropane to form 2,2-dimethyl-3-(1,1-diphenylmethoxy)-4,4-diphenyl-3-azabutane (Scheme 7; Route 2). This alkoxyamine was used to control the polymerization of styrene. The theoretical molecular weights correlated well with those calculated by SEC and displayed narrow molecular weight distributions common to NMRP ($M_w/M_n < 1.3$).

Downloaded by CORNELL UNIV on June 26, 2012 | http://pubs.acs.org
Publication Date: August 13, 2009 | doi: 10.1021/bk-2009-1024.ch006

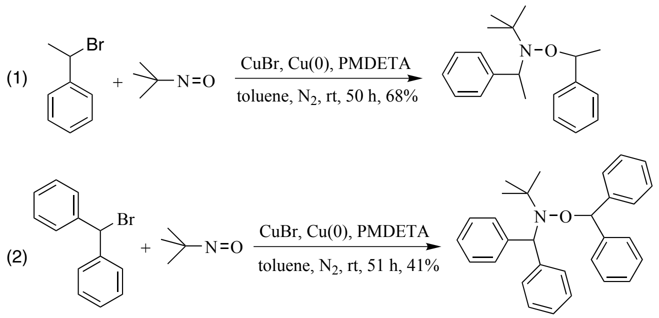

*Scheme 7. Two equivalents of benzylic radical react with 2-methyl-2-nitrosopropane to form the alkoxyamine.*

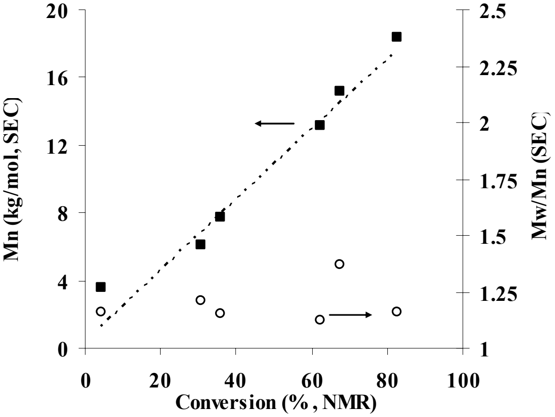

*Figure 1. Evolution of $M_n$ and $M_w/M_n$ versus conversion for [Styrene]/[Init] = 200:1. The dotted line represents the theoretical $M_n$ calculated from $^1H$ NMR.*

The initiator, 2,2-dimethyl-3-(1,1-diphenylmethoxy)-4,4-diphenyl-3-azabutane, was also able to control the polymerization of isoprene. For instance, heating 300 equivalents of isoprene with this initiator yielded molecular weight distributions in the range of 1.2-1.35 up to moderate conversions ($p$ = 65%). Polymerization of *n*-butyl acrylate without the addition of free nitroxide resulted in a linear increase in molecular weight versus conversion, but the molecular weight distributions remained relatively broad ($M_w/M_n$ = 1.4-1.5), indicating a loss of control.

## Conclusions

The advancement of nitroxide-mediated radical polymerization relies on the development of synthetic routes to alkoxyamines initiators which are straightforward, cost-effective, and versatile. The most common synthetic method involves the coupling of a nitroxide to a carbon-centered radical. There are many methods found in the literature to generate carbon-centered radicals which include enolate oxidation, halogen abstraction, and catalytic epoxidation, amongst others. While these general methods are straightforward if the nitroxide is commercially available and shelf-stable, multiple steps are added into the overall alkoxyamine synthesis if the nitroxide must be synthesized and/or does not store well.

An alternative way of synthesizing alkoxyamines in a straightforward fashion involves the double addition of radicals across the double bond of a nitroso compound (or to a nitrone). Depending on the materials used and protocol for generating carbon-centered radicals, this method can produce initiators in moderate to high yield in one step. We have synthesized alkoxyamines from the double addition of 1-phenylethyl or diphenylmethane radicals to 2-methyl-2-nitrosopropane and shown their ability to control the polymerizations of styrene and isoprene. Additional work in this laboratory has

Downloaded by CORNELL UNIV on June 26, 2012 | http://pubs.acs.org
Publication Date: August 13, 2009 | doi: 10.1021/bk-2009-1024.ch006

shown this synthetic approach to allow the synthesis of functional initiators from a range of commercially available nitroso compounds. The continued exploration of new methods for the preparation of alkoxyamines is crucial to the further development of NMRP.

## Acknowledgements

The authors would like to thank NSF(CAREER DMR-0239697) for partial funding of the work from our laboratory discussed above. We also acknowledge Elizabeth Jackson for her contribution to the research included here.

Downloaded by CORNELL UNIV on June 26, 2012 | http://pubs.acs.org
Publication Date: August 13, 2009 | doi: 10.1021/bk-2009-1024.ch006

## References

1. Hawker, C. J.; Bosman, A. W.; Harth, E. *Chem. Rev.* **2001,** *101,* 3661-3688.
2. Matyjaszewski, K.; Xia, J. *Chem. Rev.* **2001,** *101,* 2921-2990.
3. Perrier, S.; Takolpuckdee, P. *J. Polym. Sci. Part A: Polym. Chem.* **2005,** *43,* 5347-5393.
4. Fischer, H. *Chem. Rev.* **2001,** *101,* 3581-3610.
5. Otsuka, H.; Aotani, K.; Higaki, Y.; Takahara, A. *Chem. Commun.* **2002,** *2002,* 2838-2839.
6. Otsuka, H.; Aotani, K.; Higaki, Y.; Takahara, A. *J. Am. Chem. Soc.* **2003,** *125,* 4064-4065.
7. Hawker, C. J.; Barclay, G. G.; Orellana, A.; Dao, J.; Devonport, W. *Macromolecules.* **1996,** *29,* 5245-5254.
8. Nesvadba, P. *Chimia.* **2006,** *60,* 832-840.
9. Finney, N. S.; Pospisil, P. J.; Chang, S., et al. *Angew. Chem. Int. Ed. Engl.* **1997,** *36,* 1720-1723.
10. Dao, J.; Benoit, D.; Hawker, C. J. *J. Polym. Sci. Part A: Polym. Chem.* **1998,** *36,* 2161-2167.
11. Bothe, M.; Schmidt-Naake, G. *Macromol. Rapid Commun.* **2003,** *24,* 609-613.
12. Krause, T.; Habicher, W. D.; Messerschmidt, M.; Voit, B. I. *Des. Monomers Polym.* **2004,** *7,* 391-397.
13. Thiessen, W.; Wolff, T. *Des. Monomers Polym.* **2005,** *8,* 397-407.
14. Matyjaszewski, K.; Woodworth, B. E.; Zhang, X.; Gaynor, S. G.; Metzner, Z. *Macromolecules.* **1998,** *31,* 5955-5957.
15. Braslau, R.; Burrill, L. C.; Siano, M.; Naik, N.; Howden, R. K.; Mahal, L. K. *Macromolecules.* **1997,** *30,* 6445-6450.
16. Braslau, R.; Tsimelzon, A.; Gewandter, J. *Org. Lett.* **2004,** *6,* 2233-2236.
17. Jahn, U. *J. Org. Chem.* **1998,** *63,* 7130-7131.
18. Hawker, C. J. *J. Am. Chem. Soc.* **1994,** *116,* 11185-11186.
19. Hawker, C. J.; Hedrick, J. L. *Macromolecules.* **1995,** *28,* 2993-2995.
20. Ahn, K. H.; Kim, Y. *Synth. Commun.* **1999,** *29,* 4361-4366.
21. Schämann, M.; Schäfer, H. J. *Synlett.* **2004,** *1601,* 1603.
22. Li, I.; Howell, B. A.; Ellaboudy, A.; Kastl, P. E.; Priddy, D. B. *Polym. Prepr.* **1995,** *36,* 469.

23. Connolly, T. J.; Baldoví, M. V.; Mohtat, N.; Scaiano, J. C. *Tetrahedron Lett.* **1996,** *37,* 4919-4922.
24. Miura, Y.; Hirota, K.; Moto, H.; Yamada, B. *Macromolecules.* **1998,** *31,* 4659-4661.
25. Miura, Y.; Hirota, K.; Moto, H.; Yamada, B. *Macromolecules.* **1999,** *32,* 8356-8362.
26. Bartlett, P. D.; Benzing, E. P.; Pincock, R. E. *J. Am. Chem. Soc.* **1960,** *82,* 1762-1768.
27. Sugimoto, N.; Narumi, A.; Satoh, T.; Kaga, H.; Kakuchi, T. *Polym. Bull.* **2003,** *49,* 337-340.
28. Kirner, H. J.; Schwarzenbach, F.; van der Schaaf, P.A., et al. *Adv. Synth. Catal.* **2004,** *346,* 554-560.
29. Herrera, A. J.; Studer, A. *Synthesis.* **2005,** *9,* 1389-1396.
30. Guillaneuf, Y.; Couturier, J. L.; Gigmes, D.; Marque, S. R. A.; Tordo, P.; Bertin, D. *J. Org. Chem.* **2008,** *73,* 4728-4731.
31. Moon, B.; Kang, M. *Macromol. Res.* **2005,** *13,* 229-235.
32. Anderson, J. E.; Casarini, D.; Corrie, J. E. T.; Lunazzi, L. *J. Chem. Soc. Perkin Trans. 2.* **1993,** 1299-1304.
33. Catala, J. M.; Bubel, F.; Hammouch, S. O. *Macromolecules.* **1995,** *28,* 8441-8443.
34. Maschke, A.; Shapiro, B. S.; Lampe, F. W. *J. Am. Chem. Soc.* **1963,** *85,* 1876-1878.
35. Hoffmann, A. K.; Feldman, A. M.; Gelblum, E.; Hodgson, W. G. *J. Am. Chem. Soc.* **1964,** *86,* 639-646.
36. Zink, M.-O.; Kramer, A.; Nesvadba, P. *Macromolecules.* **2000,** *33,* 8106-8108.
37. Studer, A.; Harms, K.; Knoop, C.; Muller, C.; Schulte, T. *Macromolecules.* **2004,** *37,* 27-34.
38. Grubbs, R. B.; Wegrzyn, J. K.; Xia, Q. *Chem. Commun.* **2005,** 80-82.
39. Calder, A.; Forrester, A. R.; Hepburn, S. P. *Org. Syn.* **1972,** *52,* 77-82.
40. Xia, Q.; Grubbs, R. B. *J. Polym. Sci. Part A: Polym. Chem.* **2006,** *44,* 5128-5136.
41. Benoit, D.; Chaplinski, V.; Braslau, R.; Hawker, C. J. *J. Am. Chem. Soc.* **1999,** *121,* 3904-3920.

Downloaded by CORNELL UNIV on June 26, 2012 | http://pubs.acs.org
Publication Date: August 13, 2009 | doi: 10.1021/bk-2009-1024.ch006

## Chapter 7

# New Nitroxide Mediators for Controlled Synthesis of Polystyrene, Poly(meth)acrylates and Their Copolymers

**Dmitry F. Grishin, Elena V. Kolyakina, Marina V. Pavlovskaya, Mikhail A. Lazarev, Alexander A. Shchepalov**

**Research Institute of Chemistry Nizhny Novgorod State University,**
**23 Gagarin Av., Nizhny Novgorod, 603950, Russia**

Downloaded by STANFORD UNIV GREEN LIBR on June 26, 2012 | http://pubs.acs.org
Publication Date: August 13, 2009 | doi: 10.1021/bk-2009-1024.ch007

Two different approaches to the realization of SFRP in the presence of nitroxides, namely, the introduction of stable radicals of different structure from outside, or their *in situ* generation in a polymerization of vinyl and (meth)acrylic monomers have been analyzed. First it has been ascertained that nitroxide derivatives of imidazole and piperidine are efficient agents of living polymerization of styrene. The synthesis of polymers with low polydispersity indexes (1.2-1.4) and predicted molecular weight has been performed in a temperature range of 80-130°C. The most efficient approach for polymerization of vinyl monomers is *in-situ* generation of stable radicals from nitrones and nitroso compounds. This approach allows realization of the controlled macromolecular synthesis at relatively low temperatures (50-70°C) and utilization of a variety of monomers able to be polymerized via SFRP mechanism. Quantum-chemical modeling of the processes has been performed.

In Controlled/Living Radical Polymerization: Progress in RAFT, DT, NMP & OMRP; Matyjaszewski, K.;
ACS Symposium Series; American Chemical Society: Washington, DC, 2009.

# Introduction

Nowadays, the procedures and approaches to the controlled radical polymerization (CRP) are rapidly updated and improved. This is rather clearly represented over the past 10-15 years in a large number of original publications and reviews on this topic (*1-6*). A particular interest in this extremely significant field of the polymer synthesis is caused with an increasing demand for new materials and the improvement of properties of already available polymers. Among the known methods of CRP is the Stable Free-Radical Polymerization (SFRP), which employs stable radicals as mediators. Despite the apparent loss of leading positions, the SFRP holds actually since this method is the most accessible from the standpoint of technical realization (*5, 6*).

One of main pathways of SFRP is the application of sterically hindered nitroxides. The difficulty in practical application of this CRP direction is connected with a number of substantial drawbacks: a) low process rate; b) the realization of the chain-growth control mechanism only at high-temperature conditions; c) a limited usage of controlling additives relative to a monomer; and so on. In this connection, decrease of the polymerization temperature due to the addition of efficient initiating and controlling agents, the search for multipurpose regulators based on nitroxides, which are able to control effectively the polymerization of some types of monomers, are of obvious interest (*6-9*).

Downloaded by STANFORD UNIV GREEN LIBR on June 26, 2012 | http://pubs.acs.org
Publication Date: August 13, 2009 | doi: 10.1021/bk-2009-1024.ch007

# Experimental

Nitroxides such as 2,2,5,5-tetramethyl-4-phenyl-2,5-dihydroimidazole-1-oxyl (N1), 2,2-diethyl-4,5,5-trimethyl-2,5-dihydroimidazole-1-oxyl (N2), 2-methyl-2,3-diphenyl-1,4-diazospiro-[4,5]-deca-3-en-1-oxyl (N3), 2,2,5,5-tetramethyl-4-phenyl-2,5-dihydroimidazole-3-oxide-1-oxyl (N4), 1,2,2,4,5,5-hexamethyl-2,5-dihydroimidazole-3-oxide (N5), 2,2-dimethyl-5-phenyl-4-hydroimidazole-3-oxide (N6) have been synthesized according to the literature procedures (*10*). C-Phenyl-N-tert-butylnitrone (PBN), 2-methyl-2-nitrosopropane (MNP), nitrosodurene (ND) are commercially available (for example, Lancaster). Methyl methacrylate (MMA), styrene (St) and butyl acrylate (BA) have been washed with aqueous alkaline solution and water, dried over calcium chloride and then distilled prior to use. The purification of acrylonitrile (AN) and N-vinylpyrrolidone (VP) has been carried out by distillation. Azobisisobutyronitrile (AIBN), benzoyl peroxide (BPO) and solvents were purified by recrystallization and distillation, respectively.

Percentage of initiator and regulating additive was calculated regarding that total concentration of reaction mixture was 100%. In a standard procedure the reagents were placed in an ampoule, which was evacuated and then sealed off under vacuum. The polymerization was performed at the specified temperature (see Tables). After expiring of the fixed time the ampoule was cooled with liquid nitrogen and opened. The polymers were purified by repeated precipitation: the chloroform solution of a polymer was added step-wise into hexane or methanol.

Downloaded by STANFORD UNIV GREEN LIBR on June 26, 2012 | http://pubs.acs.org
Publication Date: August 13, 2009 | doi: 10.1021/bk-2009-1024.ch007

Block copolymerization was performed similarly to homopolymerization. After the reaction is completed the polymer mixture has been purified by precipitation method described above using isopropyl alcohol. The synthesized block-copolymers have been isolated from the polymer mixture by sequential selective extraction: polystyrene (PS) with cyclohexane, polymethyl methacrylate (PMMA) with acetonitrile, and poly-N-vinylpyrrolidone (PVP) with water.

The generation of the nitroxides from nitrones and nitroso compounds have been confirmed by ESR spectroscopy using Bruker ESR ER 200D-SRC spectrometer equipped with a high temperature controller ER 4111 VT. The molecular weights (MW) of the polymers were determined viscometrically and by size exclusion chromatography (SEC) by Knauer liquid chromatograph with Phenomenex phenogel mixed bed column Linear - 2 and calibrated by narrow PS standard kit with MW 2 900-2 570 000 Da. Eluent was chloroform with rate of 1 ml/min. The composition of copolymers has been studied by IR-spectroscopy using Infralum FT-801 spectrometer and UV-spectroscopy on a Perkin Elmer Lambda 25 spectrometer. The spectra have been recorded in UV-grade chloroform. Quantative calibration has been done using the solutions of homopolymers of defenite concentration. The $^1$H NMR spectra of block-copolymers have been recorded on Bruker DPX-200 in chloroform-$d_1$. Quantum-chemical calculations have been carried out using the program package Gaussian 98 (Revision A.3).

## Results and Discussion

In this study the controlled synthesis of PS and PMMA as well as synthesis of their copolymers with a series of vinyl monomers (BA, AN, VP) have been accomplished in two different approaches in the presence of a wide variety of nitroxides. Depending on the method of stable radical generation the SFRP techniques can be divided into two main directions: 1) an admixing of stable radicals into the polymerization system from outside (i.e. the use of stable radicals produced *ex situ*) and; 2) the generation of stable radicals directly in the polymerizing system (*in situ*). Both approaches have been realized and analyzed in the present work using various methods including quantum-chemical calculations.

### «Living» Radical Polymerization of Methyl Methacrylate and Styrene in the Presence of Nitroxides of Imidazole Type

The radical polymerization of St and MMA in the presence of a number of sterically hindered nitrogen-containing five-membered heterocyclic compounds N1 to N4 (Scheme 1) initiated by AIBN was studied in a wide temperature interval 50-130ºC. These nitroxides and temperature conditions have been chosen for the reason of comparison with those reported in the literature (*11*). It has been suggested that imidazole based nitroxides might be effective at temperature less than 90°C. But we have found that N1-N4 control effectively the polymerization process of St and molecular-weight characteristics of the synthesized polymers only at high temperatures (>100°C) similar to that of TEMPO derivatives. Although it was shown that in the presence of nitroxides N1 to N4 the process of recombination nitroxides with a growing macroradical becomes reversible even at 80ºC. The bulk polymerization of St in the presence of nitroxides N1 to N4 is accomplished at similar rates.

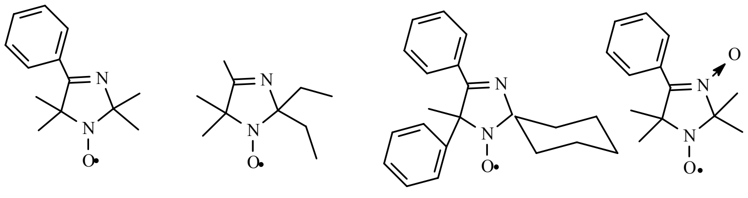

**N1** **N2** **N3** **N4**

*Scheme 1*

Molecular-weight distribution (MWD) curves of the polymers synthesized with N1-N4 are unimodal. At the same time, the MWD mode shifts towards high molecular weights with increasing of the conversion. The molecular-weight characteristics of the polymers are presented in Table I. The values of the polydispersity indexes (PDI) for polystyrene prepared at 120ºC do not exceed 1.3-1.5 all along the process. The dependence of the number-average MW on conversion in all cases is linear (Figure 1). The nitroxides structures do influence the molecular weight characteristics of polymers. The slope of linear plots $M_n$ *vs.* conversion for N1-N3 is similar in each case but different of that for N4. The later nitroxide contains nitrone and nitroxide groups simultaneously and it could provide for the formation of biradicals. This will be discussed in details below. The curves of $M_n$ *vs.* conversion for N1-N4 do not cross the origin because the difference in decomposition rates of AIBN and the generated alkoxyamines.

Downloaded by STANFORD UNIV GREEN LIBR on June 26, 2012 | http://pubs.acs.org
Publication Date: August 13, 2009 | doi: 10.1021/bk-2009-1024.ch007

Downloaded by STANFORD UNIV GREEN LIBR on June 26, 2012 | http://pubs.acs.org
Publication Date: August 13, 2009 | doi: 10.1021/bk-2009-1024.ch007

**Table I. Molecular-Weight Parameters of Polystyrene Synthesized in the Presence of AIBN (1.0 mol. %) and Nitroxides N1-N4 (1.5 mol. %) at 120ºC**

| *Nitroxide* | *Time, h* | *Conversion, %* | $M_n \times 10^{-3}$ | $M_w/M_n$ |
|---|---|---|---|---|
| - | 2 | 69 | 5.8 | 8.3 |
| N1 | 6 | 10 | 2.2 | 1.4 |
| N1 | 45 | 75 | 3.9 | 1.3 |
| N1* | 50 | 99 | 6.7 | 1.4 |
| N2 | 1 | 8 | 1.3 | 1.4 |
| N2 | 31 | 71 | 4.5 | 1.4 |
| N2** | 20 | 64 | 7.4 | 1.2 |
| N3 | 14 | 22 | 3.0 | 1.2 |
| N3 | 53 | 75 | 4.7 | 1.2 |
| N3*** | 38 | 81 | 5.2 | 1.8 |
| N4 | 1 | 17 | 4.9 | 1.5 |
| N4 | 40 | 99 | 5.5 | 1.5 |

* post-polymer formed in the presence of N1 at initial conversion 50 %, PDI = 1.3 and MW = $3.8 \times 10^{-3}$,;

** post-polymer formed in the presence of N2 at initial conversion 51 %, PDI = 1.3 and MW = $4.2 \times 10^{-3}$,;

***post-polymer formed in the presence of N3 at initial conversion 73 %, PDI = 1.3 and MW = $4.8 \times 10^{-3}$,.

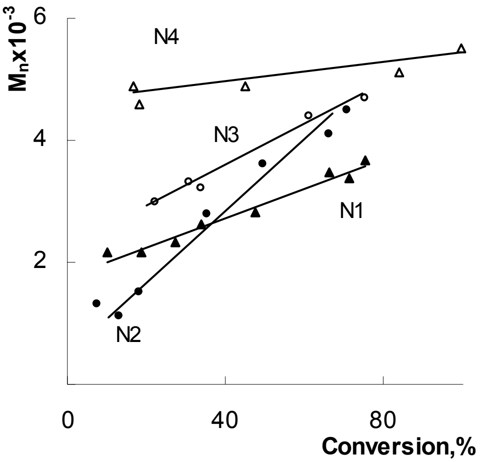

*Figure 1. Dependence of number - average molecular weight of PS vs. conversion; AIBN (1.0 mol. %), nitroxydes N1-N4 (1.5 mol. %). T = 120ºC.*

Therefore, the initial radicals formed from AIBN may add some monomers before transforming to dormant form as it takes place in the case of conventional controlled radical polymerization. After that, the molecular weight growth rate is less pronounced than in the cases described before.

In order to confirm the realization of “pseudo-living” polymerization in the presence of these nitroxides the post-polymerization of St has been studied with participation of macroinitiators synthesized at 120°C using N1–N3. Note, that polydispersity indexes of the post-polymers are relatively low, although they are somewhat high than PDI of the initiating polymer (macroinitiator) (Table I).

The polymerization of MMA under controlled conditions failed because of side reactions related to the intermolecular (Scheme 2, reaction 1) and intramolecular transfer of the hydrogen atom (Scheme 2, reactions 2, 3). Hydroxylamine being generated in reactions 1 and 3 (Scheme 2) can itself terminate chains through reaction 4. The set of processes 1-4 (Scheme 2) leads to the termination of MMA polymerization.

Downloaded by STANFORD UNIV GREEN LIBR on June 26, 2012 | http://pubs.acs.org
Publication Date: August 13, 2009 | doi: 10.1021/bk-2009-1024.ch007

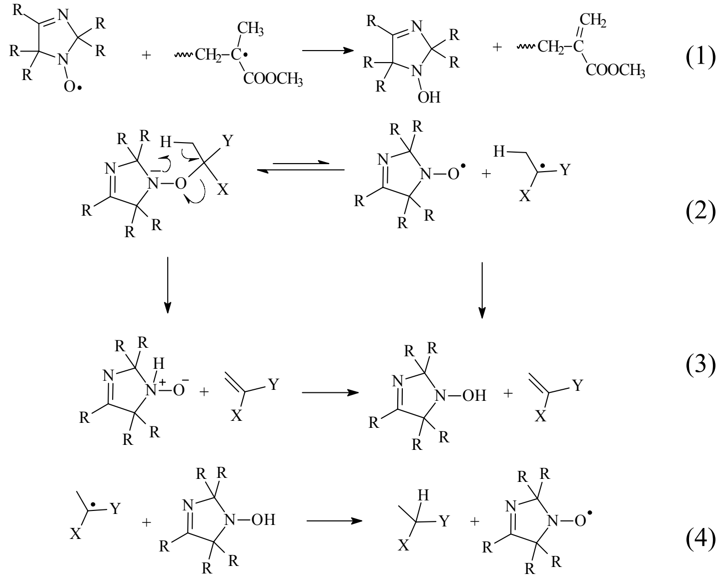

*Scheme 2*

In order to compare the efficiencies of the imidazole nitroxides with the piperidine ones the C-ON< bond dissociation energies (BDE) in alkoxyamines generated from the nitroxides N2, N3, 2,2,6,6-tetramethyl-4-oxopiperidine-1-oxyl (TEMOPO) as well as in carbon-centered radicals, which are models of the growing radicals of St and MMA, have been calculated (Table II). It has been shown that the BDE for more sterically hindered nitroxide N3 is somewhat lower than that for TEMOPO. These results are in accordance with the literature data. Thus, it is known that the sterical hindrance effects in nitroxide and alkyl fragments are affecting the C-O bond homolysis of alkoxyamines (*12, 13*).

**Table II. Quantum-Chemical Calculation of Carbon-Oxygen (>C-O) Bond Energy (kJ/mol) in [R-N] Adducts**

| *Radical* | *TEMOPO B3LYP/6-31G(d)* | *N2 B3P86/6-31G(d)* | *N3 B3P86/6-31G(d)* |
|---|---|---|---|
| St | 128 | 136 | 118 |
| MMA | - | 125 | 94 |

The data indicate that the structure of the five-membered nitrogen-containing compounds and the growing radicals exerts a direct influence on elementary stages of polymer synthesis and the molecular-weight parameters of the polymers obtained.

## Controlled Synthesis of Homopolymers of Methyl Methacrylate and Styrene and Their Copolymers with Vinyl Monomers in the Presence of Precursors of Nitroxides

Since the traditional method of SFRP with the participation of nitroxides has some restrictions the development of new approaches that allow the controlled polymerization for various monomers is of crucial importance. The application of the nitroxide mediated polymerization in the presence of the sterically hindered nitroxides has recently made possible the realization of the MMA controlled polymerization (*14*). Charleux et al. were able to polymerize MMA via SFRP at low temperatures by adding a small amount of St (*15*).

Since 1998 the in situ generation of stable nitroxides in the polymerization system has been proposed (*16-22*). This technique is emerging field of research (*23-29*). It provides the controlled polymerization not only for St but also for some (meth)acrylic monomers at temperatures suitable for industrial application (*16-29*).

The most effective technique of CRP is the generation of stable radicals in the polymerizing mixture by means of spin trapping of the growing radicals or the initiator with spin scavengers (nitrones, nitroso compounds). In this case the formation of high-molecular nitroxides is feasible (Scheme 3).

Downloaded by STANFORD UNIV GREEN LIBR on June 26, 2012 | http://pubs.acs.org
Publication Date: August 13, 2009 | doi: 10.1021/bk-2009-1024.ch007

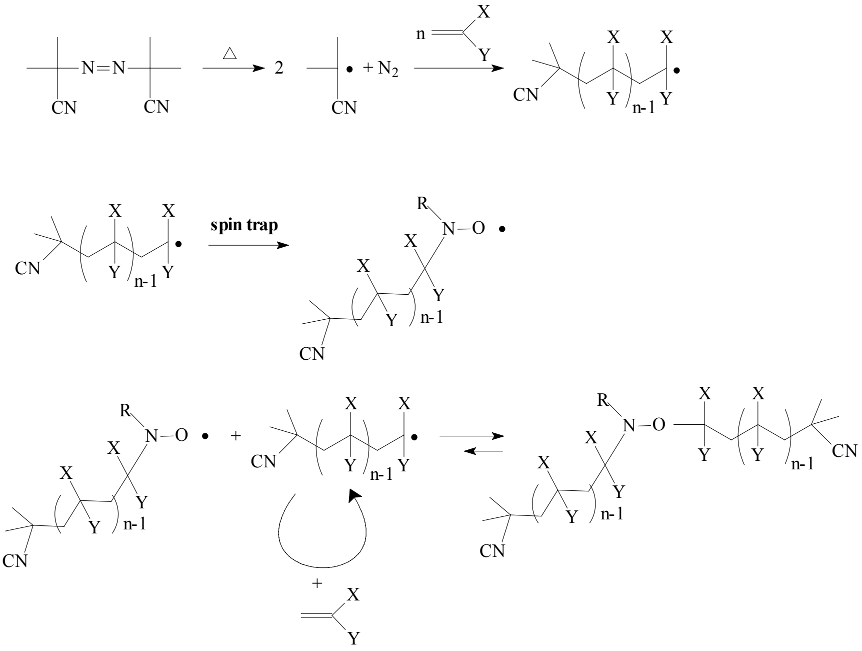

*Scheme 3*

Barner-Kowollik and co-workers (*28, 29*) have examined several nitrones (PBN, N-methyl-α-phenylnitrone, N-methyl-α-(4-bromo-phenyl) nitrone) and one nitroso compound - nitrosobenzene (NB) to control the molecular weight of PS, N-isopropylacrylamide, BA *via* so-called enhanced spin capturing polymerization method. In this technique, molecular weight control is achieved (at 60ºC or lower and [scavenger]/[initiator] from 2 to 8) *via* the reaction of a growing radical chain with a nitrone forming a macronitroxide. These nitroxides subsequently react rapidly and irreversibly with propagating macroradicals forming polymer of a certain chain length, which can be regulated by the nitrone concentration. At temperatures above 100 ºC, the reversible cleavage of the alkoxyamine group can occur, thus making a reversible activation/deactivation mechanism possible.

The Barner-Kowollik technique is similar to that proposed earlier by Grishin et al. (*16, 17, 19-21, 23, 24*). However, it is worth to note that a considerable excess of spin traps used by Barner-Kowollik and co-workers causes probably complete interception of propagating radicals and results in the low temperature synthesis of macronitroxides with constant molecular weight throughout the reaction.

In our early studies (*16, 17, 19-21, 23, 24*) concentrations of scavengers (demonstrated in Scheme 4, excluding N5 and N6) were lower and molecular weight of PMMA and PS increased linearly with conversions. As compared to low-molecular nitroxides, the polydispersity index of samples prepared with realizing this approach is slightly higher. On the other hand, the *in situ* method with the participation of the high-molecular nitroxides allows the controlled synthesis not only of PS but also various poly(meth)acrylates, in particular,

Downloaded by STANFORD UNIV GREEN LIBR on June 26, 2012 | http://pubs.acs.org
Publication Date: August 13, 2009 | doi: 10.1021/bk-2009-1024.ch007

PMMA (*16*), polybutyl methacrylate and polyBA (*19*), at the temperatures 50-90°C.

In the present work St polymerization in the presence of the nitrones N4-N6 of the imidazole series (Schemes 1 and 4) at a ratio of [initiator]:[nitrone] = 1:1.5 have been studied in details over a wide temperature interval (70-120°C). The rate of St polymerization performed in the presence of N6 is significantly lower than that carried out in the presence of N5, although it is close to the polymerization rate when the nitroxide N4 is used (Tables I, III).

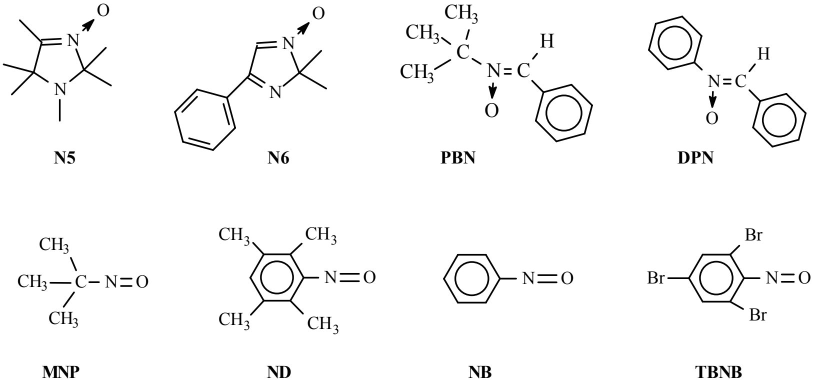

*Scheme 4*

**Table III. Molecular-Weight Characteristics of Polystyrene Synthesized in the Presence of AIBN (1.0 mol. %) and Nitrones (1.5 mol. %) at 120°C**

| *Nitrones* | *Time, h* | *Conversion,%* | $M_n x10^{-3}$ | $M_w/M_n$ |
|---|---|---|---|---|
| N5 | 0.1 | 18 | 7.7 | 1.5 |
| N5 | 0.3 | 46 | 10.1 | 1.7 |
| N5 | 1.5 | 78 | 12.8 | 2.4 |
| N6 | 1.0 | 18 | 3.4 | 1.8 |
| N6 | 7.2 | 55 | 7.3 | 3.2 |
| N6 | 12.0 | 67 | 9.4 | 3.0 |

In contrast to PS obtained at 70°C the molecular weights of PS prepared at 120°C in the presence of nitrones N4-N6 increase linearly with conversion of the monomer. Note, that with nitrones N5 and N6 the polydispersity indexes of the polymer samples are high (~2-3) (Table III) and the MWD curves have bimodal shape. The existence of two modes can be associated with different mechanisms of initiation and termination of chains. Besides, it can be explained by side reactions in the presence of nitrones. Compound N4 is the most efficient reversible inhibitor of polymerization among five-membered nitrones. It can be

Downloaded by STANFORD UNIV GREEN LIBR on June 26, 2012 | http://pubs.acs.org
Publication Date: August 13, 2009 | doi: 10.1021/bk-2009-1024.ch007

suggested that the inhibiting efficiency of this compound is caused by the presence of the nitroxide group rather than the nitrone group, since all the main features found for St polymerization in the presence of N4 are analogous to the peculiarities of vinyl monomers polymerization with imidazole nitroxides described in the section above. Thus, the polymerization of St in the presence of cyclic nitrones and nitroxides of the imidazole series indicate their direct participation in reactions with active polymer radicals. However, in comparison with the aliphatic nitrones they are less efficient as regulators of the chain growth (*16, 19*). Unfortunately, it was not possible to observe the spin-adducts between the compounds N5-N6 and the growing radicals by ESR spectroscopy. This can be explained by the extremely low concentration of the nitroxides.

As is known, the stability of the nitroxides is determined by the steric and polar effects (*30*). During the polymerization in the presence of nitrones and nitroso compounds the stable nitroxides can contain "a high-molecular part", which due to its steric bulk prevents the formation of a C-ON< bond. The electron-acceptor ester groups or a phenyl ring can stabilize nitroxide. In total, this leads to the formation of a more labile bond between the stable nitroxide and a growing macroradical, than with 2,2,6,6-tetramethylpiperidine-1-oxyl (TEMPO) and its analogs. Unfortunately, the possibilities of the direct experimental study of a growing chain in the processes of "pseudo-living" radical polymerization with the participation of high-molecular nitroxides are rather limited in technical and methodological aspects.

In this connection, the C-ON< bond dissociation energy have been calculated by the modern quantum chemistry methods. Moreover, the influence of the steric hindrances on the energy of the C-ON< bond between radical $(CH_3)_2C^{\bullet}COOCH_3$ of MMA and the nitroxides, resulting from the addition of methyl, ethyl, *iso*-propyl, *tert*-butyl and methyl methacrylate radicals to PBN, have been examined. The corresponding alkoxyamines are illustrated in Scheme 5. The calculation results are summarized in Tables IV and V.

Downloaded by STANFORD UNIV GREEN LIBR on June 26, 2012 | http://pubs.acs.org
Publication Date: August 13, 2009 | doi: 10.1021/bk-2009-1024.ch007

Downloaded by STANFORD UNIV GREEN LIBR on June 26, 2012 | http://pubs.acs.org
Publication Date: August 13, 2009 | doi: 10.1021/bk-2009-1024.ch007

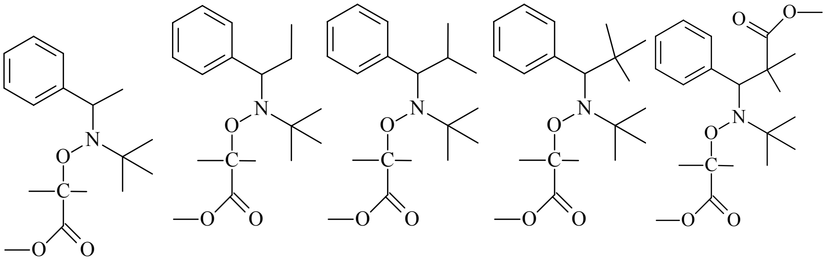

Me-PBN-MMA    Et-PBN-MMA    $^i$Pr-PBN-MMA    $^t$Bu-PBN-MMA    MMA-PBN-MMA

*Scheme 5*

**Table IV. Geometric Parameters of Alkoxyamines of PBN Derivatives (B3LYP/6-31G(d), Total Geometry Optimization)**

| *Alkoxyamine* | *Geometric parameter* | | | | |
|---|---|---|---|---|---|
| | *d(NO), nm* | *d(NC(H)), nm* | *d(NC(CH$_3$)$_3$), nm* | *a(CNC), degree* | *a(NOC), degree* |
| MMA-PBN-MMA | 0.1437 | 0.1494 | 0.1509 | 121.7 | 118.8 |
| $^t$Bu-PBN-MMA | 0.1457 | 0.1499 | 0.1525 | 115.3 | 119.3 |
| $^i$Pr-PBN-MMA | 0.1451 | 0.1497 | 0.1516 | 117.0 | 118.9 |
| Et-PBN-MMA | 0.1450 | 0.1493 | 0.1514 | 117.0 | 118.0 |
| Me-PBN-MMA | 0.1450 | 0.1489 | 0.1513 | 117.1 | 117.8 |

The computational data reveals that the sequential substitution of a methyl group with ethyl, isopropyl and *tert*-butyl group results in the lengthening of covalent N-O, N-C(H) and N-C(CH$_3$)$_3$ bonds. On going from methyl to ethyl, isopropyl and *tert*-butyl group the angle C-N-C is decreasing, while the C-O-N angles become larger. In addition, the C-ON< bond dissociation energy and enthalpy decreases from 94 to 63 kJ/mol and from 82 to 51 kJ/mol, respectively (Table V). The introduction of the electron-accepting ester group having a larger size than the *tert*-butyl group gives rise to the more pronounced weakening of the C-ON< bond (Table V). This group has an effect other than that of alkyl groups on the geometric parameters of alkoxyamine (Table IV) – the N-O bond length decreases and C-N-C angle increases. This is, probably, caused by different electronic effects of the ester group.

**Table V. Energies of C-ON< Bond (kJ/mol) in Alkoxyamines Derivatives of PBN and TEMPO (B3LYP/6-31G(d), Total Geometry Optimization)**

| *Alkoxyamine* | *Energetic parameter of C-ON< bond* | |
|---|---|---|
| | *Energy of bond, $E_{bond}$* | *Enthalpy of bond, $H_{bond}(298.15)$* |
| MMA-PBN-MMA | 43 | 31 |
| $^{t}$Bu-PBN-MMA | 63 | 51 |
| $^{i}$Pr-PBN- MMA | 82 | 69 |
| Et-PBN-MMA | 92 | 80 |
| Me-PBN-MMA | 94 | 82 |
| TEMPO-MMA | 98 | 85 |
| TEMOPO-MMA | 104 | 89 |

Downloaded by STANFORD UNIV GREEN LIBR on June 26, 2012 | http://pubs.acs.org
Publication Date: August 13, 2009 | doi: 10.1021/bk-2009-1024.ch007

The calculated values of the C-ON< bond energy for the alkoxyamine derivatives of TEMPO and TEMOPO are summarized in Table V. The calculations implies that C-ON< bond between the adduct $(CH_3)_2C^{\bullet}COOCH_3$/PBN and the growing radicals is ca. 55 kJ/mol weaker than the bond between TEMPO and the growing radicals. Such bond can dissociate reversibly at a lower temperature than in the case of TEMPO and its derivatives. Thus, the usage of PBN in the radical polymerization of (meth)acrylic monomers makes it possible to carry out the controlled synthesis of polymers under mild conditions.

It is important that the polymerization of a large variety of monomers is feasible in the presence of the proposed systems. In particular, the realization of SFRP was a difficult task in the polymer chemistry over decades for acrylic monomers (*1-6*). The realization of CRP with monomers of a different nature allowed the expansion of a variety of polymeric materials used in every possible fields of science, medicine and industry due to the modification of polymer properties by introducing the second comonomer, i.e. the statistic and block copolymerization (*5, 6, 28, 29*). Our investigations, therefore, were focused on the development of new methods of the copolymerization of vinyl monomers with a different structure at temperatures suitable for use in industrial polymer synthesis.

The system based on PBN allows the copolymerization of St-AN with an azeotropic composition of 60 mol. % St and 40 mol. % AN as well as St-VP and MMA-VP at a molar ratio 20:80 and 50:50, respectively. Addition of PBN into the polymerization system leads to a linear growth of the intrinsic viscosity of copolymers as conversion increases. In contrast to the samples synthesized using AIBN the MWD curves of the copolymers produced in the presence of PBN are unimodal. As the polymerization time increases, the maxima of the MWD curves sequentially shift towards the region of higher MW. The polydispersity indexes of such copolymers (Table VI) increase slightly with conversion growth although they remain significantly lower than those of copolymers obtained in the presence of AIBN without adding PBN ($M_w/M_n \sim 3$-4).

**Table VI. Molecular Weight Characteristics of Copolymers Synthesized in the Presence of Spin Traps**

| *Copolymer* | *T, $^0C$* | *Initiator, (mol. %)* | *Additive, (mol. %)* | *Conversion, %* | $M_n \times 10^{-3}$ | $M_w/M_n$ |
|---|---|---|---|---|---|---|
| St-AN | 70 | AIBN (0.5) | PBN (0.50) | 65 | 57 | 1.7 |
| St-AN | 70 | AIBN (0.5) | PBN (0.50) | 92 | 76 | 1.8 |
| MMA-VP[*] | 60 | AIBN (0.8) | PBN (0.10) | 3 | 134 | 1.8 |
| MMA-VP[*] | 60 | AIBN (0.8) | PBN (0.10) | 80 | 193 | 1.8 |
| St-VP[*] | 80 | AIBN (0.8) | PBN (0.05) | 7 | 7 | 1.6 |
| St-VP[*] | 80 | AIBN (0.8) | PBN (0.05) | 76 | 10 | 2.1 |
| St-AN | 100 | BPO (0.4) | MNP (0.35) | 3 | 0.6 | 1.5 |
| St-AN | 100 | BPO (0.4) | MNP (0.35) | 78 | 56 | 2.3 |
| St-MMA[**] | 70 | AIBN (0.8) | ND (0.20) | 10 | 27 | 1.4 |
| St-MMA[**] | 70 | AIBN (0.8) | ND (0.20) | 65 | 32 | 1.7 |
| St-BA[**] | 70 | AIBN (0.8) | ND (0.20) | 8 | 35 | 1.5 |
| St-BA[**] | 70 | AIBN (0.8) | ND (0.20) | 83 | 51 | 1.8 |
| St-AN[**] | 70 | AIBN (0.8) | ND (0.25) | 6 | 52 | 1.6 |
| St-AN[**] | 70 | AIBN (0.8) | ND (0.25) | 70 | 69 | 1.8 |

[*] MW of MMA-VP and St-VP copolymers were calculated by Mark-Houwink equation with using constants $K = 4.8 \times 10^{-5}$ and $\alpha = 0.8$ for PMMA and $K = 7.16 \times 10^{-5}$ and $\alpha = 0.76$ for PS (*31*), respectively.

[**] MW of copolymers were calculated by Mark-Houwink equation with use of constants $K = 7.16 \times 10^{-5}$ and $\alpha = 0.76$ for PS (*31*).

Downloaded by STANFORD UNIV GREEN LIBR on June 26, 2012 | http://pubs.acs.org
Publication Date: August 13, 2009 | doi: 10.1021/bk-2009-1024.ch007

In the copolymerization of St with VP and MMA with VP the chosen pairs of the monomers differ substantially in the reactivities. The accumulation of VP homopolymer in the system becomes possible at the end of the copolymerization process, when the active monomers (MMA, St) are practically totally exhausted. In order to estimate quantitatively the PVP content in the copolymers, PVP was isolated with distilled water and then the molecular-weight parameters of the washed copolymers have been determined. It has been established that the samples synthesized in the presence of the traditional initiator (AIBN) contain of a great amount of PVP (35-50 %) at high degrees of conversion. The copolymers prepared in the presence of PBN practically do not contain PVP. This indicates that the addition of PBN in the system allows the preparation of copolymers that do not contain of VP homopolymer impurities.

The composition of the copolymers at different degrees of conversion was studied by IR-spectroscopy. It has been ascertained the composition of copolymer obtained from MMA:VP (50:50 mol. %) as well as from St:VP (20:80 mol. %) changes with increasing conversion. The copolymers isolated at small degrees of conversion are enriched with more active comonomer (MMA or St) compared to the starting monomer mixture. However, as the conversion increases, the composition of the polymers is changing. In both cases, with PBN and without PBN the increase of the VP content is observed in the copolymers.

In order to study the effect of aliphatic nitroso compounds in polymerization, MNP as the chain growth regulator has been tested in the copolymerization of St with AN. The synthesis of alkoxyamines has been carried out *in situ* in the presence of BPO at 100ºC. In this system a linear growth of the number-average molecular weight of the copolymers with conversion and a clear shift of MWD curves towards a high-molecular region is observed. In fact the molecular-weight distribution for the copolymer is rather wide (Table VI). In addition, a low-molecular shoulder in the MWD curves at a low conversion is attributed to the oligomeric fraction in the copolymer. The portion of this fraction is decreasing with conversion and at the high conversion this oligomeric fraction is disappeared.

The influence of aromatic nitroso compounds on the copolymerization of St with various acrylic monomers (MMA, BA and AN) has been studied using ND. The copolymerization of these monomers has been investigated at monomer ratio that corresponds to azeotropic compositions. ND affects the kinetics of the process and molecular-weight parameters of the copolymers. On adding of ND into the copolymerization no autoacceleration as well as a spontaneous increase in the intrinsic viscosity and number-average MW of the copolymers are observed. The polydispersity indexes for the copolymers are listed in Table VI. Although the PDI slightly grows with increasing conversion it stays significantly lower than that of the copolymers prepared without ND ($M_w/M_n$~ 2.5-4).

The relative reactivities for St and MMA have been determined. The composition of the copolymers of St with MMA and BA at various conversions obtained by the ND-mediated synthesis was studied by the IR- and UV-spectroscopy. It has been found that the reactivity ratios for St and MMA in copolymerization in the presence of ND are almost perfectly coincide with those in conventional radical copolymerization of St with MMA. With the molar ratio of monomers [St]:[MMA]=53:47 and [St]:[BA]=77:23 the copolymer composition under the examined conditions is close to the composition of the initial mixture in the whole conversion interval.

One of the main evidence for the polymerization of vinyl monomers in the presence of PBN *via* the “pseudoliving” mechanism is the capability of high-molecular alkoxyamines to resume the polymerization process on adding a new portion of the monomer in the formed polymer, i.e. to act as macroinitiators. In this study we experimentally confirmed the ability of the high-molecular nitroxides, *in-situ* prepared on the basis of PBN, to play the role of macroinitiators. Polymers of PS, synthesized in bulk over a wide temperature range (70-120$^0$C) at a different [PBN]:[initiator] ratio, have been exploited as starting macroinitiators. The macroinitiators have been isolated at the conversions less than 30 % and these exhibit smallest PDI. The samples have been precipitated several times to purify them from residues of the initiator and the nitrone. With the macroinitiators formed in the presence of 0.8 mol. % AIBN and 0.08 mol. % PBN at 70$^0$C the curves of MWD of the reaction products were shifted towards a higher-molecular region from the curves of the starting polystyrene. This fact points to that MW of the starting polymer increases as a result of the post-polymerization reaction due to the “integration” of new monomer units through a labile bond of alkoxyamine. However, the curves of the molecular-weight distribution of the post-polymers are bimodal that testifies to a sufficient share of thermal self-initiated polymerization of the monomer. Besides, the yield of the post-polymer is strictly dependent of the process temperature. Raising temperature from 70 to 90$^0$C permits to increase the post-

Downloaded by STANFORD UNIV GREEN LIBR on June 26, 2012 | http://pubs.acs.org
Publication Date: August 13, 2009 | doi: 10.1021/bk-2009-1024.ch007

polymer portion. The part of the side process also grows although to a smaller extent. Further raise the temperature up to 120$^0$C leads to the changeover of the post-polymerization reaction to an uncontrolled condition: the polymers formed in these conditions are similar to the polymers synthesized without nitrone. The data definitively show that using high-molecular alkoxyamines based on polystyrene the temperature interval 70-90$^0$C is the most optimal.

The block copolymerization has been conducted similarly to the post-polymerization. The PS prepared at 70$^0$C in the presence of AIBN (0.8 mol. %) and PBN (0.08 mol. %) and isolated at conversions from 10 % up to extreme values, was used as macroinitiator for block copolymerization. To the purified macroinitiator a new portion of comonomer – MMA has been added. The choice of MMA as a comonomer is explained by the fact that PMMA and PS differ in properties and hence they can be easily separated. In addition, the polymerization of MMA in the presence of the PBN:AIBN pair is known (*16*) and, therefore, the block copolymerization is expected to occur.

The reaction of PS macroinitiator with MMA was provided at 70°C. After isolation the PS-b-PMMA (Scheme 6) has been characterized by IR- and NMR-spectroscopy as well as by SEC.

Downloaded by STANFORD UNIV GREEN LIBR on June 26, 2012 | http://pubs.acs.org
Publication Date: August 13, 2009 | doi: 10.1021/bk-2009-1024.ch007

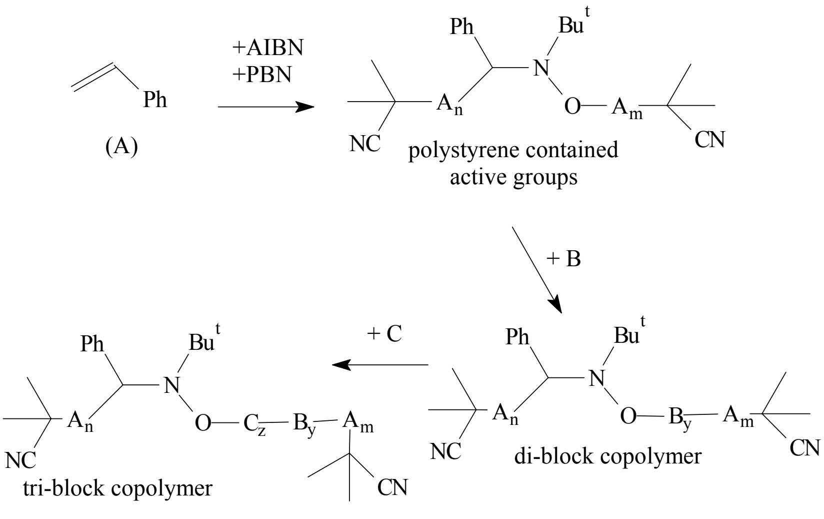

B: MMA or VP
C: St or BA

*Scheme 6*

The data obtained indicate that the block copolymer is the main component of the copolymerization products. It has been established that polystyrene successfully (about 87%) is able to initiate the block copolymerization. As expected the content of MMA units in the block copolymers slightly increases with growing yield of the block copolymer from 86 to 92 wt. %. The MW also increased with conversion of comonomer and MWD curves of PS-b-PMMA samples shifted towards high molecular weights relative to the initial polymer. The chain length of the PS-b-PMMA grows by more than a factor of $10^2$ compared to the chain length of the starting macroinitiator (Figure 2 a). The MWD curves of the macroinitiator and the block copolymer (62 % yield) do not cross (Figure 2b). It demonstrates that the latter polymer does not contain the initial polymer. The polydispersity of the block copolymers is 1.8-2.0 and it is little increased in comparison with the starting polystyrene. This means that length of polymer chains is increased due to adding of new MMA monomer units and the block copolymer was indeed obtained.

Downloaded by STANFORD UNIV GREEN LIBR on June 26, 2012 | http://pubs.acs.org
Publication Date: August 13, 2009 | doi: 10.1021/bk-2009-1024.ch007

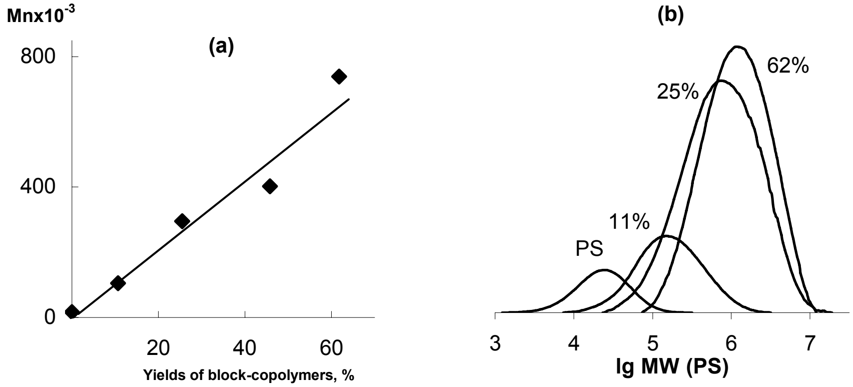

*Figure 2. Dependence of MW of PS-b-PMMA on conversion (a) and molecular-weight distribution of PS-b-PMMA (b) synthesized at 70°C in the presence of PBN. Curves are normalized to the conversion.*

It has been shown that the most of chains involved in the macroinitiator contain the active groups (>NO-C, Scheme 6) reinitiating the polymerization and being responsible for the formation of post- and block copolymers. Similar regularities have been revealed for all the samples of the starting PS independent on its yield. Consequently, the PBN-mediated polymerization of St is the controlled process till high conversions. Residual PS has been found in polymer products of reaction non-active, i.e. ”dead” and not reacted polymer.

The PMMA was formed together with the block copolymer via self-initiation reaction in small amounts. However, this reaction is untypical for pure MMA and observed only in the presence of some additives.

Our method of block copolymer synthesis differs from Detrembleur (*22,25,27*) or Barner-Kowollik (*28,29*) methods. In our case the initial polymer was obtained in the controlled polymerization conditions. This MW increased with its yield. The methods of other authors are consisted with generation of the starting polymers in the presence of PBN or other reagents at lower temperature than required to provide controlled polymerization. In consequence of it the MW of the formed macroinitiatiors did not change with conversion. As it was established, the both methods provide the synthesis of the macroinitiator but the degree of livingness of chains are different.

On the basis of the macroinitiators prepared in the presence of PBN, the synthesis of PS-b-PVP and PVP-b-PS block copolymers (Scheme 6) has been performed at 80ºC and 70ºC, respectively. First, PS synthesized at 70ºC with the use of PBN (0.8 mol. %) and AIBN (0.8 mol.%) was applied as macroinitiator for the PS-b-PVP synthesis. Thus, PVP obtained by the controlled polymerization in the presence of PBN (0.2 mol.%) and AIBN (0.8 mol.%) at 60ºC was used as the macroinitiator for the synthesis of the PVP-b-PS. The polymerization products obtained with the macroinitiators can be separated into three fractions: homo-PS, homo-PVP and the block copolymer by a sequential selective extraction of the polymer mixture in cyclohexane (for PMMA) and water (for PVP), respectively. The MWD curves of the block copolymerization products are unimodal and sequentially shifted towards a high-molecular region in comparison with the initial macroinitiator. The polydispersity indexes of the block copolymers are rather low (for PVP-b-PS, PDI = 2.1; PS-b-PVP, PDI = 1.4). These data prove the possibility of reinitiation of growing radicals when used high molecular alkoxyamines at temperatures below 80ºC

The living polymerization of MMA and its block-copolymerization mediated by TEMPO and its derivatives has not yet been reported (*1-3*). Disproportionation of nitroxide and MMA growing radical is dominanting at high temperatures. That is the consequence of inability for nitroxide-mediated polymerization to occur (*32*). On the other hand, this type of polymerization does proceed in the presence of the sterically hindered nitroxide at 100°C (*14*) and of high molecular nitroxides under low temperatures (*16*). As was mentioned above, high molecular nitroxides allow synthesis of the PS-b-PMMA block-copolymers under controlled conditions up to high conversions. In order to confirm the presence of the active groups in the diblock-copolymers capable to reinitiate polymerization the synthesis of PS-b-PMMA-b-PS as well as PS-b-PMMA-b-PBA triblock-copolymers was performed (Scheme 6). It is established that the diblock copolymer PS-b-PMMA reacts completely with third comonomer. Triblock copolymers have been characterized by SEC and $^1$H NMR. The MWD curves of the triblock copolymer samples are shown in Figure 3. The triblock copolymer MWD curves are shifted relative to precursors (the diblock copolymer and the starting polystyrene). With conversion a number of units of third comonomer is increasing. On the contrary, the content of first and second monomer units in triblock copolymers was similar to the starting diblock copolymer. Thus, in the products of the block copolymerization the active groups indeed remain, therefore a cascade synthesis of poly-block-copolymers is feasible.

Downloaded by STANFORD UNIV GREEN LIBR on June 26, 2012 | http://pubs.acs.org
Publication Date: August 13, 2009 | doi: 10.1021/bk-2009-1024.ch007

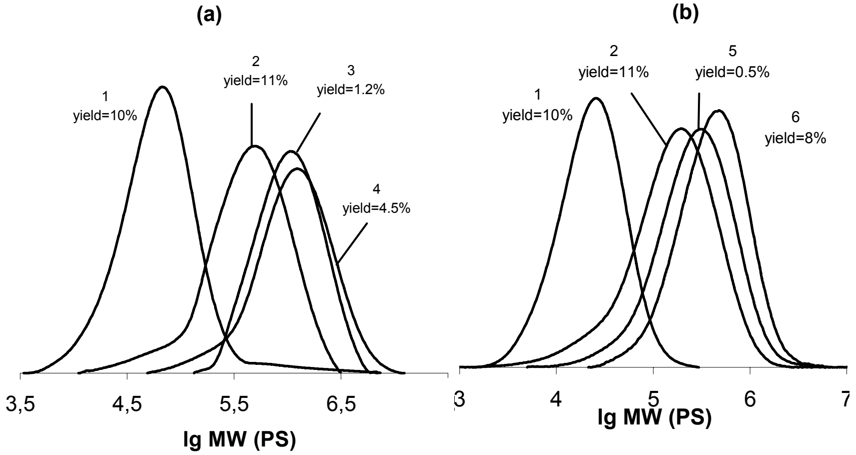

*Figure 3. Molecular-weight distribution curves of PS-b-PMMA- b-PS triblock copolymers (a, curve 3, 4) and PS-b-PMMA-b-PBA triblock copolymers (b, curve 5, 6) synthesized in bulk at 90°C in the presence of initiating diblock copolymer PS-b-PMMA (curve 2), the latter was produced by the polymerization of MMA in the presence of initiating PS (curve 1) in yield of 10 wt.%. The yields of the polymers are shown near the curve.*

## Conclusions

Thus, the approaches proposed in this study permit to realize polymerization of vinyl monomers (St, MMA, BA, VP, AN) under controlled conditions and enable preparation of homo-, post- and block copolymers with relatively low polydispersity indexes with the predetermined molecular weights. The applied techniques of the *in-situ* generation of the stable nitroxides and alkoxyamines are fairly promising for the realization of CRP at temperatures ranging from 50 to 90°C. First, this is caused with the simplicity of the process realization, the availability and efficiency of the precursors considered. A majority of the control techniques on the basis of the systems studied unlike individually synthesized alkoxyamines allow the controlled polymerization in good yields and with the considerable degree of the control of the molecular-weight parameters for an essentially short time.

Downloaded by STANFORD UNIV GREEN LIBR on June 26, 2012 | http://pubs.acs.org
Publication Date: August 13, 2009 | doi: 10.1021/bk-2009-1024.ch007

Downloaded by STANFORD UNIV GREEN LIBR on June 26, 2012 | http://pubs.acs.org
Publication Date: August 13, 2009 | doi: 10.1021/bk-2009-1024.ch007

## Acknowledgements

The work was supported by the Russian Foundation for Basic Researches (project No 08-03-00100). The authors thank Dr. I.A. Kirilyuk for giving the compounds N1-N6.

## References

1. *Handbook of Radical Polymerization*; Matyjaszewski, K.; Davis, T. P., Eds.; Wiley-Interscience: Hoboken, 2002; 936 p.
2. Goto, A.; Fukuda, T. *Prog. Polym. Sci.* **2004,** *29*, 329-385.
3. Matyjaszewski, K.; Braunecker, W.A. *Prog. Polym. Sci.* **2007,** *32*, 93-146.
4. Grishin, D. F. *Polym. Sci. Ser. A* **2008,** *50,* 221-242.
5. Hawker, C.J.; Bosman, A.W.; Harth, E. *Chem. Rev.* **2001**, *101,* 3661-3668.
6. Sciannamea, V.; Jérôme, R.; Detrembleur, C. *Chem. Rev.* **2008**, *108*, 1104-1126.
7. Studer, A.; Harms, K.; Knoop, C.; Muller, C.; Schulte, T. *Macromolecules* **2004**, *37*, 27-34.
8. Siegenthaler, K. O.; Studer, A. *Macromolecules* **2006**, *39*, 1347-1352.
9. Ruehl, J.; Hill, N. L.; Walter, E. D.; Millhauser, G.; Braslau, R. *Macromolecules* **2008**, *41*, 1972-1982.
10. Reznikov, V. A.; Volodarsky, L. B. *Russ. Chem. Bull.* **1997,** *46,* 1577–1581.
11. Zubenko, D.; Kiriluk, I.; Roshchupkina G.; Zhurko, I.; Reznikov, V.; Marque, S.R.A.; Bagryanskaya, E. *Helvetica Chimica Acta* **2006**, *89*, 2341-2353.
12. Moad, G.; Rizzardo, E. *Macromolecules* **1995**, *28*, 8722-8728.
13. Fischer, H.; Kramer, A.; Marque, S. R. A.; Nesvadba, P. *Macromolecules* **2005**, *38*, 9974-9984.
14. Guillaneuf, Y.; Gigmes, D.; Marque, S. R. A.; Astolfi, P.; Greci, L.; Tordo, P.; Bertin, D. *Macromolecules* **2007**, *40*, 3108-3114.
15. Nicolas, J.; Dire, C.; Mueller, L.; Belleney, J.; Charleux, B. *Macromolecules* **2006**, *39*, 8274-8282.
16. Grishin, D. F.; Semenycheva, L.L.; Kolyakina, E.V. *Dokl. Chem.* **1998,** *362*, 199-203.
17. Grishin, D.F.; Semyonycheva, L.L.; Kolyakina, E.V. *Mendeleev Commun.* **1999,** *6,* 250-251.
18. Zink, M-O.; Kramer, A.; Nesvadba, P. *Macromolecules* **2000**, *33,* 8106-8108.
19. Kolyakina, E.V.; Semenycheva, L.L.; Grishin, D.F. *Polym. Sci. Ser. A* **2001,** *43*, 1223-1228.
20. Pavlovskaya, M.V.; Kolyakina, E.V.; Polyanskova, V.V.; Semenycheva, L.L.; Grishin, D.F. *Russ. J. Appl. Chem.* **2002,** *75,* 1868-1872.
21. Grishin, D.F.; Pavlovskaya, M.V.; Kolyakina, E.V.; Semenycheva, L. L. *Russ. J. Appl. Chem.* **2002,** *75*, 1468-1472.

22. Detrembleur, C.; Sciannamea, V.; Koulic, C.; Claes, M.; Hoebeke, M.; Jerome, R. *Macromolecules* **2002,** *35*, 7214-7223.
23. Grishin, D.F.; Semenycheva, L.L.; Kolyakina, E.V.; Polyanskova V.V. *Polym. Sci. Ser. A* **2003,** *45,* 99-103.
24. Kolyakina, E.V.; Polyanskova, V.V.; Grishin, D.F. *Russ. Chem. Bull.* **2007,** *56*, 168-173.
25. Sciannamea, V.; Guerrero-Sanchez, C.; Schubert, U. S.; Catala, J.- M.; Jérôme, R.; Detrembleur, C. *Polymer* **2005,** *46,* 9632-9641.
26. Sciannamea, V.; Bernard, M.; Catala, J. M.; Jerome, R.; Detrembleur, C. *J. Polym. Sci., Part A: Polym. Chem.* **2006**, *44*, 6299-6311.
27. Sciannamea, V.; Catala, J. M.; Jerome, R.; Detrembleur, C. *J. Polym. Sci., Part A: Polym. Chem.* **2007**, *45*, 1219-1235.
28. Wong, E. H. H.; Junkers, T.; Barner-Kowollik, C. *J. Polym. Sci., Part A: Polym. Chem.* **2008**, *46*, 7273–7279.
29. Wong, E. H. H.; Stenzel, M. H.; Junkers, T.; Barner-Kowollik, C. *J. Polym. Sci., Part A: Polym. Chem.* **2009**, *47*, 1098–1107.
30. Marque, S. *J. Org. Chem.* **2003**, *68*, 7582–7590.
31. *Polymer Handbook;* Brandrup, J.; Immergut, E. P., Eds.; Wiley-Interscience: New York, 1975.
32. Moad, G.; Anderson, A. G.; Ercole, F.; Johnson, C. H. J.; Krstina, J.; Moad, C. L.; Rizzardo, E.; Spurling, T. H.; Thang, S. H. *ACS Symp. Ser.* **1998**, *685*, 332-360.

Downloaded by STANFORD UNIV GREEN LIBR on June 26, 2012 | http://pubs.acs.org
Publication Date: August 13, 2009 | doi: 10.1021/bk-2009-1024.ch007

Downloaded by COLUMBIA UNIV on June 26, 2012 | http://pubs.acs.org
Publication Date: August 13, 2009 | doi: 10.1021/bk-2009-1024.ch008

## Chapter 8

# Formation, Dissociation, and Radical Exchange of Organo-Cobalt Complexes in Mediating Living Radical Polymerization

**Chi-How Peng[1], Shan Li[1], and Bradford B. Wayland[2]***

**[1]Department of Chemistry, University of Pennsylvania,
Philadelphia, PA 19104**
**[2]Department of Chemistry, Temple University, Philadelphia, PA 19122**

Reactions of organic radicals (•R) with cobalt(II) metallo-radicals (Co•) and organo-cobalt complexes (Co-R′) have a central role in several pathways that produce control for radical polymerizations. Interactions of organic radicals with cobalt(II) metallo-radical produce a cobalt hydride (Co-H) via the β-hydrogen abstraction. Subsequent addition of the cobalt hydride with the olefin monomers to produce organometallic complexes (Co-R′) can give catalytic chain transfer. Reversible homolysis of the organo-metal bond in the absence of β-H transfer gives the living radical polymerization (LRP) by a reversible termination (RT) mechanism. When the exchange of freely diffusing radicals in solution with the dormant organic units in organometallic complexes is fast, a LRP can occur by a degenerative transfer (DT) mechanism. Methyl acrylate (MA) and vinyl acetate (VAc) polymerization mediated by cobalt porphyrin complexes are used to illustrate the features of these two LRP pathways. Kinetic and thermodynamic properties for several of the central reactions are evaluated by following the time evolution of the $^1$H NMR for organo-cobalt porphyrin complexes.

In Controlled/Living Radical Polymerization: Progress in RAFT, DT, NMP & OMRP; Matyjaszewski, K.;
ACS Symposium Series; American Chemical Society: Washington, DC, 2009.

# Introduction

Reactions of organic radicals with metallo-radicals and organometallic complexes have a central role in several pathways that mediate living radical polymerization (LRP).[1-16] The metal site reactions that occur when organic radicals interact with metal-centered radicals and organo-metal species in solution are shown in Scheme 1.[17,18] Interactions of organic radicals ($\bullet C(CH_3)R_1R_2$) with metal-centered radicals (M•) in solution produce a solvent caged radical pair ($M\bullet\bullet C(CH_3)R_1R_2$) (Scheme 1A) which can collapse to form an organometallic complex ($M\text{-}C(CH_3)R_1R_2$) (Scheme 1B), separate back into freely diffusing radicals ($M\bullet + \bullet C(CH_3)R_1R_2$), or react by M• abstracting a β-hydrogen from the radical ($\bullet C(CH_3)R_1R_2$) to form a metal hydride (M–H) and an olefin ($CH_2{=}CR_1R_2$) (Scheme 1C).[17]

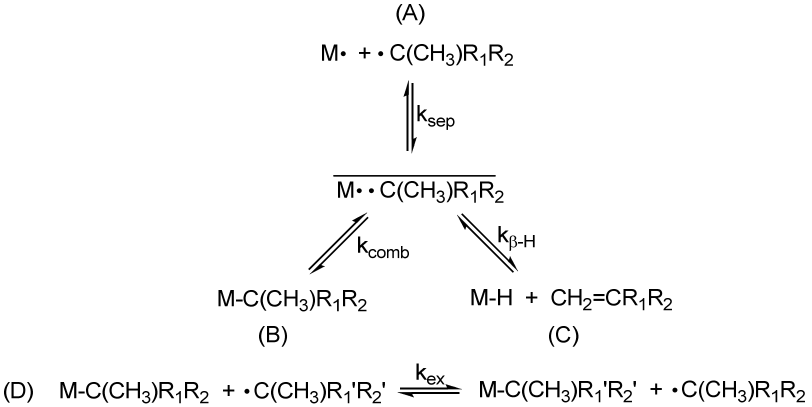

Scheme 1. Reactions of metal-centered radicals and organo-metal complexes with organic radicals.

Hydrogen abstraction by a metal-centered radical (M•) from the growing polymeric radical to form a metal hydride (M-H) (Scheme 1A, C) that subsequently adds with the monomer to produce an organometallic complex (M-R) gives catalytic chain transfer. Reversible homolysis of the organo-metal bond in the absence of β-H transfer provides an organo-metal route to obtain living radical polymerization by a reversible termination (RT) mechanism (Scheme 1A, B; eq. 1).[2,19-21] When the exchange of freely diffusing radicals in solution with the dormant organic units in organometallic complexes is fast, then a LRP can occur by a degenerative transfer (DT) mechanism (Scheme 1D, eq. 2).[4,22-24] Cobalt porphyrin complexes can achieve each of the reactions with organic radicals described in Scheme 1 and thus function as prototype systems to explore the pathways, potential scope, and limitation of living radical polymerization by both reversible termination (RT) (Scheme 1A, B) and degenerative transfer (DT) (Scheme 1D) as well as catalytic chain transfer (CCT) (Scheme 1A, C).

Downloaded by COLUMBIA UNIV on June 26, 2012 | http://pubs.acs.org
Publication Date: August 13, 2009 | doi: 10.1021/bk-2009-1024.ch008

Downloaded by COLUMBIA UNIV on June 26, 2012 | http://pubs.acs.org
Publication Date: August 13, 2009 | doi: 10.1021/bk-2009-1024.ch008

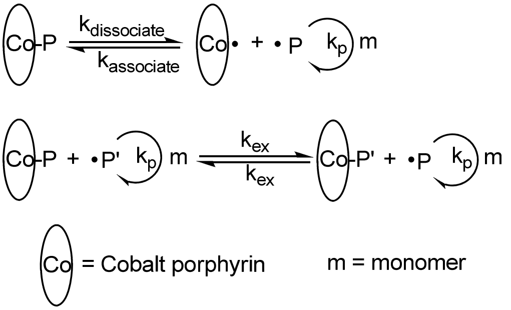

(1)

(2)

This article reports on the formation of organo-metal intermediates, hydrogen atom transfer, and radical exchange reactions that occur in the radical polymerization of methyl acrylate (MA) and vinyl acetate (VAc) mediated by organo-cobalt tetramesityl porphyrin complexes (organo-Co(TMP)).[4]

## Cobalt(II) Metallo Radical and Organo-Cobalt Complexes

Cobalt(II) tetramesityl porphyrin ((TMP)Co$^{II}$•) and cobalt(II) tetraphenyl porphyrin ((TPP)Co$^{II}$•) complexes are examples of large and small steric requirement complexes which are capable of controlling the radical polymerization of arylates and vinyl esters.[1-4] The unpaired electron in the $d_{z^2}$ orbital of cobalt(II) porphyrin complexes couples with organic radicals to form the organo-cobalt complexes (Figure 1).

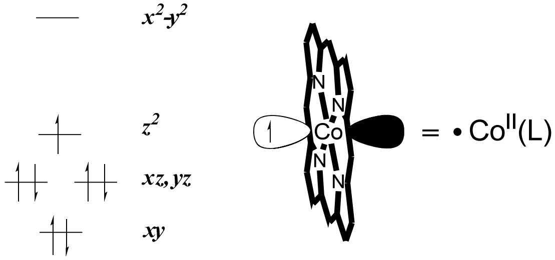

*Figure 1. d-orbitals MO diagram and schematic structure of cobalt(II) porphyrin complex illustrating its metallo radical behavior.*

Organo-cobalt porphyrin complexes are readily identified in solution by NMR because magnetic anisotropy of the aromatic porphyrin ligands results in high field NMR shifts that scale by $(3\cos^2\theta-1)/r^3$ from the center of the ring for magnetic nuclei in groups that are bonded with metal sites in metalloporphyrin (Figure 2A). Hydrogen nuclei in organic groups bonded to the cobalt centers often have large upfield shifts that place the hydrogen resonances in the clear region on the high field side of TMS (Figure 2B). $^1$H NMR thus provides a powerful method to observe the organic units bonded with the metal in organo-cobalt porphyrin complexes and investigate mechanistic issues.

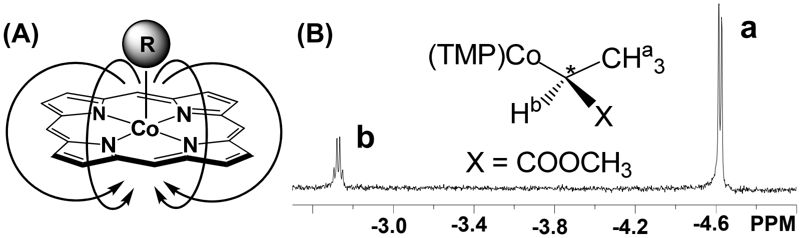

*Figure 2. (A) porphyrin ring current produces magnetic shielding for the R group bonded to cobalt. (B) NMR spectra of (TMP)Co-CH($CO_2CH_3$)$CH_3$ illustrates the ring current effect.*

Organo-cobalt porphyrins are five coordinate sixteen-electron complexes and this coordinate and electronic unsaturation provide a highly favorable situation for fast associative radical interchange (Figure 3). The rapid exchange of the radicals in solution with the dormant radicals in the organo-cobalt complexes provides an equal opportunity for the polymeric radical chains to propagate which gives low polydispersity.

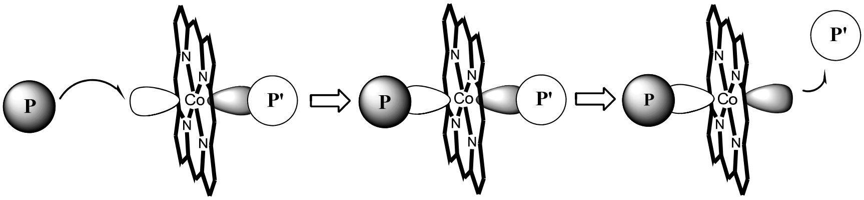

*Figure 3. Radical interchange process of organo-cobalt porphyrin complexes with the external polymeric radicals.*

## Polymerization of Methyl Acrylate

Solutions of methyl acrylate (MA) (2.2M), (TMP)$Co^{II}$• ($1.0\times10^{-3}$M), and V-70 ((($CH_3$)$_2$($OCH_3$)C($CH_2$)C($CH_3$)(CN))$_2N_2$) ($1.1\times10^{-3}$M) in $C_6D_6$ were heated to 333K and yielded the polymeric products with low polydispersity and predictable molecular weight based on one polymer chain per cobalt which are evidence that the polymerization process is “living” (Figure 4).

Downloaded by COLUMBIA UNIV on June 26, 2012 | http://pubs.acs.org
Publication Date: August 13, 2009 | doi: 10.1021/bk-2009-1024.ch008

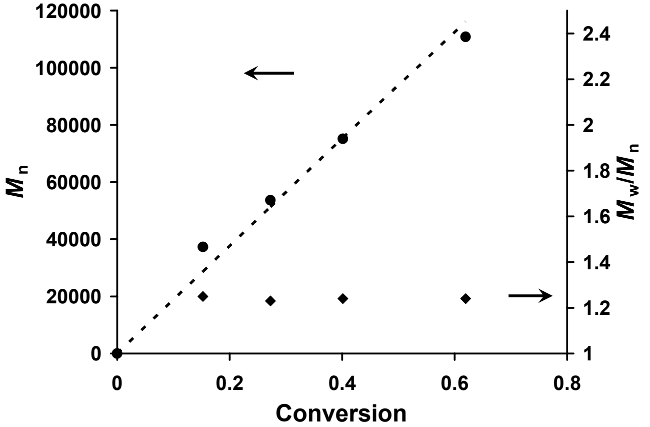

*Figure 4. Change in the number average molecular weight ($M_n$) (●) and polydispersity ($M_w/M_n$) (◆) with conversion of methyl acrylate (MA) to polymethyl acrylate (PMA) at 333K in $C_6D_6$. $[MA]_i = 2.2$ M; $[(TMP)Co^{II}]_i = 1.0\times10^{-3}$ M; $[V\text{-}70]_i = 1.1\times10^{-3}$ M. The dotted line is the theoretical line for one polymer chain per organo-cobalt complex.*

Figure 5 shows representative kinetic plots for MA radical polymerizations mediated by $(TMP)Co^{II}\bullet$ ($1.0\times10^{-3}$M) in $C_6D_6$ initiated by external azo radical source (V-70). When the ratio of total moles of radicals injected into solution from the radical source to the initial moles of $(TMP)Co^{II}\bullet$ is less than unity the polymerization process is mediated by the excess of $(TMP)Co^{II}\bullet$. There are two moles of radicals produced per mole of V-70 and sixty percent of the radicals produced enter solution such that 1.20 moles of radicals enter solution from one mole of dissociated V-70. The polymerization is relatively slow because the radical is maintained at a low concentration by a quasi-equilibrium between $(TMP)Co^{II}\bullet$ and (TMP)Co-P (Figure 5A; eq. 1). Radical polymerization of MA for the condition where the total moles of radicals that enter solution from V-70 exceeds the initial moles of $(TMP)Co^{II}\bullet$ is illustrated in figure 5B-D. An induction period where a few percent conversion of the monomer occurs is followed by the onset of rapid polymerization at the time when effectively all of the $(TMP)Co^{II}\bullet$ has been converted to (TMP)Co-P. The reaction that predominates during the post induction period where rapid polymerization occurs is given in eq. 2 (DT process). Radicals ($[R\bullet]=(k_i[V\text{-}70]/2k_t)^{1/2}$) entering solution from V-70 initiate polymerization of MA and the radicals in solution exchange with radicals in the dormant (TMP)Co-P complex by both associative and dissociative pathways.

Downloaded by COLUMBIA UNIV on June 26, 2012 | http://pubs.acs.org
Publication Date: August 13, 2009 | doi: 10.1021/bk-2009-1024.ch008

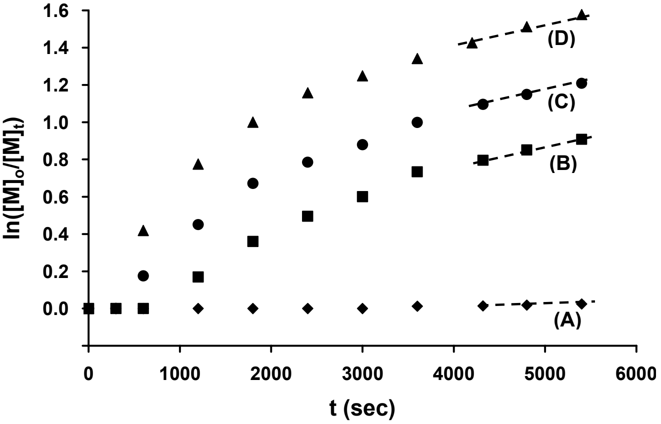

*Figure 5. Kinetic plots for polymerization of methyl acrylate (MA) in $C_6D_6$ at 333K initiated by V-70 with $[(TMP)Co^{II}]_i = 1.0\times10^{-3}M$, $[MA]_i = 2.25M$, $[V\text{-}70]_i/[(TMP)Co^{II}]_i$ = (A) 0.53; (B) 1.21; (C) 1.58; (D) 2.54, slope of the dot line = (A) $5\times10^{-4}\ s^{-1}$; (B) $8.2\times10^{-3}\ s^{-1}$; (C) $8.1\times10^{-3}\ s^{-1}$; (D) $8.3\times10^{-3}\ s^{-1}$.*

When the external radical source (V-70) is exhausted, the polymerization rate decreases because dissociation of organo-cobalt complex ((TMP)Co-P) becomes the exclusive radical source ($[P\bullet] = K_{(333K)}\ [(TMP)Co\text{-}P]/[(TMP)Co^{II}\bullet]$) which is one of the features of a reversible termination LRP. The radicals in solutions are maintained at low concentration by the quasi-equilibrium with the dormant organo-cobalt complex (eq. 1). This is illustrated by the parallel linear regions of the first order rate plots that occur when all of the V-70 radical source has dissociated (Figure 5B-D).

## Polymerization of Vinyl Acetate

Living radical polymerization mediated by cobalt(II) porphyrin complexes and organo-cobalt porphyrin complexes have been extended to vinyl esters. Radical polymerization of vinyl acetate (VAc) mediated by $(TMP)Co^{II}\bullet$ with azo radical sources (V-70 and AIBN) are illustrated in figure 6 and 7.

Downloaded by COLUMBIA UNIV on June 26, 2012 | http://pubs.acs.org
Publication Date: August 13, 2009 | doi: 10.1021/bk-2009-1024.ch008

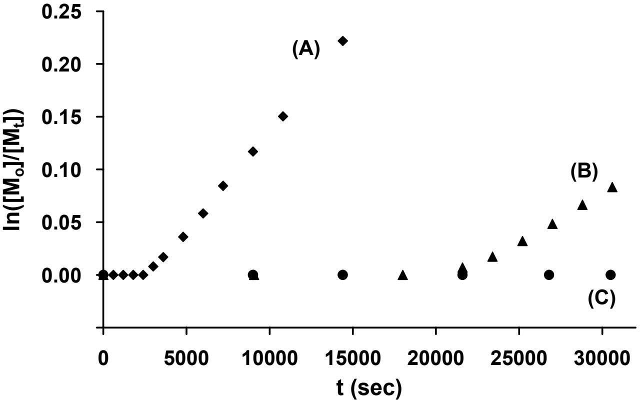

*Figure 6. Kinetics plots for the vinyl acetate (VAc) radical polymerization mediated by cobalt(II) tetramesitylporphyrin ((TMP)Co$^{II}$) in $C_6D_6$ at 333 K: (A) [(TMP)Co$^{II}$]$_i$ = 6.9×10$^{-4}$ M, [V-70]$_i$ = 8.0×10$^{-4}$ M, and [VAc]$_i$ = 5.42 M, Conv. = 10.11%, $M_w/M_n$ = 1.13, $M_n$ = 64000 ($M_n$ (Calc) = 68000); (B) [(TMP)Co$^{II}$]$_i$ = 5.9×10$^{-4}$ M, [AIBN]$_i$ = 7.6×10$^{-3}$ M, and [VAc]$_i$ = 1.74 M, Conv. = 8.00%, $M_w/M_n$ = 1.22, $M_n$ = 14000 ($M_n$ (Calc) = 20000). (C) [(TMP)Co$^{II}$]$_i$ = 5.9×10$^{-4}$ M, [V-70]$_i$ = 3.9×10$^{-4}$ M, and [VAc]$_i$ = 1.54 M.*

During the induction period radicals that enter solution from the azo radical sources react and are trapped by (TMP)Co$^{II}$• as organo-cobalt complexes. If at the end of the induction period radicals continue to enter solution from the azo radical source, then a relatively fast radical polymerization of VAc occurs (333K) (Figure 6A, B). This is the situation where the control of radical polymerization requires a degenerative transfer mechanism which is dependent on the exchange of radicals between solution and the organo-cobalt transfer agent (eq. 2). When the number of radicals from the external radical source is insufficient to convert all the (TMP)Co$^{II}$• to organo-cobalt complexes as illustrated in figure 6C, then this is the condition where the control of radical polymerization uses a reversible termination mechanism (eq. 1) and the concentration of radicals in solution is derived exclusively from dissociation of organo-cobalt complex. The vanishingly small rate of polymerization from radicals that result from Co-R bond homolysis (Figure 6C) places an upper limit of ~10$^{-14}$ on the homolytic dissociation constant ($K_{dis}$(333K) < 10$^{-14}$) for organo-cobalt complexes formed by this system.

Downloaded by COLUMBIA UNIV on June 26, 2012 | http://pubs.acs.org
Publication Date: August 13, 2009 | doi: 10.1021/bk-2009-1024.ch008

Downloaded by COLUMBIA UNIV on June 26, 2012 | http://pubs.acs.org
Publication Date: August 13, 2009 | doi: 10.1021/bk-2009-1024.ch008

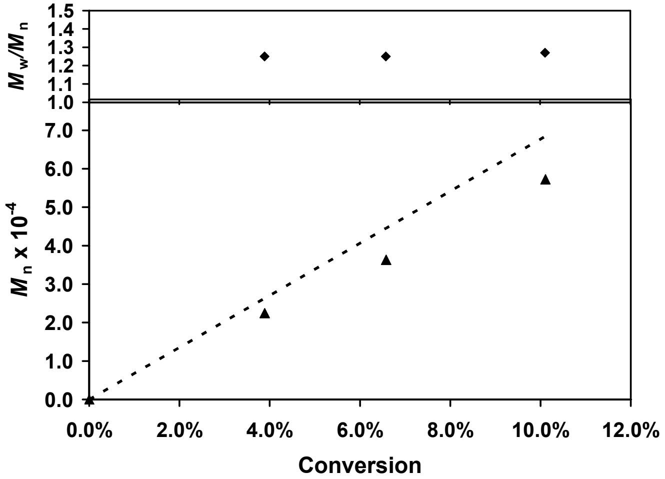

*Figure 7. Change in the number average molecular weight ($M_n$) (▲) and polydispersity ($M_w/M_n$) (◆) with conversion of vinyl acetate (VAc) to polyvinyl acetate (PVAc) at 333K in $C_6D_6$. $[VAc]_i = 5.42$ M; $[(TMP)Co^{II}]_i = 6.90\times10^{-4}$ M; $[V\text{-}70]_i = 8.00\times10^{-4}$ M. The dotted line is the theoretical line for one polymer chain per organo-cobalt complex.*

The polymerization process is observed to have living character during the period of relatively fast radical polymerization after the induction period (Figure 6A, B; Figure 7). At low vinyl acetate conversion, the number average molecular weight increases linearly with conversion and relatively small polydispersities are observed (Figure 7). The observed $M_n$ values approach the theoretical values for one living chain per organo-Co(TMP) unit, but deviations toward lower molecular weight regularly increase as the conversion increases.[4]

## Mechanisms of Cobalt Porphyrin Mediated Living Radical Polymerization

Cobalt tetramesityl porphyrin derivatives ($(TMP)Co^{II}\bullet$ and (TMP)Co-P) mediate the living radical polymerization (LRP) of acrylates[1-3] by complementary reversible termination (RT)[5,19-21] (eq. 1) and degenerative transfer (DT)[24-28] (eq. 2) pathways. Both RT and DT mechanisms utilize organo-cobalt porphyrin complexes ((TMP)Co-P) as the dormant species to store radicals for living radical polymerization. Fast interchange between the organic radicals in solution and in the dormant species gives a narrow molecular weight distribution for both pathways. Homolytic Co-C bond dissociation in the dormant complex ((TMP)Co-P) provides a dissociative route for radical exchange and controls the radical concentration in RT processes through the dissociation equilibrium constant ($K_{dis}$) ($[R\bullet] = (K_{dis}[(TMP)Co\text{-}P]/[(TMP)Co^{II}\bullet])$.

In a DT process there is a continual influx of radicals from an external radical source and the polydispersity is controlled by a near degenerate exchange of radicals between solution and the latent complex. The radical concentration in a DT process is primarily determined by the concentration of the external radical source (V-70, AIBN) and the rate constants for radicals to enter solution ($k_i$) and terminate ($k_t$) ($[R\bullet] = (k_i[I]/2k_t)^{1/2}$).

## Formation of Organo-Cobalt Complexes Through β-Hydrogen Transfer

When cyanoalkyl radicals (•C($CH_3$)(R)CN) are injected into a solution containing (TMP)$Co^{II}$• and acrylate or vinyl monomers, they can either add to monomer to form a monomer-based radical •CH(X)$CH_2$-C($CH_3$)(R)CN or react with (TMP)$Co^{II}$• to form a transient cobalt hydride (TMP)Co-H by β-H abstraction. (TMP)$Co^{II}$• reacts rapidly with the monomer-based radical to form (TMP)Co-CH(X)$CH_2$-C($CH_3$)(R)CN (Scheme 2A) and (TMP)Co-H adds with a monomer to produce an organometallic complex ((TMP)Co-CH(X)$CH_3$) (Scheme 2B).

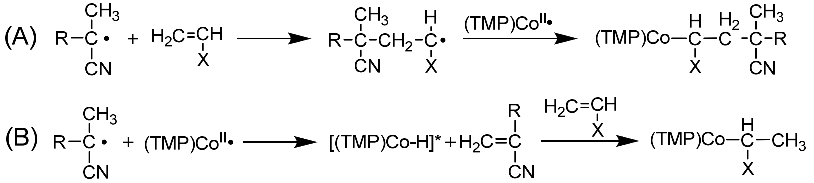

Scheme 2. *Alternate reactions of cyano radicals with (TMP)$Co^{II}$• and olefin monomers*

Addition of (TMP)Co-H to the double bond of acrylate or vinyl monomers produce the Markovnikov product ((TMP)Co-CH(X)$CH_3$) as the exclusive species observed in the $^1$H NMR (Scheme 2B). Concerted addition of (TMP)Co-H to $CH_2$=CH(X) is blocked by the porphyrin pyrrole nitrogen donors that occupy all of the *cis*-coordination sites adjacent to the Co-H unit. In benzene, the lowest energy stepwise pathway most likely involves hydrogen atom transfer to the olefin to give a radical pair that collapses to the organometallic complex. Kinetic preference for the Markovnikov product results from the relative stability of the two possible intermediate radicals •CH(X)$CH_3$ and •$CH_2CH_2$X. The enthalpy of isomerization from •CH(X)$CH_3$ to •$CH_2CH_2$X of +7 kcal mol$^{-1}$ (X=OC(O)$CH_3$) and +11 kcal mol$^{-1}$ (X=COO$CH_3$) computed at the Gaussian B3LYP 6-31G(d) level[29] is consistent with the high selectivity for (TMP)Co-CH(X)$CH_3$. The initially formed kinetic product (TMP)Co-CH(X)$CH_3$ is not observed to isomerize over extended periods of time in benzene and undoubtedly (TMP)Co-CH(X)$CH_3$ is also the thermodynamic product. The polarity of organo-metal bonds ($M^+R^-$) provides an electronic effect that gives a thermodynamic preference for placing the electron withdrawing group on the α-carbon[30] and the electronic effect in this case more than compensates for the

Downloaded by COLUMBIA UNIV on June 26, 2012 | http://pubs.acs.org
Publication Date: August 13, 2009 | doi: 10.1021/bk-2009-1024.ch008

increased steric repulsion. (TMP)Co-CH(X)$CH_3$ is thus both kinetically and thermodynamically preferred to (TMP)Co-$CH_2CH_2$X.

## Reversible Termination and Dissociative Radical Exchange illustrated by Methyl Acrylate Polymerization

Observation of organo-cobalt complexes formed in cobalt porphyrin mediated LRP of methyl acrylate (MA) by $^1$H NMR shows that the dominant reaction which occurs during the portion of the induction period when significant amounts of (TMP)$Co^{II}$• are present is the hydrogen abstraction from the cyano radicals to form a transient intermediate (TMP)Co-H. The cobalt hydride subsequently reacts with MA to produce (TMP)Co-CH($CO_2CH_3$)$CH_3$ (Co-MA) (Scheme 2B).

Scheme 3 outlines the alternative reaction pathways for (TMP)Co-CH($CO_2CH_3$)$CH_3$ (Co-MA) to mediate the polymerization process. Co-MA can transform to (TMP)Co-CH($CO_2CH_3$)$CH_2$CH($CO_2CH_3$)$CH_3$ (Co-$MA_2$) via the reversible termination (RT) pathway which occurs by the homolytic Co-C bond dissociation (Scheme 3A). Initiator radical capped organo-cobalt species (TMP)Co-CH($CO_2CH_3$)$CH_2$C($CH_3$)(R)CN (Co-MA-In) are formed through the associative interchange of the •MA-In radical with Co-MA which is associated with a degenerative transfer (DT) process (Scheme 3B).

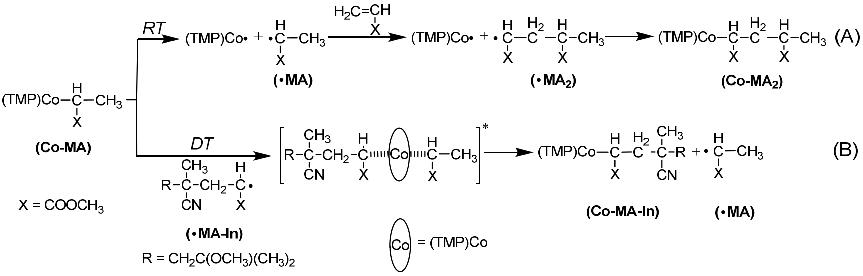

*Scheme 3. Organometallic formation and transformation through reversible termination (RT) and degenerative transfer (DT) pathways in the cobalt porphyrin mediated LRP of MA*

Kinetic studies using $^1$H NMR show that (TMP)Co-CH($CO_2CH_3$)$CH_2$CH($CO_2CH_3$)$CH_3$ (Co-$MA_2$) is the primary product during the induction period and thus homolytic dissociation is the more favorable route for controlled radical polymerization of methyl accrylate.

Downloaded by COLUMBIA UNIV on June 26, 2012 | http://pubs.acs.org
Publication Date: August 13, 2009 | doi: 10.1021/bk-2009-1024.ch008

Downloaded by COLUMBIA UNIV on June 26, 2012 | http://pubs.acs.org
Publication Date: August 13, 2009 | doi: 10.1021/bk-2009-1024.ch008

## Degenerative Transfer and Associative Radical Interchange illustrated by Vinyl Acetate Polymerization

The reversible termination pathway for cobalt porphyrin mediated LRP of vinyl acetate (VAc) is effectively quenched by the extremely small extent of homolytic dissociation that results from the relatively strong Co-CH(OAc)$CH_2$R bond. Associative interchange of radicals between solution and organo-cobalt complexes ((TMP)Co-P) provides an effective degenerative transfer route for living radical polymerization of VAc at 60°C.

Scheme 4 outlines the reactions that occur in the polymerization system containing (TMP)$Co^{II}$•, AIBN, and VAc during the early stage when substantial quantities of (TMP)$Co^{II}$• remain. Cyanoisopropyl radicals (•In′) experience a series of competitive reactions in the system containing (TMP)$Co^{II}$• and vinyl acetate which include initiating VAc polymerization (Scheme 4A), β-H transfer to form (TMP)Co-H (Scheme 4B), forming a weakly bonded organo-cobalt complex (Scheme 4C), and radical termination (Scheme 4D).

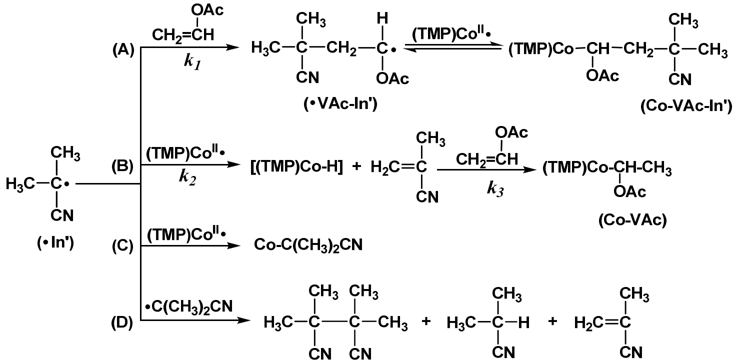
(A)
OAc
CH2=CH
k1
CH3 H
H3C—C—CH2—C•
CN OAc
(•VAc-In')
(TMP)CoII•
(TMP)Co—CH—CH2—C—CH3
OAc CN
(Co-VAc-In')
CH3
H3C—C•
CN
(•In')
(B)
(TMP)CoII•
k2
[(TMP)Co-H] + H2C=C(CH3)CN
CH2=CH(OAc)
k3
(TMP)Co-CH(OAc)-CH3
(Co-VAc)
(C)
(TMP)CoII•
Co-C(CH3)2CN
(D)
•C(CH3)2CN
H3C—C(CH3)(CN)—C(CH3)(CN)—CH3 + H3C—C(CH3)(CN)—H + H2C=C(CH3)CN

*Scheme 4. Alternate reactions of cyanoisopropyl radicals with (TMP)$Co^{II}$• and vinyl acetate during the induction period*

Scheme 5 illustrates several radical processes (propagation, exchange, and termination) that the cyanoisopropyl radical (•In′) goes through immediately following the induction period. After all of the (TMP)$Co^{II}$• is effectively converted to organo-cobalt complexes Co-VAc-In′ and Co-VAc, cyanoisopropyl radicals (•In′) from AIBN continue to flow into solution. The reactions of •In′ radical are limited to combining with the vinyl acetate monomer to form •VAc-In′ (Scheme 5A) and bimolecular termination (Scheme 5B) during this time period. The highly stabilized •C$(CH_3)_2$CN (•In′) radical

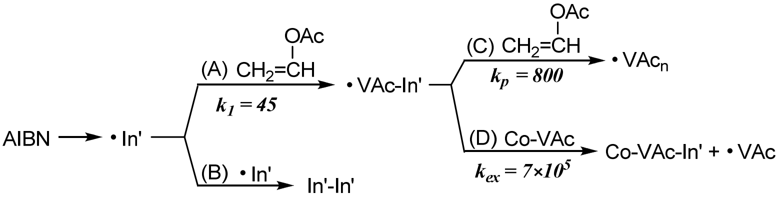

*Scheme 5. Radical propagation, exchange, and termination processes subsequent to the induction period.*

forms a weakly bonded organo-cobalt complex with (TMP)Co$^{II}$•[31] and thus is not expected to be effective in exchanging with the much more strongly bonded organo-cobalt complexes derived from the higher energy vinyl acetate radicals (•CH(OAc)CH$_2$P). The kinetics for transformation of the organo-cobalt species subsequent to the conversion of (TMP)Co$^{II}$• to organo-cobalt complexes depend on both the rate constant for reaction of the cyanoisopropyl radical (•In′) with VAc (k$_1$ in scheme 4A and 5A) (d[•VAc-In′]/dt = k$_1$[•In′][VAc]) and the rate constants for exchange of radicals in solution with the latent radicals in organo-Co(TMP) complexes (•P$_m$ + (TMP)Co-P$_n$ $\rightleftharpoons$ P$_m$-Co(TMP) + •P$_n$). The inter-conversion between organo-cobalt complexes (Co-VAc-In′, Co-VAc, Co-VAc$_2$ …, Co-VAc$_n$) after (TMP)Co$^{II}$• has been expended results from these radical exchange processes.

Figure 8 shows the quantitative evaluation of the transformation of (TMP)Co species with time for a representative polymerization process ([(TMP)Co$^{II}$•]$_i$ = 4.31×10$^{-4}$ M, [AIBN]$_i$ = 1.49×10$^{-2}$ M, and [VAc]$_i$ = 1.27 M). The kinetic simulations[32] shown in figure 8 use the kinetic model based on scheme 4 and equations 3-7. At the early induction period, complexes Co-VAc-In′ and Co-VAc are produced concomitant with the decrease of the (TMP)Co$^{II}$• concentration. The distribution of Co-VAc-In′ and Co-VAc depends on the relative rates of radical addition to monomer (Scheme 4A) and hydrogen atom transfer (Scheme 4B). At the end of induction period when the concentration of (TMP)Co$^{II}$• is approaching zero, the formation of dimer-cobalt complex (TMP)Co-CH(OAc)CH$_2$CH(OAc)CH$_3$ (Co-VAc$_2$) starts to be observed. The evolution and distribution of each organometallic species are dominated by the relative rates of radical interchange and monomer propagation (Figure 8).

Downloaded by COLUMBIA UNIV on June 26, 2012 | http://pubs.acs.org
Publication Date: August 13, 2009 | doi: 10.1021/bk-2009-1024.ch008

$$\bullet\text{In}' + \text{VAc} \xrightarrow{k_1} \bullet\text{VAc-In}' \qquad (3)$$

$$\bullet\text{VAc-In}' + \text{Co-VAc} \overset{k_4}{\rightleftharpoons} \text{Co-VAc-In}' + \bullet\text{VAc} \qquad (4)$$

$$\bullet\text{VAc} + \text{VAc} \xrightarrow{k_5} \bullet\text{VAc}_2 \qquad (5)$$

$$\bullet\text{VAc}_2 + \text{Co-VAc-In}' \overset{k_6}{\rightleftharpoons} \text{Co-VAc}_2 + \bullet\text{VAc-In}' \qquad (6)$$

$$\bullet\text{VAc}_2 + \text{Co-VAc} \overset{k_7}{\rightleftharpoons} \text{Co-VAc}_2 + \bullet\text{VAc} \qquad (7)$$

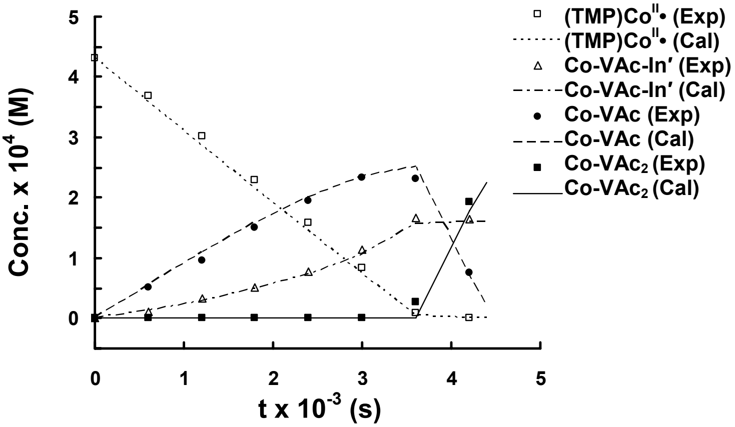

*Figure 8. Experimental points and calculated lines for the concentrations of (TMP)Co$^{II}$• and (TMP)Co-organo complexes during the early stage of the induction period. Initial concentrations: [AIBN]$_i$ = 1.49×10$^{-2}$M, [(TMP)Co$^{II}$•]$_i$ = 4.31×10$^{-4}$M, [VAc]$_i$ = 1.27M. Parameters used in the kinetic simulations for reactions at 333K can be found in reference 29.*

The observed kinetics of the formation of (TMP)Co-CH(OAc)CH$_2$-C(CH$_3$)$_2$CN (Co-VAc-In′) and (TMP)Co-CH(OAc)CH$_3$ (Co-VAc) from (TMP)Co$^{II}$• (-d[(TMP)Co$^{II}$•]/dt = k$_1$[•In′][VAc] + k$_2$[•In′][(TMP)Co$^{II}$•]) under conditions with different concentrations of VAc and (TMP)Co$^{II}$• provide an estimation of the k$_1$ to k$_2$ ratio ((k$_1$/k$_2$) = 9.0 ± 0.2×10$^{-5}$). Kinetic simulations shown in figure 8 have been done by using the ratio of k$_1$/k$_2$ (9.0×10$^{-5}$) as a constant while varying the absolute value for k$_1$ and k$_2$ and the radical exchange rate constants (k$_4$, k$_6$, and k$_7$). The change of the concentrations of Co-VAc-In′ and Co-VAc with time can only be reasonably fitted when the absolute value for k$_1$ was relatively small compared to k$_p$(VAc) (~800 M$^{-1}$ s$^{-1}$) and with rate constants for radical exchange greater than 7×10$^5$ M$^{-1}$ s$^{-1}$. The best simulation result (333K) shown as the lines in figure 8 was obtained by using k$_1$ = 45 M$^{-1}$ s$^{-1}$, k$_2$ = 5×10$^5$ M$^{-1}$ s$^{-1}$ and radical exchange rate constants k$_4$ = k$_7$ ≈ 7×10$^5$ M$^{-1}$ s$^{-1}$ and k$_6$ ≈ 5×10$^6$ M$^{-1}$ s$^{-1}$.

The similarity of the derived hydrogen atom transfer rate constant (k$_2$(333K) ~ 5×10$^5$ M$^{-1}$ s$^{-1}$) and the value of 4×10$^5$ M$^{-1}$ s$^{-1}$ reported for hydrogen transfer from methacrylonitrile oligomer radicals to cobalt(II) tetraphenyl porphyrin[33,34] provides the confidence in the kinetic analysis. The radical

Downloaded by COLUMBIA UNIV on June 26, 2012 | http://pubs.acs.org
Publication Date: August 13, 2009 | doi: 10.1021/bk-2009-1024.ch008

exchange rates are not uniquely determined by the kinetic analysis, but experimental data can only be reasonably fitted when the rate constants for near degenerate radical interchange reactions (eq. 4 and 7) are greater than $4\times10^5$ $M^{-1}$ $s^{-1}$ and less than $1\times10^6$ $M^{-1}$ $s^{-1}$. The agreement between simulation and experiment illustrated in figure 8 is obtained by using $k_4 = k_7 = 7\times10^5$ $M^{-1}$ $s^{-1}$. The rate constants deduced for radical exchange ($k_{ex}(333K) \sim 7\times10^5$ $M^{-1}$ $s^{-1}$) ($P_m\bullet$ + (TMP)Co-$P_n \rightleftharpoons$ $P_m$-Co(TMP) + $P_n\bullet$) in the (TMP)Co system are comparable to or larger than the values reported for exchange rates of radicals with dithioesters (RAFT)[24,35] and a series of organo main group species[36-38] that are observed to control living radical polymerization by degenerative transfer. The observed rate constants of the radical exchange processes in the organo-cobalt mediated LRP of VAc ($k_{ex}(333K) \sim 7\times10^5$ $M^{-1}s^{-1}$) are large enough to account for the relatively low polydispersities (Figure 6, 7).[4]

Methyl acrylate (MA) and vinyl acetate (VAc) polymerization mediated by cobalt(II) metallo-radicals (Co•) and organo-cobalt complexes (Co-R′) are used to illustrate the features of two LRP pathways of reversible termination (RT) and degenerative transfer (DT). Reactions of organic radicals with Co• produce a cobalt hydride (Co-H) via the β-hydrogen abstraction. Subsequent addition of the cobalt hydride with the olefin monomers produces organometallic complexes (Co-R′). Reversible homolysis of the organo-metal bond in the absence of β-H transfer gives the living radical polymerization (LRP) by a reversible termination (RT) mechanism. When the exchange of freely diffusing radicals in solution with the dormant organic units in organometallic complexes is fast, a LRP can occur by a degenerative transfer (DT) mechanism. Kinetic and thermodynamic properties for several of the central reactions are evaluated by following the time evolution of the $^1$H NMR for organo-cobalt porphyrin complexes.

Downloaded by COLUMBIA UNIV on June 26, 2012 | http://pubs.acs.org
Publication Date: August 13, 2009 | doi: 10.1021/bk-2009-1024.ch008

## References

1. Wayland, B. B.; Poszmik, G.; Mukerjee, S. L.; Fryd, M. *J. Am. Chem. Soc.* **1994,** *116*, 7943-7944.
2. Wayland, B. B.; Peng, C.-H.; Fu, X.; Lu, Z.; Fryd, M. *Macromolecules* **2006,** *39*, 8219-8222.
3. Peng, C.-H.; Fryd, M.; Wayland, B. B. *Macromolecules* **2007,** *40*, 6814-6819.
4. Peng, C.-H.; Scricco, J.; Li, S.; Fryd, M.; Wayland, B. B. *Macromolecules* **2008,** *41*, 2368-2373.
5. Poli, R. *Angew. Chem. Int. Ed.* **2006,** *45*, 5058-5070.
6. Maria, S.; Kaneyoshi, H.; Matyjaszewski, K.; Poli, R. *Chem. Eur. J.* **2007,** *13,* 2480-2492.
7. Debuigne, A; Caille, J-R.; Jèrôme, R. *Angew. Chem. Int. Ed.* **2005,** *44,* 1101-1104.
8. Debuigne, A; Willet, N.; Jèrôme, R.; Detrembleur, C. *Macromolecules* **2007,** *40,* 7111-7118.
9. Debuigne, A.; Champouret, Y.; Jérôme, R.; Poli, R.; Detrembleur, C. *Chem. Eur. J.* **2008,** *14,* 4046-4059.

10. Kaneyoshi, H.; Matyjaszewski, K. *Macromolecules* **2005,** *38,* 8163-8169.
11. Kaneyoshi, H.; Matyjaszewski, K. *J. Polym Sci. Part A: Polym. Chem.* **2007,** *45,* 447-459.
12. Kato, M.; Kamigaito, M.; Sawamoto, M.; Higashimura, T. *Macromolecules* **1995,** *28*, 1721-1723.
13. Wakioka, M.; Baek, K.-Y.; Ando, T.; Kamigaito, M.; Sawamoto, M. *Macromolecules* **2002,** *35,* 330-333.
14. Asandei, A. D.; Moran, I. W. *J. Am. Chem. Soc.* **2004**, *126*, 15932-15933.
15. Asandei, A. D.; Saha, G. *Macromolecules* **2006,** *39,* 8999-9009.
16. Shaver, M. P.; Allan, L. E. N.; Gibson, V. C. *Organometallics* **2007,** *26*, 4725-4730.
17. Halpern, J. *Polyhedron* **1988,** *7*, 1483-1490.
18. Ng, F. T. T.; Rempel, G. L.; Mancuso, C.; Halpern, J. *Organometallics* **1990,** *9*, 2762-2772.
19. Matyjaszewski, K.; Xia, J. H. *Chem. Rev.* **2001**, *101*, 2921-2990.
20. Kamigaito, M.; Ando, T.; Sawamoto, M. *Chem. Rev.* **2001,** *101*, 3689-3746.
21. Yoshikawa, C.; Goto, A.; Fukuda, T. *Macromolecules* **2003**, *36,* 908-912.
22. Iovu, M. C.; Matyjaszewski, K. *Macromolecules* **2003,** *36*, 9346-9354.
23. Chiefari, J.; Chong, Y. K.; Ercole, F.; Krstina, J.; Jeffery, J.; Le, T. P. T.; Mayadunne, R. T. A.; Meijs, G. F.; Moad, C. L.; Moad, G.; Rizzardo, E.; Thang, S. H. *Macromolecules* **1998**, *31*, 5559-5562.
24. Moad, G.; Rizzardo, E.; Thang, S. H. *Aust. J. Chem.* **2005**, *58*, 379-410.
25. Müller, A. H. E.; Yan, D.; Litvinenko, G.; Zhuang, R.; Dong, H. *Macromolecules* **1995**, *28,* 7335-7338.
26. Goto, A.; Kwak, Y.; Fukuda, T.; Yamago, S.; Iida, K.; Nakajima, M.; Yoshida, J. *J. Am. Chem. Soc.* **2003**, *125*, 8720-8721.
27. David, G.; Boyer, C.; Tonnar, J.; Ameduri, B.; Lacroix-Desmazes, P.; Boutevin, B. *Chem. Rev.* **2006**, *106*, 3936-3962.
28. Asandei, A. D.; Moran, I. W.; Saha, G.; Chen, Y. *J. Polym. Sci., Polym. Chem.* **2006**, *44*, 2015-2026.
29. Li, S.; de Bruin, B.; Peng, C.-H.; Fryd, M.; Wayland, B. B. *J. Am. Chem. Soc.* **2008**, *130,* 13373-13381.
30. Harvey, J. N. *Organometallics* **2001,** *20,* 4887-4895.
31. Woska, D. C; Xie, Z. D; Gridnev, A. A.; Ittel, S. D.; Fryd, M.; Wayland, B. B. *J. Am Chem. Soc.* **1996,** *118,* 9102-9109.
32. The simulation program, MacKinetics v0.9.1, was generously provided by Dr. Walter S. Leipold III.
33. Gridnev, A. A.; Ittel, S. D. *Chem. Rev.* **2001,** *101*, 3611-3660.
34. Gridnev, A. A.; Ittel, S. D. *Macromolecules* **1996**, *29*, 5864-5874.
35. Goto, A.; Sato, K.; Tsujii, Y.; Fukuda, T.; Moad, G.; Rizzardo, E.; Tang, S. H. *Macromolecules* **2001**, *34*, 402-498.
36. Kwak, Y.; Goto, A.; Fukuda, T.; Kobayashi, Y.; Yamago, S. *Macromolecules* **2006**, *39,* 4671-4679.
37. Goto, A.; Ohno, K.; Fukuda, T. *Macromolecules* **1998**, *31*, 2809-2814.
38. Kwak, T.; Goto, A.; Fukuda, T.; Yamago, S.; Ray, B. *Z. Phys. Chem.* **2005,** *219,* 283-293.

Downloaded by COLUMBIA UNIV on June 26, 2012 | http://pubs.acs.org
Publication Date: August 13, 2009 | doi: 10.1021/bk-2009-1024.ch008

Downloaded by UNIV OF GUELPH LIBRARY on June 26, 2012 | http://pubs.acs.org
Publication Date: August 13, 2009 | doi: 10.1021/bk-2009-1024.ch009

## Chapter 9

# Key Role of Metal-Coordination in Cobalt-Mediated Radical Polymerization of Vinyl Acetate

**Antoine Debuigne[1,*], Rinaldo Poli[2,3*], Robert Jérôme[1], Christine Jérôme[1], Christophe Detrembleur[1]**

**[1] Center for Education and Research on Macromolecules (CERM), University of Liège (ULG), Sart-Tilman, B6A, 4000 Liège, Belgium.**
**[2] Laboratoire de Chimie de Coordination, UPR CNRS 8241, and University of Toulouse; UPS, INPT; 31077 Toulouse, France. [3]Institut Universitaire de France, 103 bd Saint-Michel, 75005 Paris, France**

Cobalt mediated radical polymerization (CMRP) of vinyl acetate (VAc) follows a reversible termination mechanism when initiated from a preformed alkyl-cobalt(III) complex. In these particular conditions, CMRP functions as a stable free radical process and fine tuning of the Co-C bond strength becomes crucial. Increase of temperature and addition of molecules, such as water, dimethylformamide and dimethylsulfoxide, able to coordinate the cobalt complex appeared as efficient strategies to weaken the Co-C bond and thus to speed up the polymerization while maintaining a very good control of the VAc polymerization. The key role of metal-coordination was investigated by kinetic measurements combined with DFT calculations.

In Controlled/Living Radical Polymerization: Progress in RAFT, DT, NMP & OMRP; Matyjaszewski, K.;
ACS Symposium Series; American Chemical Society: Washington, DC, 2009.

Controlled radical polymerization (CRP)[1] has become a powerful technique to prepare polymers with predictable and well-defined molecular parameters. The most popular techniques are nitroxide-mediated radical polymerization (NMP),[2-4] atom transfer radical polymerization (ATRP)[5-7] and radical addition fragmentation chain transfer (RAFT)[8,9]. However, other systems have also proved their efficiency in CRP and opened new opportunities for macromolecular engineering, which justifies that efforts are still devoted to their developement. Cobalt-mediated radical polymerization (CMRP) is one of them.

Since its discovery in 1994 by Wayland [10,11] and Harwood,[12,13] CMRP has constantly developed and provides today a very high level of control for a range of vinyl monomers including acrylates,[10-15] acrylonitrile (AN)[16,17] and vinyl acetate (VAc).[18-24] Cobalt porphyrins are particularly efficient for acrylates, whereas bis(acetylacetonato)cobalt(II) ($Co(acac)_2$) has established itself as the complex of choice for VAc and AN. Besides optimizing the experimental conditions, many efforts were devoted to investigating the CMRP mechanism. Initially, the process was only considered as a stable free radical polymerization (SFRP), the cobalt complex playing the role of counter radical according to eq. 1. Under this assumption, the rate of Co-C bond cleavage at the polymer chain end relative to the back reaction regulates the equilibrium between dormant and active species ($K=[Co^{II}][P°]/[P\text{-}Co^{III}]$). More recently, a predominant contribution of a degenerative chain transfer (DT) mechanism was highlighted when an excess of radicals relative to cobalt is present in the medium.[19,21,25] The release of the radical polymer chains from the $P\text{-}Co^{III}$ complex is driven by the attack of another radical polymer chain on the cobalt free coordination site, as depicted by equation 2. These conclusions were drawn for both cobalt porphyrins and bis(diketonato)cobalt complexes. In the particular case of VAc, such a dual behavior was confirmed by using a preformed alkyl-bis(acetylacetonato)cobalt(III) complex as CMRP initiator. Indeed, when initiated at 30°C in bulk by the alkylcobalt(III) complex, the VAc polymerization proceeds very slowly. However, when this CMRP initiator was treated with additional free azo-initiator (V-70), a fast and well controlled VAc polymerization took place. Finally, as shown in equation 3, it was demonstrated that lewis bases (L), such as water or pyridine, can occupy the free coordinating sites of the cobalt(II) and cobalt(III) species, which prevents the DT mechanism to occur.[19,21] Under these conditions, the polymerization follows a reversible termination (RT) process and is considerably faster than polymerization conducted without additives while the control is not affected .

Downloaded by UNIV OF GUELPH LIBRARY on June 26, 2012 | http://pubs.acs.org
Publication Date: August 13, 2009 | doi: 10.1021/bk-2009-1024.ch009

$$P{-}[Co^{III}] \rightleftharpoons P^{\circ} + [Co^{II}] \qquad \text{eq. 1}$$

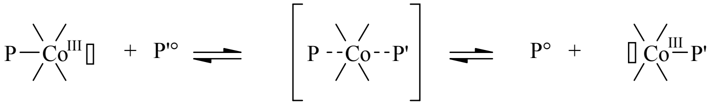
eq. 2

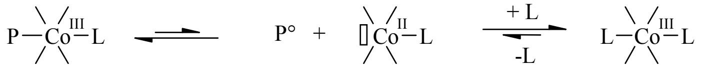
eq. 3

In this paper, we propose to focus on the CMRP of VAc conducted in the RT regime, thus in the absence of additional azo-initiator. The adjustment of Co-C bond strength has been investigated in detail. Among other things, the effect of temperature as well as amount and nature of the Lewis base additive have been examined. For example, dimethylformamide (DMF) and dimethylsulfoxide (DMSO) have been used for the first time as additive for the CMRP of VAc. DFT calculations are used to rationalize the kinetic results and to draw conclusions on the key role played by metal-coordination with these molecules.

## Experimental Section

### Materials.

Vinyl acetate (>99%, Aldrich) was dried over calcium hydride, degassed by several freeze-pump-thaw cycles before being distilled under reduced pressure and stored under argon. Dimethylsulfoxide (DMSO) was dried over calcium hydride before being distilled under reduced pressure and stored under argon. Dimethylformamide (DMF) and dichloromethane ($CH_2Cl_2$) were dried over molecular sieves and degassed by bubbling argon for 30 minutes. Doubly distilled water was degazed by several freeze-pump-thaw cycles. 2,2'-Azo-bis-(4-methoxy-2,4-dimethyl valeronitrile) (V-70) (Wako), bis(acetyl-acetonato)cobalt(II) ($Co(acac)_2$) (>98%, Acros) and 2,2,6,6-tetramethyl-piperidine 1-oxy (TEMPO) (98%, Aldrich) were used as received.

### Characterizations.

$^1H$ NMR spectra were recorded with a Bruker AM 250 Spectrometer (250 MHz) in deuterated chloroform. Inductively Coupled Plasma Mass Spectrometry (ICPMS) was carried out with a Spectrometer Elan DRC-e Perkin Elmer SCIEX. Samples were prepared according to the following procedure: evaporation of 1 ml of the cobalt adduct stock solution in dichloromethane, treatment of the residue by $HNO_3$ (65%) at 60°C for 2 h, dilution with 250 ml of doubly distilled water. Size exclusion chromatography (SEC) of poly(vinyl acetate) was carried out in THF (flow rate : 1 mL $min^{-1}$) at 40 °C with a Waters

Downloaded by UNIV OF GUELPH LIBRARY on June 26, 2012 | http://pubs.acs.org
Publication Date: August 13, 2009 | doi: 10.1021/bk-2009-1024.ch009

600 liquid chromatrograph equipped with a Waters 410 refractive index detector and styragel HR columns (four columns HP PL gel 5µm $10^5$ Å, $10^4$ Å, $10^3$ Å, $10^2$ Å) using a PS calibration.

### Preparation of the alkylcobalt(III) complex used as CMRP initiator.

The procedure for the synthesis as well as the complete characterization of the low molecular weight cobalt(III) adduct are described in detail in a recent paper.[19] As a rule, this cobalt adduct contains less than 4 vinyl acetate units on average end-capped by the $Co(acac)_2$ complex ($[Co(acac)_2(-CH(OCOCH_3)CH_2)_{<4}-R_0]$); $R_0$ being the primary radical generated by V-70). The complex was stored as a $CH_2Cl_2$ solution at -20°C under argon. The cobalt concentration of the stock solution was estimated as 0.152 M by inductively coupled plasma mass spectrometry (ICP-MS).

Downloaded by UNIV OF GUELPH LIBRARY on June 26, 2012 | http://pubs.acs.org
Publication Date: August 13, 2009 | doi: 10.1021/bk-2009-1024.ch009

### Polymerization procedures.

In a round bottom flask capped by a three-way stopcock and purged by three vacuum-argon cycles, 1 ml of the alkylcobalt(III) complex stock solution ([Co] = 0.152 M, 0.152 mmol) was introduced and evaporated to dryness under reduced pressure. The compound was then dissolved in distilled and degassed VAc (5.00 ml, 4.67 g, 54.2 mmol) under argon. The reaction mixture was then stirred at 30°C. Samples were regularly withdrawn from the medium and added with TEMPO in order to quench the polymerization. The VAc conversion and the molecular parameters of the PVAc were determined by gravimetry and SEC (THF, cal. PS) analysis, respectively. The same experiment was repeated at 40°C, 50°C and 60°C (Figure 1) but also at 30°C in the presence of degassed additives such as water (Figure 3), dimethylsulfoxide and dimethylformamide (Figure 4). In the last two cases, the monomer conversion was monitored by $^1H$ NMR.

### Computational details.

All geometry optimizations were performed with the Gaussian03 suite of programs.[26] The same functional and basis functions used in the previous study[17] were adopted for the new calculations in order to directly compare the energetics. Specifically, geometries were optimized with the B3LYP functional and the energy was obtained at this fixed geometry by use of the B3PW91* functional, which is a modified version of the B3PW91 functional with the $c_3$ coefficient changed to 0.15.[27] All energies were corrected for zero point vibrational energy and for thermal energy to obtain the bond dissociation enthalpies at 298 K. The standard approximations for estimating these corrections were used (ideal gas, rigid rotor and harmonic oscillator) as implemented into Gaussian03. The unrestricted formulation was used for open-shell molecules. All geometry optimizations were carried out without any symmetry constraint and all final geometries were characterized as local minima of the potential energy surface (PES) by verifying that all second derivatives of the energy were positive. The value of $<S^2>$ at convergence was very close to the expected value of 0.75 for the radical species and 3.75 for the spin quartet species [the greatest deviation was 3.760 for complex $Co(acac)_2(DMSO)_2$], indicating minor spin contamination.

Downloaded by UNIV OF GUELPH LIBRARY on June 26, 2012 | http://pubs.acs.org
Publication Date: August 13, 2009 | doi: 10.1021/bk-2009-1024.ch009

# Results and Discussion

Recently, we reported the synthesis and isolation of a low molecular weight oligomeric alkyl-cobalt(III) compound which mimics the dormant species of the CMRP of VAc, i.e. PVAc-$Co(acac)_2$.[19] Typically, $Co(acac)_2$ was reacted for several hours with V-70 in VAc at 30°C. The reaction was stopped before any polymerization was observed. The in-situ formed alkyl-cobalt(III) species was then isolated by chromatography under an inert atmosphere and identified as $Co(acac)_2$-capped PVAc oligomers with less than four VAc units on average [$Co(acac)_2(-CH(OCOCH_3)CH_2)_{<4}-R_0$, $R_0$ being V-70 fragment]. This compound was further used as CMRP initiator for VAc[19] but also AN[17]. No induction period was observed in these cases. Importantly, the recovered alkyl-cobalt(III) species was purified from undecomposed V-70 before use, which offers the possibility to polymerize VAc in a pure reversible-termination regime, governed by the thermal cleavage of the Co-C bond. The latter is influenced by different factors, as discussed below.

## Effect of Temperature

Since the Co-C bond cleavage is a thermal process, it is quite obvious to investigate CMRP at different temperatures. The bulk radical polymerization of VAc initiated by V-70 in the presence of $Co(acac)_2$ ($[V70]/[Co(acac)_2]= 3.25$) at higher temperature (50°C instead of 30°C) was already reported.[24] In that case, the polymerization was faster but the controlling ability was negatively affected, as signalled by significantly increased molar mass distributions ($M_w/M_n \sim 1.3$-$1.6$). This deleterious effect might be due to transfer reaction to monomer whose contribution increases with temperature. Another reason for the loss of control observed at 50°C could be the very fast decomposition of the excess of azo-initiator resulting in the occurrence of irreversible termination reactions. Indeed, for a proper control in the DT regime, only tiny amounts of radicals need to be continuously generated in order to sustain the controlled polymerization process.

Consequently, the effect of temperature on the course of the CMRP should ideally be investigated in a reversible-termination regime, thus without additional V-70 that might interfere with the process at higher temperatures. For this reason, the VAc polymerization was carried out in bulk using the preformed $Co(acac)_2(-CH(OCOCH_3)CH_2)_{<4}-R_0$ oligomeric complex as initiator at temperatures ranging from 30°C to 60°C (Figure 1).

In agreement with previously reported results, the polymerization conducted at 30°C was controlled but extremely slow.[19] Indeed, the PVAc molar mass increased with the monomer conversion, chromatograms regularly shifted towards higher molar masses with the time (Figure 2), and the molar mass distribution was low ($M_w/M_n$~1.1). However, only a 13% monomer conversion was obtained after 7 h. The slow consumption of the monomer accounts for a quite stable Co-C bond at this temperature. As reported elsewhere and discussed in the last section of this manuscript, intramolecular chelation of the metal by the ester function of the last PVAc unit leads to formation of a 5 member-ring complex which strengthens the metal-carbon bond.[19]

In order to activate the cleavage of the cobalt-carbon bond and thus increase the rate of the polymerization, higher temperatures were tested (40°C, 50°C and 60°C). As expected, the polymerization was faster at higher temperatures, as indicated by the increase of the slope of the time dependence of $\ln[M]_0/[M]$ with the temperature (See figure 1a). At 40°C, VAc conversion reached 50% after 7 h whereas the same monomer conversion was obtained after only 2.5 h and 40 min at 50°C and 60°C, respectively. The thermal activation of Co-C bond cleavage effectively allows to speed up the CMRP process by displacement of the equilibrium ($K=[Co^{II}][P°]/[P\text{-}Co^{III}]$) towards the active species. This achievement is all the more important since the increase of the polymerization rate does not negatively affect the level of control. Indeed, whatever the temperature, the molar masses increase linearly with the monomer conversion and are relatively close to the theoretical prediction calculated based on the $[VAc]_0/[Co(acac)_2(\text{-}CH(OCOCH_3)CH_2)_{<4}\text{-}R_0]_0$ initial molar ratio. The observed deviations from ideality could be due to the high sensitivity of the alkylcobalt(III) initiator which partially deactivates during the process. Moreover, the molar mass distribution remains as low as 1.1. Nevertheless, it must be noted that bimodal distributions were observed beyond 65% monomer conversion, especially at 60°C. This observation suggests that significant termination occurs by coupling reactions at this temperature and high monomer conversion.

Downloaded by UNIV OF GUELPH LIBRARY on June 26, 2012 | http://pubs.acs.org
Publication Date: August 13, 2009 | doi: 10.1021/bk-2009-1024.ch009

Downloaded by UNIV OF GUELPH LIBRARY on June 26, 2012 | http://pubs.acs.org
Publication Date: August 13, 2009 | doi: 10.1021/bk-2009-1024.ch009

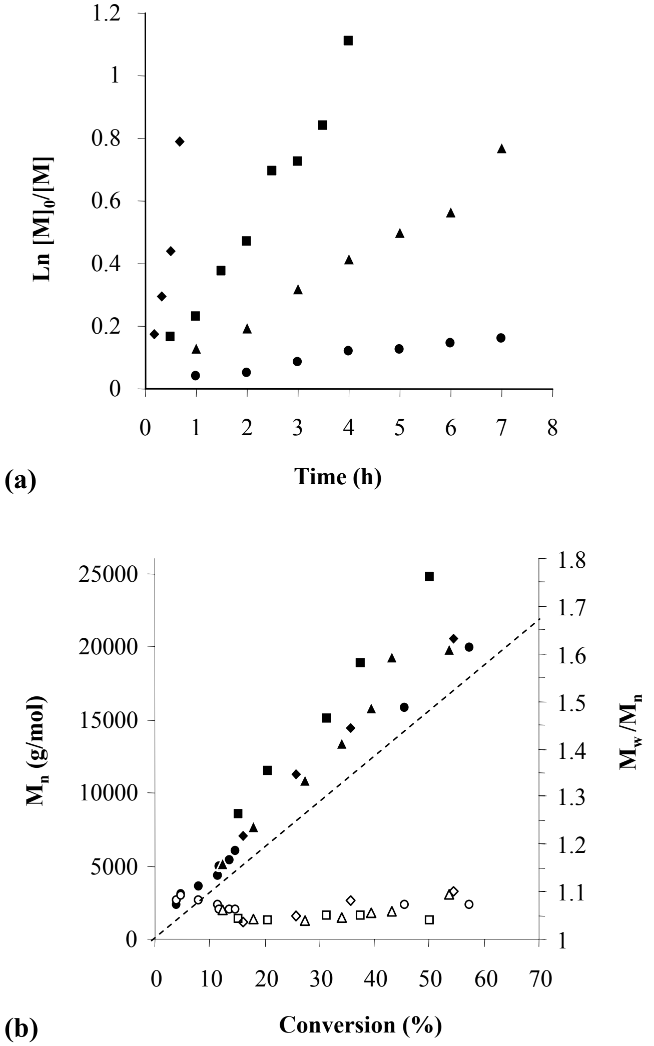

*Figure 1. (a) Time dependence of ln[M]$_0$/[M] (M: monomer); (b) dependence of the PVAc molar mass (M$_n$, full symbols) and molar mass distribution (M$_w$/M$_n$, hollow symbols) on the monomer conversion for the VAc polymerization initiated in bulk by an alkylcobalt(III) complex at various temperatures. [Co(acac)$_2$(-CH(OCOCH$_3$)CH$_2$)$_{<4}$-R$_0$)]$_0$/[VAc]$_0$ = 358. (●) 30°C,(▲) 40°C,(■) 50°C,(♦) 60°C. The dotted line represents the theoretical dependence of the molar mass vs conversion.*

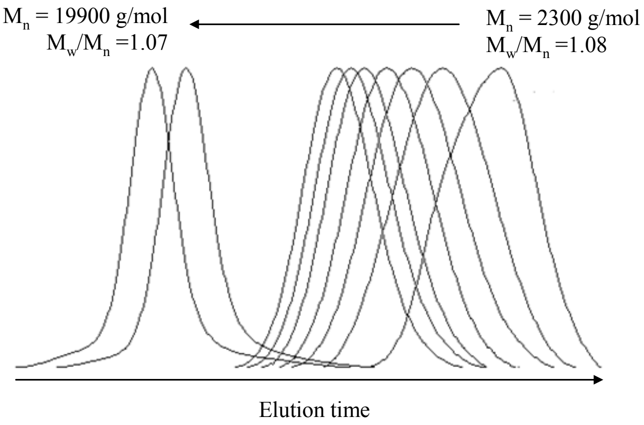

*Figure 2. SEC chromatograms for the VAc polymerization initiated in bulk by an alkylcobalt(III) complex at 30°C.* $[Co(acac)_2(\text{-}CH(OCOCH_3)CH_2)_{<4}\text{-}R_0)]_0/[VAc]_0 = 358$.

In summary, such a fast and controlled polymerization at 60°C is only possible in the reversible-termination regime using a preformed CMRP initiator free of V-70. Indeed, under degenerative chain transfer conditions, the excess of V-70 would decompose very rapidly at 60°C and generate a massive amount of radicals, which interfere with the control process.

## Effect of Water on CMRP of VAc

The beneficial effect on the polymerization kinetic of Lewis base additives has already been demonstrated.[19,21] Indeed, ligation of pyridine or water molecules on the free coordination site of the alkyl-Co(acac)$_2$ complex allows to activate the CMRP process and thus increases the polymerization rate while maintaining an excellent control of the VAc polymerization.[19]

The polymerization of VAc initiated at 30°C by the Co(acac)$_2$(-CH(OCOCH$_3$)CH$_2$)$_{<4}$-R$_0$ complex was studied in the presence of various amounts of water. In all experiments, the same [VAc]/[Co] molar ratio was used. From Figure 3a, it clearly appears that the polymerizations realized in the presence of water were faster than the reference experiment without any additives and still obeyed first order kinetics. Moreover, the increase of the polymerization rate was higher when higher concentration of water was used relative to the metal. For example, when a 120 fold excess of water was used compare to cobalt, the monomer conversion reaches 55% in 4 h at 30°C whereas only 10% conversion was observed in absence of additive in the same time interval.

From the molecular parameters point of view, similar molar masses were expected in all these experiments for a given conversion since the [VAc]/[R-Co$^{III}$] molar ratio was constant. In line with this expectation, all experiments showed the same trend with the monomer conversion and the molar masses were

Downloaded by UNIV OF GUELPH LIBRARY on June 26, 2012 | http://pubs.acs.org
Publication Date: August 13, 2009 | doi: 10.1021/bk-2009-1024.ch009

close to the theoretical prediction calculated on the basis of the monomer/initiator ratio (Figure 3b), the largest deviation being observed when 60 equivalents of water was used relative to the metal. In all these experiments, the collected PVAc samples were very well-defined, with molar mass distributions lower than 1.1. Interestingly, when water was added to activate the CMRP process, monomodal molar mass distributions were observed even beyond 60% monomer conversion, contrary to the experiments carried out at higher temperatures without additive (cfr previous section). Typically, in the experiment using a 120-fold excess of water relative to the cobalt complex initiator, polymers with molar distributions as low as 1.10 were collected (Mn = 27000 g/mol, 91%, 24 h).

These experiments confirm that addition of water to the CMRP medium is an efficient approach to speeding up the polymerization of VAc at low temperature (30°C) while maintaining a good level of control. As discussed in details in the last section, added water can compete with the intramolecular chelation of the ester group of the last monomer unit in the dormant species. The resulting alkyl-cobalt(III) complex ligated by water can undergo Co-C bond cleavage with release of the growing radical chain and $Co(acac)_2(H_2O)$ (see equation 3, where $L = H_2O$). The latter can further react with water and form $Co(acac)_2(H_2O)_2$, which shifts the CMRP equilibrium towards the actives species and leads to higher polymerization rates.

Although it clearly appears that rates are higher when more water is added, it must be mentioned that there is a limit to this strategy. Indeed, if a very large amount of water is used, the system might become heterogeneous. In this case, contribution of metal-coordination to the increase of the polymerization rate becomes minor relative to the diffusion of the controlling agent ($Co(acac)_2$) out of the VAc phase (the polymerization locus) towards the aqueous phase, as highlighted in a previous study.[19,20]

Downloaded by UNIV OF GUELPH LIBRARY on June 26, 2012 | http://pubs.acs.org
Publication Date: August 13, 2009 | doi: 10.1021/bk-2009-1024.ch009

Downloaded by UNIV OF GUELPH LIBRARY on June 26, 2012 | http://pubs.acs.org
Publication Date: August 13, 2009 | doi: 10.1021/bk-2009-1024.ch009

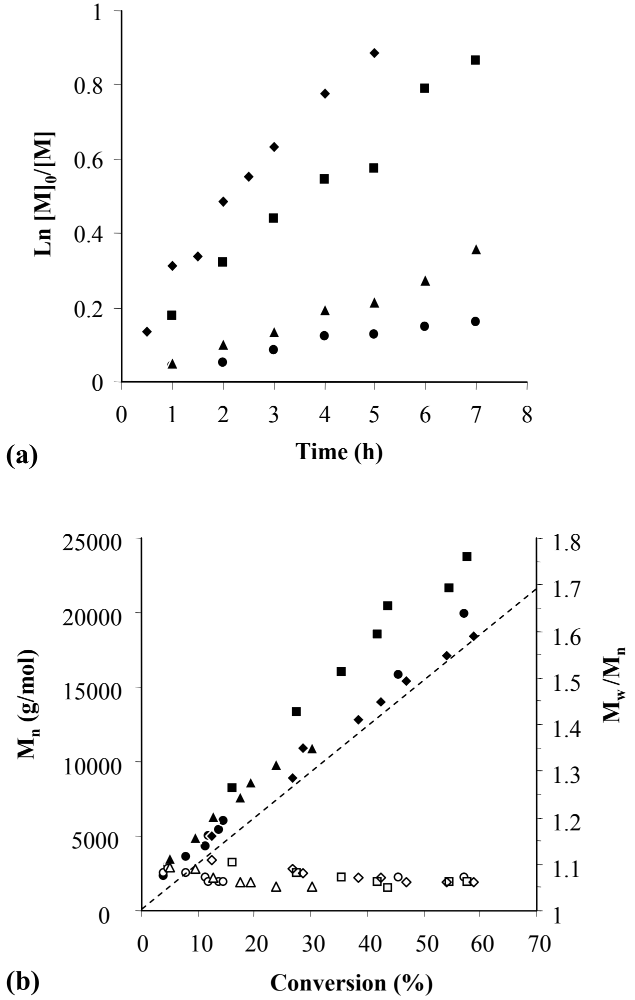

*Figure 3. (a) Time dependence of ln[M]$_0$/[M] (M: monomer); (b) dependence of the PVAc molar mass ($M_n$, full symbols) and molar mass distribution ($M_w/M_n$, hollow symbols) on the monomer conversion for the VAc polymerization initiated at 30°C by an alkylcobalt(III) complex in the presence of various amounts of water. $[Co(acac)_2(-CH(OCOCH_3)CH_2)_{<4}-R_0)]_0/[VAc]_0 = 358$. (●) no additive (▲) $[H_20]_0/[R-Co^{III}]_0=30$,(■) $[H_20]_0/[R-Co^{III}]_0=60$,(♦) $[H_20]_0/[R-Co^{III}]_0=120$. The dotted line represents the theoretical dependence of the molar mass vs conversion.*

## Effect of DMF and DMSO

Since coordination of the cobalt complex by water molecules has a drastic effect on the Co-PVAc bond strength, we investigated other molecules likely to play similar role and activate the CMRP of VAc. In this respect, previous study showed that both dimethylformamide and dimethylsulfoxide can interact with $Co(acac)_2$ via their oxygen leading to the corresponding *trans*-octahedral cobalt complexes ($Co(acac)_2L_2$, with L=DMF or DMSO)[17]. Although the beneficial effect of these additives on the CMRP of AN has already been demonstrated,[16,17,20] the impact of these molecules on the course of the CMRP of VAc has never been studied. For this reason, the polymerization of VAc was initiated at 30°C from the akyl-cobalt(III) initiator in the presence of DMF and DMSO. For these experiments, the [VAc]/[Co] and the [ligand]/[cobalt] molar ratios were maintained constant and equal to 358 and 60, respectively (see Figure 4).

The VAc polymerization always proceeded in a controlled manner when water was replaced by DMF or DMSO. In both cases, the molar masses increased linearly with the monomer conversion in an almost perfect agreement with the theoretical curve (Figure 4b). Again, the PVAc molar mass distributions were low (~1.1) up to 60% of monomer conversion. Moreover, in the presence of DMSO, the polymerization of VAc was monitored until 86% monomer conversion and the recovered PVAc was still well-defined ($M_n$= 28700 g/mol, $M_w/M_n$ = 1.15). The polymerization rate varies in the order $H_2O$ > DMSO > DMF > no additive. DMSO appeared almost as efficient as water to activate the CMRP whereas only a very slight increase of the polymerization rate was obtained upon addition of DMF. The last section is devoted to the rationalization of these kinetic observations by DFT calculations. A close link between the ability of these ligands to activate the CMRP process and their ligation power was evidenced.

Downloaded by UNIV OF GUELPH LIBRARY on June 26, 2012 | http://pubs.acs.org
Publication Date: August 13, 2009 | doi: 10.1021/bk-2009-1024.ch009

Downloaded by UNIV OF GUELPH LIBRARY on June 26, 2012 | http://pubs.acs.org
Publication Date: August 13, 2009 | doi: 10.1021/bk-2009-1024.ch009

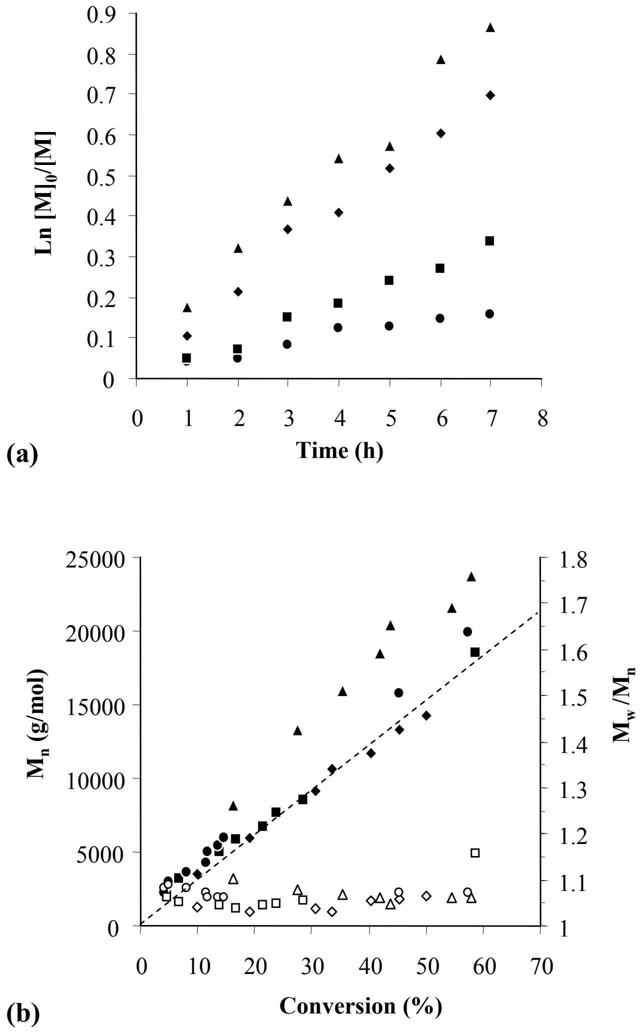

*Figure 4. (a) Time dependence of* $\ln[M]_0/[M]$ *(M: monomer); (b) dependence of the PVAc molar mass* ($M_n$*, full symbols) and molar mass distribution* ($M_w/M_n$*, hollow symbols) on the monomer conversion for the VAc polymerization initiated at 30°C by an alkylcobalt(III) complex in the presence of various additives.* $[Co(acac)_2(\text{-}CH(OCOCH_3)CH_2)_{<4}\text{-}R_0)]_0/[L]_0/[VAc]_0 = 1/60/358$*. (●) no additive (▲) L=*$H_20$*, (■) L=DMF, (♦) L=DMSO. The dotted line represents the theoretical dependence of the molar mass vs conversion.*

## DFT Calculation.

As previously reported, the [Co(acac)$_2$(-CH(OCOCH$_3$)CH$_2$)$_{<4}$-R$_0$] initiator, as well as the subsequent Co(acac)$_2$-capped polymer, [Co(acac)$_2$(PVAc)], can be satisfactorily simplified to the [Co(acac)$_2$(CH(OCOCH$_3$)CH$_3$)] model complex for computational purposes.[19] Replacement of the oligomeric or polymeric chain beyond the Co-bonded first monomer unit by an H atom is not expected to affect the calculated bond enthalpy values. Since Co$^{III}$ is known to have a strong preference for an octahedral coordination and since the Co-bonded VAc unit has a potentially coordinating ester function with the carbonyl O atom suitably placed 4 bonds away from the metal atom, intramolecular coordination of this carbonyl function to yield a 5-member chelate ring stabilized the system by 3.0 kcal mol$^{-1}$ in enthalpy at the chosen computational level. The preferred conformation of the ring-opened isomer is a square pyramid with the alkyl chain occupying the axial position and with the two chelating acetylacetonate ligands in the equatorial plane, as shown in Figure 5.

In the absence of Lewis base additives, the degenerate transfer pathway of controlled polymerization can easily take place from this 5-coordinate intermediate by addition of the free radical at the vacant site, *trans* to the Co$^{III}$-alkyl bond. The reversible termination pathway, on the other hand, requires cleavage of the Co$^{III}$ bond to yield the free radical and tetrahedral [Co(acac)$_2$], which costs an additional 10.0 kcal mol$^{-1}$. Thus, thermal activation of the [Co(acac)$_2$(PVAc)] dormant state requires 13.0 kcal mol$^{-1}$ according to the calculations on this model system.

The presence of Lewis bases (L) in the medium completely perturbs the above picture by diverting the system toward the formation of *trans*-[Co(acac)$_2$(PVAc)(L)] adducts, thus blocking the 6th coordination site on Co$^{III}$ and shutting down the DT pathway. Optimization of the *trans*-[Co(acac)$_2$(CH(OCOCH$_3$)CH$_3$)(L)] models with the L ligands of interest in this study (DMF, DMSO, H$_2$O), gives binding energies of 7.0, 3.8 and 11.3 kcal mol$^{-1}$, respectively (see Figure 5). Note that DMSO establishes a weaker bond than DMF to this Co$^{III}$ system. This difference does not appear to have an electronic origin, since DMSO is known as a slightly better base than DMF (donor numbers of 29.8 and 26.6, respectively).[28] Rather, it is probably caused by a greater steric repulsion between the acetylacetonato ligands and the SMe$_2$ group of DMSO, which carries three electron densities (the two Me groups and the S lone pair), relative to the CH(NMe$_2$) group of DMF. This steric difference is felt strongly by this system since the electronic contribution is weak (low bond strengths).

Since the 6th coordination position is now blocked by L coordination, radical polymerization may only occur by homolytic cleavage of the Co$^{III}$-alkyl bond. This process produces first a 5-coordinate [Co$^{II}$(acac)$_2$(L)] complex, together with the free radical. However, a second L molecule can saturate the coordination site left open by the radical dissociation, yielding [Co$^{II}$(acac)$_2$(L)$_2$]. Previous calculations[19,21] have shown that the 5-coordinate complex adopts a trigonal bipyramidal geometry with L occupying an equatorial position and the acac ligands spanning the angles between one equatorial and one axial position, as shown in Figure 5. The 6-coordinate Co$^{II}$ complex, on the other hand, adopts

Downloaded by UNIV OF GUELPH LIBRARY on June 26, 2012 | http://pubs.acs.org
Publication Date: August 13, 2009 | doi: 10.1021/bk-2009-1024.ch009

an octahedral *trans* structure, as also confirmed by the isolation of [$Co^{II}(acac)_2(DMSO)_2$] and by its single crystal X-ray diffraction study.[17] The energetic results of the calculations, illustrated in Figure 5, show that the relative stability of both the 5-coordinate [$Co^{II}(acac)_2(L)$] and the 6-coordinate [$Co^{II}(acac)_2(L)_2$] systems, relative to [$Co(acac)_2$] and L, follows the order DMF < DMSO < $H_2O$. The relative steric encumberance of DMF and DMSO plays a less important role in the formation of [$Co^{II}(acac)_2(L)$], because L is further away from the acac ligands in the *tbp* geometry, and the electronic factors (better basicity of DMSO) can now play a more determinant role. On going from 5-coordinate [$Co^{II}(acac)_2(L)$] to 6-coordinate [$Co^{II}(acac)_2(L)_2$], the steric factor becomes again relevant, since the relative stabilization of the DMSO system (2.8 kcal $mol^{-1}$) is less than that of the DMF system (3.3 kcal $mol^{-1}$). The overall stabilization of 6-coordinate [$Co^{II}(acac)_2(L)_2$] relative to [$Co^{II}(acac)_2$] still remains in favor of DMSO, thanks to the more favorable first coordination step. On the other hand, [$Co^{II}(acac)_2(L)_2$] is much more greatly stabilized when L is water.

In the presence of Lewis base additives, the equilibrium of interest for the radical concentration control is between the sum of *trans*-[$Co(acac)_2(PVAc)(L)$] and L on one side and the sum of *trans*-[$Co(acac)_2(L)_2$] and free $PVAc^{\bullet}$ on the other side. According to the calculations on this model system, the enthalpy cost increases in the order $H_2O$ (6.0 kcal $mol^{-1}$) < DMSO (7.1 kcal $mol^{-1}$) < DMF (10.8 kcal $mol^{-1}$), and these values are all smaller than the enthalpy cost for the thermal activation of the L-free system (13.0 kcal $mol^{-1}$). This trend reproduces the experimentally observed trend of polymerization rates. Note that the greater acceleration factor for DMSO relative to DMF is not the result of a better coordinating power of DMSO for the $Co^{II}$ center, but rather to a poorer coordinating ability for the $Co^{III}$ center, relative to DMF.

Downloaded by UNIV OF GUELPH LIBRARY on June 26, 2012 | http://pubs.acs.org
Publication Date: August 13, 2009 | doi: 10.1021/bk-2009-1024.ch009

Downloaded by UNIV OF GUELPH LIBRARY on June 26, 2012 | http://pubs.acs.org
Publication Date: August 13, 2009 | doi: 10.1021/bk-2009-1024.ch009

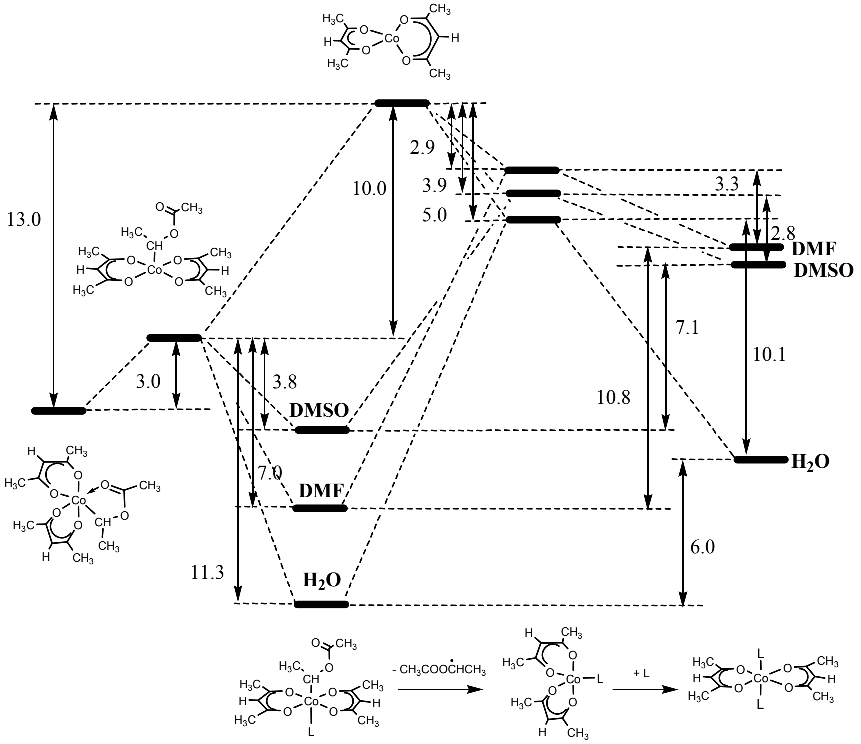

*Figure 5. Enthalpy diagram and sketch of the coordination geometries adopted by the different complexes for the processes of relevance to the VAc polymerization operated by the reversible termination mechanism.*

## Conclusion

It is now well accepted that the VAc polymerization mediated by Co(acac)$_2$ can either proceed by degenerative chain transfer or by reversible termination depending on the experimental conditions.[19,21] The latter mechanism is predominant when preformed alkyl-cobalt(III) complexes, i.e. PVAc oligomeric chains capped by Co(acac)$_2$, are used as initiators in the absence of free V-70. In this case, CMRP functions as an SFRP system for which adjustment of the Co-C bond strength is crucial since it regulates the equilibrium between dormant and active species that tempers the instantaneous concentration of growing radical chains in the medium. We have demonstrated that the Co-C bond can be labilized and thus the polymerization rate can be increased while maintaining a high level of control of the PVAc molecular parameters ($M_n$, $M_w/M_n$). This achievement was made possible either by increasing the temperature from 30°C to 60°C or by using additives able to coordinate the cobat complex such as water, DMF and DMSO. In the latter approach, water was the most efficient ligand whereas the weakest effect was observed with DMF. DFT calculations allowed us to rationalize these results and provided a detailed understanding of how the coordinating power of the added base to both the Co$^{II}$ and Co$^{III}$ center, and in particular how the different balance between electronic and steric effects for the different systems, influences the radical formation equilibrium.

## Acknowledgments

The authors from Liège are indebted to the "Belgian Science Policy" for financial support in the frame of the "Interuniversity Attraction Poles Programme (PAI VI/27) - Functional Supramolecular Systems", and to the "Fonds National de la Recherche Scientifique" (F.N.R.S., Belgium). A.D. (Chargés de Recherches FNRS) and C.D. (Maître de Recherches FNRS) are thankful to the F.N.R.S. R.P. thanks the "Agence National de la Recherche" (Contract No. NT05–2 42140), the CNRS and the IUF for funding and the "Centre Interuniversitaire de Calcul de Toulouse" (Project CALMIP) for granting free computational time. The authors thank G. Cartigny for skilful assistance and Wako for kindly providing them with V-70.

Downloaded by UNIV OF GUELPH LIBRARY on June 26, 2012 | http://pubs.acs.org
Publication Date: August 13, 2009 | doi: 10.1021/bk-2009-1024.ch009

## References

(1) Braunecker, W. A.; Matyjaszewski, K. *Prog. Polym. Sci.* **2007**, *32*, 93-146.

(2) Georges, M. K.; Veregin, R. P. N.; Kazmaier, P. M.; Hamer, G. K. *Macromolecules* **1993**, *26*, 2987-2988.

(3) Hawker, C. J.; Bosman, A. W.; Harth, E. *Chem. Rev.* **2001**, *101*, 3661-3688.

(4) Sciannamea, V.; Jerome, R.; Detrembleur, C. *Chem. Rev.* **2008**, *108*, 1104-1126.

(5) Matyjaszewski, K.; Xia, J. *Chem. Rev.* **2001**, *101*, 2921-2990.

(6) Tsarevsky, N. V.; Matyjaszewski, K. *Chem. Rev.* **2007**, *107*, 2270-2299.

(7) Kamigaito, M.; Ando, T.; Sawamoto, M. *Chem. Rev.* **2001**, *101*, 3689-3745.

(8) Lowe, A. B.; McCormick, C. L. *Prog. Polym. Sci.* **2007**, *32*, 283-351.

(9) Barner-Kowollik, C. *Handbook of RAFT polymerization* **2008**, *Ed. Wiley VCH.*

(10) Wayland, B. B.; Poszmik, G.; Mukerjee, S. L.; Fryd, M. *J. Am. Chem. Soc.* **1994**, *116*, 7943-7944.

(11) Wayland, B. B.; Mukerjee, S.; Poszmik, G.; Woska, D. C.; Basickes, L.; Gridnev, A. A.; Fryd, M.; Ittel, S. D. *ACS Symp. Ser.* **1998**, *685*, 305-315.

(12) Arvanitopoulos, L. D.; Gruel, M. P.; Harwood, H. J. *Polym. Prep.* **1994**, *35*, 549-550.

(13) Arvanitopoulos, L. D.; Greuel, M. P.; King, B. M.; Shim, A. K.; Harwood, H. J. *ACS Symp. Ser.* **1998**, *685*, 316-331.

(14) Wayland, B. B.; Basickes, L.; Mukerjee, S.; Wei, M.; Fryd, M. *Macromolecules* **1997**, *30*, 8109-8112.

(15) Lu, Z.; Fryd, M.; Wayland, B. B. *Macromolecules* **2004**, *37*, 2686-2687.

(16) Debuigne, A.; Warnant, J.; Jerome, R.; Voets, I.; de Keizer, A.; Cohen Stuart, M. A.; Detrembleur, C. *Macromolecules* **2008**, *41*, 2353-2360.

(17) Debuigne, A.; Michaux, C.; Jérôme, C.; Jérôme, R.; Poli, R.; Detrembleur, C. *Chem. Eur. J.* **2008**, *14,* 7623-7637.

(18) Debuigne, A.; Caille, J.-R.; Jerome, R. *Angew. Chem.* **2005**, *44*, 1101-1104.

(19) Debuigne, A.; Champouret, Y.; Jerome, R.; Poli, R.; Detrembleur, C. *Chem. Eur. J.* **2008**, *14*, 4046-4059.

(20) Debuigne, A.; Caille, J.-R.; Detrembleur, C.; Jerome, R. *Angew. Chem.* **2005**, *44*, 3439-3442.

(21) Maria, S.; Kaneyoshi, H.; Matyjaszewski, K.; Poli, R. *Chem. Eur. J.* **2007**, *13*, 2480-2492.

(22) Peng, C.-H.; Scricco, J.; Li, S.; Fryd, M.; Wayland, B. B. *Macromolecules* **2008**, *41*, 2368-2373.

(23) Li S; de Bruin B; Peng C-H; Fryd M; B., W. B. *J. Am. Chem. Soc.* **2008**, 13373-13381.

(24) Debuigne, A.; Detrembleur, C.; Bryaskova, R.; Caille, J.-R.; Jerome, R. *ACS Symp. Ser.* **2006**, *944*, 372-386.

(25) Wayland, B. B.; Peng, C.-H.; Fu, X.; Lu, Z.; Fryd, M. *Macromolecules* **2006**, *39*, 8219-8222.

(26) M. J. Frisch; G. W. Trucks; H. B. Schlegel; G. E. Scuseria, M. A. R., J. R. Cheeseman, J. Montgomery, J. A., T. Vreven, K. N. Kudin, J. C. Burant, J. M. Millam, S. S. Iyengar, J. Tomasi, V. Barone, B. Mennucci, M. Cossi, G. Scalmani, N. Rega, G. A. Petersson, H. Nakatsuji, M. Hada, M. Ehara, K. Toyota, R. Fukuda, J. Hasegawa, M. Ishida, T. Nakajima, Y. Honda, O. Kitao, H. Nakai, M. Klene, X. Li, J. E. Knox, H. P. Hratchian, J. B. Cross, C. Adamo, J. Jaramillo, R. Gomperts, R. E. Stratmann, O. Yazyev, A. J. Austin, R. Cammi, C. Pomelli, J. W. Ochterski, P. Y. Ayala, K. Morokuma, G. A. Voth, P. Salvador, J. J. Dannenberg, V. G. Zakrzewski, S. Dapprich, A. D. Daniels, M. C. Strain, O. Farkas, D. K. Malick, A. D. Rabuck, K. Raghavachari, J. B. Foresman, J. V. Ortiz, Q. Cui, A. G. Baboul, S. Clifford, J. Cioslowski, B. B. Stefanov, G. Liu, A. Liashenko, P. Piskorz, I. Komaromi, R. L. Martin, D. J. Fox, T. Keith, M. A. Al-Laham, C. Y. Peng, A. Nanayakkara, M. Challacombe, P. M. W. Gill, B. Johnson, W. Chen, M. W. Wong, C. Gonzalez, J. A. Pople,. *Gaussian 03, Revision C.02, Gaussian, Inc., Wallingford CT* **2004**.

(27) Harvey, J. N.; Aschi, M. *Faraday Discuss.* **2003**, *124*, 129-143.

(28) Gutmann, V. *Non Aqueous Solution,* Springer, New York, **1969**.

Downloaded by UNIV OF GUELPH LIBRARY on June 26, 2012 | http://pubs.acs.org
Publication Date: August 13, 2009 | doi: 10.1021/bk-2009-1024.ch009

Downloaded by STANFORD UNIV GREEN LIBR on June 26, 2012 | http://pubs.acs.org
Publication Date: August 13, 2009 | doi: 10.1021/bk-2009-1024.ch010

## Chapter 10

# $Cp_2TiCl$-Mediated Controlled Radical Polymerization of Isoprene Initiated by Epoxide Radical Ring Opening

**Alexandru D. Asandei,* Christopher P. Simpson, Hyun S. Yu,**
**Olumide I. Adebolu, Gobinda Saha and Yanhui Chen**

**Department of Chemistry and Institute of Materials Science, Polymer Program, University of Connecticut, 97 N. Eagleville Rd, Storrs, CT, 06269-3136, USA**

The effect of the reaction variables in the $Cp_2TiCl$-mediated controlled radical isoprene polymerizations initiated by epoxide radical ring opening was investigated over a wide range of conditions ($[Cp_2TiCl_2]/[epoxide] = 1/1-6/1$, $[Cp_2TiCl_2]/[Zn] = 1/0.5-1/8$, $[isoprene]/[epoxide] = 20/1-1000/1$, T = 70-130 °C in THF and dioxane), to reveal a linear dependence of molecular weight on conversion, linear kinetics and moderate polydispersities up to high conversions, with an optimum in initiator efficiency, rate and polydispersity for $[epoxide]/[Cp_2TiCl_2]/[Zn] = 1/3/6-1/4/8$ at 90 - 110 °C. NMR studies demonstrated the epoxide initiation and the stereoselectivity of a conventional radical polymerization. Furthermore, random and block copolymers with styrene could also be obtained.

In Controlled/Living Radical Polymerization: Progress in RAFT, DT, NMP & OMRP; Matyjaszewski, K.;
ACS Symposium Series; American Chemical Society: Washington, DC, 2009.

Downloaded by STANFORD UNIV GREEN LIBR on June 26, 2012 | http://pubs.acs.org
Publication Date: August 13, 2009 | doi: 10.1021/bk-2009-1024.ch010

# Introduction

Since their inception in the mid 90s, living radical polymerizations (LRP) have undergone a remarkable development and have become one of the most useful and dynamic synthetic methods in modern polymer chemistry.(1) The ability of LRP to control molecular weight ($M_n$) and polydispersity ($M_w/M_n$) while requiring considerably more user-friendly reaction conditions vs. water sensitive ionic and coordination polymerizations has greatly benefited the polymer synthesis toolbox and has enabled its wide use in the synthesis of complex macromolecular structures. Accordingly, such LRP applications have motivated extensive efforts in the development of novel catalytic systems.

It is currently accepted that the polymerization livingness is afforded by the reversible termination of the growing chains with persistent radicals (*2*) or degenerative transfer agents and that mechanistically, (*3*) LRP occurs by atom transfer (ATRP), dissociation-combination (DC) or degenerative transfer (DT) processes. Catalyst-wise, organic derivatives such as nitroxide (4) and iodine (5) or sulfur-based transfer agents (6) mediate LRP *via* DC and respectively DT, while organometallic complexes (7) of Co, (8) Te, (9*a*) Sb, (*9b*) Bi, (*9c*) Mo (10*a*) and Cr (*10b*) may favor both DC and DT pathways. Finally, late transition metal halide persistent radicals (*2*) (Cu, Ni, Fe, Ru, etc) (*1,3,*11) have proven very successful in ATRP.

However, current LRP systems are still somewhat limited by the restrictive choice of only activated halide or thermal initiators, which may restrict chain end functionality, and by the range of monomers polymerizable by a given method. (*1*) Thus, a broader initiator and catalyst selection would further enhance the usefulness of LRP in macromolecular synthesis. Epoxides and carbonyls are fundamental motifs in organic and polymer chemistry, and are commercially available with a wide structural variation. Moreover, they could provide alcohol polymer chain ends, useful in block or graft copolymer synthesis. Yet, none of the current late transition metal catalyzed radical polymerizations has taken advantage of these possibilities.

While the applications of early transition metals (ETM) in α-olefin coordination polymerizations (*12*) and organometallic reactions (*13*) have long been established, the unique advantages offered by the radical chemistry of Ti have only recently been recognized, (*14*) and this area of research has since witnessed an effervescent and sustained growth, (*15*) currently emerging as a powerful new strategy in organic synthesis. Thus, a representative example, the soluble, lime-green paramagnetic $Cp_2Ti(III)Cl$ (*16*) complex, inexpensively synthesized in situ by the Zn reduction of $Cp_2Ti(IV)Cl_2$ (*17*) is a very mild one electron transfer agent and mediates a variety of radical reactions (*18*) including the radical ring opening (RRO) of epoxides. (*14*)

We have recently extended the use of $Cp_2TiCl$ to polymer chemistry and introduced both epoxides (19) and aldehydes (20) as novel classes of initiators for radical polymerizations. The first examples of an ETM-mediated LRPs were demonstrated for styrene with initiation (21) from epoxide RRO, (*19*) aldehyde SET reduction, (*20*) redox reactions with peroxides (*20b*) as well as halide abstraction. This methodology was also applied in the synthesis of branched and graft copolymers.

While the ligand effect was thoroughly investigated in ETM-catalyzed coordination polymerizations, it is less documented for radical processes. Thus, in our efforts to optimize Ti-LRP, the effects of ligands, (*19b-d)* reducing agents,(*19e)* solvents and additives, (*19f)* as well as reagent ratios and temperature (*19e,f)* were also investigated. This study revealed the superiority of sandwich metallocenes over alkoxide and half-sandwich ligands, as well as the relatively weak influence of the substituents on the Cp ligands. Gratifyingly, the most promising complex ($Cp_2TiCl_2$) was also the least expensive one. (*19g)*

Interestingly, the $Cp_2ClTi$-OR alkoxides generated in-situ by epoxide RRO ([22]*a)* or aldehyde SET reduction (*22b)* were also found to mediate the living ring opening polymerization of cyclic esters such as caprolactone. Moreover, these novel initiating methodologies were applied in the $Cp_2ClTi$-mediated synthesis of graft or mixed arm brush copolymers where epoxide groups along polymer chains ([23]) were used as an initiating sites for graft copolymerizations of both olefins and cyclic esters.

Polymers derived from 1,3-dienes, such as isoprene, butadiene, and chloroprene are industrially relevant. ([24]) However, their controlled synthesis is typically accomplished only by anionic ([25]) or coordination ([26]) methods which require stringent conditions and limit the range of initiator functionalities. While ATRP works exceptionally well with styrene and (meth)acrylates (*1*), its extension to dienes, ([27]) VAc, ([28]) or VCl ([29]) has proven troublesome and, with the notable exception of nitroxide (*30*) and RAFT reagents (*31*), metal mediated LRP methods have failed to control isoprene polymerizations. Thus, as transition metal catalysts appear to be conspicuously absent from the available isoprene LRP methods, we decided to investigate the potential of the $Cp_2TiCl$/epoxide system in this application ([32]).

## Experimental

### Materials.

Bis(cyclopentadienyl)titanium dichloride ($Cp_2TiCl_2$, Acros, 97 %), styrene oxide (SO, Acros, 98%), Zn (nanosize, $d_{aver}$ = 35 nm, 99+ %), glycidyl 4-methoxyphenyl ether (MPEG, 99%), 2,2-bis[4-(glycidyloxy)phenyl]propane (DGEBA, 97%), were used as received. 1,4-dioxane (99.7 %) and tetrahydrofuran (THF, 99.9%) both from Fisher were distilled from a blue Na/benzophenone solution. Isoprene (Acros, 99%) was dried over $CaH_2$ and passed through a basic $Al_2O_3$ column.

### Techniques.

$^1$H-NMR (500 MHz) spectra were recorded on a Bruker DRX-500 at 24 °C in $CDCl_3$ (Aldrich; 0.03% v/v TMS as internal standard). GPC analyses were performed on a Waters 150-C Plus gel permeation chromatograph equipped with a Waters 410 differential refractometer, a Waters 2487 dual wavelength

Downloaded by STANFORD UNIV GREEN LIBR on June 26, 2012 | http://pubs.acs.org
Publication Date: August 13, 2009 | doi: 10.1021/bk-2009-1024.ch010

absorbance UV-VIS detector set at 254 nm, a Polymer Laboratories PL-ELS 1000 evaporative light scattering (ELS) detector and with a Jordi Flash Gel ($1x10^5$ Å, 2 x 10*4* Å, $1x10^3$ Å) column setup with THF as eluent at 2 mL/min at 40 °C. Number-average ($M_n$) and weight-average molecular weights ($M_w$) were determined from polystyrene calibration plots.

### Polymerizations.

A 35-mL Ace Glass 8648 # 15 Ace-Thread pressure tube equipped with bushing and a plunger valve and containing $Cp_2TiCl_2$ (49 mg, 0.20 mmol), Zn (26 mg, 0.40 mmol) $CaH_2$ (< 10 mg as trace moisture scavenger) and dioxane (1.0 mL) was degassed, and the Ti reduction was carried out at rt. The tube was then cooled, opened under Ar, charged with MPEG (9 mg, 0.05 mmol) and isoprene (1 mL, 9.98 mmol), re-degassed and heated at 110 °C for 24 h. Conversion and molecular weights were determined by NMR and GPC respectively. The reported $M_n$ and $M_w/M_n$ values correspond to unprecipitated samples, since MeOH precipitation seemed to artificially affect the linearity of the $M_n$ vs. conversion plots and reduce $M_w/M_n$, especially at low molecular weights (e.g. $M_n < 5{,}000$), *via* fractionation. Kinetic plots were constructed from one data point experiments.

## Results and Discussion

The mechanism of Ti-mediated isoprene LRP is presented in Scheme 1. Zn reduction of $Cp_2Ti(IV)Cl_2$ to the $Cp_2Ti(III)Cl$ metalloradical (eq. 1) is carried out in situ and proceeds readily in THF or dioxane at room temperature, as indicated by a typical red to green color change. While the reduction occurs even with stoichiometric Zn, a small excess was typically employed to accelerate the process. The strong affinity of the Ti radical towards epoxides is evidenced by the rapid color change to yellow-orange upon injection of excess initiator into the green $Cp_2TiCl$ solutions, indicating the occurrence of the corresponding SET process.

Downloaded by STANFORD UNIV GREEN LIBR on June 26, 2012 | http://pubs.acs.org
Publication Date: August 13, 2009 | doi: 10.1021/bk-2009-1024.ch010

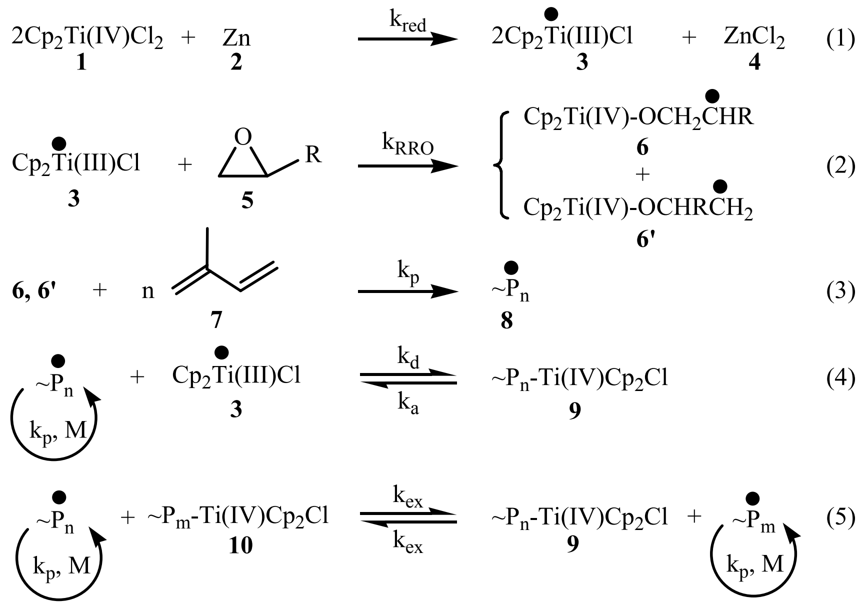

Scheme 1. *Ti-mediated isoprene LRP initiated by epoxide RRO.*

Epoxides are unique initiators as their Ti-induced RRO (*15*) occurs with the formation of a pair of very reactive primary and secondary, constitutionally isomeric *β*-titanoxy radicals derived from RRO regioselectivity (Scheme 1, eq. 2), where typically the secondary radical is favored, but both have the same thermodynamic stabilization as the corresponding alkyl radicals. (*15*) The interaction of such radicals with double bonds is well documented, (*15*), and their addition to isoprene initiates the polymerization (eq. 3) which proceeds in a living fashion, mediated by the reversible end-capping of the propagating chain end with a second equivalent of $Cp_2TiCl$. The reversible C-Ti bond homolysis most likely occurs *via* a combination of the DC and DT mechanisms (eqs. 4, 5) (*19*) and is possibly catalyzed by Zn. (*19*) Thus, one Ti equivalent is required for epoxide RRO and another one for polymerization control.

Downloaded by STANFORD UNIV GREEN LIBR on June 26, 2012 | http://pubs.acs.org
Publication Date: August 13, 2009 | doi: 10.1021/bk-2009-1024.ch010

## NMR Analysis.

Several aromatic epoxides (SO, MPEG, DGEBA) were selected as models. The demonstration of the epoxide initiation is available from the analysis of the

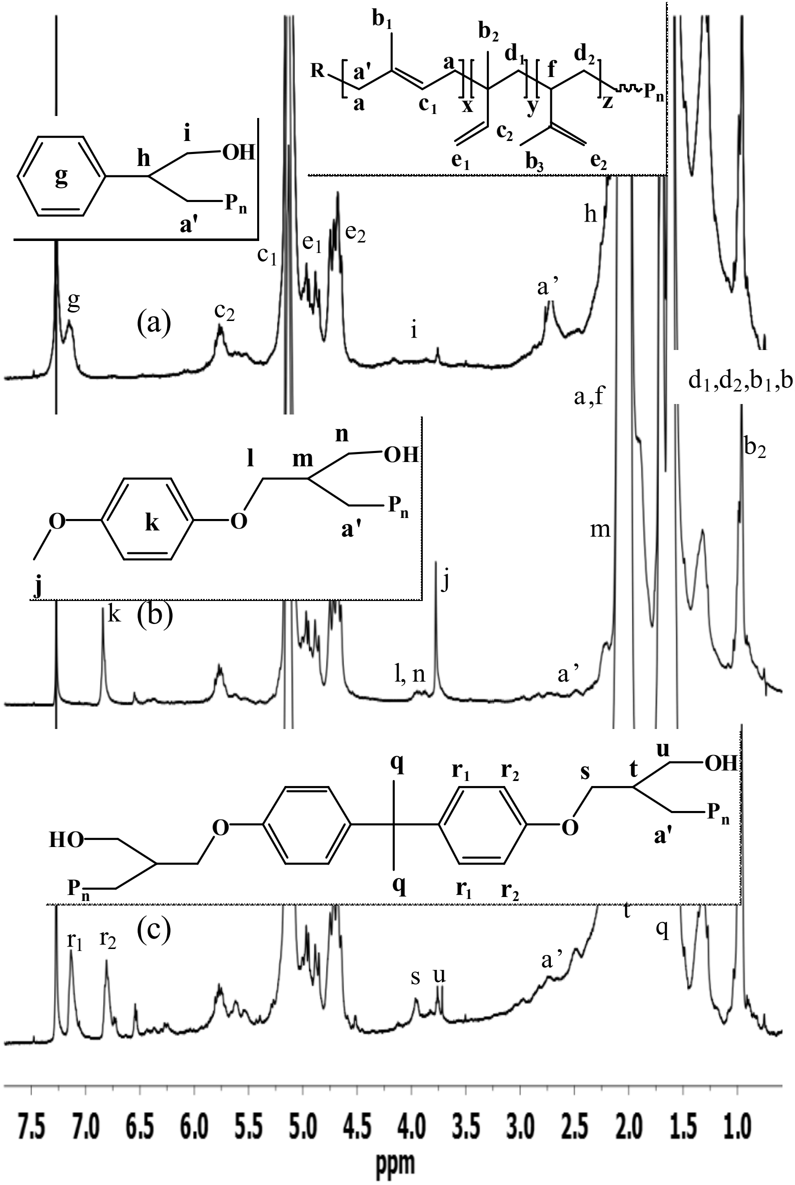

*Figure 1. 500 MHz $^1$H-NMR spectra of polyisoprene initiated from epoxides (Table 1, exp 23-25): (a) SO, $M_n^{NMR} = 4{,}400$, (b) MPEG, $M_n^{NMR} = 3{,}800$. (c) DGEBA, $M_n^{NMR} = 3{,}200$.*

Downloaded by STANFORD UNIV GREEN LIBR on June 26, 2012 | http://pubs.acs.org
Publication Date: August 13, 2009 | doi: 10.1021/bk-2009-1024.ch010

NMR spectra of the corresponding polymers in Figure 1 where, for simplicity, only the most preferred mode of epoxide RRO is depicted. The first observation is that the polyisoprene (PI) spectrum is comparable in terms of stereospecificity (peaks *a-f*) to that of PI synthesized by free radical as well as nitroxide or RAFT polymerizations at similar temperature (*30,31*; *i.e.* ~85 % 1,4 and ~ 8 % 1,2 and ~8 % 3,4), suggesting that no special coordination mediated Ti chain end control is occurring. Moreover, specific initiator resonances such as the ones derived from the aromatic regions of SO (*g*, $\delta = 7.15$ ppm), MPEG (*k*, $\delta = 6.85$ ppm), and DGEBA ($r_1$, $r_2$, $\delta = 6.85$ and 7.15 ppm) are present. In addition, -C$H_x$-O- alcohol or ether resonances corresponding to a combination of the primary and secondary alcohols derived from the two modes of epoxide RRO and to the original ether linkages in the initiator are observed as follows: SO (*i*, $\delta = 3.5$-3.8 ppm), MPEG (C$H_3$-O-, *j*, $\delta = 3.75$ ppm; *l, n*, $\delta = 3.8$ - 4 ppm) and DGEBA (*s, u*, $\delta = 3.6$ - 4 ppm). Additional signals such as the small peaks at 6.3-6.6 ppm in the MPEG and DGEBA spectra correspond to a small amount of vinyl ether formed *via* alcohol dehydration during workup.

In all cases, the connection of the initiator with polyisoprene is evidenced by a broad series of multiplets (*a'*, $\delta = \sim 2.3$-3 ppm) corresponding to one of the diastereotopic protons of the first -C$H_2$- isoprene unit located next to the –CH (*h, m, t*) stereocenter derived from both modes of epoxide RRO. Finally, the integration of the initiator peaks vs. the polymer chain also enables the calculation of $M_n^{NMR}$, which in each case is reasonably similar to $M_n^{GPC}$.

## Effect of the Reaction Variables.

Several variables such as the target degree of polymerization (DP = [Iso]/[MPEG]), the [Zn]/[$Cp_2TiCl_2$] and [$Cp_2TiCl_2$]/[MPEG] ratios, as well as the solvent and temperature were tested to optimize the polymerization. The results are presented in Figures 2 and 3, and summarized in Table 1. In all cases, a linear dependence of $M_n$ on conversion, moderate polydispersities and linear kinetics, indicative of the living character of the polymerization were observed up to high conversions. However, the reaction conditions do affect the rate, polydispersity (PDI) as well as initiator efficiency (IE).

As seen below, the effects of the [MPEG]/[$Cp_2TiCl_2$]/[Zn] ratios are closely intertwined and are detailed in Table 1, exp. 1-14 and in Figure 2, where progressively higher [$Cp_2TiCl_2$]/[MPEG] ratios were explored at various [$Cp_2TiCl_2$]/[Zn] levels, while maintaining [Iso]/[MPEG] = 200/1. According to the proposed mechanism, a minimum [$Cp_2TiCl_2$]/[MPEG] = 2/1 ratio (one Ti equiv. for radical generation, the other for control) should be enough to control the polymerization. However, excess $Cp_2TiCl$ has a beneficial effect.

Figure 2a presents selected examples of the dependence of molecular weight and polydispersity on conversion for various reagent ratios and shows that controlled polymerizations are obtained in all cases. The effect of reagent stoichiometry on initiator efficiency (IE), rate ($k_p^{app}$) and polydispersity (PDI) are further detailed in Figure 2 b-d.

Consistent with the proposed mechanism, a low [$Cp_2TiCl_2$]/[MPEG] ratio (exp 1) does not provide enough Ti for the endcapping the growing chain and

Downloaded by STANFORD UNIV GREEN LIBR on June 26, 2012 | http://pubs.acs.org
Publication Date: August 13, 2009 | doi: 10.1021/bk-2009-1024.ch010

the IE is very low but it increases with increasing [$Cp_2TiCl_2$]/[MPEG] from IE ~ 0.03 at [$Cp_2TiCl_2$]/[MPEG] = 1/1 to almost quantitative at [$Cp_2TiCl_2$]/[MPEG] = 6/1. However, even larger Ti excess may contribute to side reactions such as epoxide deoxygenation. Reasonable polymerizations are already observed at [$Cp_2TiCl_2$]/[MPEG] = 3/1-4/1.

The trends in IE are paralleled by those in the apparent rate constant of propagation ($k_p^{app}$, Fig. 2c) which is largest (~0.038 $h^{-1}$) at [$Cp_2TiCl_2$]/[MPEG] = 4/1 and in PDI, (Fig. 2d) which decreases with increasing [$Cp_2TiCl_2$]/[MPEG] and [Zn]/[$Cp_2TiCl_2$], leveling off at about 1.4.

The overall effect of Zn on the polymerization is complex and may be explained by its involvement in the mediation of both initiation and propagation steps. Since Zn is an insoluble reagent, a slight excess accelerates $Cp_2TiCl$ formation, while the resulting Lewis acidic $ZnCl_2$ coordinates the epoxide and assists the $Cp_2TiCl$ RRO process. ([33]) In addition, organozinc species may be involved in the catalysis of the reversible termination step. Thus, Zn transmetalation/reduction of the Ti endcapped dormant chains (~$P_n$-$Cp_2TiCl$) generates $Cp_2TiCl$ and transient diallyl organozinc species, (~$P_{n2}Zn$) which thermally homolyze liberating Zn(0) and the propagating radical which adds more monomers until trapped again by $Cp_2TiCl$. (*19*,[34]) The effect of the amount of Zn is more significant at low [$Cp_2TiCl_2$]/[MPEG] ratios (2/1) where Zn excess lowers IE, but it decreases in importance at higher $Cp_2TiCl$ concentrations. Thus, polymerizations can be conducted even with stoichiometric Zn ([Zn]/[$Cp_2TiCl_2$] = 0.5/1), provided that enough [$Cp_2TiCl_2$]/[MPEG] excess (*e. g.* 6/1) is present (Table 1, exp 13). Nonetheless, for large [$Cp_2TiCl_2$]/[MPEG] values, too much Zn may increase polydispersity. Overall, an optimum in terms of IE and PDI is seen for [I]/[Ti]/[Zn] = 1/4/8 but acceptable polymerizations can also be run with [I]/[Ti]/[Zn] = 1/3/6 and even 1/2/4. Finally, extra Zn and $Cp_2TiCl$ may also contribute to scavenging traces of oxygen from the polymerization.

By comparison with styrene, (where in fairness, optimization experiments were carried out at a lower DP of 50) (*19e,f, 21*), larger [$Cp_2TiCl_2$]/[epoxide] ratios are required for isoprene, and excess Zn does not seem to provide the same continuous decrease in PDI. Nonetheless, while polydispersities are still large by comparison, the do converge to about 1.4 at high conversions. This may also indicate that the side reactions associated with Ti-mediated isoprene polymerizations are harder to suppress than in the case of styrene. Interestingly, while the three modes of monomer enchainment (1,2, 1,4 and 3,4) lead to 3 different allyl titanium propagating chain ends, with different populations, steric effects and dissociation energy of the ~$P_n$-$TiCp_2Cl$ bond, the dominant 1,4-addition mode does not allow for a possible $\beta$-hydride elimination side reaction.

Downloaded by STANFORD UNIV GREEN LIBR on June 26, 2012 | http://pubs.acs.org
Publication Date: August 13, 2009 | doi: 10.1021/bk-2009-1024.ch010

Downloaded by STANFORD UNIV GREEN LIBR on June 26, 2012 | http://pubs.acs.org
Publication Date: August 13, 2009 | doi: 10.1021/bk-2009-1024.ch010

**Table I. Isoprene Polymerizations Mediated by $Cp_2TiCl$.**

| Exp. | [Iso]/[MPEG]/ $[Cp_2TiCl_2]$/[Zn] | Mn and PDI at 50% | | $k_p^{app}$ $(h^{-1})$[a] | Init. Effic.[b] | T, °C | Zn/ Ti | Ti/ Epox |
|---|---|---|---|---|---|---|---|---|
| 1 | 200/1/1/2 | 237,000 | 1.77 | 0.005 | 0.03 | 110 | 2 | 1 |
| 2 | 200/1/2/4 | 15,000 | 1.40 | 0.013 | 0.45 | 110 | 2 | 2 |
| 3 | 200/1/2/6 | 60,300 | 1.90 | 0.011 | 0.11 | 110 | 3 | 2 |
| 4 | 200/1/2/8 | 53,500 | 1.65 | 0.016 | 0.13 | 110 | 4 | 2 |
| 5 | 200/1/2/16 | 51,200 | 1.86 | 0.009 | 0.12 | 110 | 8 | 2 |
| 6 | 200/1/3/6 | 9,300 | 1.52 | 0.019 | 0.74 | 110 | 2 | 3 |
| 7 | 200/1/3/9 | 12,400 | 1.39 | 0.017 | 0.53 | 110 | 3 | 3 |
| 8 | 200/1/3/12 | 12,700 | 1.40 | 0.013 | 0.53 | 110 | 4 | 3 |
| 9 | 200/1/4/4 | 8,500 | 1.35 | 0.020 | 0.84 | 110 | 1 | 4 |
| 10 | 200/1/4/8 | 7,300 | 1.41 | 0.038 | 0.93 | 110 | 2 | 4 |
| 11 | 200/1/4/12 | 8,900 | 1.40 | 0.035 | 0.90 | 110 | 3 | 4 |
| 12 | 200/1/4/16 | 7,300 | 1.60 | 0.018 | 0.94 | 110 | 4 | 4 |
| 13 | 200/1/6/3 | 14,500 | 1.45 | 0.023 | 0.46 | 110 | 0.5 | 6 |
| 14 | 200/1/6/12 | 6,200 | 1.42 | 0.041 | 1.08 | 110 | 2 | 6 |
| 15 | 50/1/3/6 | 3,400 | 1.32 | 0.051 | 0.50 | 110 | 2 | 3 |
| 16 | 100/1/3/6 | 8,100 | 1.37 | 0.033 | 0.42 | 110 | 2 | 3 |
| 17 | 400/1/3/6 | 24,600 | 1.38 | 0.009 | 0.55 | 110 | 2 | 3 |
| 18 | 1000/1/8/12 | 45,000 | 1.60 | 0.005 | 0.76 | 110 | 1.5 | 8 |
| 19 | 200/1/4/8 | 12,100 | 1.35 | 0.016 | 0.56 | 90 | 2 | 4 |
| 20 | 200/1/4/8 | 7,800 | 1.61 | 0.045 | 0.87 | 130 | 2 | 4 |
| 21 | 200/1/4/8[c] | 7,400 | 1.30 | 0.011 | 0.93 | 70 | 2 | 4 |
| 22 | 200/1/4/8[c] | 7,900 | 1.41 | 0.036 | 0.85 | 110 | 2 | 4 |
| 23 | 20/1/3/12 | 2,900 | 1.34 | n/a | n/a | 110 | 4 | 3 |
| 24 | 20/1/3/12[d] | 3,200 | 1.45 | n/a | n/a | 110 | 4 | 3 |
| 25 | 20/1/5/15[e] | 2,500 | 1.31 | n/a | n/a | 110 | 3 | 5 |
| 26 | 200/400/1/3/6[f] | 17,000 | 1.39 | n/a | n/a | 110 | 2 | 3 |
| 27 | 75/75/1/3/6[f] | 16,000 | 1.47 | n/a | n/a | 110 | 2 | 3 |
| 28 | 100/100/1/3/6[f] | 15,000 | 1.46 | n/a | n/a | 110 | 2 | 3 |

[a] Calculated as the slope of the kinetic plot. [b] Calculated as $M_n^{theor}/M_n^{GPC}$. [c] All exp. in dioxane, except exp. 21 and 22 in THF. [d] SO, [e] DGEBA. Exp 23-28 $M_n$ and PDI not at 50%. [f] Styrene copolymers.

Downloaded by STANFORD UNIV GREEN LIBR on June 26, 2012 | http://pubs.acs.org
Publication Date: August 13, 2009 | doi: 10.1021/bk-2009-1024.ch010

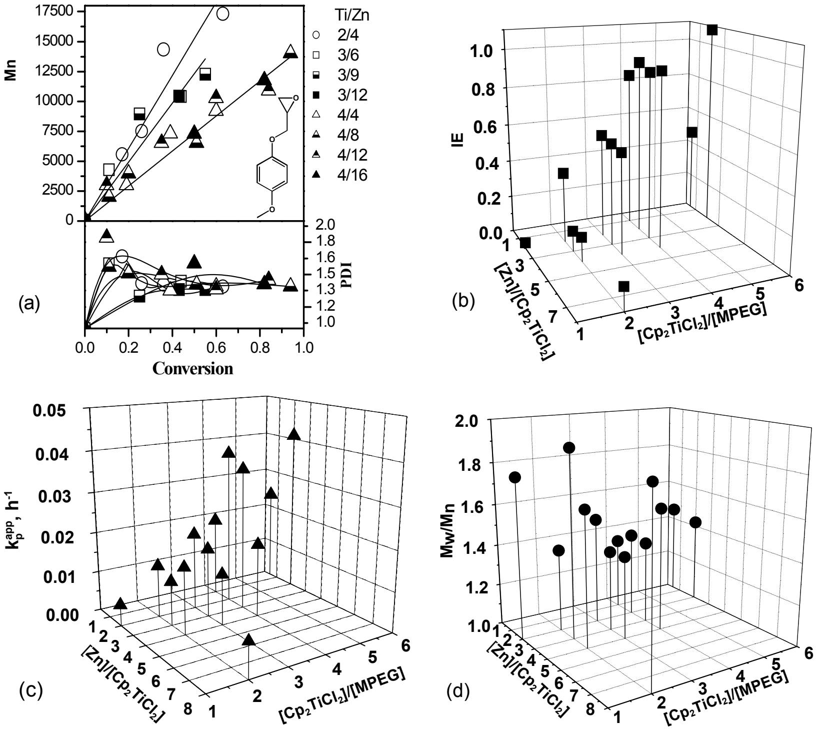

*Figure 2. Effect of the [MPEG]/[$Cp_2TiCl_2$]/[Zn] ratios: (a) conversion dependence of $M_n$ and $M_w/M_n$. (b), (c), (d): Dependence of IE (b, ■), $k_p^{app}$ (c, ▲) and PDI at ~50% conversion (d, ●) on [$Cp_2TiCl_2$][MPEG] and [Zn]/[ $Cp_2TiCl_2$]. [Iso]/[MPEG] = 200/1; T = 110 °C.*

The effect of the monomer/initiator ratio is presented in Table 1 exp. 6, 15-18 and Figure 3a. A linear dependence of molecular weight on conversion and linear kinetics are observed for a wide range of DP = [Iso]/[MPEG] ratios from 50/1 to 1000/1. The polydispersity values are about 1.4 but increase at higher conversions or for larger degrees of polymerizations. The IE is about 0.4-0.5 at low DP (50, 100) but increases to about 0.75 at DP = 200. The lower IE at low DPs can be explained by the increase in the rate of possible epoxide deoxygenation (*14*) brought about by the high $Cp_2TiCl$ concentrations. Conversely, IE decreases again at DP = 400 as the lower $Cp_2TiCl$ concentration cannot suppress epoxide related side reactions such as coupling. However, this may be corrected by increasing the amount of $Cp_2TiCl$ (*e. g.* at DP = 1,000) which brings back the IE to about 0.75. Thus, IE seems to be sensitive to the Ti concentration and it is likely that an optimization should be performed for each target DP.

The combined effect of temperature and solvent is presented in Figure 3b and in Table 1, exp. 10, 19-22. A linear dependence of $M_n$ on conversion occurs in dioxane and THF at all temperatures in the 90-130 ºC range. In both solvents, the IE is large (~0.8-0.9) and relatively independent of temperature, indicating that epoxide RRO and initiation are fast relative to initiator related side reactions. Due to the thermal suppression of termination, transfer and epoxide deoxygenation the PDIs decrease with temperature to about 1.35 at 70-90 °C. As previously described, dipolar aprotic coordinating solvents are favored in the Ti-LRP of styrene (*19*). Thus, while both are reasonably good solvents for polyisoprene, the more polar THF may allow for a faster $Cp_2TiCl_2$ reduction and higher reactivity of $Cp_2TiCl$ *via* a better solvation and dissociation of the $(Cp_2TiCl)_2$ dimer (*15-17*).

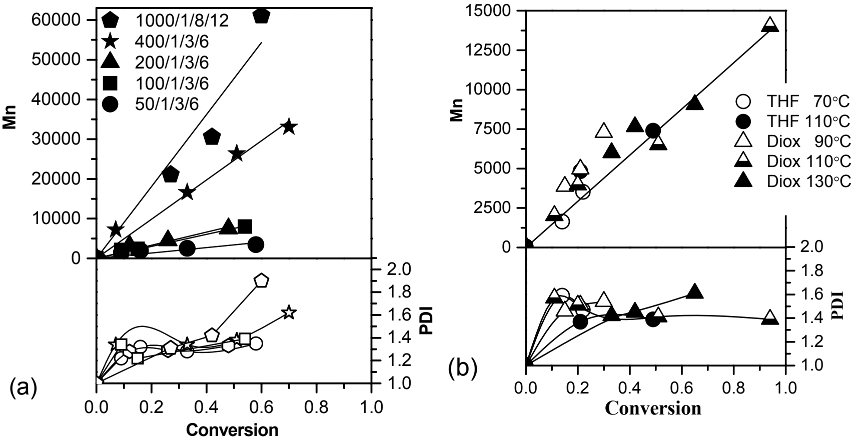

*Figure 3. Dependence of $M_n$ and $M_w/M_n$ on conversion for: (a) various [Iso]/[MPEG] ratios in dioxane at 110 °C. (b) several solvent and temperature conditions ([Iso]/[MPEG]/[ $Cp_2TiCl_2$]/[Zn] = 2001/1/4/8)*

Finally, as a further demonstration of the livingness of the polymerization, both random and block copolymers were successfully synthesized by chain extension from polyisoprene and polystyrene which was verified by a combination of GPC and NMR (Figure 4) analyses. Thus, the GPC traces of the copolymers are monomodal while the resonances associated with polystyrene, polyisoprene and MPEG are clearly visible (*e.g.* aromatic, and vinyl regions as well as the methoxy at δ = 3.75 ppm). The copolymer type is identifiable by the broadness vs. sharpness of the corresponding signals in the random and respectively block copolymers.

Downloaded by STANFORD UNIV GREEN LIBR on June 26, 2012 | http://pubs.acs.org
Publication Date: August 13, 2009 | doi: 10.1021/bk-2009-1024.ch010

Downloaded by STANFORD UNIV GREEN LIBR on June 26, 2012 | http://pubs.acs.org
Publication Date: August 13, 2009 | doi: 10.1021/bk-2009-1024.ch010

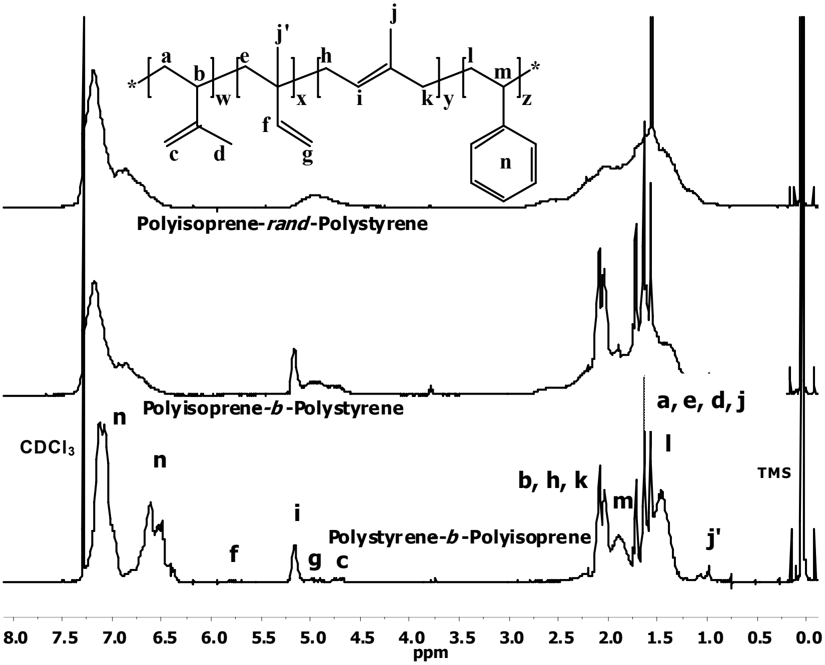

*Figure 4. 500 MHz $^{1}$H-NMR spectra of isoprene/styrene copolymers.*

## Conclusions

The first examples of transition metal mediated controlled radical polymerizations of isoprene were demonstrated using the epoxide/$Cp_2TiCl$ initiator system. The initiation was supported by NMR investigations, which indicated the presence of epoxide fragments on the chain end and the stereoselectivity of a conventional radical polymerization. The effect of the reaction variables was studied over a wide range of conditions ($[Cp_2TiCl_2]/[epoxide] = 1/1-1/6$, ($[Cp_2TiCl_2]/[Zn] = 1/0.5-1/8$ , $[Iso]/[epoxide] = 20/1-1000/1$, T = 70-130 °C in THF and dioxane) to reveal a linear dependence of molecular weight on conversion, linear kinetics as well as moderate polydispersities up to high conversions. The initiator efficiency (IE) and the rate increase, while polydispersity decreases with increasing the $[Cp_2TiCl_2]/[epoxide]$ ratios, with an optimum at $[epoxide]/[Cp_2TiCl_2]/[Zn] = 1/3/6-1/4/8$ at 90 - 110 °C. While IE is independent of temperature, lower polydispersities (1.3-1.4) were obtained at lower temperatures ~ 90 °C. Furthermore, random and block copolymers with styrene could also be obtained.

The $Cp_2TiCl_2$/epoxide methodology uses off-the-shelf reagents, and mediates isoprene LRP at lower temperatures (90-110 °C vs. 120-130 °C) than the more expensive nitroxide and dithioester LRP methods, to which it offers a convenient and inexpensive alternative. Moreover, refinement of the ligand systems using examples already available in Ti-coordination polymerization is likely to optimize the polymerization further.

## Acknowledgements

The National Science Foundation (CHEM-0518247) and the Donors of the Petroleum Research Fund (PRF-G) administered by the American Chemical Society are gratefully acknowledged for financial support.

## References

---

1. (a) Pintauer, T.; Matyjaszewski, K. *Chem. Rev.* **2008**, *37*, 1087–1097. (b) Braunecker, W. A.; Matyjaszewski, K. *Prog. Polym. Sci.* **2007**, 32, 93–146. (c) *Handbook of Radical Polymerization*; Matyjaszewski, K., Davis, T. P., Eds.; Wiley-Interscience: New York, **2002**, pp 361-462.
2. Souaille, M.; Fischer, H. *Macromolecules* **2000**, *33*, 7378.
3. Goto, A.; Fukuda, T. *Progr. Polym. Sci.* **2004**, *29*, 329-385.
4. Hawker, C. J.; Bosman, A.W.; Harth, E. *Chem. Rev.* **2001**, *101*, 3661-3688.
5. Gaynor, S.; Wang, J.; Matyjaszewski, K. *Macromolecules* **1995**, *28*, 8051.
6. Moad, G; Rizzardo, E.; Thang, S. *Acc. Chem. Res.* **2008**, 41(9), 1133-1142.
7. Poli, R. *Angew. Chem. Int. Ed. Engl.* **2006**, *45*, 5058–5070.
8. (a) Wayland, B. B.; Poszmik, G.; Mukerjee, S. L.; Fryd, M. *J. Am. Chem. Soc.* **1994**, *116*, 7943. (b) Debuigne, A.; Caille, J. R.; Jerome, R. *Angew. Chem. Int. Ed.* **2005**, *44*, 1101 –1104.
9. (a) Yamago, S.; Iida, K.; Yoshida, J. I. *J. Am. Chem. Soc.* **2002**, *124*, 2874. (b) Yamago, S.; Ray, B.; Iida, K.; Yoshida, J.; Tada, T.; Yoshizawa, K.; Kwak, Y.; Goto, A.; Fukuda, T. *J. Am. Chem. Soc.*, **2004**, *126*, 13908-13909. (c) Yamago, S.; Kayahara, E.; Kotani, M.; Ray, B.; Kwak, Y.; Goto, A.; Fukuda, T. *Angew. Chem., Int. Ed. Engl.* **2007**, *46*(8), 1304-1306.
10. (a) Le Grognec, E.; Claverie, J.; Poli, R. *J. Am. Chem. Soc.* **2001**, *123,* 9513. (b) Champouret, Y.; Baisch, U.; Poli, R.; Tang, L.; Conway, J. L.; Smith, K. M. *Angew. Chem. Int. Ed.* **2008**, *47*, 6069-6072.
11. (c) Percec, V.; Asandei, A. D.; Asgarzadeh, F.; Bera, T. K. Barboiu, B. *J. Poly. Sci: Part A: Polym. Chem.* **2000**, *38*, 3839. (d) Percec, V.; Asandei. A. D.; Asgarzadeh F.; Barboiu, B.; Holerca, M. N.; Grigoras, C. *J. Poly. Sci: Part A: Polym. Chem.* **2000**, *38*, 4353.
12. Mahanthappa, M. ; Waymouth, R. M. *J. Am. Chem. Soc.* **2001**, *123*, 12093.
13. Reetz, M. T. *In Organometallics in Synthesis: A Manual.* Schlosser, M. (Ed.). John Wiley and Sons, Chichester, England, **2002**, p 817-924. 14. (a) Rajanbabu, T.; Nugent, W. *J. Am. Chem. Soc.* **1994**, *116*, 986. (b) Rajanbabu, T.; Nugent, W.; Beattie, M. *J. Am. Chem. Soc.* **1990**, *112*, 6408-6409. (c) RajanBabu, T.; Nugent, W. *J. Am. Chem. Soc* **1989**, *111*, 4525.
15. (a) Gansauer, A.; Rinker, B. *Titanium and Zirconium in Organic Synthesis*; Wiley, **2002**. (b) Cuerva, J. M.; Oller-López, J. L.; Oltra, J. E. *Top. Curr. Chem.* **2006**, *264*, 63–91. (c) Gansäuer, A.; Justicia, J.; Fan, C. A.; Worgull, D.; Piestert, F. *Top. Curr. Chem.* **2007**, 279: 25–52.
16. Spencer, R. P.; Schwartz, J. *Tetrahedron*, **2000**, *56*, 2103-2112.

Downloaded by STANFORD UNIV GREEN LIBR on June 26, 2012 | http://pubs.acs.org
Publication Date: August 13, 2009 | doi: 10.1021/bk-2009-1024.ch010

17. Green, M. L.; Lucas, C. R. *J. Chem. Soc. Dalton Trans.* **1972**, *8*, 1000-1003.
18. Barden, M. C.; Schwartz, J. *J. Am. Chem. Soc.* **1996**, *118*, 5484.
19. (a) Asandei, A. D.; Moran, I. W. *J. Am. Chem. Soc.* **2004**, *126*, 15932. (b) Asandei, A. D.; Moran, I. W. *J. Polym. Sci. Part A: Polym. Chem.* **2005**, *43*, 6028. (c) Asandei, A. D.; Moran, I. W. *J. Polym. Sci. Part A: Polym. Chem.* **2005**, *43*, 6039. (d) Asandei, A. D.; Moran, I. W. *J. Polym Sci. Part A: Polym. Chem.* **2006**, *44*, 1060. (e) Asandei, A. D.; Moran, I. W.; Saha, G.; Chen, Y. *J. Polym. Sci. Part A: Polym. Chem.* **2006**, *44*, 2156. (f) Asandei, A. D.; Moran, I. W.; Saha, G.; Chen, Y. *J. Polym. Sci. Part A: Polym. Chem.* **2006**, *44*, 2015. (g) Asandei, A. D.; Moran, I. W.; Saha, G.; Chen, Y. *ACS Symp. Ser.* **2006***, 944,* 125-139.
20. (a) Asandei, A. D.; Chen, Y. *Macromolecules* **2006**, *39*, 7459. (b) Asandei, A. D.; Saha, G. *J. Polym. Sci. Part A: Polym. Chem.* **2006**, *44*, 1106.
21 (a) Asandei, A. D.; Chen, Y.; Moran, I. W.; Saha, G. *Tetrahedron*, **2008**, 64, 11831-11838. (b) Asandei, A. D.; Chen, Y.; Moran, I. W.; Saha, G. *J. Organomet. Chem.* **2007**, 692, 3174-3182.
22. (a) Asandei, A. D.; Saha, G. *Macromol. Rapid Commun.* **2005**, *26*, 626. (b) Asandei, A. D.; Chen, Y.; Adebolu, O. I.; Simpson, C. P. *J. Polym. Sci.: Part A: Polym. Chem.* **2008**, *46*, 2869-2877. 23. Asandei, A. D.; Saha, G. *Macromolecules,* **2006***, 39*, 8999-9009. 24. (a) Schops, M.; Leist, H.; DuChesne, A.; Wiesner, U. *Macromolecules* **1999**, *32*, 2806. (b) Li, W.; Wang, H.; Yu, L.; Morkved, T.; Jaeger, H. M. *Macromolecules* **1999**, *32*, 3034. (c) Allgaier, J.; Poppe, A.; Willner, L.; Richter, D. *Macromolecules* **1997**, *30*, 1582.
25. Hirao, A.; Hayashi, M. *Acta Polym*. **1999**, *50*, 219.
26. Evans, W. J.; Giarikos, D. G.; Allen, N. T. *Macromolecules* **2003**, *36*, 4256.
27. Wootthikanokkhan, J.; Peesan, M. *Eur. Polym. J.* **2001**, *37*, 2063.
28. Xia, J.; Paik, H.; Matyjaszewski, K. *Macromolecules* **1999**, *32*, 8310-8314.
29. Percec, V.; Popov, A.; Castillo, E.; Monteiro, M.; Barboiu, B.; Asandei A. D.; Mitchell, C. *J. Am. Chem. Soc.* **2002**, *124*, 4940-4941. (b) Asandei, A. D.; Percec, V. *J. Polym. Sci.: Part A: Polym. Chem.* **2001**, *39*, 3392.
30. (a) Grubbs, R. B.; Wegrzyn, J.; Xia, Q. *Chem. Commun.* **2005**, *1*, 80. (b) Kamachi, M.; Kajiwara, A. *Macromolecules* **1996**, *29*, 2378. (c) Keosherian, B.; Georges M.; Quinlan, M.; Vergin, R.; Goodbrand, B. *Macromolecules* **1998**, *31*, 7559.(d) Benoit, D.; Harth, E.; Fox, P.; Waymouth, R. M.; Hawker, C. J. *Macromolecules* **2000**, *33*, 363. (e) Li, I.; Howell, B.; Dineen, M.; Kastl, P.; Lyons, J.; Meunier, D.; Smith, P.; Priddt, B. *Macromolecules* **1997**, *30*, 5195. (f) Gavranovic, G.; Csihony, S.; Bowden, N. B.; Hawker, C. J.; Waymouth, R. M.; Moerner, W. ; Fuller, G. *Macromolecules* **2006,** *39,* 8121.
31. (a) Germack, D. S; Wooley, K. L. *J. Polym. Sci.: Part A: Polym. Chem.* **2007**, *45*, 4100. (b) Jitchum, V.; Perrier, S. *Macromolecules* **2007**, *40,* 1408.
32. (a) Asandei, A. D.; Simpson, C. P.; Yu, H. S. *Polym. Prepr.* **2008**, *49(2)*, 73-74. (b) Asandei, A. D.; Simpson, C. P. *Polym. Prepr.* **2008**, *49(2)*, 75-76. (c) Asandei, A.D.; Simpson C. *Polym. Prepr*. **2008**, *49(1),* 452-453. (d) Asandei, A. D.; Saha, G. *Polym. Prepr.* **2005**, *46(2)*, 474-475.

Downloaded by STANFORD UNIV GREEN LIBR on June 26, 2012 | http://pubs.acs.org
Publication Date: August 13, 2009 | doi: 10.1021/bk-2009-1024.ch010

33. Gansauer, A.; Bluhm, H. *Chem. Commun.* **1998**, 214-215.
34. Jensen, T. R.; Yoon, S. C.; Dash, A. K.; Luo, L. B.; Marks, T. J. *J. Am. Chem. Soc.* **2003**, *125*, 14482-14494.

Downloaded by STANFORD UNIV GREEN LIBR on June 26, 2012 | http://pubs.acs.org
Publication Date: August 13, 2009 | doi: 10.1021/bk-2009-1024.ch010

Downloaded by PENNSYLVANIA STATE UNIV on June 27, 2012 | http://pubs.acs.org
Publication Date: August 13, 2009 | doi: 10.1021/bk-2009-1024.ch011

## Chapter 11

# Reversible Addition Fragmentation Chain Transfer (RAFT) Mediated Polymerization of N-Vinylpyrrolidone: RAFT agent design

**Gwenaelle Pound-Lana and Bert Klumperman**

**Department of Chemistry and Polymer Science, University of Stellenbosch,**
**Private Bag X1, South Africa**
**gwen@sun.ac.za; bklump@sun.ac.za**

A selection of seven *O*-ethyl xanthates with different R groups were tested for their ability to control the polymerization of *N*-vinylpyrrolidone (NVP). Quantification of the species involved in the initialization step was achieved via *in situ* $^1$H-NMR spectroscopy by using a high concentration of xanthate compared to typical polymerization concentrations. The results pointed at 3 different initialization behaviors, namely selective, poorly selective and selective but slow initialization. The selectivity and length of the initialization period were used as criteria to classify the different R groups with respect to NVP. The classification obtained is valuable to the design of an optimized RAFT agent for the preparation of poly(*N*-vinylpyrrolidone) with narrow molar mass distribution and well-defined endgroups.

In Controlled/Living Radical Polymerization: Progress in RAFT, DT, NMP & OMRP; Matyjaszewski, K.;
ACS Symposium Series; American Chemical Society: Washington, DC, 2009.

# Introduction

Reversible addition-fragmentation chain-transfer (RAFT) mediated polymerization is the first polymerization technique reported for the preparation of poly(*N*-vinylpyrrolidone) (PVP) with a narrow molar mass distribution (polydispersity indexes (PDIs) below 1.5).[1,2] In addition, the technique enables the prediction of the molar mass of the polymer from the initial stoichiometry and selected functionalities can be introduced at the polymer chain-ends. The choice of the reversible chain transfer agent (RAFT agent) is critical for the success of a RAFT-mediated polymerization system. In order to obtain a well-defined polymer, the structure of the RAFT agent needs to be optimized for a given monomer, in terms of both the R group and the Z group. The RAFT agent Z group is designed to modulate the rates of addition and fragmentation of the intermediate radical adducts. NVP derived radicals are poorly stabilized. The Z group must therefore be a poorly stabilizing group to enable fast fragmentation of the intermediate radical adducts.

Xanthates and dithiocarbamates have been identified as suitable candidates for the RAFT-mediated polymerization of NVP.[1-4] As we pointed out in a recent publication, the structure of the R group is also determining.[5] For a series of xanthates where Z=OEt, a change in the R group structure can lead to a polymerization system where (1) molar masses increase linearly with conversion or (2) a system with hybrid behavior[6] and poor control over the molar mass distribution or (3) a system where a high degree of control is obtained but where a delay in the onset of polymerization is observed. In the last two cases the ability to predict the molar mass from the initial stoichiometry and/or the level of control over the endgroups can be compromised.

The data available in the literature concerning the R group design for NVP is scarce. Classical techniques used for the determination of conversion as well as a high ratio of monomer to RAFT agent, as is typically used in polymerizations, do not enable quantification of the monomer nor the RAFT agent conversion during the pre-equilibrium or initialization step. Ideally, initialization should be selective and fast. Fast and selective initialization ensures that all chains are initiated from the beginning of the polymerization by the R group. Initialization studies have enabled us to identify situations where initialization is slow and/or poorly selective. Therefore the use of a low ratio of monomer to RAFT agent and quantification of the RAFT agent and monomer concentrations via NMR spectroscopy is valuable to elucidate the kinetics and mechanism of RAFT mediated polymerizations. In addition, this type of experiments, which we call initialization studies, can be used for screening various RAFT agents for a given monomer and thus for optimizing the RAFT agent structure.

In the present chapter we extend the range of *O*-ethyl xanthate R groups used to mediate the polymerization of NVP (Figure 1). A systematic variation of the R group substituents and their influence on the initialization step during xanthate mediated polymerization of NVP are presented, as probed via *in situ* NMR spectroscopy.

Downloaded by PENNSYLVANIA STATE UNIV on June 27, 2012 | http://pubs.acs.org
Publication Date: August 13, 2009 | doi: 10.1021/bk-2009-1024.ch011

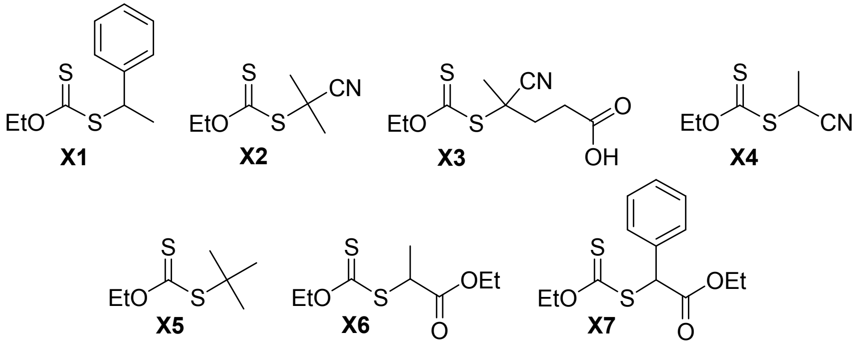

*Figure 1: xanthate structures*

## Experimental section

### Materials

*N*-vinylpyrrolidone (Aldrich, 99%) was dried over anhydrous magnesium sulfate and purified by distillation under reduced pressure. 2,2'-Azobis(isobutyronitrile) (AIBN) (Riedel de Haen) was used without further purification for the preparation of X2, whereas it was recrystallized twice from methanol for use as the initiator in initialization experiments. Potassium *O*-ethyl xanthate (95%, Merck or Fluka), *2*-bromopropionic acid (99%, Aldrich), ethyl *2*-bromo propionate (98%, Fluka), α-chlorophenylacetylchloride (90%, Aldrich), 1-bromoethyl benzene (Aldrich, 97%), 2-bromopropionitrile (Aldrich, 97%), *tert*-butyl mercaptan (Aldrich, grade), ethylene glycol (Aldrich, 99+%), the deuterated solvent $C_6D_6$ (99.6%, Aldrich) and 4,4'-azobis(4-cyanopentanoic acid) (ACPA, Fluka, ≥ 98%) were used without further purification. Silica gel (Fluka, particle size 0.063 – 0.2 mm, Brockmann 2-3) was used for column chromatography.

### RAFT agent synthesis

*S*-(2-phenylethyl) *O*-ethyl xanthate (X1), *S*-(1-cyanoethyl) *O*-ethyl xanthate (X4), *S*-(2-propionic acid) and *O*-ethyl xanthate (X6) were prepared from potassium *O*-ethyl xanthate and the suitable alkyl bromide and purified by column chromatography where necessary. A typical procedure was as follows (preparation of X1): 1-bromoethyl benzene (5 mL, 6.8 g, $3.7 \cdot 10^{-2}$ mol) was added dropwise to a solution of potassium *O*-ethyl xanthate (6.46 g, $4.0 \cdot 10^{-2}$ mol) in ethanol (40 mL). After 6 h of reaction under magnetic stirring a white precipitate was filtered off. Solvents were evaporated under vacuum. Diethyl ether was added (200 mL). The filtrate was washed with distilled water (4×50 mL) and was dried with anhydrous magnesium sulfate. The solvents were evaporated under vacuum. Yield: 91%. Purity (NMR) > 96%.

Downloaded by PENNSYLVANIA STATE UNIV on June 27, 2012 | http://pubs.acs.org
Publication Date: August 13, 2009 | doi: 10.1021/bk-2009-1024.ch011

*S*-(2-cyano-2-propyl) *O*-ethyl xanthate (X2, Purity (NMR) > 97%) and *S*-(4-cyano-4-pentanoic acid) *O*-ethyl xanthate (X3, Purity (NMR) > 98%) were prepared from *O*,*O*-diethyl bisxanthate[7] and the azo initiators AIBN and ACPA, respectively, according to the method of Zard and coworkers.[8]

*S*-(*tert*-butyl) *O*-ethyl xanthate (X5): 1. Preparation of *S*-(2-propionic acid) *O*-ethyl xanthate. Potassium *O*-ethyl xanthate (10.08 g, $6.25 \cdot 10^{-2}$ mol) was dissolved in distilled water (30 mL). 3.3 M NaOH (15 mL) was added under stirring. The mixture was cooled with an ice bath. *2*-Bromopropionic acid (4.50 mL, 7.6 g, $5.0 \cdot 10^{-2}$ mol) was added dropwise. The reaction mixture was stirred for 16 h at room temperature. The pH of the solution (pH = 7 at the end of the reaction) was adjusted with 2 M HCl to pH = 1. The product was extracted with diethyl ether (2×200 mL), then from the ethereal phase with aqueous sodium carbonate (25 g in 250 mL water, 2×50 mL). The pH was readjusted to pH = 3 with 1 M HCl. The product was extracted with diethyl ether (200 mL). The ethereal phase was dried over anhydrous magnesium sulfate and the solvent was evaporated under reduced pressure. The product, a pale yellow solid (9.22 g, $4.75 \cdot 10^{-2}$ mol), crystallized during solvent evaporation. Yield: 76%. Purity (NMR) > 97%. $^1$H-NMR (300 MHz, $CDCl_3$): δ[ppm] = 11.10, 1H, broad, (COO*H*), 4.64, 2H, 2×q, $^3J_A$=7.3 Hz, $^3J_B$=7.1 Hz ($CH_2$), 4.41, 1H, q, $^3J$=7.3 Hz (C*H*), 1.60, 3H, d, $^3J$=7.3, ($CH_3$CH), 1.41, 3H, t, $^3J_A$=7.3 Hz, $^3J_B$=7.1 Hz ($CH_3CH_2$). 2. *S*-(2-propionic acid) *O*-ethyl xanthate (8.0 g, $4.1 \cdot 10^{-2}$ mol) was dissolved in dilute alkaline solution containing 4 equivalents of sodium hydroxide (300 mL). Then *tert*-butyl mercaptan (1.53 g, $1.7 \cdot 10^{-2}$ mol) was added under stirring at room temperature. The mixture became turbid, then milky after a few minutes, and was stirred for 20 h at room temperature. *tert*-Butyl xanthate separated out as a yellow viscous oil. It was extracted with diethyl ether (2×200 mL). The ethereal phase was washed with dilute NaOH (0.1 M, 3×50 mL), with distilled water (50 mL), dried over anhydrous magnesium sulfate and the solvent was evaporated under reduced pressure. The product was purified by Kugelrohr distillation (3 mbar, thermostat at 70 ºC) to yield 4.08 g ($2.30 \cdot 10^{-2}$ mol, yield = 55%) of yellow oil (purity (NMR) > 96%). $^1$H-NMR (300 MHz, $CDCl_3$): δ[ppm] = 4.68, 2H, q, $^3J$=7.3 Hz, ($CH_2$), 1.49, 9H, s, $C(CH_3)_3$, 1.46, 3H, t, $^3J$=7.3 Hz, ($CH_3$-$CH_2$).

*S*-(2-ethyl phenylacetate) *O*-ethyl xanthate (X7) was prepared according to the procedure reported in a previous publication.[9] Purity (NMR) > 95%.

## *In situ* NMR initialization experiments

In a typical *in situ* NMR spectroscopy polymerization experiment, the desired amount of initiator (AIBN), xanthate, monomer ([monomer]:[xanthate]:[AIBN] = 5.0:1.0:0.12) and deuterated solvent $C_6D_6$ (0.25 g, 50 wt%) were weighed. The solutions were transferred to NMR tubes. The tubes were flushed with ultra-high purity argon for 5 minutes. A sealed glass insert containing the integration reference standard (formic acid in $C_6D_6$) was inserted. *In situ* $^1$H-NMR experiments were carried out on a 600 MHz Varian $^{Unity}$Inova spectrometer. A 5 mm inverse detection PFG probe was used for the experiments and the probe temperature was calibrated using an ethylene

Downloaded by PENNSYLVANIA STATE UNIV on June 27, 2012 | http://pubs.acs.org
Publication Date: August 13, 2009 | doi: 10.1021/bk-2009-1024.ch011

glycol sample in the manner suggested by the manufacturer. $^1$H spectra were acquired with a 3 μs (40°) pulse width and a 4 sec acquisition time. The tube containing the sample was inserted into the magnet at 25 °C and the magnet fully shimmed on the sample. A spectrum was collected at 25 °C to serve as a reference. The sample was then removed from the magnet and the cavity of the magnet was raised to the required temperature (60 °C or 70 °C). Once the magnet cavity had stabilized at the required temperature, the sample was re-inserted (time zero) and allowed to equilibrate for 3 to 5 min. Additional shimming was then carried out to fully optimize the system and the first spectra were recorded approximately 5 to 7 min after the sample was inserted into the magnet. Integration of the spectra was carried out using ACD labs 7.0 1-D $^1$H-NMR processor®. All FID files were processed at once. Phase correction and baseline correction were applied to the Fourier-transformed spectra and peaks were integrated manually. The concentrations were determined relative to the internal reference (formic acid) contained in the glass insert.

Downloaded by PENNSYLVANIA STATE UNIV on June 27, 2012 | http://pubs.acs.org
Publication Date: August 13, 2009 | doi: 10.1021/bk-2009-1024.ch011

## Results and discussion

### Selective initialization

Selective initialization occurs when the monomer is consumed in an equimolar amount with the RAFT agent for the sole formation of the RAFT agent single monomer adduct (see Scheme 1, where *n* = 1). Typical examples of selective initialization are with *S*-(2-cyano-2-propyl) *O*-ethyl xanthate (X2) and *S*-(2-ethyl phenylacetate) *O*-ethyl xanthate (X7) (Figure 2).

Downloaded by PENNSYLVANIA STATE UNIV on June 27, 2012 | http://pubs.acs.org
Publication Date: August 13, 2009 | doi: 10.1021/bk-2009-1024.ch011

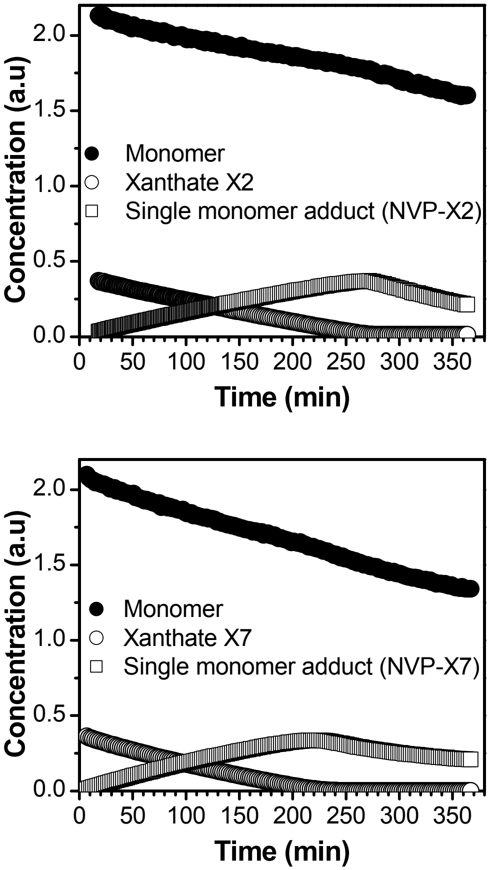

*Figure 2: concentration profiles in the X2 (top) and X7 (bottom) mediated polymerization of NVP*

The initialization reaction sequence (Scheme 1) consists of the addition of a monomer derived radical (RM•) onto the RAFT agent, subsequent fragmentation of the intermediate radical towards the release of the R group and the formation of the single monomer adduct. The overall reaction consists of the incorporation of one monomer unit in the RAFT agent to form the RAFT agent single monomer adduct.

The RAFT agent is efficient if it provides a fast equilibrium between active and dormant species, *i.e.* fast radical addition and fast fragmentation of adduct radicals (see Scheme 1). This requires a subtle adjustment between the rates of addition ($k_{add}$ and $k_{-\beta}$) and fragmentation ($k_{\beta}$ and $k_{-add}$) with respect to the rates of reinitiation ($k_i$) and propagation ($k_p$). Experimentally, rate constants are not available separately due to the interconnection among several competing reactions where the product of one reaction becomes the reagent of another one.

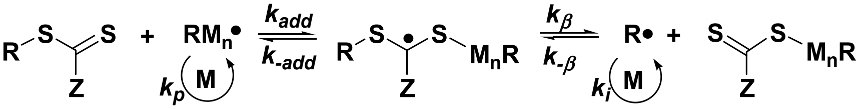

*Scheme 1: RAFT pre-equilibrium and rate constants of radical reactions.*

Selectivity during initialization implies that a maximum of one monomer unit is incorporated in the RAFT agent between two consecutive addition-fragmentation cycles, i.e. $k_{add}$ is high compared to $k_p$, and also that fragmentation from the intermediate radical releases the R group rather than the incoming radical, i.e. $k_\beta$ is high compared to $k_{-add}$. Hence, the R group must be a better leaving group than the monomer derived species. The R and Z groups must ensure a high rate of addition to the RAFT agent in comparison with the rate of propagation. Initialization studies also pointed out that the R group radical must be a good reinitiating group, i.e. $k_i$ must be higher than or in the same range as $k_p$. In a system where initialization is selective, the initial xanthate concentration decreases linearly with time. It is the rate of reinitiation that determines the length of the initialization period.

## Slow initialization

Slow initialization takes place when xanthate X1 is used with NVP. As seen in Figure 3, the monomer and RAFT agent X1 are consumed in an equimolar amount at a much lower rate than in the case of X2.

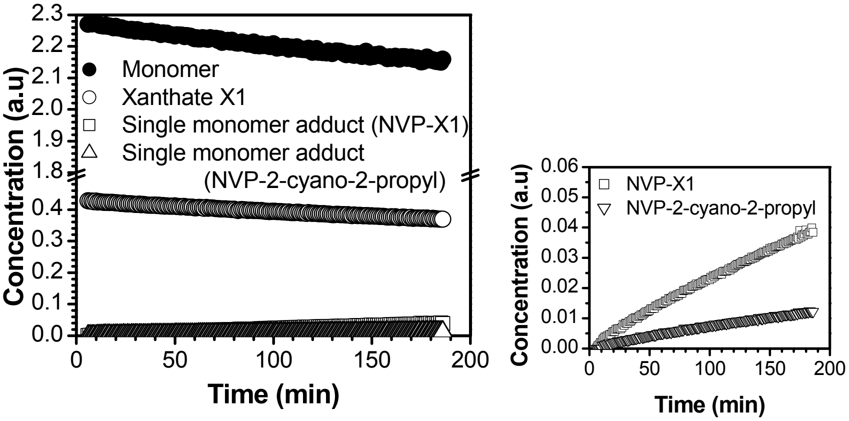

*Figure 3: concentration profiles in the X1 mediated polymerization of NVP. Right: enlargement in the low concentration region.*

Slow initialization occurs in systems where the rate of reinitiation (crosspropagation between the R group radical and the monomer) is significantly lower than the rate of propagation. Long initialization time is due to the R group radical having a low crosspropagation rate constant with the monomer, which can be explained mostly in terms of radical stability. In the

Downloaded by PENNSYLVANIA STATE UNIV on June 27, 2012 | http://pubs.acs.org
Publication Date: August 13, 2009 | doi: 10.1021/bk-2009-1024.ch011

present example the R group phenethyl is significantly more stable than the NVP derived radical, therefore the rate of addition of phenethyl radicals to NVP is low. Other factors than the radical stability (steric hindrance, polarity) also contribute to the crosspropagation step.

Selective but slow initialization may result in a significant fraction of chains being initiated by the primary radical source. As seen in Figure 3 (right), the single monomer adduct resulting from the addition of 2-cyano-2-propyl (from the initiator AIBN) to NVP accounts for approximately one fourth of all single monomer adduct species. Slow initialization may therefore be a problem where chain-end functionality needs to be introduced in the polymer via an R group functional RAFT agent.

Downloaded by PENNSYLVANIA STATE UNIV on June 27, 2012 | http://pubs.acs.org
Publication Date: August 13, 2009 | doi: 10.1021/bk-2009-1024.ch011

## Poorly selective initialization

An extreme case of poorly selective initialization can be illustrated with the use of *S*-(*tert*-butyl) *O*-ethyl xanthate (X5). In this system, the single monomer adduct could not be identified. From the concentration profiles presented in Figure 4 it is clear that more than one molar equivalent of monomer per RAFT agent was consumed before complete conversion of the initial RAFT agent, indicating that propagation had already occurred to a significant extent.

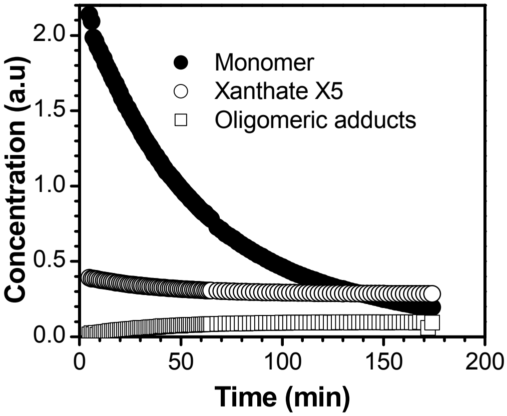

*Figure 4: concentration profiles in the X5 mediated polymerization of NVP*

The formation of oligomeric adducts from the beginning of the reaction can be due, in some cases, to the monomer-derived radicals having better leaving group ability than the R group. The *tert*-butyl radical being stabilized by 3 methyl substituents, it is unlikely that it has poorer leaving group ability than NVP-derived radicals. A more likely explanation is that the rate of addition of the propagating radical to the RAFT agent is lower than the rate of propagation. This could be due to the *tert*-butyl R group stabilizing the thiocarbonyl thio compound, resulting in low $k_{add}$. In this case, radicals can undergo multiple monomer additions prior to addition to the RAFT agent.

X4 and X6 showed a somewhat intermediate behavior between selective and poorly selective initialization. As can be seen in Figure 5, the xanthate is consumed in a close to equimolar ratio with the monomer. Nonetheless, second monomer adducts and higher (oligomeric) adducts were detected before the end of the initialization period, indicating a slight loss in selectivity. The xanthate concentration did not decrease linearly with time, but instead a curvature was observed, which was more pronounced in the case of X6 than of X4. These results indicate that the leaving group radicals and NVP derived radicals have similar reactivities. A sudden decrease in the rate of monomer consumption occurred upon completion of initialization with X4. This indicates that the radical 2-propionitrile from X4 has slightly better leaving group ability and/or a higher rate of addition to NVP (crosspropagation) than the rate of propagation.

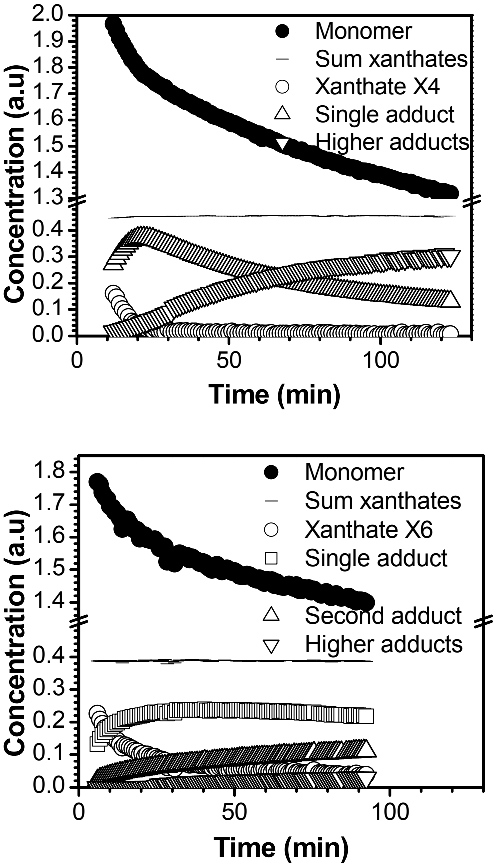

*Figure 5: concentration profiles in the X4 (top) and X6 (bottom) mediated polymerization of NVP*

Downloaded by PENNSYLVANIA STATE UNIV on June 27, 2012 | http://pubs.acs.org
Publication Date: August 13, 2009 | doi: 10.1021/bk-2009-1024.ch011

## Initialization and side-reactions

Initialization studies have enabled us to identify radical and non-radical side-reactions affecting the monomer and xanthate species.[9] These include consumption of NVP for the formation of an unsaturated dimer, hydration products due to the presence of traces of water, and more. In the case of X3, which R group contains a carboxylic acid functionality, esterification took place with NVP.[9] The concentration profiles in the X3 mediated polymerization of NVP (Figure 6) were affected by such side-reactions. The initialization behavior was expected to be similar to initialization with X2 due to the comparable nature of the substituents on the R group radical center. Although the rates of monomer and xanthate consumption and single adduct formation compare well, the concentration profiles do not follow a linear trend as is the case with X2. Also a higher than equimolar amount of NVP to xanthate was consumed. Consumption of NVP for side-reactions which are not related to the RAFT mechanism can explain this curvature. Until the end of this experiment, the only new xanthate species observed was the single monomer adduct, which confirmed the selectivity of the initialization step.

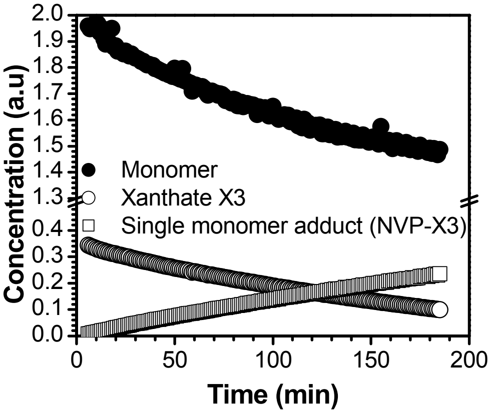

*Figure 6: concentration profiles in the X3 mediated polymerization of NVP*

Downloaded by PENNSYLVANIA STATE UNIV on June 27, 2012 | http://pubs.acs.org
Publication Date: August 13, 2009 | doi: 10.1021/bk-2009-1024.ch011

## Selectivity of initialization at low RAFT agent concentration

The selectivity of initialization is affected by the RAFT agent concentration. Van den Dungen *et al.* demonstrated that initialization can remain selective even at low RAFT agent concentrations.[10] At low RAFT agent concentrations, as is usually the case for polymer preparation, long initialization time can be mistaken for inhibition. Inhibition would suggest that no polymerization takes places. In systems where initialization is selective but slow, the monomer is consumed for the conversion of the RAFT agent into its single monomer adduct, however the change in monomer conversion can generally not be detected.

Although selectivity may not be retained at lower RAFT agent concentrations, poorly selective initialization observed at high RAFT agent concentration guarantees a “hybrid behavior” at low RAFT agent concentration. In such a “hybrid” system, higher molar mass material is obtained from the beginning of the reaction and new xanthate endcapped chains are formed late in the polymerization, leading to broad molar mass distribution of the resulting polymer.[5]

## Classification of the R groups with respect to NVP reactivity

The R group classification presented here is based on initialization studies. R groups on the left side of the scale gave selective initialization. R groups on the right side of the scale gave poorly selective initialization. The initialization time and selectivity decreased from left to right. This classification provides an indication of how the rate of fragmentation of the R group from the intermediate radical compares with that of the monomer derived species. It also gives an indication of how the rate of crosspropagation or addition of the R group radical to the monomer compares with the rate of propagation.

It is noteworthy to mention that our experimentally obtained classification slightly differs from that of Rizzardo *et al.* in the “Handbook of RAFT Polymerization”.[11] In particular, R groups producing stabilized radicals were found to be inadequate for NVP and VAc (results not shown) due to impractically long initialization times, *e.g.* $R=CH(CH_3)C_6H_5$. The present classification provides an explanation for long initialization times reported by other authors.

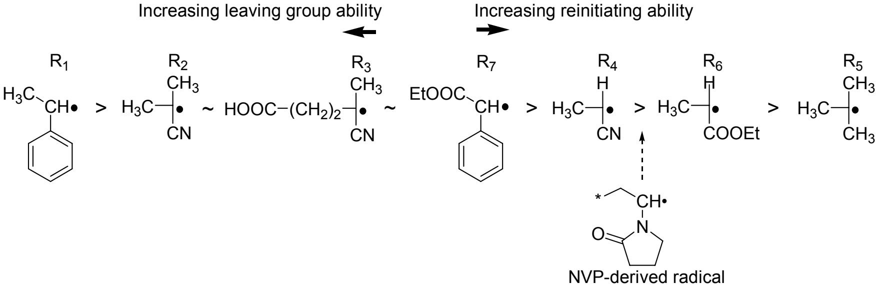

*Figure 7: Classification of R groups with respect to NVP reactivity*

There is currently a strong interest for the preparation of chain-end functional PVP including PVP with alpha chain-end functionality introduced via the RAFT agent R group. The classification of the R groups with respect to their ability to provide fast and selective initialization with NVP may serve as a guide for the design of RAFT agents for such applications. It can also be extrapolated to the preparation of block copolymers via polymerization of NVP in the presence of a macromolecular RAFT agent.

Downloaded by PENNSYLVANIA STATE UNIV on June 27, 2012 | http://pubs.acs.org
Publication Date: August 13, 2009 | doi: 10.1021/bk-2009-1024.ch011

## Conclusions

*In situ* NMR initialization experiments enabled screening xanthate RAFT agents with different R groups for their ability to control the polymerization of NVP. Three types of initialization behavior were identified, depending on the R group structure.

Selective initialization occurred with $R_1$=$C_6H_5CH(CH_3)$-, $R_2$=$(CH_3)_2C(CN)$-, $R_3$=$(HOOC(CH_2)_2C(CN)(CH_3)$- and $R_7$=$C_6H_5CH(CO_2Et)$. However, the rate of initialization with $R_1$ was very low compared to the rate of polymerization. Such a behavior was attributed to the poor ability of $R_1$ to reinitiate the polymerization of NVP. It is therefore recommended to avoid the use of $R_1$ with NVP in order to prevent the occurrence of a long induction period and loss of chain-end functionality, even at low xanthate concentrations. On the contrary, $R_2$ and $R_3$ and $R_7$ provide relatively fast and selective initialization and therefore are suitable to mediate the polymerization of NVP. Functionality can be introduced via the R group by using a xanthate prepared from a functional azo initiator, as is the case with X3.

$R_5$=$C(CH_3)_3$- displayed an extreme case of poorly selective initialization, where long oligomers were formed from the beginning of the reaction and only a fraction of the initial xanthate was used at close to 90% monomer conversion. $R_4$=$CH_3CH(CN)$- and $R_6$=$CH_3CH(CO_2Et)$- showed a slight hybrid behavior, where a small excess of monomer (less than 2 molar equivalents) was used for the conversion of the initial xanthate. Initialization was fast with $R_4$ and $R_6$, which suggests that they are good candidates to mediate the polymerization of NVP, although a hybrid behavior may be observed at low RAFT agent concentrations. $R_4$ has been identified as an R group with similar reactivity as the monomer NVP towards fragmentation from the intermediate radicals and addition to NVP.

A classification of the R group was provided according to the selectivity and length of the initialization step. The leaving group ability decreased and reinitiating group ability increased in the order: $C_6H_5CH(CH_3)\bullet$ > $R'CH_2C(CN)(CH_3)\bullet$ ~ $C_6H_5CH(CO_2Et)\bullet$ > $CH_3CH(CN)\bullet$ > NVP• > $CH_3CH(CO_2Et)\bullet$ > $C(CH_3)_3\bullet$.

Downloaded by PENNSYLVANIA STATE UNIV on June 27, 2012 | http://pubs.acs.org
Publication Date: August 13, 2009 | doi: 10.1021/bk-2009-1024.ch011

# References and notes

1. Devasia, R.; Bindu, R. L.; Borsali, R.; Mougin, N.; Gnanou, Y. *Macromol. Symp.* **2005**, *229*, 8-17.
2. Wan, D.; Satoh, K.; Kamigaito, M.; Okamoto, Y. *Macromolecules* **2005**, *38*, 10397-10405.
3. Nguyen, T. L. U.; Eagles, K.; Davis, T. P.; Barner-Kowollik, C.; Stenzel, M. H. *J. Polym. Sci. Part A: Polym. Chem.* **2006**, *44*, 4372–4383.
4. Postma, A.; Davis, T. P.; Li, G.; Moad, G.; O'Shea, M. S. *Macromolecules* **2006**, *39*, 5307-5318.
5. Pound, G.; McLeary, J. B.; McKenzie, J. M.; Lange, R. F. M.; Klumperman, B. *Macromolecules* **2006**, *39*, 7796 - 7797.
6. Barner-Kowollik, C.; Quinn, J. F.; Nguyen, T. L. U.; Heuts, J. P. A.; Davis, T. P. *Macromolecules* **2001**, *34*, 7849-7857.
7. Shi, L.; Chapman, T. M.; Beckman, E. J. *Macromolecules* **2003**, *36*, 2563-2567.
8. Bouhadir, G.; Legrand, N.; Quiclet-Sire, B.; Zard, S. Z. *Tetr. Lett.* **1999**, *40*, 277-280.
9. Pound, G.; Eksteen, Z.; Pfukwa, R.; McKenzie, J. M.; Lange, R. F. M.; Klumperman, B. *J. Polym. Sci. Part A: Polym. Chem.* **2008**, *46*, 6575-6593.
10. van den Dungen, E. T. A.; Matahwa, H.; McLeary, J. B.; Sanderson, R. D.; Klumperman, B. *J. Polym. Sci. Part A: Polym. Chem.* **2008**, *46*, 2500-2509.
11. Rizzardo, E.; Moad, G.; Thang, S. H. In *Handbook of RAFT polymerization*; Barner-Kowollik, C., Ed.; Wiley, 2008.

Downloaded by PENNSYLVANIA STATE UNIV on June 27, 2012 | http://pubs.acs.org
Publication Date: August 13, 2009 | doi: 10.1021/bk-2009-1024.ch011

Downloaded by DUKE UNIV on June 26, 2012 | http://pubs.acs.org
Publication Date: August 13, 2009 | doi: 10.1021/bk-2009-1024.ch012

## Chapter 12

# Gelation Kinetics of RAFT Radical Copolymerization of Methacrylate and Dimethacrylate

**Qiang Yu [1*], Qian Gan [1], Hongwen Zhang[1], and Shiping Zhu [2*]**

**[1.] School of Materials Science & Engineering, Jiangsu Polytechnic University, Changzhou, Jiangsu, China 213164**
**[2.] Department of Chemical Engineering, McMaster University, 1280 Main Street West, Hamilton, Ontario, Canada L8S 4L7**

The gelation kinetics and network development in the RAFT copolymerization of oligo(ethylene glycol) methyl ether methacrylate (OEGMEMA) and oligo(ethylene glycol) dimethacrylates (OEGDMA) were investigated using differential scanning calorimetry, solvent extraction/swelling technique, and dynamic mechanical analysis. A significant autoacceleration was observed in the RAFT copolymerization processes. For the RAFT systems with 2.56, 5.26, 8.11, and 11.11 mol% OEGDMA, the vinyl conversions at the onset of autoacceleration were ~26, 21, 17, and 15%, respectively, very close to the corresponding microgel points. This suggested that the highly branched chains and gels restricted the mobilities of propagating radicals and RAFT-capped chains, resulting in the autoacceleration. The gelation behavior in the RAFT process was different from that in conventional free radical polymerization. The slow chain growth in the RAFT process allowed sufficient chain relaxation and uniform distribution of reacting species, which reduced intramolecular crosslinking and limited microgel formation. Increasing OEGDMA concentration level resulted in earlier gelation and faster network development, giving rise to network products with higher crosslinking densities, higher glass transition temperatures, and deteriorated structural homogeneities.

In Controlled/Living Radical Polymerization: Progress in RAFT, DT, NMP & OMRP; Matyjaszewski, K.;
ACS Symposium Series; American Chemical Society: Washington, DC, 2009.

# Introduction

Reversible addition-fragmentation chain transfer (RAFT) polymerization is one of the most efficient and versatile polymerization techniques in the syntheses of well-defined polymers with controlled chain topology, composition, microstructure and functionality.[1-6] The mechanistic feature of RAFT is the establishment of an addition-fragmentation (propagating radical deactivation /activation) equilibrium.[1,5] A propagating radical adds to a dormant species (RAFT agent molecule or RAFT-capped chain) to form an intermediate radical, followed by fragmentation of the intermediate radical into another propagating radical, which, in the presence of monomers, propagates until it adds to a dormant species again. Frequent addition/fragmentation cycles between a small number of propagating radicals and a large number of dormant species provide all chains with an equal probability to grow, and thus give good control over the development of chain microstructure, such as molecular weight and composition. Current activities in the RAFT research are mainly focused on precise control of chain structure of linear and branched polymers, as well as on development of novel RAFT agents.[2-3]

Very recently, there has been an increasing interest in developing homogeneous polymer gel materials with controlled network micro-structural properties.[7-14] Conventional free radical polymerization (FRP) of various vinyl monomers in the presence of a small amount of divinyl cross-linker has been widely used for preparation of polymer networks. However, this process offers little control over the micro-structural properties of primary chains and resulting networks. Due to slow initiation, fast propagation and fast termination, it takes only seconds for individual chains in the FRP to fully grow from initiation to termination. Rapid reactions between propagating radicals and pendant double bonds in their vicinity yield highly crosslinked micro-domains (so-called microgels) at an early stage of polymerization, which subsequently results in structural heterogeneity in the network product.[15-18]

RAFT polymerization, as well as the other types of controlled/living radical polymerization (CLRP), has advantages over FRP in preparation of homogeneous polymer networks. The fast exchange between propagating radical and dormant species temporarily and frequently interrupts chain growth through propagation, and ensures that only few monomers add to a growing chain in each activation/deactivation cycle. During a long dormant period, the chain experiences sufficient relaxation and diffusion, giving rise to a uniform distribution of reaction species (radicals, monomers, primary chains, and pendant double bonds). The uniform distribution of reaction species minimizes microgel formation by suppressing intramolecular reactions such as cyclization and by facilitating intermolecular reactions such as crosslinking. More homogeneous polymer networks are thus produced.

Several groups have applied various CLRP techniques to syntheses of crosslinked polymers.[8-11,19-25] Norisuye and Fukuda[19] compared the structural and dynamic properties of polystyrene networks prepared by FRP and RAFT respectively using a time-resolved dynamic light scattering. Striking differences in gelation mechanism were observed between the two types. In the FRP system, cyclization or intramolecular crosslinking reactions dominated the early stage of

Downloaded by DUKE UNIV on June 26, 2012 | http://pubs.acs.org
Publication Date: August 13, 2009 | doi: 10.1021/bk-2009-1024.ch012

polymerization, thus introduced severe heterogeneities into the network product. In contrast, crosslinking reactions occurred more randomly in the RAFT system, resulting in a more homogeneous gel product. Our group studied the reaction behaviors and network structures in the RAFT polymerization of dimethacrylates using DSC and DMA.[21] We found that the RAFT polymerization of dimethacrylates showed significantly different reaction behaviors from its FRP counterpart. The restricted mobilities of propagating radical and RAFT-capped chain species induced diffusion-controlled addition reactions, resulting in a mild autoacceleration. The networks prepared by RAFT were more homogeneous than those prepared by FRP.

Polymerization kinetics plays an important role in determining the microstructural properties of primary chains and resulting network. Although the studies reported in literature revealed significant improvement in network homogeneity by applying CLRP technologies, the polymerization kinetics and its influence on the development of polymer networks have not been well understood. In this work, we report an experimental investigation on the RAFT copolymerization of a methacrylate/dimethacrylate system. The kinetic behavior, gelation, and network structural evolution with different divinyl concentration levels were examined systematically.

Downloaded by DUKE UNIV on June 26, 2012 | http://pubs.acs.org
Publication Date: August 13, 2009 | doi: 10.1021/bk-2009-1024.ch012

## Experimental Part

Materials. Oligo(ethylene glycol) methyl ether methacrylate (OEGMEMA, 99%) and Oligo(ethylene glycol) dimethacrylate (OEGDMA, 99%) were purchased from Aldrich and were used without further purification. The number-average molecular weights of OEGMA and OEGDMA measured by $^{1}$H NMR were 300 and 330 g/mol, respectively. Azobis-isobutyronitrile (AIBN, Aldrich, 97%) was used as radical initiator and was purified by recrystallization from chloroform-methanol. Benzyl dithiobenzoate (BDTB) was used as RAFT agent. It was synthesized according to an established procedure.[26-27]

Reaction recipe. The molar ratio of vinyl group to initiator and RAFT agent was set to 100:0.25:1. Take the RAFT system with OEGDMA molar fraction of 2.56% (5.0% based on vinyl groups) as a real synthetic example: 2.88 gram (9.5 mmol of vinyl group) of OEGMA, 83.3 mg (0.5 mmol of vinyl group) of OEGDMA, 4.1 mg (0.025 mmol) of AIBN, and 27.1 mg (0.1 mmol) of BDTB were added to a dry 10 mL glass ampoule. The ampoule was then sealed with a rubber septum and was degassed with ultrahigh-purity nitrogen for 10 min.

Kinetic measurement. The RAFT copolymerization was conducted in a differential scanning calorimeter (DSC, Pyris-1, Perkin-Elmer) in an isothermal mode. Approximately 20 mg of the reaction mixture was placed in an aluminum pan and the DSC cell was purged with ultrahigh-purity nitrogen for 5 min before the DSC was equilibrated at the reaction temperature (80 °C). During the isothermal DSC scanning, a 50 mL/min nitrogen flow was maintained to prevent intervention by oxygen. The heat flow evolving from the exothermic reaction was measured as a function of time. Since the heat evolved from consumption of vinyl groups is very large compared to possible heats from other reactions, it was assumed that other reactions would not have a significant effect on the amount of heat released. The theoretical enthalpy (-54.8 kJ/mol)[28] of methacrylate double bond in the complete conversion was used to calculate the rate of polymerization in terms of vinyl conversion (note: it is different from monomer conversion). Integrating the polymerization rate curve with respect to time provided the vinyl conversion as a function of time.[21]

Rheological measurement. The RAFT copolymerization was also conducted in a strain-controlled rheometer (Physica, MCR-301, Anton Paar) with parallel plate geometry (25 mm in diameter) and in an environmental chamber. Approximately 1 g reaction mixture, same as in the kinetic study, was put onto the lower plate. The upper parallel plate was lowered to tightly press the sample with a gap adjusted to 1.0 mm. A 5 L/min nitrogen flow was maintained as heating medium and protection atmosphere. After the chamber was quickly heated to the required temperature (80 °C), a time sweep was run in an oscillatory mode at a constant frequency of 1 Hz and a constant strain of 0.5%. The variation in the complex viscosity of the sample during the RAFT copolymerization was recorded.

Gel characterization. The glass ampoules containing the same reaction mixture as in the kinetic study were immersed into an oil bath parallel to the DSC and rheological measurements. The reaction was stopped at different time intervals by immersing an ampoule into an ice-water bath. The resulting product was put into a bottle containing 50-fold THF to extract residual monomers and sol polymers (note: oligomeric, linear, and branched polymer chains are soluble in THF). The solvent was replaced every other day over a period of at least one week until no more extractable polymer was detected. The insoluble portion (gel) was collected in a stainless metal screen with a pore size of 20 μm, and then dried to constant weight in a vacuum oven at 50 °C. The gel fraction ($f_g$) was then obtained by $f_g = W_g/W_p$, where $W_g$ is the dried gel weight, and $W_p$ is the total sample weight. The dried gel was put into THF at 25 °C for at least one week to reach swelling equilibrium. The swollen gel was then weighed to determine the swelling ratio ($S_g$), which was defined by $S_g = (W_s-W_g)/W_g$, where $W_s$ is the swollen gel weight, and $W_g$ is the dried gel weight. This measurement also provided information about the moment that gels started to appear during the RAFT copolymerization.

DMA measurement. The reaction mixture, same as in the kinetic study, was also introduced into a mould made of two glass plates separated by a 1 mm silicone gasket. The mould was then immersed to an oil bath for polymerization. The resulting products were used for structure characterization. Dynamic mechanical measurement was performed on the samples using a dynamic mechanical analyzer (Physica, MCR-301, Anton Paar) in a torsion model by applying a sinusoidal stress of 1 Hz frequency. The specimen was a thin rectangular sheet of 1 mm thick and 10 mm × 40 mm dimension. The storage modulus and loss tangent were recorded as a function of temperature with a ramping rate of 5 °C /min.

Downloaded by DUKE UNIV on June 26, 2012 | http://pubs.acs.org
Publication Date: August 13, 2009 | doi: 10.1021/bk-2009-1024.ch012

## Results and Discussion

### Kinetic Behavior of RAFT with Crosslinking

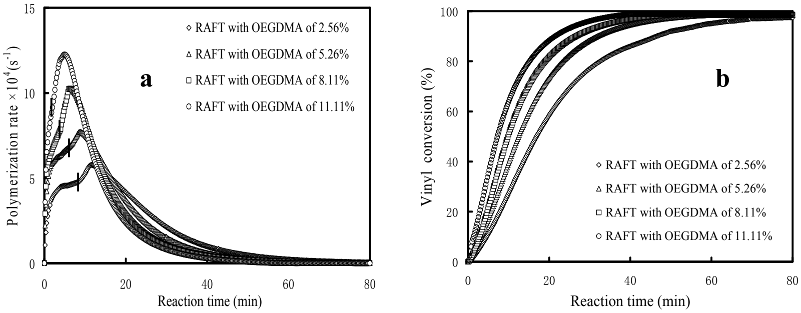

*Figure 1 (a) Polymerization rate and (b) vinyl conversion profiles for the RAFT copolymerization of OEGMEMA with different molar fractions of OEGDMA at 80 °C. Experimental conditions: [vinyl]:[AIBN]:[BDB] = 100:0.25:1 (The black bar represents the onset of autoacceleration).*

Figures 1a and b present the polymerization rate and vinyl conversion profiles for the RAFT copolymerization of OEGMA with four OEGDMA molar fraction levels (2.56, 5.26, 8.11, 11.11% based on monomer molecules, equivalent to 5.0, 10, 15, and 20 % based on vinyl groups). Some important kinetic features were observed. The copolymerization experienced an initial increase in the polymerization rate at the beginning of the reaction with the quick decomposition of the radical initiator, followed by a significant increase of Rp (autoacceleration) when the vinyl conversion reached a certain level. After that, Rp decreased gradually with time as vinyl groups were depleted.

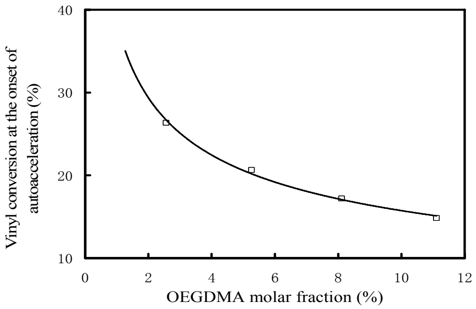

*Figure 2 Relationship between vinyl conversion at the onset of autoacceleration and OEGDMA molar fraction in the RAFT system under the same reaction conditions as in Figure 1.*

Downloaded by DUKE UNIV on June 26, 2012 | http://pubs.acs.org
Publication Date: August 13, 2009 | doi: 10.1021/bk-2009-1024.ch012

The rate autoacceleration in the network-forming RAFT system has been observed in the RAFT polymerization of dimethacrylates and it was attributed to diffusion-controlled addition reactions.[21] There are two types of radical populations involved in the RAFT process, propagating radical and intermediate radical. While the total radical concentration is determined by a pseudo steady-state equilibrium between initiation and termination, the propagating radical population is controlled by the addition-fragmentation equilibrium.[29] This equilibrium depends on the relative rates of the addition of propagating radicals to RAFT-capped dormant chains and the fragmentation of the formed intermediate radicals. In the network-forming system, with the generation of highly branched polymer chains and gels as the RAFT polymerization reached a certain vinyl conversion level, the mobilities of the propagating radicals and RAFT-capped chains were restricted, resulting in a diffusion-controlled addition reaction. This diffusion-controlled addition slowed down the deactivation of propagating radicals, resulting in an increase in the propagating radical concentration, and thus an increase in the polymerization rate. It should be pointed out that the radical termination reaction also becomes diffusion-controlled at the same time, due to its bimolecular nature and involvement of two macromolecular species. However, its effect on the increase in propagating radical population is compromised by the addition/fragmentation equilibrium and is thus minor.

If this explanation is valid, the onset of rate autoacceleration in the RAFT copolymerization of OEGMEMA/OEGDMA should be a function of the OEGDMA amount. Figure 2 shows the relation between vinyl conversion at the onset of autoacceleration and OEGDMA molar fraction in the RAFT copolymerization system under the same reaction conditions as in Figure 1. It can be observed that for the RAFT systems with OEGDMA of 2.56, 5.26, 8.11, and 11.11 mol%, the autoacceleration occurred at ~26, 21, 17, and 15% of vinyl conversion, respectively, and the rate increased with the OEGDMA molar fraction. Obviously, a higher concentration level of OEGDMA introduced more pendant groups into polymer chains, promoted branching and crosslinking, and gave rise to an earlier and stronger autoacceleration.

The vinyl conversion increased at different rates, depending on the OEGDMA molar fraction in the feed. The highest rate was found in the 11.11 mol% OEGDMA system, and the lowest was with 2.56 mol% OEGDMA. However, their final vinyl conversions were close up to 97 %, as shown in Figure 1b.

Downloaded by DUKE UNIV on June 26, 2012 | http://pubs.acs.org
Publication Date: August 13, 2009 | doi: 10.1021/bk-2009-1024.ch012

## Gelation

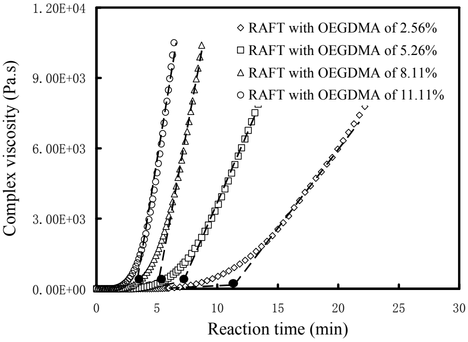

*Figure 3 Variation of the complex viscosity during the RAFT copolymerization of OEGMEMA with different molar fractions of OEGDMA under the same reaction conditions as in Figure 1 (The black circle represents the onset of macro-gelation).*

Gelation represents an abrupt transition from a viscous liquid of linear and branched polymer chains to an elastic gel. The gel point is defined as time (or vinyl conversion) at which the polymerization reaches this transition. In the literature, some researchers defined the gel point as the moment when the reaction mixture lost its mobility in an upside-down position held for 10 s,[9,22-23] whereas others determined the gel point as the moment that gel materials can be collected by solvent extraction.[11,14] In FRP with crosslinking, the experimental data obtained by the two methods were very different because of an involvement of microgels. In our experiment, the gelation process was examined by both rheological and solvent extraction measurements. The former followed the variation in complex viscosity of the reaction medium. It was found that the complex viscosity increased steadily at the beginning of reaction and this increase accelerated abruptly due to network formation (see Figure 3). This abrupt acceleration in the increase of complex viscosity was taken as the onset of macro-gelation (macrogel point).[30] The solvent extraction provided the information on gel amounts at different time intervals, as well as time when gels started to appear, which was defined as the onset of micro-gelation (microgel point).

Figure 4 correlates the vinyl conversions at the onset of micro-gelation, determined by the solvent extraction, and at the onset of macro-gelation, measured in the rheological test, to the OEGDMA molar fraction. Figure 5a and b present the gel fraction and swelling ratio data, respectively.

Downloaded by DUKE UNIV on June 26, 2012 | http://pubs.acs.org
Publication Date: August 13, 2009 | doi: 10.1021/bk-2009-1024.ch012

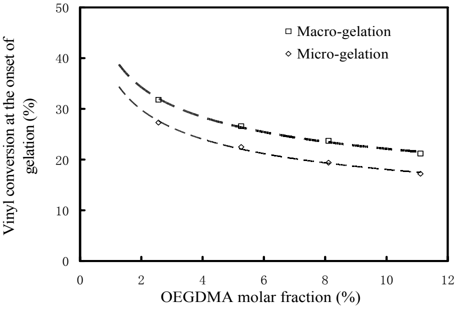

*Figure 4 Vinyl conversions at the onset of the gelation for the RAFT copolymerization of OEGMEMA with different molar fractions of OEGDMA under the same reaction conditions as in Figure 1.*

Gelation in the conventional FRP crosslinking systems has been extensively studied.[9,15-18,31-32] Due to slow initiation, fast propagation and fast termination, polymer chains with full length and pendant double bonds are formed from the beginning of polymerization. Since polymer chains in the system are very diluted at this moment, and the diffusion of chains is relatively slow compared to the fast propagation, the reaction between radical and pendant double bonds mostly occurs within the same molecule, producing various cycles in the chain. As the reaction proceeds, the number of such chains increases, and the intermolecular reactions between these chains result in the formation of densely crosslinked domains (microgels) at a very early stage of polymerization.[31-32] Microgels quickly grow through reacting with other chains, and become detectable by solvent extraction (microgel point), while the reaction system remains its fluidity. At a higher conversion, these microgels react with each other via intermolecular crosslinking to form huge polymer networks (macrogel point). The reaction medium loses its mobility. Ide and Fukuda found that insoluble gels were detected at a very early stage of copolymerization of styrene and divinyl biphenyl, while the macro-gelation occurred much later.[9]

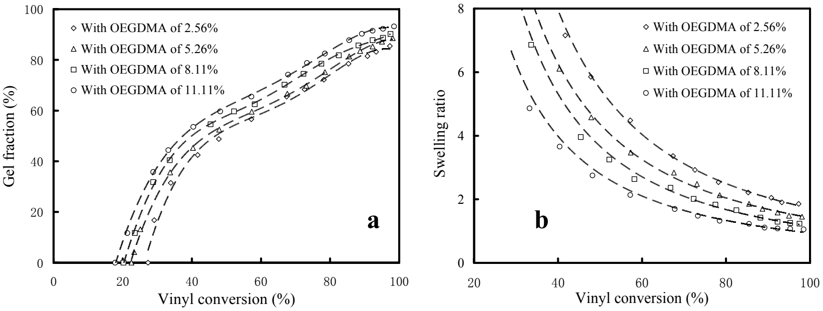

*Figure 5 Development of gel fraction (a) and swelling ratio (b) versus vinyl conversion during the RAFT copolymerization of OEGMEMA with different molar fractions of OEGDMA under the same conditions as in Figure 1.*

Downloaded by DUKE UNIV on June 26, 2012 | http://pubs.acs.org
Publication Date: August 13, 2009 | doi: 10.1021/bk-2009-1024.ch012

The experimental data in Figure 4 to Figure 5 showed that the gelation behavior in RAFT process was different from that in FRP. No gel materials were collected from the low conversion samples. The vinyl conversions at the onsets of micro- and macro-gelation were very close. This indicated that intramolecular cyclization and microgel formation were greatly suppressed, and the network was formed mainly through the intermolecular reactions between highly branched chains. In the RAFT, the majority of primary chains (radical and dormant) were initiated within a short period of time at the early stage of polymerization. The fast and frequent exchange of propagating radicals with dormant chains interrupted chain growth, leading to slow but simultaneous growth of the primary chains. The slow chain growth gave sufficient time for chain relaxation and diffusion of reacting species. With more uniform distribution of vinyl groups (pendant and monomeric) in the reaction medium, the propagating radicals reacted with monomers, crosslinkers, and pendant double bonds in a more statistically random manner proportional to their concentrations, which limited intramolecular cyclization and microgel formation at the early stage of the reaction. The intermolecular reaction between propagating radicals and pendant double bonds generated branched polymer chains. The branched polymers had enhanced possibility to react with each other than the linear counterpart because the branched polymers contained more pendant double bonds and/or radical centers. The successive intermolecular reactions between branched chains eventually yielded the polymer network having an “infinite” large weight-average molecular weight (macro-gelation). After that, the network further developed through the propagation of gel radicals with monomers and the incorporation of sol polymers via the reactions between radicals and pendant double bonds of both gel and sol populations. The gel fraction and the network crosslinking density gradually increased, and the gel swelling ratio reduced.

Divinyl concentration level significantly influenced the gelation process and the network development. It was observed that the macrogel points appeared at ~32, 26, 23, and 21 % of vinyl conversion, respectively, as the molar fraction of OEGDMA increased from 2.56 to 5.26, 8.11, and 11.11%. The final gel fraction and the network crosslinking density also increased with the OEGDMA molar fraction. Increasing divinyl concentration resulted in an increased number of pendant groups in the polymer chains, which induced a more rapid gelation and faster development of the network. It was also interesting to note that the micro-gelation occurred at the same conversion region as did the autoacceleration. Clearly, the highly branched chains and gels restricted the mobilities of propagating radicals and RAFT-capped chains, resulting in a diffusion-controlled addition reaction. It provides further experimental evidence to support the origination of the rate autoacceleration in the RAFT crosslinking system.

## RAFT-crosslinked network structure

The structural properties of the network products resulted from the RAFT copolymerization of OEGMEMA with different levels of OEGDMA were characterized by dynamic mechanical analyzer (DMA). Figures 6a and b show

Downloaded by DUKE UNIV on June 26, 2012 | http://pubs.acs.org
Publication Date: August 13, 2009 | doi: 10.1021/bk-2009-1024.ch012

the evolution of storage modulus and loss tangent as a function of temperature. It was observed that the networks experienced a transition from a glassy state to a rubbery state in the range of -70 to 0 ℃. The storage modulus in the rubbery region is an indication of network crosslinking density. The rubbery moduli of the samples with OEGDMA of 2.56, 5.26, 8.11, and 11.11 mol% at 20 ℃ were 0.558, 0.889, 1.21, and 1.48 ($\times 10^6$) Pa, respectively. Flory's theory of elasticity was used to estimate the crosslinking density from the rubbery modulus. Figure 7 shows the crosslinking density and glass transition temperature as a function of OEGDMA molar fraction. The glass transition temperature was obtained from the peak maximum of the tanδ curves in Figure 6b.

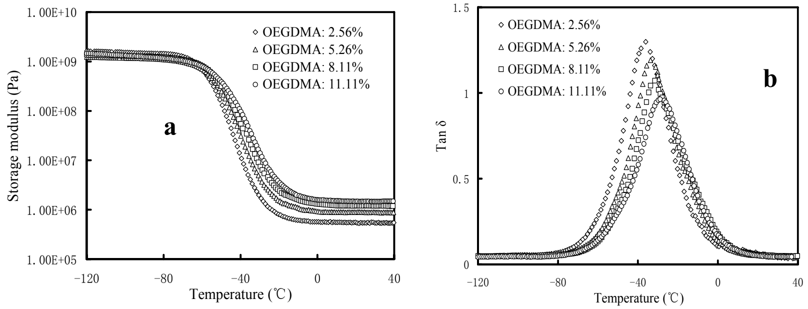

*Figure 6 Storage modulus (a) and loss tangent (b) versus temperature for the polymer networks prepared by the RAFT in Figure 5.*

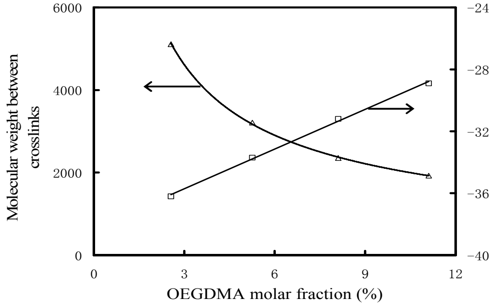

*Figure 7 Crosslinking density and glass transition temperature of RAFT network as a function of OEGDMA molar fraction.*

The networks prepared with higher OEGDMA molar fractions had higher crosslinking densities and thus higher glass transition temperatures. This increase in crosslinking density was expected because an increased divinyl crosslinker concentration level introduced more pendant double bonds, which contributed to the increased number of effective crosslinks, resulting in the denser network structure. The dense network restricted the mobility of chains and thus gave higher glass transition temperature.

It has been suggested[15,18,20,33] that the height of glass transition peak in a tanδ-temperature curve depends on the number of kinetic units adequately mobile to contribute to transition, while the breadth of transition region is

Downloaded by DUKE UNIV on June 26, 2012 | http://pubs.acs.org
Publication Date: August 13, 2009 | doi: 10.1021/bk-2009-1024.ch012

related to the extent of structural heterogeneity. The tanδ peak height of the network samples in Figure 6a decreased with the higher molar fraction of OEGDMA, which was ascribed to increased crosslinking density and shortened chain length between the crosslinks. It was also observed that the half-width of the tanδ peak increased with the OEGDMA mole concentration. The half-width values were 26.7, 28.3, 29.7, and 30.6 °C, respectively, for the polymer networks prepared with 2.56, 5.26, 8.11, and 11.11 mol% OEGDMA. This indicated that the degree of structural heterogeneity increased with the network crosslinking density and that the networks with high crosslinking density levels had broader distributions of chain segmental mobilities.

## Conclusion

Based on the experimental investigation on the reaction kinetics and evolution of polymer networks in the RAFT copolymerization of OEGMEMA/OEGDMA, the following conclusions can be drawn.

(1) The RAFT copolymerization of OEGMA with four OEGDMA molar fraction levels all experienced a significant rate autoacceleration, and this autoacceleration came earlier with higher OEGDMA concentration level. The autoacceleration and micro-gelation process occurred at the same conversion region. It is confirmed that the autoacceleration in the RAFT crosslinking system originated from the restricted mobilities of propagating radicals and RAFT-capped chains.

(2) The vinyl conversions corresponding to gel appearance (solvent extraction) and macro-gelation (abrupt increase in viscosity) were very close in the RAFT copolymerizations, indicating that the intermolecular cyclization and microgel formation were suppressed in the RAFT crosslinking system. RAFT copolymerization with higher concentration of OEGDMA resulted in more rapid gelation and faster development of the network.

(3) The structural properties of the networks resulted from the RAFT copolymerization of OEGMEMA/OEGDMA were related to the divinyl molar concentration. The RAFT copolymerization with higher levels of OEGDMA concentration produced polymer networks with higher crosslinking density, higher glass transition temperature and higher degree of structural heterogeneity.

Downloaded by DUKE UNIV on June 26, 2012 | http://pubs.acs.org
Publication Date: August 13, 2009 | doi: 10.1021/bk-2009-1024.ch012

## Acknowledgment

The authors thank National Natural Science Foundation of China for the financial support of this research (No. 20674032).

## References

1 Chiefari, J.; Chong, Y. K.; Ercole, F.; Krstina, J.; Le, T. P. T.; Mayadunne, R. T. A.; Meijs, G. F.; Moad, G.; Moad, C. L.; Rizzardo, E.; Thang S. H. *Macromolecules* **1998**, *31*, 5559.

2 Moad, G.; Rixxard E.; Thong S. H. *Aust. J. Chem.* **2005,** *58*, 379.

3 Perrier, S.; Takolpuckdee, P. *J. Polym. Sci. Part A: Polym. Chem.* **2005,** *43*, 5347.

4 Barner-Kowollik, C.; Buback, M.; Charleux, B.; Coote, M. L.; Drache, M.; Fukuda, T.; Goto, A.; Klumperman, B.; Lowe, A. B.; McLeary, J. B.; Moad, G.; Monteiro, M. J.; Sanderson, R. D.; Tonge, M. P.; Vana, P. *J. Polym. Sci. Part A: Polym. Chem.* **2006,** *44*, 5809.

5 Cowe, A. B.; McCormick, C. L. *Prog. Polym. Sci.* **2007,** *32*, 283.

6 Braunecker, W. A.; Matyjaszewski, K. *Prog. Polym. Sci.* **2007,** *32*, 93.

7 Abrol, S.; Caulfield, M. J.; Qiao, G. G.; Solomon, D. H. *Polymer* **2001,** *42*, 5987.

8 Ward, J. H.; Shahar, A.; Peppas, N. A. *Polymer* **2002,** *43*, 1745.

9 Ide, N.; Fukuda, T. *Macromolecules* **1999,** *32*, 95.

10 Yu, Q.; Zeng, F.; Zhu, S. *Macromolecules* **2001,** *34*, 1612.

11 Jiang, C. F.; Shen, Y. Q.; Zhu, S.; Hunkeler, D. *J. Polym. Sci. Part A: Polym. Chem.* **2001,** *39*, 3780.

12 Anseth, K. S.; Metters, A. T.; Bryant, S. J. *J. Controlled Release* **2002,** *78*, 199.

13 Rydholm, A. E.; Bowman, C. N.; Anseth, K. S. *Biomaterials* **2005,** *26*, 4495.

14 Yu, Q.; Zhang, J.; Cheng, M; Zhu, S. *Macromol. Chem. Phys.* **2006,** *207*, 287.

15 Kannurpatti, A. R.; Anseth, J. W.; Bowman, C. N.. *Polymer* **1998,** *39*, 2507.

16 Bastide, J.; Leibler, L. *Macromolecules* **1988,** *21*, 2647.

17 Rey, L.; Duchet, J.; Galy, J.; Sautereau, H.; Vouagner, D.; Carrion, L. *Polymer* **2002,** *43*, 4375.

18 Allen, P. E. M.; Simon, G. P.; Williams, D. R. G.; Williams, E. H. *Macromolecules* **1989,** *22*, 809.

19 Norisuye, T.; Morinaga, T; Tran-Cong-Miyata, Q.; Goto, A.; Fukuda, T.; Shibayama, M. *Polymer* **2005,** *46*, 1982.

20 Yu, Q.; Zhou, M.; Ding, Y.; Jiang, B.; Zhu, S. *Polymer* **2007,** *48*, 7058.

21 Yu, Q.; Zhu, Y; Ding, Y; Zhu, S. *Macromol. Chem. Phys.* **2008,** *209*, 551.

22 Gao, H.; Min, K.; Matyjaszewski, K. *Macromolecules* **2007,** *40*, 7763.

23 Gao, H.; Li, W.; Matyjaszewski, K. *Macromolecules* **2008,** *41*, 2335.

24 Krasia, T. C.; Patrickios, C. S. *Macromolecules* **2006,** *39*, 2467.

25 Achilleos, M.; Krasia, T. C.; Patrickios C. S. *Macromolecules* **2007,** *40*, 5575.

Downloaded by DUKE UNIV on June 26, 2012 | http://pubs.acs.org
Publication Date: August 13, 2009 | doi: 10.1021/bk-2009-1024.ch012

26 Moad, G.; Chiefari, J.; Chong, Y. K.; Krstina, J.; Mayadunne, R. T. A.; Postma, A.; Rizzardo, E.; Thang, S. H. *Polym. Int.* 2000, *49*, 993.

27 Ganachaud, F.; Monteiro, M. J.; Gilbert, R. G.; Dourges, M. A.; Chang, S. H.; Rizzardo, E. *Macromolecules* **2000,** *33*, 6738.

28 Ansenth, K. S.; Wang, C. M.; Bowman, C. N. *Polymer* **1994,** *35*, 3243.

39 Calitz, F. M.; Tong, M. P.; Sanderson, R. D. *Macromolecules* **2003,** *36*, 5.

30 Winter, H. H.; Chambon, F. *Journal of Rheology*, **1986**, *32*, 367.

31 Tobita, H.; Hamielec, A. E. *Macromolecules* **1989,** *22*, 3098.

32 Zhu, S.; Hamielec, A. E. *Macromolecules* **1992,** *25*, 5457.

33 Robert, GE.; Waite, EF. *The Physics of Glassy Polymers;* RN. Haward; New York, Wiley: **1973**.

Downloaded by DUKE UNIV on June 26, 2012 | http://pubs.acs.org
Publication Date: August 13, 2009 | doi: 10.1021/bk-2009-1024.ch012

Downloaded by DUKE UNIV on June 27, 2012 | http://pubs.acs.org
Publication Date: August 13, 2009 | doi: 10.1021/bk-2009-1024.ch013

## Chapter 13

# Amphiphilic Block Copolymers Synthesized via RAFT: Stimulus-Induced Nanoscale Assembly and Cross-linking in Aqueous Media

**Matthew G. Kellum,[1] Adam E. Smith,[1] Xuewei Xu,[1] and Charles L. McCormick[1,2]**

**Departments of [1]Polymer Science and [2]Chemistry and Biochemistry,
The University of Southern Mississippi, 118 College Drive,
Hattiesburg, MS 39406**

In this chapter we present an overview of amphiphilic block copolymer systems synthesized via reversible addition fragmentation chain transfer (RAFT) polymerization in our group. The solution behavior of these systems as a function of temperature, pH, or electrolyte concentration is discussed. In addition, an overview of the cross-linking of such systems utilizing covalent cross-linking, interpolyelectrolyte complexation, or in situ metal chelation is presented.

In Controlled/Living Radical Polymerization: Progress in RAFT, DT, NMP & OMRP; Matyjaszewski, K.;
ACS Symposium Series; American Chemical Society: Washington, DC, 2009.

## Introduction

Amphiphilic block copolymers that reversibly assemble into nanostructures in response to stimuli such as temperature, pH, ionic strength, etc. have been the subject of extensive research for over two decades. The recent advent of controlled radical polymerization (CRP) techniques has led to exquisite control of polymer architecture, molecular weight, and polydispersity. Of particular note is the facility by which reversible addition-fragmentation chain transfer (RAFT) polymerization can be utilized to prepare di- and triblock copolymers with thermally responsive, amphoteric, or electrolyte character, allowing the stimuli-induced formation of well-defined nanostructures in aqueous media. A number of unprotected functional monomers, which can be subsequently used for in situ conjugation or cross-linking reactions, can be polymerized directly in aqueous media. In this chapter, we review recent progress towards synthesis of diblock and triblock copolymers capable of reversible assembly into micelles, vesicles, or other nanostructures in water. We also overview efforts in "locking" such assemblies via covalent cross-linking, interpolyelectrolyte complexation, or in situ metal chelation.

Downloaded by DUKE UNIV on June 27, 2012 | http://pubs.acs.org
Publication Date: August 13, 2009 | doi: 10.1021/bk-2009-1024.ch013

### Morphological Transitions in Dilute Aqueous Block Copolymer Solutions

Amphiphilic block copolymers can assemble into a variety of complex morphologies in dilute aqueous solution including micelles, vesicles, tubules, and large complex micelles. These morphologies are dictated by a number of factors including the length of both the hydrophilic and hydrophobic blocks, polymer concentration in solution, and the nature of the solution used for aggregate formation. A variety of techniques have been utilized to promote assembly of these aggregates. Initial procedures relied on dissolution of the polymer in a common solvent for both blocks followed by dialysis against a selective solvent for one block. In most studies, an organic solvent (e.g. N,Ndimethylformamide (DMF), tetrahydrofuran (THF), or dioxane) was used to molecularly dissolve the block copolymers. Aggregation was then promoted by the addition of water followed by dialysis to remove the organic solvent.

Eisenberg and coworkers were the first to report a variety of morphologies from block copolymers consisting of long hydrophobic polystyrene (PS) blocks and short hydrophilic poly(acrylic acid) (PAA) blocks (1). Numerous morphologies were achieved by maintaining a constant PS block length of 200 while varying the PAA block length from 4 to 21 repeat units. Decreasing the PAA block length led to morphological transitions from micelles to rods to vesicles to large compound micelles. Eisenberg and coworkers later reported similar morphology changes utilizing block copolymers containing a PS block, 240 repeat units, and shorter poly(ethylene oxide) (PEO) blocks ranging from 15 to 180 repeat units (2). By increasing the hydrophilic block length, transitions from spherical to rod-like or vesicular structures were observed.

The Eisenberg group also showed that alteration of solution properties (i.e. pH or salt concentration) can dramatically affect solution morphology (3). By adding HCl or NaCl to dilute aqueous PS-b-PAA copolymer solutions, morphological transitions were observed. The presence of by-ions decreases both steric and electrostatic repulsions in the charged PAA coronas. Increasing HCl or NaCl concentration leads to morphological transitions from spheres to rods to vesicles and even to a new morphology termed large compound vesicles. Similar transitions have been observed with the addition of $CaCl_2$ and are attributed to binding or bridging of the charged PAA coronas.

Since Eisenberg's discovery of these polymeric morphologies, other research groups have observed unique morphologies in dilute aqueous solutions using other amphiphilic block copolymer systems. For instance, Bates et al. found that manipulating the block lengths of polybutadiene (PB) and PEO led to multiple morphologies (4). These results presented along with previous data (5) show that as the weight percent of PEO incorporated within the block copolymer increases, a trend from vesicles to cylinders to spheres is observed.

Downloaded by DUKE UNIV on June 27, 2012 | http://pubs.acs.org
Publication Date: August 13, 2009 | doi: 10.1021/bk-2009-1024.ch013

## Stimuli-Responsive Morphological Transitions

## Controlled Radical Polymerization Techniques

Advances in CRP techniques provide a synthetic route to achieve well-defined polymers with complex architectures, controlled molecular weights, and narrow molecular weight distributions, thus allowing the tailorinig of polymers for specific technological applications (6-8). The most significant CRP techniques include stable free radical polymerization (SFRP) (9,10), atom transfer radical polymerization (ATRP) (11-13), and RAFT polymerization (1418). The levels of control achieved by these polymerization techniques are comparable to traditional living techniques; however, wider monomer selection and less stringent reaction conditions make these techniques more versatile than conventional living techniques.

Many researchers have utilized these CRP techniques for the synthesis of homopolymers, block copolymers, and post-reaction-modified polymers for use in aqueous media(19-22). A wide range of monomers have been used to produce anionic, cationic, zwitterionic, and neutral polymers. Much of the work in this area is focused on the preparation of stimuli-responsive block copolymers which can reversibly assemble in aqueous solution in response to environmental changes (temperature, pH, electrolyte concentration). Such systems are capable of producing morphologies previously reported by the Eisenberg group with the advantage of direct dissolution in aqueous conditions and reversible aggregation.

Responsive Morphologies

Numerous stimuli-responsive block copolymer systems have been shown to aggregate into spherical and vesicular assemblies in aqueous solutions; however, interest has shifted as to how these morphologies respond to varying environmental conditions. For example, Armes and coworkers reported a block copolymer consisting of a hydrophilic PEO block and a pH-responsive poly[2(diethylamino)ethyl methacrylate-stat-3-(trimethoxysilyl) propyl methacrylate] (P(DEA-stat-TMSPMA)) block (23). This block copolymer assembled into vesicles which were then cross-linked using the siloxane groups to permanently retain the morphology. Utilizing the pH-responsive nature of the DEA groups, the permeability and size of the vesicles could be altered by varying the pH.

Another important contribution to stimuli-responsive morphologies was that by Grubbs et al. who reported that a triblock copolymer could transition from micelles to vesicles via a change in temperature (24). A triblock copolymer consisting of a permanently hydrophilic PEO block, a temperature-responsive poly(N-isopropyl acrylamide) (PNIPAM) block, and a permanently hydrophobic poly(isoprene) (PI) was utilized in the study. Initially, micelles were observed in solution due to aggregation caused by the PI blocks. Upon heating, the PNIPAM block became hydrophobic, thus increasing the total hydrophobic portion of the block copolymer. This in situ change resulted in a transition from micellar to vesicular aggregates.

Downloaded by DUKE UNIV on June 27, 2012 | http://pubs.acs.org
Publication Date: August 13, 2009 | doi: 10.1021/bk-2009-1024.ch013

## Drug Transport Vehicles

### Stimuli-Responsive Morphologies for Drug Delivery

Although polymeric transport vehicles for drugs targeted to specific organs were envisioned by Ringsdorf over 30 years ago (25), only recently have CRP techniques, in particular RAFT, become available for preparing structures with the appropriate architectures for use in biological media (22). Over the past few years, research has focused on advanced design of precisely structured, responsive polymer-drug conjugates, micelles, polymersomes, and other nanoparticles capable of payload delivery.

Polymeric vesicles have great potential for the delivery of hydrophilic drugs due to the aqueous core within the assembly. Many research groups have shown the facility by which drugs can be incorporated into vesicles followed by either a burst release due to in situ stimuli or slow release related to diffusion through the vesicle wall. Eisenberg and coworkers loaded vesicles with doxorubicin (DOX), a potent antibiotic used against tumors and leukemias, and showed a tunable release pattern (26). In this study $PS_{310}$-b-$PAA_{36}$ copolymers, shown to form vesicles, were loaded with DOX under varying solution compositions of water and dioxane. The dioxane increases the permeability of the vesicles and hence increased the amount of DOX incorporated within the vesicles. Release profiles were then generated which showed that the rate of DOX released could be altered by changing the solution environment. Armes et al. prepared pH-responsive DOX-loaded vesicles (27) from a permanently hydrophilic, biocompatible zwitterionic block and a pH-responsive block, used to trigger vesicle formation. They show that without the presence of vesicles DOX release is rapid (80 % within 5 minutes) while DOX-loaded vesicles are able to release the drug in a slower and more controlled manner. The above examples illustrate the potential and versatility of utilizing complex morphologies as tunable releasing agents.

### Shell Cross-linking of Drug Delivery Vehicles

Despite the recognized potential of block copolymer assemblies such as micelles or vesicles as drug delivery vehicles, clinical application has been limited. Upon injection of a polymeric drug carrier into the bloodstream, a large dilution effect occurs, resulting in concentrations below the critical aggregation concentration (CAC); once the concentration decreases below the CAC, a burst release of the drug occurs as the aggregate undergoes dissolution (28). This drawback can be overcome by cross-linking the nanostructure. Unfortunately, the core cross-linking of a micelle decreases the drug carrying capacity and thus limits its application as a drug delivery vehicle (29). An alternative approach is to cross-link the shell of the self-assembled aggregate. The first example of shell cross-linked micelles was reported by Wooley and co-workers, who oligomerized pendant styrene groups using free radical chemistry (30). Numerous strategies have since been developed for the shell cross-linking of micelles including carbodiimide coupling (31-34); cross-linking with 1,2-bis(2iodoethoxy)ethane (35-37), divinyl sulfone (38), or glutaraldehyde (39); interpolyelectrolyte complexation (40-43); metal-catalyzed cross-linking (44) and click chemistry (45).

## Shell Cross-linking of Stimuli-Responsive Morphologies Using RAFT Polymers

### Shell Cross-linking via Interpolyelectrolyte Complexation

Since the seminal work by Armes and coworkers (41) in 2004, our group has investigated a number of stimuli-responsive copolymer systems capable of forming shell cross-linked micelles and vesicles through interpolyelectrolyte complexation. In 2006, we reported the formation of vesicles prepared from the self-assembly of poly(N-(3-aminopropyl) methacrylate hydrochloride (APMA))b-PNIPAM in water (Scheme 1) (40). At room temperature, the diblock copolymer readily dissolves in aqueous solution; however, upon increasing the solution temperature above the LCST of the PNIPAM block, the diblock copolymer self-assembles into uniform aggregates with hydrodynamic diameters of approximately 280 nm, indicative of vesicles (Figure 1). Since APMA is pH-responsive, the vesicle stability was investigated at varying pH values. The vesicles remained intact over the studied pH range while the size varied with the degree of protonation of the APMA units (310 nm at pH 3.0 and 220 nm at pH 10.8).

Downloaded by DUKE UNIV on June 27, 2012 | http://pubs.acs.org
Publication Date: August 13, 2009 | doi: 10.1021/bk-2009-1024.ch013

Downloaded by DUKE UNIV on June 27, 2012 | http://pubs.acs.org
Publication Date: August 13, 2009 | doi: 10.1021/bk-2009-1024.ch013

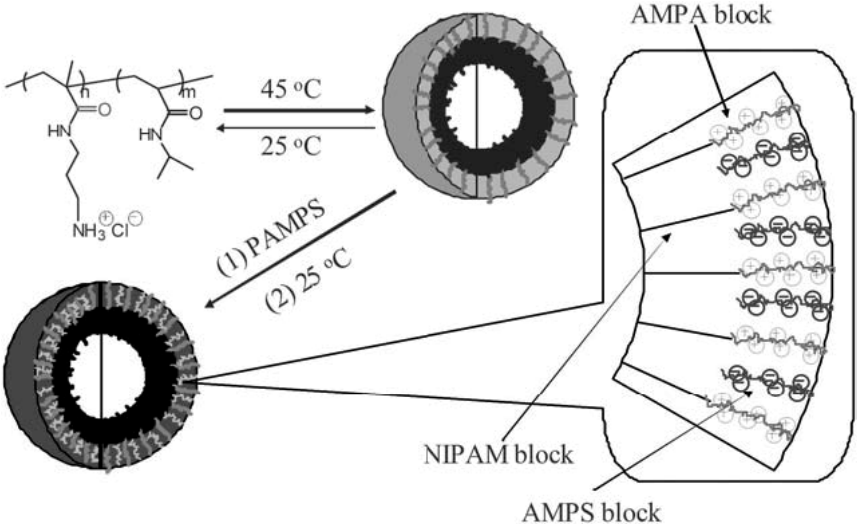

*Scheme 1. Formation of vesicles from PAPMA-PNIPAM diblock copolymers and their subsequent ionic cross-linking. PAPMA: poly(N-(3-aminopropyl) methacrylamide hydrochloride). (Reproduced from reference 40. Copyright 2006 John Wiley & Sons LTD.)*

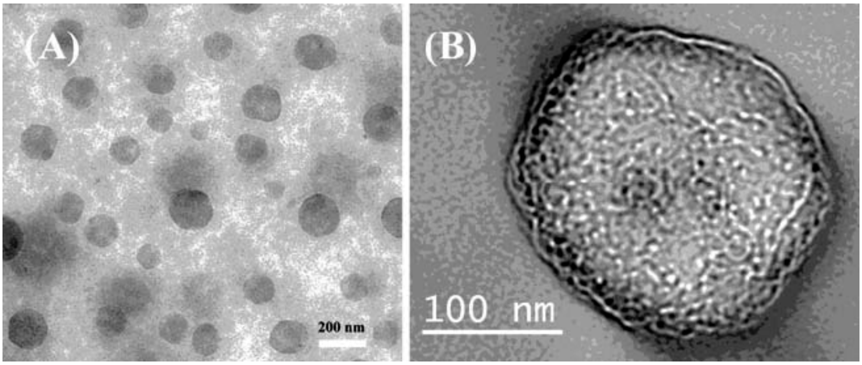

*Figure 1. Transmission electron microscopy images of (A) vesicles prepared from PAPMA88-PNIPAM50 via rapid increase of solution temperature from 25 °C to 45 °C. (B) Single vesicle. (Reproduced from reference 40. Copyright 2006 Science.)*

The cationic PAPMA shells of the vesicles were subsequently cross-linked through interpolyelectrolyte complexation (IPEC) with an anionic polyelectrolyte, poly(sodium 2-acrylamido-2-methylpropane sulfonate) (PAMPS). After shell cross-linking, the size of the vesicles decreased from 270 to 140 nm due to the charge neutralization of the shell. Successful cross-linking was demonstrated as the vesicles remained intact at low temperatures. The resulting cross-linked vesicles were stable over a wide pH range and moderate electrolyte concentration. The vesicles could be dissociated by increasing the electrolyte concentration to 0.8 M NaCl.

We have also demonstrated the successful shell cross-linking of block copolymer derived from amino acid based monomers. Tri- and pentablock copolymers of N-acryloyl alanine (AAL), NIPAM, and DMA reversibly self-assemble into PNIPAM-cored micelles in response to changes in temperature (42). The presence of the anionic carboxylate groups in the PAAL shell makes such a system amenable to shell cross-linking through interpolyelectrolyte complexation (Scheme 2). Addition of an equimolar amount of cationic poly((ar-vinylbenzyl)trimethylammonium chloride) (PVBTAC) led to the shell cross-linking of the micelles. The slight decrease in size of the shell cross-linked micelles upon cooling to room temperature was attributed to the reduced electrostatic repulsion of the carboxyl groups, leading to more efficient packing.

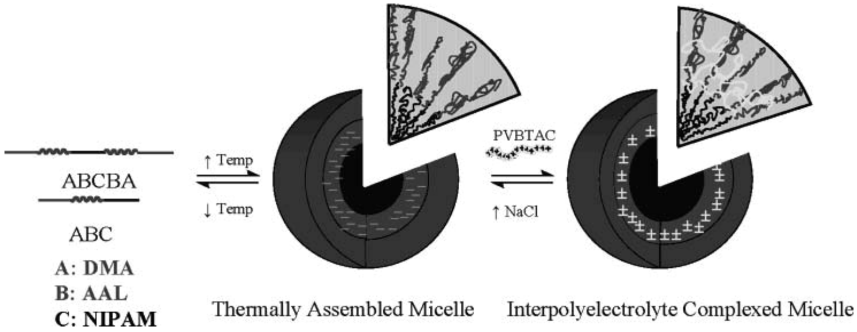
ABCBA
ABC
A: DMA
B: AAL
C: NIPAM
↑ Temp
↓ Temp
PVBTAC
↑ NaCl
Thermally Assembled Micelle
Interpolyelectrolyte Complexed Micelle

*Scheme 2. Temperature-responsive micellization of block copolymers and reversible interpolyelectrolyte-complexed micelle formation. (Reproduced from reference 42. Copyright 2006 American Chemical Society.)*

Downloaded by DUKE UNIV on June 27, 2012 | http://pubs.acs.org
Publication Date: August 13, 2009 | doi: 10.1021/bk-2009-1024.ch013

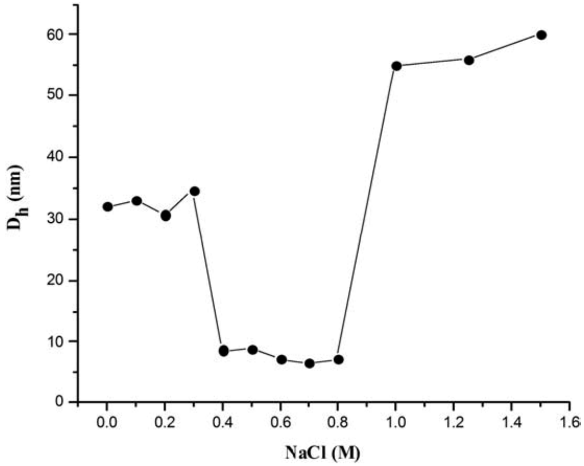

*Figure 2. Apparent hydrodynamic diameters (Dh) as a function of sodium chloride concentration ([NaCl]) for ionically cross-linked DMA100-b-AAL65-bNIPAM165 triblock copolymer micelles. (Reproduced from reference 42. Copyright 2006 American Chemical Society.)*

The reversibility of the electrostatically cross-linked micelles was investigated by introducing simple salts. The cross-linked micelles remain intact in aqueous solutions with NaCl concentrations as high as 0.3 M. At 0.4 M NaCl concentration, the shell cross-linked micelles dissociate to unimers, demonstrating the reversible nature of the interpolyelectrolyte complexed shell. Interestingly, above 0.8 M NaCl, aggregates reform as the PNIPAM blocks are "salted out" (Figure 2).

Block copolymers of P(AMPS-b-AAL) have also been synthesized by our group. These block copolymers exhibit a pH-responsive behavior due to protonation of the PAAL block. Specifically, a P($AMPS_{225}$-b-$AAL_{200}$) copolymer was synthesized and shown to form aggregates with sizes around 120 nm at pH 1. These aggregates were cross-linked via interpolyelectrolyte complexation utilizing the anionic PAMPS corona and cationic quaternarized poly(4-vinylpyridine) (QP4VP). After cross-linking, the aggregates increased in size to around 150 nm. As seen in Figure 3, the cross-linked aggregates at pH 1 appear to be hexagonally packed. This may be attributed to the association between the anionic and cationic segments of the respective blocks.

Downloaded by DUKE UNIV on June 27, 2012 | http://pubs.acs.org
Publication Date: August 13, 2009 | doi: 10.1021/bk-2009-1024.ch013

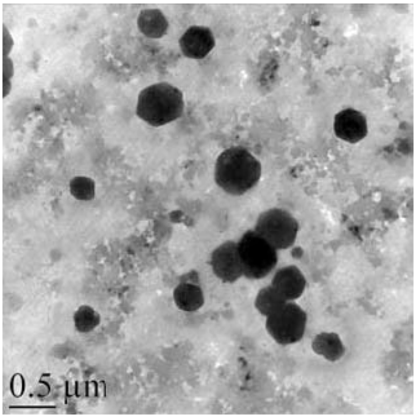

*Figure 3. TEM image of P(AMPS$_{225}$-b-AAL$_{200}$)/QP4VP interpolyelectrolyte complexes at pH 1.*

P(AMPS$_{225}$-b-AAL$_{200}$) has been cross-linked with a RAFT-generated poly(N-[3-(dimethylamino)propyl]acrylamide) (PDMAPA). Upon interpolyelectrolyte complexation, sizes of 192 nm are observed by DLS. "Locking" of the assembly is demonstrated by increasing the pH above the pKa of PAAL (3.5). The nanoassemblies remain "locked" as indicated by the average apparent hydrodynamic diameter of 189 nm. Dissociation of the assemblies occurs when the solution pH is increased to values at which PDMAPA is completely deprotonated. Upon removal of the cationic charge, the interpolyelectrolyte complexation is reversed resulting in unimers of 19 nm (Figure 4).

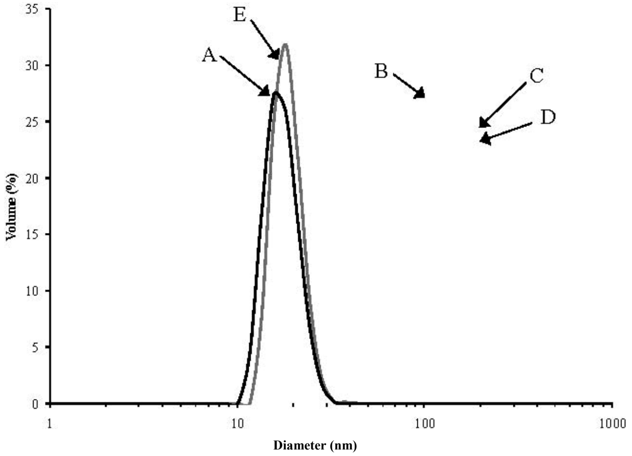

*Figure 4. Size distribution (measured by dynamic light scattering) of P(AMPS$_{225}$-b-AAL$_{200}$) under specific conditions: unimers at pH 7.0 (A), vesicles at pH 1.0 (B), after formation of IPEC at pH 1 (C), IPEC at pH 9.0 (D), unimeric complex components at pH 12.0 (E).*

Downloaded by DUKE UNIV on June 27, 2012 | http://pubs.acs.org
Publication Date: August 13, 2009 | doi: 10.1021/bk-2009-1024.ch013

## Shell Cross-linking via Incorporation of Activated Esters

The reaction of a difunctional amine with an activated ester moiety incorporated in the shell of nanoassemblies provides a facile and efficient method for the formation of SCL nanoassemblies. Recently, we reported the synthesis of PEO-b-P((DMA-stat-N-acryloxysuccinimide (NAS))-b-PNIPAM) which self-assembles into micelles in response to temperature changes (46). The NAS moieties, located in the shell of the micelles, were subsequently reacted with ethylene diamine to cross-link micelle coronas (Scheme 3). This reaction proceeds rapidly, reaching over 95 % completion in 2 h. The aggregate structure of the SCL micelles is conserved after reducing the solution temperature below the critical aggregation temperature (CAT) as confirmed by DLS and AFM (Figure 5).

Downloaded by DUKE UNIV on June 27, 2012 | http://pubs.acs.org
Publication Date: August 13, 2009 | doi: 10.1021/bk-2009-1024.ch013

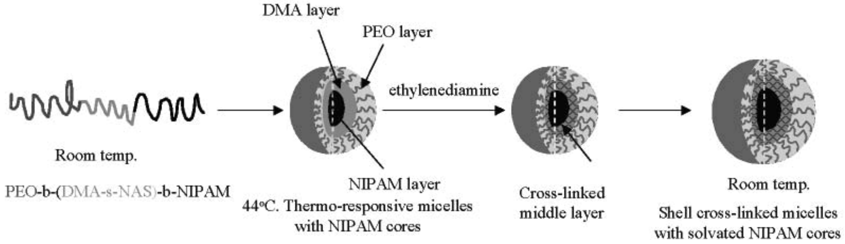
DMA layer
PEO layer
ethylenediamine
Room temp.
PEO-b-(DMA-s-NAS)-b-NIPAM
NIPAM layer
44°C. Thermo-responsive micelles with NIPAM cores
Cross-linked middle layer
Room temp.
Shell cross-linked micelles with solvated NIPAM cores

*Scheme 3. Self-assembly into micelles and shell cross-linked micelles of PEO-b-P((DMA-stat-NAS)-b-NIPAM) triblock copolymers. (Reproduced from reference 46. Copyright 2006 American Chemical Society.)*

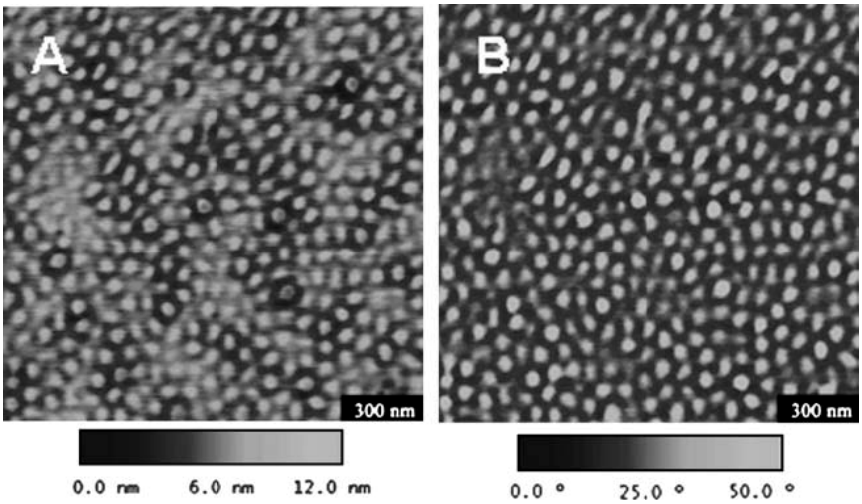
A
B
300 nm
300 nm
0.0 nm
6.0 nm
12.0 nm
0.0 °
25.0 °
50.0 °

*Figure 5. Tapping-mode AFM images of PEO-b-P((DMA-s-NAS)-b-NIPAM) micelles after cross-linking with ethylenediamine. (A) Height image; (B) Phase image. Samples were prepared by drop deposition (5 mL, 0.01% concentration) onto freshly cleaved mica and allowed to dry in air. (Reproduced from reference 46. Copyright 2006 American Chemical Society.)*

While reacting the NAS moiety with ethylene diamine proved to be a facile method for producing SCL micelles, the cross-linking reaction is not reversible. The use of a cleavable functionality, however, should allow the breakdown of SCL micelles and subsequent dissociation to unimers in situ. To demonstrate the feasibility of such a process, a micelle-forming triblock copolymer, PEO$_{45}$-b-P(DMA$_{98}$-s-NAS$_{30}$)-b-PNIPAM$_{87}$, was synthesized by RAFT polymerization (47). After heating a solution of the block copolymer above the CAT, the micelles were cross-linked with cystamine, a disulfide-containing diamine (Scheme 4). The resulting disulfide cross-links were then cleaved through chemical reduction by either a thiol exchange reaction with dithiothreitol (DTT) or tris(2-carboxyethyl)phosphine hydrochloride (TCEP). Using either reagent leads to dissociation of the SCL micelles into unimers as confirmed by DLS. After removal of the excess reducing agent, addition of cystamine results in the reformation of the SCL micelles through a thiol/disulfide exchange reaction.

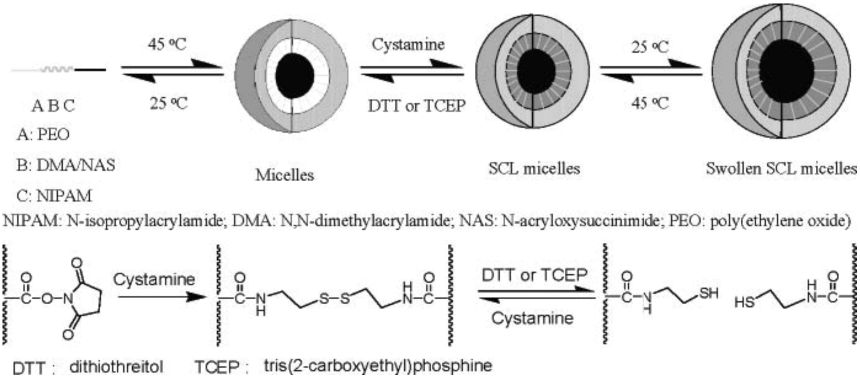
45 °C
25 °C
A B C
A: PEO
B: DMA/NAS
C: NIPAM
Micelles
Cystamine
DTT or TCEP
SCL micelles
25 °C
45 °C
Swollen SCL micelles
NIPAM: N-isopropylacrylamide; DMA: N,N-dimethylacrylamide; NAS: N-acryloxysuccinimide; PEO: poly(ethylene oxide)
Cystamine
DTT or TCEP
Cystamine
SH
HS
DTT : dithiothreitol
TCEP : tris(2-carboxyethyl)phosphine

*Scheme 4. Formation of reversible shell cross-linked micelles from PEO-b-P((DMA-stat-NAS)-b-NIPAM) triblock copolymers by reaction with cystamine. (Reproduced from reference 47. Copyright 2006 American Chemical Society.)*

The drug delivery of the reversible SCL micelles was assessed by the release of a model drug, dipyridamole (DIP). DIP was loaded into the hydrophobic micelles core at 45 °C. Lowering the solution temperature to 25 °C led to dissociation of micelles to unimers resulting in the burst release of the DIP (Figure 6). Cross-linking of the micellar structure led to significant retardation of release of the drug, both at 25 and 45 °C, suggesting the possibility of tuning drug release based on the degree of cross-linking.

Downloaded by DUKE UNIV on June 27, 2012 | http://pubs.acs.org
Publication Date: August 13, 2009 | doi: 10.1021/bk-2009-1024.ch013

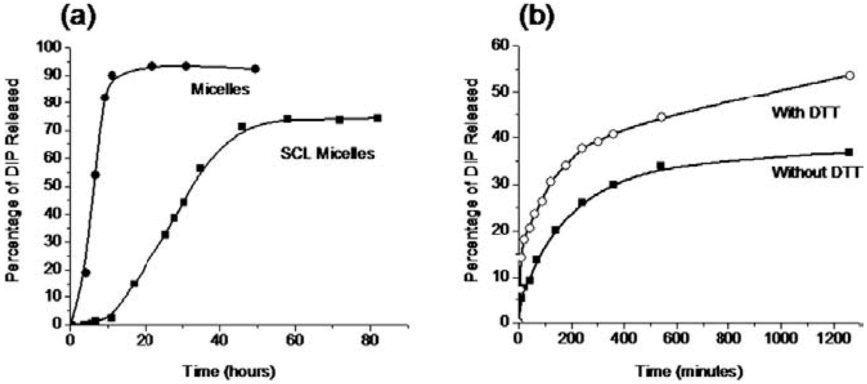

*Figure 6. Cumulative DIP release to PBS buffer from (a) shell cross-linked (SCL) and un-cross-linked micelles at 25 °C and (b) SCL micelles at 37 °C in the presence of DTT and without DTT. (Reproduced from reference 47. Copyright 2006 American Chemical Society.)*

Our most recent report utilizing an activated ester for the formation of SCL micelles details the use of a cleavable, temperature-responsive polymeric cross-linker (48). In this study, micellization of the pH-responsive triblock copolymer, α-methoxyPEO-b-PAPMA-b-poly[2-(diisopropylamino)ethyl (mPEO-b-PAPMA-b-PDPAEMA), was induced by increasing the solution pH above 6.0, thus rendering the PDPAEMA block hydrophobic (Scheme 5). To produce the polymeric cross-linking agent, the RAFT polymerization of NIPAM was mediated by a difunctional CTA with carboxylic acid R-groups. The end groups were subsequently functionalized with an activated ester via carbodiimide coupling to give (α,ω-N-hydroxysuccinimidyl ester)PNIPAM (NHS-PNIPAMNHS). The primary amine functionality in the PAPMA shell was subsequently reacted with the temperature-responsive cross-linking agent, NHS-PNIPAMNHS. The SCL micelles produced were both pH- and temperature-responsive and because the polymeric cross-linking agent contains a trithiocarbonate core, the cross-links can easily be cleaved to allow dissociation of the micelles back to unimers.

Downloaded by DUKE UNIV on June 27, 2012 | http://pubs.acs.org
Publication Date: August 13, 2009 | doi: 10.1021/bk-2009-1024.ch013

Downloaded by DUKE UNIV on June 27, 2012 | http://pubs.acs.org
Publication Date: August 13, 2009 | doi: 10.1021/bk-2009-1024.ch013

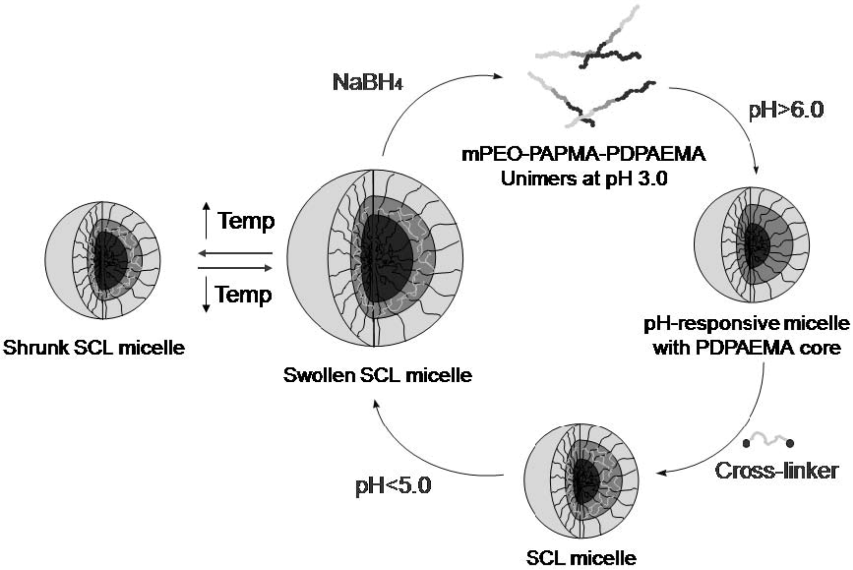
NaBH4
mPEO-PAPMA-PDPAEMA
Unimers at pH 3.0
pH>6.0
↑ Temp
↓ Temp
Shrunk SCL micelle
Swollen SCL micelle
pH-responsive micelle
with PDPAEMA core
Cross-linker
pH<5.0
SCL micelle

*Scheme 5. pH-Responsive micellization of mPEO-PAPMA-PDPAEMA triblock copolymer and formation of SCL micelles via cross-linking with NHS-PNIPAMNHS.*

Recently, our group achieved the “one-pot” synthesis of reversible SCL micelles. A water-soluble, reversibly cleavable and membrane permeable cross-linker, dimethyl 3,3'-dithiobispropionimidate (DTBP) was employed to “lock” the mPEO-PAPMA-PDPAEMA micelles via the process presented in Scheme 6. The disulfide-containing cross-linker provides a reversibly cleavable site in the SCL micelles; DTT was used as a cleaving agent while SCL micelles were reformed under oxidizing conditions (Figure 7).

Downloaded by DUKE UNIV on June 27, 2012 | http://pubs.acs.org
Publication Date: August 13, 2009 | doi: 10.1021/bk-2009-1024.ch013

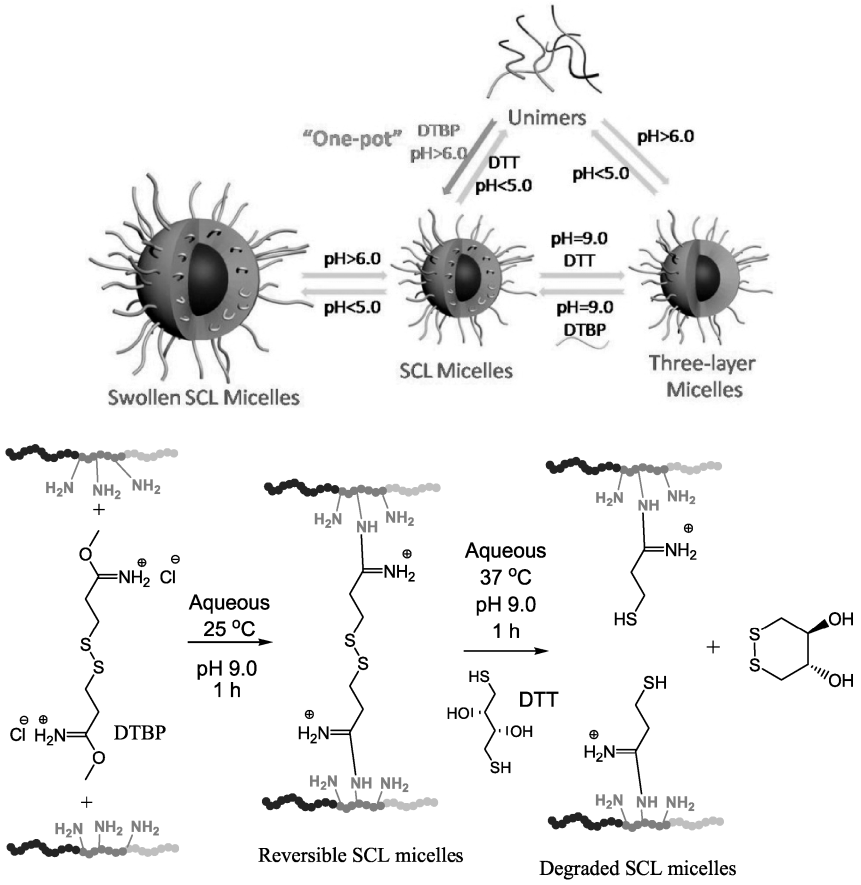
Unimers
"One-pot" DTBP pH>6.0
DTT pH<5.0
pH>6.0
pH<5.0
pH>6.0
pH<5.0
pH=9.0 DTT
pH=9.0 DTBP
Swollen SCL Micelles
SCL Micelles
Three-layer Micelles
H2N NH2 NH2
DTBP
Aqueous 25 °C pH 9.0 1 h
Reversible SCL micelles
Aqueous 37 °C pH 9.0 1 h
DTT
Degraded SCL micelles

Scheme 6. *Micellization of mPEO-PAPMA-PDPAEMA triblock copolymer and formation of reversible SCL micelles via a water-soluble, membrane permeable cross-linker, DTBP.*

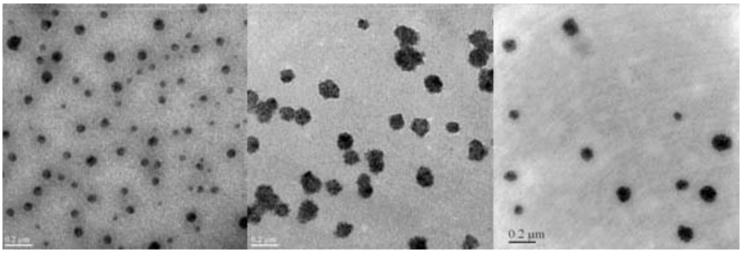
0.2 μm
0.2 μm
0.2 μm

*Figure 7. TEM image of the SCL micelles at pH 9.0 (Left), pH 3.0 (Middle) and re-cross-linked micelles at pH 9.0 (Right) (Triblock copolymer concentration: 0.05 wt%).*

## Shell Cross-linking via in situ Nanoparticle Formation

A number of reports have recently shown the ability of certain amine-containing polymers to act as both reducing and stabilizing agents for the formation of gold nanoparticles (49-53). We synthesized an amine-containing diblock copolymer, $PDMAEMA_{73}$-b-$PNIPAM_{99}$, capable of self-assembling into vesicles with hydrodynamic diameters of 140 nm above the CAT. The gold nanoparticle-decorated vesicles were synthesized by mixing the block copolymer with $NaAuCl_4$ at 50 °C in solution (Scheme 7) (54). The formation of the gold nanoparticles in the PDMAEMA domains acts as a cross-linking agent due to the anchoring of multiple polymer chains to the surface of the nanoparticles. After the formation of the gold nanoparticle cross-links, the vesicular structure remains intact even when the solution temperature is reduced to 25 °C. The size and size distribution of the vesicles increase slightly which can be attributed to the increased hydrophilicity of the PNIPAM block.

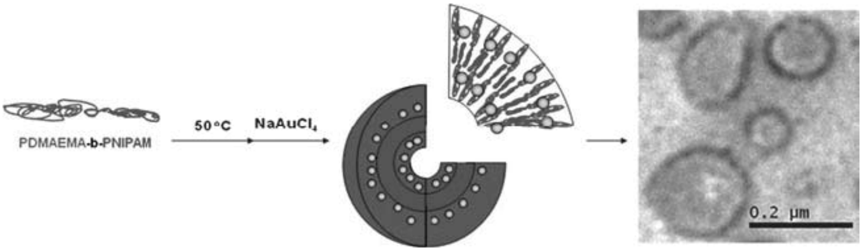

*Scheme 7. Formation of thermally responsive vesicles decorated with gold nanoparticles. (Reproduced from reference 54. Copyright 2007 American Chemical Society.)*

Block copolymers of PDMAEMA and PNIPAM represent an interesting class of responsive polymers which respond to two or more stimuli. PNIPAM is among the most widely studied thermally-responsive monomers while PDMAEMA is itself responsive towards changes in pH, temperature, and ionic strength. Such systems provide a facile manner for the investigation of factors responsible for dictating the solution morphology of stimuli-responsive, self-assembling systems. By tuning the solution properties, the relative hydrophilic mass fraction can be tuned to produce various solution morphologies (Scheme 8) (55). Recently, a series of PDMAEMA-b-PNIPAM copolymers was synthesized by sequential RAFT polymerizations according to Scheme 9 (56). First, the RAFT polymerization of DMAEMA was mediated by CTP to synthesize a PDMAEMA macroCTA. The polymerization was stopped below 70 % conversion to maintain end group fidelity and molecular weight control. This macroCTA was then chain extended with NIPAM yielding a well defined series of PDMAEMA-b-PNIPAM diblock copolymers.

Downloaded by DUKE UNIV on June 27, 2012 | http://pubs.acs.org
Publication Date: August 13, 2009 | doi: 10.1021/bk-2009-1024.ch013

Downloaded by DUKE UNIV on June 27, 2012 | http://pubs.acs.org
Publication Date: August 13, 2009 | doi: 10.1021/bk-2009-1024.ch013

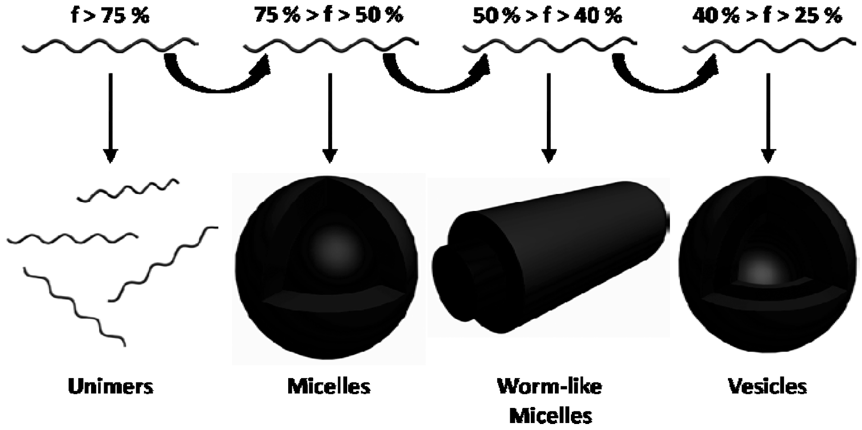

*Scheme 8. Formation of various solution morphologies by controlling the relative hydrophilic mass of block copolymers.*

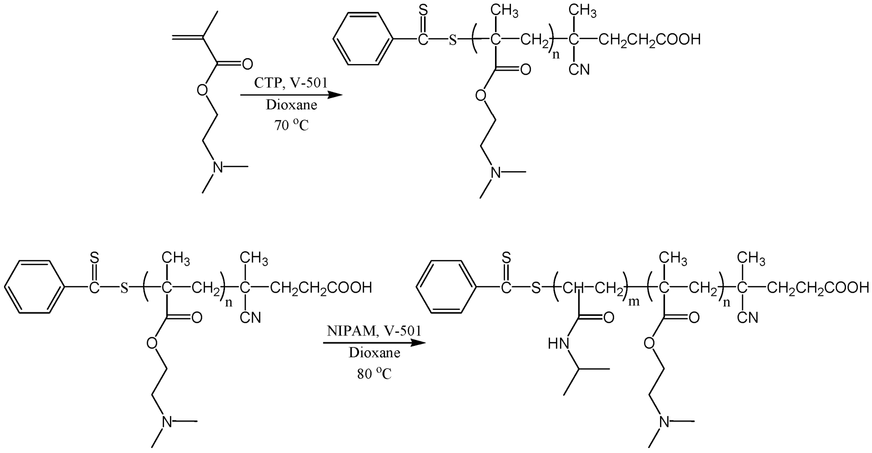

*Scheme 9. RAFT synthesis of multi-responsive PDMAEMA-b-PNIPAM copolymers.*

Dynamic light scattering was used to investigate the effect of copolymer composition, solution pH, and electrolyte concentration on the temperature-responsive self-assembly of the PDMAEMA-b-PNIPAM copolymers in aqueous media. For the copolymer series derived from a PDMAEMA$_{165}$ macroCTA, as the degree of polymerization (DP) of the PNIPAM block increased, the critical aggregation temperature decreased. At pH 5, the copolymer with the shortest PNIPAM block (DP = 102) did not aggregate over the temperature range studied. Increasing the length of the PNIPAM block leads to aggregation of the block copolymer at 38 and 36 °C for the block copolymers with PNIPAM block lengths of 202 and 435, respectively, with the aggregate sizes being approximately 200 nm at 50 °C. Since PDMAEMA can be reversibly protonated, changes in solution pH should drastically affect the aggregation behavior. For the block copolymer PDMAEMA$_{165}$-b-PNIPAM$_{102}$, as discussed above, at pH 5 no aggregation is seen over the temperature range studied. Increasing the pH to 7 leads to aggregates of 250 nm above a critical aggregation temperature of 50 °C. At pH 9, the PDMAEMA stabilizing blocks become increasingly hydrophobic due to the deprotonation of the tertiary amine functionality. Under these conditions, the block copolymers self-assemble into aggregates of 570 nm above a CAT of 38 °C. Similar to variations in the pH, the presence of added electrolyte can drastically alter the self-assembly behavior of PDMAEMA-b-PNIPAM copolymers. Increasing the NaCl concentration in an aqueous solution of PDMAEMA$_{165}$-b-PNIPAM$_{102}$ from 0 to 200 mM changes the aggregate sizes from 230 to 60 nm (Figure 8).

Downloaded by DUKE UNIV on June 27, 2012 | http://pubs.acs.org
Publication Date: August 13, 2009 | doi: 10.1021/bk-2009-1024.ch013

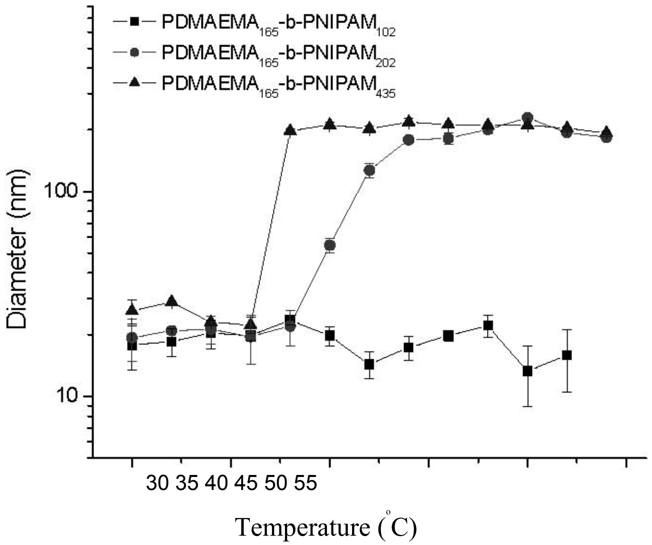

*Figure 8. Hydrodynamic diameter vs. temperature data for PDMAEMA$_{165}$-bPNIPAM$_{102}$ (■),PDMAEMA$_{165}$-b-PNIPAM$_{102}$ (●), and PDMAEMA$_{165}$-bPNIPAM$_{102}$ (▲) copolymers showing the effect of block copolymer composition on the self-assembly behavior in aqueous solution (0.01 % (w/w) concentration, pH 5.0).*

The self-assembled nanostructures were subsequently cross-linked by the in situ reduction of NaAuCl4 to AuNPs in the PDMAEMA shells to "lock" in the solution morphology. The resulting aggregate morphology was observed using TEM and compared to the hydrodynamic sizes obtained from DLS. A solution of PDMAEMA165-b-PNIPAM102 dissolved in 200 mM NaCl at a pH of 7.0 was found to form aggregates of 58 nm at 50 °C. After the AuNP cross-linking, the solution temperature was lowered to 25 °C and the aggregate size increased to 72 nm due to the swelling of the PNIPAM core. From the TEM images and the DLS data, it was determined that the block copolymers were forming simple core-shell micelle morphology. Increasing the DP of the PNIPAM block increases the hydrophobicity of the block copolymer above the CAT. At pH 7, two aggregate size populations (61 nm and 276 nm) are observed in dynamic light scattering when an aqueous solution of PDMAEMA165-b-PNIPAM202 is heated to 50 oC. When the solution is cross-linked with AuNPs, TEM shows both spherical micelles of approximately 70 nm and worm-like micelles with diameters of 50 to 100 nm and lengths of 500 nm. Further increasing the PNIPAM block length leads to the formation of vesicular aggregates with an average hydrodynamic diameter of 179 nm as seen in the TEM micrograph shown in Figure 9.

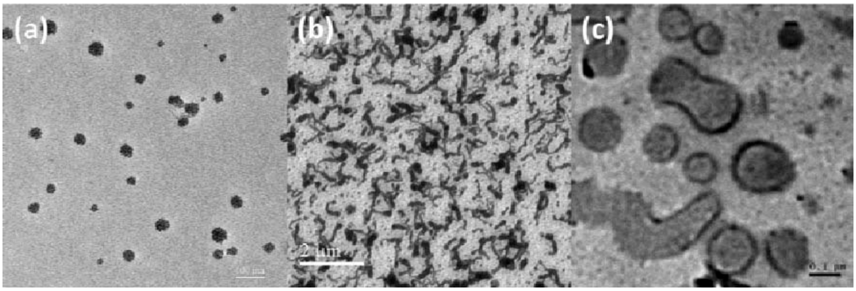

*Figure 9. TEM micrographs showing (a) spherical micelles from PDMAEMA$_{165}$-b-PNIPAM$_{102}$ (0.01 wt%, pH 7.0, 200 mM NaCl) (b) worm-like micelles of PDMAEMA$_{75}$-b-PNIPAM$_{175}$ (0.01 wt%, pH 7.0) and (c) vesicles derived from of PDMAEMA$_{165}$-b-PNIPAM$_{202}$ (0.01 wt%, pH 7.0).*

## Summary/Conclusions

In this chapter we have highlighted the aqueous solution properties, cross-linking methods, and potential applications of selected block copolymer systems. The RAFT technique is a powerful tool for the synthesis of block copolymers which can self-assemble into various solution morphologies utilizing changes in environmental conditions including solution pH, temperature, and salt concentration. Once assembled, these structures can be “locked” by a wide variety of methods including interpolyelectrolyte complexation, chemical cross-linking, and in situ formation of metal nanoparticles.

Downloaded by DUKE UNIV on June 27, 2012 | http://pubs.acs.org
Publication Date: August 13, 2009 | doi: 10.1021/bk-2009-1024.ch013

## Acknowledgments.

Support for this research by the U.S. Department of Energy (DE-FC26-01BC15317) and the MRSEC program of the National Science Foundation (DMR-0213883) is gratefully acknowledged.

## References

1. Zhang, L.; Eisenberg, A. Science **1995**, 268, 1728-1731.
2. Yu, K.; Eisenberg, A. Macromolecules **1996**, 29, 6359-6361.
3. Zhang, L.; Yu, K.; Eisenberg, A. Science **1996**, 272, 1777-1779.
4. Jain, S.; Bates, F.S. Science **2003**, 300, 460-464.
5. Won, Y.Y.; Brannan, A.K.; Davis, H.T.; Bates, F.S. J. Phys. Chem. B **2002**, 106, 3354-3364.
6. Controlled Radical Polymerization; Matyjaszewski, K., ed. ACS Symposium Series 685; American Chemical Society: Washington, DC, 1998.
7. Controlled/Living Radical Polymerizations: Progress in ATRP, NMP, and RAFT; Matyjaszewski, K., ed. ACS Symposium Series 768; American Chemical Society: Washington, DC, 2000.
8. Advances in Controlled/Living Radical Polymerization; Matyjaszewski, K., ed. ACS Symposium Series 854; American Chemical Society: Washington, DC, 2003.
9. Hawker, C.J.; Bosman, A.W.; Harth, E. Chem. Rev. **2001**, 101, 3661-3688.
10. Sciannamea, V.; Jerome, R.; Detrembleur, C. Chem. Rev. **2008**, 108, 11041126.
11. Controlled synthesis of polymers with ionic or ionizable groups using atom transfer radical polymerization; Tsarevsky, N.V.; Matyjaszewski, K., ed. ACS Symposium Series 937; American Chemical Society: Washington, DC, 2006.
12. Matyjaszewski, K.; Xia, J. Chem. Rev. **2001**, 101, 2921-2990.
13. Veerle, C.; Tomislav, P.; Matyjaszewski, K. Prog. Polym. Sci. **2001**, 26, 337-377.
14. Faveir, A.; Charreyre, M.-T. Macromol. Rapid Commun. **2006**, 27, 653, 692.
15. Moad, G.; Rizzardo, E.; Thang, S.H. Aust. J. Chem. **2005**, 58, 379-410.
16. Moad, G.; Rizzardo, E.; Thang, S.H. Aust. J. Chem. **2006**, 59, 669-692.
17. Barner-Kowollik, C., ed.; John Wiley & Sons Ltd: Southern Gate, Chichester, West Sussex, England, 2008.
18. Perrier, S.; Takolpuckdee, P. J. Polym. Sci., Part A: Polym. Chem. **2005**, 43, 5347-5393.
19. McCormick, C.L.; Sumerlin, B.S.; Lokitz, B.S.; Stempka, J.E. Soft Matter **2008**, 4, 1760-1773.
20. McCormick, C.L.; Lowe, A.B. Acc. Chem. Res. **2004**, 37, 312-325.
21. Lowe, A.B.; McCormick, C.L. Prog. Polym. Sci. **2007**, 32, 283-351.
22. York, A.W.; Kirkland, S.E.; McCormick, C.L. Adv. Drug Delivery Rev. **2008**, 60, 1018-1036.

Downloaded by DUKE UNIV on June 27, 2012 | http://pubs.acs.org
Publication Date: August 13, 2009 | doi: 10.1021/bk-2009-1024.ch013

23. Du, J.; Armes, S.P. J. Am. Chem. Soc. **2005**, 127, 12800-12801.
24. Sundararaman, A.; Stephan, T.; Grubbs, R.B. J. Am. Chem. Soc. **2008**, 130, 12264-12265.
25. Ringsdorf, H. J. Polym. Sci. Symp. **1975**, 51, 135-155.
26. Choucair, A.; Soo, P.L.; Eisenberg, A. Langmuir **2005**, 21, 9308-9313.
27. Du, J.; Tang, Y.; Lewis, A.L.; Armes, S.P. J. Am. Chem. Soc. **2005**, 127, 17982-17983.
28. Kwon, G.S.; Okano, T. Adv. Drug Delivery Rev. **1996**, 21, 107-116.
29. Hales, M.; Barner-Kowolik, C.; Davis, T.P.; Stenzel, M.H. Langmuir **2004**, 20, 10809.
30. Thurmond, K.B.; Kowalewski, T.; Wooley, K.L. J. Am. Chem. Soc. **1997**, 119, 6656-6665.
31. Huang, H.; Kowalewski, T.; Remsen, E.E.; Gertzmann, R.; Wooley, K.L. J. Am. Chem. Soc. **1997**, 119, 11653-11659.
32. Remsen, E.E.; Thurmond, K.B.; Wooley, K.L. Macromolecules **1999**, 32, 3685-3689.
33. Zhang, Q.; Remsen, E.E.; Wooley, K.L. J. Am. Chem. Soc. **2000**, 122, 3642-3651.
34. Wooley, K.L. J. Polym. Sci., Part A: Polym. Chem. **2000**, 38, 1397-1407.
35. Butun, V.; Lowe, A.B.; Billingham, N.C.; Armes, S.P. J. Am. Chem. Soc. **1999**, 121, 4288-4289.
36. Butun, V.; Billingham, N.C.; Armes, S.P. J. Am. Chem. Soc. **1998**, 120, 12135-12136.
37. Liu, S.Y.; Weaver, J.V.M.; Tang, Y.Q.; Billingham, N.C.; Armes, S.P.; Tribe, K. Macromolecules **2002**, 35, 6121-6131.
38. Liu, S.Y.; Ma, Y.H.; Armes, S.P. Langmuir **2002**, 18, 7780-7784.
39. Rodriguez-Hernandez, J.; Babin, J.; Zappone, B.; Lecommandoux, S. Biomacromolecules **2005**, 6, 2213-2220.
40. Li, Y.; Lokitz, B.S.; McCormick, C.L. Angew. Chem., Int. Ed. **2006**, 45, 5792-5795.
41. Weaver, J.V.M.; Tang, Y.; Liu, S.; Iddon, P.D.; Grigg, R.; Armes, S.P.; Billingham, N.C.; Hunter, R.; Rannard, S.P. Angew. Chem., Int. Ed. **2004**, 43, 1389-1392.
42. Lokitz, B.S.; Convertine, A.J.; Ezell, R.G.; Heidenreich, A.; Li, Y.; McCormick, C.L. Macromolecules **2006**, 39, 8594-8602.
43. Lokitz, B.S.; York, A.W.; Stempka, J.E.; Treat, N.D.; Li, Y.; Jarrett, W.L.; McCormick, C.L. Macromolecules **2007**, 40, 6473-6480.
44. Matsumoto, K.; Hirabayashi, T.; Harada, T.; Matsuoka, H. Macromolecules **2005**, 38, 9957-9962.
45. Joralemon, M.J.; O'Reilly, R.K.; Hawker, C.J.; Wooley, K.L. J. Am. Chem. Soc. **2005**, 127, 16892-16899.
46. Li, Y.; Lokitz, B.S.; McCormick, C.L. Macromolecules **2006**, 39, 81-89.
47. Li, Y.; Lokitz, B.S.; Armes, S.P.; McCormick, C.L. Macromolecules **2006**, 39, 2726-2728.
48. Xu, X.; Smith, A.E.; Kirkland, S.E.; McCormick, C.L. Macromolecules **2008**, ASAP Alert.
49. Yuan, J.-J.; Schmid, A.; Armes, S.P. Langmuir **2006**, 22, 11022-11027.

Downloaded by DUKE UNIV on June 27, 2012 | http://pubs.acs.org
Publication Date: August 13, 2009 | doi: 10.1021/bk-2009-1024.ch013

50. Bronstein, L.M.; Sidorov, S.N.; Gourkova, A.Y.; Valetsky, P.M.; Hartmann, J.; Breulmann, M.; Colfen, H.; Antonietti, M. Inorg. Chim. Acta **1998**, 280, 348-354.
51. Yu, S.; Colfen, H.; Mastai, Y. Nanosci. Nanotechnol. **2004**, 4, 291-298.
52. Sun, X.; Dong, S.; Wang, E. Mater. Chem. Phys. **2006**, 96, 29-33.
53. Ishii, T.; Otsuka, H.; Kataoka, K.; Nagasaki, Y. Langmuir **2004**, 20, 561, 564.
54. Li, Y.; Smith, A.E.; Lokitz, B.S.; McCormick, C.L. Macromolecules **2007**, 40, 8524-8526.
55. Discher, D.E.; Ahmed, F. Annu. Rev. Biomed. Eng. **2006**, 8, 323-341.
56. Smith, A.E.; Xu, X.; Abell, T.U.; Kirkland, S.E.; Hensarling, R.M.; McCormick, C.L. **2008**, Submitted for Publication.

Downloaded by DUKE UNIV on June 27, 2012 | http://pubs.acs.org
Publication Date: August 13, 2009 | doi: 10.1021/bk-2009-1024.ch013

Downloaded by UNIV OF GUELPH LIBRARY on June 26, 2012 | http://pubs.acs.org
Publication Date: August 13, 2009 | doi: 10.1021/bk-2009-1024.ch014

## Chapter 14

# Mechanism of Z-RAFT Star Polymerization

**D. Boschmann[1], M. Mänz[1], M. G. Fröhlich[2], G. Zifferer[2], P. Vana[1,]***

**[1]Institut für Physikalische Chemie, Universität Göttingen, Tammannstr. 6,
D-37077 Göttingen, Germany**
**[2]Institut für Physikalische Chemie, Universität Wien, Währinger Str. 42.,
A-1090, Wien, Austria**

Z-RAFT star polymerizations of styrene and several acrylates using multifunctional star-shaped RAFT agents, in which up to six controlling dithioester-moieties are irreversibly linked to the core via their Z-group, were characterized in-depth both experimentally and by simulations with respect to their mechanism. Methods for obtaining absolute molar masses of star polymers via conventionally calibrated SEC and for tracing the initialization of arm growth via NMR using fully deuterated monomer are detailed. These studies revealed a significant impact of the pre-equilibrium, i.e., the choice of the leaving group, on the star polymer topology. Monte Carlo simulations of the shielding effect occurring in the main equilibrium indicated that steric congestion is not affecting the process to a major extent. Unexpected star-star coupling in Z-RAFT star polymerization of acrylates was identified as a result of intermolecular chain transfer to polymer. Finally, a novel octagonal Z-RAFT agent that bases on a silsesquioxane core is presented.

In Controlled/Living Radical Polymerization: Progress in RAFT, DT, NMP & OMRP; Matyjaszewski, K.;
ACS Symposium Series; American Chemical Society: Washington, DC, 2009.

## Introduction

Complex polymer topologies from controlled radical polymerization are only available after prudential design of mediating compounds and after careful optimization of process parameters. This calls for a fundamental understanding of the underlying reaction mechanisms. Among possible polymer topologies (*1*), star polymers are of special interest, because they exhibit extraordinary rheological characteristics which arise from their spatial shape (*2*). This is, e.g., exploited in oils and lubricants for automotives *(2,3)*, in adhesives *(4)*, and for flocculation (5). Star polymers are also becoming increasingly important in life sciences, where they find applications for drug release *(6)* and serve as unimolecular polymeric micelles (*7*). When aiming at very well-defined star polymers using controlled radical Reversible Addition-Fragmentation Chain Transfer (RAFT) polymerization (*8-12*), a multifunctional star-shaped RAFT agent needs to be employed, in which the stabilizing group (Z-group) constitutes the core (*13-18*). The mechanism of this so-called Z-RAFT star polymerization (see Scheme 1), in principle, prevents star-star coupling reactions as well as the formation of linear living polymer, which both are distinct mechanistic features when performing RAFT polymerization with star-shaped RAFT agents, in which the active RAFT-groups are linked to the central core via their respective leaving groups (R-groups) (*17,19-24*). For a more detailed description of the mechanistic principles of core-first RAFT star polymerizations, including the differences between Z- and R-group approaches, the reader is referred to ref. (*14*). Our interest in Z-RAFT star polymerization is driven by our efforts to construct well-defined, unimolecular, and cored nano-carriers, which base on star-shaped RAFT polymers as scaffold. The Z-RAFT star polymerization was consequently studied in detail with respect to its mechanism, which provides the necessary foundation for rational polymer design.

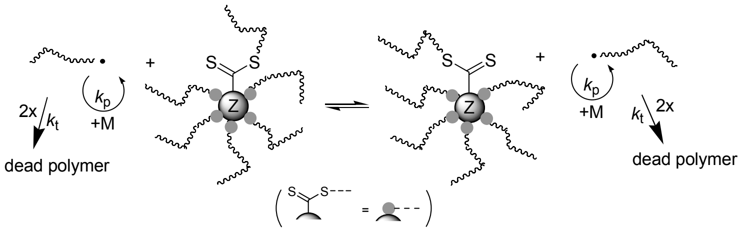

*Scheme 1. Main equilibrium of Z-RAFT star polymerization.*

For the studies of Z-RAFT star polymerization, mono- and multifunctional trithiocarbonates were chosen as RAFT agents (see Chart 1). Trithiocarbonates become increasingly popular as RAFT agents, due to their easy preparation and due to the absence of potentially disturbing rate retardation effects, which are observed with more reactive RAFT agents such as dithiobenzoates (*19*). Mayadunne *et al.* (*20*) were the first who introduced pentaerythritol-based multifunctional trithiocarbonates as Z-RAFT star agents. Since then, the synthesis protocols for this class of star-shaped RAFT agents were adapted by us (*14*) and others (*21*), providing easy access to multifunctional mediating agents.

Downloaded by UNIV OF GUELPH LIBRARY on June 26, 2012 | http://pubs.acs.org
Publication Date: August 13, 2009 | doi: 10.1021/bk-2009-1024.ch014

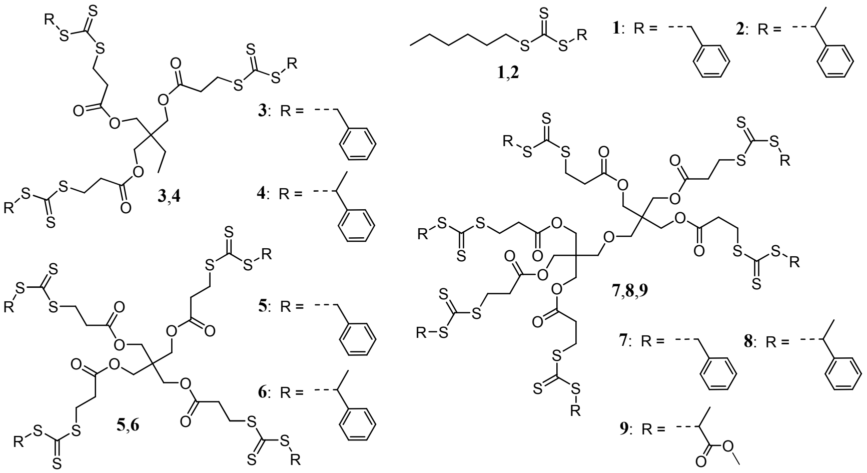

*Chart 1. Mono- and multifunctional RAFT agents used for mechanistic studies of Z-RAFT star polymerization*

## Characterization of Z-RAFT star polymer

Absolute molecular weights of star polymers cannot be obtained via conventionally calibrated size-exclusion chromatography (SEC) using linear standards, as star polymers have distinctively different hydrodynamic volumes in comparison to linear polymer chains. The most straight-forward technique for obtaining such absolute molecular weights of star polymers is of course light-scattering (LS). Since LS-detectors may not be available in all laboratories, we developed alternative ways for measuring molar masses of star polymers (*22*). As the arms of an individual star polymer from Z-RAFT star polymerization are interlinked at the core via relatively weak S–C-bonds, they may be detached with relative ease. The outcome of such destructive experiments, however, sometimes remains obscure, since the cleavage reactions are difficult to perform quantitatively in all systems (*23*). We thus developed a novel method of characterizing star polymers from Z-RAFT star polymerization via SEC, which rests on the fact that the arms of the star polymers are occurring as free linear chains during propagation (see Scheme 1). It is hence possible, by using a cocktail of conventional and star-shaped RAFT agents, to let the arms take part in two individual RAFT equilibriums (see Scheme 2).

Downloaded by UNIV OF GUELPH LIBRARY on June 26, 2012 | http://pubs.acs.org
Publication Date: August 13, 2009 | doi: 10.1021/bk-2009-1024.ch014

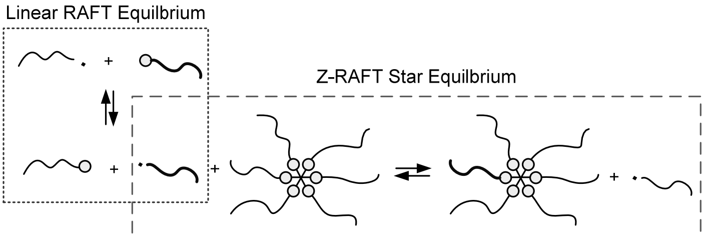

*Scheme 2. The interwoven equilibriums of concurrently proceeding linear and Z-RAFT star polymerization. Thiocarbonylthio-moieties are indicated by circles. (Reproduced from ref. (22). Copyright 2008 Elsevier)*

Downloaded by UNIV OF GUELPH LIBRARY on June 26, 2012 | http://pubs.acs.org
Publication Date: August 13, 2009 | doi: 10.1021/bk-2009-1024.ch014

The equilibrium between dormant linear polymer and dormant stars guarantees that the arms have identical chain lengths, no matter if they occur within the star or outside. Since the SEC is calibrated against linear standards, a determination of the average molecular weight of the linear arm polymer is easily achieved. Molar mass distributions of polymer formed in the presence of such a RAFT agent cocktail are distinctively bimodal (see Figure 1). The true molecular weights of star polymeric material can be obtained by multiplying the molar mass of the linear polymer by the known number of arms. Comparison of the apparent and the expected molecular weight of polystyrene stars, which have been generated by usage of RAFT agents **4**, **6**, and **8** (see Chart 1), indicated that 3-arm star polymer seems to have only 2.58 arms, that 4-arm stars appear as having only 3.05 arms and that 6-arm stars seem to have 3.94 arms (*22*). This indicates the contraction of star polymer coils in solution in comparison to linear chains (*24*) and is in excellent agreement with previous reported data (*25,26*). Application of this method in Z-RAFT star polymerization of styrene revealed that when using trithiocarbonate-type RAFT agents with phenylethyl as the leaving group, the number of arms remain constant between 30 % and full monomer conversion. This indicates a rapid passing of the pre-equilibrium, i.e., a quick initialization of arm growth, and proves that the stars are stable throughout the polymerization. The absolute molar masses of the Z-RAFT stars obtained via this characterization method perfectly matches the theoretical predictions as well as absolute molar masses from LS-measurements (*22*). This finding allows for the following conclusions: (i) the number of arms is identical to the functionality of the star-shaped RAFT agent, i.e., all RAFT groups have initiated arm growth after 30 % of monomer conversion, and (ii) even at very high monomer conversions (thus yielding large star molecules), there is no shielding effect operational that hampers the RAFT process. Otherwise, deviations from theoretical predictions would occur.

Downloaded by UNIV OF GUELPH LIBRARY on June 26, 2012 | http://pubs.acs.org
Publication Date: August 13, 2009 | doi: 10.1021/bk-2009-1024.ch014

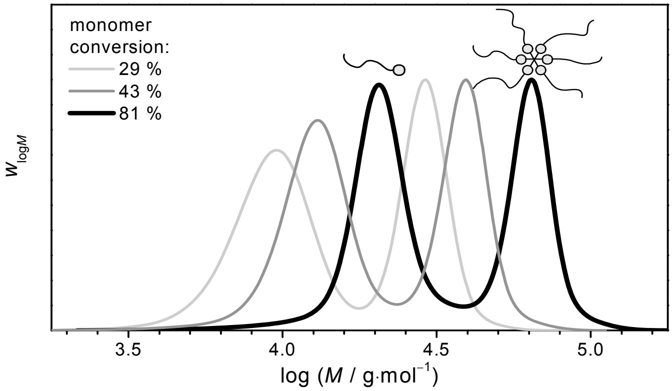

*Figure 1. Molecular weight (SEC) distributions, $w_{\log M}$, of polystyrene generated in styrene bulk polymerization in the presence of 19 mmol·L$^{-1}$ of linear RAFT agent **2**, 4.8 mmol·L$^{-1}$ of tetrafunctional RAFT agent **6**, and 3.0 mmol·L$^{-1}$ 1,1'-azobis(cyanocyclohexane) as the initiator at 80 °C after various monomer conversions.*

However, when using benzyl as the leaving group, i.e., employing RAFT agents **3**, **5**, and **7** (see Chart 1) in conjunction with **1** as linear RAFT agent, a pronounced impact of monomer conversion on the number of arms was observed (*22*). In this case, the apparent arm numbers are steadily increasing with monomer conversion and do reach the expected and confirmed values for the anticipated arm numbers only at very high monomer conversions. Stenzel and coworkers made similar observations in Z-RAFT star polymerizations with benzyl-trithiocarbonates in one of their early publications (*15*) in which they found qualitative evidence for increasing arm numbers with progressive reaction. Interestingly, this effect was not considered since then and benzyl-type star-shaped RAFT agents were uncritically used in many Z-RAFT star polymerizations (*16,18,21,27*). It seems to be clear that the imperfect pre-equilibrium when using benzyl as the leaving group hampers the rapid initialization of arm growth in styrene polymerization, which apparently not only affects polydispersity, but more importantly influences the star polymer topology. This remarkable effect is due to the multi-functionality of the star-shaped RAFT agent, which effectively needs to be initialized several times in a row before becoming a star. It should however be noted that this detrimental effect is dependent on the polymerization system and that, e.g., benzyl as well as methyl-2-propionate as leaving groups show a quick passing of the pre-equilibrium in Z-RAFT star polymerization of acrylates, which lead to topological correct acrylate stars already in early polymerization phases (*23*).

## Initialization of arm growth

The above described method (*22,23*) for obtaining true molecular weights of star polymers is not able to detect apparent arm numbers at very low monomer conversions, because linear arm polymer and star polymer species are not well separated by SEC in the low molar mass regime. We thus designed a method, in which the topological evolution of stars can be traced from the very beginning of Z-RAFT star polymerization using $^1$H-NMR spectroscopy (*28*). When tracing the NMR-signals of the R-group during a Z-RAFT star polymerization in fully deuterated styrene-$d_8$ (see Figure 2), the insertion of monomers between the R- and the thiocarbonylthio-moiety, i.e., the initialization of arm growth, can clearly be observed via the signal intensity disappearance of **H**$_β$-atoms, which become separated from the sulfur (see inset of Figure 3) and thus significantly change their chemical shift.

Downloaded by UNIV OF GUELPH LIBRARY on June 26, 2012 | http://pubs.acs.org
Publication Date: August 13, 2009 | doi: 10.1021/bk-2009-1024.ch014

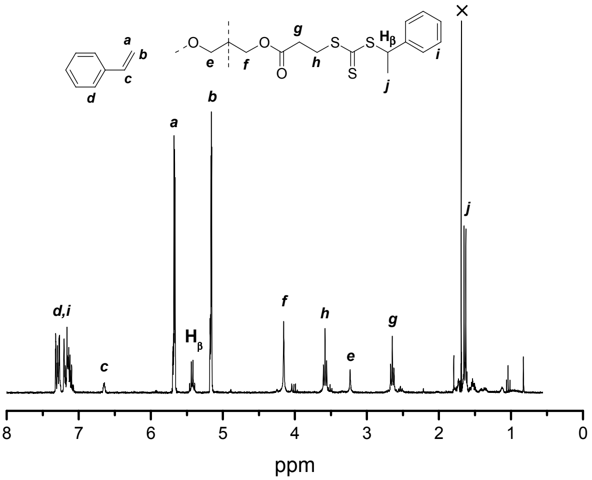

*Figure 2. $^1$H-NMR spectrum of star-shaped RAFT agent **8** (6.3 mmol·L$^{-1}$) and 1,1'-azobis(cyanocyclohexane) (2.9 mmol·L$^{-1}$) in solution of styrene-d$_8$.(Reproduced from ref. (28). Copyright 2008 Wiley Periodicals, Inc.)*

Since styrene-$d_8$ is exhibiting only small $^1$H-NMR signals, which originate from residual non-deuterated sites (see signals **a** to **d** in Figure 2), the process can be monitored directly within the polymerization mixture. In addition, both the low concentrated RAFT agent and the RAFT agent derived polymer end-groups can be observed without significant disturbance by polymer signals.

This approach (*28*) revealed that using phenyl ethyl as the leaving group induced formation of completely initialized stars already after ca. 8 % of monomer conversion, which can be deduced from the depletion of signal intensity of **H**$_β$-atoms (see Figure 3). This finding proves that complete stars are generated already at very low monomer conversions when using phenyl ethyl as the leaving group and nicely complements the above described studies (*22*).

Downloaded by UNIV OF GUELPH LIBRARY on June 26, 2012 | http://pubs.acs.org
Publication Date: August 13, 2009 | doi: 10.1021/bk-2009-1024.ch014

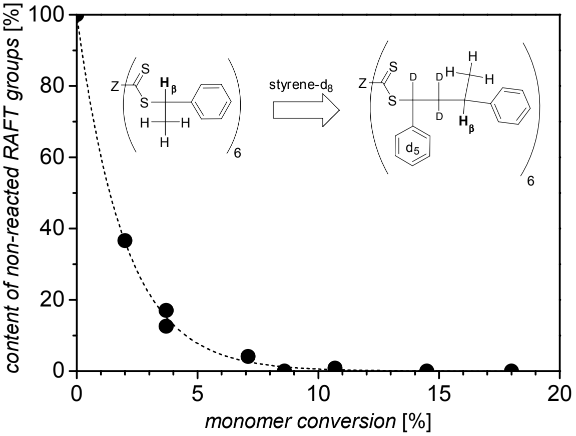

*Figure 3. Content of non-reacted (original) RAFT groups vs. monomer conversion in Z-RAFT star polymerization of styrene-$d_8$ in bulk at 80 °C using 2.9 mmol·L$^{-1}$ 1,1'-azobis(cyanocyclohexane) as the initiatior and 6.3 mmol·L$^{-1}$ of hexa-functional RAFT agent **8**. The inset illustrates the arm-growth initialization reaction.*

Benzyl as the leaving group, i.e., using **7** as the RAFT agent, was found to drastically slow down arm-growth initialization, resulting in fully initialized stars only after ca. 60 % of monomer conversion (*28*). Below that value, star-polystyrene of the expected topology cannot be generated with benzyl as the leaving group, which is in line with the above reported studies using conventionally calibrated SEC (*22*). It should be noted that the evolution of the number of initiated arms is independent of the polymerization rate, as the underlying process is chain transfer. The slow arm-growth initialization with benzyl leaving groups leads to stars with very disparate arm lengths. Nevertheless, the molecular weight distribution of the overall star polymer is remarkably narrow, which is due to the livingness of the early initiated arms. Although no complete stars have been generated at low monomer conversion, low polydispersity indices (*PDI*) are observed: At 13.8 % of monomer conversion, for instance, the *PDI* is 1.17, although only four out of six arms have been initialized on average (*28*). It is thus evident that the topological defects occurring in Z-RAFT star polymerization using an inadequate R-group cannot easily be identified from the polydispersity, which masquerades a successful process in terms of topological control.

## Monte Carlo simulations of shielding effects

In Z-RAFT star polymerization, the growing radical is located at the end of a linear chain (i.e., the arm) and the equilibrating reaction between active and dormant species happens near the core where the RAFT-moieties stay attached throughout the entire polymerization. Consequently, this reaction site is increasingly shielded by polymer segments with proceeding polymerization, during which the length both of growing macroradicals and star polymer arms increases steadily. It is, however, experimentally found that Z-RAFT star polymerization is well controlled up to almost complete monomer conversions (*14,22*). We consequently started to question frequently reported arguments about the detrimental shielding of growing arms, which was accused to increasingly hamper the RAFT process (*15,16,29,30*). In order to quantify the shielding effect of growing arms, we performed simulations of star/chain pairs that mimic the steric situation occurring in the main equilibrium of Z-RAFT star polymerization (see Scheme 1). Shielding factors $K_{i,e}$ (see Figure 4), describing the contact probability between specific segments $i$ along the arms of star-shaped $F$-arm polymers ($2 \leq F \leq 6$) and the terminal end $e$ of a linear chain (where the radical centre is located in real systems) were calculated by exact enumeration of star/chain pair samples prepared by Monte Carlo techniques (*31,32*). $K_{i,e}$ may also be interpreted as a rate constant relative to the rate constant between the same reactive centers *not* located at a polymer and can hence be employed for kinetic simulations.

Inspection of Figure 4 indicates that the contact probability between the end of a linear chain (of the same length $n$ as each arm of the star) and specific positions in the star polymer is minimal in the center of the star at $i/n = 0$, where the reactive RAFT-moieties sit. The reduction of $K_{i,e}$ is getting more pronounced with increasing number of arms $F$ as well as with chain lengths of the participating species (not shown) (*31,32*). The obtained data indeed indicate a progressive steric congestion. Please note that the simulations were performed on a cubic lattice, which artificially reduces the contact probability for 6-arm stars directly with the center to zero (see Figure 4).

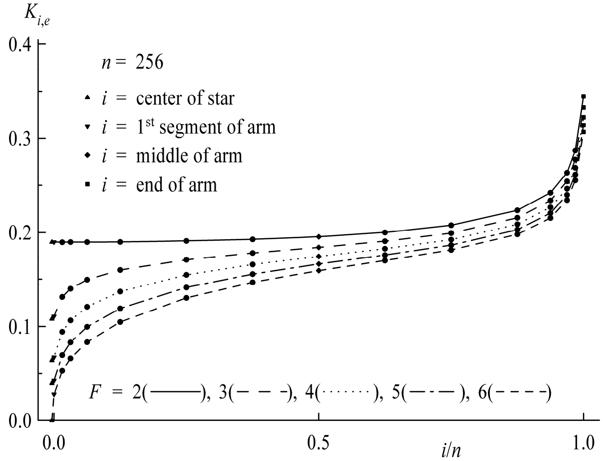

*Figure 4. Shielding factors $K_{i,e}$ vs. reduced position i/n for the interaction between the end of the linear chain and specific segments i within stars of different arm numbers F. i/n = 0: center of the star, i/n = 1: arm tips.*

Downloaded by UNIV OF GUELPH LIBRARY on June 26, 2012 | http://pubs.acs.org
Publication Date: August 13, 2009 | doi: 10.1021/bk-2009-1024.ch014

The $K_{i,e}$ values, however, rapidly increase when considering locations along the star polymer arms that are farther away from the actual center. This finding was translated into dedicated simulations, in which the core unit was expanded in order to account for actual chemical structures being used in Z-RAFT star polymerizations. It was found that by slightly expanding the core, steric crowding can substantially be relieved. Inspection of Figure 5 shows that the largely reduced contact probability directly at the core is substantially less pronounced in the case of RAFT-moieties being separated from the actual center by spacers. This finding helps to explain the good performance of Z-RAFT agents **3** to **9** in terms of polymerization control, because the active sites in these compounds are separated from the actual center by eight covalent bonds.

In all cases, the chain length dependence of $K_{i,e}$ can adequately be described by the use of power laws (*31,32*). For segments which are remote from the center of the star the exponent of such a power law is fairly independent of the functionality $F$ and reads ca. –0.16 for $i = n$ and –0.27 for $i = n/2$, as has also been found for linear chains (*33*). For positions near the center of the star, however, a rather strong dependence of the exponent on $F$ has been found; for $F = 6$, e.g., the exponent is –0.6.

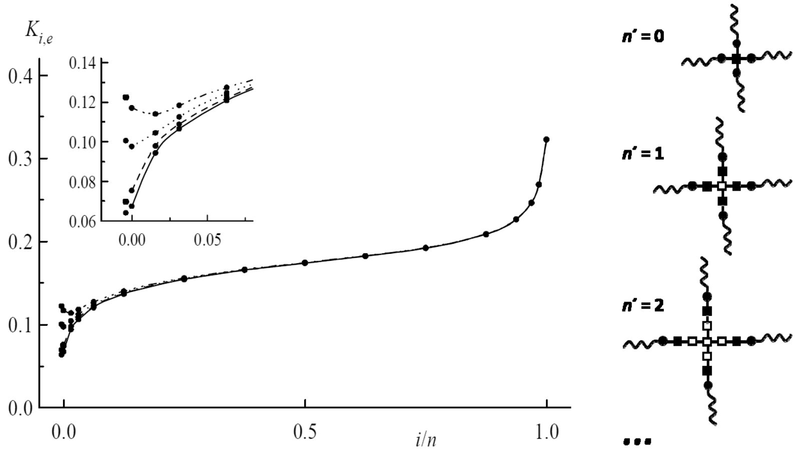

*Figure 5. Shielding factors $K_{i,e}$ vs. reduced position i/n for the interaction between the end of the linear chain and specific segments i within 4-arm stars for a chain length n = 256 for different values of core enlargement n'=0 (full line), n' = 1 (dashed line), n' = 2 (dotted line) and n' = 3 (chain dotted line). A close-up of the central region is shown in the inset. (Adapted with permission from ref. (32). Copyright 2008 Wiley Periodicals, Inc.)*

From the shielding factors obtained for various numbers of arms and chain lengths up to $F \times 512$ segments (which e.g. relates to a 6-arm polystyrene of 1.5 to 3 million Da considering that one simulated monomer unit relates to 5 to 10 real units, depending on their actual persistence lengths) it could be estimated that the addition reaction in Z-RAFT star polymerization with chain lengths of several hundred monomer units, which is typical for controlled polymerizations, is roughly three to maximal ten times slower (depending on $F$, chain length, and

Downloaded by UNIV OF GUELPH LIBRARY on June 26, 2012 | http://pubs.acs.org
Publication Date: August 13, 2009 | doi: 10.1021/bk-2009-1024.ch014

the size of the core) than in linear RAFT polymerization, which basically would relate to the data found for $i/n = 1$. Such a relatively small decrease of the addition rate coefficient, $k_{ad}$, is not sufficient to impede the overall RAFT process, as has been demonstrated in earlier kinetic simulation studies into RAFT polymerization using PREDICI® (*34*). Diminishing control found in some Z-RAFT star polymerization systems (*13*) is thus more likely effected by non-optimal reaction conditions or other still unidentified effects than being caused by steric effects. To what extent, however, the drop in the addition rate is affecting polydispersity and molecular weight evolution in detail waits to be studied.

Downloaded by UNIV OF GUELPH LIBRARY on June 26, 2012 | http://pubs.acs.org
Publication Date: August 13, 2009 | doi: 10.1021/bk-2009-1024.ch014

## Star-star coupling

By using Z-RAFT star polymerization of several acrylates (methyl acrylate (MA), butyl acrylate (BA), and dodecyl acrylate(DA)) using RAFT agent **9**, well-defined 6-arm star polymers with molecular weights of more than 1 million Da could be generated (*14*). Narrow and monomodal molecular weight distributions were found up to intermediate monomer conversions, as indicated in Figure 6a. The living process was found to be very effective up to high monomer conversions, again indicating that steric congestion next to the star polymer core is not hampering the Z-RAFT star polymerization.

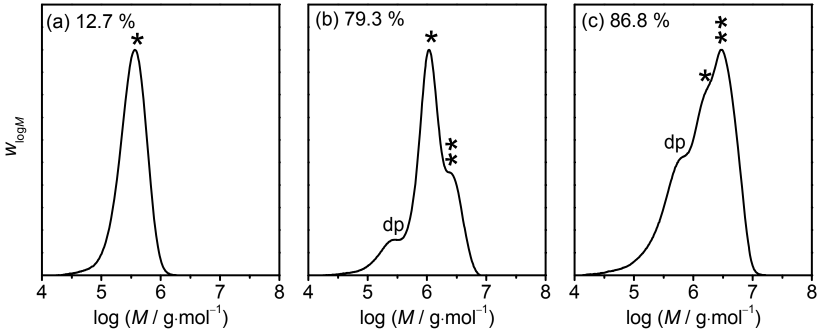

*Figure 6. Molecular weight (SEC) distributions of polymer from a* ***9****-mediated ($0.44 \times 10^{-3}$ mol·L$^{-1}$) AIBN-initiated ($1.71 \times 10^{-3}$ mol·L$^{-1}$) 6-arm Z-RAFT star polymerization of BA in bulk at 60 °C after various monomer conversions. (dp) dead polymer; (*) 6-arm star polymer; (**) star-star couple.(Reproduced from ref. (14). Copyright 2007 American Chemical Society)*

At relatively high monomer conversions, however, an unexpected high molecular weight component occurred, indicated by ** in Figure 6b and Figure 6c, which has double the molecular weight of the 6-arm star polymer, *. Dead polymer, dp, from conventional termination between two growing arms occurs on the low molecular weight side of the living star polymer, naturally becoming more prominent throughout the polymerization. By using a dual detection

Downloaded by UNIV OF GUELPH LIBRARY on June 26, 2012 | http://pubs.acs.org
Publication Date: August 13, 2009 | doi: 10.1021/bk-2009-1024.ch014

approach with RI- and UV-detection after SEC, with the UV-detection set to 310 nm, at which only the RAFT-moieties absorb and the polymer backbone remains invisible, the high molecular weight material was identified as a star-star couple containing exactly two living cores (*14*). The structure of these star-star couples was confirmed via cleavage experiments, in which the arm polymer was separated from the two cores. These experiments yielded arm polymer with molar masses that were identical for the 6-arm star as well as for the star-star couple.

The formation of star-star couples is clearly not in accordance with the basic Z-RAFT star polymerization mechanism (see Scheme 1), but could be assigned to *inter*molecular chain transfer to polymer, which becomes significant in acrylate polymerization at high monomer conversions. The reaction mechanism leading to star-star couples is depicted in Scheme 3: *Inter*molecular chain transfer to polymer generates radical sites on the Z-RAFT star polymer, which then in turn undergo RAFT reaction with other star polymer species, generating doubled stars. This mechanism has recently been supported by ESI-MS studies by Barner-Kowollik and co-workers (*35*).

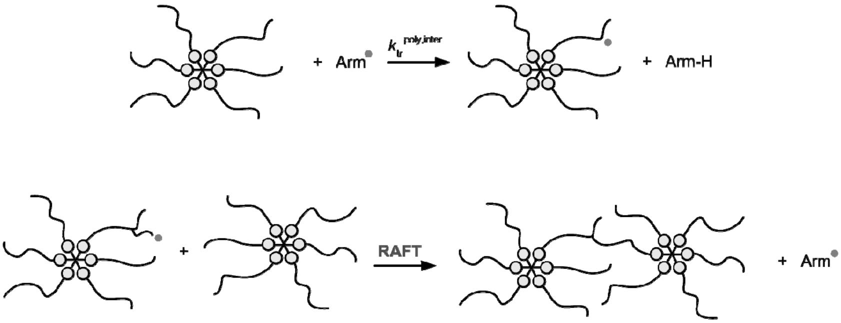

*Scheme 3. Reaction pathways leading to star-star couples in Z-RAFT star polymerization of acrylates.(Adapted with permission from ref. (14). Copyright 2007 American Chemical Society)*

The amount of star-star couples, which is a direct measure for the amount of long-chain branches originating from *inter*molecular chain transfer to polymer, i.e., every couple relates to one long-chain branch point, was quantified via diligent peak separation of the multimodal SEC peaks into peaks relating to the individual species. Thereby obtained amounts of star-star couples as function of monomer conversion were modeled via kinetic computer simulations using PREDICI© (*36*). By this approach, which turns an unavoidable side-reaction into a benefit, the rate coefficient of *inter*molecular transfer to polymer, $k_{tr}^{inter,poly}$, could be measured directly for the first time. The data obtained for BA and DA polymerization reads (*14*):

$$k_{tr}^{poly,inter}\ (\text{BA, 60 °C}) = (0.33 \pm 0.11)\ \text{L}\cdot\text{mol}^{-1}\cdot\text{s}^{-1}.$$
$$k_{tr}^{poly,inter}\ (\text{DA, 60 °C}) = (7.1 \pm 1.6)\ \text{L}\cdot\text{mol}^{-1}\cdot\text{s}^{-1}.$$

Alternative methods are mainly able to determine the sum of *inter*- and *intra*molecular chain transfer to polymer. It should be noted that *intra*molecular chain transfer to polymer (back-biting) does not lead to star-star couples, but induces short-chain branching of the polymer chains only.

## Expanding the arm numbers

The pentaerythritol-based star RAFT agents are generally limited to six arms. Since a systematic expansion of the arm numbers appears desirable in order to continue the systematic studies of Z-RAFT star polymerizations, alternative cores need to be implemented. We consequently developed a new octa-functional trithiocarbonate-type RAFT agent that bases on an inorganic silsesquioxane core. Silsesquioxane as building block for star polymers has recently been used for controlled atom-transfer polymerization (ATRP) (*37,38*) providing well defined organic/inorganic composite materials. It thus seems beneficial to apply this approach to Z-RAFT star polymerization in order to further increase the homogeneity of such materials. Considering the results of Monte Carlo studies reported above, we designed the novel RAFT agent 10 (see Chart 2) with substantial spacers between the core and the active RAFT-groups, which is anticipated to alleviate steric shielding effects.

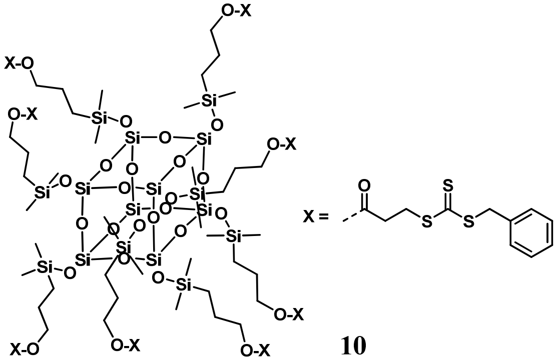

*Chart 2. Octa-functional silsesquioxane-type Z-RAFT agent (octakis-dimethyl-3(3-benzyl-trithiocarbonyl-propionic-acid)propane-1,3-diylsilylbicycloocta-siloxane)*

The Z-RAFT agent was synthesized in a two step reaction (see below) and showed good controlling behavior in preliminary styrene polymerizations (see Figure 7), which is indicated by steadily increasing molar masses and polydispersities below 1.5. Please note that the molecular weight data are apparent values only, since they were obtained via conventional calibration against linear standards. It should be noted that the employed benzyl R-group is not optimal to generate pure 8-arm star polystyrene, as has been reported above, and it is anticipated that the number of arms increases during this preliminary polymerization studies. The synthesis procedure, however, allows easy

Downloaded by UNIV OF GUELPH LIBRARY on June 26, 2012 | http://pubs.acs.org
Publication Date: August 13, 2009 | doi: 10.1021/bk-2009-1024.ch014

substitution by more effective R-groups. The resulting octa-functional RAFT agents wait to be used in Z-RAFT star polymerizations leading to inorganic/organic hybrid star polymers. The properties and usage of these star polymers will be reported in forthcoming studies.

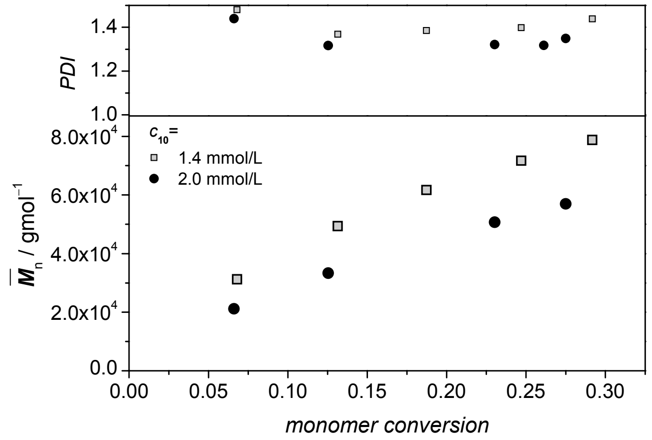

*Figure 7. Apparent number average molecular weight, $\overline{M}_n$, and polydispersity index, PDI, vs. monomer conversion in Z-RAFT star polymerization of styrene in bulk at 80 °C using 3.0 mmol·L$^{-1}$ 1,1'-azobis(cyanocyclohexane) as the initiatior and octa-functional RAFT agent **10**.*

Synthesis of octakis-dimethyl-3(3-benzyl-trithiocarbonyl-propionic-acid)propane-1,3-diylsilylbicycloocta-siloxane **10**: To a KOH solution (23.0 g, 0.410 mol, in 125 mL $H_2O$), 3-mercaptopropionic acid (10 mL, 0.130 mol) was added at room temperature. After 30 min, $CS_2$ (15 mL) was slowly added. After stirring at room temperature for 12 h, benzyl bromide (15.4 mL, 0.130 mol) was added. The reaction mixture was then heated to 80 °C and stirred for additional 12 h. Afterwards, the mixture was acidified with concentrated HCl and extracted with $CH_2Cl_2$ (4 × 40 mL). The combined organic phases were treated with a saturated aqueous solution of $K_2CO_3$. The aqueous phase was then again acidified with concentrated HCl and extracted with $CH_2Cl_2$ (3 × 40 mL). The solvent was removed under reduced pressure and the raw product was then purified via column chromatography using silica (pentane/THF/acetic acid 100/10/1, *Rf* = 0.33). 3-3-Benzyl-sulfanyl-thiocarbonyl-sulfanyl-propionic-acid (*15*) (6.50 g, 0.024 mmol, 18 % yield) were obtained as light yellow crystals. The purity was 93 % according to NMR.

$^1$H–NMR (200 MHz; $CDCl_3$) δ (ppm): 2.83 (t, 2H, $C_2CO$, $J$ = 7.0 Hz), 3.61 (t, 2H, $C\mathit{H}_2S$, $J$ = 7.0 Hz), 4.61 (s, 2H, $CH_2$), 7.27 (m, 5H, $C_6\mathit{H}_5$), 10.1 (b, 1H, COOH).

In $CCl_4$ (10 mL), 3-3-Benzyl-sulfanyl-thiocarbonyl-sulfanyl-propionic-acid (0.60 g, 2.2 mmol, 10 eq) was dissolved. Thionylchloride (0.6 mL) was then added drop-wise. The reaction mixture was heated slowly and refluxed for 12 h.

Downloaded by UNIV OF GUELPH LIBRARY on June 26, 2012 | http://pubs.acs.org
Publication Date: August 13, 2009 | doi: 10.1021/bk-2009-1024.ch014

After removal of the solvent under reduced pressure, the obtained product was added to a solution of octakis-dimethyl-3-propanol-1,3-diylsilylbicycloocta-siloxane (0.31 g, 0.211 mmol) in *N,N*-dimethyl-acetamide (50 mL). After adding pyridine (0.18 mL, 17.4 g, 2.2 mmol, 10 eq), the reaction was stirred under nitrogen atmosphere for 6 h at 60°C. After reducing the volume of the reaction mixture to 1/3, it was added to a methanol/water mixture. The yellow precipitate was filtrated, dried under reduced pressure, put on ice and extracted with $CHCl_3$. The organic phases were dried over $Na_2SO_4$ and the raw product was then purified via column chromatography using silica (pentane/acetic acid 3:1, *Rf* = 0.25). 0.32 g (41%) **10** were obtained as yellow oil. The purity was 98 % according to NMR.

$^1$H-NMR (200 MHz, $CDCl_3$) $\delta$ (ppm): 0.00 (s, *48* H, $C\underline{H}_3$), 0.44 (m, 16 H, $C\underline{H}_2$), 1.51 (m, 16 H, $C\underline{H}_2$), 2.60 (t, *J* = 6.8 Hz, 16 H, $C\underline{H}_2$), 3.47 (t, *J* = 6.8 Hz, 16 H, $C\underline{H}_2$), 3.90 (m, 16 H, $C\underline{H}_2$), 4.45 (s, 16 H, $C\underline{H}_2$), 7.16 (m, 40 H, $\underline{H}_{ar}$).

$^{13}$C-NMR (75 MHz, $CDCl_3$) $\delta$ (ppm): −0.38 ($\underline{C}H_3$), 13.53 ($\underline{C}H_2$), 22.22 ($\underline{C}H_2$), 31.37 ($\underline{C}H_2$), 33.05 ($\underline{C}H_2$), 41.47 ($\underline{C}H_2$), 67.22 ($\underline{C}H_2$), 127.79 ($\underline{C}_{ar}H$), 128.70 ($\underline{C}_{ar}H$), 129.24 ($\underline{C}_{ar}H$), 134.83 ($\underline{C}_{ar}H$), 171.34 ($\underline{C}$=O), 222.94 ($\underline{C}$=S).

ESI-MS**:** exp. *m*/*z* 3598.3 (M + 2×MeOH + $NH_4^+$), 3603.2 (M + 2×MeOH + $Na^+$), 1797.2 (M + MeOH + 2×$Na^+$); calc: *m*/*z* 3598.31 (M + 2×MeOH + $NH_4^+$), 3603.27 (M + 2×MeOH + $Na^+$), 1797.12 (M + MeOH + 2×$Na^+$).

## Acknowledgements

Financial support by the *Deutsche Forschungsgemeinschaft* for project VA226/3 and within the frame of the European Graduate School “Microstructural Control in Free-Radical Polymerization” is gratefully acknowledged. P.V. acknowledges receipt of a Heisenberg-Professorship (DFG). We thank M. Buback (Univ. of Göttingen) for support and stimulating discussions and P. Schoenmakers and R. Edam (Univ. of Amsterdam) for help with the light-scattering measurements.

Downloaded by UNIV OF GUELPH LIBRARY on June 26, 2012 | http://pubs.acs.org
Publication Date: August 13, 2009 | doi: 10.1021/bk-2009-1024.ch014

# References

1. Tezuka, Y.; Oike, H. *Prog. Polym. Sci.* **2002**, *27*, 1069.
2. Lee, J. H.; Goldberg, J. M.; Fetters, L. J.; Archer, L. A. *Macromolecules* **2006**, *39*, 6677.
3. McLeish, T. C. B. *Chem. Eng. Res. Des.* **2000**, *78*, 12.
4. Hadjichristidis, N.; Pispas, S.; Pitsikalis, M.; Iatrou, H.; Vlahos, C., Asymmetric star polymers: Synthesis and properties. In *Branched Polymers I*, 1999; Vol. 142, pp 71.
5. Li, J. S.; Modak, P. R.; Xiao, H. N. *Colloids Surf., A* **2006**, *289*, 172.
6. Qiu, L. Y.; Bae, Y. H. *Pharm. Res.* **2006**, *23*, 1.
7. Kul, D.; Van Renterghem, L. M.; Meier, M. A. R.; Strandman, S.; Tenhu, H.; Yilmaz, S. S.; Schubert, U. S.; Du Prez, F. E. *J. Polym. Sci., Part A: Polym. Chem.* **2008**, *46*, 650.
8. Chiefari, J.; Chong, Y. K.; Ercole, F.; Krstina, J.; Jeffery, J.; Le, T. P. T.; Mayadunne, R. T. A.; Meijs, G. F.; Moad, C. L.; Moad, G.; Rizzardo, E.; Thang, S. H. *Macromolecules* **1998**, *31*, 5559.
9. Barner-Kowollik, C.; Davis, T. P.; Heuts, J. P. A.; Stenzel, M. H.; Vana, P.; Whittaker, M. *J. Polym. Sci., Part A: Polym. Chem.* **2003**, *41*, 365.
10. Moad, G.; Rizzardo, E.; Thang, S. H. *Aust. J. Chem.* **2005**, *58*, 379.
11. Perrier, S.; Takolpuckdee, P. *J. Polym. Sci., Part A: Polym. Chem.* **2005**, *43*, 5347.
12. Moad, G.; Rizzardo, E.; Thang, S. H. *Aust. J. Chem.* **2006**, *59*, 669.
13. Boschmann, D.; Vana, P. *Polym. Bull. (Heidelberg, Ger.)* **2005**, *53*, 231.
14. Boschmann, D.; Vana, P. *Macromolecules* **2007**, *40*, 2683.
15. Stenzel, M. H.; Davis, T. P. *J. Polym. Sci., Part A: Polym. Chem.* **2002**, *40*, 4498.
16. Darcos, V.; Dureault, A.; Taton, D.; Gnanou, Y.; Marchand, P.; Caminade, A. M.; Majoral, J. P.; Destarac, M.; Leising, F. *Chem. Commun. (Cambridge, U. K.)* **2004**, 2110.
17. Bernard, J.; Favier, A.; Zhang, L.; Nilasaroya, A.; Davis, T. P.; Barner-Kowollik, C.; Stenzel, M. H. *Macromolecules* **2005**, *38*, 5475.
18. Hao, X. J.; Malmstrom, E.; Davis, T. P.; Stenzel, M. H.; Barner-Kowollik, C. *Aust. J. Chem.* **2005**, *58*, 483.
19. Barner-Kowollik, C.; Buback, M.; Charleux, B.; Coote, M. L.; Drache, M.; Fukuda, T.; Goto, A.; Klumperman, B.; Lowe, A. B.; Mcleary, J. B.; Moad, G.; Monteiro, M. J.; Sanderson, R. D.; Tonge, M. P.; Vana, P. *J. Polym. Sci., Part A: Polym. Chem.* **2006**, *44*, 5809.
20. Mayadunne, R. T. A.; Jeffery, J.; Moad, G.; Rizzardo, E. *Macromolecules* **2003**, *36*, 1505.
21. Johnston-Hall, G.; Monteiro, M. J. *Macromolecules* **2008**, *41*, 727.
22. Boschmann, D.; Edam, R.; Schoenmakers, P. J.; Vana, P. *Polymer* **2008**, *49*, 5199.
23. Boschmann, D.; Edam, R.; Schoenmakers, P. J.; Vana, P. *Macromol. Symp.* **2008**, accepted.
24. Burchard, W. *Adv. Polym. Sci.* **1999**, *143*, 113.
25. Radke, W.; Gerber, J.; Wittmann, G. *Polymer* **2003**, *44*, 519.
26. Douglas, J. F.; Roovers, J.; Freed, K. F. *Macromolecules* **1990**, *23*, 4168.

Downloaded by UNIV OF GUELPH LIBRARY on June 26, 2012 | http://pubs.acs.org
Publication Date: August 13, 2009 | doi: 10.1021/bk-2009-1024.ch014

27. Dureault, A.; Taton, D.; Destarac, M.; Leising, F.; Gnanou, Y. *Macromolecules* **2004**, *37*, 5513.
28. Boschmann, D.; Mänz, M.; Pöppler, A.-C.; Sörensen, N.; Vana, P. *J. Polym. Sci., Part A: Polym. Chem.* **2008**, *46*, 7280.
29. Jesberger, M.; Barner, L.; Stenzel, M. H.; Malmstrom, E.; Davis, T. P.; Barner-Kowollik, C. *J. Polym. Sci., Part A: Polym. Chem.* **2003**, *41*, 3847.
30. Barner-Kowollik, C.; Davis, T. P.; Stenzel, M. H. *Aust. J. Chem.* **2006**, *59*, 719.
31. Fröhlich, M. G.; Vana, P.; Zifferer, G. *J. Chem. Phys.* **2007**, *127*.
32. Fröhlich, M. G.; Vana, P.; Zifferer, G. *Macromol. Theory Simul.* **2007**, *16*, 610.
33. Olaj, O. F.; Zifferer, G. *Makromol. Chem.* **1988**, *189*, 1097.
34. Vana, P.; Davis, T. P.; Barner-Kowollik, C. *Macromol. Theory Simul.* **2002**, *11*, 823.
35. Hart-Smith, G.; Chaffey-Millar, H.; Barner-Kowollik, C. *Macromolecules* **2008**, *41*, 3023.
36. Wulkow, M. *Macromol. Theory Simul.* **1996**, *5*, 393.
37. Costa, R. O. R.; Vasconcelos, W. L.; Tamaki, R.; Laine, R. M. *Macromolecules* **2001**, *34*, 5398.
38. Hussain, H.; Tan, B. H.; Gudipati, C. S.; Xaio, Y.; Liu, Y.; Davis, T. P.; He, C. B. *J. Polym. Sci., Part A: Polym. Chem.* **2008**, *46*, 7287.

Downloaded by UNIV OF GUELPH LIBRARY on June 26, 2012 | http://pubs.acs.org
Publication Date: August 13, 2009 | doi: 10.1021/bk-2009-1024.ch014

Downloaded by STANFORD UNIV GREEN LIBR on June 27, 2012 | http://pubs.acs.org
Publication Date: August 13, 2009 | doi: 10.1021/bk-2009-1024.ch015

## Chapter 15

# Iodine Transfer Radical Polymerizations of Vinylidene Fluoride in Supercritical Carbon Dioxide and Polymer Functionalization via Click Chemistry

**Muhammad Imran-ul-haq, Nadja Förster, Radovan Vukicevic, Kristin Herrmann, Rebekka Siegmann, Sabine Beuermann***

**Institute of Chemistry, University of Potsdam,**
**Karl-Liebknecht-Str. 24-25, D-14476 Golm, Germany,**

Vinylidene fluoride polymerizations were carried out in solution with supercritical carbon dioxide using mono and diiodo perfluorinated hexane as chain transfer agents. Characteristics of controlled radical polymerizations were observed leading to polymers with low polydispersities in the range from 1.2 to 1.4. Polymers with iodine end groups were subsequently functionalized with sodium azide and symmetrical alkynes to yield poly(vinylidene fluoride) with triazol end groups.

In Controlled/Living Radical Polymerization: Progress in RAFT, DT, NMP & OMRP; Matyjaszewski, K.;
ACS Symposium Series; American Chemical Society: Washington, DC, 2009.

Downloaded by STANFORD UNIV GREEN LIBR on June 27, 2012 | http://pubs.acs.org
Publication Date: August 13, 2009 | doi: 10.1021/bk-2009-1024.ch015

Controlling the molecular structure of polymers is a key issue for modern polymer synthesis, because more and more complex macromolecules are needed in the rapidly growing fields of nanotechnology or nanobiotechnology (*i*). To fulfill this demand versatile techniques of macromolecular engineering were developped, enabling work at the interface between polymer science and other synthetic fields such as biochemistry or inorganic chemistry (*ii*-*v*). The control over polymer functionalities (side groups or chain ends) is essential, since functional groups can be used for performing further modifications such as the reinitiation of polymerizations, creation of supramolecular linkages, conjugation of macromolecules or adsorption of polymers on surfaces.

Sharpless and coworkers popularized the 1,3-dipolar cycloaddition of azides and terminal alkynes, catalyzed by copper(I), in organic synthesis (*vi*). Such reactions were proven to be very practical, because they can be performed in high yield, in multiple solvents (including water), and in the presence of numerous other functional groups (*vii*). Moreover, the formed 1,2,3-triazol is chemically very stable. Due to their efficiency and simplicity, these cycloadditions were classified as ‘‘click’’ reactions (*viii*). Combination of chain-end functionality control via iodine transfer polymerization (ITP) and the efficiency of click chemistry is an interesting pathway for the synthesis of end-functional polymers, because iodine chain ends originating from ITP are expected to be easily transformed into azides, and a plethora of functional alkynes is commercially available.

Fluorinated polymers are of large interest for technical applications due to their unique properties, e.g., excellent chemical, thermal and mechanical stability as well as electroactivity (*ix*). Frequently, these polymers are synthesized in heterogeneous phase employing fluorinated stabilizers, which have a high potential for bioaccumulation. Supercritical carbon dioxide ($scCO_2$) has emerged as an attractive alternate solvent (*x,xi*). To avoid the use of surfactants homogeneous phase polymerizations of vinylidene fluoride in $scCO_2$ were studied. Homogeneity was established for polymerizations leading to polymers with number average molecular weights, $M_n$, below 10000 $g{\cdot}mol^{-1}$. In case of molecular weight control via initiation up to 10 wt.% of initiator had to be used (*xii*). To reduce the amount of initiator alternately molecular weights were controlled by chain transfer reactions (*xiii*, *xiv*). Degenerative transfer polymerizations are particularly interesting since they lead to controlled polymerization conditions giving access, e.g., to block copolymers. In this contribution the syntheses of poly(vinylidene fluoride), PVDF, with iodine end groups in solution with supercritical $CO_2$ and subsequent functionalization of the polymer by click reactions is reported.

# Experimental

## Materials

All reagents were used without further purification: the monomer vinylidene fluoride (VDF, Solvay Solexis), carbon dioxide ($CO_2$, grade 4.5, Messer Griesheim), perfluorinated hexyl iodide ($C_6F_{13}I$, Dyneon), diiodoperfluorohexane ($IC_6F_{12}I$, Dyneon), di-*tert* butyl peroxide (DTBP, Akzo Nobel), N,N-dimethyl acetamide (DMAc, 99 % pure, Acros*)* and LiBr (Sigma-Aldrich, 99 %).

## Polymer Characterization

Size-exclusion chromatography (SEC) of the polymers was carried out with DMAc containing 0.1 % LiBr as eluent and a column temperature of 45 °C. The samples were analyzed on a SEC set-up consisting of an Agilent 1200 isocratic pump, an Agilent 1200 refractive index detector, and two GRAM columns (10µm, 8 x 300mm, pore sizes 100 and 1000) from Polymer Standards Services. The SEC set-up was calibrated using low polydispersity polystyrene standards (PSS), since PVDF standards were not available. Polymer end groups were determined via NMR spectroscopy (Bruker, 300 MHz), Fourier Transform Infrared (FTIR, Vertex 70, Bruker) spectroscopy and electrospray ionization mass spectrometry (ESI-MS, Micromass Manchester, UK). NMR spectra were measured at room temperature using DMSO-$d_6$ or acetone-$d_6$ as solvent and TMS as an internal reference.

Downloaded by STANFORD UNIV GREEN LIBR on June 27, 2012 | http://pubs.acs.org
Publication Date: August 13, 2009 | doi: 10.1021/bk-2009-1024.ch015

## Iodine Transfer Polymerizations of VDF using $C_6F_{13}I$ and $IC_6F_{12}I$

VDF was polymerized in solution with around 73 wt.% $CO_2$ at 120 °C and 1500 bar with 0.06 mol·L$^{-1}$ DTBP in the presence of variant amounts of $C_6F_{13}I$ or $IC_6F_{12}I$. Monomer concentrations were around 3.7 mol·L$^{-1}$ in all cases. The reactions were carried out in optical high-pressure cells allowing for in-line measurement of monomer conversion via Fourier Transform Near Infrared (FT-NIR) spectroscopy (Vertex 70, Bruker). Details of the experimental set-up and preparation of the reactions mixtures are given in refs. xii and xiv.

## General Procedure for the Functionalization of PVDF with Iodine End Groups

PVDF synthesized using perfluorinated hexyl iodide as chain transfer ($M_n$ = 2040 g·mol$^{-1}$, 200 mg, 0.10 mmol), sodium azide (200 mg, 3.07 mmol), symmetrically alkyl substituted alkyne (2-butyne, 0.5 ml, 6.4 mmol), and 15 ml of DMF were added in a flask. The flask was connected with a reflux condenser and the reaction mixture was stirred for 72 hours at 90 °C. As the reaction proceeds the colour of the solution changes from transparent to brown. Functionalized poly(vinylidene fluoride) was precipitated in water, filtered and washed with diethyl ether to remove the unreacted organic reactants and side products. The final product was dried under vacuum. The polymers were analyzed by $^1$H-NMR and FTIR spectroscopy.

## Results and Discussion

Based on previous VDF polymerizations, in which molecular weights were controlled by initiation, polymerizations in the presence of $C_6F_{13}I$ or $IC_6F_{12}I$ were carried out at 120 °C and 1500 bar in solution with around 70 wt.% of $CO_2$. FT-NIR spectra recorded during the polymerization are depicted in Figure 1. The peak at 6303 $cm^{-1}$ is assigned to the CH-stretching vibration at the double bond of the monomer. As conversion increases with reaction time the intensity of the peak decreases until the peak disappears completely. The two small peaks at 6214 and 6332 $cm^{-1}$ referring to the absorbances of $CO_2$ remain unchanged. The spectra in Figure 1 indicate that the reaction mixture stayed homogeneous until complete monomer conversion was reached.

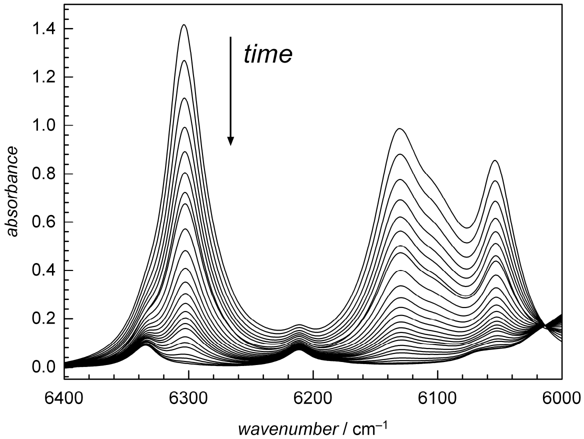

*Figure 1: FT-NIR spectra series recorded during a polymerization at 120 °C and 1500 bar in the presence of 0.21 mol·L$^{-1}$ $C_6F_{13}I$ as degenerative chain transfer agent.*

For end group analyses of the polymers $^1$H-NMR and ESI-MS spectra were recorded. As detailed in ref. xiii predominantly chains are seen that were initiated by a $C_6F_{13}$-group and terminated by transfer of an iodine atom. The finding is in accordance with a controlled radical polymerization ($^{xv}$):

$$C_6F_{13}\text{-(VDF)}_n\cdot + C_6F_{13}\text{-(VDF)}_m\text{–I} \rightleftharpoons C_6F_{13}\text{-(VDF)}_n\text{–I} + C_6F_{13}\text{-(VDF)}_m\cdot$$

Molecular weight analyses of polymers obtained from polymerizations with 0.2 mol·L$^{-1}$ $C_6F_{13}I$ resulted in a number average molecular weight of $M_n$ = 1800 g·mol$^{-1}$ and a polydispersity of 1.2. According to eq (1) an $M_n$ of 1600 g·mol$^{-1}$ is calculated, which is in good agreement with the experimental value.

$$M_n = [\text{VDF}]/[C_6F_{13}I]\cdot x\cdot M(\text{VDF}) + M(C_6F_{13}I), \qquad (1)$$

Downloaded by STANFORD UNIV GREEN LIBR on June 27, 2012 | http://pubs.acs.org
Publication Date: August 13, 2009 | doi: 10.1021/bk-2009-1024.ch015

with VDF concentration, [VDF], $C_6F_{13}I$ concentration, [$C_6F_{13}I$], monomer conversion, $x$, and the molar masses of VDF, $M$(VDF), and $C_6F_{13}I$, $M(C_6F_{13}I)$. To test for livingness VDF polymerizations with a fixed amount of $C_6F_{13}I$ were stopped at different conversions. Since the VDF polymerizations are rather fast and the chain transfer agent contributes to the initiation (*xiv*), a comparably low $C_6F_{13}I$ concentration of 0.081 mol·L$^{-1}$ leading to polydispersities of 1.4 had to be chosen. At higher concentrations of $C_6F_{13}I$ and associated lower polydispersities stopping the reaction at rather low conversions was not possible. The molecular weight distributions (MWDs) are shown in Figure 3. As expected for living radical polymerizations the MWDs are shifted in direction of higher molecular weights with increasing conversion. The MWDs given in Figure 2 refer to 23, 54 and 86 % of VDF conversion. Considering that the SEC was calibrated against polystyrene standards, the $M_n$ values of 1800, 2900, and 4700 g·mol$^{-1}$ are in reasonable agreement with the theoretical values of 1100, 2000, and 3000 g·mol$^{-1}$, respectively. It is remarkable to note that controlled radical polymerization conditions are not restricted to low or intermediate conversions.

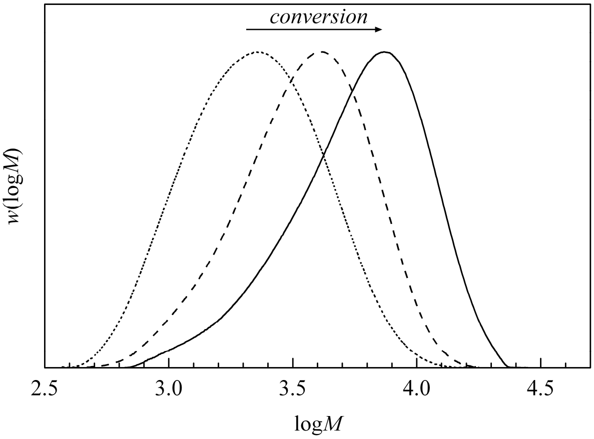

*Figure 2: Molecular weight distributions of PVDF obtained from polymerizations at 120 °C and 1500 bar in around 70 wt.% $CO_2$ with 0.081 mol·L$^{-1}$ $C_6F_{13}I$ stopped at different reaction times.*

For VDF polymerizations with 0.2 mol·L$^{-1}$ $C_6F_{13}I$ up to complete monomer conversion polydispersities as low as 1.2 were obtained. This is remarkable, because for various systems employing degenerative transfer agents, e. g., using dithiobenzoates, control of molecular weight decreases with conversion, as indicated by higher polydispersities ($^{xvi}$). One reason for the livingness up to very high conversion may be seen in the high pressure used. Due to high pressure the diffusion controlled rate coefficient of the termination reaction is significantly reduced, which is reflected by typical activation volumes $\Delta V^{\#}$ of 20 cm$^3$mol$^{-1}$ for termination rate coefficients ( $^{xvii}$ ). Thus, unfavorable bimolecular termination reactions associated with a loss of control are suppressed. Previously it was shown that high pressure may significantly increase the conversion range in which reversible addition fragmentation transfer polymerizations led to low polydispersity (~1.1) polymer material (*xvi*).

Downloaded by STANFORD UNIV GREEN LIBR on June 27, 2012 | http://pubs.acs.org
Publication Date: August 13, 2009 | doi: 10.1021/bk-2009-1024.ch015

Just recently, the favorable influence of high pressure on AGET (activators generated by electron transfer) atom transfer radical polymerizations was reported ($^{xviii}$).

In addition to $C_6F_{13}I$ the corresponding diiodo compound, $IC_6F_{12}I$, was used for molecular weight control. Polymerizations were also carried out at 120 °C, 1500 bar and with 70 wt.% $CO_2$. The experimental details and results are listed in Table 1.

**Table 1: Experimental details and results for VDF polymerizations at 120 °C and 1500 bar with 0.06 mol·L$^{-1}$ DTBP and the indicated amounts of $IC_6F_{12}I$ as chain transfer agent.**

| exp. | $c(IC_6F_{12}I)$/ mmol·L$^{-1}$ | c(VDF)/ mol·L$^{-1}$ | c($CO_2$)/ wt.% | $t$ / min | $x$ / % | $M_n$ / g·mol$^{-1}$ | *PDI* |
|---|---|---|---|---|---|---|---|
| 1 | 14 | 3.7 | 76 | 54 | 47 | 13200 | 1.4 |
| 2 | 29 | 3.6 | 76 | 18 | 48 | 12900 | 1.2 |
| 3 | 29 | 3.6 | 76 | 42 | 87 | 29500 | 1.3 |
| 4 | 63 | 3.6 | 74 | 41 | 82 | 7600 | 1.2 |
| 5 | 64 | 3.6 | 74 | 185 | 96 | 9100 | 1.4 |
| 6 | 80 | 3.6 | 74 | 60 | 99 | 6100 | 1.2 |
| 7 | 79 | 3.6 | 74 | 109 | 82 | 11200 | 1.4 |
| 8 | 235 | 3.5 | 68 | 114 | 97 | 2650 | 1.1 |

Table 1 shows that again polymers with very narrow MWDs were obtained. As for $C_6F_{13}I$ as chain transfer agent at high conversions low PDI values were obtained. For example, polymerizations up to conversions of more than 90 % lead to polymer material with PDI values below 1.2. It is interesting to note that rather high molecular weights of $M_n > 10000$ g·mol$^{-1}$ were accessible. In case of experiment 3 the reaction mixture showed two phases at the end of the reaction. Still a low polydispersity of 1.3 was obtained.

Downloaded by STANFORD UNIV GREEN LIBR on June 27, 2012 | http://pubs.acs.org
Publication Date: August 13, 2009 | doi: 10.1021/bk-2009-1024.ch015

Downloaded by STANFORD UNIV GREEN LIBR on June 27, 2012 | http://pubs.acs.org
Publication Date: August 13, 2009 | doi: 10.1021/bk-2009-1024.ch015

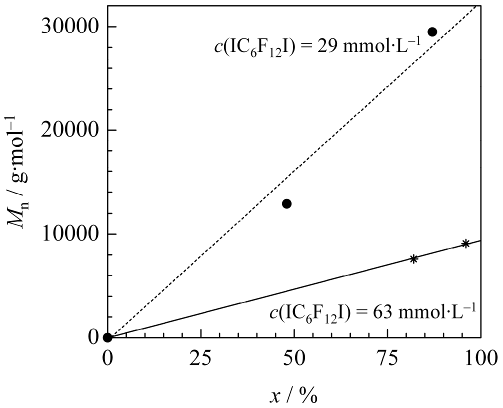

*Figure 3: Increase of $M_n$ with conversion for VDF polymerizations at 120 °C, 1500 bar and $IC_6F_{12}I$ concentrations as indicated.*

PVDF with $C_6F_{13}I$-derived end groups, $M_n$ = 2040 g·mol$^{-1}$ and $M_w/M_n$ = 1.3 was used for functionalization. Due to the rather labile C−I bond it was expected that these polymers can be transformed into various triazol functional end groups with alkyl substituents (methyl, ethyl and propyl) by a one-pot reaction: substitution of the terminal iodine atom by an azide function as intermediate and subsequent 1,3-dipolar cycloaddition of the terminal azide and functional alkynes (methyl, ethyl and propyl). The scheme for the functionalization with 2-butyne is shown in Scheme 1.

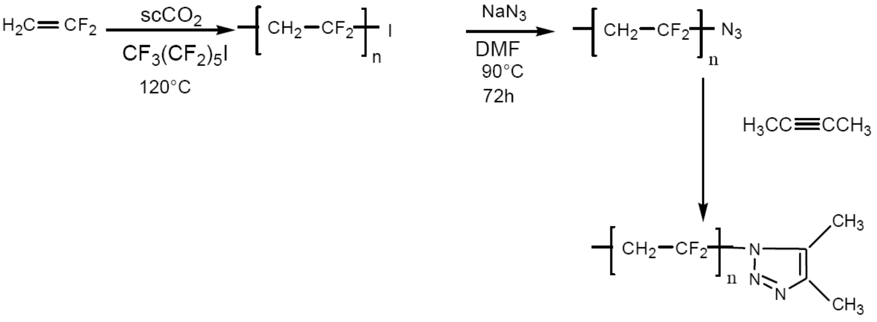

*Scheme 1: Synthesis of end functionalized PVDF.*

The so-called ‘‘click’’ cycloaddition (*xix*) was performed without any catalyst because of the symmetric nature of the alkynes employed. The polymer end groups were determined by $^1$H-NMR, FT-IR spectroscopy and by ESI-MS analyses.

For functionalization of PVDF with 2-butyne, 3-hexyne, and 4-octyne polymers with number average molecular weights ranging from 1500 to 2700 g·mol$^{-1}$ were used. The reaction temperature was always 90 °C. After carrying out the first experiments with 2-butyne and 3-hexyne for 72 hours, for reactions with 1-octyne it was tested whether the reaction time may be lowered. It turned out that already after 24 hours the majority of iodine end groups is transformed to triazol end groups. Further, it was found that variations in $M_n$ do not affect the functionalization.

## End Group Analyses

A poly(vinylidene fluoride) sample with iodine end groups from polymerization in $scCO_2$ was purified and analyzed by $^1$H-NMR. The spectrum (A) is given in lower part of Figure 4. The two signals centered at 3.62 and 3.87 ppm (a, b) are due to methylene protons of the terminal VDF unit carrying an iodine atom as end group either attached to $CF_2$ or to $CH_2$, respectively. (*xv*). The signals from 2.6 to 3.2 ppm are due to the methylene protons present in the polymer backbone (d). The peak at 3.25 ppm corresponds to protons of the methylene group directly attached to $CF_3(CF_2)_5$ (c). For a detailed description of the peak assignments and the influence of head to tail, head to head, and tail to tail addition on the polymer microstructure the reader is referred to the original work by Boyer et al. (*xv*). The $^1$H-NMR spectra do not show any indication of initiator-derived end groups, which was confirmed by ESI-MS analysis (*xiii*). To perform a 1,3-dipolar azide/alkyne cycloaddition at the iodide-chain end, the iodide functional PVDF was transformed into an azide functional polymer by nucleophilic substitution. The obtained azide functional PVDF was subsequently involved in ‘‘click’’ reactions with three symmetric alkynes to prepare PVDF with triazol end groups. Typically, in the absence of an appropriate catalyst, the reaction between azides and terminal alkynes is quite slow, because these alkynes are poor 1,3-dipole acceptors.

The upper spectrum in Figure 4 was recorded for PVDF after reaction between the azide group and a methyl substituted alkyne. After the click reaction, in all cases the signals assigned to the methylene protons in the terminal VDF unit were shifted to slightly higher field at 3.90 and 4.08 ppm (f, g). When 2-butyne is used for the cycloaddition the methyl group directly attached to the triazol ring should give rise to a peak between 2.5 and 3 ppm (h). Using 3-hexyne as alkyne the methyl protons occur at 1.14 ppm and in case of 4-octyne at 0.96 ppm.

A:

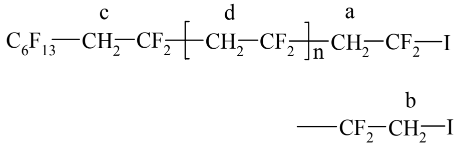

$$C_6F_{13}-\overset{c}{CH_2}-CF_2-\overset{d}{\left[CH_2-CF_2\right]_n}-\overset{a}{CH_2}-CF_2-I$$

$$-CF_2-\overset{b}{CH_2}-I$$

B:

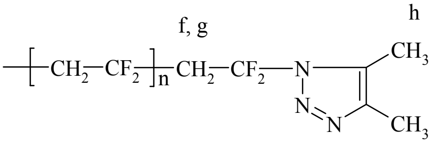

Downloaded by STANFORD UNIV GREEN LIBR on June 27, 2012 | http://pubs.acs.org
Publication Date: August 13, 2009 | doi: 10.1021/bk-2009-1024.ch015

Downloaded by STANFORD UNIV GREEN LIBR on June 27, 2012 | http://pubs.acs.org
Publication Date: August 13, 2009 | doi: 10.1021/bk-2009-1024.ch015

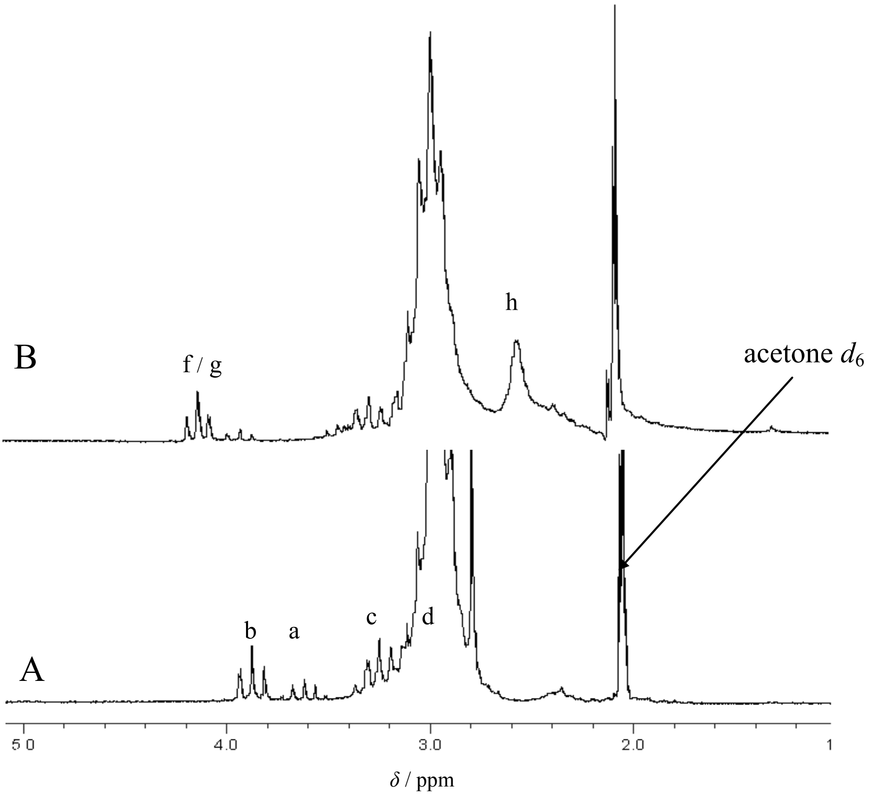

*Figure 4: $^1$H-NMR spectrum of purified poly(vinylidene fluoride) with iodine end groups (A) and a triazol end group (B) obtained after functionalization with $NaN_3$ and 2-butyne. Spectra were recorded at room temperature in acetone-d6.*

The existence of triazol end groups was confirmed by electrospray-ionization mass spectrometry. Characteristic peaks referring to a VDF chain with a $C_6F_{13}$ end group originating from the chain transfer agent and the second end group being a triazol group with two methyl substituents were found at e.g. *m/z* of 608.1, 672.1 and 736.1. Contributions from species with iodine end groups were negligible. Further, FTIR spectra of PVDF with iodine end groups show a characteristic peak at 613 cm$^{-1}$. After transformation to an azide the peak disappears and an absorbance at 2112 cm$^{-1}$ assigned to the azide is observed. After formation of the triazol a peak at 1654 cm$^{-1}$ occurs, which may be assigned to C=C and C=N of the triazol ring ($^{xx}$).

## Molecular weight analyses

Molecular weight distributions of the original PVDF material with iodine end groups and of the final material after performing the “click” reactions with three different symmetrical alkynes were measured by SEC. The results listed in

Table 2 indicate that $M_n$ is slightly enhanced with increasing size of the end groups. Further, Table 2 shows that polydispersities, $M_w/M_n$, of the material after performing the click reaction are slightly lower than the original material. The lowering in $M_w/M_n$ should be due to additional purification steps.

**Table 2: SEC results of the original PVDF sample (PVDF-I) and after performing "click" reactions with the alkynes indicated.**

| alkynes | $M_n$ / g·mol$^{-1}$ | $M_w/M_n$ |
|---|---|---|
| PVDF-I | 2040 | 1.4 |
| 2-butyne | 2200 | 1.2 |
| 3-hexyne | 2640 | 1.2 |
| 4-octyne | 2800 | 1.3 |

## Conclusions

PVDF obtained from homogeneous phase iodine transfer polymerization in supercritical $CO_2$ with iodide end groups allows for efficient functionalization of the polymer. After substitution of the iodine end group by an azide goup 1,3-dipolar cycloadditions with alkynes yield polymers with 1,2,3-triazol end groups. Using symmetrical alkynes the reactions may be carried out in the absence of any catalyst. In future, the work will be extended to functionalization of the end groups with non-symmetric alkynes. With respect to applications, e.g., as liquid crystalline materials, the introduction of mesogenic end groups into the polymer appears to be attractive.

## Acknowledgements

The authors thank Dyneon GmbH for financial support of this research. Additional support by the Deutsche Forschungsgemeinschaft within the European Graduate School on „Microstructural Contral in Free-Radical Polymerization“ is acknowledged.

## References

---

[i]. Langer, R.; Tirrell, D. A.; *Nature* **2004,** *428*, 487-492.

[ii]. Klok, H. A.; *J. Polym. Sci., Part A: Polym. Chem.* **2005,** *43*, 1-17.

[iii]. Pyun, J.; Matyjaszewski, K.; *Chem. Mater.* **2001**, *13*, 3436-3448.

[iv]. Gress, A.; Smarsly, B.; Schlaad, H.**;** *Macromole. Rapid Commun.* **2008**, *29*, 304-308.

[v]. Lutz, J.-F.; Boerner, H. G.; *Prog. Poly. Sci.* **2008**, *33*, 1-39.

Downloaded by STANFORD UNIV GREEN LIBR on June 27, 2012 | http://pubs.acs.org
Publication Date: August 13, 2009 | doi: 10.1021/bk-2009-1024.ch015

---

[vi]. Rostovtsev, V. V.; Green, L. G.; Fokin, V. V.; Sharpless, K. B.; *Angew. Chem. Int. Ed.* **2002**, *41*, 2596-2599.

[vii]. Link, A. J.; Vink, M. K. S.; Tirrell, *D. A.; J. Am. Chem. Soc.* **2004**, *126*, 10598-10602.

[viii]. Kolb, C.; Finn, M. G.; Sharpless, K. B.; *Angew. Chem. Int.Ed.* **2001**, *40*, 2004-2021.

[ix]. Scheirs, J. (Ed.), Modern Fluoropolymers, High Performance Polymers for Diverse Applications, Wiley, New York, 1997.

[x]. Wood, C. D.; Yarbrough, J. C.; Roberts, G.; DeSimone, J. M. in Kemmere, M. F.; Meyer, T. eds. Supercritical Carbon Dioxide in Polymer Reaction Engineering, Wiley-VCH, 2005, 189-204.

[xi]. Tai, H.; Wang,W.; Martin, R.; Liu, J.; Lester, E.; Licence, P.; Woods, H. M.; Howdle, S. M. *Macromolecules* **2005**, *38*, 355.

[xii]. Beuermann, S.; Imran-ul-haq, M.; *J. Polym. Sci., Polym Chem. Ed.* **2007**, *45*, 5626-5635.

[xiii]. Imran-ul-haq, M.; Tiersch, B.; Beuermann, S.; *Macromolecules* **2008,** *41*, 7453-7462.

[xiv]. Beuermann, S.; Imran-ul-haq, M.; *Macromol. Symp.* **2007**, *259*, 210-217.

[xv]. Boyer, C.; Valade, D.; Lacroix-Desmazes, P.; Ameduri, B.; Boutevin, B. J. *Polym. Sci., Polym. Chem. Ed.* **2006**, *44*, 5763-5777.

[xvi]. Arita, T.; Buback, M.; Janssen, O.; Vana, P.; *Macromol. Rapid Commun.* **2004**, *25*, 1376–1381.

[xvii]. Beuermann, S.; Buback, M.; *Prog. Polym. Sci.* **2002**, *27*, 191-254.

[xviii]. Kwiatkowski, P.; Jurczak, J.; Pietrasik, J.; Jakubowski, W.; Mueller, L.; Matyjaszewski, K.; *Macromolecules* **2008**, *41*, 1067-1069.

[xix]. Huisgen, R.; *1,3-Dipolar cycloaddition - introduction, survey, mechanism,* in 1,3-Dipolar Cycloaddition Chemistry, A. Padwa, Ed., Wiley, NewYork, **1984.**

[xx]. Imran-ul-haq, M.; *PhD thesis*, Potsdam, 2008.

Downloaded by STANFORD UNIV GREEN LIBR on June 27, 2012 | http://pubs.acs.org
Publication Date: August 13, 2009 | doi: 10.1021/bk-2009-1024.ch015

Downloaded by OHIO STATE UNIV LIBRARIES on June 26, 2012 | http://pubs.acs.org
Publication Date: August 13, 2009 | doi: 10.1021/bk-2009-1024.ch016

## Chapter 16

# SG1 and BLOCBUILDER® technology: a versatile toolbox for the elaboration of complex macromolecular architectures

**Didier Gigmes[1,]*, Jerôme Vinas[1,2], Nelly Chagneux[1], Catherine Lefay[1], Trang N. T. Phan[1], Thomas Trimaille[1], Pierre-Emmanuel Dufils[1], Yohann Guillaneuf[1], Géraldine Carrot[2], François Boué[2] and Denis Bertin[1,]***

**[1] UMR 6264 "Laboratoire Chimie Provence" CNRS et Universités d'Aix-Marseille 1, 2 et 3, Faculté des Sciences de Saint Jérôme, Av. Escadrille Normandie-Niemen, Case 542, 13397 Marseille cedex 20, France.**
**[2] Laboratoire Léon Brillouin, CEA-CNRS, CEA Saclay 91191 Gif-sur-Yvette, France.**
*** To whom correspondence should be addressed. E-mail: denis.bertin@univ-provence.fr; didier.gigmes@univ-provence.fr**

During the last decade, Nitroxide Mediated Polymerization using the SG1 nitroxide was recognized as an efficient technique to prepare controlled/living polymers *via* free radical polymerization. However, in order to go further in the synthesis of complex architectures, it was necessary to develop convenient chain-end functionalization strategies. Indeed, the preparation of telechelic polymers is of paramount importance for the synthesis of reactive building blocks, either to prepare polymer conjugates (biomaterials, surface modification,…) or to elaborate novel materials by coupling reaction. Due to both the radical reactivity and the presence of carboxylic acid function, the alkoxyamine BlocBuilder® represents a major breakthrough for macromolecular engineering. In this work, we illustrate two strategies to introduce valuable functional groups at the α position, namely the 1,2 intermolecular radical addition of BlocBuilder® on activated olefins and the coupling reaction *via* the BlocBuilder® *N*-succinimidyl activated ester derivatives.

In Controlled/Living Radical Polymerization: Progress in RAFT, DT, NMP & OMRP; Matyjaszewski, K.; ACS Symposium Series; American Chemical Society: Washington, DC, 2009.

Conjugates and block copolymers were then further prepared by these two techniques. Introduction of functionalities in ω position was also investigated *via* the radical reactivity of the SG1 macroalkoxyamine.

Downloaded by OHIO STATE UNIV LIBRARIES on June 26, 2012 | http://pubs.acs.org
Publication Date: August 13, 2009 | doi: 10.1021/bk-2009-1024.ch016

# Introduction

Nitroxide Mediated Polymerization (NMP) as well as Atom Transfer Radical Polymerization (ATRP) and Reversible Addition Fragmentation chain Transfer (RAFT) are powerful controlled radical polymerization (CRP) techniques which allow the synthesis of well-defined polymers, in composition and architecture.([i]) However, emerging technologies such as optics, microelectronics, and biomaterials are always looking for new materials exhibiting continuously more sophisticated properties and performance. To enhance their mechanical, thermal, or solubility behavior properties, the combination of polymers prepared by CRP with other polymers obtained from different techniques (such as Ring Opening Polymerization (ROP), Ring Opening Methathesis Polymerization (ROMP), Coordination Polymerization,…) is imperative to obtain a real synergy between chemically different and often immiscible macromolecules.([ii]) Apart from the combination of polymer with different chemical compositions, the architecture of the macromolecular species is also a crucial parameter. Indeed star, grafted, comb, cyclic complex architectures exhibit in many cases completely different properties than their linear analogues.([iii])

The development of the acyclic β-phosphorylated *N*-(2-methylpropyl)-*N*-(1-diethylphosphono-2,2-dimethyl propyl)-*N*-oxyl (so-called SG1) nitroxide introduced by Tordo *et al.([iv])* and now industrially developed by Arkema, represents a major breakthrough in NMP. This nitroxide was proven to be efficient for the controlled radical polymerization of various monomers([v]) such as styrene derivatives, acrylates derivatives, acrylic acid, *N,N*-dimethylacrylamide, acrylamides, *N*-isopropylacrylamide, …

From this nitroxide, numerous alkoxyamines were synthesized and among them, *N*-(2-methylpropyl)-*N*-(1-diethylphosphono-2,2-dimethylpropyl)-*O*-(2 carboxylprop-2-yl)hydroxylamine so-called MAMA-SG1 represents also a significant advance in NMP.([vi]) It has to be noted that this compound is commercially available from ARKEMA under the name of BlocBuilder® (Scheme 1). Indeed due to its particularly fast dissociation rate constant,([vii]) BlocBuilder® allows to improve the quality of the control of the polymerization, and offers the possibility to perform polymerization reactions in aqueous media.([viii]) These properties lead to the design and the obtention of novel block copolymers that were not accessible *via* the TEMPO nitroxide.(*v*)

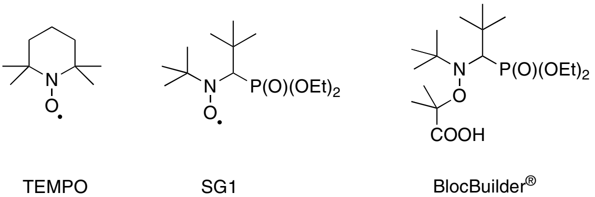

*Scheme 1.*

All controlled radical polymerization techniques are suited to the synthesis of functional polymers, nevertheless the *α* and *ω* position functionalization techniques have to be distinguished. The *α*-functionalization of the polymer chains is readily done by using the appropriate initiator prior to polymerization.(*v*) In that case ATRP is the more convenient system since a large number of α-brominated ester or amide compounds, are already either, commercially available or easy to prepare. Regarding the RAFT technique, the preparation of 100 % α-functionalized chains, implies that both the transfer agent and the radical initiator have to be functionalized prior to the polymerization step. In the case of NMP, functionalized alkoxyamines could be prepared but need generally multi-steps syntheses.

The *ω*-functionalization is mostly more difficult to perform since it requires chemical transformation after the polymerization step. The more common techniques are described in Scheme 2.(*v*) While the nucleophilic substitution of the halogen end-group represents a very convenient way to prepare end-functional polymers using ATRP, the NMP and RAFT techniques are less prone to end-functionalization. In the RAFT process, the thiocarbonylthio function could be transformed by different ways into a thiol group,(*v*) but the introduction of other groups is less straightforward. However, S. Perrier *et al.*([*ix*]) reported an approach for end-functionalization of polymers performed by RAFT that notably allows introduction of carboxylic acid group at the chain-end. A few methods is available to remove or transform the nitroxide moiety from polymers prepared by NMP. Moreover these techniques are not efficient for all nitroxides.

The lack of convenient alternatives applicable to chain-end functionalization of polymers prepared by NMP, prompted us to develop a methodology to achieve *α*-*ω* telechelic polymers based on the SG1 and the corresponding BlocBuilder® technology. The obtained polymers were then used as precursors for the elaboration of macromolecular complex architectures.

Downloaded by OHIO STATE UNIV LIBRARIES on June 26, 2012 | http://pubs.acs.org
Publication Date: August 13, 2009 | doi: 10.1021/bk-2009-1024.ch016

Downloaded by OHIO STATE UNIV LIBRARIES on June 26, 2012 | http://pubs.acs.org
Publication Date: August 13, 2009 | doi: 10.1021/bk-2009-1024.ch016

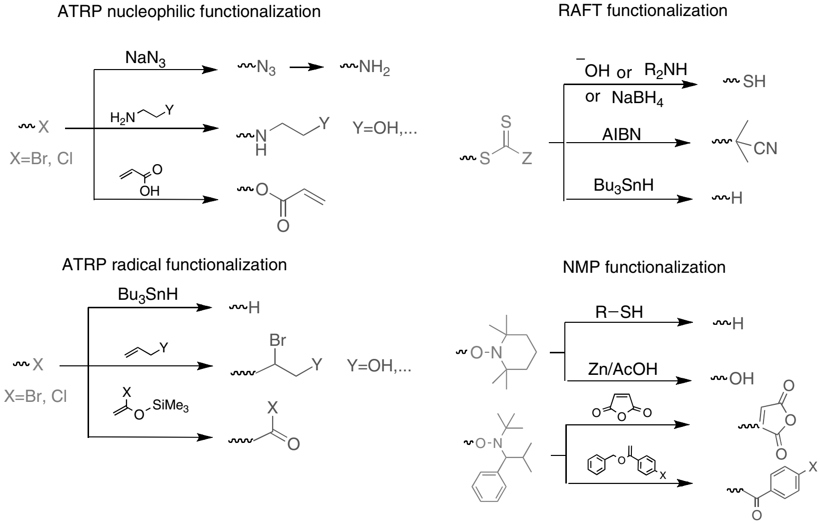
ATRP nucleophilic functionalization
NaN3
X=Br, Cl
Y=OH,...
RAFT functionalization
⁻OH or R2NH or NaBH4
AIBN
Bu3SnH
ATRP radical functionalization
Bu3SnH
X=Br, Cl
Y=OH,...
SiMe3
NMP functionalization
R−SH
Zn/AcOH

*Scheme 2. Usual end-functionalization technique for polymers prepared by CRP.*

The potential offered by BlocBuilder® has been recently highlighted for the synthesis of $\alpha$-functionalized polymers (Scheme 3). In a first series of experiments, we investigated the coupling reaction between amino-terminated compounds with the corresponding *N*-succinimidyl activated ester of BlocBuilder®.(x) Secondly, due to its high dissociation rate constant, BlocBuilder® was used successfully in clean 1,2 radical intermolecular addition on activated olefins.(xi) Recently, we also studied the $\omega$ chain-end functionalization of polymers prepared by SG1 mediated NMP to produce telechelic polymers.(xii)

The aim of this work is to illustrate the versatility of BlocBuilder® mediated polymerization for both the synthesis of telechelic polymers and complex architectures.

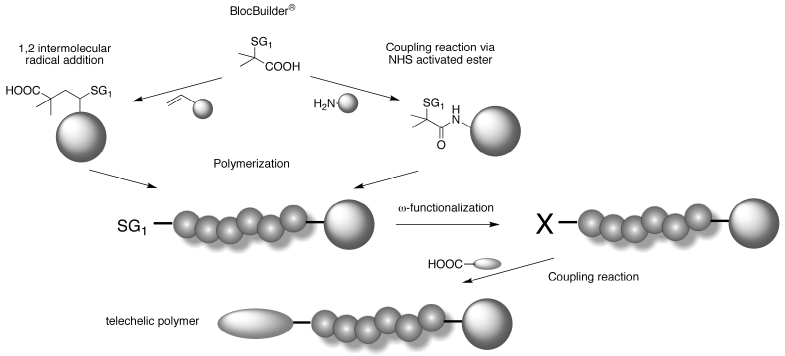
BlocBuilder®
1,2 intermolecular radical addition
Coupling reaction via NHS activated ester
HOOC
SG1
COOH
H2N
Polymerization
SG1
ω-functionalization
X
HOOC
Coupling reaction
telechelic polymer

*Scheme 3. Functionalization methodology developed from the BlocBuilder® technology*

## Experimental Section

### Materials.

All reagents and solvents were used without further purification. Poly(ethylene oxide) POE monomethyl ether ($M_n$ = 2000 g/mol, data given by supplier) was purchased from Sigma-Aldrich Chemical Co. Poly(etherimide) PEI (2950 g.mol$^{-1}$) was synthesized by polycondensation of 1,3-phenylene diamine and 4,4'-(4,4'-isopropylidenediphenoxy)bis(phtalic anhydride). Alkoxyamine BlocBuilder® was kindly provided by ARKEMA. The MAMA-NHS alkoxyamine was synthesized as already described in reference (*x*). The *N*-acryloyl-glucosamine has been synthesized as described in reference ([xiii]).

### Coupling reaction using DCC/DMAP.

The experimental procedure for the coupling between PEO and alkoxyamine has been previously described in reference ([xiv]).

### Synthesis of *N*-(2-hydroxyethyl)pivalamide.

Pivalic acid (5 g, 49 mmol) and *N*-hydroxysuccinimide NHS (6.76 g, 58.8 mmol) were dissolved in THF (45 mL). Then, a solution of dicyclocarbodiimide DCC (11.11 g, 54 mmol) in THF (5 mL) was added. After stirring at 0°C for 1.5 h, the precipitated *N,N*'-dicyclohexylurea (DCU) was removed by filtration. The filtrate was then concentrated under reduced pressure. The purification was performed two more times and yielded finally to 6.74 g (62 % yield) of a white powder. $^1$H NMR (300 MHz, $CDCl_3$): 1.39 (s, 9H), 2.83 (s, 4H). This compound was directly used for the synthesis of *N*-(2-hydroxyethyl)pivalamide: 1 g of pivalic succidimyl ester (5 mmol) and 336 mg of aminoethanol (5.5 mmol) were dissolved in 50 mL of acetonitrile. After stirring at RT for one hour, the product precipitated and was recovered by filtration. After drying under vacuum, 0.7 g (> 95 % yield) of a white powder was obtained. $^1$H NMR (300 MHz, DMSO-*d6*): 2.51 (s, 9H), 2.60 (t, 2H), 3.38 (t, 2H). ESI-MS: $C_7H_{15}NO_2$, M = 145 g.mol$^{-1}$; m/z: $[M+H]^+$ 146.

### 2-methyl-2-[*N-tert*-butyl-*N*-(1-diethoxyphosphoryl-2,2-dimethylpropyl) aminoxy]-*N*-(3-triethoxysilylpropyl) propionamide MAMA-NH-Si.

(3-aminopropyl) triethoxysilane (1.02g, 4.61 mmol) was added through a syringe to a solution of MAMA-NHS (2 g, 4.18 mmol) in THF (40 mL) at 0°C under inert atmosphere. After 1 h under stirring, the precipitated *N*-hydroxysuccinimide was removed by filtration. The filtrate was then concentrated under reduced pressure to about 2 mL volume and added in cold diethyl ether (30 mL). The precipitated product was filtrated off. This

Downloaded by OHIO STATE UNIV LIBRARIES on June 26, 2012 | http://pubs.acs.org
Publication Date: August 13, 2009 | doi: 10.1021/bk-2009-1024.ch016

precipitation step was repeated twice. After evaporation of the solvent, silylated alkoxyamine was obtained (74 % yield) as a yellow wax. $^{31}$P NMR (121.59 MHz, $CDCl_3$) : 27.82. $^{1}$H NMR (300 MHz, $CDCl_3$) : 0.58 (m, 2H), 1.05 (s, 9H), 1.12-1.19 (m, 18H), 1.23-1.33 (m, 6H), 1.52 (s, 3H), 1.62 (m, 5H), 2.99 (m, 1H), 3.32 (m, 2H), 3.75 (q, $J$ = 6 Hz, 6H), 3.92-4.27 (m, 4H).

### Grafting of silylated alkoxyamine onto silica nanoparticles in water.

Silica dispersion (30 g of 2 wt % $SiO_2$ particles in water), obtained using the Persello procedure, was introduced in a 100 mL two neck round-bottom flasks, fitted with septum, condenser, and deoxygenated for 20 min by nitrogen bubbling. In parallel, silylated alkoxyamine (0,21g, 0,36 mmol) was dissolved in cold DMF (2g) and deoxygenated in the same way. The alkoxyamine solution was then slowly added to the silica *sol*. After stirring at room temperature during 2h, the functionalized silica sol was characterized by both $^{29}$Si NMR and small-angle neutron scattering (SANS).

### General procedure for the 1,2 radical addition.

The experimental procedure has been previously described in reference (*xi*).

### 2,2-Dimethyl-4-[N-*tertio*butyl-N-(1-diethoxyphosphoryl-2,2-dimethylpropyl)aminoxy]-4-pyridin-4-yl butanoic acid MAMA-4VP-SG1.

Yield: 54%. $^{1}$H NMR (300.13 MHz, $CDCl_3$): 8.13-8.20 (m, 2H), 7.28-7.45 (m, 2H), 5.23 (major diastereoisomer, m, 0.65H), 4.97 (minor diastereoisomer, m, 0.35H), 4.45-3.78 (m, 2.8H), 3.48 (major diastereoisomer, d, $J$=27.5 Hz, 0.65H), 3.41 (minor diastereoisomer, d, $J$=26.5 Hz, 0.35H), 3.23–2.29 (m, 3.2H), 1.44–0.77 (m, 30H). $^{31}$P NMR (121.49 MHz, $D_2O$): 26.11 (55 %) ; 24.75 (45 %). $^{31}$P NMR (121.49 MHz, $CDCl_3$): 24.52 (65 %) ; 25.76 (35 %). ESI-MS: $C_{24}H_{43}N_2O_6P$, M = 486 g.mol$^{-1}$; m/z: $[M+H]^+$ 487; $[M+NH_4]^+$ = 509 ; $[M+K]^+$= 525.

### 2,2-Dimethyl-4-[N-tertiobutyl-N-(1-diethoxyphosphoryl-2,2-dimethylpropyl)aminoxy]-4-(4-(sodium sulfonate)phenyl) butanoic acid MAMA-SSNa-SG1.

Yield: 66%. $^{1}$H NMR (300.13 MHz, $CDCl_3$): 7.77–7.37 (m, 4H), 5.09 (major diastereoisomer, m, 0.55H), 4.87 (minor diastereoisomer, m, 0.45H), 4.26–3.75, 3.34 (m, 4H), 3.40 (major diastereoisomer, d, $J$= 27 Hz, 0.55H), 3.35 (minor diastereoisomer, d, $J$=27 Hz, 0.45H), 2.68–2.53 (m, 1H), 2.37–2.20 (m, 1H), 1.40–0.80 (m, 30H). $^{31}$P NMR (121.49 MHz, $D_2O$): 26.11 (55 %) ; 24.75 (45 %).

Downloaded by OHIO STATE UNIV LIBRARIES on June 26, 2012 | http://pubs.acs.org
Publication Date: August 13, 2009 | doi: 10.1021/bk-2009-1024.ch016

### 2,2-Dimethyl-4-[N-tertiobutyl-N-(1-diethoxyphosphoryl-2,2-dimethylpropyl)aminoxy]-4-(N-(2,4,5-trihydroxy-6-(hydroxymethyl) tetrahydro-2H-pyran-3-yl)carbamoyl) butanoic acid MAMA-NAG-SG1.

Yield: 40%. $^1$H NMR (300.13 MHz, DMSO-d$_6$): 8.04–7.07 (m, 1H), 6.44-5.55 (m, 1H), 5.20-3.09 (m, 16H), 2.68–2.53 (m, 1H), 2.30–1.90 (m, 2H), 1.40–1.0 (m, 30H). $^{31}$P NMR (121.49 MHz, DMSO-d$_6$): 25.83 (5 %) ; 25.05 (10 %); 24.89 (15 %); 24.81 (20 %); 24.51 (10 %); 24.10 (40 %).

### Synthesis of PEI-diacrylate.

In a three-neck round bottom flask equipped with a water cooled condenser, PEI (0.9 g) and triethylamine (0.857 mL) were mixed in 10 mL of $CH_2Cl_2$. 0.52 mL of acryloyl chloride in 5 mL of $CH_2Cl_2$ was added dropwise at 0 °C under dry nitrogen. After this addition was complete, the reaction solution was allowed to warm to room temperature and the reaction mixture was stirred overnight. The solution was then filtered to remove the triethylammonium chloride. Then, the solution was washed three times with 20 mL of saturated $NaHCO_3$ solution. The product was dried over $MgSO_4$ and the solvent was removed by rotary evaporation. The PEI-diacrylate was then precipitated in cold diethyl ether. It was then filtered and dried under vacuum to a constant mass.

### Synthesis of PEI-dialkoxyamine.

In a two-neck round bottom flask equipped with a water cooled condenser, PEI-diacrylate (0.5 g) was mixed with 6 mL of THF. The BlocBuilder® (1.2 g) was then added to the solution. After complete dissolution, the mixture was deoxygenated by nitrogen bubbling for 20 min and then the reaction was performed at 100 °C for 1 h. The solution was then cooled down in iced water bath and precipitated in cold diethyl ether. It was then filtered, washed with cold diethyl ether and dried under vacuum to a constant mass.

### Synthesis of PS-PEI-PS.

PEI-macroinitiator (0.35 g, 0.12 mmol), 2.52 g of styrene and 5.6 g of N-methyl pyrrolidone were placed in a three-neck round bottom flask equipped with a water cooled condenser. The solution was purged with nitrogen for 20 min. The mixture was immersed in an oil bath at 120 °C. Samples were taken periodically for conversion analysis using $^1$H NMR. The solution was then cooled to room temperature and precipitated in cold methanol. The copolymer was dried under high vacuum to a constant mass.

Downloaded by OHIO STATE UNIV LIBRARIES on June 26, 2012 | http://pubs.acs.org
Publication Date: August 13, 2009 | doi: 10.1021/bk-2009-1024.ch016

### Synthesis of PS-Ketone.

PS-TEMPO described in reference (*xii*) ($M_n$ = 4,900 g.mol$^{-1}$, PDI = 1.2, 250 mg) and *m*-chloroperbenzoic acid *m*CPBA powder (27 mg) in 3 mL of toluene were introduced in a 20 mL round bottom flask. The flask was stirred at room temperature for one day. The polymer was then purified by precipitation in cold methanol and dried over vacuum.

### Preparation of PS-DNPH conjugate.

The PS-Ketone synthesized previously (100 mg) was dissolved in 1 mL of a 5% trifluoroacetic acid (TFA) in THF; 25 mg of 2,4-dinitrophenylhydrazine (DNPH0 was added. A yellow color formed immediately. The PS-DNPH conjugate was then purified by precipitation in cold methanol and dried over vacuum.

## Results and Discussion

### *α*-functionalization of polymer chains

#### *Via coupling reaction*

The coupling reaction between an initiator bearing a carboxylic acid end-group and a compound with an alcohol or amine function, before or after polymerization, has been extensively used to prepare block copolymers.(*xv*) The amphiphilic polystyrene-*block*-poly(ethylene oxide) (PS-*b*-PEO) is one of these copolymers, combining very different and interesting properties for many industrial applications: polymeric surfactants, compatibilizers in polymer blends, stabilizers, and as templates for the preparation of inorganic nanoparticles such as mesoporous silica. In order to prepare such polymers, we investigated the coupling reaction between a commercial hydroxy-terminated PEO with 2-[*N*-tertiobutyl-*N*-(1-diethoxyphosphoryl-2,2-dimethylpropyl) aminooxy]propanoic acid AMA-SG1 (Scheme 4). (*xiv*)

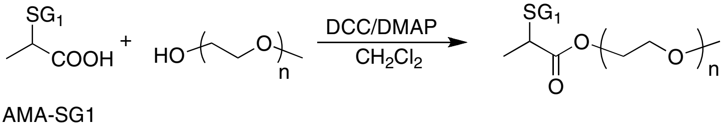

*Scheme 4. Coupling reaction between AMA-SG1 and hydroxy terminated PEO.*

Downloaded by OHIO STATE UNIV LIBRARIES on June 26, 2012 | http://pubs.acs.org
Publication Date: August 13, 2009 | doi: 10.1021/bk-2009-1024.ch016

The results obtained with the AMA-SG1 encouraged us to study the coupling between hydroxy-terminated PEO and BlocBuilder®. Two different procedures were used: first *via* the thionyl chloride and secondly *via* the dicyclocarbodiimide DCC/ dimethylaminopyridine DMAP pair, both reactions were performed in dichloromethane. The results reported in Table 1 showed that the introduction of a extra methyl group drastically decreases the yield of the coupling reaction.

| Acid compound | Coupling Conditions | Yield |
|---|---|---|
| AMA-SG1 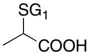 | DCC/DMAP/ $CH_2Cl_2$ | 43 % |
| BlocBuilder® 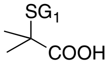 | DCC/DMAP/ $CH_2Cl_2$ | 5 % |
| BlocBuilder® 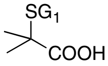 | Thionyl Chloride | < 5 % |
| Propionic acid 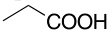 | DCC/DMAP/ $CH_2Cl_2$ | 65 % |
| Isobutyric acid 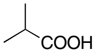 | DCC/DMAP/ $CH_2Cl_2$ | 60 % |
| Pivalic acid 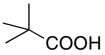 | DCC/DMAP/ $CH_2Cl_2$ | 20 % |

*Table 1.Yield of coupling between different acid compounds and hydroxy terminated PEO (Mn =1,800 g.mol$^{-1}$).*

This result could be explained by the combination of a higher steric hindrance and at the same time an increase of the dissociation rate constants for BlocBuilder® compared to AMA-SG1. In order to clarify which parameters could be responsible for such results, we studied the esterification of three model carboxylic acids exhibiting different steric hindrance, namely propanoic, isobutyric and pivalic acid with PEO ($M_n$ = 1800 g.mol$^{-1}$).

The results obtained (Table 1) showed that in the selected experimental conditions, when the α-carbon of the carboxylic acid is primary or secondary the yield of coupling is close to 60-70 % but decrease to 20 % in case of a tertiary one. As expected a too high steric hindrance leads to a decrease of the coupling yield, however in the case of the BlocBuilder® the increase of the dissociation rate constants plays also probably a role, since the yield of the reaction was below 5 %.

It is well known that amino compounds are more nucleophilic reagents than the corresponding alcohols, therefore we tried to react pivalic acid as a model of BlocBuilder® with aminoethanol using the DCC/DMAP pair. Aminoethanol was chosen with the view to prepare a dual functional initiator allowing the combination of ROP and NMP techniques. Unfortunately, the amidification

Downloaded by OHIO STATE UNIV LIBRARIES on June 26, 2012 | http://pubs.acs.org
Publication Date: August 13, 2009 | doi: 10.1021/bk-2009-1024.ch016

reaction only lead to the starting reagents and to achieve such transformation, new coupling conditions had to be used.

Activated esters are very useful derivatives to bind covalently amines with carboxylic acids yielding to the corresponding amides and have thus found broad application in peptide chemistry for instance.(xvi) Among the different activated moieties, the *N*-hydroxy succinimide group is very efficient to introduce functionalities in polymer science through the use of *N*-acryloxysuccinimide or the methacrylate analogue.(xvii)

Therefore, we extrapolated this synthetic route for the reaction of pivalic acid with aminoethanol (Scheme 5). First, the pivalic NHS activated ester was obtained in 60 % yield. The coupling of the latter with aminoethanol produced the *N*-(2-hydroxyethyl)pivalamide with near quantitative yield.

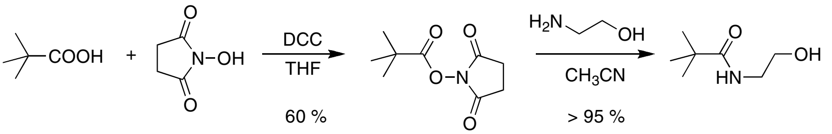

*Scheme 5.*

This result prompted us to prepare the *N*-succinimidyl derivative of BlocBuilder® (*x*) so-called MAMA-NHS (Scheme 6a). We showed that this compound exhibits a dissociation rate constant 15 times higher than BlocBuilder® and behaves also as an efficient initiator for NMP polymerizations (*x*). MAMA-NHS alkoxyamine was then reacted with ethanolamine to provide the corresponding OH-functional alkoxyamine. From this initiator we were able to prepare a di-block copolymer PLA-*b*-PS (*x*) by combining sequentially the NMP of styrene and the ring opening polymerization of D,L-lactide with the alcohol function (Scheme 6b).

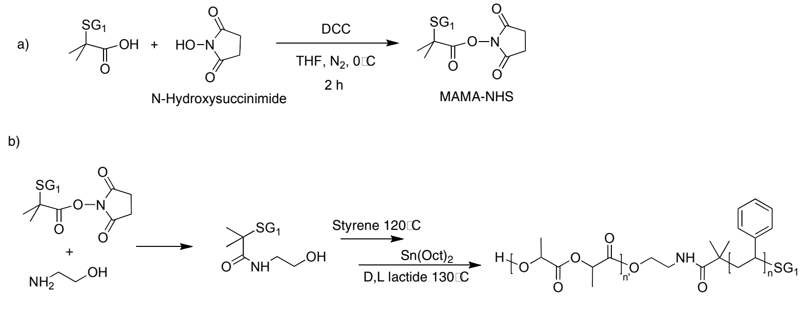

*Scheme 6.*

The MAMA-NHS was also reacted with the commercially available amino terminated poly(propylene glycol) (PPO) leading to a PPO macroalkoxyamine.

Downloaded by OHIO STATE UNIV LIBRARIES on June 26, 2012 | http://pubs.acs.org
Publication Date: August 13, 2009 | doi: 10.1021/bk-2009-1024.ch016

The potential of MAMA-NHS was further illustrated with the synthesis of hybrid nanoparticles. Indeed this kind of materials could be very interesting in a broad field of applications, from optoelectronics and sensing to catalysis and medicine because of the synergy between optical, thermal and electric properties of the inorganic particles and physicochemical properties of polymeric materials. Several examples in the literature describe the use of NMP from inorganic particles for the elaboration of these hybrid objects. Usually the synthesis of silylated initiator/controller is required to initiate CRP at the surface of silica nanoparticles. Beyou *et al.*(*xviii*) and Hawker *et al.*(*xix*) have for example synthesized silylated alkoxyamines in several steps.

As many aminosilylated compounds are commercially available, we easily obtained in 74 % yield the silylated alkoxyamine MAMA-NH-Si from the coupling reaction of MAMA-NHS with the (3-amino propyl)triethoxysilane (Scheme 7).

Downloaded by OHIO STATE UNIV LIBRARIES on June 26, 2012 | http://pubs.acs.org
Publication Date: August 13, 2009 | doi: 10.1021/bk-2009-1024.ch016

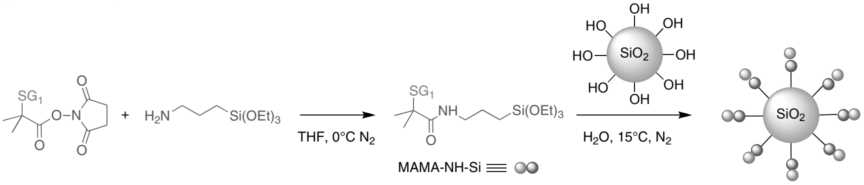

*Scheme 7.*

The other advantage of our approach is that the overall synthesis is performed in aqueous media and this has a particular interest regarding potential bio-related applications.

The silylated alkoxyamine MAMA-NH-Si was therefore grafted in aqueous media to the surface of silica nanoparticles, previously prepared using the procedure of Persello.( *xx* ) Both initial and functionalized particles were characterized by quantitative solid state $^{29}$Si NMR, and small-angle neutron scattering (SANS). The radius of the bare silica particles was calculated to be 35 Å, from the fit of the SANS spectrum in the Guinier regime. According to the $^{29}$Si NMR analysis, the grafting efficiency was found to be close to 90%, for a target density of 0.9 initiators per nm$^2$. The SANS analysis also showed that the condensation of the NMP precursor leads to an increase of the scattered intensity, suggesting some aggregation during the grafting reaction. The radius of alkoxyamine-grafted-particles was estimated around 78 Å (with the Guinier approximation), that means that this aggregation seems to be limited to 12 particles per aggregates (determined using the ratio of the volume (diameter)$^3$ before and after grafting). To our knowledge, this result represents the first example of alkoxyamine covalently grafted to silica particles in aqueous solution. Polymerization using these functionalized silica particles will be described in a forthcoming article.

In conclusion we showed that, the transformation of carboxylic acid moiety of the BlocBuilder® alkoxyamine with several valuable molecular or macromolecular compounds bearing an amino group, was achievable by using the corresponding MAMA-NHS as intermediates. This reaction leaded to polymer-conjugates, diblock copolymer or hybrid nanoparticles. Nevertheless this coupling strategy is limited to primary amines and another functionalization technique was necessary to broaden again the range of complex architecture. To reach this goal, we have developed a strategy based on the 1,2 intermolecular radical addition of BlocBuilder® onto activated olefins.

### *Via 1,2 Intermolecular Radical Addition*

During the last decade, 1,2 intermolecular radical addition using alkoxyamine has been developed in organic chemistry as an alternative of the radical addition using tin-chemistry.(*xxi*)

In the case of activated olefins, the challenge consists to avoid the multiple addition. Therefore to circumvent any undesired polymerization, the thermal stability of the starting and obtained alkoxyamines has to be tuned carefully (Scheme 8). The corresponding alkoxyamine resulting from the radical addition on the olefin double bond bears a less stabilized and bulky secondary radical moiety compare to the 1-carboxy-1-methyl ethyl alkyl radical moiety of the BlocBuilder®. Therefore, owing to the lower C-ON bond dissociation energy (BDE) of the latter compare to the targeted product, BlocBuilder® was expected to lead to a clean 1,2-intermolecular radical addition onto various olefins.(*xi*)

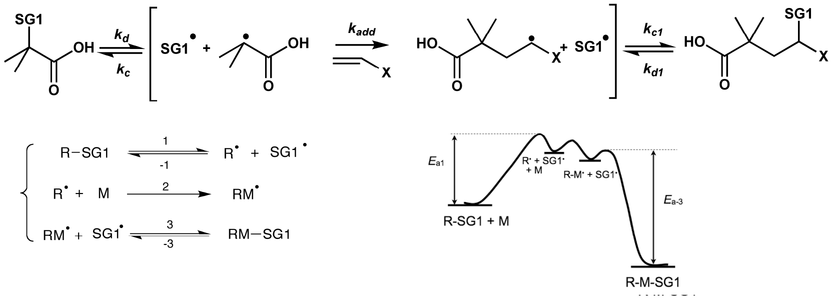

*Scheme 8. 1,2 Intermolecular radical addition mechanism.*

This reaction was already successfully performed at 100 °C in solution with styrene, *n*-butyl acrylate, hydroxyethyl acrylate, acrylic acid.(*xi*) In this paper, we extended this methodology to other activated olefins, namely 4-vinylpyridine, sodium styrene sulfonate and a glycomonomer the *N*-acryloyl-glucosamine (Scheme 9).

Downloaded by OHIO STATE UNIV LIBRARIES on June 26, 2012 | http://pubs.acs.org
Publication Date: August 13, 2009 | doi: 10.1021/bk-2009-1024.ch016

Downloaded by OHIO STATE UNIV LIBRARIES on June 26, 2012 | http://pubs.acs.org
Publication Date: August 13, 2009 | doi: 10.1021/bk-2009-1024.ch016

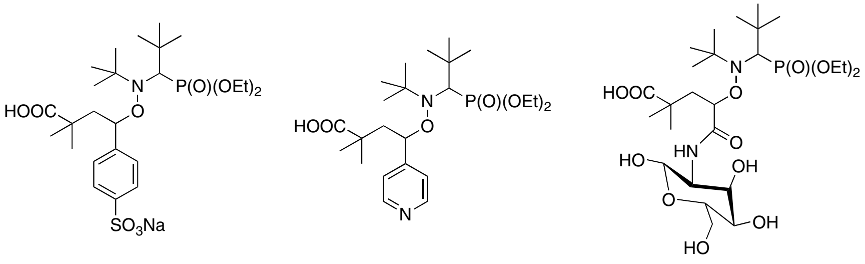

BB-SSNa-SG1 BB-4VP-SG1 BB-NAG-SG1

*Scheme 9.*

For each case, the monomer conversion was above 90 % and the yields were good (66 % for BB-SSNa-SG1) to moderate (40 % for BB-NAG-SG1 and 54 % for BB-4VP-SG1). This result showed that a totally water soluble (BB-SSNa-SG1), a water soluble under acidic conditions (BB-4VP-SG1) and glucosylated alkoxyamines were conveniently prepared in a one-step procedure from the commercially available BlocBuilder®.

The 1,2 intermolecular radical addition is also useful to prepare di or tri-block copolymers. In that case the vinylic function introduced by, esterification or amidification of acryloyl chloride with a polymer bearing a terminal alcohol or amino moiety, can be easily converted into a macroalkoxyamine. Starting from this macroalkoxyamine, a further polymerization step could lead to the corresponding di or triblock copolymers. To illustrate this strategy, we prepared a triblock copolymer of PS-*b*-poly(etherimide)-*b*-PS (Scheme 10). The poly(etherimide) (PEI) terminated by two amino groups was first reacted with acryloyl chloride to obtain the corresponding PEI-diacrylate in 74 % yield determined by $^1$H NMR.

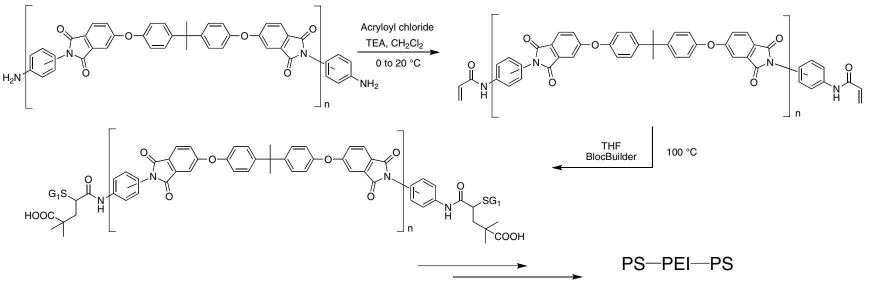

*Scheme 10. Synthesis of PS-b-PEI.*

Typically, the 1,2 addition was performed at 100 °C with a large excess of BlocBuilder® (10 equivalents per acrylate function) to ensure a qualitative functionalization as proved by $^{31}$P NMR. The macroalkoxyamine was finally used as macroinitiator for styrene polymerization in 30 w% *N*-methyl pyrrolidone solution. The good agreement between experimental and theoretical evolution of $M_n$ versus conversion ensured that styrene polymerization was well controlled (Figure 1).

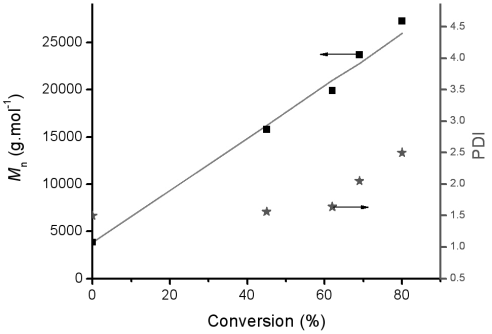

*Figure 1. Evolution of $M_n$ and PDI (determined both by SEC) Vs conversion (determined by $^1H$ RMN) for the styrene (30 w% in N-methylpyrrolidone) polymerization at 120°C with targeted $M_n$ of 28,000 g.mol$^{-1}$.*

## *ω*-functionalization of polymer chains

The *α* functionalization of polymer chains has been extensively used for preparing complex architecture and polymer conjugates.(*xxii*) Nevertheless to use the control radical polymerization process as a tool to prepare reactive building blocks, it is compulsory to study the *ω* functionalization. This method could enable for example to prepare either multisegmented polymers or surface active micelles combined with a functionalized core for applications such as drug delivery, imaging, …

As already mentioned, the chain-end functionalization is difficult to perform and especially for polymers prepared by NMP. Rizzardo(*xxiii*) and Pionteck(*xxiv*) showed that TEMPO is prone to oxidation/reduction reactions to produce hydroxy or ketone functionalized polymers. Hawker(*xxv*) and Braslau(*xxvi*) used a radical trap, either a monomer unable to homopolymerize or a monomer that underwent a fragmentation to produce stable polymer chains.

The nitroxide SG1 as a chain end is more difficult to work with and one of our research topic deals with the ω-functionalization of SG1-based polymers. Preliminary studies to extrapolate the oxidation/reduction methods to the SG1 end-group were non conclusive and only the starting polymers were recovered.(*xxvii*) Polymers bearing hydroxy group are nevertheless of high interest for the preparation of multisegmented polymers for example. Recently, we proposed new radical pathways to produce end functional polymers starting from SG1-based polymers.(*xii*) In particular hydroxy-functional polystyrenes could be prepared easily by two different pathways: an exchange with TEMPO nitroxide followed by a Zn/AcOH reduction or by a direct radical hydroxylation methodology (Scheme 12).

Downloaded by OHIO STATE UNIV LIBRARIES on June 26, 2012 | http://pubs.acs.org
Publication Date: August 13, 2009 | doi: 10.1021/bk-2009-1024.ch016

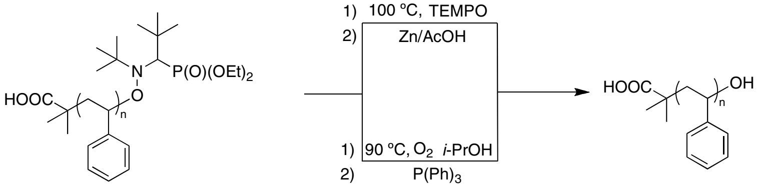

*Scheme 12. Radical chain-end functionalization of SG1-based polystyrenes.*

Among the different reactive groups that could be useful to introduce at polymer chain end, the ketone moiety is a convenient functional group for biological applications. Many authors used this functional group to perform ligation reactions in order to attach compounds of interest to saccharides on cell surfaces for instance.([xxviii])

To replace the SG1 moiety by a ketone function, we first performed a nitroxide exchange with TEMPO on the polymer-SG1 chain, followed by an oxidation of the obtained macroalkoxyamine in presence of *meta*-chloroperbenzoic acid (*m*CPBA) as described by Pionteck (Scheme 13).(*xxiv)*

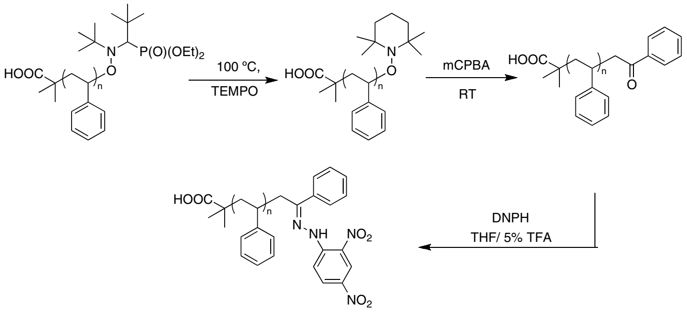

*Scheme 13. Synthesis of a polystyrene – DNPH conjugate.*

As previously described, the exchange between TEMPO and SG1 was carried out at 100 ºC with two equivalents of TEMPO. This reaction was quantitative as demonstrated by Electron Spin Resonance (ESR) and Liquid Chromatography at the Critical condition (LC-CC). We showed previously that in pure dimethylformamide (DMF) at temperature above 70 ºC, polystyrene could be eluted at the critical conditions and in that case functional polymers could be separated.([xxix]) This technique was also used here to follow the chain-end chemical transformations and the chromatograms obtained after injection of PS-SG1, PS-TEMPO and PS-ketone are presented in Figure 2.

Downloaded by OHIO STATE UNIV LIBRARIES on June 26, 2012 | http://pubs.acs.org
Publication Date: August 13, 2009 | doi: 10.1021/bk-2009-1024.ch016

Downloaded by OHIO STATE UNIV LIBRARIES on June 26, 2012 | http://pubs.acs.org
Publication Date: August 13, 2009 | doi: 10.1021/bk-2009-1024.ch016

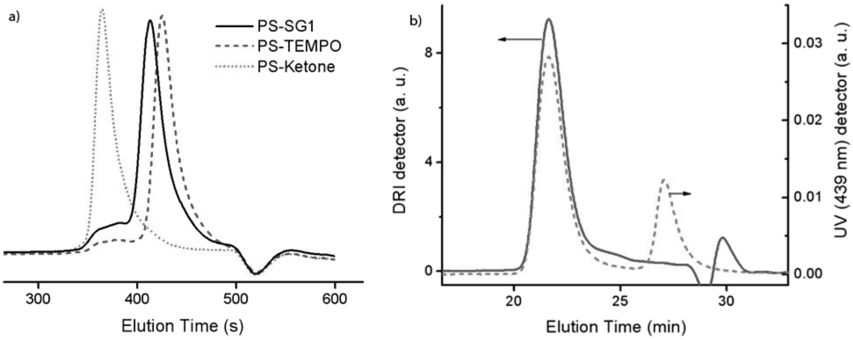

*Figure 2.a) LC-CC Chromatogram (DMF, 82.5°C, C18 nucleodur columns) of the exchange/oxidation reaction. b) Comparison between DRI and UV (439 nm) detection for the PS-DNPH conjugate.*

We then prepared a polymer conjugate using the reactivity of the obtained ω ketone chain-end functionalized polymer.

Braslau *et al.*(*xxvi*) investigated the reactivity of the ketone on the polymer terminus by derivatization reaction with 2,4-dinitrophenylhydrazine (DNPH). This method is well studied, and the preparation of hydrazones is not difficult to perform. 2,4-Dinitrophenylhydrazones have intense molar absorptivities at 439 nm, which provides a method of quantification of functionalized polymer endgroup through UV-visible spectroscopy. The coupling between DNPH and the PS-ketone was then performed using the procedure of Braslau and monitored by LC-CC and dual detection (DRI and 439 nm UV) SEC. The quantitative shift of the LC-CC chromatograms and the overlay of the two detectors response proved the good efficiency of this multi-steps reaction and a quantitative production of PS-DNPH conjugate.

The use of *ω*-functionalized polymers to create block copolymer will be investigated in a forthcoming article.

# Conclusion

The aim of this article was to illustrate the preparation of telechelic polymers using the BlocBuilder® technology. Two strategies to introduce functionality at the α position were developed: the 1,2 intermolecular radical addition of BlocBuilder® on activated olefins and the coupling reaction *via* the BlocBuilder® N-succinimidyl activated ester. Using the coupling reaction with amino compounds, we were then able to prepare conveniently conjugates with aminoethanol, block copolymers with PPO and functionalized silica nanoparticles. The 1,2 intermolecular radical addition allowed the preparation of other functionalized initiator/control agent such as water soluble or glucosilated alkoxyamines. The *ω*-functionalization was also investigated to develop a tool to prepare reactive building blocks, enhancing the range of complex macromolecular architecture. We showed that the quantitative introduction of a ketone group by nitroxide exchange followed by oxidation of the TEMPO moiety was possible. A conjugate with a hydrazone linkage was then prepared.

## Acknowledgments

Authors would like to thank Arkema, the University of Provence and the CNRS for financial support. Dr. Sarah Querelle and Pr. Andre Deratani from the Institut Européen des Membranes of Montpellier (France) are acknowledged for the PEI synthesis.

Downloaded by OHIO STATE UNIV LIBRARIES on June 26, 2012 | http://pubs.acs.org
Publication Date: August 13, 2009 | doi: 10.1021/bk-2009-1024.ch016

## References

---

[i] Braunecker, W. A.; Matyjaszewski, K. *Prog. Pol. Sci.* **2007**, 32, 93-146.

[ii] Bernaerts, K. V.; Du Prez, F. E. *Prog. Pol. Sci.* **2006**, 31, 671-722.

[iii] Tezuka, Y.; Oike, H. *Prog. Pol. Sci.* **2002**, 27, 1069-1122.

[iv] a) Finet, J.-P.; Le Moigne, F.; Gnanou, Y.; Nicol, P.; Grimaldi, S.; Plechot, N.; Tordo, P. 1996, Int PCT WO 96/24620 b) Benoit, D.; Grimaldi, G.; Robin, S.; Finet, J.-P.; Tordo, P.; Gnanou, Y. *J. Am. Chem. Soc.* **2000**, 122, 5929-5939.

[v] Chapter 9 Living Radical Polymerization in The Chemistry of Free Radical Polymerization 2nd Edn., Moad, G.; Solomon, D. H.; Elsevier: Amsterdam, 2006.

[vi] Gigmes, D.; Marque, S.; Guerret, O.; Couturier, J.-L.; Chauvin, F.; Dufils, P.-E.; Bertin, D.; Tordo, P. WO Patent 2004, 2004/014926.

[vii] Chauvin, F.; Dufils, P. E.; Gigmes, D.; Guillaneuf, Y.; Marque, S. R. A.; Tordo, P.; Bertin, D. *Macromolecules* **2006**, 39, 5238-5250.

[viii] Charleux, B.; Nicolas, J. *Polymer* **2007**, 48, 5813-5833.

[ix] Perrier, S.; Takolpuckdee, P.; Mars, C. A. *Macromolecules* **2005**, 38, 2033-2036.

[x] Vinas, J.; Chagneux, N.; Gigmes, D.; Trimaille, T.; Favier, A.; Bertin, D. *Polymer* **2008**, 49, 3639-3647.

[xi] Dufils, P. E.; Chagneux, N.; Gigmes, D.; Trimaille, T.; Marque, S. R. A.; Bertin, D.; Tordo, P. *Polymer* **2007**, 48, 5219-5225.

[xii] Guillaneuf, Y.; Dufils, P. E.; Autissier, L.; Rollet, M.; Gigmes, D.; Bertin D. *Macromolecules submitted.*

[xiii] Klein, J.; Herzog, D. *Makromol. Chem.* **1987**, 188, 1217-1232.

[xiv] Beaudoin, E.; Dufils, P. E.; Gigmes, D.; Marque, S.; Petit, C.; Tordo, P.; Bertin, D. *Polymer* **2006**, 47, 98-106.

[xv] a) Nguyen, H. A.; Marechal, E. *J. Macromol. Sci. –Rev. Macromol. Chem. Phys.* **1988**, C28, 187-291. b) Jerome, R.; Henrioullegranville, M.; Boutevin, B.; Robin, J. J. *Prog. Pol. Sci.* **1991**, 16, 837-906.

---

[xvi] Montalbetti, C. A. G. N.; Falque, V. *Tetrahedron* **2005**, 61, 10827-10852.

[xvii] Theato, P. *J. Pol. Sci. Part A: Pol. Chem.* **2008**, 46, 6677-6687.

[xviii] Bartholome, C.; Beyou, E.; Bourgeat-Lami, E.; Chaumont, P.; Zydowicz, N. *Macromolecules* **2003**, 36, 7946-7952.

[xix] Blomberg, S.; Ostberg, S.; Harth, E.; Bosman, A. W.; Van Horn, B.; Hawker, C. J. *J. Polym. Sci: Part A: Polym. Chem*. **2002**, 40, 1309-1320.

[xx] Persello, J. 2000 Int. PCT WO 00/69976.

[xxi] Studer, A. *Chem. Soc. Rev*. **2004**, 33, 267-273.

[xxii] a) Johnson, J. A.; Finn, M. G.; Koberrstein, J. T.; Turro, N. J. *Macromol. Rapid Commun*. **2008**, 29, 1052-1072. b) Nicolas, J.; Mantovani, G.; Haddleton, D. M. *Macromol. Rapid Commun*. **2007**, 28, 1083-1111.

[xxiii] Solomon, D. H.; Rizzardo, E.; Cacioli, P. *US Patent* **1985**, 4,581,429.

[xxiv] Malz, H.; Komber, H.; Voigt, D.; Pionteck, J. *Macromol. Chem. Phys.* **1998**, 199, 583-588.

[xxv] Harth, E.; Hawker, C. J.; Fan, W.; Waymouth, R. M. *Macromolecules* **2001**, 34, 3856-3862.

[xxvi] Chau, W.; Turner, R.; Braslau, R. *React. Funct. Polym*. **2008**, 68, 396-405.

[xxvii] Arkema *Personal communication*.

[xxviii] Hang, H.C.; Bertozzi, C.R. *Acc. Chem. Res.* **2001**, 34, 727.

[xxix] Petit, C.; Luneau, B.; Beaudoin, E.; Gigmes, D.; Bertin, D. *J. Chromatogr. A* **2007**, 1163, 128-137.

Downloaded by OHIO STATE UNIV LIBRARIES on June 26, 2012 | http://pubs.acs.org
Publication Date: August 13, 2009 | doi: 10.1021/bk-2009-1024.ch016

Downloaded by UNIV OF DELAWARE MORRIS LIB on June 27, 2012 | http://pubs.acs.org
Publication Date: August 13, 2009 | doi: 10.1021/bk-2009-1024.ch017

## Chapter 17

# Bioconjugates of polymers and sequence-defined peptides by reversible addition fragmentation chain transfer radical polymerization

**Hans G. Börner**

**Max Planck Institute of Colloids and Interfaces, Colloid Department, MPI KGF Golm, 14424 Potsdam, Germany**
**hans.boerner@mpikg.mpg.de**

A synthesis platform is described to access defined peptide-polymer conjugates by reversible addition fragmentation chain transfer polymerization (RAFT) routes. Different strategies are summarized to introduce a chain transfer agent (CTA) to a supported peptide, yielding peptide-CTAs. The approaches rely on dithioesters or trithiocarbonates as CTAs. Particularly the latter were evidenced to be robust against nucleophiles. Kinetic investigations are presented, revealing that both peptide-CTA types control the polymerization of various monomers, effectively. Thus, RAFT allows for the access of a broad range of peptide-polymer conjugates to design bio-relevant materials and functional polymer systems.

In Controlled/Living Radical Polymerization: Progress in RAFT, DT, NMP & OMRP; Matyjaszewski, K.;
ACS Symposium Series; American Chemical Society: Washington, DC, 2009.

# Introduction

The combination of monomer-sequence defined peptides and common synthetic polymers proved to result in an interesting class of (multi)functional block copolymers.(1-5) These bioconjugates are referred to as peptide-polymer conjugates.(6) Prospectively they are of importance for biomedical applications such as drug or DNA delivery, and bio-host systems, but also for realizing functional nanostructures, or nanoelectronics.(7-9)

Peptide-polymer conjugates exhibit significantly different properties compared to established amphiphilic or double hydrophilic block copolymers. Most evident differences result from the monodisperse character of the peptide segment. The defined amino acid sequence of a peptide allows to encode specific information into the peptide-polymer conjugates.(10) Recent work demonstrated that the microstructure formation of peptide-polymer conjugates could be programmed by predefining the self-assembly properties of the peptide segments. Besides the utilization of α-helical, coiled-coil, or elastin organization motifs,(11, 12) peptide segments that exhibit high propensities to adopt the β-sheet secondary structure have proved to be highly suitable. Depending on the type of peptide-organizer and the amino acid sequence, anisotropic (nano)objects such as superhelical fibrils, planar nanotapes, nanotubes or flat macrotapes could be realized.(13-19) Moreover, responsiveness of structural transitions to external stimuli, molecular recognition and active interfacing to both inorganic, or organic surfaces could be realized with bioconjugates.(12, 20-24) The diversity in structure, functionality and function makes the peptide-guided self-assembly of peptide-polymer conjugates to a versatile biomimetic route, which certainly enlarges the structural and functional space available for polymer science.(25) Besides programming of microstructure, biological activity can be integrated, making peptide-polymer conjugates versatile tools for designing bioactive materials, constituting active interfaces between synthetic materials and biology.(26, 27)

The combination of multifunctional bioorganic segments *e. g.* peptide and synthetic polymer blocks made the development of novel synthetic strategies mandatory. Ideally, the developed routes should envelope a wide range of different synthetic polymers with adjustable molecular weights and low polydispersity indices. Moreover, suggested routes should proceed independently of the peptide primary structure. This requires strategies that are highly sequence (regio) selective and compatible to the multifunctional character of peptides. In order to provide bioconjugates for materials science applications, the introduction of a wide range of organo-soluble synthetic polymers with diverse functionalities and functions has to be addressed and multi-gram scale synthesis have to be realized, without the usually required chromatographic purification steps.

Two different synthetic approaches to integrate sequence-controlled polypeptides into synthetic polymers are described (*cf.* Figure 1). These comprise (1) the direct coupling (17, 28, 29) of peptides to synthetic polymers, and (2) the polymerization from a peptidic macro-"initiator". Due to a decrease in chain end-group reactivity with increasing molecular weight of the polymer or the peptide, the direct coupling approach becomes less suitable for high

Downloaded by UNIV OF DELAWARE MORRIS LIB on June 27, 2012 | http://pubs.acs.org
Publication Date: August 13, 2009 | doi: 10.1021/bk-2009-1024.ch017

molecular weight bioconjugates.(20) This inherent difficulty could be detoured by the utilization of the polymerization approach, applying the “grafting from” method.

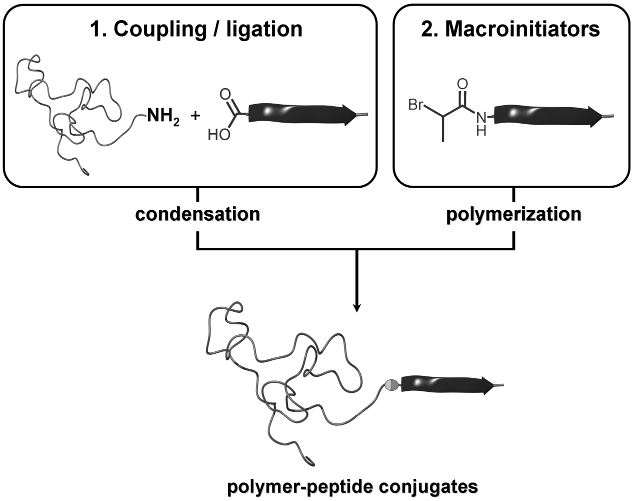

*Figure 1. Schematic illustration of the principal synthesis strategies to AB-block structured polymer-peptide conjugates.*

Controlled radical polymerization (CRP) (30-32) techniques seem to be most suited for the synthesis of the bioconjugates. Due to the control over molecular weight and molecular weight distribution as well as the high tolerance to diverse functional groups, CRP methods are promising for the syntheses of well-defined conjugates with a broad variety of compositions, topologies and architectures.(33) The three major methods of CRP proved to be successfully applicable for the synthesis of peptide-polymer conjugates. The utilization of sequence-defined polypeptides as macroinitiators for CRP methods have been described,(34-36) including nitroxide-mediated radical polymerization (NMP (37)) and atom transfer radical polymerization (ATRP (38, 39)). Recently, the reversible addition-fragmentation chain transfer radical polymerization (RAFT (33, 40)) could be applied, successfully, too.

Nitroxide mediated polymerization (NMP) is considered as the first, widespread CRP method and Wooley *et al.* investigated alkoxyamine-functionalized peptides as macroinitiators for NMP.(41) The strategy involved the solid-phase supported introduction of a functional alkoxyamine moiety to the terminal amino group of a supported peptide. The resulting peptide initiator stared and controlled a solid-phase supported NMP. Two different triblock copolymers were accessed, combining an amphiphilic block copolymer with a functional peptide. After polymerization, the ABC-bioconjugates were liberated from the support, suggesting that NMP is a promising tool for bioconjugation.

ATRP is considered as the most studied and applied method of CRP.(38, 42, 43) Therefore, peptide ATRP-macroinitiators have been applied, proving

Downloaded by UNIV OF DELAWARE MORRIS LIB on June 27, 2012 | http://pubs.acs.org
Publication Date: August 13, 2009 | doi: 10.1021/bk-2009-1024.ch017

that both solid-phase supported polymerization and homogeneous polymerization in solution can be applied to access well-defined peptide-polymer conjugates. Studies of the polymerization kinetics reveal interactions between the catalyst and the peptide. However, they were not critical in terms of synthesis control of the desired polymer and hence ATRP became a powerful tool to integrate peptides into a variety of different polymers or copolymers.

In this chapter, the recent developments in the "grafting from" polymerization approaches using the RAFT technique to obtain peptide-polymer conjugates are summarized. To keep focus, we will not discuss related conjugation strategies as they have been addressed by recent reviews.(6, 44)

## Results and Discussions

Analyzing the advantages but also the method immanent difficulties of the other CRP methods, the reversible addition fragmentation transfer radical polymerization (RAFT) has been investigated as a promising tool to access peptide-polymer conjugates. The RAFT radical polymerization technique proved to be a versatile CRP tool.(45-47) Particularly the tolerance against many functional groups, the absence of metal catalysts and the close relation of the RAFT process to conventional free radical polymerizations are advantages for the synthesis of bioconjugates.

### Synthesis of the peptide macrotransfer agents (Peptide-CTAs)

The first amide-based RAFT chain transfer agents (CTAs) have been described by McCormick *et al.* followed by Perrier *et al.*, demonstrating that amidic CTAs can mediate the RAFT polymerization, effectively.(48-50) Taking this into account, the RAFT polymerization technique could be extended to synthesize peptide-polymer conjugates.(15, 51)

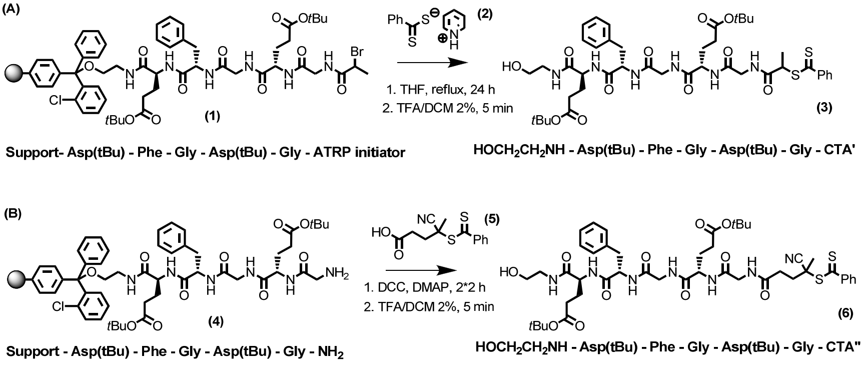
(A)
(1)
(2)
1. THF, reflux, 24 h
2. TFA/DCM 2%, 5 min
(3)
Support- Asp(tBu) - Phe - Gly - Asp(tBu) - Gly - ATRP initiator
HOCH$_2$CH$_2$NH - Asp(tBu) - Phe - Gly - Asp(tBu) - Gly - CTA'
(B)
(4)
(5)
1. DCC, DMAP, 2*2 h
2. TFA/DCM 2%, 5 min
(6)
Support - Asp(tBu) - Phe - Gly - Asp(tBu) - Gly - NH$_2$
HOCH$_2$CH$_2$NH - Asp(tBu) - Phe - Gly - Asp(tBu) - Gly - CTA"

*Scheme 1. Synthetic routes to peptide chain transfer agents (3, 6) either via functionality transformation of a peptide ATRP-macroinitiator into a peptide macro-CTA (route A)) or by coupling of a carboxylate functionalized CTA (5) to*

Downloaded by UNIV OF DELAWARE MORRIS LIB on June 27, 2012 | http://pubs.acs.org
Publication Date: August 13, 2009 | doi: 10.1021/bk-2009-1024.ch017

*the N-terminus of a supported peptide (route B); (peptide ATRP-macroinitiator attached to a pS-(2-Cl-trityl) resin as solid support (1), supported peptide (4) and peptide-based CTAs after liberation from the support (3, 6)).*

Peptide-based CTAs can be obtained by solid-phase supported synthesis, which makes the usually required chromatographic purification steps obsolete. This is an important criterion, significantly improving the flexibility of the synthesis route. While purification of peptide-CTAs via high-pressure liquid chromatography (HPLC) is certainly possible, such a purification step would require adaptation to the peptide sequence, making it time and material consuming. Two different synthesis pathways have been established, providing (*i.*) peptide-dithiobenzoate CTAs (51) and (*ii.*) peptide-trithiocarbonate CTAs(26) in almost quantitative yields (*cf.* Scheme 1 and 2). Dithiobenzoate CTAs have been accepted as rather universal RAFT transfer agents, mediating the polymerization of a broad variety of functional monomers, effectively. Peptide-dithiobenzoate CTAs can be accessed by functionality transformation of a resin-bound peptide ATRP macroinitiator(36) (Scheme 1, route a).(51)

The alternative approach involves the coupling of 4-cyano-4-((thiobenzoyl)sulfanyl)pentane carboxylic acid to the N-terminal amine group of a supported peptide(Scheme 1 b). This approach would allow the regio-selective introduction of the transfer group either at the N-terminal amine group or at a specific sequence-position by the modification of an ε-amine group of a lysine residue.(51) However, besides the peptide chain transfer agent **6** the formation of a byproduct was observed. This resulted from the nucleophilic attack of the peptide amine terminus on the dithioester, leading to a thioamide structure. The thioamide was present in significant amounts (~24%), but was not found to interfere with a subsequent CRP process (data not shown).(51) Nevertheless, the method could be applied to the coupling of RAFT agents via hydroxyl moieties, *e. g.* to side chain functionalities of serine or threonine residues, where the particular side reaction is not expected. This would lead to a hydrolytically labile ester-linkage between the peptide and the polymer that might be interesting for the predefined degradation of peptide-polymer conjugates or for the liberation of peptide segments as bio-functional units in *e. g.* medical applications.

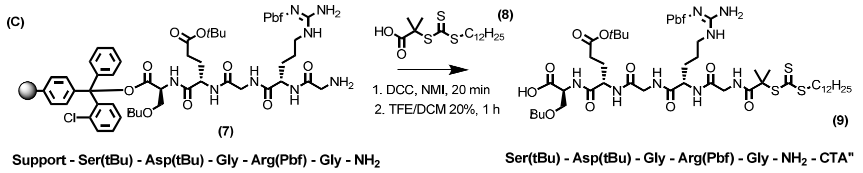
(C)
(7)
(8)
(9)
1. DCC, NMI, 20 min
2. TFE/DCM 20%, 1 h
Support - Ser(tBu) - Asp(tBu) - Gly - Arg(Pbf) - Gly - NH2
Ser(tBu) - Asp(tBu) - Gly - Arg(Pbf) - Gly - NH2 - CTA"

*Scheme 2. Synthesis route to peptide chain transfer agent (9) by coupling of carboxylate functionalized CTA (8) to the N-terminus of a supported peptide (route C); (supported peptide (7) and peptide-based CTAs after liberation from the support (9)).*

Downloaded by UNIV OF DELAWARE MORRIS LIB on June 27, 2012 | http://pubs.acs.org
Publication Date: August 13, 2009 | doi: 10.1021/bk-2009-1024.ch017

Despite the advantages and potentials of the RAFT methodology to access bioconjugates, the synthesis protocol for the introduction of the dithiobenzoate CTA group to a supported peptide could not be automated and hence remains relatively time-consuming. Therefore, a convenient and fully-automated one-step approach was developed to synthesize peptide CTAs, while strongly reducing the synthetic efforts and the costs.(26) Particularly this strategy is of advantage if large and/or multifunctional peptide CTAs are synthesized, because longer treatments at increased temperatures and chromatographic purification steps are not required. This enables the straightforward synthesis of polymers with multifunctional and potentially bio-functional peptide segments.

The strategy does not rely on standard dithioester-based CTAs, but on trithiocarbonates (*cf.* Scheme 2 route C). The latter have been evidenced to exhibit a higher tolerance against nucleophiles than the dithiobenzoate analoges.(52, 53) Additionally, while the synthesis of RAFT CTAs often require multi-step reactions and chromatographic purifications, the S-1-dodecyl-S'-(R,R'-dimethyl-R''-acetic acid) trithiocarbonate (Scheme 2 (8)) is readily accessible from commodity compounds (acetone, chloroform, carbon disulfide and 1-dodecanethiol) in a one pot reaction. The ease of synthesis, the absence of further purification steps and the cost-effective large scale accessibility (100 g scales) makes this CTA an appealing candidate for the design of peptide-based CTAs. The S-1-dodecyl-S'-(R,R'-dimethyl-R''-acetic acid) could be treated like a Fmoc amino acid derivative and was coupled to the N-terminus of a supported peptide in a fully automated manner. Substitution side products like *e. g.* dithiourea (R-SC(S)NH-R') were practically negligible, as they were limited to ~0.3% (HPLC), indicating the high tolerance of the trithiocarbonate functionality against nucleophiles.

Two solid-phase supported synthesis routes to peptide-based CTAs have been established in the recent years, allowing for the quantitative introduction of either a dithiobenzoate or a trithiocarbonate CTA moiety. While the latter proved to be easily accessible in larger scale and robust towards nucleophiles, the first is considered as a rather universal CTA, allowing the mediation of the polymerization of a broad range of different monomers. However, the trithiocarbonate gets progressively more popular as evidenced by an increasing number of publications studying and applying trithiocarbonates.

## The RAFT polymerization

An inherent difficulty of ATRP, involving oligopeptide structures is the interaction between the copper catalyst and the peptide. These interactions depend strongly on the length and on the amino acid sequence of the oligopeptide, requiring adaptation of the polymerization conditions on each peptide system. Such interactions might be successfully reduced or even completely suppressed by adjusting the ligand sphere of the ATRP catalyst. This however, makes further studies mandatory.

Considering the fact, that RAFT radical polymerization proceeds without the presence of a metal catalyst, it has been proven to be a valuable tool to access well-defined polymer-peptide conjugates.(51) The RAFT process allows

Downloaded by UNIV OF DELAWARE MORRIS LIB on June 27, 2012 | http://pubs.acs.org
Publication Date: August 13, 2009 | doi: 10.1021/bk-2009-1024.ch017

Downloaded by UNIV OF DELAWARE MORRIS LIB on June 27, 2012 | http://pubs.acs.org
Publication Date: August 13, 2009 | doi: 10.1021/bk-2009-1024.ch017

for the controlled polymerization of a broad variety of monomers and is a facile method because the involved components are not air or moisture sensitive. Hence, the components can be straightforward dissolved and deoxygenated prior to the polymerization. Moreover, racemization and thermal degradation is expected to be limited because the RAFT polymerizations are performed at moderate reaction temperatures or even at room temperature and basic conditions, that might cause racemization, have to be anyhow avoided.

The poly(*n*-butyl acrylate)-*block*-polypeptide was synthesized to examine the RAFT radical polymerization of *n*BA.(51) The macrotransfer agent **3** was used homogeneously in solution for CRP of *n*-butyl acrylate with 20 mol%, but also 5 mol% AIBN as source of the primary radicals.

The polymerization proceeds in a controlled manner, providing well-defined peptide-polymer conjugates with molecular weights that increase linearly with monomer consumption and polydispersities remain low during the process ($M_w/M_n \approx 1.1$) (Figure 2 b). Moreover, the semi-logarithmic plot shows a first order kinetics after a retardation period of about 8 hours (Figure 2 a). Retardation times should be taken into consideration for controlled polymerizations, especially when low molecular weight polymers are targeted.

A comparable retardation period was observed when only 5 mol% of AIBN was used, excluding the possibility that potential impurities retard the polymerization of *n*BA with **3**. The slope of the first order kinetics plot was, expectedly, 4 times smaller (dashed line in Figure 2b), indicating that the overall rate of polymerization directly correlates to the amount of formed radicals.

Downloaded by UNIV OF DELAWARE MORRIS LIB on June 27, 2012 | http://pubs.acs.org
Publication Date: August 13, 2009 | doi: 10.1021/bk-2009-1024.ch017

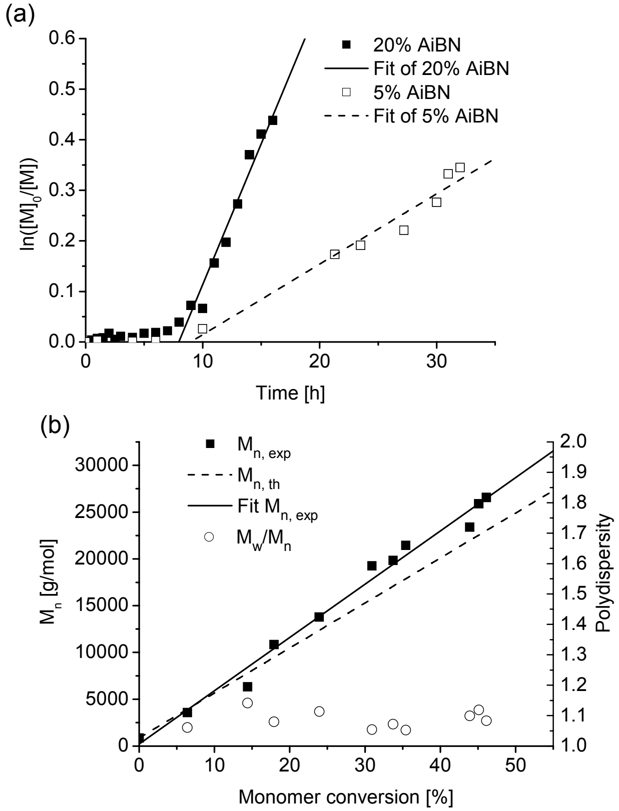

*Figure 2. RAFT polymerization of nBA controlled by* ***6*** *at 60 °C: first-order kinetic plot ln($[M]_0$/[M]) vs reaction time (a) and $M_{n,\ GPC}$ vs conversion (b) (Conditions: $[nBA]_0/[\mathbf{3}]_0/[AiBN]_0$ = 375/1/0.2, DMF = 60 vol %.)*

To confirm the incorporation of the peptide segment into the polymer, a low molecular weight conjugate with $M_{\mathrm{n,NMR}}$ = 4.6 kDa ($\mathrm{DP}_{\mathrm{n,NMR}}$ = 29) was synthesized and precipitated multiple times in MeOH/$H_2O$. Since this is a good solvent mixture for the peptide CTA (3), the absence of peptides that are not bound to a polymer can be ensured. The formation of the poly(*n*-butyl acrylate)-*block*-peptide conjugate was conclusively demonstrated by $^1$H NMR spectroscopy, showing the characteristic resonances for the protons of the peptide, the p*n*BA segment, as well as the RAFT moiety. Since both the RAFT and peptide end-group functionalities were quantified in a ratio 1:1, formation of the dimerization product, resulting from termination via radical coupling can be excluded within the experimental error of the analytical method. Since the RAFT moiety remains quantitatively at the end of the polymer chain of the isolated conjugates, the polymer chain-end can be modified by further block extension or functionality transformation. This may allow access of polymers with advanced architectures.

Trithiocarbonates proved to be very efficient CTAs for controlling the polymerization of various monomers. Recent reports described the successful utilization of the S-1-dodecyl-S'-(R,R'-dimethyl-R''-acetic acid) or related derivatives to polymerize *e. g.* St,(54) MMA,(45) *n*BA,(55) or NIPAM (53). Taking this in account, the tritiocarbonate peptide-CTA was evaluated to mediate the homogeneous polymerization of *n*BA in solution. After liberation of the peptide-CTA from the support, **9** could be isolated by simple precipitation and was directly applied in the polymerization reaction. The *n*BA polymerization was performed under highly dilute conditions in N,N-dimethylformamide at 65 °C to prevent peptide aggregation, which might result in an increased rate of termination. 10 mol% AIBN was used as a source of primary radicals and the reaction kinetics could be followed by GPC and $^1$H NMR. As shown in Figure 3 (b), the semi logarithmic plot of conversion *versus* time was linear. Moreover, the polydispersity index $M_w/M_n$ of the formed bioconjugate remains low at ~1.1 throughout the process of polymerization. The molecular weight $M_n$ increased linearly with monomer conversion indicating that the polymerization proceeds in a controlled manner. Hence the RAFT polymerization of *n*BA process was efficiently mediated by **9**, providing peptide-polymer conjugates with adjustable molecular weight and low polydispersity index.

Downloaded by UNIV OF DELAWARE MORRIS LIB on June 27, 2012 | http://pubs.acs.org
Publication Date: August 13, 2009 | doi: 10.1021/bk-2009-1024.ch017

Downloaded by UNIV OF DELAWARE MORRIS LIB on June 27, 2012 | http://pubs.acs.org
Publication Date: August 13, 2009 | doi: 10.1021/bk-2009-1024.ch017

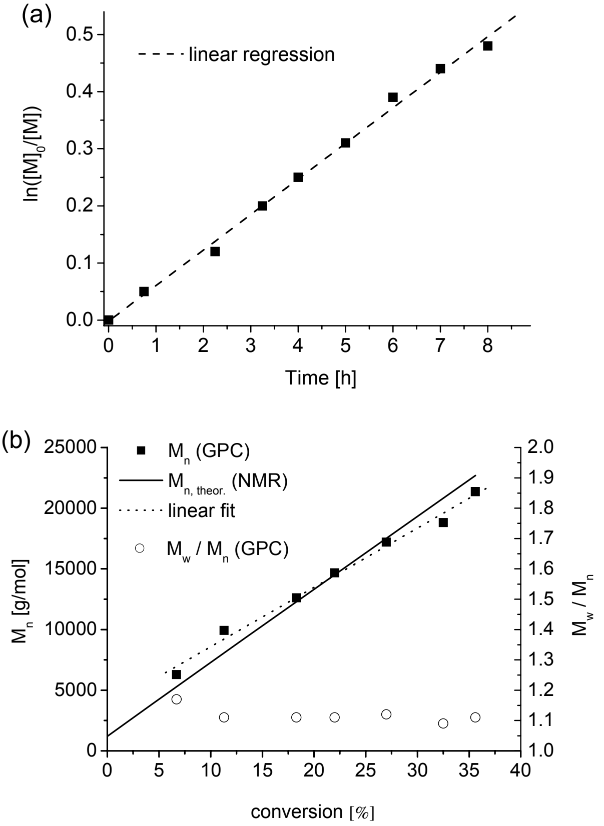

*Figure 3. RAFT polymerization of nBA controlled by* ***XX*** *at 65 °C: $M_{n,\ GPC}$ vs conversion (a) and first-order kinetic plot ln($[M]_0/[M]$) vs reaction time (b) (Conditions: $[nBA]_0/[\mathbf{9}]_0/[AIBN]_0$ = 470/1/0.1, DMF = 90 vol.%).*

After the initial report of the feasibility of a peptide-based CTA to mediate RAFT polymerization processes, RAFT became rapidly a valuable tool to design peptide-polymer conjugates and protein-polymer conjugates. Several groups contributed to this field, significantly expanding the scope of the process.

Börner *et al.* exploited the methodology to realize elaborated functional systems by describing a straightforward method to realize *e. g.* thermo responsive surface modifications with biological activity or interfacial positioning of functional peptide segments in micellar assemblies of ABC-peptide-polymer conjugates.(26, 56) Cameron and coworkers demonstrated first the applicability of the “grafting through” route by polymerizing elastin-based peptide-macromonomers.(57) As a result well-defined graft copolymers with pendent elastin side chains have been obtained. The peptide grafts result in an interesting lower critical solution temperature (LCST) behavior, where the critical temperature was adjustable by the pH-value. Bulmus and Davis, reported the first *in situ* synthesis of protein-polymer conjugates via RAFT.(58) They generated well-defined bioconjugates in a one-step approach, by introducing a water soluble CTA to bovine serum albumin by the Z-group anchor and used this protein based CTA to control the polymerization of NIPAM. Sumerlin *et al.* expanded this *in situ* approach, successfully, by demonstration the value of an "R-group" anchored CTA.(59) A thrithiocarbonete CTA was coupled to a model protein by applying a straightforward thiol-maleimide immobilization. The resulting protein based CTA shows effective control over a NIPAM polymerization at room temperature that provides well-controlled protein conjugates with interesting catalytic activity.

## Conclusion

It was shown that well-defined bioconjugates comprising sequence-defined peptides and synthetic polymers could be obtained by utilizing RAFT radical polymerization. Two different strategies were evaluated for the synthesis of peptide-based chain transfer agents (CTAs); namely, (*i.*) the transformation of an ATRP initiator moiety of a supported peptide ATRP-macroinitiator into a peptide-CTA functionality and (*ii.*) the coupling of a carboxylate functionalized CTA to the N-terminal amino group of a supported peptide. The functionality transformation of a resin-bound oligopeptide ATRP macroinitiator into an oligopeptide transfer agent proceeds in a clean manner. However, it requires increased temperature and longer reaction times. As an alternative, the coupling of the carboxylic acid functionalized dithiobenzoate based CTA to the supported peptide was accompanied by the formation of a thioamide side product that could not be significantly suppressed. However, the coupling of the more robust carboxylic acid functionalized trithiocarbonate CTA preserves the simplicity of the method by not suffering from side reactions, making it highly suited for the generation of peptide-CTAs.

The RAFT radical polymerization of *n*-butyl acrylate in solution using either the dithiobenzoate or the trithiocarbonate peptide-CTAs show an efficient control of the polymerization processes. In both cases, peptide-polymer conjugates could be accessed that exhibit a narrow molecular weight distribution ($M_w/M_n \approx 1.1$) and controllable molecular weights. The presented polymerization kinetics indicated a highly controlled polymerization process. Moreover, the peptide segments were quantitatively incorporated into the bioconjugates and the CTA groups remain at the ω-end of the polymer chain after isolation of the conjugates. This allows further modification of the conjugates by block extensions or functionality transformation.

It is expected, that the highly robust trithiocarbonates will be exploited further in the synthesis of complex bioconjugates, integrating functional peptides, proteins and sequence-defined oligosaccharides to the established world of polymer and material sciences. The RAFT synthesis route provides straightforward and inexpensive access to even complex bioconjugates and thus has the potential to be developed to a platform technology. This might drive research in various fields such as biomedicine, pharmaceutical technology, nanomaterials e.g. ceramics, membrane research or nanoelectronics.

Downloaded by UNIV OF DELAWARE MORRIS LIB on June 27, 2012 | http://pubs.acs.org
Publication Date: August 13, 2009 | doi: 10.1021/bk-2009-1024.ch017

## Acknowledgements

J. Hentschel, K. Bleek, M. ten Cate, H. Rettig, E. Krause, K. Ostwald, J. Brandt, M. Gräwert, O. Niemeyer and Erich C. are thanked for their contributions to this work. HGB would like to thank M. Antonietti for his continuous support and helpful discussions. Financial support was received from the German Research Foundation through the Emmy Noether Program (BO 1762/2-1-3) and the Max Planck Society.

Downloaded by UNIV OF DELAWARE MORRIS LIB on June 27, 2012 | http://pubs.acs.org
Publication Date: August 13, 2009 | doi: 10.1021/bk-2009-1024.ch017

## References

1. Börner, H. G.; Schlaad, H. *Soft Matter* **2007,** *3*, 394.
2. Nicolas, J.; Mantovani, G.; Haddleton, D. M. *Macromol. Rapid Commun.* **2007,** *28*, 1083.
3. Klok, H.-A. *J. Polym. Sci. Part A: Polym. Chem.* **2005,** *43*, 1.
4. van Hest, J. C. M.; Tirrell, D. A. *Chem. Commun.* **2001**, 1897.
5. Heredia, K. L.; Maynard, H. D. *Org. Biomol. Chem.* **2007,** *5*, 45.
6. Lutz, J.-F.; Börner, H. G. *Prog. Polym. Sci.* **2008,** *33*, 1.
7. Hartmann, L.; Häfele, S.; Peschka-Suess, R.; Antonietti, M.; Börner, H. G. *Chem. Europ. J.* **2007**, 2025.
8. Vandermeulen, G. W. M.; Tziatzios, C.; Duncan, R.; Klok, H. A. *Macromolecules* **2005,** *38*, 761.
9. Dünne, A. A.; Börner, H. G.; Kukula, H.; Schlaad, H.; Werner, J. A.; Wiegand, S.; Antonietti, M. *Anticancer Res.* **2007,** *27* 3935.
10. Vandermeulen, G. W. M.; Klok, H. A. *Macromol. Biosci.* **2004,** *4*, 383.
11. Schlaad, H.; Kukula, H.; Smarsly, B.; Antonietti, M.; Pakula, T. *Polymer* **2002,** *43*, 5321.
12. Ayres, L.; Vos, M. R. J.; Adams, P.; Shklyarevskiy, I. O.; van Hest, J. C. M. *Macromolecules* **2003,** *36*, 5967.
13. Eckhardt, D.; Groenewolt, M.; Krause, E.; Börner, H. G. *Chem. Commun.* **2005**, 2814.
14. Couet, J.; Jeyaprakash, J. D.; Samuel, S.; Kopyshev, A.; Santer, S.; Biesalski, M. *Angew. Chem. Int. Ed.* **2005,** *44*, 3297.
15. ten Cate, M. G. J.; Severin, N.; Börner, H. G. *Macromolecules* **2006,** *39*, 7831.
16. Couet, J.; Biesalski, M. *Macromolecules* **2006,** *39*, 7258.
17. Hentschel, J.; Krause, E.; Börner, H. G. *J. Am. Chem. Soc.* **2006,** *128*, 7722.
18. Hentschel, J.; Börner, H. G. *J. Am. Chem. Soc.* **2006,** *128*, 14142.
19. Hentschel, J.; ten Cate, M. G. J.; Börner, H. G. *Macromolecules* **2007,** *40*, 9224.
20. Vandermeulen, G. W. M.; Tziatzios, C.; Klok, H. A. *Macromolecules* **2003,** *36*, 4107.

21. Geng, J.; Mantovani, G.; Tao, L.; Nicolas, J.; Chen, G. J.; Wallis, R.; Mitchell, D. A.; Johnson, B. R. G.; Evans, S. D.; Haddleton, D. M. *J. Am. Chem. Soc.* **2007,** *129*, 15156.
22. Kessel, S.; Thomas, A.; Börner, H. G. *Angew. Chem., Int. Ed.* **2007,** *46*, 9023.
23. Ma, Y.; Börner, H. G.; Hartmann, J.; Cölfen, H. *Chem. Eur. J.* **2006,** *12*, 7682.
24. Page, M. G.; Nassif, N.; Börner, H. G.; Antonietti, M.; Cölfen, H. *Cryst. Growth Des.* **2008,** *8*, 1792.
25. Whitesides, G. M. *Small* **2005,** *1*, 172.
26. Hentschel, J.; Bleek, K.; Ernst, O.; Lutz, J.-F.; Börner, H. G. *Macromolecules* **2008,** *41*, 1073.
27. Tugulu, S.; Silacci, P.; Stergiopulos, N.; Klok, H. A. *Biomaterials* **2007,** *28*, 2536.
28. Roberts, M. J.; Bentley, M. D.; Harris, J. M. *Adv. Drug Deliv. Rev.* **2002,** *54*, 459.
29. Rosler, A.; Klok, H. A.; Hamley, I. W.; Castelletto, V.; Mykhaylyk, O. O. *Biomacromolecules* **2003,** *4*, 859.
30. Matyjaszewski, K.; Davis, T. P., *Handbook of Radical Polymerization*. Wiley-Interscience: 2002.
31. Matyjaszewski, K. *Prog. Polym. Sci.* **2005,** *30*, 858.
32. Braunecker, W. A.; Matyjaszewski, K. *Prog. Polym. Sci.* **2007,** *32*, 93.
33. Chiefari, J.; Rizzardo, E., Control of Free-Radical Polymerization by Chain Transfer Methods. In *Handbook of Radical Polymerization*, Matyjaszewski, K.; Davis, T. P., Eds. Wiley-Interscience: 2002; pp 629.
34. Becker, M. L.; Liu, J.; Wooley, K. L. *Biomacromolecules* **2005,** *6*, 220.
35. Mei, Y.; Beers, K. L.; Byrd, H. C. M.; van der Hart, D. L.; Washburn, N. R. *J. Am. Chem. Soc.* **2004,** *126*, 3472.
36. Rettig, H.; Krause, E.; Börner, H. G. *Macromol. Rapid Commun.* **2004,** *25*, 1251.
37. Hawker, C. J.; Bosman, A. W.; Harth, E. *Chem. Rev.* **2001,** *101*, 3661.
38. Matyjaszewski, K.; Xia, J. *Chem. Rev.* **2001,** *101*, 2921.
39. Wang, J. S.; Matyjaszewski, K. *J. Am. Chem. Soc.* **1995,** *117*, 5614.
40. Chiefari, J.; Chong, Y. K.; Ercole, F.; Krstina, J.; Jeffery, J.; Le, T. P. T.; Mayadunne, R. T. A.; Meijs, G. F.; Moad, C. L.; Moad, G.; Rizzardo, E.; Thang, S. H. *Macromolecules* **1998,** *31*, 5559.
41. Becker, M. L.; Liu, J. Q.; Wooley, K. L. *Chem. Commun.* **2003**, 180.
42. Kamigaito, M.; Ando, T.; Sawamoto, M. *Chem. Rev.* **2001,** *101*, 3689.
43. Tsarevsky, N. V.; Matyjaszewski, K. *Chem. Rev.* **2007,** *107*, 2270.
44. van Hest, J. C. M. *Polym. Rev.* **2007,** *47*, 63.
45. Moad, G.; Rizzardo, E.; Thang, S. H. *Aust. J. Chem.* **2005,** *58*, 379.
46. Barner, L.; Davis, T. P.; Stenzel, M. H.; Barner-Kowollik, C. *Macromol. Rapid Commun.* **2007,** *28*, 539.
47. Favier, A.; Charreyre, M. T. *Macromol. Rapid Commun.* **2006,** *27*, 653.
48. Donovan, M. S.; Lowe, A. B.; Sumerlin, B. S.; McCormick, C. L. *Macromolecules* **2002,** *35*, 4123.
49. Takolpuckdee, P.; Mars, C. A.; Perrier, S.; Archibald, S. J. *Macromolecules* **2005,** *38*, 1057.

Downloaded by UNIV OF DELAWARE MORRIS LIB on June 27, 2012 | http://pubs.acs.org
Publication Date: August 13, 2009 | doi: 10.1021/bk-2009-1024.ch017

50. Zhao, Y. L.; Perrier, S. *Chem. Commun.* **2007**, 4294.
51. Ten Cate, M. G. J.; Rettig, H.; Bernhardt, K.; Börner, H. G. *Macromolecules* **2005,** *38*, 10643.
52. Lai, J. T.; Filla, D.; Shea, R. *Macromolecules* **2002,** *35*, 6754.
53. Convertine, A. J.; Ayres, N.; Scales, C. W.; Lowe, A. B.; McCormick, C. L. *Biomacromolecules* **2004,** *5*, 1177.
54. Mahanthappa, M. K.; Bates, F. S.; Hillmyer, M. A. *Macromolecules* **2005,** *38*, 7890.
55. Wang, R.; McCormick, C. L.; Lowe, A. B. *Macromolecules* **2005,** *38*, 9518.
56. ten Cate, M. G. J.; Börner, H. G. *Macromol. Chem. Phys.* **2007,** *208*, 124.
57. Fernandez-Trillo, F.; Dureault, A.; Bayley, J. P. M.; van Hest, J. C. M.; Thies, J. C.; Michon, T.; Weberskirch, R.; Cameron, N. R. *Macromolecules* **2007,** *40*, 6094.
58. Boyer, C.; Bulmus, V.; Liu, J. Q.; Davis, T. P.; Stenzel, M. H.; Barner-Kowollik, C. *J. Am. Chem. Soc.* **2007,** *129*, 7145.
59. De, P.; Li, M.; Gondi, S. R.; Sumerlin, B. S. *J. Am. Chem. Soc.* **2008,** *130*, 11288.

Downloaded by UNIV OF DELAWARE MORRIS LIB on June 27, 2012 | http://pubs.acs.org
Publication Date: August 13, 2009 | doi: 10.1021/bk-2009-1024.ch017

Downloaded by PENNSYLVANIA STATE UNIV on June 26, 2012 | http://pubs.acs.org
Publication Date: August 13, 2009 | doi: 10.1021/bk-2009-1024.ch018

## Chapter 18

# RAFT Polymerization, a Versatile Tool for the Production of Functional Soft Nanoparticles

**Varangkana Jitchum, Hamilton Kakwere, Vincent Ladmiral, Sébastien Perrier***

**Key Centre for Polymers & Colloids**
**School of Chemistry**
**Building F11, Eastern Avenue**
**The University of Sydney**
**NSW 2006, Australia**

Block copolymers showing a hydrophilic and a hydrophobic segment were synthesized via reversible addition fragmentation chain transfer (RAFT) polymerization, and their amphiphilic properties were exploited to generate polymeric micelles in water. The hydrophilic corona was subsequently crosslinked covalently to yield surface functional soft nanoparticles showing hydroxyl groups in the case of poly(ethyl acrylate–*b*–hydroxethyl acrylate) and carboxylic acid groups when using poly(acrylic acid–*b*–isoprene) .

In Controlled/Living Radical Polymerization: Progress in RAFT, DT, NMP & OMRP; Matyjaszewski, K.;
ACS Symposium Series; American Chemical Society: Washington, DC, 2009.

## Introduction

Diblock copolymers are well–known for their abilities to spontaneously assemble into nano-ordered structures. When block copolymers with incompatible blocks are dissolved in a thermodynamically good solvent for one block but bad solvent for the other block, the copolymer chains associate reversibly to form aggregates. Various structures such as spherical, cylindrical 'worm–like' micelles and vesicles have been developed via this approach, for applications in the field of materials science[1,2,3] and bioengineering,[4,5] and in industry, especially for pharmaceutical applications.[6,7] Using block copolymers to produce such nanostructures is a versatile approach, as the nature of the aggregate can be determined by controlling the weight fraction of the hydrophilic block relative to the total copolymer molecular weight.[8,9] This technique has been exploited to produce functional polymeric soft nanoparticles from the self assembly of block copolymers into micelles. However, the micellar structures only exist above the copolymer critical micelle concentration (CMC), and they are not very robust to changes in their environment, thereby limiting their applicability. For example, micelles can easily be destroyed upon variation in concentration, pH, temperature or ionic strength of their environment.[10] An elegant route towards structures stabilization is the crosslinking of the core[11] or the shell[12] of the micelles. Synthesis of shell crosslinked polymeric nanoparticles was pioneered by Wooley,[12] and exploited by several research groups since then.[13] Most routes use living polymerization techniques such as anionic polymerization to produce well defined amphiphilic block copolymers, presenting reactive groups in the block corresponding to the shell of the micelle, or at the chain end of the polymer located at the periphery of the micelle. These reactive groups can react with each other under given conditions, or can be reacted with difunctional small molecules to trigger the desired crosslinking.

The advance in living radical polymerization (LRP) has had a large impact on the design of polymeric nanoparticles, as the aptitude of LRP to proceed in presence of virtually any functionality now allows the design of multifunctional copolymers of controlled structures. The major LRP techniques include atom transfer radical polymerization (ATRP)[14], stable free radical polymerization (SFRP)[15] and reversible addition-fragmentation chain transfer (RAFT) polymerization,[16,17] including the specialized area of aqueous RAFT polymerization.[18] While each of these techniques has its inherent advantages and limitations, the RAFT process is possibly the most versatile system, due to the wide range of functional monomers that can be polymerized without requiring protecting group chemistry, and the mild reaction conditions required for polymerization.[19] Indeed, the process relies on the simple introduction of a small amount of dithioester (chain transfer agent, CTA) in a classic free radical system (monomer + initiator). The transfer of the CTA between growing radical chains, present at very low concentration, and dormant polymer chains, present at higher concentration, will regulate the growth of the molecular weight, and limit the termination reactions.

In here, we show how RAFT polymerization can be used to produce functional amphiphilic block copolymers poly(ethyl acrylate–*b*–hydroxethyl acrylate), P(EA–b–HEA), and poly(acrylic acid–*b*–isoprene), P(tBA–*b*–I),

Downloaded by PENNSYLVANIA STATE UNIV on June 26, 2012 | http://pubs.acs.org
Publication Date: August 13, 2009 | doi: 10.1021/bk-2009-1024.ch018

which can self assemble into micelles in aqueous solution. The micelles are stabilized by cross-linking of the hydrophilic segment, which forms the shell of the micelles, leading to soft nanoparticles showing either hydroxyl or carboxylic acid functional groups on their surfaces.

## Experimental Section

*Materials.* All solvents, monomers, and other chemicals were purchased at the highest purity available and used as received unless otherwise stated. All monomers were filtered before utilization through a basic alumina (Brockmann I) column, to eliminate the radical inhibitor. Isoprene (I) and hydroxyethyl acrylate (HEA) were distilled *in vacuo*. Tetrahydrofuran (THF, Riedel-deHaën, HPLC grade), dimethylformamide (DMF, Ajax Fine Chemicals) and methanol (Ajax Fine Chemicals) were dried over molecular sieves (4Å) before use. 2,2-Azobisisobutyronitrile (AIBN, 99%, Fisher) was recrystallized twice from ethanol. N-acryloxysuccinimide (NAS) was synthesized based on the method described in literature by Pollak et al.[20] The trithiocarbonate RAFT agent, 2-ethylsulfanylthiocarbonylsulfanyl-propionic acid ethyl ester (ETSPE) was synthesized in accordance to the method described by Wood et al.[21] Dialysis experiments were carried out using Spectra/Por dialysis tubing with MWCO 12000-14000. NMR analyses were done using Bruker Ultra Shield Avance spectrometers (400 and 300 MHz). SEC analyses using THF with 0.5% (v/v) TEA as eluent (1mL/min) were carried out at room temperature using a Polymer Laboratories SEC system consisting of a guard column and two Polymer Laboratories PLgel 5mm Mixed-C columns (molecular weight range of 2,000,000-500 g/mol) connected to a differential refractive index (DRI) detector (Shodex, RI-101). SEC analyses using DMF with 0.5% (w/v) LiBr as eluent (0.8 mL/min) were carried out at ambient temperature using a system comprising of a guard column and two Polymer Laboratories PolarGel-M columns connected to an Optilab DSP refractive index detector with a P10 cell (Wyatt Technology). Gradient polymer elution chromatography (GPEC) analyses were performed using a Polymer Laboratories system equipped with a normal phase column attached to an evaporative light scattering detector (ELSD) PL-ELS 1000. The solvent combination employed was hexane/THF at 1mL/min. Pure hexane was the initial solvent system and pumped at 1ml/min for 10 minutes before the composition of the solvent was changed gradually to pure THF. The ELSD nebulizer temperature was set at 50 °C and the evaporation temperature was set at 90 °C. Particle size measurements were carried out by dynamic light scattering (DLS) using a Malvern Instruments Zetasizer nano series instrument. At least five measurements were made for each sample with an equilibration time of 5 minutes before each measurement. Samples for transmission electron microscopy (TEM) analyses were made by placing a drop of sample onto a carbon coated copper grid followed by addition of a drop of the staining solution (uranyl acetate or osmium tetroxide). Excess solution was carefully blotted off using filter paper and samples were air dried for a few minutes or overnight, depending on staining conditions, before analysis. TEM images were obtained using a JEOL 1200 EX, Philips CM12 and Philips CM120 electron microscopes.

Downloaded by PENNSYLVANIA STATE UNIV on June 26, 2012 | http://pubs.acs.org
Publication Date: August 13, 2009 | doi: 10.1021/bk-2009-1024.ch018

Hydrodynamic chromatography (HDC) was used to measure particle size using a Varian/Polymer Laboratories particle size distribution analyzer (PL-PSDA). The system was calibrated using monodisperse polystyrene latex standards with vary narrow particle size distribution. The particles were detected after elution from the HDC column by a UV detector operating at 254 nm. The eluent was a solution of proprietary surface active agents in water.

*Typical RAFT polymerization.* A toluene (6.5 mL) solution containing ETSPE (0.420 g, 1.76 mmol), monomer (EA, 16.7 g, 167 mmol) and AIBN (0.030 g, 0.180 mmol) was placed in a schlenk tube cooled in dry ice. Oxygen was removed by nitrogen bubbling for 10 minutes. After degassing, the polymerization system was placed into a heated oil bath maintained at 60 °C for the length of the reaction. The resulting macro chain transfer agent (macro CTA) was purified by repeated precipitation into cold hexane from THF. Drying of the purified macroCTAs was carried out under reduced pressure in a vacuum oven at 40 °C for 24 hours. After drying, the polymeric CTAs were analyzed by $^1$H NMR and SEC.

*Typical synthesis of a block copolymer; P(EA–b–HEA).* Weighed amounts of poly(EA) macroCTAs (0.180 mmol) were left to dissolve in measured amounts of DMSO overnight (3 mL). After dissolution, known amounts of HEA (0.615 g, 5.30 mmol) and AIBN (0.003 g, 0.018 mmol) were added and the polymerization solutions were placed in ampoules which were sealed using rubber septa. Each system was purged using nitrogen gas for 30 minutes before being placed in a heated oil bath maintained at 55 °C for the length of the reaction. At the end of the reaction period (16 hours), polymerizations were stopped by placing the reaction vessels into an ice bath followed by $^1$H NMR analyses using d-DMSO as solvent. Purification of the polymers was effected by repeated precipitation (3 times) of the polymer in a cold solvent mixture of hexane : diethyl ether : toluene (8:2:0.1, v/v) followed by filtration and drying under reduced pressure overnight in a vacuum oven. The intended composition in final products was 50 % of poly(EA) and 50% of poly(HEA) and the degrees of polymerization of the block copolymer products were determined by $^1$H NMR. The block copolymers were also characterized using GPEC, FT-IR and SEC.

*Typical procedure for the micellization of P(EA–b–HEA) and P(EA–b–(HEA–co–NAS)).* Polymers were weighed (0.189 g) and left to dissolve in 10.5 mL aliquots of dry methanol overnight to give 18 g/L solutions. These solutions were then filtered through 0.2 micron membrane filters. MilliQ water was then added at a rate of 0.04 mL/min using an auto dispenser under constant stirring to yield 0.75 g/L polymer solution.

*Typical crosslinking reaction of P(EA–b–(HEA–co–NAS)) micelles; P($EA_{117}$–b–($HEA_{85}$–co–$NAS_{16}$)).* The pH of each micelle solutions was first adjusted to 9-9.5 using a few drops of phosphate buffer. 1.04 mL of a HMDA solution in water was filtered through 0.2 micron membrane filters and added to 125 mL aliquots of stirred aqueous micelle solutions at a rate of 0.1 mL/min which were then left to stir for 24 hours. The amount of HMDA (3.5 mg/mL, $3\times10^{-2}$ mmol/mL) added to each micelle solution was such that only 85% of the NAS residues got crosslinked and the reactants ratio of NAS:HMDA units in solution was 2:1. The amount of HMDA solution required to reach 100% NAS

Downloaded by PENNSYLVANIA STATE UNIV on June 26, 2012 | http://pubs.acs.org
Publication Date: August 13, 2009 | doi: 10.1021/bk-2009-1024.ch018

crosslinking was added after 24 hours at a rate of 0.04mL/min and the solution was left to stir for 4 hours.

*Typical synthesis of a block copolymer; P(tBA–b–I).* The diblock copolymer was synthesized by using P*t*BA as macro CTA. The polymerization was carried out in a dry ampoule equipped with a magnetic stirring bar. The ampoule was charged with P*t*BA macro-RAFT (2.11 g, 0.217 mmol), dicumyl peroxide (0.012 g, 0.043 mmol) and isoprene monomer (7.39 g, 109 mmol). The mixture was allowed to stir at room temperature for 10 min to ensure homogeneity before the ampoule was placed in dry ice and the reaction mixture degassed by nitrogen bubbling. The reaction vessel was then sealed and placed in an oil bath at 115 °C for 24 h. The tube was immersed in an ice bath to quench the polymerization. Excess isoprene monomer was removed under reduced-pressure. The resulting polymer was precipitated in a dichloromethane/acetone mixture and dried under vacuum overnight to give yellow $PtBA_{74}$-*b*-$PI_{132}$ diblock copolymer.

*Typical synthesis of P(AA–b–I).* P*t*BA-*b*-PI was added to a 250-mL two-necked round-bottom flask equipped with a stir bar and a condenser. The polymer was dissolved into a 10% HCl solution in water. The solution was stirred to reflux overnight. The resulting product was dried under vacuum for 24 hours.

*Micellization of P($AA_{74}$–b–$I_{132}$).* To a solution of $PAA_{74}$-*b*-$PI_{132}$, diblock copolymer, in 1 ml of DMF (0.010 mg, 0.003 mg/mL), 10 mL of MilliQ water was added dropwise via a syringe pump over the course of four hours. The reaction mixture was further stirred overnight at ambient temperature before being transferred to a pre-soaked dialysis tube (MWCO ca. 12000 – 14000 Da), and dialyzed against MilliQ water for two days, to afford a micelle solution with a final polymer concentration of 0.265 mg/mL.

*Typical crosslinking reaction of P(AA–b–I) micelles; P($AA_{74}$–b–$I_{132}$).* A 0.1 mL solution of 2,2’-(ethylenedioxy)bis(ethylamine) (0.657 mg, 0.004 mmol) in water was added dropwise to a 49.6 mL PAA-*b*-PI micelle solution (1.28 mg, 0.018 mmol acid residues). 0.3 mL of a solution of 1-[3’-(dimethylamino)-propyl]-3-ethylcarbodiimide methiodide (2.64 mg, 0.009 mmol) was then added dropwise to the micelle solution. The reaction mixture was further stirred for a few days at ambient temperature and dialyzed against deionized water for three additional days using 12 – 14 kDa MWCO membranes.

## Results and Discussion

The strategy adopted to form soft nanoparticles follows that published by Wooley and coworkers,[12] with the synthesis of diblock copolymers, using RAFT polymerization in our case, followed by their self assembly in water and the crosslinking of the shells of the micelles leading to stable particles. RAFT polymerization of acrylate monomers has been extensively studied.[16,177,22] Good control over molecular weight distribution can be achieved in presence of dithiobenzoates and trithiocarbonate CTAs. In this work, we use ETSPE,[21] as it has been reported to have good thermal stability,[23] and to efficiently control the RAFT polymerization of acrylates.[24]

Downloaded by PENNSYLVANIA STATE UNIV on June 26, 2012 | http://pubs.acs.org
Publication Date: August 13, 2009 | doi: 10.1021/bk-2009-1024.ch018

### OH–Functionalized Soft Nanoparticles – P(EA–*b*–HEA)

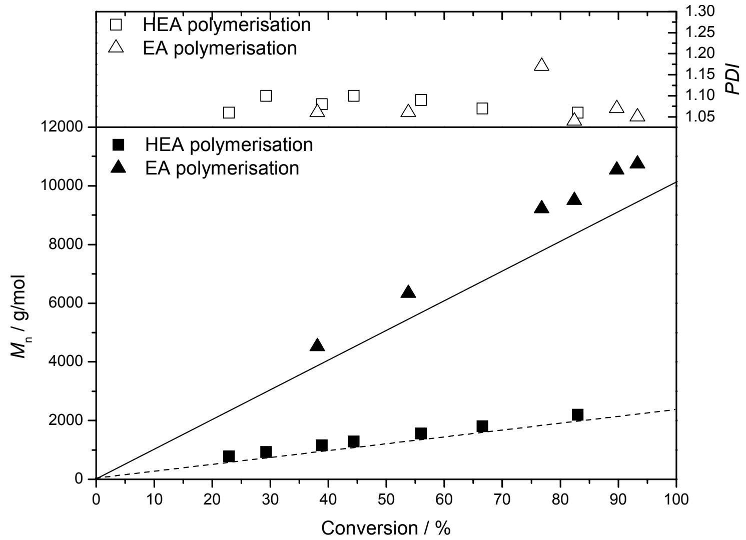

*Figure 1. Evolution of $M_n$ and PDI with conversion for the polymerizations of EA (triangles) and HEA (squares) mediated by ETSPE. The plain line is the theoretical evolution of $M_n$ for EA. The dashed line is the theoretical evolution of $M_n$ for HEA. (Reaction conditions: EA/ETSPE/AIBN: 100/1/0.1 at 60 °C in toluene (30 % v/v); HEA/ETSPE/AIBN: 20/1/0.1 at50 °C in DMSO (30 % v/v)).*

P(EA) was synthesized as the first block, followed by chain extension with HEA. To synthesize well-defined block copolymers by RAFT polymerization, it is essential to ensure that the first block has a high proportion of living chains. The EA polymerizations were therefore not taken to high conversions, to limit termination events, which lead to the formation of dead polymer chains, without ω functionality. $^1$H NMR analysis of the purified P(EA) blocks confirmed the presence of the RAFT end groups and the complete removal of unreacted monomer. Chain extension with HEA was undertaken and GPEC analyses were used to characterize the resulting block copolymers. Analyses of the purified block copolymers and macroCTAs by GPEC demonstrated the successful chain extension of P(EA) into P(EA–*b*–HEA), as the retention time of the copolymer eluted at higher retention time than the macro chain transfer agent (macroCTA), with no peak observable at the macroCTA retention time, thus showing that no macroCTA remained in the block copolymer (Figure 2). The expected effect of polymer molecular weight on solubility was also observed from the GPEC chromatograms of the macroCTAs. Indeed, the observed peak retention times were found to increase along with the macroCTAs molecular weight. This dependence of solubility on molecular weight was however not as clear in the case of the block copolymers, probably due to their amphiphilic properties.

Downloaded by PENNSYLVANIA STATE UNIV on June 26, 2012 | http://pubs.acs.org
Publication Date: August 13, 2009 | doi: 10.1021/bk-2009-1024.ch018

Downloaded by PENNSYLVANIA STATE UNIV on June 26, 2012 | http://pubs.acs.org
Publication Date: August 13, 2009 | doi: 10.1021/bk-2009-1024.ch018

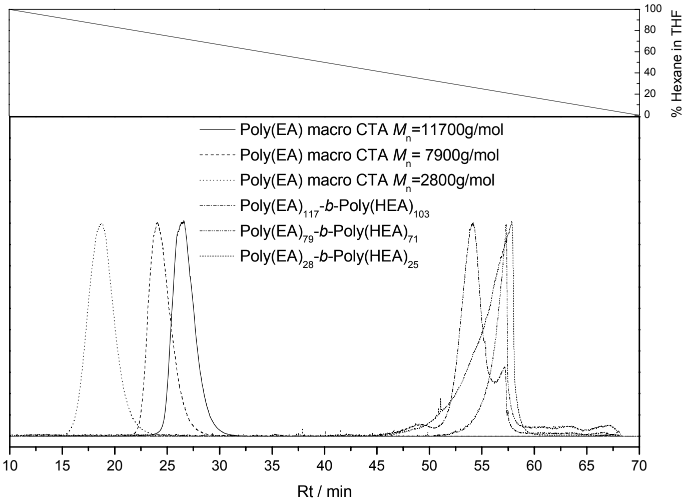

*Figure 2. GPEC chromatograms of macroCTAs and P(EA–b–HEA) diblock copolymers.*

SEC analyses of the block copolymers were undertaken using DMF as eluent. LiBr was added to the eluent to break down the hydrogen bonds in the polymer that may affect the analysis.[25,26,27,28] The SEC results clearly showed chain extension of the P(EA) chains with HEA, with good control over molecular weight distribution (Figure 3).

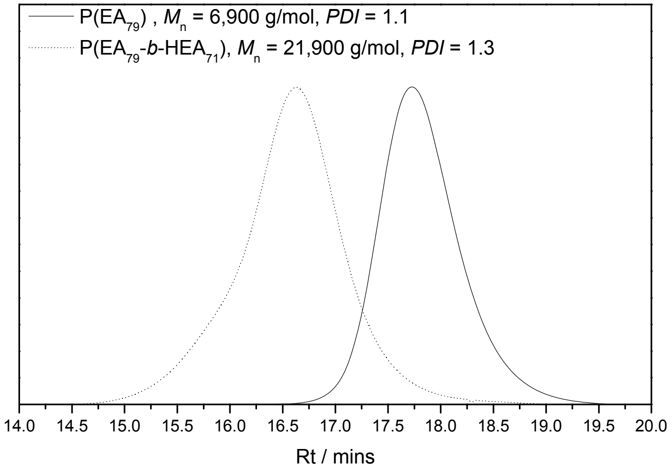

*Figure 3. Typical SEC traces of a chain extension experiment of P(EA) with HEA analyzed using DMF with 0.5 % w/v LiBr as the eluent.*

P(EA–*b*–HEA) block copolymers were initially dissolved in methanol, a solvent which solubilizes both hydrophilic and hydrophobic blocks. Slow addition of water, a non-solvent for P(EA), was then used to trigger micellization. The resulting micelle solutions were analyzed by DLS and TEM. Particle size analysis by DLS showed monomodal symmetrical and narrow distributions (<0.1) indicating that the sizes of the micelles were nearly uniform with an average diameter of 23.4 nm for the P(EA$_{79}$–*b*–HEA$_{71}$) copolymer and 18.6 nm for the P(EA$_{28}$–*b*–HEA$_{25}$) copolymer. Differences in the particle sizes can be explained by the difference in the chain lengths of the copolymers. TEM measurements confirmed these observations, and gave an average particle diameter of 18±1 nm and 13±1 nm for P(EA$_{79}$–*b*–HEA$_{71}$) and P(EA$_{28}$–*b*–HEA$_{25}$), respectively (Figure 4). The slight discrepancy between DLS and TEM analyses may be attributed to the micelles being fully hydrated in solution for DLS measurement, whilst they are dry under TEM conditions.[29,30] Additional evidence of formation of micelles was obtained by the determination of the critical micelle concentration (CMC). Surface tension measurements were undertaken at various concentrations of P(EA$_{79}$–*b*–HEA$_{71}$), using the Du Noüy ring method. The surface tension of the aqueous solution was plotted against concentration, and the CMC was determined as the concentration in block copolymer for which surface tension remains constant upon increase of the copolymer concentration (Figure 5). A CMC of 4.8 g/L was obtained, which is comparable to values of low molecular weight surfactants.[31]

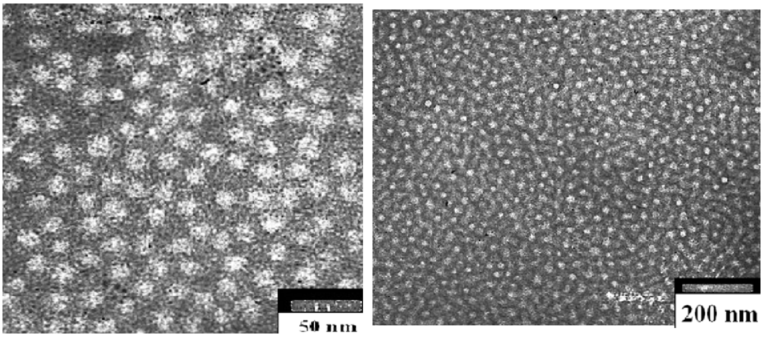

*Figure 4. TEM images of P(EA$_{28}$-b-HEA$_{25}$) (left) and P(EA$_{79}$-b-HEA$_{71}$) (right) micelle solutions.*

Downloaded by PENNSYLVANIA STATE UNIV on June 26, 2012 | http://pubs.acs.org
Publication Date: August 13, 2009 | doi: 10.1021/bk-2009-1024.ch018

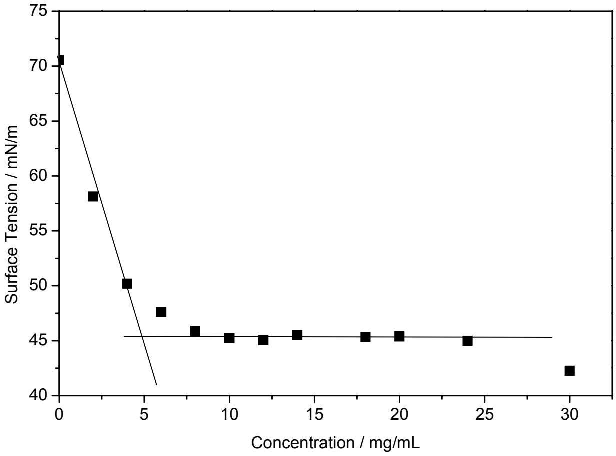

*Figure 5. Surface tension against concentration graph for CMC determination.*

In order to ensure efficient crosslinking of the micelle shell, a succinimide group was introduced in the hydrophilic segment by copolymerization of *N*–acryloxysuccinimide (NAS) with HEA. The reaction of NAS with hexamethylenediamine (HMDA) to crosslink micelles shells is well documented and quantitative.[32] A hydrophobic P(EA) block ($M_n$ = 23000 g/mol, *PDI* = 1.10) was chain–extended with HEA and different amounts of NAS to yield block copolymers P(EA$_{117}$–*b*–(HEA$_{92}$–*co*–NAS$_9$)) and P(EA$_{117}$–*b*–(HEA$_{85}$–*co*–NAS$_{16}$)). Average diameters of 38.5 nm (DLS) and 34 nm (TEM) were found for P(EA$_{117}$–*b*–(HEA$_{92}$–*co*–NAS$_9$)), and 59.1 nm (DLS) and 38 nm (TEM) for P(EA$_{117}$–*b*–(HEA$_{85}$–*co*–NAS$_{16}$)). The increase in the size of the micelles by comparison to micelles of P(E–*b*–HEA) is due to the difference in size of the block copolymer chains and the hydrolysis of NAS. This hydrolysis leads to carboxylic acid pendant groups, which are more polar than the hydroxyl groups of HEA, and increase the hydration of the shells of the micelles by water.[30] In this case again, the discrepancy between DLS and TEM analyses can be attributed to the difference in the analysis conditions: dry state for TEM and in solution for DLS. The difference in size between DLS and TEM analyses was more significant for the particles containing a higher proportion of NAS, P(EA$_{117}$-*b*-(HEA$_{85}$-*co*-NAS$_{16}$)), thus confirming the effect of the hydrolyzed NAS on the solvatation of the micelle shell. Shell crosslinking was performed in presence of HMDA at pH 9. $^1$H NMR showed that 85 % of the NAS units had reacted. DLS and TEM analyses revealed a single population of particles which size was close to that of the micelles before crosslinking (41.7 nm (DLS) and 30 nm (TEM) for P(EA$_{117}$–*b*–(HEA$_{92}$–*co*–NAS$_9$)) and 60.6 nm (DLS) and 28 nm (TEM) for P(EA$_{117}$–*b*–(HEA$_{85}$–*co*–NAS$_{16}$))), thus demonstrating that intermicellar crosslinking did not occur.

This route is an efficient and versatile approach to the synthesis of spherical nanoparticles of tunable size, showing a high concentration in hydroxyl groups at their surface. The hydroxyl groups ensure the particles are hydrophilic, and provide a versatile handle for further functionalization of the nanoparticles surface.

Downloaded by PENNSYLVANIA STATE UNIV on June 26, 2012 | http://pubs.acs.org
Publication Date: August 13, 2009 | doi: 10.1021/bk-2009-1024.ch018

## $CO_2H$–Functionalized Soft Nanoparticles – P(AA–*b*–I)

The carboxylic acid decorated soft nanoparticles were designed following the strategy described above: crosslinking of the shell of micelles formed by self-assembly of amphiphilic diblock copolymers. In this case the copolymer chosen was poly(acrylic acid–*b*–isoprene) (P(AA–*b*–I)). *tert*–Butyl acrylate (*t*BA) was first polymerized via RAFT polymerization mediated by ETSPE to produce a P(*t*BA) macroCTA. The polymerization was well controlled with molecular weight increasing linearly with conversion, and *PDI* remained below 1.2 at all time (results not shown). The P(*t*BA) macroCTA ($M_n$ = 9,600 g/mol, *PDI* = 1.06) was then used to mediate the RAFT polymerization of isoprene following a procedure previously published by our group.[33] This led to well-defined P(*t*BA–*b*–I) diblock copolymers. THF GPC analysis of this diblock copolymer revealed a $M_n$ of 19,000 g/mol and a *PDI* of 1.23 (Figure 6). $^1$H NMR analyses allowed to calculate the DP of the isoprene block, P(*t*$BA_{74}$–*b*–$I_{132}$). The obtained P(*t*BA–*b*–I) diblock copolymer was converted into P($AA_{74}$–*b*–$I_{132}$) via hydrolysis in a solution of HCl (10%). The chemical structure of P($AA_{74}$–*b*–$I_{132}$) was confirmed by ATR-FTIR, with characteristic signals at 3300-2500 cm$^{-1}$ (O–H of carboxylic acid), 1760-1690 cm$^{-1}$ (C=O of carboxylic acid), 1470-1450 cm$^{-1}$ (C–H bend of alkanes),1100-650 cm$^{-1}$ (C–H bend of alkenes) and 725-720 cm$^{-1}$ (C–H rock of alkanes). The completion of the hydrolysis was confirmed by $^1$H NMR. Hydrolysis of *t*BA was chosen over direct polymerization of acrylic acid because PAA is not miscible in isoprene, thus making the block extension reaction more difficult from a technical point of view.

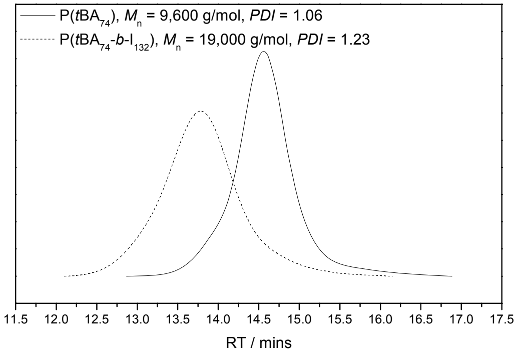

*Figure 6. SEC traces of a chain extension experiment of P(tBA) with isoprene analyzed using THF as the eluent.*

Downloaded by PENNSYLVANIA STATE UNIV on June 26, 2012 | http://pubs.acs.org
Publication Date: August 13, 2009 | doi: 10.1021/bk-2009-1024.ch018

Downloaded by PENNSYLVANIA STATE UNIV on June 26, 2012 | http://pubs.acs.org
Publication Date: August 13, 2009 | doi: 10.1021/bk-2009-1024.ch018

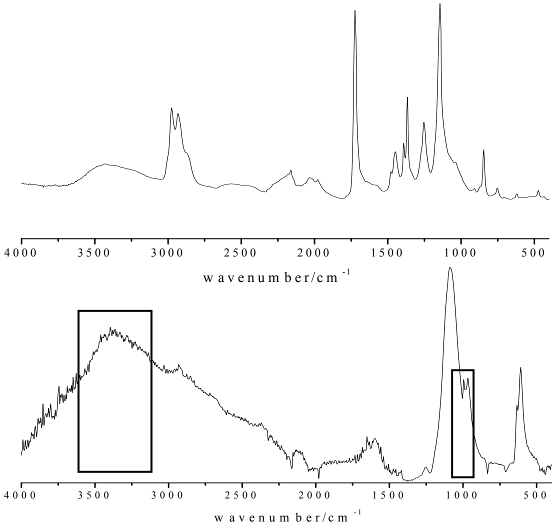

*Figure 7. FTIR spectrum of 50% shell cross-linked micelle, micelle (above) and (bottom) cross-linked nanoparticle.*

The amphiphilic block copolymer was first dissolved in DMF, a good solvent for both blocks, and subsequent addition of water triggered the formation of micelles. Dialysis ensured the removal of DMF and the stabilization of the micelles in water. The aggregates were analyzed by DLS (89 nm), hydrodynamic chromatography (HDC) (55 nm) and TEM (50 nm), and all techniques agreed well with each other (within the limits discussed above). Figure 8 shows a typical TEM picture of the micelles. The effect of the carboxylic acid functionality on the hydration of the shell is well illustrated here. Indeed, at similar degree of polymerization, P(AA–*b*–I) generate bigger micelles than that obtained from P(EA–*b*–HEA) and P(EA–*b*–(HEA–*co*–NAS)), clearly demonstrating the increase in the hydration of the shell by water in presence of carboxylic acid groups.[30]

The crosslinking of the shell of P($AA_{74}$–*b*–$I_{132}$) was performed by reacting the carboxylic acid groups of the PAA block with 2,2’-(ethylenedioxy)bis(ethylamine) following a procedure published in the literature.[34] The chemical reaction was confirmed by FTIR, Figure 7, which showed the appearance of a peak at 3400-3250 cm$^{-1}$, characteristic of the N-H stretch of amides. The C-O stretch peak of ethers group in cross-linker molecule was also observed at 1000 cm$^{-1}$. The shape and size of the carboxylic acid decorated soft nanoparticles were investigated by TEM and DLS. TEM pictures gave a size of 25 nm while DLS measurement showed a uniform distribution centered on 34 nm. Figure 8 shows a typical TEM picture of the nanoparticles after crosslinking. The decrease in size of the particles after crosslinking reaction is due to the tightening of the shell upon reaction of the carboxylic acid pendant groups with a high concentration of diamine linker, as has been reported previously.[12]

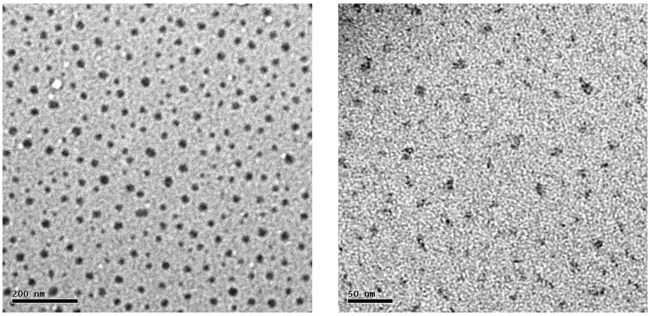

*Figure 8. Typical TEM images of micelles (left) and shell crosslinked micelles (right) of P($AA_{74}$–b–$I_{132}$) stained with $OsO_4$.*

Downloaded by PENNSYLVANIA STATE UNIV on June 26, 2012 | http://pubs.acs.org
Publication Date: August 13, 2009 | doi: 10.1021/bk-2009-1024.ch018

In this approach, the carboxylic acid functionality confers hydrophilic properties to the particle surface, and it is used for both crosslinking reaction and further functionalization of the particle. By comparison to the route used to produce hydroxyl functional particles, this approach does not require the use of a specific group for the crosslinking reaction, and the degree of crosslinking relies solely on the amount of crosslinker used. However, it follows that a shell showing dense crosslinking has a lower concentration in carboxylic acid group at its surface, thus reducing the number of sites available for further functionalization of the particle. Further functional groups can also be introduced via the RAFT agent. Indeed, in this work we have used 2-ethylsulfanylthiocarbonylsulfanyl-propionic acid ethyl ester as chain transfer agent. However, by mediating polymerizations with functionalized RAFT agents such as dithiobenzoate derivatives of *S*–methoxycarbonylphenylmethyl dithiobenzoate,[35] or by modification of the dithioester moiety after reaction,[36] one could introduce new reactive groups at the polymeric chain end situated at the surface of the particles. The combination of these approaches provides an almost infinite number of possible functionalization of the soft nanoparticle surfaces.

## Conclusions

We presented the synthesis of well-defined amphiphilic diblock copolymers using RAFT polymerization and the use of their self-assembly in solution to produce micelles and soft nanoparticles. RAFT polymerization is very efficient to control the polymerization of functional acrylates, and can also mediate the polymerization of other less common vinyl monomers such as isoprene. This characteristics was use to synthesize P(EA–*b*–HEA), P(EA–*b*–(HEA–*co*–NAS)) and P(AA–*b*–I) diblock copolymers. These copolymers spontaneously self assembled in water to form micelles with narrow size distributions. These nanostructures were then stabilized by crosslinking of the functional hydrophilic blocks. This method enabled the synthesis of well-defined soft nanoparticles. This work demonstrates the strong versatility of RAFT polymerization to synthesize functional polymeric nanostructures with high precision and control.

# References

---

1. Antonietti, M.; Forster, S., *Adv. Mat.* **2003**, *15*, 1323.
2. Park, M.; Harrison, C.; Chaikin, P.M.; Registe, R.A.; Adam, D. H. *Science* **1997**, *276*, 1401.
3. Stupp, S.I.; LeBonheur, V.; Walker, K.; Li, L.S.; Huggins, K. E.; Keser, M.; Amstutz, A. *Science* **1997**, *276*, 384.
4. Collier, J.H.; Messermith, P.B. *Annu. Rev. Mater. Res.* **2001,** *31*, 237.
5. Silva, G.A.; Czetster, C.; Niece, K.L.; Beniash, E.; Harrington, D.A.; Kesster, J.A.; Stupp, S. I. *Science* **2004,** *303*, 1352.
6. Savic, R.; Luo, R.B.; Eisenberg, A.; Maysinger, D. *Science* **2003,** *300*, 615.
7. Yu, K.; Eisenberg A. *Macromolecules* **1998,** *31*, 3509.
8. Won, Y.Y.; David, H.T.; Bates, F.T. *Science* **1999,** *283*, 960.
9. Dalhaimer, P.; Engler A.J.; Parthasarathy R.; Discher, D.E. *Biomacromolecules* **2004,** *5*, 1714.
10. Read, E.S.; Armes, S. P. *Chem. Commun.* **2007**, 3021.
11. Guo, A.; Liu, G.; Tao, J. *Macromolecules* **1996**, *29*, 2487.
12. Thurmond, K.B.; Kowalewski, T.; Wooley, K. L. *J. Am. Chem. Soc.* **1996**, *118*, 7239.
13. (a) O'Reilly, R.K.; Hawker, C.J.; Wooley, K.L. *Chem. Soc. Rev.* **2006**, *35*, 1068; (b) Read, E.S.; Armes, S.P. *Chem. Commun.* **2007**, 3021; (c) Stenzel, M.H. *Chem. Commun.* **2008**, 3486.
14. Matyjaszewski, K.; Xia, J. *Chem. Rev.* **2001**, *101*, 2921.
15. Hawker, C.J.; Bosman, A.W.; Harth, E. *Chem. Rev***. 2001**, *101*, 3661.
16. Moad, G. ; Rizzado, E.; Thang, S.H. *Aust. J. Chem.* **2006**, *59*, 669.
17. Perrier, S.; Takolpuckdee, P. *J. Polym. Sci. Part A: Polym. Chem.* **2005**, *43*, 5347.
18. Lowe, A.B.; McCormick, C.L. *Prog.Polym.Sci.* **2007**, *32*, 283.
19. (a) Moad, G.; Rizzardo, E.; Thang, S.H., *Acc. Chem. Res.* **2008**, *41*, 1133; (b) Barner-Kowollik, C.; Davis, T.P.; Heuts, J.P.A.; Stenzel, M.H.; Vana, P.; Whittaker, M. *J. Polym. Sci. Part A: Polym. Chem.* **2003***, 41*, 365; (c) Takolpuckdee, P.; Westwood, J.; Lewis, D. M.; Perrier, S., *Macromol. Symp.* **2004,** *216*, 23.
20. Pollak, A.; Blumenfeld, H.; Wax, M.; Baughn, R.L.; Whitesides, G. M. *J. Am. Chem. Soc.* **1980**, *102*, 6324.
21. Wood, M.R.; Duncalf, D.J.; Rannard, S.P.; Perrier, S. *Org. Lett.* **2006**, *8*, 553.
22. Shipp, D. A. *Polym. Rev.* **2005**, *45*, 171.
23. Legge, T.M.; Slark, A.T.; Perrier, S., *J. Polym. Sci., Part A: Polym. Chem.* **2006,** *44*, 6980.
24. Wood, M.R.; Duncalf, D.J.; Findlay, P.; Rannard, S.P.; Perrier, S. *Aust. J. Chem.* **2007**, *60*, 772.
25. Zhang, Q.; Zhan, X.; Chen, F.; Shi, Y.; Wang, Q. *J. Polym. Sci. Part A: Polym. Chem.* **2007**, *45*, 1585.
26. Coca, S.; Jasieczek, C.B.; Beers, K. L.; Matyjaszewski, K. *J. Polym. Sci. Part A: Polym. Chem.* **1998**, *36*, 1417.

Downloaded by PENNSYLVANIA STATE UNIV on June 26, 2012 | http://pubs.acs.org
Publication Date: August 13, 2009 | doi: 10.1021/bk-2009-1024.ch018

27. Segudovic, N.; Sertic, S.; Kovacfilipovic, M.; Jarm, V. *J. Chromato. A* **1995**, *704*, 149.
28. Tokuda, T.; Mori, M.; Yamada, T. *J. Chromato. A* **1996**, *722*, 123.
29. Madsen, J.; Armes, S.P.; Bertal, K.; Lomas, H.; MacNeil, S.; Lewis, A.L. *Biomacromolecules* **2008**, *9*, 2265.
30. Terreau, O.; Luo, L.B.; Eisenberg, A. *Langmuir* **2003**, *19*, 5601.
31. *Surfactant science and technology;* Myers, D., Ed.; New York, 2nd ed., 1992; p. 334.
32. Li, Y.; Lokitz, B. S.; McCormick, C.L. *Macromolecules***2006**, *39*, 81.
33. Jitchum, V.; Perrier, S., *Macromolecules* **2007,** *40*, 1408.
34. Turner, J.L.; Chen, Z.; Wooley, K.L., *J. Controlled Release* **2005,** 109, 189.
35. (a) Perrier, S.; Takolpuckdee, P.; Westwood, J.; Lewis, D.M. *Macromolecules* **2004,** *37*, 2709; (b) Takolpuckdee, P.; Mars, C.A.; Perrier, S.; Archibald, S.J. *Macromolecules* **2005,** *38*, 1057.
36. (a) Moad, G.; Chong, Y.K.; Postma, A.; Rizzardo, E.; Thang, S.H. *Polymer* **2005**, *46*, 8458; (b) Xu, J.; He, J.; Fan, D.; Wang, X.; Yang, Y. *Macromolecules* **2006**, *39*, 8616; (c) Lima, V.; Jiang, X.; Brokken-Zijp, J.; Shoenmakers, P.J.; Klumperman, B.; Van der Linde, R. *J Polym Sci Part A: Polym Sci* **2005**, *43*, 959; (d) Patton, D.L.; Mullings, M.; Fulghum, T.; Advincula, R.C. *Macromolecules* **2005**, *38*, 8597; (e) Chen, M.; Giggino, K.P.; Smith, T.A.; Thang, S.H.; Wilson, G. *J. Aust J Chem* **2005**, *57*, 1175; (f) Segui, F.; Qiu, X.-P.; Winnik, F.M. *J Polym Sci Part A: Polym Sci* **2008**, *46*, 314; (g) Li, M.; De, P.; Gondi, S.R.; Sumerlin, B.S. *J Polym Sci Part A: Polym Chem* **2008**, *46*, 5093; (h) Chong, B.; Moad, G.; Rizzardo, E.; Skidmore, M.; Thang, S.H. *Aust J Chem* **2006**, *59*, 755; (i) Perrier, S.; Takolpuckdee, P.; Mars, C.A. *Macromolecules* **2005**, *38*, 2033.

Downloaded by PENNSYLVANIA STATE UNIV on June 26, 2012 | http://pubs.acs.org
Publication Date: August 13, 2009 | doi: 10.1021/bk-2009-1024.ch018

Downloaded by COLUMBIA UNIV on June 27, 2012 | http://pubs.acs.org
Publication Date: August 13, 2009 | doi: 10.1021/bk-2009-1024.ch019

## Chapter 19

# Kinetics and Colloidal Stability of Raft/Miniemulsion Polymerization of MMA Using Comblike Polymeric Surfactants

**Peihong Ni*, Xiulin Zhu*, and Xiaodong Zhou**

**Key Laboratory of Organic Synthesis of Jiangsu Province,
College of Chemistry, Chemical Engineering and Materials Science,
Soochow University, Suzhou 215123, China**

Three comblike amphiphilic copolymers have been prepared via conventional free-radical random copolymerization of [2-(acryloyloxy)ethyl]trimethylammonium chloride (AETMAC), and stearyl methacrylate (SMA) with different feed ratios in ethanol solution. Subsequently, these copolymers were used as polymeric surfactants in the RAFT/miniemulsion polymerization of methyl methacrylate (MMA). The effects of the composition and amount of the polymeric surfactants on the controlled/living polymerization of MMA such as kinetics and colloidal stability in the systems have been investigated.

In Controlled/Living Radical Polymerization: Progress in RAFT, DT, NMP & OMRP; Matyjaszewski, K.;
ACS Symposium Series; American Chemical Society: Washington, DC, 2009.

Downloaded by COLUMBIA UNIV on June 27, 2012 | http://pubs.acs.org
Publication Date: August 13, 2009 | doi: 10.1021/bk-2009-1024.ch019

The reversible addition-fragmentation chain transfer (RAFT) mediated polymerization process in heterogeneous systems such as emulsion and miniemulsion polymerization may provide process and economic advantages over the bulk and solution systems.[1-5] In recent years, some researchers have focused on RAFT/emulsion polymerization to solve problems, e.g. colloid instability, retardation, and broad molecular weight distributions.[4,6-8] Amphiphilic copolymers or hydrophilic macro-RAFT agent have been used in RAFT emulsion polymerization to stabilized the colloid systems. Gilbert et al. synthesized an amphipathic RAFT agent, $(AA)_x$-$(BA)_y$-RAFT, to form micelles as "seeds" for further emulsion polymerization.[9] Hawkett et al. developed a self-assembly approach in which micelle-forming amphipathic block copolymers terminated with the desired RAFT agent (acrylic acidb-*block*-butyl acrylate-RAFT) was used.[10] Charleux et al. reported that poly[2-(diethylamino)ethyl methacrylate], made by RAFT polymerization using (4-cyanopentanoic acid)-4-dithiobenzoate as a chain transfer agent, was used in the surfactant-free polymerization of styrene.[11] Addition of styrene units would lead to in situ formation of an amphiphilic block copolymer capable of stabilizing polymer particles. Charleux and coworkers also studied that in surfactant-free styrene emulsion polymerization, sodium acrylate was added as co-monomer. Styrene-*co*-(sodium acrylate) random copolymers were formed in situ and provided sufficient stabilization to give stable latexes.[12] Nevertheless, for a RAFT/emulsion polymerization system, the phase separation resulting from the poor solubility of the oil-soluble oligmer-RAFT in aqueous solution is supposed to be unavoidable when the RAFT agents transport from the monomer droplets through an aqueous phase to micelles or propagating particles.

It has been found that RAFT/miniemulsion polymerization can eliminate the transport of the RAFT agent during the whole polymerization process because a hydrophobic RAFT agent or macro-RAFT polymers can be equally dispersed into the nanosize droplets, that is, polymerization loci, before polymerization.[13,14] In some researches, functions of a series of surfactants and RAFT agents, for example, a nonionic polymeric surfactant,[15] a high-surfactant-concentration ionic miniemulsion,[16] a water-soluble RAFT agent,[17] and even cationic and anionic amphiphilic surfmers,[18] have been studied and applied in the RAFT/miniemulsion polymerization.

However, in some cases, the RAFT/miniemulsion polymerization process would deviate from the ideal RAFT miniemulsion polymerization. The colloidal instability was still a major issue when an ionic surfactant was used, and the particle size distribution was usually broader than that of a conventional miniemulsion polymerization.[19,20] In resolving the problem of transporting RAFT agent among an aqueous phase from droplets to particles, our group used β-cyclodextrin as a phase transfer agent in the miniemulsion polymerization of butyl methacrylate or styrene to ensure homogeneous distribution of the RAFT agent in all particles, in which 2-cyanoprop-2-yl dithiobenzoate was utilized as the chain-transfer agent.[21,22] In the presence of the β-cyclodextrin, phase separation leading to formation of a red layer, i.e. monomer/oligomer surface layer, as previously documented,[23] was not observed (or was significantly reduced), coagulum formation was reduced and narrower molecular weight distributions were observed. We also prepared a water-soluble macro-RAFT agent based on poly[2-(diethylamino)ethyl methacrylate] (PDMAEMA) and then used in MMA RAFT/miniemulsion polymerization, which allowed the latex well stable.[24] In our previous study, we have proved that cationic polymeric surfactant based on PDMAEMA can improve the stability of conventional miniemulsion polymerization.[25]

In this work, a series of comblike amphiphilic copolymers have been synthesized and used as polymeric surfactants in the RAFT/miniemulsion polymerization of MMA. These polymeric surfactants were prepared via conventional free-radical random copolymerization of [2-(acryloyloxy)ethyl] trimethyl ammonium chloride (AETMAC) and stearyl methacrylate (SMA) to yield poly(AETMAC-*co*-SMA) copolymers with different molar ratio of the two units, in which feed ratios of AETMAC:SMA (molar ratios) equal to 9:1, 8:2, and 7:3, respectively. The kinetics and colloidal stability of the RAFT polymerization have been investigated.

Downloaded by COLUMBIA UNIV on June 27, 2012 | http://pubs.acs.org
Publication Date: August 13, 2009 | doi: 10.1021/bk-2009-1024.ch019

# Experimental

## Materials

Stearyl methacrylate (SMA, 99%, Aldrich) was recrystallized from ethanol. [2-(acryloyloxy)ethyl]trimethylammonium chloride (AETMAC, 80% in water) were purchased from ATOFINA, France. 1-Dodecanethiol (98%) was purchased from Sinopharm Chemical Reagent Co., Ltd. Hexadecane (HD; Merck), sodium dodecyl sulfate (SDS; Farco Chemical Supplies; 99%), tetrahedronfuran (THF) and hydroquinone were of reagent grade and used as received from suppliers. 2, 2'-Azobis(isobutyronitrile) (AIBN; Shanghai Chemical Reagent; 98%) was recrystallized from ethanol and kept in a refrigerator under 4 ºC. 2-Cyanoprop-2-yl dithiobenzoate (CPDB) was prepared according to the previous literatures reported by Mitsukami et al.[26] and Thang et al.[27]

## Instrumentation

The number-average molecular weights ($M_n$) and molecular weight distribution indexes (denoted PDIs) of the dried latex PMMA polymers were recorded on a Waters 1515 gel permeation chromatographer (GPC) instrument using a PLgel 5.0 μm-bead-size guard column (50×7.5 $mm^2$), followed by two linear PLgel columns (500 Å and Mixed-C) and a differential refractive index detector. The eluent was tetrahydrofuran (THF) at 30 °C with a flow rate of 1.0 mL $min^{-1}$. The molecular weights were determined with standard methyl methacrylate calibration used for the calculation.

The chemical structures of copolymers were determined on a 400-MHz NMR instrument (INOVA-400) with $CDCl_3$ and $D_2O$ solvents containing 1% TMS as an internal reference.

Surface tension measurements were carried out using a JK99C automatic surface tensiometer (Shanghai Zhongchen Co., China) equipped with a platinum ring.

The particle sizes and size distributions of the polymer latices were determined with an HPPS hpp5001 high-performance particle size instrument (Malvern) at 25 °C. Before the measurement, the original latex samples were diluted with deionized water to adjust the light strength suitable to the measurement conditions. The cumulant method was chosen for measuring the *z*-average hydrodynamic diameter ($D_z$) and size polydispersity index (size PDI).

## Synthesis of Poly(AETMAC-*co*-SMA) Polymeric Surfactants

Poly(AETMAC-*co*-SMA) copolymers were synthesized via a conventional free radical copolymerization of AETMAC and SMA using ethanol as solvent. The molar ratios of AETMAC to SMA were in the range of 9:1 to7:3. AIBN and dodecylthiol were used as initiator and chain transfer agent, respectively. The products were purified using a rotary evaparator under reduced pressure, then the copolymers were precipitated in cold hexane three times and dried in vacuo. Three samples of copolymers, designated as AS-I, AS-II and AS-III (corresponding to the feed mole radios of [AETMAC]/[SMA] as 9:1, 8:2, and 7:3, respectively), were selected as polymeric emulsifiers in the further RAFT/miniemulsion polymerization of MMA.

## RAFT/Miniemulsion Polymerization of MMA

Methyl methacrylate (MMA, 20 g) was first mixed with AIBN, HD and CPDB. This oil phase was thoroughly mixed by magnetic stirring until homogeneous. Then the oil phase was slowly added into an aqueous solution which dissolved the poly(AETMAC-*co*-SMA) polymeric surfactant. After agitation, the emulsion was ultrasonicated by a probe (JYD-650, Shanghai Zhixin Instrument Co., China) for 40 times with the lifetime of 2 s and an interval of 1 s. The obtained miniemulsion was transferred to a 250 mL four-necked, round-bottom flask. After bubbling $N_2$ for 30 min, the miniemulsion was heated to 70 ºC to start the polymerization. The conversion of MMA to the polymer was determined via a gravimetric method. Samples were taken from the reactor at regular time intervals throughout the reaction, immediately quenched with hydroquinone in a bath of ice water, and then dried in an oven at 50 °C for ananlysis.

## De-emulsification of PMMA Latex

The final PMMA latex was dropped into methanol to yield white precipitate, and then filtrated to attain solid product. The raw sample was washed with deionized water, centrifugated, and filtrated. The process was repeated at least

Downloaded by COLUMBIA UNIV on June 27, 2012 | http://pubs.acs.org
Publication Date: August 13, 2009 | doi: 10.1021/bk-2009-1024.ch019

three times to remove the water-soluble polymeric surfactants. The resultant PMMA sample was dried under vacuum at 40 °C for 24 h.

## Results and Discussion

The free-radical copolymerization of AETMAC and SMA is carried out in ethanol solution at 60 °C with 10 wt% ethanol based on the monomer using 1-dodecanethiol as a chain transfer agent and AIBN as an initiator. Figure 1 depicts the synthesis of poly(AETMAC-*co*-SMA) copolymers. The reaction mixture was homogeneous all along the polymerization. From the element analysis, the compositions of these copolymers based on the unit ration between AETMAC and SMA can be calculated as 88/12 for AS-I, 77/23 for AS-II, and 71/29 for AS-III, respectively. Table 1 shows the typical recipes for the preparation of thc polymeric surfactants and the composition of the copolymers .

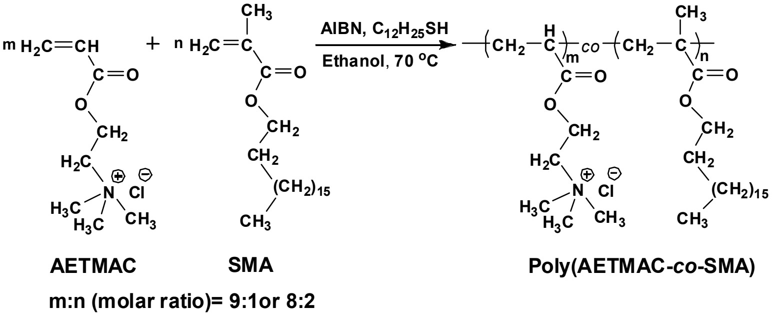

*Figure 1. A Representative reaction procedure for the synthesis of highly charge-density amphiphilic random copolymers poly(AETMAC-co-SMA) via conventional free radical polymerization.*

**Table I. Typical Recipes for the Preparation of Polymeric Surfactants Poly(AETMAC-*co*-SMA) and the Composition of Copolymers**

| *Sample ID* | *Feed Mixture* [a] | | *Composition of copolymer (Molar ratio)* | |
|---|---|---|---|---|
| | *AETMAC (g / mmol)* | *SMA (g / mmol)* | *AETMAC* | *SMA* |
| AS-I | 4.79/ 27 | 1.01/ 3 | 88 | 12 |
| AS-II | 4.26/ 24 | 2.02/ 6 | 77 | 23 |
| AS-III | 3.73/ 21 | 3.03/ 9 | 71 | 29 |

[a] The amounts of 1-dodecanethiol and AIBN were respectively 0.3 g and 0.06 g in each experiment.

Downloaded by COLUMBIA UNIV on June 27, 2012 | http://pubs.acs.org
Publication Date: August 13, 2009 | doi: 10.1021/bk-2009-1024.ch019

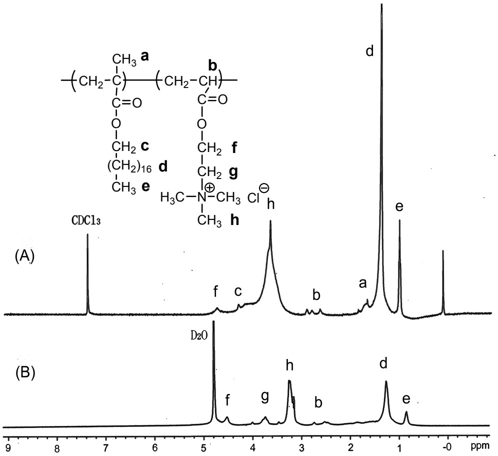

*Figure 2. $^1$H NMR spectra of poly(AETMAC-co-SMA) copolymer (AS-II) measured in the solvents (A) $CDCl_3$ and (B) $D_2O$.*

The chemical structure of AS-II was characterized by $^1$H NMR spectroscopy as shown in Figure 2. Referring to AETMAC and SMA units, the assignments were carried out and given in the figure. The chemical shifts of all the protons in the copolymers can be clearly found. For the demonstration of microsphere structure, two pre-weighted amounts of the copolymer sample AS-II (5.0 mg for each one, purified prior to use) were filled into two NMR testing tubes. One was dissolved into 0.5 mL of deuterated water ($D_2O$), and the other was dissolved in 0.5 mL of deuterated chloroform ($CDCl_3$). Figure 2(A) shows the $^1$H NMR spectrum of AS-II in $CDCl_3$. The characteristic chemical shift ascribed to the protons ($–C\boldsymbol{H}_2–$) of SMA (peak d) is at 1.3 ppm, while the peak weakens in $D_2O$, as shown in Figure 2(B), indicating that the amphiphilic copolymer can form micells in $D_2O$.

The average molecular weights of the poly(AETMAC-*co*-SMA) copolymers were recorded on an aqueous GPC instrument (HP-1100) equipped with a GMPW(XL) no. B3287 column connected to a refractive index detector (G 1362A). The standard narrow distribution of PEO was used in the calibration. The $M_n$ values were approximately 3000 g mol$^{-1}$, and PDI around 1.45-1.47. The critical aggregating concentrations (cac) of the three polymeric surfactants were around 3.4 g L$^{-1}$.

In a typical RAFT miniemulsion polymerization, the amounts of monomer MMA and deionized water were kept as 20 g (0.20 mol) and 80 g, respectively. The molar ratio of [MMA]:[CPDB]:[AIBN] was kept at 600:2:1. Hexadecane (HD) was used as a costabilizer to prevent Ostwald ripening. The comblike polycationic surfactant was utilized as the stabilizer to prevent the latex from coalescing. Theoretically, the addition of the polycationic surfactant can improve the stability of the miniemulsion polymerization for two main reasons: (i) the positive charge from AETMAC units provide a repulsive force between the droplets and so improve the stability of miniemulsion through electrostatic stabilization; and (ii) the stearyl group can anchor into the monomer droplets or latex particles to avoid the oil-soluble RAFT agent, oligomer, or monomer diffusing readily through aqueous phase in the early stage of polymerization and

Downloaded by COLUMBIA UNIV on June 27, 2012 | http://pubs.acs.org
Publication Date: August 13, 2009 | doi: 10.1021/bk-2009-1024.ch019

causing the occurrence of a superswelling state.[28] Figure 3 depicts the process of stabilization.

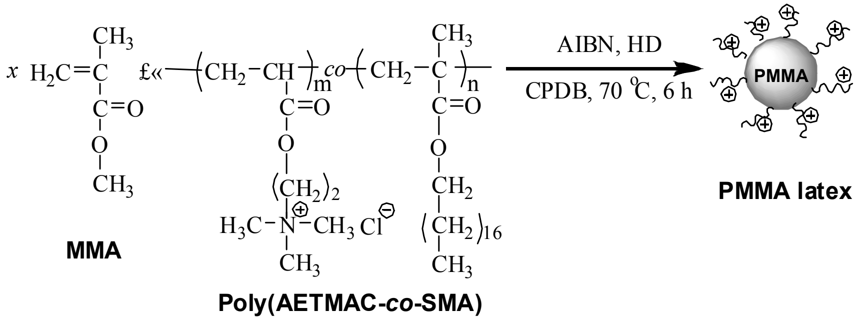

*Figure 3. Scheme for the adsorption of the amphiphilic polymeric surfactant poly(AETMAC-co-SMA) on the surface of droplets and latex particles.*

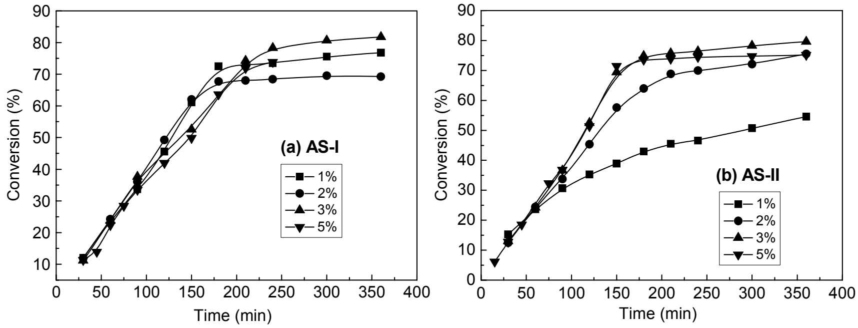

*Figure 4. Conversion-time profiles for MMA miniemulsion polymerizations with different amounts of polymeric surfactants of (a) AS-I and (b) AS-II.*

Figure 4 shows the kinetics of the RAFT/miniemulsion polymerization of MMA stabilized by AS-I and AS-II, respectively, at the different concentrations of the polymeric surfactants. On the whole, the polymerization rate increased with the increasing amounts of polymeric surfactants because of the increasing droplet number would result in many more polymerization loci and a faster rate of RAFT miniemulsion polymerization of MMA. Meanwhile, the colloidal stability was greatly improved. In the cases of AS-I and AS-II used, no red organic layer was present during polymerization, and the latex product was shelf stable for several months. However, AS-III did not act well in the RAFT miniemulsion polymerization. The reason is due to that there are less positive charge groups in AS-III and weaker repulsion between particles comparing to the other two systems above-mentioned.

Considering the concentrations of polymeric surfactants affect the kinetics of RAFT miniemulsion polymerization, the molecular weights of latexes and PDIs, we studied the first-order linear relationship between $M_n$ and conversion of MMA at different concentrations of AS-I and AS-II. Figure 5 shows that the RAFT miniemulsion polymerization of MMA in the presence of 2 to 5 wt% AS-I or AS-II have a better living polymerization character. The experimental $M_n$ data fit well with the theoretical molecular weights. In the case of AS-I, all the

Downloaded by COLUMBIA UNIV on June 27, 2012 | http://pubs.acs.org
Publication Date: August 13, 2009 | doi: 10.1021/bk-2009-1024.ch019

PDI values were fairly below the benchmark of 1.3. In the system of AS-II, the PDI values are also very low, except for the system used 1 wt% AS-II as stabilizer. These results indicate that the polymeric surfactants containing cationic polyelectrolyte and hydrophobic long alkyl chain are efficient stabilizer for RAFT-mediate polymerization in heterogeneous system.

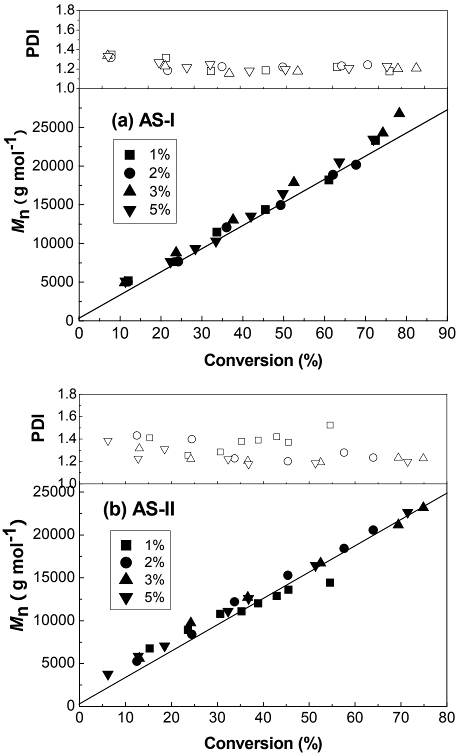

*Figure 5. The evolution of $M_n$ and the PDI as a function of conversion with different amounts of (a) AS-I and (b) AS-II.*

The particle size and particle size distribution (size PDI) of the PMMA latexes were monitored after the polymerization. Figure 6 shows the typical statistic graphs of size distributions at the different concentrations of AS-I and AS-II, respectively. It is very obvious that the monomerdal peaks appeare for size PDIs in the range of 2 to 5 wt% surfactants based on the amount of MMA. The results can be attributed to the electrostatic effect and anchoring function of the polymeric surfactants to the latex particles.

Downloaded by COLUMBIA UNIV on June 27, 2012 | http://pubs.acs.org
Publication Date: August 13, 2009 | doi: 10.1021/bk-2009-1024.ch019

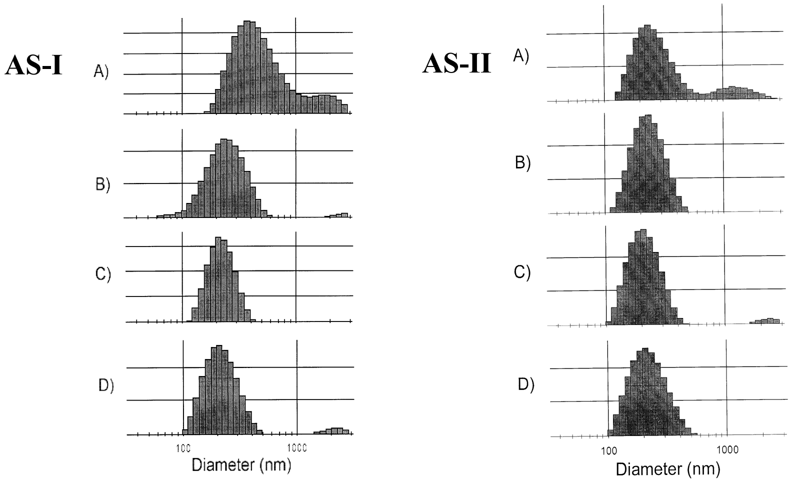

*Figure 6. The typical statistic graphs of particle size distributions of the microspheres prepared by RAFT/miniemulsion polymerization using polymeric surfactants AS-I and AS-II, respectively. The corresponding amounts of polymeric surfactant based on the amount of monomer MMA were A) 1%, B) 2%, C) 3%, and D) 5%, respectively.*

## Conclusions

Living radical polymerization of MMA in a miniemulsion by reversible addition-fragmentation chain transfer (RAFT) has been successfully realized in the presence of polymeric surfactants, namely poly{[(acryloyloxy)ethyltrimethyl ammonium chloride]-*co*-stearyl methacrylate}. The linear relationship between the MMA monomer conversion and the molecular weight, as well as lower polydispersity index (PDI), shows that these polymerization processes were under control. This method demonstrates that the comblike cationic polyelectrolyte is efficient stabilizer for RAFT miniemulsion polymerization.

## Acknowledgements

The authors gratefully acknowledge the financial supports from the Natural Science Foundation of Jiangsu Province (BK2008157), the National Natural Science Foundation of China (20474041), and Qing Lan Project for Innovation Team of Jiangsu Province, China.

## References

1. Per Zetterlund, B.; Kagawa, Y.; Okubo, M. *Chem. Rev.* **2008,** *108,* 3747-3794.

Downloaded by COLUMBIA UNIV on June 27, 2012 | http://pubs.acs.org
Publication Date: August 13, 2009 | doi: 10.1021/bk-2009-1024.ch019

2. Cunningham, M. F. *Prog. Polym. Sci.*, **2008**, *33*, 365–398.
3. Save, M.; Guillaneuf, Y.; Gilbert, R. G. *Aust. J. Chem.* **2006**, *59*, 693.
4. McLeary J. B.; Klumperman, B. *Soft Matter*, **2006**, *2*, 45-53.
5. Cunningham, M. F. *Prog. Polym. Sci.*, **2002**, *27*, 1039-1067.
6. Barner-Kowollik, C.; Davis, T. P.; Heuts, J. P. A.; Stenzel, M. H.; Vana, P.; Whittaker, M. *J. Polym. Sci. Part A: Polym. Chem.* **2003**, *41*, 365-375.
7. Monteiro, M. J.; Hodgson, M.; de Brouwer, H. *J. Polym. Sci. Part A: Polym. Chem.* **2000**, *38*, 3864-3874.
8. Prescott, S. W.; Ballard, M. J.; Rizzardo, E.; Gilbert, R. G. *Aust. J. Chem.* **2002**, *55*, 415-424.
9. Ferguson, C. J.; Hughes, R. J.; Pham, B. T. T.; Hawkett, B. S.; Gilbert, R. G.; Serelis, A. K. *et al. Macromolecules* **2002**, *35*, 9243-9245.
10. Ferguson, C. J.; Hughes, R. J.; Nguyen, D.; Pham, B. T. T.; Gilbert, R. G.; Serelis, A. K. *et al. Macromolecules* **2005**, *38*, 2191-2204.
11. Manguian, M.; Save, M.; Charleux, B. *Macromol. Rapid Commun.* **2006**, *27*, 399-404.
12. Freal-Saison, S.; Save, M.; Bui, C.; Charleux, B.; Magnet, S. *Macromolecules* **2006**, *39*, 8632-8638.
13. Lansalot, M.; Davis, T.P.; Heuts, J.P.A. *Macromolecules*, **2002**, *35*, 7582-7591.
14. Zhou X.D.; Ni P. H., Yu Z. Q., *Polymer*, **2007**, *48*, 6262-6271.
15. de Brouwer, H.; Tsavalas, J.G.; Schork, F.J.; Monteiro, M.J. *Macromolecules* **2000**, *33*, 9239-9246.
16. Mcleary, J. B.; Tonge, M. P.; de Wet-Roos, D.; Sanderson, R. D.; Klumperman, B. *J. Polym. Sci. Part A: Polym. Chem.* **2004**, *42*, 960- 974.
17. Shim, S. E.; Lee, H.; Choe, S. *Macromolecules* **2004**, *37*, 5565-5571.
18. Matahwa, H.; McLeary, J. B.; Sanderson, R. D. *J. Polym. Sci. Part A: Polym. Chem.* **2006**, *44*, 427-442.
19. Tsavalas, J. G.; Schork, F. J.; de Brouwer, H.; Monteiro, M. J. *Macromolecules* **2001**, *34*, 3938-3946.
20. Yang, L.; Luo, Y. W.; Li, B. G. *Polymer* **2006**, *47*, 751-762.
21. Zhang, F.; Ni, P. H.; Xiong, Q. F.; Yu, Z. Q. *J. Polym. Sci. Part A: Polym. Chem.* **2005**, *43*, 2931-2940.
22. Yu, Z. Q.; Ji, X. L.; Ni, P. H. *Colloid Polym. Sci.* **2006**, *285*, 211-218.
23. Monteiro, M. J.; Hodgson, M.; de Brouwer, H. *J. Polym. Sci. Part A: Polym. Chem.* **2000**, *38*, 3864-3874.
24. Xiong Q. F.; Ni, P. H.; Zhang, F.; Yu, Z.Q. *Polym. Bull. (Heidelberg)* **2004**, *53*, 1-8.
25. Ni, P. H.; Zhang, M. Z.; Ma, L. H.; Fu, S. K. *Langmuir* **2006**, *22*, 6016-6023.
26. Mitsukami, Y.; Donovan, M. S.; Lowe, A. B.; McCormick, C. L. *Macromolecules* **2001**, *34*, 2248-2256.
27. Thang, S. H.; Chong, Y. K.; Mayadunne, R. T. A.; Moad, G.; Rizzardo, E. *Tetrahedron Lett.* **1999**, *40*, 2435-2438.
28. Luo, Y. W.; Tsavalas, J.; Schork, F. J. *Macromolecules* **2001**, *34*, 5501-5507.

Downloaded by COLUMBIA UNIV on June 27, 2012 | http://pubs.acs.org
Publication Date: August 13, 2009 | doi: 10.1021/bk-2009-1024.ch019

Downloaded by COLUMBIA UNIV on June 26, 2012 | http://pubs.acs.org
Publication Date: August 13, 2009 | doi: 10.1021/bk-2009-1024.ch020

## Chapter 20

# Nitroxide-Mediated Controlled Free-Radical Copolymerization of Poly(ethylene glycol) Methyl Ether Methacrylate and Methacrylic Acid. Toward New Water-Soluble Macroinitiators

**Charlotte Dire,[1] Julien Nicolas,[2,]* Ségolène Brusseau,[1] Bernadette Charleux,[1,]* Stéphanie Magnet,[3] Laurence Couvreur[3]**

**[1] UPMC Paris 6, CNRS, UMR 7610, Laboratoire de Chimie des Polymères, 4 place Jussieu, 75252 Paris cedex 05, France**
**[2] Univ Paris-Sud, CNRS, UMR 8612, Laboratoire de Physico-Chimie, Pharmacotechnie et Biopharmacie, Faculté de Pharmacie, 5 rue Jean-Baptiste Clément, 92296 Châtenay-Malabry, France**
**[3] Arkema, Groupement de Recherches de Lacq, RN 117, B.P. n°34, 64170, Lacq, France**

New water-soluble macroalkoxyamines were synthesized via nitroxide-mediated controlled free-radical copolymerization of poly(ethylene glycol) methyl ether methacrylate with a low percentage of styrene and terpolymerization with methacrylic acid at a temperature below 80 °C. They were employed as macroinitiators for the synthesis of amphiphilic block copolymers, either in bulk or in aqueous emulsion polymerization. In the latter process, PEG-coated, amphiphilic diblock copolymer micelles were generated in situ.

In Controlled/Living Radical Polymerization: Progress in RAFT, DT, NMP & OMRP; Matyjaszewski, K.;
ACS Symposium Series; American Chemical Society: Washington, DC, 2009.

# Introduction

Controlled radical polymerization (CRP) in emulsion (*1,2,3*) has recently witnessed a significant improvement with the use of purposely designed water-soluble alkoxyamines based on the nitroxide SG1 (*4*), one of the most efficient control agents for nitroxide-mediated polymerization (NMP) (*5*). As opposed to the use of low molar mass, water-soluble alkoxyamines in emulsion polymerization (*6,7,8,9*), which require the addition of a classical surfactant to ensure the colloidal stability, the use of the macromolecular counterpart (the so-called macroalkoxyamine) is a way to achieve surfactant-free batch process at high solids content (*10,11*). Indeed, the water-soluble macroalkoxyamine acts equally as the initiator, the stabilizer and the control agent. The concept is based on chain extension by a controlled/living free-radical polymerization process simultaneously with self-assembly of the amphiphilic block copolymer formed in situ. In other words, the method leads to direct formation of amphiphilic block copolymer micelles and the system requires neither the addition of a classical initiator, nor that of a surfactant. It therefore corresponds to a breakthrough in controlled/living free-radical emulsion polymerization with a reduction of the number of reagents (only two, i.e. the monomer and the macroalkoxyamine) and the formation of self-stabilized polymer particles.

In this view, the synthesis of novel macroalkoxyamines and their use for surfactant-free, batch emulsion polymerization are of high interest as they may allow the particle colloidal properties to be finely tuned due to any subtle changes in the stabilizing corona (i.e. the macroalkoxyamine moiety). The first example in this field reported the use of SG1-terminated poly(sodium acrylate) water-soluble macroalkoxyamines for surfactant-free emulsion polymerization of styrene and *n*-butyl acrylate at 20 wt.% solids (*10,11*). Even though the macroinitiator efficiency was below 100%, very stable particles were eventually recovered, exhibiting very small diameters and narrow particle size distributions.

Thanks to the latest advances in NMP of methacrylic esters, the synthesis of well-defined polymethacrylates mediated by the nitroxide SG1 is now conceivable (*12,13*). To overcome the main drawback of such a polymerization (i.e. the too large activation-deactivation equilibrium constant, $K$, increasing the concentration of propagating radicals and hence the occurrence of irreversible termination reactions), the simplest available solution is to add a very small amount of styrene (4.4–8.8 mol.%) to the polymerization medium in order to drastically drop $K$ and to promote the reversible deactivation process. We recently made the most of this result by performing surfactant-free emulsion polymerization of methyl methacrylate with a small amount of styrene (8.8 mol.% or below) at low temperature (60–90 °C) via the use of a poly(sodium methacrylate-*co*-styrene) (P(NaMA-*co*-S)) macroalkoxyamine exhibiting a high dissociation rate constant (*14*,*15*). In a similar way as observed previously, small particles composed of amphiphilic diblock copolymer chains were recovered.

Poly(ethylene glycol) (PEG), also called poly(ethylene oxide) (PEO) or poly(oxyethylene) (POE), is a hydrophilic and flexible polymer often used as a steric stabilizer for latex particles. In our case, combining PEG and NaMA in the macroalkoxyamine in order to perform both steric and electrostatic stabilization

Downloaded by COLUMBIA UNIV on June 26, 2012 | http://pubs.acs.org
Publication Date: August 13, 2009 | doi: 10.1021/bk-2009-1024.ch020

might be advantageous. Besides, PEG is deeply employed in the pharmaceutical area as a key material, especially for drug delivery purposes such as polymer-protein/peptide bioconjugates (termed PEGylation) (*16,17*) or “stealth” long-circulating nanoparticles (*18*). Recently, it has been shown that the above-mentioned nitroxide-mediated copolymerization approach with a low percentage of styrene was also successfully applied to poly(ethylene glycol) methyl ether methacrylate (MePEGMA), yielding well-defined comblike polymethacrylates with PEG side-chains (*19*). The purpose of this work is now to investigate the behavior of novel SG1-terminated, water-soluble macroalkoxyamines combining both MePEGMA and NaMA monomer units for bulk and surfactant-free emulsion polymerization.

Downloaded by COLUMBIA UNIV on June 26, 2012 | http://pubs.acs.org
Publication Date: August 13, 2009 | doi: 10.1021/bk-2009-1024.ch020

## Experimental Part

### Materials

Methacrylic acid (MAA, purest grade, Acros) and poly(ethylene glycol) methyl ether methacrylate (MePEGMA, average $M_n$ = 300 g.mol$^{-1}$, Aldrich) were used without further purification. Styrene (S, 99%, Aldrich) and methyl methacrylate (MMA, 99%, Aldrich) were distilled under reduced pressure before use. The *N*-(2-methylpropyl)-*N*-(1-diethylphosphono-2,2-dimethylpropyl)-*O*-(2-carboxyl prop-2-yl) hydroxylamine initiator (the so-called BlocBuilder®, 99%) and the *N*-tert-butyl-*N*-(1-diethyl phosphono-2,2-dimethylpropyl) nitroxide (SG1, 85%) were kindly supplied by Arkema. 1,4-Dioxane (synthesis grade, SDS), ethanol (synthesis grade, VWR Prolabo), trimethylsilyldiazomethane (2 M solution in hexane, Aldrich), sodium carbonate ($Na_2CO_3$, pure, Prolabo), NaOH 1 M (1 M solution in water, SDS) and diethyl phosphite (98%, Aldrich) were used as received. For emulsion polymerizations, deionized water was used (USF Regeneration).

### Analytical techniques

$^1$H NMR spectroscopy was performed on Bruker spectrometers, either an Avance 300 (300 MHz) or an AC250 (250 MHz). Deuterated solvents were used ($CDCl_3$ for the P(MePEGMA-*co*-S) copolymers and DMSO-$d_6$ for the P(MePEGMA-*co*-MAA-*co*-S) copolymers). Composition of the precipitated copolymers containing methacrylic acid units was determined by quantitative $^{13}$C NMR spectroscopy in DMSO-$d_6$ solution using a Bruker Avance 300 spectrometer operating at a frequency of 75 MHz. The $^{31}$P NMR spectra were recorded in 10 mm diameter tubes at 25 °C, on a Bruker Avance 300 spectrometer operating at the frequency of 121.44 MHz. Spectra were recorded applying the following conditions: spectral width of 75 ppm, flip angle of 10°, relaxation delay of 90 s, digital resolution of 0.27 Hz.pt$^{-1}$ and suppression of the NOE. The chemical shift scale was calibrated on the basis of the added diethyl phosphite at $\delta = 7.1$ ppm.

Size exclusion chromatography (SEC) was used for molar mass analysis of the copolymers. The set-up is composed of two PSS linear M columns thermostated at 40 °C with THF as an eluent at a flow rate of 1 $mL.min^{-1}$. Detection was made with a refractometer Refracto Monitor IV (LDC analytical). This technique allowed $M_n$ (the number-average molar mass), $M_w$ (the weight-average molar mass) and $M_w/M_n$ (the polydispersity index, PDI) to be determined. Before injecting the polymer samples containing methacrylic acid units, a reaction of methylation was performed, to turn the acid groups into methyl esters, using trimethylsilyldiazomethane. The Viscotek OmniSEC software was used for data analysis. The calibration curve was based on poly(methyl methacrylate) (PMMA) or on polystyrene (PS) standards from Polymer Laboratories and toluene was used as a flow-rate marker.

Glass transition temperatures ($T_g$) of the copolymers were determined by differential scanning calorimetry (DSC) on a TA Instrument 9900 equipped with a DSC910 module. Samples were heated between –150 and +150 °C at a heating rate of 20 $°C.min^{-1}$.

The z-average diameter ($D_z$) of the latex particles and the polydispersity factor ($\sigma$) were measured by dynamic light scattering (DLS) at a temperature of 25 °C and an angle of 90 ° using a Zetasizer Nano Series (S90) from Malvern Instrument. Before measurements, the latex samples were diluted in deionized water.

Downloaded by COLUMBIA UNIV on June 26, 2012 | http://pubs.acs.org
Publication Date: August 13, 2009 | doi: 10.1021/bk-2009-1024.ch020

## Synthesis of a P(MePEGMA-*co*-S)-SG1 macroalkoxyamine

Synthesis of the P(MePEGMA-*co*-S)-SG1 macroalkoxyamine **M1** (Table 1) was adapted from literature procedure (*19*). Briefly, a mixture of MePEGMA (18.75 g, 0.83 $mol.L^{-1}$), styrene (0.63 g, 0.08 $mol.L^{-1}$, initial molar fraction: $f_{S0}$ = 0.088), SG1 (0.023 g, $1.04 \times 10^{-3}$ $mol.L^{-1}$, 11.8 mol.% based on the initiator) and ethanol (57 mL) was deoxygenated by nitrogen bubbling for 20 min at room temperature. The BlocBuilder® alkoxyamine initiator (0.25 g, $8.72 \times 10^{-3}$ $mol.L^{-1}$) was added and nitrogen bubbling was carried out for an additional 10 min. The mixture was then introduced into a 250 mL three-neck round-bottom flask heated at 78.5 °C during 3 h. Time zero of the reaction was triggered when the temperature in the reactor reached 75 °C. The copolymer was then precipitated in diethyl ether and dried under high vacuum until constant weight.

## Synthesis of P(MePEGMA-*co*-MAA-*co*-S)-SG1 macroalkoxyamines

A typical experimental procedure was applied and experiment **M2** (Table 1) is described in detail below. A mixture of MePEGMA (45.05 g, 1.0 $mol.L^{-1}$, initial molar fraction: $f_{MePEGMA0}$ = 0.456), MAA (12.92 g, 1.0 $mol.L^{-1}$, initial molar fraction: $f_{MAA0}$ = 0.456), S (3.01 g, 0.19 $mol.L^{-1}$, initial molar fraction: $f_{S0}$ = 0.088) and free SG1 (0.0955 g, $2.17 \times 10^{-3}$ $mol.L^{-1}$, 10.5 mol.% based on the initiator) in the solvent (ethanol, 92.42 mL) was deoxygenated with a nitrogen stream for 20 min at room temperature. The BlocBuilder® initiator was then added (1.178 g, $2.06 \times 10^{-2}$ $mol.L^{-1}$), and nitrogen bubbling was carried out for an additional 10 min. The so-formed solution was then added into a 250 mL three-neck round-bottom flask, immersed in a thermostated oil bath and fitted with a reflux condenser, a nitrogen inlet and a thermometer. The polymerization was carried out at 78.5 °C. Time zero of the polymerization was chosen when the temperature of the mixture reached 70 °C. Samples were periodically withdrawn and cooled in an ice-water bath to stop the reaction. The overall monomer conversion was determined by $^1$H NMR. Before using the copolymers as macroinitiators, the polymerization medium was precipitated in cold diethyl ether and dried under vacuum at room temperature for 3 days to eliminate monomers and solvent. Experimental conditions are summarized in Table 1.

### Bulk polymerization of styrene initiated by a P(MePEGMA-*co*-S)-SG1 macroalkoxyamine

Downloaded by COLUMBIA UNIV on June 26, 2012 | http://pubs.acs.org
Publication Date: August 13, 2009 | doi: 10.1021/bk-2009-1024.ch020

Synthesis of the P(MePEGMA-*co*-S)-*b*-PS block copolymer (**C2**) was as follows. The P(MePEGMA-*co*-S)-SG1 macroalkoxyamine **M1** (1.52 g, $9.17 \times 10^{-5}$ mol, $4.9 \times 10^{-2}$ mol.L$^{-1}$), styrene (1.72 g, $1.65 \times 10^{-2}$ mol, 8.74 mol.L$^{-1}$) and free SG1 (0.0027 g, $9.25 \times 10^{-6}$ mol, 10.0 mol.% based on **M1**) were placed in a Schlenk tube, sealed with a rubber septum. The mixture was then deoxygenated by nitrogen bubbling during 30 min and the Schlenk tube was placed in an oil bath at 110 ºC, triggering the beginning of the polymerization. Samples were removed periodically using degassed syringes and quenched in iced water bath for conversion and molecular weight analysis. Final copolymer was precipitated in hexane and dried under high vacuum.

A similar protocol was employed for the synthesis of the P(MePEGMA-*co*-S)-*b*-PS block copolymer (**C1**), excepted that no free SG1 was initially introduced in the reaction mixture, the reaction temperature was increased up to 120 °C and a high molar mass copolymer was targeted. Experimental conditions are summarized in Table 2.

### Polymerization of styrene initiated by a P(MePEGMA-*co*-MAA-*co*-S)-SG1 macroalkoxyamine in 1,4-dioxane solution

A typical experiment is as follows (experiment **C3**, Table 2). The purified P(MePEGMA-*co*-MAA-*co*-S)-SG1 copolymer **M2** (0.3295 g, $8 \times 10^{-3}$ mol.L$^{-1}$), styrene (2.122 g, 4.86 mol.L$^{-1}$) and 1,4-dioxane (1.93 mL) were placed in a Schlenk tube. After degassing by six freeze-pump-thaw cycles, the polymerization was run at 120 °C for 7 h. The tube was then sunk in an ice-water bath to quench the reaction. Monomer conversion was calculated by gravimetry and the obtained copolymer was analyzed by size exclusion chromatography. The various experimental conditions are reported in Table 2.

Downloaded by COLUMBIA UNIV on June 26, 2012 | http://pubs.acs.org
Publication Date: August 13, 2009 | doi: 10.1021/bk-2009-1024.ch020

**Table 1. Experimental conditions for the SG1-mediated copolymerizations of poly(ethylene glycol) methyl ether methacrylate (MePEGMA) and methacrylic acid (MAA) with a low proportion of styrene (S) in ethanol at 78.5 °C.**

| Entry | $[\mathrm{MePEGMA}]_0$ (mol.L$^{-1}$) | $[\mathrm{MAA}]_0$ (mol.L$^{-1}$) | $[\mathrm{S}]_0$ (mol.L$^{-1}$) | $f_{\mathrm{MePEGMA0}} / f_{\mathrm{MAA0}} / f_{\mathrm{S0}}$[a] | $[\mathrm{BlocBuilder}^{®}]_0$ (mol.L$^{-1}$) | $r$[b] (%) | Target $M_n$ at 100% conversion (g.mol$^{-1}$) | Time (h) |
|---|---|---|---|---|---|---|---|---|
| **M1** | 0.83 | 0 | 0.08 | 0.912 / 0 / 0.088 | $2.06 \times 10^{-2}$ | 11.8 | 30 100 | 3 |
| **M2** | 1.0 | 1.0 | 0.19 | 0.456 / 0.456 / 0.088 | $2.06 \times 10^{-2}$ | 10.5 | 20 100 | 4 |
| **M3** | 0.3 | 2.7 | 0.30 | 0.09 / 0.82 / 0.09 | $3.60 \times 10^{-2}$ | 11.3 | 10 800 | 3.4 |

[a] Initial molar fractions of MePEGMA, MAA and S.

[b] $r = 100 \times [\mathrm{SG1}]_0 / [\mathrm{BlocBuilder}^{®}]_0$.

Downloaded by COLUMBIA UNIV on June 26, 2012 | http://pubs.acs.org
Publication Date: August 13, 2009 | doi: 10.1021/bk-2009-1024.ch020

**Table 2. Experimental conditions for the chain extensions of the SG1-capped P(MePEGMA-*co*-S) and P(MePEGMA-*co*-MAA-*co*-S) copolymers with styrene.**

| Entry | Macroinitiator; concentration ($mol.L^{-1}$) | $[S]_0$ ($mol.L^{-1}$) | $r^e$ (%) | Target $M_n$ at 100 % conversion ($g.mol^{-1}$) | Time (h) |
|---|---|---|---|---|---|
| **C1**[a] | **M1**[c]; $1.1 \times 10^{-2}$ | 8.74 | 0 | 99 300 | 7 |
| **C2**[b] | **M1**[c]; $4.9 \times 10^{-2}$ | 8.74 | 10.0 | 35 150 | 4.5 |
| **C3**[a] | **M2**[d]; $8 \times 10^{-3}$ | 4.86 | 0 | 72 000 | 7 |
| **C4**[a] | **M3**[d]; $5.5 \times 10^{-3}$ | 3.59 | 0 | 72 000 | 7 |

[a] 120 °C; [b] 110 °C; [c] bulk; [d] in 1,4-dioxane solution.
[e] $r = 100 \times [SG1]_0 / [macroinitiator]_0$.

## Surfactant-free emulsion copolymerization of methyl methacrylate and styrene initiated by P(MePEGMA-*co*-MAA-*co*-S)-SG1 macroalkoxyamines

A typical polymerization procedure was applied and experiment **E2** (Table 3) is described in detail below. A mixture of water (98.84 g), the P(MePEGMA-*co*-MAA-*co*-S)-SG1 macroinitiator **M3** (3.184 g, $6.19 \times 10^{-3}$ $mol.L^{-1}$), NaOH 1 M (21.43 g, $1.78 \times 10^{-1}$ $mol.L^{-1}$, i.e. 1 equiv. NaOH based on the carboxylic acid groups) and $Na_2CO_3$ (0.445 g, $3.5 \times 10^{-2}$ $mol.L^{-1}$) was introduced in a 250 mL round-bottom flask and stirred at room temperature until complete solubilization of the P(MePEGMA-*co*-MAA-*co*-S)-SG1 macroinitiator. The comonomer mixture (MMA (27.36 g, $2.736 \times 10^{-1}$ mol) and S (2.77 g, $2.66 \times 10^{-2}$ mol, initial molar fraction of S in the comonomer mixture: $f_{S0} = 0.088$), 19.46 wt.% based on water) was then added to the aqueous solution and the obtained unstable biphasic system was deoxygenated by nitrogen bubbling for 20 min. This mixture was introduced into a 300 mL thermostated glass reactor (PARR / Equilabo), which corresponds to time zero of the polymerization, and was heated at 85 °C for 6 h. Samples were periodically withdrawn to follow the overall monomer conversion by gravimetry and to analyze the copolymers and the particles by methods described below. The various experimental conditions are reported in Table 3.

**Table 3. Experimental conditions for the surfactant-free emulsion copolymerizations of methyl methacrylate with a small fraction of styrene ($f_{S0} = 0.088$) initiated by P(MePEGMA-*co*-MAA-*co*-S)-SG1 macroinitiator.**[a]

| Entry | Macroinitiator; concentration ($mmol.L^{-1}_{water}$) | Monomer content (wt.%) | Target $M_n$ at 100% conversion ($g.mol^{-1}$) |
|---|---|---|---|
| **E1** | **M2**; 6.64 | 19.0 | 47 200 |
| **E2** | **M3**; 6.19 | 19.5 | 44 800 |

[a] $T = 85$ °C; $[Na_2CO_3]_0 = 35$ $mmol.L^{-1}_{water}$; 1 equivalent NaOH based on the COOH groups; pH = 8.

## Results and Discussion

### SG1-terminated macroalkoxyamines based on MAA and MePEGMA

Water-soluble macroalkoxyamines based on MePEGMA (**M1**, Tables 1 and 4) and on MePEGMA and MAA (**M2-M3**, $f_{\mathrm{MAA0}}$ = 0.456 and 0.82, Tables 1 and 4) were synthesized by SG1-mediated solution copolymerization in ethanol at 78.5 °C with 8.8 mol.% of styrene in the initial feed. The polymerization time was kept rather short (2–4 h) so as to recover copolymers with the highest chain-end functionality. As expected, SG1-mediated copolymerizations of styrene and MePEGMA proceeded via a controlled fashion and yielded a well-defined copolymer with a polydispersity index as low as 1.26 (Table 4). In addition, experiments **M2** and **M3** did not seem to be affected by the terpolymerization process. Indeed, linear evolutions of logarithmic conversions with time and of molar masses with conversion were noticed together with high initiating efficiencies and rather low PDI (Table 4 and Figure 1).

Downloaded by COLUMBIA UNIV on June 26, 2012 | http://pubs.acs.org
Publication Date: August 13, 2009 | doi: 10.1021/bk-2009-1024.ch020

**Table 4. Characteristics of the SG1-based macroalkoxyamines used in this work.**

| Entry | Structure of the copolymer | $M_n$ (g.mol$^{-1}$) | $M_w/M_n$ |
|---|---|---|---|
| **M1** | P(MePEGMA-*co*-S)-SG1 | 16 400 | 1.26 |
| **M2** | P(MePEGMA-*co*-MAA-*co*-S)-SG1 | 9 400 | 1.38 |
| **M3** | P(MePEGMA-*co*-MAA-*co*-S)-SG1 | 4 400 | 1.32 |

### *Chain-end analysis and extensions*

The **M1** macroalkoxyamine was analyzed by $^{1}$H and $^{31}$P NMR spectroscopy to investigate the chain-end structure. On the $^{1}$H NMR spectrum (Figure 2a), the effective incorporation of styrene in the copolymer was demonstrated with a good agreement with the initial feed ratio (styrene in the copolymer is 12 mol.%). Besides, chain-end protons were partially visible. Indeed, even though the methyl protons peak from the 2-(hydroxycarbonyl)prop-2-yl moiety is almost entirely covered by the polymer peak in the 1.5–2.0 ppm region, the peak from the *tert*-butyl groups of the SG1, clearly visible around 0.5–0.6 ppm, qualitatively demonstrated the chain-end functionalization of the copolymer by the nitroxide. This result is corroborated by the $^{31}$P NMR spectrum, on which characteristic peaks of the SG1-based alkoxyamine were detected in the 23–25 ppm region (Figure 2b). However, a discrepancy between the real molar mass of the macroalkoxyamines and the experimental one derived from SEC analysis (with a calibration curve based on PMMA standards) is highly expected, which prevents the use of $^{31}$P NMR for the estimation of the living chain fraction. Therefore, chain extension experiments were performed to better assess the chain-end functionality of the P(MePEGMA-*co*-S)-SG1 copolymers.

Downloaded by COLUMBIA UNIV on June 26, 2012 | http://pubs.acs.org
Publication Date: August 13, 2009 | doi: 10.1021/bk-2009-1024.ch020

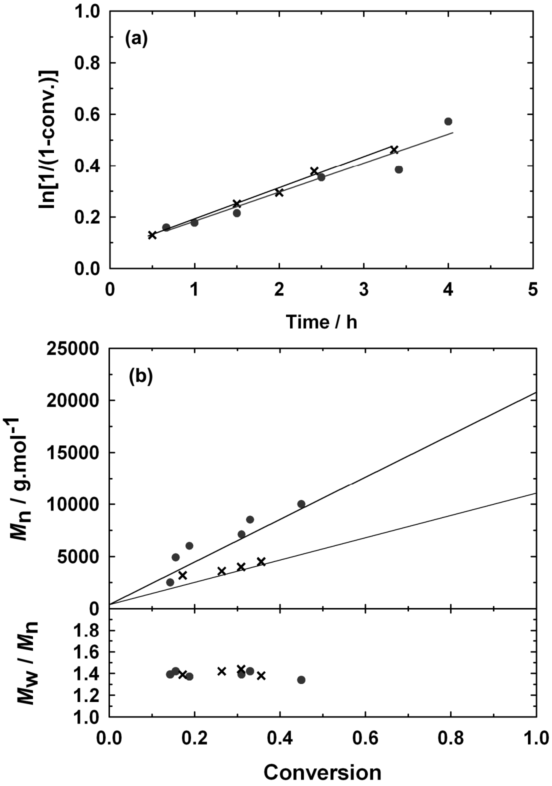

*Figure 1. Logarithmic molar conversion vs time plot (a) and evolution of $M_n$ and $M_w/M_n$ vs weight conversion (the full lines represent the theoretical $M_n$) (b) for the SG1-mediated copolymerizations **M2** (●) and **M3** (×).*

The macroalkoxyamine **M1** was first subjected to a reinitiation step in the bulk polymerization of styrene at 120 °C during 7 h in order to allow a complete shift of the SEC peak toward higher molar mass via chain extension. It is unambiguous on Figure 3 that a P(MePEGMA-*co*-S)-*b*-PS diblock copolymer (**C1**) was indeed obtained. A nearly complete shift of the SEC peak was noticed in very good agreement with previous chain-extensions of SG1-terminated polymethacrylates (*13,14*). Only a tiny shoulder was observed at the macroinitiator elution volume accounting for a small fraction of dead chains. This result reinforced the idea of a high living-chain fraction of such MePEGMA-based macroalkoxyamine, very similar to those obtained with MMA or MAA as the main monomer. SEC (PS standards) of the resulting block copolymer gave $M_n$ = 121 400 g.mol$^{-1}$ with a high polydispersity index of 2.5, not surprising since the experimental conditions of the chain-extension step were not appropriate for a controlled growth of the second block (high target $M_n$). Identical results were obtained with the terpolymers **M2** and **M3** containing different proportions of methacrylic acid upon chain extension with styrene in

1,4-dioxane solution (experiments **C3** and **C4** in Table 4, Figure 4). The very good crossover efficiency makes thus possible the application of those copolymers as macroinitiators for the synthesis of well-defined, amphiphilic block copolymers, either in bulk, or in emulsion polymerization.

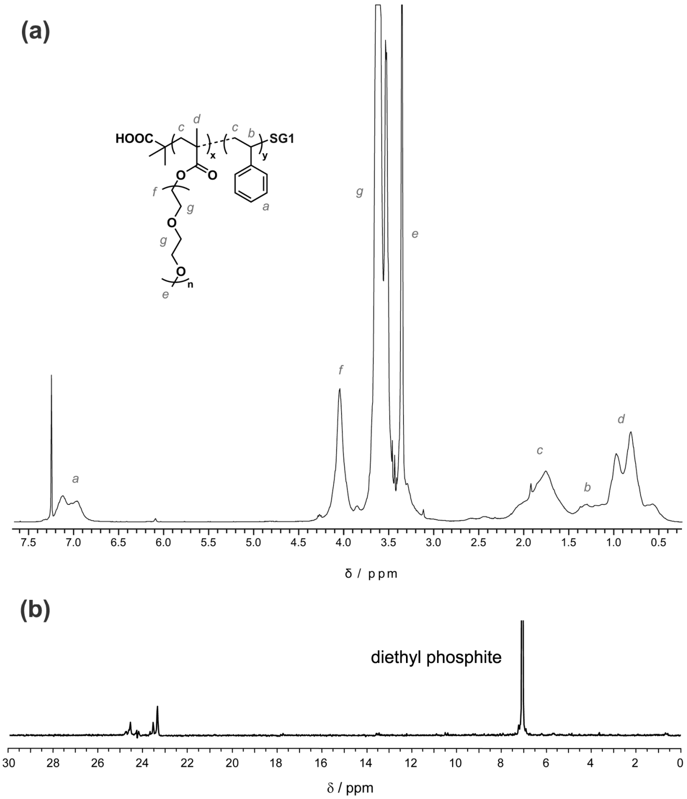

*Figure 2. $^{1}H$ (a) and $^{31}P$ (b) NMR spectra of the macroalkoxyamine **M1** in $CDCl_3$.*

*Synthesis of a well-defined block copolymer*

The synthesis of a well-defined P(MePEGMA-*co*-S)-*b*-PS block copolymer from the macroalkoxyamine **M1** was then considered (**C2**). Reaction temperature was slightly lowered to 110 °C, 10.0 mol.% of free SG1 was initially added to the reaction mixture and a more reasonable, low molar mass was targeted. As expected, first-order kinetic plot was linear throughout the polymerization, accounting for a constant number of propagating radicals (Figure 5a). A linear evolution of the number-average molar mass with the overall monomer conversion together with low polydispersity indexes were also obtained (Figure 5b). After 4.5 h, the final conversion was 43% and from SEC (PMMA standards), $M_n$ = 24 300 g.mol$^{-1}$ and $M_w/M_n$ = 1.36. From $^{1}$H NMR, the overall molar composition of the copolymer was 58/42 (MePEGMA/S; mol.%/mol.%).

Downloaded by COLUMBIA UNIV on June 26, 2012 | http://pubs.acs.org
Publication Date: August 13, 2009 | doi: 10.1021/bk-2009-1024.ch020

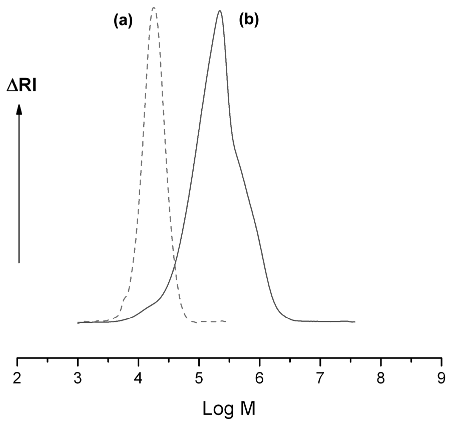

*Figure 3. Size-exclusion chromatography analysis of the P(MePEGMA-co-S)-SG1 macroalkoxyamine* ***M1*** *(a) and the P(MePEGMA-co-S)-b-PS block copolymer* ***C1*** *(b).*

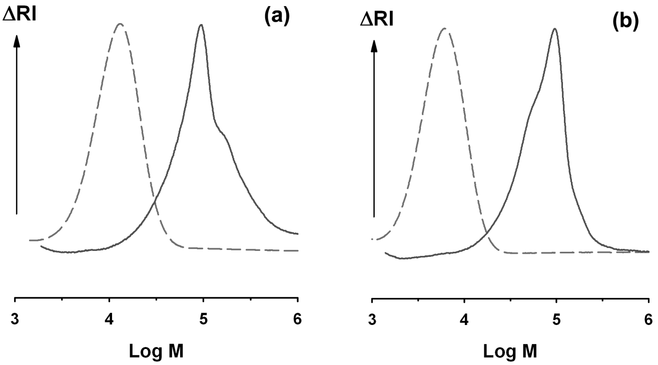

*Figure 4. Size-exclusion chromatography analysis of the P(MePEGMA-co-MAA-co-S)-SG1 macroalkoxyamine* ***M2*** *(dotted line), the P(MePEGMA-co-MAA-co-S)-b-PS block copolymer* ***C3*** *(solid line) (a), the P(MePEGMA-co-MAA-co-S)-SG1 macroalkoxyamine* ***M3*** *(dotted line) and the P(MePEGMA-co-MAA-co-S)-b-PS block copolymer* ***C4*** *(solid line) (b).*

DSC analysis of the P(MePEGMA-*co*-S)-SG1 macroalkoxyamine **M1** was performed (Figure 6) and a $T_g$ of –54 °C was observed, in very good agreement with the value reported in the literature ($T_g$ = –57.6 °C) for a PMePEGMA homopolymer synthesized from the same molar mass monomer ( *20* ). Interestingly, this also demonstrated that the $T_g$ of the copolymer does not seem to be affected by the few styrene subunits incorporated into the chain structure. As expected, the block copolymer **C2** exhibited two distinct glass transition temperatures at –52 and 112 °C, corresponding to PEG and PS domains, respectively.

Downloaded by COLUMBIA UNIV on June 26, 2012 | http://pubs.acs.org
Publication Date: August 13, 2009 | doi: 10.1021/bk-2009-1024.ch020

Downloaded by COLUMBIA UNIV on June 26, 2012 | http://pubs.acs.org
Publication Date: August 13, 2009 | doi: 10.1021/bk-2009-1024.ch020

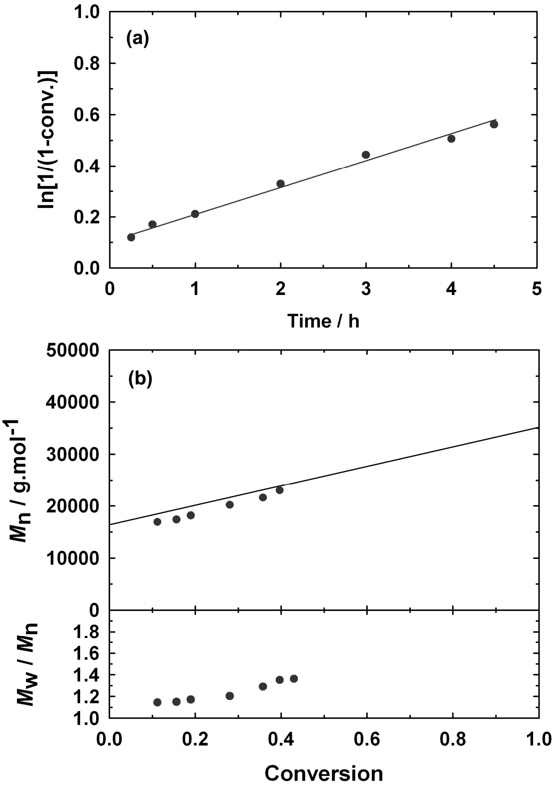

*Figure 5. P(MePEGMA-co-S)-b-PS block copolymer* ***C2*** *synthesized by SG1-mediated bulk polymerization of styrene initiated by the P(MePEGMA-co-S)-SG1 macroalkoxyamine* ***M1*** *at 110 °C. Ln[1/(1-conv.)] vs time plot (a) and evolution of $M_n$ and $M_w/M_n$ vs conversion (full line: theoretical $M_n$) (b).*

## Use of MePEGMA-based macroalkoxyamines M2 and M3 in surfactant-free emulsion polymerization

The surfactant-free batch emulsion copolymerizations of methyl methacrylate with a small percentage of styrene ($f_{S0}$ = 0.088) were performed at 85 °C in alkaline conditions using the P(MePEGMA-*co*-MAA-*co*-S)-SG1 macroalkoxyamines **M2** and **M3** as water-soluble initiators (Table 3). In the polymerization medium, those hydrophilic macroalkoxyamines are composed of MePEGMA and NaMA subunits in various proportions and may then contribute to the electrosteric stabilization of the particles. Both polymerizations were fast and 90% conversion was reached within 3 h (Figure 7a) as previously observed with the P(MAA-*co*-S)-SG1 macroinitiators (*15*). The controlled character of the polymerizations is illustrated in Figure 7b with the linear increase of $M_n$ with monomer conversion and the relatively low polydispersity indexes. More important is the complete shift of the SEC peaks indicating a complete

Downloaded by COLUMBIA UNIV on June 26, 2012 | http://pubs.acs.org
Publication Date: August 13, 2009 | doi: 10.1021/bk-2009-1024.ch020

reinitiation step and then the highly efficient synthesis of amphiphilic block copolymers, with a long hydrophobic block and a short hydrophilic one. Stable particles were created in the system upon self-assembly of the so-formed copolymers and exhibited a very small average diameter with, however, a low fraction of aggregates (leading to high values of the polydispersity factor). Moreover, the latex **E1**, initiated by the terpolymer macroalkoxamine **M2** with the highest proportion of MePEGMA was highly viscous (it had the texture of homogeneous, white cream).

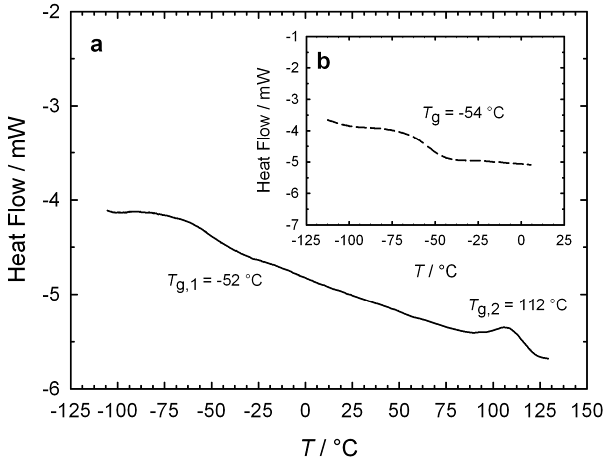

*Figure 6. DSC thermograms of the copolymer **C2** (a) and the macroalkoxyamine **M1** (b).*

**Table 5. Experimental results for the surfactant-free emulsion copolymerizations of methyl methacrylate with a small fraction of styrene ($f_{S0}$ = 0.088) initiated by a P(MePEGMA-*co*-MAA-*co*-S)-SG1 macroinitiator**

| Entry | Time | Conversion | $M_{n,th}$ | $M_{n,SEC}$ | PDI | DLS | |
|---|---|---|---|---|---|---|---|
| | (h) | (%) | (g.mol$^{-1}$) | (g.mol$^{-1}$) | | $D_z$ (nm) | σ[a] |
| **E1** | 2.9 | 90.3 | 43 900 | 47 800 | 1.5 | [b] | 1 |
| **E2** | 3.3 | 89.7 | 41 300 | 41 600 | 1.3 | 32 | 0.3 |

[a] Polydispersity factor

[b] The value measured by dynamic light scattering (DLS) is not correct because of too high a polydispersity factor (σ = 1).

Downloaded by COLUMBIA UNIV on June 26, 2012 | http://pubs.acs.org
Publication Date: August 13, 2009 | doi: 10.1021/bk-2009-1024.ch020

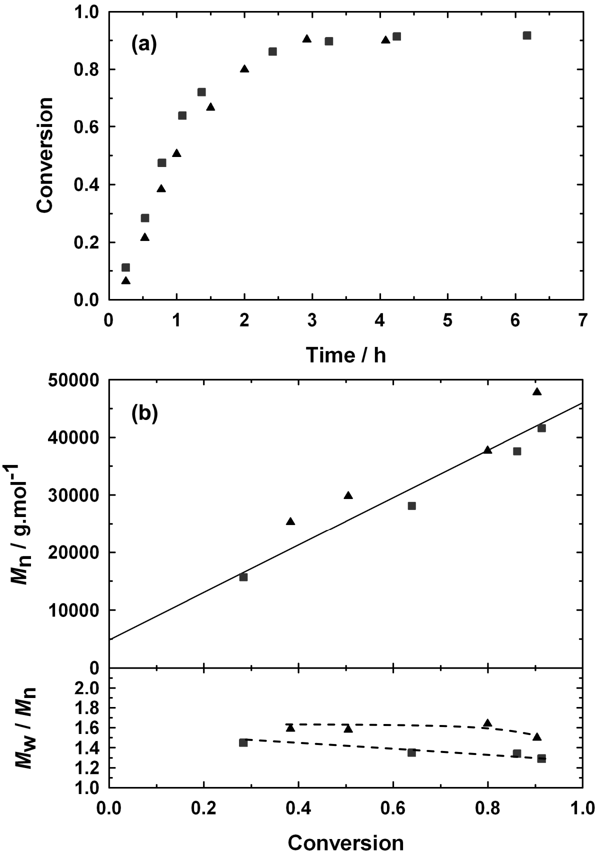

*Figure 7. Overall conversion vs time (a) and number-average molar mass, $M_n$, and polydispersity index, $M_w/M_n$, vs conversion (the full line represents the theoretical $M_n$) (b) for the SG1-mediated surfactant-free emulsion copolymerizations of methyl methacrylate and styrene ($f_{S0}$ = 0.088)* ***E1*** *(▲) and* ***E2*** *(■) (see Table 3).*

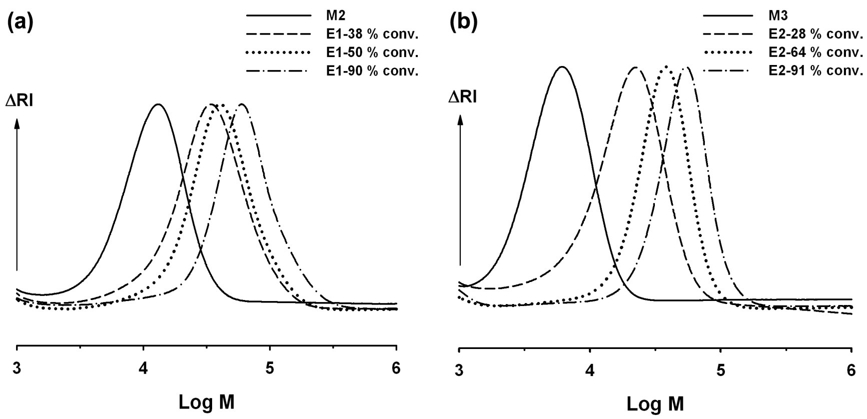

*Figure 8. Evolution of the size exclusion chromatograms with conversion for the SG1-mediated surfactant-free emulsion copolymerizations of methyl methacrylate and styrene ($f_{S0}$ = 0.088)* ***E1*** *(a) and* ***E2*** *(b) (see Table 3).*

# Conclusions

New water-soluble, comb-like macroalkoxyamines with PEG side chains and, for some of them, methacrylic acid subunits were synthesized via nitroxide-mediated controlled free-radical copolymerization of poly(ethylene glycol) methyl ether methacrylate with a low percentage of styrene and terpolymerization with methacrylic acid at a temperature below 80 °C. High chain-end functionality was assessed and allowed us to employ them as macroinitiators for the synthesis of amphiphilic block copolymers, either in bulk or in aqueous emulsion polymerization. In the latter process, PEG-coated, amphiphilic diblock copolymer micelles were generated in situ exhibiting both satisfying macromolecular and colloidal characteristics.

# Acknowledgements

The authors wish to thank Arkema for the financial support of CD's PhD thesis and for kindly providing the nitroxide SG1 and the BlocBuilder®. They are also grateful to Dr. Hervé Lefebvre for his help in differential scanning calorimetry.

Downloaded by COLUMBIA UNIV on June 26, 2012 | http://pubs.acs.org
Publication Date: August 13, 2009 | doi: 10.1021/bk-2009-1024.ch020

# References

1. Qiu, J. ; Charleux, B.; Matyjaszewski ; K. *Prog. Polym. Sci.* **2001**, *26*, 2083.
2. Cunningham, M. F. *Prog. Polym. Sci.* **2008**, *33*, 365.
3. Zetterlund, P.B.; Kagawa, Y.; Okubo, M. *Chem. Rev.* **2008**, *108*, 3747.
4. Charleux, B.; Nicolas, J. *Polymer* **2007**, *48*, 5813.
5. Hawker, C.J.; Bosman, A.W.; Harth, E. *Chem. Rev.* **2001**, *101*, 3661.
6. Nicolas, J.; Charleux, B.; Guerret, O.; Magnet, S. *Angew. Chem., Int. Ed.* **2004**, *43*, 6186.
7. Nicolas, J.; Charleux, B.; Guerret, O.; Magnet, S. *Macromolecules* **2005**, *38*, 9963.
8. Nicolas, J.; Charleux, B.; Magnet, S. *J. Polym. Sci., Part A: Polym. Chem.* **2006**, *44*, 4142.
9. Nicolas, J.; Ruzette, A.-V.; Farcet, C.; Gerard, P.; Magnet, S.; Charleux, B. *Polymer* **2007**, *48*, 7029
10. Delaittre, G.; Nicolas, J.; Lefay, C.; Save, M.; Charleux, B. *Chem. Commun* **2005**, 614.
11. Delaittre, G.; Nicolas, J.; Lefay, C.; Save, M.; Charleux, B. *Soft Matter* **2006**, *2*, 223.
12. Charleux, B.; Nicolas, J.; Guerret, O. *Macromolecules* **2005**, *38*, 5485.
13. Nicolas, J.; Dire, C.; Mueller, L.; Belleney, J.; Charleux, B.; Marque, S. R. A.; Bertin, D.; Magnet, S.; Couvreur, L. *Macromolecules* **2006**, *39*, 8274.
14. Dire, C.; Charleux, B.; Magnet, S.; Couvreur, L. *Macromolecules* **2007**, *40*, 1897.
15. Dire, C.; Magnet, S.; Couvreur, L.; Charleux, B. *Macromolecules* **2009***, 42,* 95.
16. Veronese, F. M. *Biomaterials* **2001**, *22*, 405.
17. Duncan, R. *Nat. Rev. Drug Discovery* **2003**, *2*, 347.
18. Stolnik, S.; Illum, L.; Davis, S. S. *Adv. Drug Delivery Rev.* **1995**, *16*, 195.
19. Nicolas, J.; Couvreur, P.; Charleux, B. *Macromolecules* **2008**, *41*, 3758.
20. Zhang, Y.; Costantini, N.; Mierzwa, M.; Pakula, T.; Neugebauer, D.; Matyjaszewski, K. *Polymer* **2004**, *45*, 6333.

Downloaded by COLUMBIA UNIV on June 26, 2012 | http://pubs.acs.org
Publication Date: August 13, 2009 | doi: 10.1021/bk-2009-1024.ch020

Downloaded by COLUMBIA UNIV on June 26, 2012 | http://pubs.acs.org
Publication Date: August 13, 2009 | doi: 10.1021/bk-2009-1024.ch021

## Chapter 21

# Synthesis and Reaction of Well-defined Copolymers with Thermally Exchangeable Dynamic Covalent Bonds in the Side Chains

**Hideyuki Otsuka,[1,2,]* Yoshifumi Amamoto,[2] Yasuhiro Matsuda,[1]**
**Takeshi Maeda,[1] and Atsushi Takahara[1,2,]***

**[1]Institute for Materials Chemistry and Engineering, Kyushu University,**
**Motooka, Nishi-ku, Fukuoka 819-0395, Japan**
**[2]Graduate School of Engineering, Kyushu University,**
**Motooka, Nishi-ku, Fukuoka 819-0395, Japan**

Synthesis of well-defined linear copolymers with thermally exchangeable dynamic covalent bonds in their side chains and their structural interconversion system were demonstrated. The well-defined linear polymers with alkoxyamine moieties in their side chains were successfully prepared by the atom transfer radical polymerization (ATRP) method by tuning the reaction conditions. Random copolymer was successfully converted into macroscopic gel due to the cross-linking reaction between complementarily-reactive alkoxyamine units. From the results of gel permeation chromatography – multi-angle laser light scattering (GPC-MALLS) and small angle X-ray scattering (SAXS) measurements, it was made clear that the star-like nanogels are formed as the most stable structure in the diblock copolymer system. The molecular weights of the nanogels at equilibrium are clearly controlled by initial concentrations as well as the composition and molecular weights of the diblock copolymers. The structures of the nanogels were observed by scanning force microscopy (SFM) observation, which revealed that nanogels consisted of both a gel part and branching molecular chains. By controlling the stoichiometric ratio of added alkoxyamine, structural conversion from nanogels to diblock copolymer also proceeded, as the structures of the compounds depend on the equilibrium state.

In Controlled/Living Radical Polymerization: Progress in RAFT, DT, NMP & OMRP; Matyjaszewski, K.;
ACS Symposium Series; American Chemical Society: Washington, DC, 2009.

Downloaded by COLUMBIA UNIV on June 26, 2012 | http://pubs.acs.org
Publication Date: August 13, 2009 | doi: 10.1021/bk-2009-1024.ch021

# Introduction

With the recent advancement of controlled polymerization methods such as atom transfer radical polymerization (ATRP),[1] well-defined copolymers with uniform molecular weight and designed composition can be synthesized. Such well-defined copolymers are good candidates to form molecular assembled structures such as nanogels. Nanogels are defined as internally cross-linked single macromolecules of molecular weight and dimensions similar to the parent linear polymer chains, but having a number of transverse covalent bonds between the chain segments.[2]

We have already developed dynamic covalent polymers with 2,2,6,6-tetramethylpiperidinyl-1-oxy (TEMPO)-based alkoxyamine moieties.[3-7] Although the central C–O bonds in alkoxyamine derivatives behave as typical covalent bonds under normal conditions, the alkoxyamine unit can reversibly dissociate into a styryl radical and a TEMPO derivative upon heating and reach an equilibrium state via radical crossover processes (Scheme 1).[4,5]

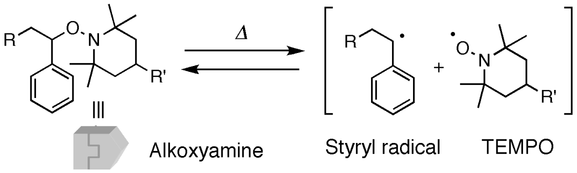

*Scheme 1. Reversible dissociation/association reaction of an alkoxyamine.*

Because of their exchanging ability, the C–O bonds in alkoxyamine derivatives are regarded as dynamic covalent bonds.[8] In addition, radical reaction is tolerant of many functional groups. In this chapter, we describe the synthesis of well-defined copolymers with thermally exchangeable dynamic covalent bonds and a smart structural interconversion system between linear copolymers and nanogels based on the exchange reaction of alkoxyamine units as shown in Scheme 2. A molecular design in which two types of complementarily-reactive alkoxyamine units are integrated into "single" polymer chains enables the formation "self build-up" molecular systems, and we discuss the influence of the primary structure of linear polymers on the structures of nanogels.

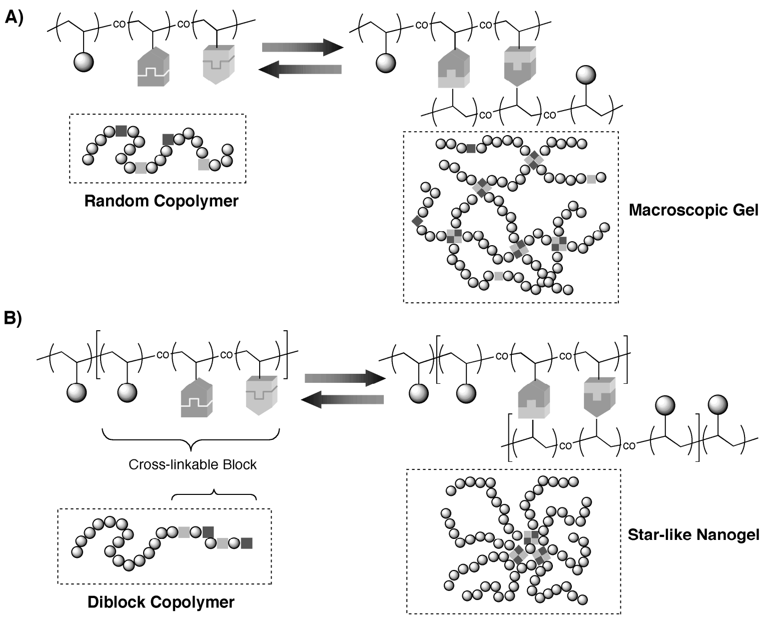

*Scheme 2. Reversible formation of A) macroscopic gel and B) star-like nanogels from linear copolymers by dynamic covalent exchange.*

# Experimental

## Materials

Methacrylate monomers with alkoxyamine groups (**1** and **2**) were prepared by addition reaction of 2-methacryloyloxyethyl isocyanate (Showa Denko) to the corresponding alkoxyamine derivatives with hydroxyl groups in the presence of dibutyltin dilaurate at room temperature.[6] PMMA prepolymers were prepared by the ATRP method initiated from ethyl ethyl 2-bromoisobutylate[2-(EiB)Br] in the presence of CuBr/sparteine system.

### *Poly(MMA-co-**1**-co-**2**)*

In a typical run, Cu(I)Br (5.0 mg, 0.035 mmol) was charged into a round-bottom flask containing a magnetic stirring bar, and the air was removed by evacuation and backfilled with argon three times. Then, MMA (0.535 mL, 5.00 mmol), methacrylic esters **1** (0.433 g, 1.00 mmol) and **2** (0.463 g, 1.00 mmol), anisole (1.0 mL), and sparteine[9] (16.1 μL, 0.0700 mmol) were added. The mixture was degassed by five freeze-pump-thaw cycles and the round-bottom flask was immersed in an oil bath thermostatted at 50 ºC under argon, and 2-(EiB)Br (6.83 mg, 0.035 mmol) was added. The samples for reaction trace were picked from the reaction system via syringes, and their conversion was

Downloaded by COLUMBIA UNIV on June 26, 2012 | http://pubs.acs.org
Publication Date: August 13, 2009 | doi: 10.1021/bk-2009-1024.ch021

evaluated by $^1$H-NMR measurement. After 4 h, the reaction mixture was quenched rapidly to 0 ºC and diluted with acetone, and solution was filtered through a neutral $Al_2O_3$ column. The filtrate was concentrated, and poured into excess methanol. The precipitation was then collected and dried in vacuo to give the purified polymer as a white powder (555.5 mg, 39.0 %): $M_n$ = 27 600 g/mol, $M_w/M_n$ = 1.23.

### *PMMA-b-poly(MMA-co-**1**-co-**2**) (**3**)*

In a typical run, Cu(I)Br (5.0 mg, 0.035 mmol) was charged into a test tube containing a magnetic stirring bar, and the air was removed by evacuation and backfilled with argon three times. Then, MMA (0.534 mL, 5.00 mmol), methacrylic ester with alkoxyamine moieties **1** (0.433 g, 1.00 mmol) and **2** (0.463 g, 1.00 mmol), anisole (1.60 mL), and sparteine[9] (16.1 µL, 0.0700 mmol) were added. The mixture was degassed by five freeze-pump-thaw cycles and the test tube was immersed in an oil bath thermostatted at 50 ºC under argon atmosphere, and the PMMA prepolymer (0.809 g, $M_n$ = 23 100 g/mol, $M_w/M_n$ = 1.11) dissolved in degassed anisole (4.4 mL) was added. After 30 min, the reaction mixture was quenched rapidly to 0 ºC and diluted with acetone, and solution was filtered through a neutral $Al_2O_3$ column. The filtrate was concentrated, and poured into excess hexane. The precipitation was then collected and dried in vacuo to give the purified polymer (**3a**) as a white powder. $M_n$ = 39 000 g/mol, $M_w/M_n$ = 1.07.

### *Polymer Reaction of Diblock Copolymer **3**.*

In a typical run, a 5.0 wt % anisole solution of block copolymer **3a** was charged into a glass tube, degassed by seven freeze-pump-thaw cycles, and sealed off under vacuum. The solution was heated at 100 ºC for 24 h. No macrogelation was observed, and the reaction mixture was reprecipitated from hexane to afford core cross-linked polymer (nanogel) **4a** in 95% yield. In this experiment, alkoxyamine [4-methoxy-1-((1'-phenylethyl)oxy)-2,2,6,6-tetramethylpiperidine, **5**] was generated as a result of a radical exchange reaction.

### *Polymer Reaction of Nanogel to Linear Copolymers.*

In a typical run, nanogel **4d** (5 mg) was dispersed in anisole solution (5 wt %) with an excess of alkoxyamine **5** (9.0 mg, 0.031 mmol, 40 equiv./alkoxyamine) and charged into a glass tube. The solution was degassed by seven freeze-pump-thaw cycles, sealed off under vacuum, and heated at 100 ºC for 48 h.

Downloaded by COLUMBIA UNIV on June 26, 2012 | http://pubs.acs.org
Publication Date: August 13, 2009 | doi: 10.1021/bk-2009-1024.ch021

### Measurements

The absolute molecular weight of nanogels was measured by gel permeation chromatography – multiangle laser light scattering (GPC-MALLS) in THF at 40 ºC on a Dawn EOS instrument (Wyatt Technology; Ga-As laser, λ = 690 nm). The morphology of nanogels on mica was observed in air at room temperature by a SFM (SII Nanotechnology Inc., SPA 400) in a dynamic force microscopy (DFM) mode. Small-angle X-ray scattering (SAXS) was carried out at the BL40B2 beam line of SPring-8 using an incident X-ray with the wavelength λ = 0.150 nm. The measured samples were 5 mg/mL concentrations of nanogels in anisole contained in 2-mm diameter glass capillaries.

## Results and Discussion

### Design and Synthesis of Diblock Copolymers with Alkoxyamines

Random copolymers of MMA and monomers with alkoxyamine moieties and linear diblock copolymers consisting of PMMA block and random block of MMA and monomers with alkoxyamine moieties were designed as the parent polymers. As the monomers with alkoxyamine moieties, we prepared methacrylic esters **1** and **2** containing the alkoxyamine units. They have potential reactivity with each other above 60 °C via a radical crossover reaction, but they are expected to remain stable at room temperature.

Random copolymers that consist of MMA/**1**/**2** and linear diblock copolymers composed of poly(methyl methacrylate) block [PMMA block] and random copolymer block of MMA/**1**/**2** [PMAL block] were synthesized by the ATRP method. For example, in the case of diblock copolymers, linear PMMA prepolymer with a bromine atom at the chain end was prepared initially by ATRP using 2-(EiB)Br and Cu(I)Br/Sp system.[1] Subsequently, random copolymerization of MMA/**1**/**2** (5/1/1 or 20/1/1) mixture was carried out in anisole at 50 °C using PMMA prepolymer and Cu(I)Br/Sp as the catalyst complex to afford diblock copolymer **3** as shown in Scheme 3.

Downloaded by COLUMBIA UNIV on June 26, 2012 | http://pubs.acs.org
Publication Date: August 13, 2009 | doi: 10.1021/bk-2009-1024.ch021

Downloaded by COLUMBIA UNIV on June 26, 2012 | http://pubs.acs.org
Publication Date: August 13, 2009 | doi: 10.1021/bk-2009-1024.ch021

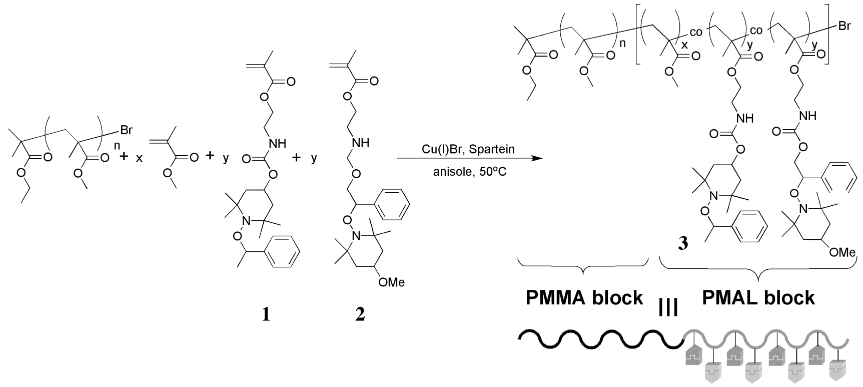

*Scheme 3. Synthesis of well-defined diblock copolymer with thermally exchangeable alkoxyamine units.*

Table 1 summarizes the molecular weights and polydispersities of four types of diblock copolymers with differences in the primary structure such as the molecular weight of each block and the composition in the PMAL block. On the basis of diblock copolymer **3a**, the structure of diblock copolymer **3b** was designed to have a higher molecular weight PMMA block, and diblock copolymer **3c** to have a lower molecular weight PMAL block. Diblock copolymer **3d** has a lower composition ratio of **1** and **2** to the MMA unit in PMAL block. The other parameters of primary structure are almost identical to diblock copolymer **3a**. Furthermore, the polydispersities of the diblock copolymers were relatively low ($M_w/M_n < 1.2$).

Downloaded by COLUMBIA UNIV on June 26, 2012 | http://pubs.acs.org
Publication Date: August 13, 2009 | doi: 10.1021/bk-2009-1024.ch021

**Table 1. Preparation of diblock copolymers 3a-3d by ATRP with different in molecular weights, polydispersities, and composition[a]**

| *Diblock copolymer (Schematic representation)* | *PMMA prepolymer* | *Block copolymer* | |
|---|---|---|---|
| | $M_n$ [g/mol] ($M_w/M_n$) | $M_n$[g/mol] ($M_w/M_n$) | $[MMA]_0/[\mathbf{1}]_0/[\mathbf{2}]_0$ |
| 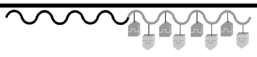<br>**3a** | 23100<br>(1.11) | 39000<br>(1.07) | 5/1/1 |
| 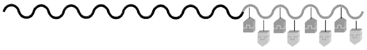<br>**3b** | 55400<br>(1.13) | 70000<br>(1.08) | 5/1/1 |
| 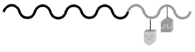<br>**3c** | 23100<br>(1.11) | 29700<br>(1.08) | 5/1/1 |
| 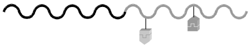<br>**3d** | 22100<br>(1.11) | 35400<br>(1.11) | 20/1/1 |

a. Number-average molecular weights of the polymers were determined by conventional GPC with an RI detector.

## Radical Crossover Reaction of Copolymers.

The radical crossover reaction of random copolymers and diblock copolymers was carried out by heating anisole solutions of the copolymers at 100 °C at various concentrations. In the case of random copolymers, at high concentrations above 5 wt %, the solution transformed into a macroscopic gel after heating for 4 hours, suggesting that the intermolecular cross-linking reaction occurred preferentially. In contrast, at low concentration conditions, no gelation was observed during the reaction, even for 24 hours. The relative molecular weight of the polymer after the reaction was evaluated by GPC. At 0.5 wt % concentration, the relative molecular weight did not increase, but rather decreased. This result suggests that the intramolecular radical crossover reaction occurred preferentially and that the radius of gyration as well as the relative molecular weight of the polymer was decreased after the reaction.

In the case of radical crossover reaction of diblock copolymers **3a**-**3d**, no macroscopic gelation of the system was observed even at high concentrations such as 10 wt %. Because of the existence of PMMA block in block copolymer, the cross-linking reaction did not occur on a macroscale but did on a nanoscale. No coloration of the solution was observed after heating in any of the experiments, suggesting that the radical crossover reaction proceeded without detectable side reactions by naked eyes due to the Persistent Radical Effect.[10]

Figure 1 shows time-coursed GPC curves of the reaction mixture after a cross-linking reaction of diblock copolymers **3a** at 5 wt % condition. The molecular weight increased and peaks for the diblock copolymers gradually disappeared with increasing reaction time. By reacting at the 5 wt % concentration condition, intermolecular cross-linking reaction of the diblock copolymer preferentially proceeded to afford the corresponding core cross-linked nanogel, and almost all diblock copolymers were converted to nanogels. Moreover, the GPC curve became constant after 12 h, indicating that the reaction seems to reach equilibrium at 12 h under these conditions. In the case of diblock copolymer **3b**-**3d**, the same results were observed.

The absolute weight average molecular weight ($M_w$) and radius of gyration ($<S^2>^{1/2}$) were also determined by GPC-MALLS and SAXS measurements, respectively. As shown in Figure 1, until 8 hours, $M_w$ and $<S^2>^{1/2}$ drastically increased as increasing reaction time. In contrast, after 8 hours, $M_w$ and $<S^2>^{1/2}$ had gradually decreased. The $M_w$ determined by GPC-MALLS was larger than that of the GPC instrument, suggesting that nanogels have a branched structure.

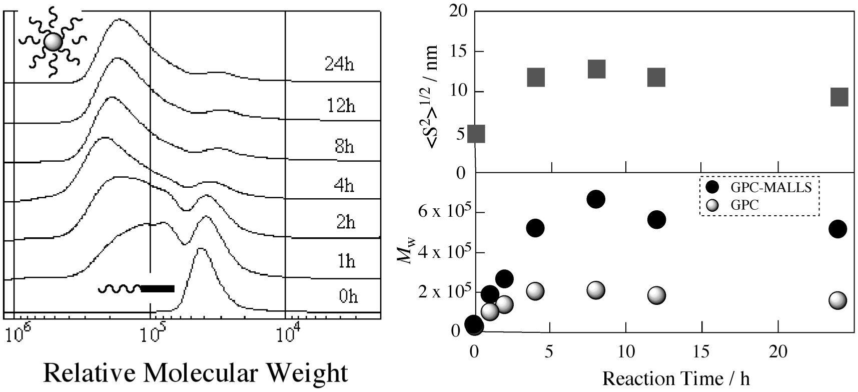

*Figure 1. Time dependence of GPC curves of the crossover reaction product **4** after heating **3a** in anisole (5 wt %) at 100 °C (left) and time dependence of $M_w$ and $<S^2>^{1/2}$ of the crossover reaction product **4** after heating **3d** in anisole (5 wt %) at 100 °C (right).*

The cross-linking reaction of diblock copolymers **3a**-**3d** was also carried out at various concentrations for 24 h. With increasing concentration, high molecular weight nanogels were formed in all cases. Similarly, the $M_w$ values of cross-linking polymers by GPC-MALLS instrument were larger under high concentration conditions.

The topology of star polymers can be directly visualized by using scanning force microscopy (SFM). The morphologies of the nanogels were analyzed by SFM observations in dynamic force microscopy (DFM) mode on a mica surface. Figure 2 shows the typical SFM height images and the line profiles of nanogels **4a** and **4b** obtained by heating diblock copolymers **3a** and **3b** in anisole at 100 °C for 24 h under the 10 wt % concentration condition. The morphologies of the nanogels with a gel part and branching chains were clearly observed, supporting our hypothesis that the nanogels have a star-like architecture. The

Downloaded by COLUMBIA UNIV on June 26, 2012 | http://pubs.acs.org
Publication Date: August 13, 2009 | doi: 10.1021/bk-2009-1024.ch021

branching chains seem to be longer in the case of nanogel **4b** as compared to nanogel **4a** due to the higher molecular weight of PMMA block in nanogel **4b**.

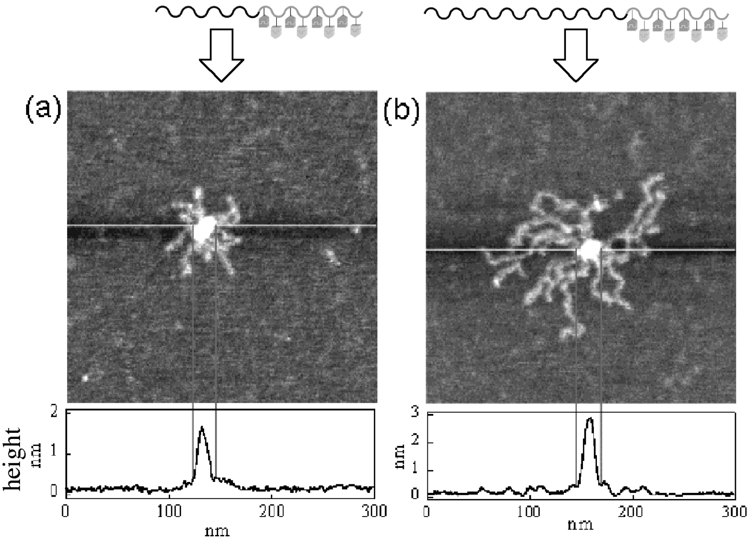

*Figure 2. SFM height images and their line profiles of nanogels on mica substrate deposited from solution obtained by heating (a)* ***4a*** *and (b)* ***4b****, at 100 °C for 24 h under the 10 wt % concentration condition.*

## Structural Transformation from Nanogels to Linear Polymers

The reverse reaction, structural conversion from nanogel to diblock copolymer, was examined by changing the stoichiometry of alkoxyamine derivative in the systems. The nanogel **4d** was added to anisole solution (5 wt %) with an excess of alkoxyamine **5** (40 equiv/alkoxyamine unit in the side chain) and heated at 100 °C. The de-cross-linking reaction of nanogel **4d** proceeded successfully. As shown in GPC profiles (Figure 3), the relative molecular weight decreased and peaks for the diblock copolymers gradually appeared with increasing reaction time. After 48 h, the polymer product exhibited unimodal peak in GPC profile ($M_n$ = 34 100 g/mol, $M_w/M_n$ = 1.14), and the GPC curve is almost identical to the GPC curve of the parent diblock copolymer (**3d**). The results of GPC-MALLS and SAXS measurements and SFM observation also strongly supported the progress of de-cross-linking reaction.

Downloaded by COLUMBIA UNIV on June 26, 2012 | http://pubs.acs.org
Publication Date: August 13, 2009 | doi: 10.1021/bk-2009-1024.ch021

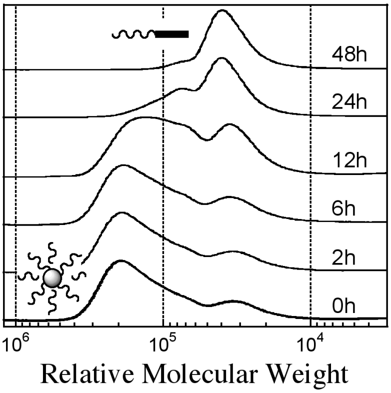

*Figure 3. Time dependence of GPC curves of the de-cross-linking reaction of nanogel **4d** in the presence of excess alkoxyamine molecule after heating in anisole at 100 °C.*

## Conclusions

We have demonstrated a thermodynamic structural interconversion system between copolymers with exchangeable dynamic covalent bonds in the side chain and star-like nanogels. Although random copolymers composed of MMA and methacrylates with complementarily-reactive alkoxyamine moieties afforded macroscopic gel, diblock copolymers successfully gave star-like nanogels. By controlling the stoichiometric ratio of alkoxyamine, structural conversion from nanogels to diblock copolymers also proceeded, as the structures of the compound depend on the equilibrium state. Such a kind of dynamic covalent macromolecular system can afford various polymer architectures through programming of the parent dynamic covalent polymers and polymer reaction conditions.

## Acknowledgments

The authors gratefully acknowledge the financial supports by Grant-in-Aid for Scientific Research (17685011, 20350057) from The Ministry of Education, Culture, Science, Sports and Technology of Japan. The present work is also supported by a Grant-in-Aid for the Global COE Program, “Science for Future Molecular Systems” from the Ministry of Education, Culture, Science, Sports and Technology of Japan. Drs. Sono Sasaki and Hiroyasu Masunaga of Japan Synchrotron Radiation Research Institute are acknowledged for their help on SAXS measurement at SPring-8 (Proposal No. 2006B1098).

Downloaded by COLUMBIA UNIV on June 26, 2012 | http://pubs.acs.org
Publication Date: August 13, 2009 | doi: 10.1021/bk-2009-1024.ch021

# References

1. (a) Matyjaszewski, K.; Xia, J. *Chem. Rev.* **2001**, *101*, 2921. (b) Tsarevsky, N. V.; Matyjaszewski, K. *Chem. Rev.* **2007**, *107*, 2270.
2. This class of polymers is also referred to as "core cross-linked star polymers" in the literature, for example: Xia, J.; Zhang, X.; Matyjaszewski, K. *Macromolecules* **1999**, *32*, 4482.
3. (a) Otsuka, H.; Aotani, K.; Higaki, Y.; Takahara, A. *Chem. Commun.* **2002**, 2838. (b) Otsuka, H.; Aotani, K.; Higaki, Y.; Amamoto, Y.; Takahara, A. *Macromolecules* **2007**, *40*, 1429.
4. (a) Otsuka, H.; Aotani, K.; Higaki, Y.; Takahara, A. *J. Am. Chem. Soc.* **2003**, *125*, 4064. (b) Higaki, Y.; Otsuka, H.; Endo, T.; Takahara, A. *Macromolecules* **2003**, *36*, 1494. (c) Higaki, Y.; Otsuka, H.; Takahara, A. *Macromolecules* **2004**, *37*, 1696.
5. Higaki, Y.; Otsuka, H.; Takahara, A. *Macromolecules* **2006**, *39*, 2121.
6. (a) Amamoto, Y.; Higaki, Y.; Matsuda, Y.; Otsuka, H.; Takahara, A. *Chem. Lett.* **2007**, *36*, 774. (b) Amamoto, Y.; Higaki, Y.; Matsuda, Y.; Otsuka, H.; Takahara, A. *J. Am. Chem. Soc.* **2007**, *129*, 13298.
7. TEMPO-based alkoxyamine derivatives were well known as initiators for nitroxide-mediated living radical polymerization. For example: Hawker, C. J.; Bosman, A. W.; Harth, E. *Chem. Rev.* **2001**, *101*, 3661.
8. (a) Rowan, S. J.; Cantrill, S. J.; Cousins, G. R. L.; Sanders, J. K. M.; Stoddart, J. F. *Angew. Chem. Int. Ed.* **2002**, *41*, 898. (b) Otto, S.; Furlan, R. L. E.; Sanders, J. K. M. *Science* **2002**, *297*, 590. (c) Nishinaga, T.; Tanatani, A.; Oh, K.; Moore, J. S. *J. Am. Chem. Soc.* **2002**, *124*, 5934. (d) Glink, P. T.; Oliva, A. I.; Stoddart, J. F.; White, A. J. P.; Williams, D. J. *Angew. Chem., Int. Ed.* **2001**, *40*, 1870 (e) Furusho, Y.; Oku, T.; Hasegawa, T.; Tsuboi, A.; Kihara, N.; Takata, T. *Chem. Eur. J.* **2003**, *9*, 2895. (f) Skene, W. G.; Lehn, J.-M. *Proc. Natl. Acad. Sci. U.S.A.* **2004**, *101*, 8270. (g) Kudo, H., Makino, S., Nishikubo, T. *J. Polym. Sci., Part A: Polym. Chem.* **2007**, *45*, 680.
9. Yu, B.; Ruckenstein, E. *J. Polym. Sci., Part A: Polym. Chem.* **1999**, *37*, 4191.
10. (a) Fischer, H. *Chem. Rev.* **2001**, *101*, 3581. (b) Studer, A. *Chem. Eur. J.* **2001**, *7*, 1159. (c) Studer, A. *Chem. Soc. Rev.* **2004**, *33*, 267. (d) Studer, A.; Schulte, T. *Chem. Rec.* **2005**, *5*, 27. (e) Tang, W.; Fukuda, T.; Matyjaszewski, K. *Macromolecules* **2006**, *39*, 4332.

Downloaded by COLUMBIA UNIV on June 26, 2012 | http://pubs.acs.org
Publication Date: August 13, 2009 | doi: 10.1021/bk-2009-1024.ch021

## Chapter 22

# Borane-mediated radical polymerization; Preparation of Fluoropolymers for High Energy Density Capacitors

**Zhi-Cheng Zhang and T. C. Mike Chung***

**Department of Materials Science and Engineering**
**The Pennsylvania State University**
**University Park, PA 16802**

Downloaded by STANFORD UNIV GREEN LIBR on June 26, 2012 | http://pubs.acs.org
Publication Date: August 13, 2009 | doi: 10.1021/bk-2009-1024.ch022

This paper discusses two closely relative areas, including the borane-mediated radical polymerization mechanism and the formed fluoropolymers used as the dielectrics thin films in high energy density capacitors for energy storage. The system of borane/oxygen control radical initiators are surprisingly effective for initiating polymerization of fluoromonomers, such as vinylidene fluoride (VDF), trifluoroethylene (TrFE), chlorotrifluoroethylene (CTFE), etc., at ambient temperature. Mechanistic study indicates that the in situ formed alkyl radical (C*) is responsible for the initiation, and the borinate radical (B-O*) forms a reversible bond with the propagating radical to prolong the polymerization. The control polymerization is characterized by predictable molecular weight, narrow molecular weight distribution, formation of diblock copolymer and chain end functionalized polymers, and tolerance to many functional groups that usually cause chain transfer reactions in regular free radical polymerization. The other aspect of this paper is to apply this control polymerization to prepare a whole family of PVDF copolymers. By systematically tuning the polymer chain conformation and crystal structure, we have identified the most suitable fluoropolymer for thin film capacitor that exhibits high energy density and low energy loss.

In Controlled/Living Radical Polymerization: Progress in RAFT, DT, NMP & OMRP; Matyjaszewski, K.;
ACS Symposium Series; American Chemical Society: Washington, DC, 2009.

Downloaded by STANFORD UNIV GREEN LIBR on June 26, 2012 | http://pubs.acs.org
Publication Date: August 13, 2009 | doi: 10.1021/bk-2009-1024.ch022

# Introduction

Despite the known autoxidation reaction of trialkylborane ($BR_3$) by oxygen which results in quantitative formation of the three corresponding alcohols (R-OH) after hydrolysis, (*1,2*) the detailed oxidation mechanism is complicated. Following the initial formation of a B-O-O-C moiety, one suggested mechanism is asymmetric cleavage of the C-O bond to produce B-O-O* and C* radicals. (*3-5*) Some reports suggest an intramolecular rearrangement of the $R_2B$-O-O-R intermediate to form a $RB(O\text{-}R)_2$ molecule. (*6-8*) Others point to homolytic cleavage of the O-O bond to form B-O* and R-O* radicals. (*9-10*) The problem relates to the complexity of the oxidation products from three reactive B-C bonds and the formation of two possible moieties (B-O-R and B-O-O-R). The reaction intermediates are too unstable to permit isolation. In this paper, we compare two oxidation adducts of $B(C_2H_5)_3$ and $B(OCH_3)(C_2H_5)_2$, and carry out the oxidation reactions in the presence of VDF monomers to form PVDF polymers. The idea is to capture the unstable intermediate radicals that *in situ* initiate the polymerization and are incorporated in the beginning of polymer chains. The distinctive chemical shifts of PVDF, separated from those of borane oxidation fragments, greatly help the end group analysis by the NMR technique.

One of the interests in this borane/$O_2$ initiator is the preparation of fluoro copolymers with well-controlled molecular structures that can be fabricated into the dielectric thin films in capacitors for energy storage applications. Opposite to battery technology, which has high energy density and low power density, capacitors (*11-13*) usually exhibit high powder density but very low energy density that limits their applications. The capacitor energy density is directly governed by the dielectric material that separates the opposite static charges. The energy density can be estimated by the equation ($J/cm^3$) = ½ ε $E^2$ = ½ ε $(V/d)^2$, wherein ε is the dielectric constant of the dielectric and E is the applied electric field. The ideal dielectric material should be able to form uniform (defect-free, impurity-free, and mechanic-strong) thin film with a small thickness (d) and the morphology that allows the application of high voltage (V) across the film

# Experimental

## Oxidation of $B(C_2H_5)_3$ and $B(OCH_3)(C_2H_5)_2$ with $O_2$

The oxidation reactions were conducted in a 100 mL flask equipped with a magnetic stirrer. After adding 2 mmol of borane, either $B(C_2H_5)_3$ or $B(OCH_3)(C_2H_5)_2$, and 20 mL ethylether under nitrogen, about 8 mmole of $O_2$ was then injected into the flask to start the oxidation reaction. The reaction was carried out at room temperature under vigorous agitation for 4 hours. The solution was directly subjected to $^{11}B$ NMR measurements. Both spectra are very similar, containing 3 chemical shifts between 35-30 ppm range, which correspond to three di-oxidized species (Et)(OR)B-O-O-B(OR)(Et), (Et)(OR)B-O-O-R, and (Et)(OR)B-O-R, respectively. Only a very low content of fully oxidized (tri-oxidized) species (near 19 ppm) is observed under this oxidation condition at room temperature with [oxygen]/[borane] = 4/1.

## Synthesis of Fluoro Co- and Ter-polymers Using Borane/Oxygen Initiator

The polymerization reactions were carried out in a 75 mL stainless steel autoclave equipped with a magnetic stirrer. In a typical reaction, 0.3 mmol of triethylboron initiator and 30 mL of acetonitrile solvent were added into the autoclave under an inert atmosphere. The autoclave was then cooled by liquid nitrogen before vacuum distilling in certain amounts of monomers. About 0.4 mmol of oxygen was introduced into the autoclave in order to oxidize organoborane and initiate polymerization before the mixture was warmed to the ambient temperature. Then the mixture was stirred constantly for a certain period of time at the ambient temperature before the reaction was terminated via venting the unreacted monomers. The resulting polymer was obtained by removing the solvent under a vacuum, subsequently purified by precipitating from the polymer solution in acetone with excess hexane. It was washed three more times with hexane, and finally dried in a vacuum oven at 70 °C for 8 h.

To obtain high quality co- and ter-polymers, with high purity and narrow molecular weight and composition distributions, the polymerization reactions were usually terminated at a low monomer conversion (< 30%) to assure a constant monomer feed ratio during the polymerization. Note that CTFE shows similar (slightly higher) reactivity with VDF, but TrFE exhibits a significantly lower reactivity than VDF.

## Thin Film Preparation and Measurements

The polymer thin films were prepared by two steps. First, the polymer film (thickness = 30-40 μm) was obtained by a solution casting method, in which the copolymer or terpolymer (8-10 wt%) was dissolved in acetone, and cased on a glass slide. After evaporating the solvent at the ambient temperature overnight, the resulting film was annealed in a vacuum oven at melting temperature for 2-3 hours to obtain uniform thin film (thickness = 10-15 μm). Gold electrodes (thickness = 50 nm) were sputtered on both surfaces of the polymer film for the measurements of the dielectric constant and D-E polarization-depolarization cycles.

The dielectric constant was measured by a HP multifrequency LCR meter, equipped with a temperature chamber. The electric displacement-electric field was measured by the displacement of the polymer film thickness, using a modified Sawyer-Tower circuit and a linear variable differential transducer (LVDT), driven by a lock-in amplifier (Stanford Research Systems, Model SR830). Electric fields ranging from 50 to 600 MV/m were applied across the polymer film using an amplified ramp waveform at 10 Hz.

Downloaded by STANFORD UNIV GREEN LIBR on June 26, 2012 | http://pubs.acs.org
Publication Date: August 13, 2009 | doi: 10.1021/bk-2009-1024.ch022

## Results and Discussion

### Borane Oxidation/Polymerization Mechansim (*14*)

In this paper, we compare two oxidation adducts of $B(C_2H_5)_3$ and $B(OCH_3)(C_2H_5)_2$, and carry out the oxidation reactions in the presence of VDF monomers to form PVDF polymers under various conditions. The idea is to capture the unstable intermediate radicals that *in situ* initiate the polymerization and are incorporated in the beginning of polymer chains. The distinctive chemical shifts of PVDF, separated from those of borane oxidation fragments, greatly help the end group analysis by the NMR technique. Figure 1 compares two sets of the $^{11}B$ NMR spectra of the oxidation adducts of $B(Et)_3$ and $B(OMe)(Et)_2$ by varying amounts of oxygen at ambient temperature.

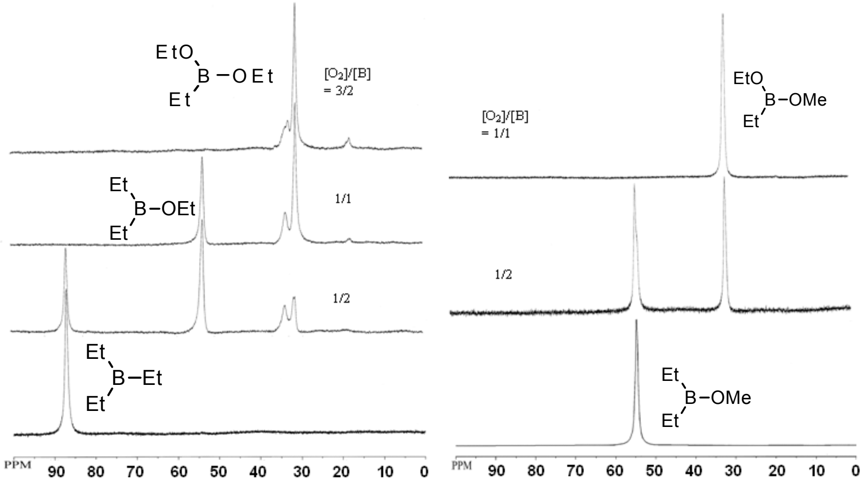

*Figure 1. $^{11}B$ NMR spectra of the oxidation adducts of (left) $B(Et)_3$ and (right) $B(OMe)(Et)_2$ by varying amount of oxygen at ambient temperature. [Reproduced with permission from Macromolecules **2006**, 39, 5187-5189. Copyright 2006 Am. Chem. Soc.]*

The oxidation adducts are quite complicated in $B(Et)_3$ yet are better controlled in $B(OMe)(Et)_2$. With an incremental amount of oxygen, two new chemical shifts are located at 56 and 32 ppm, corresponding to $B(OEt)(Et)_2$ and $B(OEt)_2Et$, and a minor peak at 36 ppm associated with B-O-B. Increasing $[O_2]/[B(Et)_3]>1$, the $B(Et)_3$ completely disappears, and the main oxidation products become di-oxidation adducts with a very small amount of tri-oxidization one at around 19 ppm. On the other hand, the incremental oxidation of $B(OMe)(Et)_2$ with oxygen ($[O_2]/[B(OMe)(Et)_2]$ <0.5) is a clean reaction. Only a new chemical shift at 32 ppm for B(OMe)(OEt)Et is shown with the presence of the unreacted $B(OMe)(Et)_2$ at 56 ppm. After increasing oxygen concentration to a stoichiometric amount, the $B(OMe)(Et)_2$ is completely converted to B(OMe)(OEt)Et without any detectable tri-oxidization adducts.

Downloaded by STANFORD UNIV GREEN LIBR on June 26, 2012 | http://pubs.acs.org
Publication Date: August 13, 2009 | doi: 10.1021/bk-2009-1024.ch022

Almost no peroxyl species of B(O-O-Et)$Et_2$ (II) and B(OEt)(OOEt)Et (IV) were observed in both cases, although they should form before intermolecular reactions (Scheme 1). In one-shot addition of excess oxygen ([oxygen]/[borane] = 4/1) to both $B(Et)_3$ and $B(OMe)(Et)_2$ they result in almost identical $^{11}$B NMR spectra with a chemical shift at 34 ppm, corresponding to B(OR)(OOEt)(Et) (IV) intermediate species, which were captured before having a chance to engage in an intermolecular reaction with B-C bonds. However, the mono-oxidized peroxide B(OOEt)$Et_2$ (II) is too unstable to survive during this oxidation process.

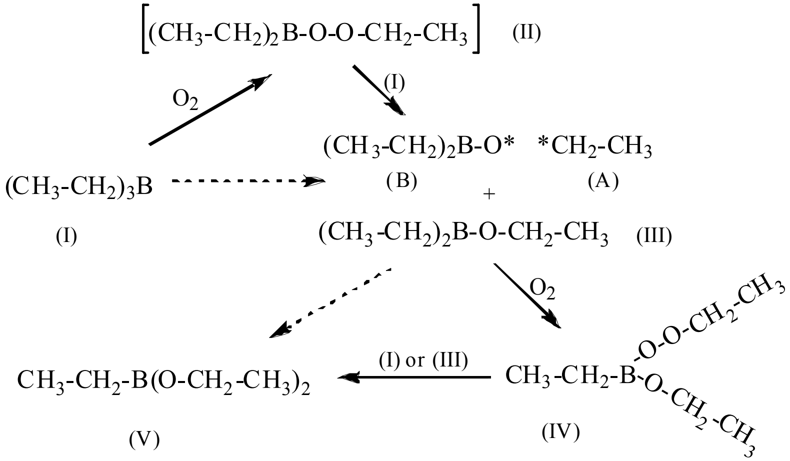
[(CH3-CH2)2B-O-O-CH2-CH3] (II)
O2
(I)
(CH3-CH2)2B-O* *CH2-CH3
(CH3-CH2)3B
(B)
(A)
+
(I)
(CH3-CH2)2B-O-CH2-CH3 (III)
O2
(I) or (III)
CH3-CH2-B(O-CH2-CH3)2
CH3-CH2-B(-O-O-CH2-CH3)(O-CH2-CH3)
(V)
(IV)

*Scheme 1. Oxidation mechanism of triethylborane*

Downloaded by STANFORD UNIV GREEN LIBR on June 26, 2012 | http://pubs.acs.org
Publication Date: August 13, 2009 | doi: 10.1021/bk-2009-1024.ch022

Downloaded by STANFORD UNIV GREEN LIBR on June 26, 2012 | http://pubs.acs.org
Publication Date: August 13, 2009 | doi: 10.1021/bk-2009-1024.ch022

**Table 1** Summary of VDF Polymerization Conditions and Results by $B(Et)_3/O_2$ Radical Initiator at Room Temperature

| Run | $TEB/O_2$ mmol | Time hrs | Yield g | Cov % | End groups | | | | Molecular weight | |
|---|---|---|---|---|---|---|---|---|---|---|
| | | | | | $CH_3CH_2$* / $CH_2CF_2$ & $CF_2CH_2$ | $CH_3CH_2$-O- | $CF_2CH_2$-OH | $CF_2COX$ (X=F or OH) | Mn (NMR) | Mv |
| A-1 | 2.4/1.6 | 0.25 | 1.6 | 11.9 | 1.58 (95.2%) | 0.08 (4.8%) | n.d. | n.d. | 9,700 | 14,500 |
| A-2 | 2.4/1.6 | 0.5 | 3.2 | 23.9 | 1.49 (96.1%) | 0.06 (3.9%) | n.d. | n.d. | 13,900 | 29,000 |
| A-3 | 2.4/1.6 | 0.75 | 5.1 | 38.1 | 1.48 (95.5%) | 0.07 (4.5%) | n.d. | n.d. | 14,100 | 27,457 |
| A-4 | 2.4/1.6 | 1 | 5.6 | 41.8 | 1.51 (96.8%) | 0.05 (3.2%) | n.d. | n.d. | 14,900 | 31,000 |
| A-5 | 2.4/1.6 | 2.5 | 7.5 | 56.0 | 1.30 (97.0%) | 0.04 (3.0%) | n.d. | n.d. | 17,100 | 66,000 |
| A-6 | 2.4/1.6 | 5 | 9.1 | 67.9 | 1.49 (98.0%) | 0.03 (2.0%) | n.d. | n.d. | 17,500 | 78,000 |
| B-1 | 2.4/0.8 | 5 | 5.4 | 40.3 | 1.38 (96.5%) | 0.05 (3.5%) | n.d. | n.d. | 18,300 | 47,000 |
| B-2 | 2.4/1.6 | 5 | 9.1 | 67.9 | 1.49 (98.0%) | 0.03 (2.0%) | n.d. | n.d. | 17,500 | 78,000 |
| B-3 | 2.4/2.4 | 5 | 11.5 | 85.8 | 1.39 (92.7%) | 0.11 (7.3%) | n.d. | n.d. | 14,000 | 63,000 |
| B-4 | 2.4/2.8 | 5 | 12.8 | 95.5 | 1.34 (91.2%) | 0.13 (8.8%) | n.d. | n.d. | 28,600 | 100,000 |
| B-5 | 2.43.2 | 5 | 12.0 | 89.6 | 1.33 (85.8%) | 0.15 (9.7%) | 0.04 (2.6%) | 0.03 (1.9%) | 36,600 | 101,000 |
| B-6 | 2.4/3.6 | 5 | 10.8 | 80.6 | 1.33 (82.6%) | 0.17 (10.6%) | 0.06 (3.7%) | 0.05 (3.1%) | 42,200 | 100,000 |
| B-7 | 2.4/4.0 | 5 | 6.0 | 44.8 | 1.40 (64.2%) | 0.20 (9.2%) | 0.25 (11.5%) | 0.33 (15.1%) | 49,000 | 127,000 |
| B-8 | 2.4/4.4 | 5 | 4.9 | 36.6 | 1.17 (40.2%) | 0.34 (11.7%) | 0.60 (20.6%) | 0.80 (27.5%) | 48,400 | 97,000 |
| B-9 | 2.4/4.8 | 5 | 4.7 | 35.1 | 1.17 (41.5%) | 0.37 (13.1%) | 0.50 (17.7%) | 0.78 (27.7%) | 35,600 | 110,000 |
| B-10 | 2.4/5.2 | 5 | 4.5 | 34.3 | 1.23 (62.4%) | 0.27 (13.7 %) | 0.25 (12.7%) | 0.22 (11.2%) | 55,900 | 101,000 |
| B-11 | 2.4/6.0 | 5 | 0 | 0 | -- | -- | -- | -- | -- | -- |

Downloaded by STANFORD UNIV GREEN LIBR on June 26, 2012 | http://pubs.acs.org
Publication Date: August 13, 2009 | doi: 10.1021/bk-2009-1024.ch022

The best way to observe the initial oxidation adduct of $B(OOEt)(Et)_2$ (II) and its subsequent reaction with $B(Et)_3$ (I) is to carry out this control oxidation in the presence of large amounts of VDF monomers ($[VDF]/[B(Et)_3] > 100$). The unstable intermediates containing free radicals during the intermolecular reaction should *in situ* initiate the radical polymerization to form poly(vinylidene fluoride) (PVDF) and deposit the adduct in the beginning of the PVDF chain. Table 1 summarizes the experimental results. The polymerization is effective at ambient temperature to obtain PVDF with an almost quantitative yield in five hours. Comparing a set (A-1 to A-6), the molecular weight increases with the monomer conversion. However, plots of the polymer molecular weight vs. the monomer conversion, the line is above the theoretical line. Some uncontrolled radical polymerization may take place in the beginning of polymerization. The protecting borinate radical (B) (Scheme 1), may not have a sufficient quantity to mediate all propagating radicals. Usually, excess mediates are needed to have a successful control radical polymerization. (15-17)

The polymer molecular weight reaches Mv >63,000 g/mole in about 5 hours. The relatively slow propagating rate, compared to that of the regular free radical polymerization mechanism, removes the safety concern for heat transport and temperature control usually associated with bulk or solution polymerization of fluoromonomers. In addition, this process produces fluoropolymers with high purities, without any contaminants from surfactants or suspension agents in most of commercial fluoropolymers, which are difficult to remove but detrimental in electric applications.

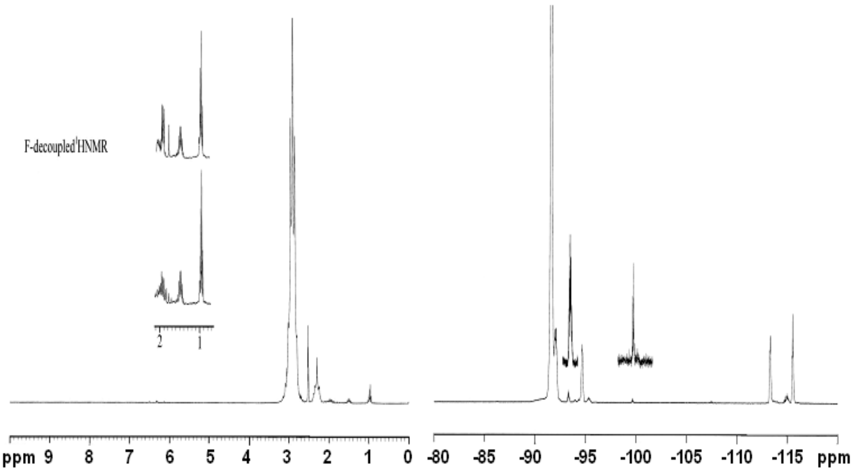

*Figure 2, (left) $^1H$ and (right) $^{19}F$ NMR spectra of a PVDF polymer (run A-6) prepared by a $B(Et)_3/O_2$ initiator (mole ratio= 3/2). [Reproduced with permission from Macromolecules **2006**, 39, 5187-5189. Copyright 2006 Am. Chem. Soc.]*

Figure 2 shows the $^1H$ and $^{19}F$ NMR spectra of a typical PVDF polymer (run A-6). In addition to two major chemical shifts at 2.9 and 2.3 ppm, corresponding to ($CF_2$-$C\mathbf{H}_2$-$CF_2$-$C\mathbf{H}_2$) and ($CF_2$-$C\mathbf{H}_2$-$C\mathbf{H}_2$-$CF_2$), respectively, three minor chemical shifts at 1, 1.5, and 2.0 ppm are associated with three types of protons at the $C\mathbf{H}_3$-$C\mathbf{H}_2$-$C\mathbf{H}_2$-$CF_2$- end group, which is originated from the oxidation adduct ($CH_3$-$CH_2$*) of $B(Et)_3$. The same chain end assignments were observed in the $^{19}F$ NMR spectrum. In addition to several main chain peaks at near 91, 95, 113, and 116 ppm, there were several weak chain end peaks near 93 ppm ($C\mathbf{F}_2$-$CH_2$-$CH_2$-$CH_3$) and 100 ppm ($C\mathbf{F}_2$-$CH_2$-$CH_3$). In fact, all reaction runs with $[O_2]/[B(Et)_3] <1$ (Table 1) show the same $CH_3$-$CH_2$- polymer chain end structure. There is no detectable $CH_3$-$CH_2$-O- group and borane fragment existing at the polymer chain end.

Scheme 1 illustrates the possible oxidation mechanism of $B(Et)_3$ (I) that can explain all our observations. In the early stage of the oxygen reaction ($[O_2]/[B(Et)_3] <1$), the first oxidation adduct shall be $B(OOEt)(Et)_2$ (II) that is very unstable and immediately reacts with the unreacted $B(Et)_3$ (I) to form a $B(OEt)(Et)_2$ (III) and two intermediate radicals, including $CH_3$-$CH_2$* radical (A) and borinate radical (B). Without monomers presence, two radicals just combine to form another $B(OEt)(Et)_2$ (III). With VDF monomers, the $CH_3$-$CH_2$* radical (A) *in situ* initiates the radical polymerization of VDF at ambient temperature. However, borinate radical (B) may be too stable to react with the monomer due to electron back-donating to the empty p-orbital of boron. But it may serve as the end-capping agent to form a reversible bond with the growing PVDF chain end to prolong the propagating process. Evidently, the mono-oxidation product $B(OEt)(Et)_2$ (III) is still very reactive, which is subjective to further oxidation, either by oxygen to form B(OOEt)(OEt)Et (VI), or by another $B(OOEt)(Et)_2$ (II) to form $B(OEt)_2Et$ (V). After the di-oxidation reaction, the peroxyl group in B(OOEt)(OEt)Et (VI) is still unstable, but is a little bit more stable than that in the mono-oxidized $B(OOEt)(Et)_2$ (II). The observed amount of B(OOEt)(OEt)Et (VI) is dependent on the availability of B-C bonds in $B(Et)_3$ (I) and $B(OEt)(Et)_2$ (III). With the further increase of oxygen concentration and reaction temperature, all three B-C bonds in $B(OMe)(Et)_2$ and $B(Et)_3$ are eventually oxidized to form tri-oxidation species.

The combined information from oxidation adducts and the polymer chain end structure, presents a complete picture of oxidation and the initiation mechanism of broane/oxygen mediated radical polymerization of fluoromonomers at ambient temperature. This borane/oxygen initiator offers a safe and effective route to prepare fluoropolymers with high molecular weights and high purities. It also provides the control of polymer chain end structure by initiator.

## Fluoropolymer Dielectric for High Energy Density capacitors (*18, 19*)

This borane/oxygen initiator was applied to prepare PVDF-based random copolymers for energy storage capacitors. The chemistry shows advantages of narrow molecular weight and composition distribution (*20*). For this study, we have prepared a family of PVDF polymers (Scheme 2) that contains vinylidene difluoride (VDF), trifluoroethylene (TrFE), and chlorotrifluoroethylene (CTFE) units. The consecutive VDF units provide strong polarization, the randomly distributed TrFE units (co-crystallizable with VDF units) direct the VDF

Downloaded by STANFORD UNIV GREEN LIBR on June 26, 2012 | http://pubs.acs.org
Publication Date: August 13, 2009 | doi: 10.1021/bk-2009-1024.ch022

Downloaded by STANFORD UNIV GREEN LIBR on June 26, 2012 | http://pubs.acs.org
Publication Date: August 13, 2009 | doi: 10.1021/bk-2009-1024.ch022

sequence to all-trans (polar) conformation, and the small amount of bulky Cl atoms in CTFE units serve as the kinks to reduce the crystalline size without significantly reducing the overall crystallinity. Some terpolymers exhibit high dielectric constant and relaxed ferroelectric behaviors. (*21-23*) It's logical to think that this type of terpolymer with a particular composition might show high energy density (due to high dielectric constant and breakdown voltage) and low energy loss (due to relax ferroelectric behavior).

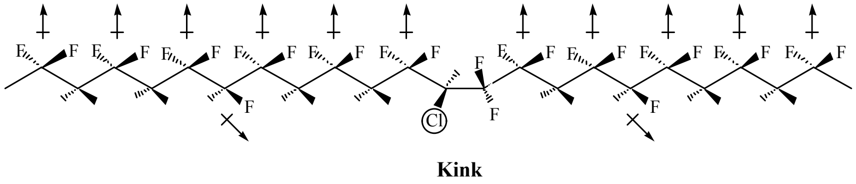

*Scheme 2. Chain conformation of VDF.TrFE/CTFE terpolymer.*

Table 2 summarizes two comparative sets of VDF/TrFE/CTFE terpolymers with a systematic variation of TrFE and CTFE contents, respectively. To obtain high quality terpolymers (high purity and narrow molecular weight and composition distributions), we employed borane/oxygen mediated control radical polymerization in a homogeneous acetonitrile solution at ambient temperature. The thermal transitions of terpolymers were examined by DSC. (*18, 19*) The relatively sharp melting peak in all co- and terpolymers implies a relatively uniform molecular structure and morphology. The increase of CTFE units (by substituting TrFE units) systematically reduces both melting ($T_m$) and Curie ($T_c$) temperatures, but maintaining high heat of fusion ($\Delta H$) that starts its diametrical descent after the CTFE content reaches > 8 mol%. The terpolymers with ~7.5 mol% CTFE units and various VDF/TrFE mole ratios maintain an overall high crystallinity. The VDF/TrFE (63.3/36.7 mol%) copolymer shows an expected Curie temperature at 65 °C. With ~7.5 mole% of CTFE content, the terpolymer Curie temperature shifts to near ambient temperature and the intensity becomes very weak, indicating a relaxed ferroelectric behavior.

Downloaded by STANFORD UNIV GREEN LIBR on June 26, 2012 | http://pubs.acs.org
Publication Date: August 13, 2009 | doi: 10.1021/bk-2009-1024.ch022

**Table 2. Summary of two comparative sets of VDF/TrFE/CTFE terpolymers prepared by triethylborane/oxygen radical initiator.**

| Run | VDF/TrFE/CTFE (%) | Tm (°C) | Tc (°C) | ΔH(J/g) |
|---|---|---|---|---|
| A-1 | 58.4/34.2/7.4 | 121.5 | 19.8 | 20.6 |
| A-2 | 65.6/26.7/7.7 | 123.6 | 23.8 | 22.0 |
| A-3 | 80.7/11.6/7.7 | 120.1 | N.A | 27.9 |
| A-4 | 92.0/0.0/8.0 | 145.0 | N.A | 25.9 |
| B-1 | 63.3/36.7/0.0 | 151.7 | 64.6 | 30.1 |
| B-2 | 58.3/37.4/4.3 | 134.6 | 31.2 | 23.3 |
| B-3 | 56.2/37.0/6.8 | 121.3 | 18.8 | 21.3 |
| B-4 | 58.4/34.2/7.4 | 121.5 | 19.8 | 20.6 |
| B-5 | 57.1/31.4/11.5 | 106.4 | N.A | 17.0 |

Figure 3 compares the dielectric constant between VDF/CTFE (92/8 mol%) copolymer and VDF/TrFE/CTFE (65.6/26.7/7.7 mol%) terpolymer. The dielectric constant profile provides a sharp Curie transition temperature. The polymers containing less than 15 mole% TrFE units show no Curie temperature. It's necessary to have more than 20 mole% of TrFE units to observe the Curie temperature, which shifts rapidly toward the ambient temperature as the TrFE content increases toward 35%. In other words, the dielectric constant profile (polarization of $CF_2$ dipoles) can be effectively controlled by terpolymer composition and thermal energy. It's engrossing to understand the similar polarization-depolarization effect under the applied electric field.

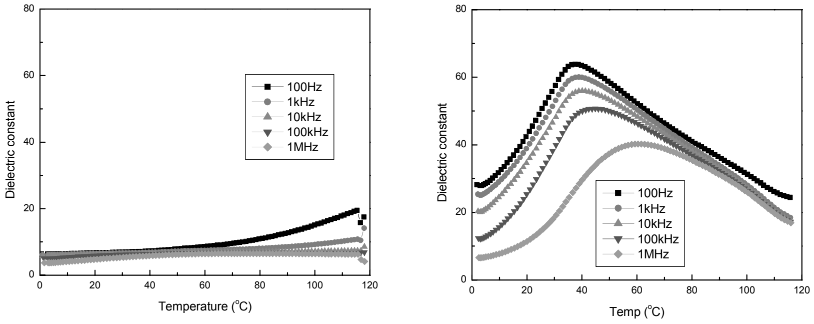

*Figure 3, Dielectric constant of (a) VDF/CTFE (92/8 mol%) copolymer (run A-1) and (b) VDF/TrFE/CTFE (65.6/26.7/7.7 mol%) terpolymer (run A-3). [Reproduced with permission from Macromolecules **2007**, 40, 783-785. Copyright 2007 Am. Chem. Soc.]*

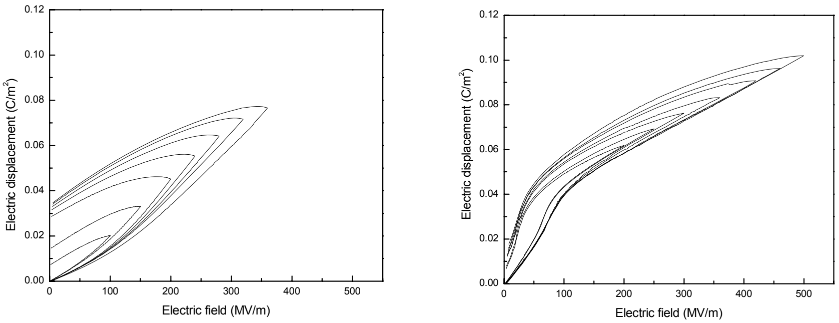

*Figure 4, Unipolar D-E hysteresis curves of (left) VDF/CTFE (92/8 mol%) copolymer (run A-1) and (right) VDF/TrFE/CTFE (65.6/26.7/7.7 mol%) terpolymer (run A-3). [Reproduced with permission from Macromolecules **2007**, 40, 783-785. Copyright 2007 Am. Chem. Soc.]*

Figure 4 compares unipolar D-E (charge displacement vs. unipolar electric field) hysteresis curves of the same set of VDF/CTFE and VDF/TrFE/CTFE polymers, with similar CTFE content (7.7-8.0 mol%). The charging-discharging cycles were first applied to 100 MV/m, then increasing 50 MV/m intervals until reaching the breakdown electric field. It's important to note that the thin film quality has a great effect on the breakdown electric field. To assure uniform and defect-free thin films for side-by-side comparison at equilibrium state, all polymers were solution cased into approximately 30-40 μm thick films. The films were then conditioned in a vacuum oven at melting temperature for a few hours before slowly cooling to room temperature in order to obtain transparent uniform films 10-15 μm thick. Without TrFE unit, the breakdown electric field for VDF/CTFE (92/8 mol%) copolymer (A-1) is typically 350 MV/m, and the copolymer shows a large hysteresis in polarization-depolarization curves with high energy loss and large remnant polarization at the end of each cycle (zero electric field). The initial increase of the TrFE content seems to have a very small effect to the D-E hysteresis curves. The significant changes were only observed while the TrFE content reached >20 mol%. The VDF/TrFE/CTFE (65.6/26.7/7.7) terpolymer (A-3), with the Curie temperature at around 35-40 $^{o}$C, shows the highest breakdown electric field at > 500 MV/m and slim polarization-depolarization curves with low energy loss and almost no remnant polarization. The electric displacement reaches to about 0.1 C/m$^2$ at 500 MV/m. Compared with the theoretical electric displacement of 0.13 C/m$^2$ for the fully polarized (β-phase) PVDF homopolymer (*24*), this terpolymer is almost at its limit with almost all VDF and TrFE units polarized along the electric field. With the further increase of the TrFE content (> 30%), the polarization-depolarization curves broaden again.

Figure 5 compares two sets of unipolar D-E loops of PVDF co- and ter-polymers with a fixed CTFE or TrFE content, respectively. The results show that certain content of TrFE is necessary to keep the polymer confirmation in polar phase, which makes the crystal easier to be polarized and depolarized. Introduction of CTFE is reducing the crystal phase content as well as cutting the

Downloaded by STANFORD UNIV GREEN LIBR on June 26, 2012 | http://pubs.acs.org
Publication Date: August 13, 2009 | doi: 10.1021/bk-2009-1024.ch022

crystal in small pieces, which allows the polar crystals to be polarized under high electric field and leaves enough free space for them to

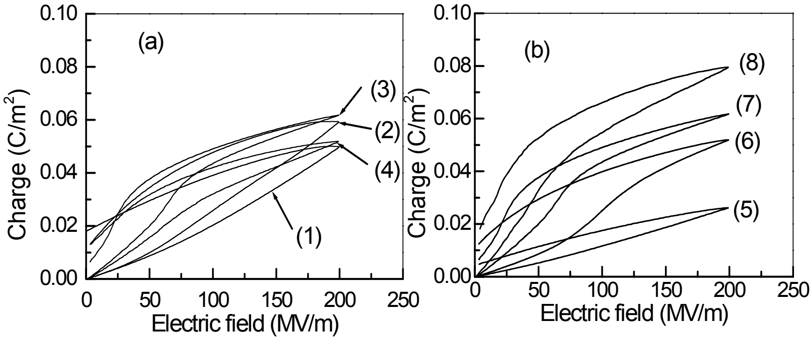

*Figure 5. Unipolar D-E hysteresis loops of copolymers with fixed CTFE content (a) 1. VDF/CTFE=92.0/8.0; 2. VDF/TrFE/CTFE= 80.7/11.6/7.7; 3. VDF/TrFE/CTFE=65.6/26.7/7.7; 4. VDF/TrFE/CTFE=58.4/34.2/7.4) and fixed TrFE content (b) (5.VDF/TrFE/CTFE=63.3/36.7/0.0; 6. VDF/TrFE/CTFE=67.3/27.2/5.5; 7.VDF/TrFE/CTFE=65.6/26.7/7.7; 8. VDF/TrFE/CTFE=68.2/22.5/9.3) [Reproduced with permission from Macromolecules **2007**, 40, 9391-9397. Copyright 2007 Am. Chem. Soc.]*

Figure 6 compares releasing energy density and energy loss of the polarization-depolarization cycle (with the maximum electric field) for the same set of co- and ter-polymers with CTFE content ~7.5 mole%. In most cases (except A-4, discussed later), the energy density closely follows the same master curve. The releasing energy density increases with the increase of the applied electric field, and the higher breakdown electric field offers the higher energy density. Both VDF and TrFE units in the polymer chain contribute to the electric displacement and energy density. However, the energy loss is dramatically different. For the VDF/CTFE (92/8 mole%) copolymer (A-1) and VDF/TrFE/CTFE (80.7/11.6/7.7) (A-2), with no and low TrFE content and without observing the Curie temperature, the energy loss is very high (even higher than the energy released in all cycles), which is unacceptable in the capacitor design. A dramatic improvement is shown in the VDF/TrFE/CTFE (65.6/26.7/7.7) terpolymer (A-3). It shows not only the highest breakdown electric field (> 500 MV/m) and highest energy density (13 J/cm$^3$), but also lowest energy loss. On the other hand, the energy density curve of the VDF/TrFE/CTFE (58.4/34.2/7.4) terpolymer (A-4) shows a clear deviation from the master curve, with saturation of about 200 MV/m and maximum releasing energy density of only about 4 J/cc. The energy loss also shapely increases after 200 MV/m, indicating that all the energy charged is lost after 200 MV/m.

Downloaded by STANFORD UNIV GREEN LIBR on June 26, 2012 | http://pubs.acs.org
Publication Date: August 13, 2009 | doi: 10.1021/bk-2009-1024.ch022

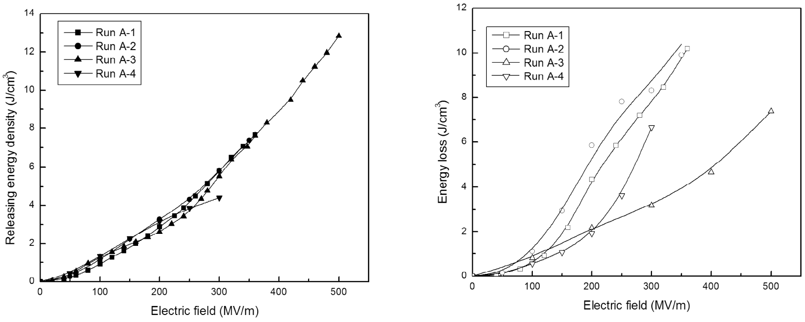

*Figure 6. (left) Releasing energy density and (right) energy loss of VDF/CTFE copolymer and three VDF/TrFE/CTFE terpolymers (runs A-2, A-3, A-4). The solid curves are only for guiding the eyes in order to see the trend. [Reproduced with permission from Macromolecules **2007**, 40, 9391-9397. Copyright 2007 Am. Chem. Soc.]*

In summary, this paper systematically studies PVDF-based co- and terpolymers to tune its polarization profile for capacitor applications. The desirable terpolymer (VDF/TrFE/CTFE = 65.6/26.7/7.7), exhibiting a high dielectric constant (□ ~ 60) at the Curie temperature (35 °C), shows a high breakdown electric field > 500 MV/m, high energy density (releasing > 13 J/cm$^3$), relatively small energy loss, and almost no remnant polarization at zero electric field.

## Conclusion

The borane-mediated control radical polymerization allows the preparation of random copolymers with high purity. They are stable under high electric fields, which are the key to achieve high energy density. Terpolymer with optimized composition shows high energy density and low energy loss.

## Acknowledgements

The authors would like to thank the Office of Naval Research and Daikin Corporation for their financial support.

Downloaded by STANFORD UNIV GREEN LIBR on June 26, 2012 | http://pubs.acs.org
Publication Date: August 13, 2009 | doi: 10.1021/bk-2009-1024.ch022

## References

1. Brown, H. C. "*Organic Synthesis via Boranes*" Wiley-Interscience, New York, **1975**.
2. Mikhailov, B. M.; Bubnov, Y. N. "*Organoboron Compounds in Organic Synthesis*" Harwood Academic Publishers, Switzerland, **1984**.
3. Davies, A. G.; Roberts, B. P. *J. Chem. Soc. B*, **1969**, 311.
4. Davies, A. G.; Ingold, K. U.; Roberts, B. P.; Tudor, R. *J. Chem. Soc. B,* **1971**, 60, 698.
5. Arimoto, F. S. *J. Polymer Sci.* **1966**, 4A, 275.
6. Davies, A. G.; Hare, D. G,; White, F. M. *J. Chem. Soc*. **1960**, 1040.
7. Mirviss, S. B. *J. Am. Chem. Soc.* **1961**, 83, 3051.
8. Davies, A. G.; Hare, D. G,; White, F. M. *J. Chem. Soc*. **1961**, 341.
9. Hansen, R. L.; Hamann, R. *J. Phys. Chem.* **1963**, 67, 2868.
10. Welch, F. J. *J. Poly. Sci.* **1962**, 61, 243.
11. Winter, M.; Brodd, R. J. *Chem Rev*. **2004**, 104, 4245.
12. Sarjeant, W. J. *IEEE Trans. Electr. Insul.* **1990**, 25, 861.
13. Sarjeant, W. J.; Zirnheld, J.; MacDougall, F. W. *IEEE Trans. on Plasma Sci.* **1998**, 26, 1368.
14. Zhang, Z. C.; Chung, T. C. *Macromolecules* **2006**, 39, 5187.
15. Hawker, C. J.; Bosman, A. W.; Harth, E. *Chem. Rev.* **2001**, 101, 3661.
16. Kamigaito, M.; Ando. T.; Sawamoto, M. *Chem Rev*. **2001**, 101, 3689.
17. Wang, J. S.; Matyjaszewski, K. *J. Am. Chem. Soc.* **1995**, 117, 5614.
18. Zhang, Z. C.; Chung, T. C. *Macromolecules* **2007**, 40, 783.
19. Zhang, Z. C.; Chung, T. C. *Macromolecules* **2007**, 40, 9391.
20. Wang, Z. M.; Zhang, Z. C.; Chung, T. C. *Macromolecules* **2006**, 39, 4268.
21. Chung, T. C.; Petchsuk, A. U. S. Patent 6,355,749.
22. Chung T. C.; Petchsuk A. *Ferroelectrics Lett.* **2001**, 28, 135.
23. Chung T. C.; Petchsuk A. *Macromolecules* **2002**, 35, 7678.
24. Furukawa, T. *Adv. Colloid and Interface Sci.* **1997**, 71, 183.

Downloaded by STANFORD UNIV GREEN LIBR on June 26, 2012 | http://pubs.acs.org
Publication Date: August 13, 2009 | doi: 10.1021/bk-2009-1024.ch022

Downloaded by CORNELL UNIV on June 26, 2012 | http://pubs.acs.org
Publication Date: August 13, 2009 | doi: 10.1021/bk-2009-1024.ch023

## Chapter 23

# MADIX Technology: from Innovative Concepts to Industrialization of Block Copolymers for Emulsion Stabilization

**Mathias Destarac,[1,2,*] Sophie Deroo,[1,*] Hélène Lannibois-Dréan,[1]**
**Alain Sénéchal,[1] Wojciech Bzducha[1]**

**[1] Rhodia Opérations, Centre de Recherches et Technologies d'Aubervilliers, 52 rue de la Haie Coq, 93308 Aubervilliers Cedex, France**
**[2] Université de Toulouse, UPS, LHFA, 118 route de Narbonne, F-31062 Toulouse, France and CNRS, LHFA UMR 5069, F-31062 Toulouse, France**

The development of controlled radical polymerization (CRP) technologies paved the way for the design of a nearly infinite array of complex polymer architectures, among which amphiphilic block copolymers have been shown to exhibit interesting interfacial properties in liquid formulations. We illustrate the potential of CRP-derived diblock copolymers as emulsion stabilizers against coalescence for water-in-oil (w/o) emulsions. P(alkyl acrylate)-*b*-P(acrylic acid) copolymers of varying $M_n$, block ratio and nature of the acrylate monomer were evaluated either as single emulsifiers or in combination with conventional surfactants. It is shown that a well-chosen diblock copolymer of adapted $M_n$ and hydrophilic-lipophilic balance presents specific features that makes it a nearly universal stabilizer for w/o emulsions, suitable for a very broad range of solvent polarity. This work led to the industrial development and commercialization of the Rhodibloc® RS copolymer as a powerful surfactant booster for inverse emulsions.

In Controlled/Living Radical Polymerization: Progress in RAFT, DT, NMP & OMRP; Matyjaszewski, K.; ACS Symposium Series; American Chemical Society: Washington, DC, 2009.

Downloaded by CORNELL UNIV on June 26, 2012 | http://pubs.acs.org
Publication Date: August 13, 2009 | doi: 10.1021/bk-2009-1024.ch023

# Introduction

Coalescence is a phenomenon of emulsion destabilization that consists in multiple fusions of droplets yielding eventually to a total phase separation between the initial dispersed and continuous phases. This phenomenon often causes limitations in the use of emulsions in particularly demanding conditions such as long shelf life, elevated temperature, high shear, high concentration … One possible way to fight against this destabilization is to use macromolecular surfactants as emulsifiers, and for example amphiphilic block copolymers (*1-5*). Over the past ten years, we developed and industrialized a proprietary xanthate-mediated controlled radical polymerization technology coined MADIX, providing access to new amphiphilic block copolymers with a very versatile chemistry *(6-7)*.

The objective of this study is to investigate the potentialities of amphiphilic diblock copolymers (DBs) as emulsifiers, fighting against coalescence. Some background on emulsion destabilization mechanisms will be introduced in order to better precise the interest and scope of our study. The chemistry and advantages of our novel amphiphilic DBs will then be presented. We will see how our DBs can be used either alone or mixed with conventional surfactants, by evaluating and understanding the benefits they can provide in terms of emulsion stabilization, mainly for w/o emulsions. We will then focus on the critical point of adaptation of the hydrophobic block to the oil phase, and look for a universal DB stabilizer.

# Results and Discussions

## Emulsion Destabilization Mechanisms

Emulsions consist of an aqueous phase and an oily phase (which is not water-miscible), one phase being dispersed in the other one. When the oily phase is dispersed in the aqueous phase, they are called “direct” or “o/w”. When the aqueous phase is dispersed in the oily phase, they are called “reverse”, “inverse” or “w/o” emulsions. These systems are out of equilibrium: they will always move more or less quickly to a macroscopic phase separation. Emulsions can be produced using emulsifiers which are amphiphilic surfactants, having one hydrophilic and one hydrophobic part. These molecules decrease the interfacial tension between the oily and aqueous phases, enabling the emulsification. The balance between the hydrophilic and hydrophobic parts of the surfactants determines which type of emulsion it will create. Bancroft‘s empiric rule tells that the continuous phase is the one in which the emulsifier is the most soluble *(8-9)*. Several phenomenons can induce emulsion destabilization (Figure 1) (*10*):

- *Flocculation* can appear and consists in the aggregation of droplets. However, it is a reversible phenomenon: the aggregates can be destroyed by shaking the emulsion.

Downloaded by CORNELL UNIV on June 26, 2012 | http://pubs.acs.org
Publication Date: August 13, 2009 | doi: 10.1021/bk-2009-1024.ch023

- *Sedimentation or creaming* of the droplets are due to the density difference between the different phases. This phenomenon is also reversible and a well dispersed emulsion can be recovered by applying shear.
- Over a long period of time, emulsions can be subject to *Ostwald ripening*, which consists in the solubilization of small droplets in the bigger ones. This phenomenon is irreversible and leads to an increase of droplet size. It is due to a higher Laplace pressure in the smaller droplets: $P=2\gamma/r$, with $\gamma$ the droplets interfacial tension and $r$ their radius. This can be strongly limited by introducing in the droplets a molecule that is very insoluble in the continuous phase. The transfer of the dispersed solvent from one droplet to a bigger one would then induce a difference in chemical potential that would fight against this transfer. In the case of w/o emulsions, a salt like NaCl is often used.
- *Coalescence* is a phenomenon of droplet fusion. This happens when droplets are not well covered and protected by the emulsifier. This phenomenon is irreversible and is the most problematic one.

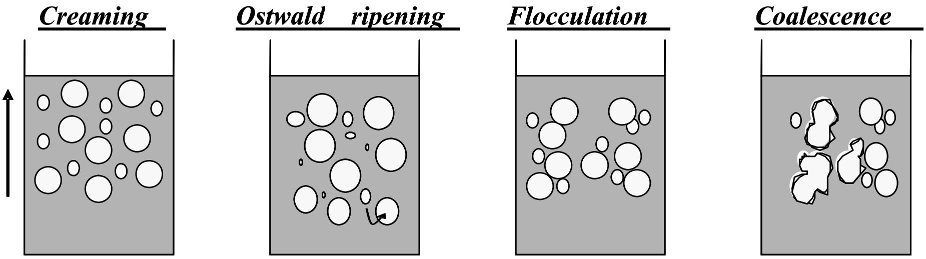

*Figure 1: Mechanisms of emulsion destabilization*

We will focus our work on the fight against emulsion coalescence for w/o emulsions. It is the area in which we have had the most unmet needs in terms of stabilization, probably due to a more limited choice in terms of conventional surfactants compared to o/w emulsions.

The objective of our work was to investigate the potentialities of CRP-derived amphiphilic DBs as emulsifiers, used either alone or in mixture with conventional surfactants, and to evaluate the benefits they could provide in terms of emulsion stabilization. In this respect, the MADIX process was implemented.

## MADIX Technology: Opportunities for the Synthesis of Amphiphilic Block Copolymers.

The MADIX process (*6-7*) has attracted a great deal of attention over the last few years because of its ability to produce polymers with well-controlled macromolecular properties from numerous monomer types. This controlled free radical polymerization (CRP) technique, based on a reversible addition-fragmentation transfer of xanthates R-S(C=S)OZ during polymerization, is undoubtedly one of the most promising approaches for the industrialization of complex, laboratory scale, polymer architectures. The advantages of MADIX for synthesizing (co)polymers with controlled architectures are numerous, amongst which:

- the possibility for fine-tuning of R and Z groups of the xanthate to vary its reactivity according to the monomer used,
- with Z=OEt,(*7*) the negligible effect of the initial xanthate concentration on the overall rate of polymerization of most of the monomers,
- its tolerance towards water as the polymerization medium (homogeneous or dispersed),
- an easy access to many types of controlled architectures, including linear diblock and triblock copolymers, but also controlled branched (co)polymers like comb-shaped, star-like, nanogels and hyperbranched (co)polymers,
- the very broad range of functional monomers suitable for this process.

Downloaded by CORNELL UNIV on June 26, 2012 | http://pubs.acs.org
Publication Date: August 13, 2009 | doi: 10.1021/bk-2009-1024.ch023

### *Block Copolymer Design*

The MADIX process enables the direct synthesis of a broad range of amphiphilic DBs via a two-step process. The $M_n$ and copolymer composition are controlled by the initial xanthate and monomer concentrations. Thus, the hydrophilic-lipophilic balance (HLB) of the macromolecular surfactant can be easily varied. Advantageously, monomers can be converted to a very high level in such a way that no polymer purification is required after the synthesis of the first block. Various functional monomers can be readily polymerized in a controlled manner without resorting to protection chemistry. They can be (co)polymerized either in the hydrophobic or in the hydrophilic block, depending on the targeted property in the final application.

The composition of the hydrophobic block can be varied in order to obtain an appropriate glass transition temperature or polarity. This block may be comprised of one single monomer or a combination of several monomers polymerized in a statistical way. The main hydrophobic monomers compatible with MADIX technology are listed below:

- styrene and derivatives,
- alkyl acrylates ($C_nH_{2n+1}$ group, with $1<n<18$),
- hydrophobic acrylamido monomers, e.g. N-octyl acrylamide.
- vinyl esters, e.g. vinyl acetate or vinyl neodecanoate.

The hydrophilic block can be either neutral or charged. Neutral monomers are usually chosen in the range of hydrophilic acrylates like 2-hydroxyethyl acrylate, acrylamide and derivatives, or vinyl lactams like N-vinyl pyrrolidone (VP). Anionically charged blocks are obtained through the polymerization of monomers bearing carboxy groups (e.g. acrylic acid), sulfonate (e.g. 2-acrylamido-2-methylpropane sulfonic acid) or phosphonate groups (like vinyl phosphonic acid (*11*). Cationic blocks are usually synthesized from monomers bearing either dialkylamino groups or permanent cationic charges (like acrylamidopropyltrimethylammonium chloride (*12*) or diallyldimethylammonium chloride (*13*)).

For the present study, PAA-P(alkyl acrylate) diblock copolymers were synthesized in ethanol at 70°C by a sequential polymerization of the two monomers initiated by AIBN and controlled by O-ethyl-S-((1-methoxycarbonyl)ethyl) xanthate (Rhodixan A1®) as the MADIX agent (*14*). The final copolymer composition was confirmed by $^1$H NMR. The good control over $M_n$ values was checked by size exclusion chromatography (SEC) for both PAA (water eluent) and PAA-PBA (THF eluent) after methylation of the PAA block in the latter case. The polydispersity indexes are relatively high for a CRP process and lie in the range 1.5-2.0 depending on both $M_n$ and composition of the copolymers. This well-established feature of the MADIX polymerization of acrylates is mainly due to the slow chain transfer to O-ethyl xanthate groups during polymerization (*15-16*).

Downloaded by CORNELL UNIV on June 26, 2012 | http://pubs.acs.org
Publication Date: August 13, 2009 | doi: 10.1021/bk-2009-1024.ch023

## Emulsion system and emulsification process.

Unless otherwise stated, the chosen DB chemistry was poly(butyl acrylate)–poly(acrylic acid) (PBA-PAA). The hydrophobic block is always significantly longer than the hydrophilic one in order to induce the formation of w/o emulsions. Therefore, PBA-PAA with respective $M_n$ of 6000-1000, 12000-3000, 8000-2000 g/mol were considered. All these DBs were synthesized under their acidic form and were used without any neutralization.

The continuous phase was a polar oil, namely the methyl ester of rape seed oil (Phytorob or Lubrirob 926-65), so that the DBs were well soluble in it. The dispersed phase consists in a 0.1M NaCl water solution in order to limit Ostwald ripening in water droplets. As conventional low HLB surfactants, we used sorbitan monooleate (Alkamuls S80) or an ethoxylated castor oil (Alkamuls OR10). As for the emulsification process, surfactant and/or diblock copolymers were solubilized in the oil phase. The water-to-oil phase ratio w/o was usually 20/80. All emulsions were prepared using an Ultraturrax during 10min at 10000rpm. Stability of these emulsions was evaluated under various conditions by following the droplet size and looking at the possible appearance of water at the bottom of the sample, both phenomena resulting from possible coalescence.

### *Diblocks as sole emulsifiers.*

Emulsions were prepared using different levels of PBA-PAA relative to the water phase (Figure 2). Good emulsification is obtained with DB levels as low as 0.5% relative to the aqueous phase. This shows that the DB is well inserted at the oil/water interface. Droplet size decreases as the DB level is increased, from approximately 5μm down to 1 μm at 5% DB. The time stability at room temperature of these emulsions has been evaluated. After one month, no water separation appeared for any DB. Only a slight droplet size increase was observed in all cases. Sedimentation of the droplets is of course observed but the emulsions re-disperse easily after 2 or 3 inversions. After 9 months, no water phase separation is observed for DB levels equal to or greater than 1%/w. Only traces of coalescence are observed at 0.5%.

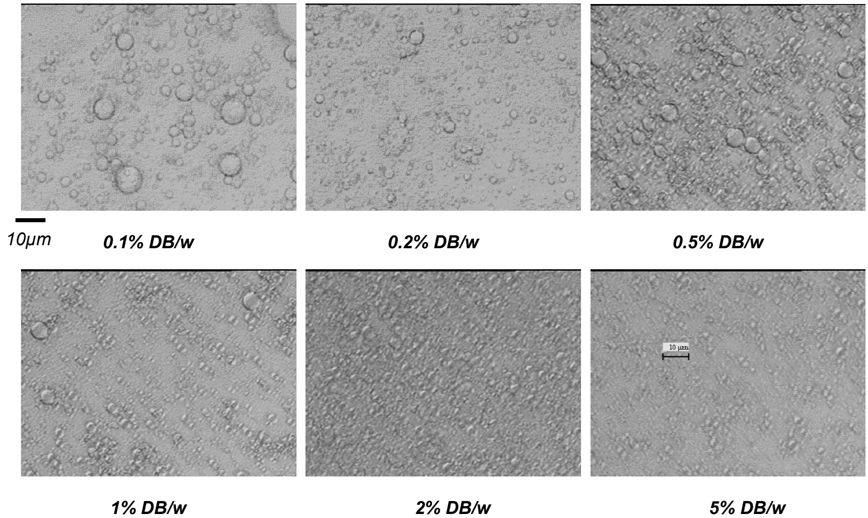

0.1% DB/w 0.2% DB/w 0.5% DB/w

1% DB/w 2% DB/w 5% DB/w

*Figure 2: Influence of the DB level on emulsification.*
*Composition: water/oil=20/80. Oil:Phytorob 926-65 (methyl ester of rape seed oil). Water:0.1M NaCl. Rhodibloc®: PBA-PAA 6000-1000*

Temperature stability was assessed on 50/50 w/o emulsions prepared with 1% or 2% PBA-PAA. After 1 week at 80°C, only a slight droplet size increase was observed for 1% DB. After 1 month at 80°C, a very slight macroscopic separation of water was seen in both cases, corresponding to less than 2% of the initial internal phase. This shows the good temperature stability of emulsions stabilized by DBs.

### *Diblocks as boosters: stabilization of w/o emulsions against coalescence*

We started from the emulsion prepared with the ethoxylated castor oil: this surfactant used at 5% relative to the water phase provides fluid emulsions of 1-2µm, but of poor stability, yielding a total coalescence after 4 days at room temperature. The replacement of 10% of the surfactant by an equal amount of DB leads to an emulsion which is as fine as the preceding one (see Figure 3), and which now shows a constant droplet size and no macroscopic coalescence over more than one month. The same performance is obtained if we reduce the total emulsifier level down to 2%/w. An interesting observation is that an emulsion produced with the DB alone has clearly a larger droplet size. Of course, we could obtain the same size (1 µm) with 5% of the DB alone but the cost-effectiveness for such a system would be altered.

Downloaded by CORNELL UNIV on June 26, 2012 | http://pubs.acs.org
Publication Date: August 13, 2009 | doi: 10.1021/bk-2009-1024.ch023

Downloaded by CORNELL UNIV on June 26, 2012 | http://pubs.acs.org
Publication Date: August 13, 2009 | doi: 10.1021/bk-2009-1024.ch023

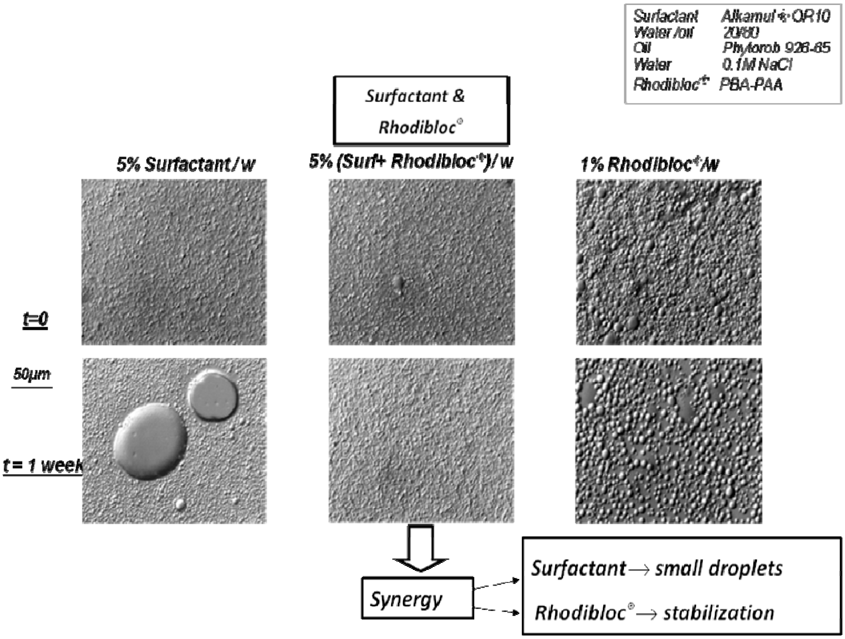
Surfactant Alkamuls OR10
Water/oil 20/80
Oil Phytorob 926-65
Water 0.1M NaCl
Rhodibloc® PBA-PAA
Surfactant & Rhodibloc®
5% Surfactant/w
5% (Surf+ Rhodibloc®)/w
1% Rhodibloc®/w
t=0
50µm
t= 1 week
Synergy
Surfactant → small droplets
Rhodibloc® → stabilization

*Figure 3: Emulsions with PBA-PAA 8000-2000 and/or ethoxylated castor oil*

This system shows a synergy between DB and surfactant: the surfactant provides a small droplet size, probably due to a low interfacial tension, whereas the DB provides the emulsion stability against coalescence.

### *Respective roles of surfactant and diblock.*

This synergy has been investigated by interfacial tension measurements using a falling drop apparatus (Figure 4). It is well-known that there is a direct correlation between the decrease of the interfacial tension by means of an amphiphile and the ability of the latter to generate small emulsion droplets. The data show that in the case of surfactant alone or used in mixture with DB, low interfacial tensions are obtained and are correlated with small emulsion droplets. In the case of DB used as single emulsifier, higher interfacial tensions are obtained for DBs of various nature, $M_n$ and composition, and correlated with emulsions of bigger droplets. This demonstrates that the main role of the conventional surfactant is to lower the interfacial tension in order to produce small droplets.

Downloaded by CORNELL UNIV on June 26, 2012 | http://pubs.acs.org
Publication Date: August 13, 2009 | doi: 10.1021/bk-2009-1024.ch023

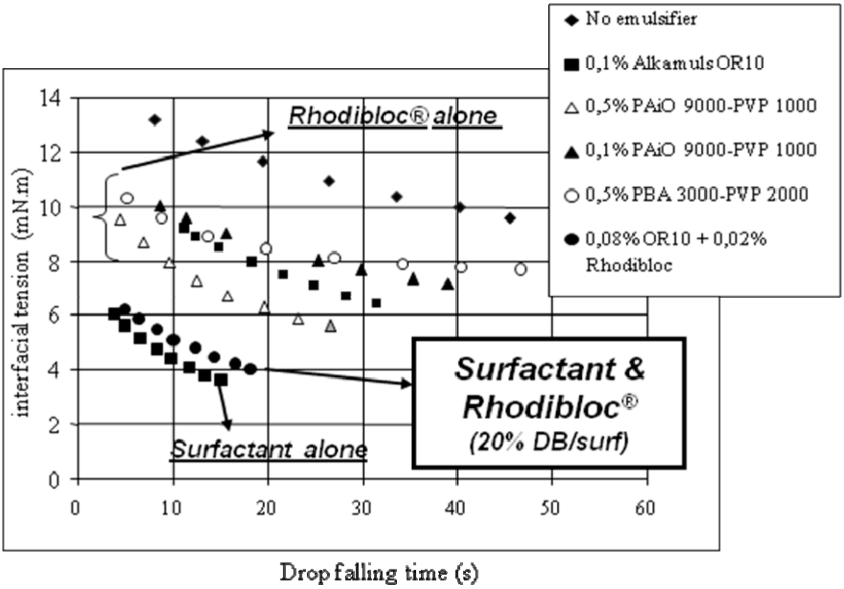

*Figure 4: Interfacial tensions for DB and/or surfactant.*
*Surfactant : Alkamuls ® OR10. Conditions of Figure 2.*

*NB : The concentrations of surfactants and diblocks indicated in the legend refer to interfacial tension measurements.*

Considering the DB, performance at such a low level can be explained by looking at its conformation at the droplet surface: amphiphilic DB polymers can be anchored in the surfactant film (Figure 5). The distance between 2 DB anchoring sites and the size of the PBA chain in the oil can be calculated and their comparison will tell us if the polymer is in a mushroom or brush conformation (*17-18*). The configuration depends on both DB structure and level. The distance D is calculated as a function of the molar fraction in DB, x, and the surface area of a surfactant molecule, A (typically 60Å²): $A=D^2x$. We will make here the hypothesis that the DB/surfactant ratios introduced in the sample and present in the interfacial film are equal, supposing an equal partition coefficient for the surfactant and the DB between the continuous phase and the interface.

Since PBA is well soluble in the oil, the extension of the PBA chain can be estimated on the basis of two times the Flory radius: $R = N^{3/5}a$, where N is the polymerization degree of the PBA block and a the length of one monomer unit (approx. 2.5Å).

For a PBA-PAA 8000-2000 at a DB level of 10%/w (corresponding to the preceding example), x=0.44 mol%, N=62, so that 2R =59Å and D=116Å. This means that the hydrophobic PBA block is in a mushroom conformation at the droplet surface, and that 2 mushrooms are separated by a distance equal to the size of one mushroom (the scale on the figure is correct).

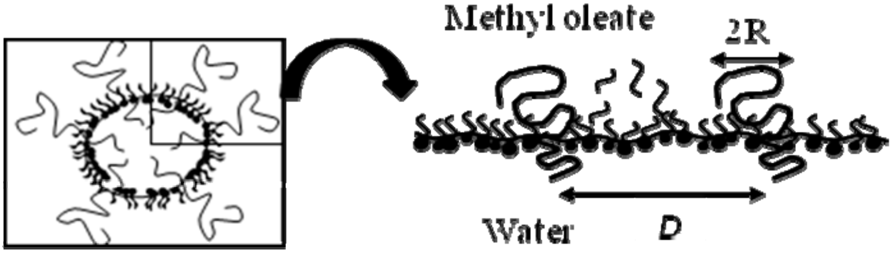

*Figure 5: Diblock conformation in the surfactant film*

Downloaded by CORNELL UNIV on June 26, 2012 | http://pubs.acs.org
Publication Date: August 13, 2009 | doi: 10.1021/bk-2009-1024.ch023

The DB polymer chains anchored at the interfacial film provide thus steric repulsions between water droplets : they protect the emulsion from flocculation and fight against droplet approach. Moreover, the mixed interfacial film is also denser, thicker and better solvated on the oil side, so that phenomena inducing coalescence such as local lack of emulsifier, adjacent film mixing or curvature inversion are prevented. This anchoring density of DB is very favorable because it provides a good covering of the droplet surface without modifying too much the film rigidity. Moreover, minimum interface coverage by the polymer chains is required: poorer stabilization is observed below 7.5% DB relative to surfactant.

### *Influence of the diblock structure*

By varying the DB structure, we have seen that several parameters have an influence on the stabilization through several mechanisms.

The *diblock length* impacts DB anchorage and repulsions between droplets. Emulsion stabilization has been investigated at a constant PBA/PAA weight ratio equal to 80/20 for diblocks of total $M_n$ ranging from 5000 to 15000 g/mol. An emulsion stabilized by 2% (DB+surfactants)/w and 10%DB/(DB+surfactants) shows a coalescence level of 50% after 1 month for a PBA-PAA 4000-1000, whereas no macroscopic water separation is observed for a PBA-PAA 8000-2000 or 12000-3000. A same trend is seen after a temperature treatment of 4 days at 80°C. A DB of minimal $M_n$ equal to 10000 g/mol provides thus a better stability, both with time and in temperature.

The *ratio of hydrophobic/hydrophilic blocks* plays on the DB partitioning between the interface and both phases, in other terms on the DB anchorage in the interfacial film. Best stability results were obtained in the weight ratio range of 80/20 to 90/10.

In the same way, the *nature of the hydrophilic monomer* influences the DB anchorage due to a more or less good solubilization of the hydrophilic block in the oil phase: for instance, a PVP block provides better stabilization than a PAA of same $M_n$.

The *nature of the hydrophobic monomer* has an important role on repulsions through the quality of the solvation in oil of the hydrophobic block. We observed that no stabilization of emulsions in non polar oils (such as Isopar M, Exxsol D100 ...) can be obtained with PBA-based diblocks, which appears to be due to the poor solubility of the hydrophobic block in this type of oil. By replacing butyl acrylate by a more hydrophobic monomer such as isooctyl acrylate, we managed to obtain DB polymers able to stabilize emulsions in non polar oils, thanks to a good solvation of the hydrophobic block in the oil. This shows that the adaptation of the hydrophobic block to the oil is crucial for the stabilization of w/o emulsions (5,*19*). We will return to this point in the next part.

### *Versatile Diblocks for Various Oil Media.*

We have seen that in order to provide an efficient stabilization, the hydrophobic block has to be well adapted to the continuous oil phase, meaning well solubilized in the oil in order to be optimally swollen. It would be thus very interesting to find a hydrophobic block adapted to a broad range of oil polarity, so that various application domains could be treated with the same diblock. This is what has been investigated in the following section.

### *Nature of Oils and Hydrophobic Blocks.*

We chose the following oils in order to cover a broad range of polarity: hexadecane, isopropyl myristate, methyl oleate, isopropyl palmitate and benzyl benzoate.

For the hydrophobic blocks, three monomers of increasing hydrophobicity have been chosen: isooctyl acrylate (A, C8), isodecyl acrylate (B, C10) and lauryl acrylate (C, C12). All have been polymerized to give a diblock with $M_n$ equal to 9000-1000. According to the monomer structures, the homopolymer A is less hydrophobic than B which is less hydrophobic than C.

All hydrophobic homopolymers are soluble in all oils. All 3 diblocks are soluble or well dispersible (slightly turbid solutions) in all oils. None of the diblock is soluble in water. According to Bancroft rule, they are thus well adapted to formulate w/o emulsions.

### *Emulsion stability*

All emulsions have been realized using a diblock as the single emulsifier, at a 2% level relative to the aqueous phase. We obtain droplet diameters ranging between 1 and 10μm. All emulsions are fluid. The stability at room temperature of the fluid emulsions is presented in Table 1.

Downloaded by CORNELL UNIV on June 26, 2012 | http://pubs.acs.org
Publication Date: August 13, 2009 | doi: 10.1021/bk-2009-1024.ch023

**Table 1. Level of Emulsion Coalescence in the Various Oils as a Function of the Nature of the Hydrophobic Block, after 2 Weeks at Room Temperature**

| | **Hexadecane** | **Isopropyl myristate** | **Methyl oleate** | **Isopropyl palmitate** | **Benzyl benzoate** |
|---|---|---|---|---|---|
| *A* | 0 | 0 | 0 | 0 | 0 |
| *B* | Trace | 2.5% | 2% | 5% | 10% |
| *C* | 0 | 0 | 2% | 2% | 2.5% |

The diblock based on B is the poorest stabilizer, as emulsion coalescence already begins after one day. The C block stabilizes emulsions in the least polar oils, but is not efficient for the most polar ones. A very good stabilization is obtained with the A block in the whole range of oil polarity. The unexpected greater stability observed in the most polar oils for C compared to B suggest that not only the number of carbon atoms of the alkyl chain but also its branched versus linear nature are parameters of importance.

After 1 day at 80°C, a relatively good stability is achieved with the diblock made of A: we obtain either a perfect stability or a very slight coalescence in some oils, as described in Table 2. But the level of coalescence in the different emulsions is much higher after 2 weeks except for hexadecane.

**Table 2. Level of Emulsion Coalescence in the Various Oils for the A Block, After 1 Day at 80°C**

| *Hexadecane* | *Isopropyl myristate* | *Isopropyl palmitate* | *Benzyl benzoate* |
|---|---|---|---|
| 0 | Trace | 0 | Trace |

We also investigated emulsion stability after freeze-thaw cycles which consist of 1-day storage at 4°C and back at room temperature. Most emulsions resist well to the first freeze-thaw cycle, but are destabilized after the second one.

A diblock based on the A hydrophobic block is thus quite universal for the stabilization of w/o emulsions in a wide range of oil polarities. We noticed that the best diblock is the one with the least hydrophobic block among the three we have tried. Furthermore, this diblock is also the most polar. We can imagine that when the solubilization of the diblock in the oil is too high (examples of B and C), the diblock can easily leave the interface and this leads to coalescence and destabilization of the emulsion.

On the basis of this study, we were able to finely tune and optimize the chemical structure and composition of a DB copolymer suitable for an application as a surfactant booster for inverse emulsion polymerization.

## Conclusions

Our expertise in polymer design and emulsion science allowed us to develop the desired DB structures through the choice of the chemical nature of blocks, the block ratio, and the length of the polymer. MADIX has shown its robustness

Downloaded by CORNELL UNIV on June 26, 2012 | http://pubs.acs.org
Publication Date: August 13, 2009 | doi: 10.1021/bk-2009-1024.ch023

and compatibility with industrial development : the Rhodibloc RS® block copolymer is today produced at industrial scale by Rhodia Novecare. It provides stabilization of water-in-oil emulsions, preventing coalescence and flocculation.

In this study, we have shown that purposely designed DBs can be used as boosters with conventional surfactants or as a single emulsifiers, providing stabilization of the emulsion: low interfacial tension and small droplet size is provided by the conventional surfactant, while steric stabilization is provided by the DB.

The DB structure can be optimized to obtain the best performance thanks to the versatility of MADIX technology. Particularly, for w/o emulsions, the key parameter is the choice of the hydrophobic block to optimize its solvation in the oil continuous phase. We managed also to find a nearly universal DB, well adapted for a wide range of oil polarities, from hexadecane to benzyl benzoate, and providing stabilization for various types of w/o emulsions. These properties have been patented and are valuable in various applications (20). Emulsion stabilization can also be valorized in all applications requiring emulsion stability in particularly demanding conditions such as long shelf life, elevated temperature, high shear, high concentration (*20-24*)... In the frame of w/o emulsions, the DBs can be used to stabilize: i) some cosmetic emulsions, ii) inverse emulsion polymerization processes, iii) oil-based muds for drilling fluids, iiii) green diesel, which is a diluted water/diesel emulsion.

Downloaded by CORNELL UNIV on June 26, 2012 | http://pubs.acs.org
Publication Date: August 13, 2009 | doi: 10.1021/bk-2009-1024.ch023

## Acknowledgement.

The authors are grateful to the Rhodia teams who contributed to this work, in particular the synthesis, analysis, applicability and application laboratories of the Rhodia R&D Center in Aubervilliers, France.

## References

1. *Polymeric surfactants (Surfactant Science Series, Vol. 42)*; Piirma, I; Marcel Dekker, Inc., New York, 1992.
2. Tadros, T., *Annu. Surfactants Rev.* **1998**, *1*, 179.
3. Holmberg, K. In *Amphiphilic block. copolymers*: *self assembly and applications*, Alexandridis P, Lindman B, Eds., Elsevier:Amsterdam: Chapter 13, p 305, 2000.
4. Pons, R. In *Amphiphilic block. copolymers*: *self assembly and applications*, Alexandridis P, Lindman B, Eds., Elsevier:Amsterdam: Chapter 17, p 409, 2000.
5. Riess, G. *Prog. Polym. Sci.* **2003**, *28*, 1107.
6. Corpart, P.; Charmot, D.; Biadatti, T.; Zard, S.Z.; Michelet, D. WO 9858974, Rhodia Chimie. [*Chem. Abstr.* **1999**, *130*, 82018].
7. Taton, D.; Destarac, M.; Zard, S.Z. In *Handbook of RAFT Polymerization*, Barner-Kowollik, C, Eds., Wiley-VCH: Weinheim, p. 373, 2008.
8. Bancroft, W.D. *J. Phys. Chem.* **1913**, *17*, 501.
9. Bancroft, W.D. *J. Phys. Chem.* **1913**, *19*, 275.

10. Evans D.F., Wennerström H.: *The Colloidal Domain. 2nd Ed.* Wiley-VCH, Inc., New York, 1999.
11. (a) Destarac, M. WO 2006/125892, Rhodia Recherches et Technologies; (b) Destarac, M.; Van Gramberen, E.; Dupuis, P.; Vila, X. *Polym. Prepr. (Am. Chem. Soc., Div. Polym. Chem.*) **2008**, *49(2)*, 173.
12. Atallah, P.; Wilson, J.; Gonzalez, I.; Chavanne, J.; Bacquet, G.; Destarac, M. *Polym. Prepr. (Am. Chem. Soc., Div. Polym. Chem.*) **2008**, *49(2)*, 175.
13. (a) Destarac, M. WO 2008/000766, Rhodia Recherches et Technologies; (b) Destarac, M.; Van Gramberen, E.; Boutin, C.; Guinaudeau, A.; Chadel, S. *Polym. Prepr. (Am. Chem. Soc., Div. Polym. Chem.*) **2008**, *49(2)*, 177.
14. Destarac, M. ; Pavageau, B.; Tolla, B. WO 2006117476, Rhodia Chimie.
15. Destarac, M. ; Bzducha, W. ; Taton, D.; Gauthier-Gillaizeau, I. ; Zard, S. Z. *Macromol. Rapid. Commun.* **2002**, *23*, 1049.
16. Jacquin, M. ; Muller, P. ; Lizarraga, G. ; Bauer, C. ; Cottet, H. ; Theodoly, O. *Macromolecules* **2007**, *40*, 2672.
17. Alexander, S. *J. Phys. (Paris)* **1977**, *38*, 983.
18. De Gennes, P.G. *Macromolecules* **1980**, *13*, 1069.
19. Napper, D.H., *Polymeric Stabilization of Colloidal Dispersions.* 1983. Academic Press, London.
20. Deroo, S.; Morvan, M. WO 03/068848, Rhodia Chimie.
21. Joanicot, M.; Kiplinger, J.D.; Morvan, M.; Adam; H. WO 03/068827, Rhodia Chimie.
22. Lannibois-Dréan, H.; Ricca, J-M.; Destarac, M.; Olier, P. WO 03/000396, Rhodia Chimie.
23. Lannibois-Dréan, H.; Ricca, J-M.; Destarac, M.; Olier, P. WO 03/002636, Rhodia Chimie.
24. Deroo, S.; Morvan, M.; Destarac, M. WO 03/090916, Rhodia Chimie.

Downloaded by CORNELL UNIV on June 26, 2012 | http://pubs.acs.org
Publication Date: August 13, 2009 | doi: 10.1021/bk-2009-1024.ch023

Downloaded by UNIV OF DELAWARE MORRIS LIB on June 26, 2012 | http://pubs.acs.org
Publication Date: August 13, 2009 | doi: 10.1021/bk-2009-1024.ch024

## Chapter 24

# Controlled Architecture Polymers at Arkema: Synthesis, Morphology and Properties of All-Acrylic Block Copolymers

**Pierre Gerard[1], Laurence Couvreur[1*], Stephanie Magnet[1], Jason Ness[2] and Scott Schmidt[2*]**

**[1]GRL, Arkema, B.P. 34, 64170 Lacq, France**
**[2]Arkema Inc., King of Prussia, PA19406, U.S.A.**
***To whom correspondence should be addressed. E-mail: laurence.couvreur@arkema.com ; scott.schmidt@arkema.com**

Over the past decade, Arkema has developed a controlled radical polymerization (CRP) technology that facilitates the production of materials with highly controlled architecture, such as block copolymers, using standard free radical polymerization techniques. The CRP technique based on NMP (Nitroxide Mediated Polymerisation) currently constitutes a remarkable tool for the design of compounds with different architectures and compositions: functionalised macromolecules, block copolymers, grafted copolymers, gradient copolymers, hybrid organic/inorganic systems, hyper-branched polymers, star polymers, polymer brushes, etc. The potential CRP products of immediate commercial impact are dominated by block copolymers, due to their ability to form nanostructured objects in solution or in solid state. Examples of possible uses are the encapsulation and release of active compounds, oil and lubricant modification, the stabilization of dispersion (cosmetic, inks, paints and mineral content, etc.), microelectronics, composites, the modification of surface properties (in the adhesives sector), the modification of mass properties in polymers (toughness, improvement of optical qualities) and in elastomers, etc.

In Controlled/Living Radical Polymerization: Progress in RAFT, DT, NMP & OMRP; Matyjaszewski, K.;
ACS Symposium Series; American Chemical Society: Washington, DC, 2009.

# Introduction

Nanotechnology developments through the preparation of complex macromolecules have seen rapid growth over the past several years due to recent advances in synthetic polymer chemistry. The growth is further fueled by the need for economical polymers designed with precise control and capable of filling intricate applications. Unfortunately, the synthetic routes employed often require stringent methods and/or costly post-polymerization modifications to obtain a given target molecule. Over the past decade, Arkema has developed a controlled radical polymerization (CRP) technology that facilitates the production of materials with highly controlled architecture, such as block copolymers, using standard free radical polymerization techniques. Block copolymers are characteristically comprised of two or more covalently linked immiscible polymer pairs that phase-separate into morphologies on the nanometer length-scale. The biphasic nature of these materials leads to composite materials containing characteristic properties inherent to each of the parent polymer phases that ultimately allows for control over the final end-use properties.

Arkema's controlled polymer technology platform derives from a basic molecule, trademarked as BlocBuilder®[1], which consists of an initiating species and a nitroxide controller combined into one molecule. The nitroxide significantly limits chain termination reactions by intermittently trapping the growing radical species. While copolymerizing two or more monomers with traditional radical initiators leads to polymers with random structures (properties are an average of the monomers used), BlocBuilder® provides a straightforward, robust method to produce novel block copolymer structures with tailored end-use properties. The advantages of Arkema's nitroxide-mediated technology include: process flexibility (bulk, solvent, and aqueous dispersed media), broad selection of monomer types (styrenic, acrylic, methacrylic, etc.), and innocuous nitroxide by-products. Other CRP techniques like Atom Transfer Radical Polymerization (ATRP) and Reversible Addition-Fragmentation chain Transfer (RAFT) typically require the removal of the control compounds from the final polymer (metallic and sulfur by-products, respectively).

The nitroxide-based CRP technique[2, 3] enables the design of compounds with very different architectures and compositions including: block copolymers, functionalized macromolecules, graft copolymers, gradient copolymers, hybrid organic/inorganic systems, star polymers, polymer brushes, etc. To realize the enormous commercial potential of this simplistic chemistry one must employ the judicial selection of segment composition and employ a rational design of polymer architecture, which ultimately defines the end-use application properties. The potential CRP products of immediate commercial impact are dominated by block copolymers, due to their ability to form nanostructured objects in solution or in solid state. Examples of possible uses include: encapsulation and release of active compounds, oil and lubricant additives, dispersion stabilizers (cosmetics, inks, paints, and mineral content), the modification of surface properties (e.g., adhesives and coatings), the modification of mass properties (impact strength, improvement of optical qualities), microelectronics, compatibilization, composites, etc.

Downloaded by UNIV OF DELAWARE MORRIS LIB on June 26, 2012 | http://pubs.acs.org
Publication Date: August 13, 2009 | doi: 10.1021/bk-2009-1024.ch024

Arkema recently announced the official launch of a new family of acrylic triblock copolymers, Nanostrength® polymers, which comprise methacrylic outer blocks that are miscible with a wide range of polymers, including most major industrial thermoset resins. Nanostrength polymers consist of two main classes; 1) all acrylic block copolymers produced by the aforementioned CRP technology and 2) polystyrene-b-polybutadiene-b-poly(methyl methacrylate) (SBM) triblock copolymers produced via "living" anionic polymerization techniques. The thermodynamically governed nano-scale morphology results in significant mechanical reinforcement without losing any of the important properties of the parent matrix material (chemical resistance, rigidity, glass transition temperature, transparency, etc.). The Nanostrength® range has natural applications in many industrial sectors such as cosmetics, composites (sports equipment, automotive, and aerospace), surface coatings, electronics and adhesives. Arkema has demonstrated commercial-scale feasibility through a pilot facility where block copolymer products have been produced on the ton scale.

Downloaded by UNIV OF DELAWARE MORRIS LIB on June 26, 2012 | http://pubs.acs.org
Publication Date: August 13, 2009 | doi: 10.1021/bk-2009-1024.ch024

## Experimental

Free-radical chemistry is the most widely used industrial polymerization process as it is cost effective, extremely robust, can employ a wide range of initiating species and reactive monomers, can be used in a wide range of operating conditions and can be utilized in emulsion systems. Unfortunately, this process does not allow for the control of molecular properties such as chemical composition, molecular weight, branching and/or for the formation of block copolymers. The inability to tailor the design of those features led to a compromise of properties often limiting the scope of applications. Aware of the intrinsic limitations of free-radical polymerization (FRP), scientists have been developing ways to overcome the lack of control in the free-radical processes by introducing the concept of CRP. Arkema has participated in this ambitious project because of its interest in free-radically produced polymers and in initiating and chain transfer systems in particular.[1] Furthermore, the project objective, to control the molecular structure of polymers, was well defined and due to the wide spread industrial use of free-radical chemistry the path to commercialization appeared less hindered than following the lead of anionic or cationic processes. The efforts of Arkema's researchers mainly concentrated on controlling the reactivity during the initiation and propagation phases of the polymerization process, in order to eliminate/reduce transfer and termination reactions and therefore access a precise control of the chain dimensions and the chain end functionality. These characteristics are then advantageously used to develop and construct more complex polymers: block copolymers, functional polymers, polymers with branched and hyper-branched chain architecture, etc.

---

[1] Arkema is integrated into the organic peroxide (Luperox) and mercaptan business

Radical polymerization pertains to polymerization which propagate through free radicals. Independent of propagation mode, we simply define that a controlled living polymerization occurs when the growth of the polymer chains continues until there are no more monomers present i.e., the addition of more monomers at the end of a living polymerization process must reactivate the process (which allows for sequenced polymerization). Furthermore, a radical polymerization process is generally considered "controlled" if the polymers obtained have the following characteristics:

- The conversion increases linearly as a function of time,
- The molecular weights change proportionally to the monomer conversion,
- The polymer has an experimental polydispersity index of less than 2 according to the law Ip = 1 + 1/Xn, where Xn is the polymerization index.

## NMP method

The simple idea of momentarily trapping the growing radical species and protecting them from non-controlled deactivations led to the development of CRP methods. The primary method Arkema chose to develop is based on a Nitroxide Mediated Polymerization (NMP) approach in which radicals are coupled with nitroxides to provide end users with a tool to enable the control over free-radical chemistry processes. In order to justify this approach commercially, it was essential to be able to concentrate developments on a limited number of molecules. The primary challenge was to develop a molecule capable of meeting the control requirements of a variety of monomers in various types of processes (from bulk processes to emulsion processes). In a certain respect, the many challenges that enabled us to converge towards the final molecule, epitomized a quest for simplicity.

The principle of trapping carbon radicals by means of nitroxides is described in Scheme 1.

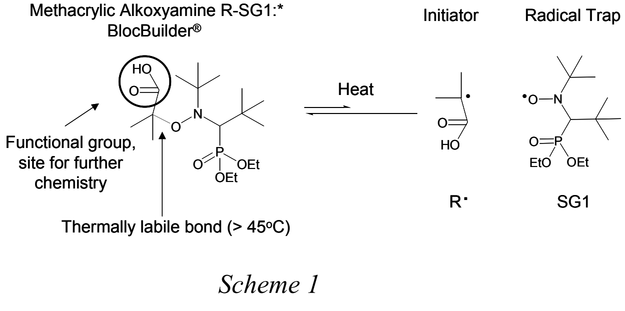
Methacrylic Alkoxyamine R-SG1:*
BlocBuilder®
Initiator
Radical Trap
HO
O
N
O
P
O
OEt
OEt
Heat
Functional group, site for further chemistry
Thermally labile bond (> 45°C)
O
HO
•O—N
O=P
EtO
OEt
R·
SG1

*Scheme 1*

The implementation of the NMP technology is very straightforward in the case where alkoxyamines are used directly. These molecules act both as initiators and as controllers and are released by thermolysis in stoichiometric proportions. It is possible to control the core architecture of the polymer thanks to the initiation fragment. Unlike standard peroxide or azoic type radical initiators, the initiator fragment can be easily transformed (see Scheme 2) using standard organic chemical reactions and it becomes possible to obtain polymer

Downloaded by UNIV OF DELAWARE MORRIS LIB on June 26, 2012 | http://pubs.acs.org
Publication Date: August 13, 2009 | doi: 10.1021/bk-2009-1024.ch024

architectures such as diblock, triblock, star, graft, hyperbranch or even telechelic copolymers, by using simple chemistry.

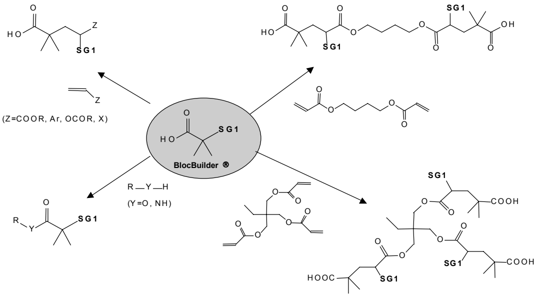

*Scheme 2*

The designed alkoxyamine and its derivatives therefore provide access to straightforward controlled radical polymerization processes, using only organic molecules and not requiring any post-processing of the polymers. This scheme is easily transferred to industrial processes provided the correct alkoxyamine selection is made. The latest generation of alkoxyamines developed by Arkema is that of "methacryl" type alkoxyamines. The product in this family with the best compromise of properties has a carboxylic acid function on the initiator fragment. This molecule has been commercialized and registered under the trade name BlocBuilder®. Carboxylic acid incorporation provides several benefits, such as, allows for the isolation of a solid product, allows for solubilization in aqueous media, provides a functional handle for further chemical modification, etc.

The thermal activation of BlocBuilder® (see Scheme 1) generates, by homolytic cleavage, a methacrylic acid radical (initiates the polymerization) and the SG1 nitroxide (controls the polymer chains growth). BlocBuilder® (mono-alkoxyamine) gives access to either gradient or block copolymers such as diblock A-B or triblock structures (symmetric A-B-A or asymmetric A-B-C). Symmetric A-B-A triblock copolymers can also be readily obtained in 2 steps starting from a previously formed di-alkoxyamine species (sometimes referred to as “Diamins”) that is generated *in-situ* by reacting 2 moles of BlocBuilder® with butanediol diacrylate in alcohol medium at 80 °C (Scheme 3)[4].

Downloaded by UNIV OF DELAWARE MORRIS LIB on June 26, 2012 | http://pubs.acs.org
Publication Date: August 13, 2009 | doi: 10.1021/bk-2009-1024.ch024

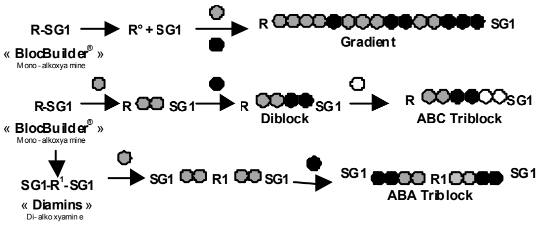

*Scheme 3*

A wide variety of block copolymers with acrylate/methacrylate or acrylate/styrenic structures have been produced. Moreover, due to the tolerance of the nitroxide chemistry towards functional groups, functionalized monomers such as (meth)acrylic acid, hydroxyethyl acrylate, glycidyl methacrylate, dimethyl acrylamide, etc. can be easily copolymerized with the hydrophobic moieties. These functionalities bring specific properties to the resultant copolymers such as compatibilization or miscibility with external matrices (through reactive or non-reactive interactions). The broad range of commodity, specialty, and functional monomers available allow for a wide range of freedom in tailoring composition which, along with the architectural control, leads to controlled end-use polymer and application properties (see Table 1).

**Table 1**

| Specialty / Functional (as co-monomers) | Applications |
|---|---|
| Acrylic acid (AA) | Polymeric surfactants, Amphiphilic Block Copolymers for cosmetic, wound care, hydrogels, … |
| Methacrylic acid (MAA) | High Tg Acrylic Block Copolymers, Elastomeric ionomers |
| Hydroxyethyl methacrylate (HEMA) | Reactive Hot Melt – Pressure Sensitive Adhesives |
| Dimethyl acrylamide (DMA) | Miscibility with High Tg Epoxy systems, Amphiphilic Block Copolymers |
| Maleic anhydride (MAH) | Compatibilizers for EP, Supramolecular chemistry |
| Glycidyl methacrylate (GMA) | Cross-linked Pressure Sensitive Adhesives |
| Polyethylene glycol methacrylate (PEGMA) | Paint & Ink dispersants |
| Tertiobutyl aminoethyl methacrylate (TBAEMA) | Decorative paints, Wood / Metal coatings |

Downloaded by UNIV OF DELAWARE MORRIS LIB on June 26, 2012 | http://pubs.acs.org
Publication Date: August 13, 2009 | doi: 10.1021/bk-2009-1024.ch024

It should also be noted that polymers obtained from BlocBuilder® have the carboxylic acid function located at the end of the chain, which means that it is possible, by chemically modifying this function, to access block copolymers comprising non-free-radical block segments, e.g. hydrophilic-hydrophobic copolymers such as polystyrene-polyethylene oxide (PS-PEO) or semi-crystalline-*b*-elastomer-*b*-amorphous block copolymers such as polycaprolactone-b–poly(butyl acrylate)-b-poly(methyl methacrylate) block copolymers (PCL-PBA-PMMA) or with one hydrolyzable/biocompostable block like polylactide (PLA) (Scheme 4)[5].

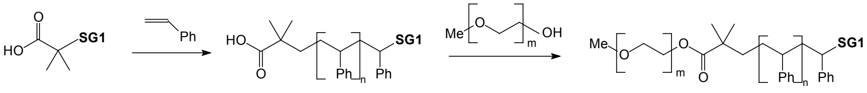

*Scheme 4*

As evidenced by the preceding text, BlocBuilder® is a highly versatile tool for the control over free-radical based polymerizations. It can be used to synthesize a wide variety of architectures, allows access to a wide range of monomer types (including functional monomers), and can be combined with other polymerization techniques through chain end functionality. Furthermore, it is highly versatile from a process point of view as it can be employed in bulk, solvent, suspension, and emulsion polymerization processes, without the prerequisite of stringent purification techniques. Furthermore, it can be used in standard equipment (no or little capital investment required) and the nitroxide chemistry employed is relatively innocuous.

## Results and Discussion

### From tough thermoplastics to “soft acrylic” thermoplastic elastomers

All acrylic triblock copolymers of poly(methyl methacrylate) – *b* – poly(butyl acrylate) – *b* –poly(methyl methacrylate) (MAM), comprising rigid and rubbery blocks tethered together and having a volume fraction of soft poly(butyl acrylate) phase included between 20% (thermoplastic materials) to 80% (elastomeric behavior) are routinely prepared by NMP[6].

One interesting aspect of these materials is that the PMMA blocks are not perfectly controlled by the nitroxide used herein and have a polydispersity index of ~ 2 to 3. This is due to the high rate of disproportionation of MMA, which ultimately leads to chain termination in a fraction of the growing block copolymer chains. Charleux and co-workers[7] have developed a process to allow for enhanced control over methacrylate polymerizations to greatly increase “livingness” and reduce polydispersity.

Despite the lack of complete MMA control, macrophase separation was never observed in any of the systems investigated and the final products revealed, as expected, nanoscale morphologies indicative of the thermodynamically controlled block copolymer self-assembly process. Lamellar

Downloaded by UNIV OF DELAWARE MORRIS LIB on June 26, 2012 | http://pubs.acs.org
Publication Date: August 13, 2009 | doi: 10.1021/bk-2009-1024.ch024

and poorly ordered bicontinuous, cylindrical, or spherical morphologies could be revealed by TEM on solvent cast films.

The morphologies of solvent cast and annealed copolymer films present little long-range order and grains of a given microdomain orientation are small. More importantly, interfacial curvature does not follow the classical evolution with composition observed for ideal monodisperse block copolymers. Hence, lamellar are observed around 65 – 55 vol % PMMA, while perfectly symmetric copolymers adopt a curved interface concave toward PMMA and form cylinders or cylindrical micelles with poor lattice order. This is likely a result of the conformational asymmetry[8].

These results suggest that unbalanced polydispersity between the two blocks can induce interfacial curvature toward to broadest molecular weight distribution. This effect is consistent with other literature results on polydisperse block copolymers which indicate lower mean interfacial curvature when increasing the PDI of the majority domain segment[9]. This co-surfactant effect might be expected to be encountered in radical or hybrid block copolymer syntheses whenever control cannot be optimized for all blocks. The morphological trends were observed under static conditions as close as possible to thermodynamic equilibrium. In practice, however, such copolymers are more likely to be used directly after processing from the melt in extruders and injection molders or in blends with homopolymers. This raises an important question regarding the effect of complex flow fields in polymer processing tools on the self-assembly of these polydisperse systems and the related impact on end-use properties. It is important to note that while the morphological behavior of polydisperse systems deviates from the analogous low polydispersity systems, they still undergo nano-scale separation and impart the desired balance of properties. Furthermore, the ever improving understanding of these systems allows greater prediction over the resultant morphology and properties one can attain. These findings are helping to further shape the way polymer chemists design composition and structure to tailor end use properties i.e., perfect control is not necessary to obtain target properties which opens up new composition possibilities and further simplifies process developments.

## New tough thermoplastic material

Poly(methyl methacrylate) (PMMA), which has a glass transition temperature (Tg) of about 110°C, is one of the more brittle amorphous thermoplastic materials. The molecular mobility in the glassy state is low and the polymer chains are unable to undergo large scale molecular motions in response to rapidly applied external stresses or impacts. Thus, at ambient temperature, PMMA is brittle and notch sensitive. Fracture proceeds by the formation of isolated crazes, associated with localized stress concentrations, a phenomenon which has been extensively described in the literature [10-12].

Owing to its transparency, PMMA is often used in applications, requiring good optical properties. However, its brittleness is a limiting factor in many cases (such as in the transport business for example). Indeed, even for high molecular weights, the energy dissipated during the fracture of commercial

Downloaded by UNIV OF DELAWARE MORRIS LIB on June 26, 2012 | http://pubs.acs.org
Publication Date: August 13, 2009 | doi: 10.1021/bk-2009-1024.ch024

grades of unmodified PMMA is significantly lower than for polycarbonate (PC), which is one of its main competitors for optical applications. However, as with many other polymers, a significant improvement in the toughness of PMMA can be obtained by combining it with a secondary phase which has a sub-ambient Tg. The size of these domains should be chosen to maximize their influence on the intrinsic deformation mechanisms of the matrix in such a way as to optimize the rate of energy dissipation during crack development. While numerous methods are currently employed in the preparation of rubber-toughened polymers, a highly attractive alternative is to use all acrylic block copolymers comprising rigid and rubbery blocks tethered together. The self-assembly of block copolymers at the molecular scale produces transparent composites (rubber domains do not scatter light) that are thermodynamically robust and can be processed repeatedly, while maintaining favorable properties. The abovementioned high molecular weight polydisperse acrylic block copolymers are able to form ordered nanostructures owing to the segregation of incompatible monomer sequences or blocks that are linked together. The domain size is of the order of magnitude of the chain length, ranging typically from 10 to 50 nm. Such tailor made morphologies open new perspectives to finely tune valuable new compromises of properties, for example between stiffness, toughness and processability.

Besides ductility, due to confinement, nanostructuration of high molecular weight polydisperse acrylic block copolymers can trigger new types of deformation mechanisms under dynamic loading and improve the toughness properties. For example, un-notched impact results are quite high without any macroscopic stress whitening, which is an interesting property in common with polycarbonate. For the notched impact properties, the critical parameter is argued to be the ratio of the length of the PMMA blocks to the entanglement length, since the PMMA effectively anchors the poly(butyl acrylate) (PBA) chains in the glassy phase. An extensive PBA shear deformation with the presence of "chevrons" morphology has been observed. Thus, it has been demonstrated that fracture properties can be substantially improved by increasing the molar masses of the blocks while maintaining the relative proportion of PBA. The molar mass of the PMMA would appear to be a key factor in the mechanical performance, which could be easily reached with high molecular weight polydisperse acrylic block copolymers prepared by NMP[13].

All-acrylic block copolymers are good commercial candidates since they have potential advantages as substitutes for contemporary commodity plastics in that their synthesis is not only well controlled, but also economically attractive for the industry.

## New additives for thermoset and composite materials

Applications of epoxy-based thermosets are often limited by an inherent brittle behavior of the matrix. The prevalence of epoxy polymers in composite materials and engineering adhesives indicates the importance to know, understand, and be able to reinforce their end-use performance. The case of static/dynamic loading is of particular significance in many applications,

Downloaded by UNIV OF DELAWARE MORRIS LIB on June 26, 2012 | http://pubs.acs.org
Publication Date: August 13, 2009 | doi: 10.1021/bk-2009-1024.ch024

especially in aerospace products. Their toughness is conventionally improved by the addition of a rubber or a thermoplastic phase. The selection of the type of organic toughening agent is often influenced by the amount of crosslinking in the epoxy polymer[14]. Thereby, soft rubbery polymers are often added as toughening agents for lightly crosslinked epoxies. The yield strengths for these materials are relative low, i.e. such materials display an inherent ability to shear yield. In these systems, the most efficient tougheners are the ones containing a high level of rubber phase that can cavitate to initiate shear bands in the epoxy matrix at the crack tip. The most widely used is the reactive liquid rubber type, e.g. CTBN (Carboxyl terminated butadiene acrylonitrile). The use of rigid thermoplastic particles has been successful in improving the fracture toughness of highly crosslinked epoxies. The yield strengths for these materials are relative high, i.e. such materials do not possess an inherent ability to shear yield, thus other mechanisms are responsible for the energy dissipation (crack bridging, crack pinning, crack deflection, etc). The tougheners used in these systems are high Tg thermoplastics such as poly(ether sulfone) (PES). However, the increase of toughening brought in these highly crosslinked epoxies is more limited than what can be obtained in lightly crosslinked epoxies. One type of toughener is thus usually devoted to reinforce only one type of thermoset family. An alternative approach to the toughening of epoxy network consists of the addition of acrylic block copolymers, comprising rigid and rubbery blocks tethered together. An immiscible or partially miscible block with thermoset precursor causes structuration by a phenomenon of segregation and a second PMMA-based miscible block stabilizes the formed structure both in lightly crosslinked systems and in more polar highly crosslinked epoxies[15]. Nanostrength® acrylic block copolymers form a regular network of nano-elastomeric domains in reactive systems by a self-assembly process governed through thermodynamics. In a thermoset resin compatible with the PMMA block, it is possible to significantly improve the intrinsic properties of the neat resins via the nanostructuration of the block copolymer additive, while at the same time preserving other key properties such as Tg, solvent resistance, stiffness, etc ...

In DGEBA (diglycidyl ether of bisphenol A)-MDEA (4,4-methylenebis-(2,6-diethyl)-aniline), the PMMA block remains miscible up to the end of the reaction and stabilizes a nanostructured morphology, while in DGEBA-DDS (4,4'-diaminodiphenyl sulfone), the PMMA block is not miscible enough to stabilize and a flocculation (macrophase separation) occurs. A new block copolymer with reactive functionalities[16], has been developed by increasing the hydrophilic character of the PMMA block. These block copolymers are able to form ordered nanostructures, such as vesicles, spherical micelles, or wormlike micelles in epoxy resins, depending on the block copolymer composition and/or concentration. Dependant on the type of epoxy system used (both the resin and the hardener), these morphologies are retained with the full curing of the resins. The domain size is always on order of magnitude of the chain length, ranging typically from 10 to 50 nm. The nano-scale morphology allows one to modify toughness in ultra-thin applications where the thickness of the epoxy layer (or inter fiber spacing between fibers in composites) is in the micron range.

Downloaded by UNIV OF DELAWARE MORRIS LIB on June 26, 2012 | http://pubs.acs.org
Publication Date: August 13, 2009 | doi: 10.1021/bk-2009-1024.ch024

Downloaded by UNIV OF DELAWARE MORRIS LIB on June 26, 2012 | http://pubs.acs.org
Publication Date: August 13, 2009 | doi: 10.1021/bk-2009-1024.ch024

As demonstrated unequivocally by Gerard and co-workers[17], acrylic block copolymers provide excellent toughness to different epoxy thermosets while maintaining other favorable properties such as Tg, modulus, transparency, etc.

The self-assembly of block copolymers at a molecular scale in epoxy-based glassy polymers produces transparent nanostructures of small rubbery domains that prevent rapid crack propagation and make acrylic block copolymers an excellent candidate for improving the damage tolerance of composites for demanding applications.

### New thermoplastic elastomers

High molecular weight polydisperse acrylic block copolymers having high levels of BA content (>50%) are of interest in various fields, including: thermoplastic elastomers either as a bulk material or as a modifier, reinforcement of engineering polymers, adhesives, paint and coatings through emulsions, etc.

MAM-based triblocks offer a given number of properties that are not fulfilled with the current TPE systems. For example, the industry is particularly active in the search for TPE’s with improved adhesion, improved oil resistance, and improved processing conditions, of which all may be addressed with the aforementioned block copolymers.

## Conclusions

Stimulated by increasing demands for polymers, the quest for products that are more economically competitive and new increasingly sophisticated applications for polymer materials, macromolecular synthesis has responded through significant progress both in the preparation processes and in the precise control of the macromolecular structures and architectures. The idea of momentarily trapping the growth of radical species, while protecting them from non-controlled deactivation, has made it possible to develop a controlled radical polymerization (CRP) method based on nitroxides (NMP). The underlying "material" concept is to progress from polymers with random structures and "average" properties, to evenly structured polymers with specific and tailored properties. This was particularly necessary because standard radical initiators did not allow this compromise, no matter which polymerization conditions (pressure, temperature, duration, medium, etc.) were employed.

Arkema's research and development department had been progressing on this effort for over 10 years prior to 2004 when the significant breakthrough with the introduction of BlocBuilder® was announced. Due to the relative ease in which it produces a wide range of block copolymers, it was quite logical to use the name - BlocBuilder®. As described throughout this chapter, BlocBuilder® provides the qualities of the initiator and controller that Arkema researchers had strived to obtain. Arkema is therefore the first and only chemical company to develop and commercialize a stable free radical initiator that fully controls families of monomers as different as styrenic, acrylic and partially methacrylic monomers. The CRP technique based on NMP currently constitutes a remarkable tool for the design of compounds with different architectures and compositions: functionalised macromolecules, block copolymers, grafted copolymers, gradient copolymers, hybrid organic/inorganic systems, hyper-branched polymers, star polymers, polymer brushes, etc. and all of these structures can now be produced using BlocBuilder®. The potential uses of CRP products essentially concern block copolymers, due to their ability to form nanostructured objects in solution or in solid state. Of course, to realize the enormous commercial potential of this relatively simplistic chemistry, the end user must employ the judicial selection of segment composition and employ a rational design of polymer architecture, which ultimately defines the end-use application properties. Examples of possible uses include: encapsulation and release of active compounds, oil and lubricant additives, compatibilizers, thermoplastic elastomers (adhesives or bulk materials), dispersion stabilizers (cosmetics, inks, paints, and mineral content), the modification of surface properties (coatings), the modification of mass properties (impact strength, improvement of optical qualities), microelectronics, composites, etc.

Downloaded by UNIV OF DELAWARE MORRIS LIB on June 26, 2012 | http://pubs.acs.org
Publication Date: August 13, 2009 | doi: 10.1021/bk-2009-1024.ch024

## Acknowledgements

The authors wish to thank Professor B. Charleux & her team, Professor D. Bertin & his team, Dr Anne-Valerie Ruzette from ESPCI and Dr Laure Lalande from EPFL and also many scientists from Arkema who have all contributed to this work by providing data and fruitful debate/discussions.

## References

[1] Couturier, J.L. ; Guerret, O. ; Bertin, D. ; Gigmes, D. ; Marque, S. ; Tordo, P. ; Chauvin, F. ; Dufils, P.E. ; **WO 2004**/014926.

[2] Matyjaszewski, K. and Spanswick, J. ; *Materials Today*, **2005**, 8, issue 3, 26-33.

[3] Matyjaszewski, K. ; *Prog. Polym. Sci.*, **2007**, 32, 93-146.

[4] Lefay, C. ; Belleney, J. ; Charleux, B. ; Guerret, O. ; Magnet, S. ; *Macromol. Rapid Commun.* **2004**, *25,* 1215.

[5] Guillaneuf, Y. ; Dufils, P.E. ; Autissier, L. ; Rollet, M. ; Gigmes, D. and Bertin, D. ; submitted to *Macromolecules*, **2008**.

[6] Ruzette, A.V. ; Chauvin, F. ; Guerret, O. ; Bertin D. ; Vuillemin B. ; Leibler, L. ; Gérard, P. ; **WO 2003**/062293.

[7] Charleux, B. ; Nicolas, J. and Guerret, O. ; *Macromolecules*, **2005**, 38, 5485-5492.

[8] Ruzette, A.V. ; Tencé-Girault, S. ; Leibler, L. ; Chauvin, F. ; Bertin, D. ; Guerret, O. ; Gérard, P. ; *Macromolecules*, **2006**, 39, 5804-5814.

[9] Lynd, N. A. ; Hillmyer, M.A. : *Macromolecules*, **2005**, 38, 8803-8810.

[10] Kramer, E. J. ; Kausch, H. H. ; *Advances in Polymer Science*, **1990**, 91/92, 1-68.

[11] Beguelin, Ph.; PhD thesis N°1572, EPF Lausanne, **1996**.

[12] Plummer, C., J., G. ; Beguelin, Ph. and Kausch H.H. ; *Colloids Surfaces A* : Physiochem. Eng. Aspects, **1999**, 153, 551-566.

[13] Lalande, L. ; Plummer, C.J.G. ; Manson, J.A. ; Gérard, P. ; submitted to *Polymer*, **2009**.

[14] Pearson, R.A., "An overview of organic toughening agents for epoxy resins", *ERFD Spring 2000 Conference*, April 16-18, **2000**, San Antonio, Texas.

[15] Ritzenthaler, S. ; Court, F. ; Girard-Reydet, E. ; Leibler, L. ; Pascault, J.P. ; *Macromolecules*, **2002**, 36, 118-126.

[16] Phang, T.N.T. ; Maiez-Tribut, S. ; Pascault, J.P. ; Bonnet, A. ; Gérard, P. ; Guerret, O. and Bertin, D. ; *Macromolecules*, **2007**, 40, 4516 - 4523.

[17] Gérard, P. ; Passade-Boupat, N. ; Fine, T. ; Gervat, L. and Pascault, J.P. ; *Macromol. Sympo.*, **2007**, 256, 55-64.

Downloaded by UNIV OF DELAWARE MORRIS LIB on June 26, 2012 | http://pubs.acs.org
Publication Date: August 13, 2009 | doi: 10.1021/bk-2009-1024.ch024

# Author Index

Adebolu, O. I., 149–163
Amamoto, Y., 319–329
Asandei, A. D., 149–163

Bertin, D., 245–262
Beuermann, S., 233–243
Börner, H. G., 265–278
Boschmann, D., 217–232
Boué, F., 245–262
Brusseau, S., 303–318
Bzducha, W., 347–359

Carrot, G., 245–262
Chagneux, N., 245–262
Charleux, B., 303–318
Chen, Y., 149–163
Chong, Y. K., 3–18
Chung, T. C. M., 331–344
Couvreur, L., 303–318, 361–373

Debuigne, A., 131–147
Deroo, S., 347–359
Destarac, M., 347–359
Detrembleur, C., 131–147
Dire, C., 303–318
Dufils, P.-E., 245–262

Förster, N., 233–243
Fröhlich, M. G., 217–232

Gan, Q., 181–193
Gerard, P., 361–373
Gigmes, D., 245–262
Greene, A. C., 81–93
Grishin, D. F., 95–114
Grubbs, R. B., 81–93
Guillaneuf, Y., 245–262

Herrmann, K., 233–243

Imran-ul-haq, M., 233–243

Jérôme, C., 131–147
Jérôme, R., 131–147
Jitchum, V., 279–292
Johnston-Hall, G., 19–35

Kakwere, H., 279–292
Kamigaito, M., 49–63
Kellum, M. G., 195–215
Klumperman, B., 167–179
Kolyakina, E. V., 95–114

Lacroix-Desmazes, P., 65–79
Ladmiral, V., 279–292
Lannibois-Dréan, H., 347–359
Lazarev, M. A., 95–114
Lefay, C., 245–262
Li, S., 115–129

Mänz, M., 217–232
McCormick, C. L., 195–215
Maeda, T., 319–329
Magnet, S., 303–318, 361–373
Malepu, V., 37–47
Matsuda, Y., 319–329
Moad, G., 3–18
Monteiro, M. J., 19–35
Mulder, R., 3–18
Murayama, H., 49–63

Ness, J., 361–373
Ni, P., 293–302
Nicolas, J., 303–318

Otsuka, H., 319–329

Pavlovskaya, M. V., 95–114
Peng, C.-H., 115–129
Perrier, S., 279–292
Petruczok, C. D., 37–47
Phan, T. N. T., 245–262
Poli, R., 131–147
Pound-Lana, G., 167–179

Rizzardo, E., 3–18

Saha, G., 149–163

Downloaded by 89.163.34.136 on June 25, 2012 | http://pubs.acs.org
Publication Date: August 13, 2009 | doi: 10.1021/bk-2009-1024.ix001

Satoh, K., 49–63
Schmidt, S., 361–373
Sénéchal, A., 347–359
Shchepalov, A. A., 95–114
Shipp, D. A., 37–47
Siegmann, R., 233–243
Simpson, C. P., 149–163
Smith, A. E., 195–215

Takahura, A., 319–329
Thang, S. H., 3–18
Thopasridharan, M., 37–47
Tonnar, J., 65–79
Tran, T., 37–47
Trimaille, T., 245–262

Vana, P., 217–232
Vinas, J., 245–262
Vukicevic, R., 233–243

Wayland, B. B., 115–129

Xu, X., 195–215

Yu, H. S., 149–163
Yu, Q., 181–193

Zhang, H., 181–193
Zhang, T., 37–47
Zhang, Z.-C., 331–344
Zhou, X., 293–302
Zhu, S., 181–193
Zhu, X., 293–302
Zifferer, G., 217–232

Downloaded by 89.163.34.136 on June 25, 2012 | http://pubs.acs.org
Publication Date: August 13, 2009 | doi: 10.1021/bk-2009-1024.ix001

# Subject Index

**A**

Acrylamides. *See* Stereospecific radical polymerization
Acrylates
  all-acrylic block copolymers, 368–369
  triblock copolymers, 367
  Z-RAFT star polymerization, 226–228
  *See also* BlocBuilder® technology; *N,N*-Dithiocarbamates (DTCs); Z-RAFT star polymerization
Acrylic acid
  application as co-monomer, 366*t*
  block copolymers with isoprene, 288–290
  *See also* Soft nanoparticles
*N*-Acryloyl alanine (AAL), block copolymers of, 201–203
Activators generated by electron transfer, atom transfer radical polymerization (ATRP), 67
Acyclic β-phosphorylated *N*-(2-methylpropyl)-*N*-(1-diethylphosphono-2,2-dimethyl propyl)-*N*-oxyl (SG1) nitroxide
  development, 246
  structure, 247
  *See also* SG1 and Blocbuilder® technology
Alkoxyamine synthesis
  addition of radicals to 2-methyl-2-nitrosopropane, 89–91
  addition of radicals to nitroso-*t*-octane, 89
  benzylic halide abstraction for, 84, 85
  dithiane based initiators, 88
  enolate oxidation, 85, 86
  generating C-centered radicals with nitroxide trapping, 83–88
  hydrocarbon oxidation synthetic protocols, 87
  initiators for nitroxide-mediated radical polymerization (NMRP), 82
  Mn(III) based epoxidation, 83–84
  photodecomposition of azo-initiator or dithiocarbamate, 88
  radical abstraction from hydrocarbons, 86–87
  radicals from organic halides, 84, 85
  trapping C-based radicals with nitroso compounds or nitrones, 89–91
Alkyl halides, alkoxyamine synthesis, 84, 85
Alkynes. *See* Poly(vinylidene fluoride) (PVDF)
Amphiphilic block copolymers
  controlled radical polymerization techniques, 197–198
  drug transport, 198–199
  macromolecular design by interchange of xanthates (MADIX) technology, 349–351
  morphological transitions in dilute aqueous solutions, 196–197
  RAFT polymerization for functional, 280–281
  shell cross-linking for drug delivery, 199
  shell cross-linking via incorporation of activated esters, 204–207
  shell cross-linking via in situ nanoparticle formation, 209–212

Downloaded by 89.163.34.136 on June 25, 2012 | http://pubs.acs.org
Publication Date: August 13, 2009 | doi: 10.1021/bk-2009-1024.ix002

- shell cross-linking via interpolyelectrolyte complexation, 199–203
- stimuli for reversible assembly, 196
- stimuli-responsive morphological transitions, 197–198
- stimuli-responsive morphologies for drug delivery, 198
- *See also* Soft nanoparticles

Architectures, macromolecular design by interchange of xanthates (MADIX), 350

Arkema, Inc.. *See* BlocBuilder® technology

Arm growth, initialization of, in Z-RAFT star polymerization, 222–223

Ascorbic acid, reductor for nitroxide, 66

Atom transfer radical addition (ATRA), alkoxyamine synthesis, 84, 85

Atom transfer radical polymerization (ATRP)
- activators generated by electron transfer (AGET), 67
- controlled method, 82, 132
- end functionalization techniques, 248
- miniemulsion polymerization, 67

Autoacceleration, kinetic behavior, 185–186

1,1-Azobis(cyclohexanecarbonitrile) (VAZO88)
- conversion, molecular weight and polydispersity index for styrene polymerization, 24, 25*f*
- initiator for styrene polymerization, 21, 23*t,* 24*t*
- termination rate coefficients for RAFT polymerization of styrene, 25–26, 28*f*

Azobis(isobutyronitrile) (AIBN)
- rate of decomposition, 7, 8*f*
- reversible addition fragmentation chain transfer (RAFT) polymerization, 5–6
- thermal decomposition, 6, 7
- *See also* Reversible addition fragmentation chain transfer (RAFT) polymerization

**B**

Batch emulsion polymerization. *See* Water-soluble macroinitiators

Benzylic halide, abstraction for alkoxyamine synthesis, 84, 85

Bioconjugates. *See* Peptide-polymer conjugates

BlocBuilder® technology
- Arkema's controlled polymer technology, 362
- carbon radical trapping by nitroxides, 364
- end-use polymer and applications, 366*t*
- experimental, 363–367
- new additives to thermoset and composite materials, 369–371
- new thermoplastic elastomers, 371
- nitroxide mediated polymerization (NMP) method, 364–367
- thermal activation, 364, 365
- tough thermoplastic materials, 368–369
- tough to "soft acrylic" thermoplastic elastomers, 367–368
- *See also* SG1 and Blocbuilder® technology

Block copolymers
- all-acrylic, 368–369
- design using MADIX, 350–351
- di- or tri-, by 1,2-intermolecular radical addition, 257–258

Downloaded by 89.163.34.136 on June 25, 2012 | http://pubs.acs.org
Publication Date: August 13, 2009 | doi: 10.1021/bk-2009-1024.ix002

Downloaded by 89.163.34.136 on June 25, 2012 | http://pubs.acs.org
Publication Date: August 13, 2009 | doi: 10.1021/bk-2009-1024.ix002

- macromolecular design by interchange of xanthates (MADIX) technology, 349–351
- poly(butyl acrylate), 76, 77*f*
- PS macroinitiators with MMA using nitroxides, 109–111, 112*f*
- vesicles formation using, and ionic cross-linking, 199–203
- *See also* Amphiphilic block copolymers; *N,N*-Dithiocarbamates (DTCs); Nitroxide mediators for controlled polymers; Soft nanoparticles

Block copolymers for emulsion stabilization. *See* Macromolecular design by interchange of xanthates (MADIX) technology

Borane-mediated radical polymerization
- autoxidation reaction of triaklylborane ($BR_3$), 332
- $^{11}B$ NMR spectra of oxidation adducts of triethylborane ($B(Et)_3$) and $B(OMe)(Et)_2$, 334*f*
- conditions for vinylidene fluoride (VDF) polymerization, 336*t*
- experimental, 332–333
- fluoro copolymers with well-controlled structures, 332
- $^1H$ and $^{19}F$ NMR spectra of PVDF, 337–338
- mechanism, 334–338
- oxidation mechanism of $B(Et)_3$, 335, 338
- synthesis of fluoro co- and ter-polymers, 333
- thin film preparation and measurements, 333
- *See also* Fluoropolymers

Butyl acrylate (BA)
- *ab initio* emulsion polymerization RITP, 68
- anchoring poly(BA) to poly(methyl methacrylate) (PMMA), 369
- block copolymerization, 76, 77*f*
- block copolymers with isoprene, 288
- copolymerization with styrene and MMA, 107*t,* 108
- iodine concentration for, polymerization, 74–75
- molecular weight distributions (MWD) of PBA, 75*f*
- procedure for miniemulsion polymerization, 69–70
- RAFT polymerization of poly(*n*-butyl acrylate), 272*f,* 274*f,* 275
- reverse iodine transfer polymerization, 74
- *See also* Reverse iodine transfer polymerization (RITP)

*t*-Butyl acrylate (tBA)
- RAFT polymerization of styrene, methyl acrylate (MA) and, 43*t*
- *See also N,N*-Dithiocarbamates (DTCs)

**C**

Cage reactions, azobisisobutyronitrile (AIBN), 6, 7

Carbon-based radicals
- addition to 2-methyl-2-nitrosopropane, 89–91
- addition to nitroso-*t*-octane, 89

Carboxyl terminated butadiene acrylonitrile (CTBN), toughening epoxies, 370

Chain length dependent termination (CLD-T). *See* Reversible addition–fragmentation chain transfer with chain length dependent termination (RAFT-CLD-T)

Chain transfer, RAFT polymerization, 4, 5
Chemically induced dynamic nuclear polarization (CIDNP), ketenimine (K), 7, 8*f*
Chlorotrifluoroethylene (CTFE). *See* Fluoropolymers
"Click" reactions
  cycloadditions, 234
  functionalizing end groups with, 241–242
  *See also* Poly(vinylidene fluoride) (PVDF)
Coalescence
  emulsion destabilization, 349
  stabilization of emulsions against, 352–353
Cobalt-mediated radical polymerization (CMRP)
  characterizations, 133–134
  cobalt complex as counter radical, 132, 133
  computational details, 134–135
  density functional theory (DFT) calculation, 143–144
  dimethylformamide (DMF) and dimethylsulfoxide (DMSO) solvent effects, 141, 142*f*
  enthalpy diagram and sketch of coordination geometries, 145*f*
  experimental, 133–135
  mechanism, 132, 133
  molar mass vs. vinyl acetate (VAc) conversion by temperature, 137*f*
  polymerization procedures, 134
  preparation of alkylcobalt(III) complex, 134
  size exclusion chromatograms for VAc polymerization, 138*f*
  temperature, 135–138
  water effects on VAc, 138–139, 140*f*
Cobalt porphyrin mediated living radical polymerization
  degenerative transfer and associative radical interchange, 125–128
  organo-cobalt complexes through β-hydrogen transfer, 123–124
  reversible termination and dissociative radical exchange, 124
Combination reactions, azobisisobutyronitrile (AIBN), 6, 7
Composite additives, BlocBuilder® technology, 369–371
Controlled/living radical polymerization (CLRP)
  advantages over free radical polymerization (FRP), 182
  vinyl acetate (VAc), 38
Controlled radical polymerization (CRP)
  amphiphilic block copolymers, 196
  macromolecular design by interchange of xanthates (MADIX) technology, 348
  stimuli-responsive morphological transitions, 197–198
  techniques, 66, 132, 246
  *See also* Nitroxide mediators for controlled polymers; Water-soluble macroinitiators
Copolymerization of methacrylate and dimethacrylate
  complex viscosity during RAFT, of oligo(ethylene glycol) methyl ether methacrylate (OEGMEMA) with oligo(ethylene glycol) dimethacrylate (OEGDMA), 187*f*
  crosslinking density vs. OEGDMA molar fraction, 190*f*
  dynamic mechanical analysis (DMA) measurement, 184
  experimental, 183–184
  gelation, 187–189
  gelation behavior in RAFT process, 189

Downloaded by 89.163.34.136 on June 25, 2012 | http://pubs.acs.org
Publication Date: August 13, 2009 | doi: 10.1021/bk-2009-1024.ix002

  gel characterization method, 184
  gel fraction development and swelling ratio vs. vinyl conversion, 188*f*
  glass transition temperature vs. OEGDMA molar fraction, 190*f*
  kinetic behavior of RAFT with crosslinking, 185–186
  kinetic measurement, 183–184
  microgels, 188
  polymerization rate and vinyl conversion, 185*f*
  RAFT-crosslinked network, 189–191
  rate autoacceleration, 186
  rheological measurement, 184
  storage modulus and loss tangent vs. temperature, 190*f*
  vinyl conversion at autoacceleration onset and OEGDMA molar fraction, 185*f*
  vinyl conversion at gelation onset, 188*f*
Copolymers
  block copolymerization of poly(butyl acrylate), 76, 77*f*
  isoprene/styrene, 159, 160*f*
  radical crossover reaction of, 325–327
  *See also* Amphiphilic block copolymers; *N,N*-Dithiocarbamates (DTCs); Fluoropolymers; Nitroxide mediators for controlled polymers; Water-soluble macroinitiators
Copolymers with covalent bonds in side chains
  copolymer of methyl methacrylate (MMA) and alkoxyamines **1** and **2** (poly(MMA-*co*-**1**-**2**)), 321–322
  de-cross-linking reaction of nanogel, 327, 328*f*
  design and synthesis of diblock copolymers with alkoxyamines, 323–324
  dissociation/association reaction of alkoxyamine, 320
  dynamic covalent polymers with 2,2,6,6-tetramethylpiperidinyl-1-oxy (TEMPO)-based alkoxyamine, 320
  experimental, 321–323
  measurements, 323
  molecular design, 320
  molecular weights and polydispersities of diblock copolymers, 324, 325*t*
  morphologies of nanogels, 326–327
  PMMA-b-poly(MMA-*co*-**1**-*co*-**2**) (**3**), 322
  polymer reaction of diblock **3**, 322
  polymer reaction of nanogel to linear copolymers, 322
  radical crossover reaction of copolymers, 325–327
  reversible formation of macroscopic gel and star-like nanogels, 321
  time dependence of molecular weight in crossover reaction, 326*f*
  topology of star polymers, 326
  transformation from nanogels to linear polymers, 327, 328*f*
  well-defined diblock with thermally exchangeable alkoxyamines, 324
  Covalent bonds. *See* Copolymers with covalent bonds in side chains
Creaming, emulsion destabilization, 349
Crosslinked polymers
  controlled living radical polymerization techniques, 182–183

Downloaded by 89.163.34.136 on June 25, 2012 | http://pubs.acs.org
Publication Date: August 13, 2009 | doi: 10.1021/bk-2009-1024.ix002

  RAFT-crosslinked network structure, 189–191
  time dependence of molecular weight of diblocks to, 326
  *See also* Shell cross-linking; Soft nanoparticles
Cycloadditions, "click" reactions, 234

**D**

De-cross-linking. *See* Copolymers with covalent bonds in side chains
Degenerative chain transfer (DT), mechanism in cobalt-mediated process, 132
Degenerative transfer (DT)
  methyl acrylate polymerization, 124
  vinyl acetate polymerization, 125–128
Density functional theory (DFT)
  cobalt-mediated radical polymerization (CMRP), 143–144, 145*f*
  computational details, 134–135
Design, block copolymers by macromolecular design by interchange of xanthates, 350–351
Destabilization, emulsion, mechanisms, 348–349
Diblock copolymers
  conformation in surfactant film, 355*f*
  emulsifiers, 351–352
  functional amphiphilic, 280–281
  influence of level on emulsification, 352*f*
  influence of structure, 355–356
  interfacial tension, 354*f*
  macromolecular design by interchange of xanthates (MADIX) for amphiphilic, 349–351
  nano-ordered structures, 280
  PS macroinitiators with MMA using nitroxides, 110–111
  stabilization emulsions against coalescence, 352–353
  *See also* Macromolecular design by interchange of xanthates (MADIX) technology; Soft nanoparticles
Dielectric, fluoropolymer, for high energy density capacitors, 338–343
Differential scanning calorimetry (DSC), RAFT polymerization of styrene, 21, 22
Dimethacrylate. *See* Copolymerization of methacrylate and dimethacrylate
*N,N*-Dimethylacrylamide (DMAM)
  application as comonomer, 366*t*
  experimental, 59–61
  $^1$H NMR spectra of poly(DMAM), 53*f*
  interaction of thioureas with DMAM monomer and dimer, 55–56
  radical polymerization of, with thioureas, 52*t*, 54*t*
  RAFT polymerization in presence of thioureas, 57–59
  stereospecific radical polymerization of, with thiourea derivatives, 51–55
  tacticity control, 58–59
  *See also* Stereospecific radical polymerization
Dimethylformamide (DMF), cobalt-mediated radical polymerization, 141, 142*f*
Dimethylsulfoxide (DMSO), cobalt-mediated radical polymerization, 141, 142*f*
Dipyridamole (DIP), delivery of model drug, 205, 206*f*
Disproportionation, azobisisobutyronitrile (AIBN), 7
Dissociative radical exchange, methyl acrylate polymerization, 124

Downloaded by 89.163.34.136 on June 25, 2012 | http://pubs.acs.org
Publication Date: August 13, 2009 | doi: 10.1021/bk-2009-1024.ix002

Downloaded by 89.163.34.136 on June 25, 2012 | http://pubs.acs.org
Publication Date: August 13, 2009 | doi: 10.1021/bk-2009-1024.ix002

Dithiane based initiators,
  alkoxyamine synthesis, 88
Dithiobenzoates
  chain transfer agent, 270
  possible side reactions of benzyl, 11–12
  RAFT polymerization of styrene, 5–6
  signal intensities of $^{13}$C NMR in styrene polymerization, 10*f*, 11
  structures, 6
  *See also* Reversible addition fragmentation chain transfer (RAFT) polymerization
Dithiocarbamate
  photodecomposition,
  alkoxyamine synthesis, 88
Dithiocarbamates, RAFT-mediated
  polymerization, 168
*N,N*-Dithiocarbamates (DTCs)
  diphenyl vs. methyl phenyl derivatives, 41
  experimental, 38–40
  $^1$H NMR spectrum of poly(methyl acrylate)-*b*-poly(vinyl acetate) (PMA-*b*-PVAc) using malonate *N,N*-diphenyldithiocarbamate (MDP)–DTC RAFT agent, 45, 46*f*
  instrumentation, 39
  MDP–DTC, 40, 41
  MDP–DTC RAFT agent for block copolymers, 43, 44*f*
  MDP–DTC RAFT polymerization of styrene with MA and t-butyl acrylate (tBA), 42–43
  PMA macroinitiator for block copolymer synthesis, 44–45
  procedure for RAFT polymerization of monomers, 40
  PVAc macroinitiator for block copolymer synthesis, 43, 44*f*
  RAFT agent syntheses, 39–40
  RAFT polymerization of vinyl acetate (VAc), 40–41, 42*f*
  *See also* Reversible addition fragmentation chain transfer (RAFT) polymerization
Divinyl cross-linker
  influencing gelation process, 189
  networks in free radical polymerization, 182
Doxorubicin (DOX), stimuli-
  responsive morphology for
  delivery, 198
Drug transport
  reversible shell cross-linked micelles, 205, 206*f*
  shell cross-linking of drug delivery vehicles, 199
  stimuli-responsive morphologies, 198
  Dynamic covalent bonds. *See* Copolymers with covalent bonds in side chains
Dynamic light scattering (DLS),
  temperature responsive block
  copolymer, 210–211
Dynamic mechanical analysis
  (DMA)
  measurement, 184
  RAFT-crosslinked network structure, 189–191

**E**

Early transition metals, living
  radical polymerizations, 150–151
Efficient initialization,
  phenomenon, 5
Elastomers, thermoplastic
  BlocBuilder® technology, 371
  tough thermoplastics to soft, 367–368
Emulsion polymerization
  macroalkoxyamines in surfactant-free, 314–315, 316*f*, 317*f*

- *See also* RAFT/miniemulsion polymerization of methyl methacrylate (MMA); Water-soluble macroinitiators

Emulsions
  - DB (diblock copolymer) conformation in surfactant film, 355*f*
  - DBs as boosters, 352–353
  - DBs as sole emulsifiers, 351–352
  - destabilization mechanisms, 348–349
  - influence of DB level on emulsification, 352*f*
  - influence of DB structure, 355–356
  - interfacial tensions of DB and surfactant, 354*f*
  - nature of oils and hydrophobic blocks, 356
  - roles of surfactant and DBs, 353–355
  - stability, 356–357
  - stabilization against coalescence, 352–353
  - versatile DBs for various oil media, 356

*See also* Macromolecular design by interchange of xanthates (MADIX) technology

End-functionalized polymers
  - α-functionalization of polymer chains, 252–258
  - ω-functionalization of polymer chains, 258–260
  - *See also* SG1 and BlocBuilder® technology

End group analyses
  - iodine transfer polymerization (ITP), 236, 239, 240–241
  - *See also* Poly(vinylidene fluoride) (PVDF)

Energy density capacitors. *See* Fluoropolymers

Enolate oxidation, alkoxyamine synthesis, 85, 86

Epoxides radical ring opening
  - nuclear magnetic resonance (NMR) analysis, 154–155
  - *See also* Isoprene polymerization

Epoxy-based thermosets, BlocBuilder® technology, 369–371

Ethyl acrylate (EA)
  - block copolymers with hydroxyethyl acrylate (HEA), 285–287
  - evolution of Mn and polydispersity during polymerization, 284*f*
  - *See also* Soft nanoparticles

**F**

Flocculation, emulsion destabilization, 348, 349

Fluorinated polymers. *See* Poly(vinylidene fluoride) (PVDF)

Fluoropolymers
  - charging-discharging cycles, 341
  - dielectric constants of vinylidene fluoride/chlorotrifluoroethylene (VDF/CTFE) and VDF/trifluoroethylene/CTFE (VDF/TrFE/CTFE), 340*f*
  - dielectric for high energy density capacitors, 338–343
  - releasing energy density and energy loss of VDF/CTFE and VDF/TrFE/CTFE terpolymers, 342, 343*f*
  - unipolar charge displacement vs. unipolar electric field hysteresis curves, 341*f*, 342*f*
  - VDF/TrFE/CTFE terpolymers comparisons, 339, 340*t*
  - *See also* Borane-mediated radical polymerization

Fragmentation, RAFT polymerization, 4–5

Downloaded by 89.163.34.136 on June 25, 2012 | http://pubs.acs.org
Publication Date: August 13, 2009 | doi: 10.1021/bk-2009-1024.ix002

Free radical polymerization (FRP)
  gelation behavior in RAFT vs., 189
  gelation in, vs. RAFT, 187–189
  networks using divinyl-crosslinker, 182

**G**

Gelation
  characterization method, 184
  controlled copolymerization, 187–189
  vinyl conversions, 191
  *See also* Copolymerization of methacrylate and dimethacrylate
Gel effect
  molecular weight vs. conversion at onset of, 31, 32*f*
  polydispersity index and onset of, 29–32
Glass transition temperature, RAFT-crosslinked network structure, 190–191
Glycidyl methacrylate (GMA), application as co-monomer, 366*t*
Gold nanoparticles, thermally responsive vesicles, 209

**H**

Hydrocarbons, alkoxyamine synthesis, 86–87
Hydrogen abstraction, metal-centered radical, 116
β-Hydrogen transfer, organo-cobalt complex formation, 123–124
Hydroxyethyl acrylate (HEA)
  block copolymers with ethyl acrylate (EA), 285–287
  chain extension experiment of poly(ethyl acrylate) with, 285*f*
  evolution of Mn and polydispersity during polymerization, 284*f*
  *See also* Soft nanoparticles
Hydroxyethyl methacrylate (HEMA), application as co-monomer, 366*t*

**I**

Imidazole-type nitroxides, living radical polymerization of styrene and methyl methacrylate, 97–101
Impurities, RAFT polymerization, 5
Initialization
  arm growth in Z-RAFT star polymerization, 222–223
  *See also* *N*-Vinylpyrrolidone (NVP)
Initiation, RAFT polymerization, 4
Initiators. *See* Alkoxyamine synthesis
Interconversion of structure. *See* Copolymers with covalent bonds in side chains
Interpolyelectrolyte complexation, shell cross-linking via, 199–203
Iodine transfer polymerization (ITP)
  controlled radical polymerization (CRP), 66
  end-functional polymers, 234
  mechanism for reverse ITP, 68
  miniemulsion polymerization, 67
  vinylidene fluoride (VDF), 235
  *See also* Poly(vinylidene fluoride) (PVDF); Reverse iodine transfer polymerization (RITP)
Isoprene polymerization
  block copolymers with acrylic acid (AA), 288–290

Downloaded by 89.163.34.136 on June 25, 2012 | http://pubs.acs.org
Publication Date: August 13, 2009 | doi: 10.1021/bk-2009-1024.ix002

- controlled radical polymerization (CRP), 151, 152
- $Cp_2TiCl$ mediating, 157*t*
- effect of reaction variables, 155–159
- epoxides as initiators, 153
- experimental, 151–152
- $^1H$ NMR spectra of isoprene/styrene copolymers, 159, 160*f*
- $^1H$ NMR spectra of polyisoprene from epoxides, 154*f*
- mechanism of Ti-mediated, 152, 153
- monomer/initiator ratio, 158, 159*f*
- NMR analysis, 154–155
- procedure, 152
- reagent stoichiometry, 155–156, 158*f*
- target degree of polymerization, 155
- temperature and solvent effects, 158–159
- zinc involvement, 156, 157*t*
- *See also* Soft nanoparticles

**K**

Ketenimine (K)
- byproduct formation from, 9
- chemically induced dynamic nuclear polarization (CIDNP), 7, 8*f*
- formation, 6

Kinetics
- factors influencing RAFT, 4–5
- formation of Co-organo complexes during vinyl acetate polymerization, 127–128
- methyl acrylate radical polymerization using organo-cobalt complexes, 119, 120*f*
- methyl methacrylate miniemulsion polymerization, 71, 72*f*
- peptide-polymer conjugates by RAFT, 272*f*, 274*f*
- polymerization, and networks, 183
- RAFT with crosslinking, 185–186
- rate autoacceleration, 185–186
- styrene consumption with time in RAFT, 12, 13*f*
- vinyl acetate radical polymerization using organo-cobalt complexes, 121*f*
- *See also* Copolymerization of methacrylate and dimethacrylate

**L**

Living radical polymerization (LRP)
- design of polymeric nanoparticles, 280
- methyl acrylate, 118–120
- molecular weight control, 150
- pathways mediating, 116
- vinyl acetate, 120–122
- *See also* Cobalt porphyrin mediated living radical polymerization; Organo-cobalt complexes

**M**

Macroalkoxyamines. *See* Water-soluble macroinitiators

Macroinitiators
- polystyrene, with MMA using nitroxides, 109–110
- *See also* Water-soluble macroinitiators

Macromolecular design by interchange of xanthates (MADIX) technology

Downloaded by 89.163.34.136 on June 25, 2012 | http://pubs.acs.org
Publication Date: August 13, 2009 | doi: 10.1021/bk-2009-1024.ix002

Downloaded by 89.163.34.136 on June 25, 2012 | http://pubs.acs.org
Publication Date: August 13, 2009 | doi: 10.1021/bk-2009-1024.ix002

- advantages, 350
- block copolymer design, 350–351
- controlled radical polymerization, 348
- emulsion system and emulsification process, 351–357
- synthesis of amphiphilic block copolymers, 349–351

Maleic anhydride (MAH), application as co-monomer, 366*t*

Malonate *N,N*-diphenyl dithiocarbamate (MDP–DTC)
- block copolymers, 43–45
- polymerization of styrene and acrylate monomers, 42–43
- RAFT agent syntheses, 39–40
- RAFT polymerization of vinyl acetate (VAc), 40–41, 42*f*

Manganese(III) epoxidation, alkoxyamine synthesis, 83–84

Mechanisms
- borane oxidation/polymerization, 334–338
- coupling reactions for α-functionalizations, 252–256
- degenerative chain transfer, in cobalt-mediated process, 132
- emulsion destabilization, 348–349
- 1,2-intermolecular radical addition for α-functionalization, 256–258
- pseudo-living, of vinyl monomers with nitroxides, 108–109
- RAFT polymerization, 4–5
- reverse iodine transfer polymerization (RITP), 68
- selectivity during initialization in RAFT, 171–173
- star-star coupling in Z-RAFT star polymerization, 227
- Ti-mediated isoprene polymerization, 152, 153
- Z-RAFT star polymerization, 218
- *See also* Cobalt porphyrin mediated living radical polymerization; *N*-Vinyl pyrrolidone (NVP)

Metal-catalyzed radical polymerization, controlled radical polymerization (CRP), 66

Methacrylate. *See* Copolymerization of methacrylate and dimethacrylate

Methacrylic acid (MAA)
- application as co-monomer, 366*t*
- *See also* Water-soluble macroinitiators

Methyl acrylate (MA)
- block copolymer using poly(vinyl acetate) macroinitiator, 43, 44*f*
- living radical polymerization, 118–120
- Mn and polydispersity vs. conversion using Co-organo complexes, 119*f*
- RAFT polymerization of styrene, MA and tBA, 43*t*
- reversible termination and dissociative radical exchange, 124
- *See also* *N,N*-Dithiocarbamates (DTCs)

Methyl methacrylate (MMA)
- controlled synthesis using nitroxide precursors, 101–103
- copolymerization with styrene and *N*-vinyl pyrrolidone (VP), 106–108
- energy of bond between MMA radical and nitroxides, 104–106
- iodine concentration for, polymerization, 72–73
- kinetics, 71, 72*f*

- living radical polymerization with imidazole-type nitroxides, 97, 100–101
- molecular weight distributions (MWD) of PMMA, 74*f*
- monomer conversion with time for RITP, 72*f*
- procedure for miniemulsion polymerization, 69–70
- PS macroinitiator with, for block copolymers, 109–110
- reverse iodine transfer polymerization (RITP), 71
- side reactions of controlled polymerizations, 100
- *See also* RAFT/miniemulsion polymerization of methyl methacrylate (MMA); Reverse iodine transfer polymerization (RITP)

Micelles
- crosslinking reactions of, 282–283
- esters in shell of nanoassemblies, 204–207, 208*f*
- micellization procedure for block copolymers, 282, 283
- shell-crosslinking via interpolyelectrolyte complexation, 199–203
- *See also* Soft nanoparticles

Micro-gelation
- RAFT copolymerization, 187–188
- *See also* Gelation

Miniemulsion polymerization
- block copolymer, 76, 77 *f*
- Ostwald ripening, 66
- problems, 66
- *See also* Emulsion polymerization; Emulsions; RAFT/miniemulsion polymerization of methyl methacrylate (MMA); Reverse iodine transfer polymerization (RITP)

"Missing steps"
- formation of dithioester, 9
- RAFT polymerization, 5

Molecular orbitals (MO), d-orbitals of cobalt(II) porphyrin complex, 117

Molecular weight
- controlling, and steric structure, 50
- targeted, of reverse iodine transfer polymerization, 67–68

Molecular weight distribution (MWD)
- change in, with conversion for difunctional RAFT agent, 24–25, 27*f*
- poly(vinylidene fluoride) (PVDF) with iodine end groups, 241–242
- polystyrene using AIBN and nitroxides, 98, 99*t*
- termination rate coefficients, 20
- *See also* Reversible addition-fragmentation chain transfer with chain length dependent termination (RAFT-CLD-T)

Monte Carlo simulations, shielding effects, 223–226

Morphologies
- nanogels, 326–327
- transitions in dilute block copolymer solutions, 196–197

**N**

Nanogels
- morphology, 326–327
- transformation to linear polymers, 327, 328*f*
- *See also* Copolymers with covalent bonds in side chains

Nanoparticles
- assembling nano-ordered structures, 280
- designing polymeric, 280
- shell cross-linking via in situ, 209–212

Downloaded by 89.163.34.136 on June 25, 2012 | http://pubs.acs.org
Publication Date: August 13, 2009 | doi: 10.1021/bk-2009-1024.ix002

Downloaded by 89.163.34.136 on June 25, 2012 | http://pubs.acs.org
Publication Date: August 13, 2009 | doi: 10.1021/bk-2009-1024.ix002

- *See also* Soft nanoparticles
- Nanostrength® polymers, 363
- N-isopropylacrylamide (NIPAM)
  - $^1$H NMR spectra of poly(NIPAM), 55*f*
  - radical polymerization of, with thioureas, 54*t*
  - stereospecific radical polymerization of, with thiourea derivatives, 51–55
  - *See also* Stereospecific radical polymerization
- Nitrones, controlled synthesis of styrene and methyl methacrylate, 101–104
- Nitroso compounds, trapping C-based radicals with, 89–91
- Nitroxide-mediated radical polymerization (NMRP)
  - alkoxyamines as initiators, 82
  - ascorbic acid, 66
  - controlled method, 66, 82, 132, 246
  - end functionalization techniques, 248
  - SG1 nitroxide, 246, 247
  - successful protocol, 82
  - *See also* Alkoxyamine synthesis; SG1 and Blocbuilder® technology
- Nitroxide mediators for controlled polymers
  - aromatic nitroso compounds and copolymerization of styrene (St) with acrylic monomers, 108
  - bond dissociation energy of MMA and nitroxides, 104–105
  - copolymerization of styrene with acrylonitrile (AN), *N*-vinyl pyrrolidone (VP) and MMA with VP, 106–108
  - efficiencies of imidazole nitroxides, 100, 101*t*
  - experimental, 96–97
  - geometric parameters of alkoxyamines, 105–106
  - living radical polymerization of methyl methacrylate and styrene with imidazole types, 97–101
  - macroinitiators for block copolymers, 111, 112*f*
  - MMA and block copolymerization, 111, 112*f*
  - MMA and styrene homopolymers and their copolymers, 101–111
  - Mn of PS vs. conversion, 98, 99*f*
  - molecular weight characteristics of PS using AIBN and nitrones, 103*t*
  - molecular weight parameters of PS using AIBN and nitroxides, 98, 99*t*
  - MWD curves of triblock copolymers, 112*f*
  - nitrones, 102–103
  - nitrones and nitroso compounds, 104
  - polydispersity indexes of copolymers, 106, 107*t*
  - pseudo-living mechanism, 108–109
  - PS macroinitiator with MMA, 109–110
  - reinitiating polymerization for post- and block copolymers, 110–111
  - side reactions of MMA polymerization, 100
- Nuclear magnetic resonance (NMR)
  - initialization experiments, 170–171
  - real time, for RAFT polymerization, 5, 15
- NVP (*N*-vinyl pyrrolidone). *See N*-Vinyl pyrrolidone (NVP)

**O**

- Oligo(ethylene glycol) dimethacrylate (OEGDMA). *See*

  Copolymerization of methacrylate and dimethacrylate
Oligo(ethylene glycol) methyl ether methacrylate (OEGMEMA). *See* Copolymerization of methacrylate and dimethacrylate
Organic halides, alkoxyamine synthesis, 84, 85
Organo-cobalt complexes
  cobalt(II) metallo radical and, 117–118
  d-orbitals molecular orbital diagram, 117*f*
  kinetic plots for vinyl acetate (VAc) radical polymerization, 121*f*
  kinetic plots of MA radical polymerization with, 119, 120*f*
  magnetic shielding, 118*f*
  Mn (number average molecular weight) and polydispersity with conversion of MA, 119*f*
  Mn and polydispersity with conversion of VAc, 122*f*
  polymerization of methyl acrylate (MA), 118–120
  polymerization of vinyl acetate (VAc), 120–122
  radical interchange of, with external polymeric radicals, 118*f*
  reactions of metal-centered radicals or, 116
  *See also* Cobalt porphyrin mediated living radical polymerization
Ostwald ripening
  emulsion destabilization, 349
  miniemulsion polymerization, 66

**P**

Particle size, poly(methyl methacrylate) (PMMA) latex, 300, 301*f*
Peptide-polymer conjugates
  atom transfer radical polymerization (ATRP), 267–268
  controlled radical polymerization (CRP), 267
  dithiobenzoate, 270
  kinetic plots, 272*f,* 274*f*
  nitroxide mediated polymerization (NMP), 267
  poly(*n*-butyl acrylate by RAFT polymerization, 272*f,* 274*f,* 275
  properties, 266
  RAFT polymerization, 270–275
  responding to stimuli, 266
  synthesis approaches, 266–267
  synthesis of peptide macrotransfer agents (peptide-CTAs), 268–270
  trithiocarbonates, 270, 273
pH, response of shell cross-linked micelles, 207, 208
Photodecomposition of dithiocarbamate, alkoxyamine synthesis, 88
Poly(acrylic acid) (PAA), morphology transitions in dilute block copolymer solutions, 196–197
Poly(*N*-3-aminopropyl) methacrylate hydrochloride (P(APMA))
  block copolymers with *N*-acryloyl alanine (AAL), 202–203
  pH-responsive micellization of triblock copolymer, 207, 208
  shell cross-linking of micelles with, 199–203
Polybutadiene (PB), morphology in dilute block copolymer solutions, 197
Poly[2-(dimethylamino)ethyl methacrylate] (PDMAEMA)
  block copolymers with poly(*N*-isopropyl acrylamide) (PNIPAM), 209–212

Downloaded by 89.163.34.136 on June 25, 2012 | http://pubs.acs.org
Publication Date: August 13, 2009 | doi: 10.1021/bk-2009-1024.ix002

  - pH-responsive micellization of triblock copolymer, 206–207, 208

Polydispersity index (PDI)
  - controlling, 20
  - evolution for polymerization of ethyl acrylate (EA) and hydroxyethyl acrylate (HEA), 284*f*
  - gel onset and increasing, 29–32
  - living radical polymerization (LRP), 150
  - molecular weight vs. conversion at onset of gel effect, 31, 32*f*
  - peptide-polymer conjugates by RAFT polymerization, 272*f,* 273, 274*f*
  - poly(vinylidene fluoride) (PVDF), 237–238
  - RAFT polymerization of styrene, 29*t*
  - unbalanced, between blocks in copolymer, 368
  - *See also* Reversible addition-fragmentation chain transfer with chain length dependent termination (RAFT-CLD-T)

Polyethylene glycol methacrylate (PEGMA), application as co-monomer, 366*t*

Poly(ethylene glycol) methyl ether methacrylate (MePEGMA). *See* Water-soluble macroinitiators

Poly(ethylene oxide) (PEO)
  - morphology transitions in dilute block copolymer solutions, 196–197
  - pH-responsive micellization of triblock copolymer, 207, 208
  - stimuli-responsive morphologies in block copolymer, 197–198

Polyisoprene
  - stimuli-responsive morphologies in triblock, 198
  - *See also* Isoprene polymerization

Poly(*N*-isopropyl acrylamide) (PNIPAM)
  - shell cross-linking micelles and vesicles, 199, 200*f,* 201
  - stimuli-responsive morphologies in block copolymer, 198

Polymer properties, molecular weight and steric structure, 50

Polymethacrylates
  - well-defined, 304
  - *See also* Nitroxide mediators for controlled polymers; Water-soluble macroinitiators

Poly(methyl methacrylate) (PMMA)
  - all-acrylic triblock copolymers, 367–368
  - new tough thermoplastic, 368–369
  - stabilizing thermosets with PMMA block, 370
  - *See also* BlocBuilder® technology

Polystyrene (PS)
  - block copolymer with poly(etherimide) (PEI), 257
  - morphology transitions in dilute block copolymer solutions, 196–197
  - PS–2,4-dinitrophenylhydrazine (PS–DNPH), 252, 259, 260*f*
  - *See also* Nitroxide mediators for controlled polymers

Poly(vinyl acetate) (PVAc)
  - controlled/living radical polymerization, 38
  - *See also N,N*-Dithiocarbamates (DTCs)

Poly(vinylidene fluoride) (PVDF)
  - end group analyses, 236, 240–241
  - experimental, 234–235
  - experimental details and results, 238*t*
  - Fourier transform–near infrared (FT–NIR) spectra during polymerization, 236*f*
  - functionalization with 2-butyne, 3-hexyne, and 4-octyne polymers, 239–240

Downloaded by 89.163.34.136 on June 25, 2012 | http://pubs.acs.org
Publication Date: August 13, 2009 | doi: 10.1021/bk-2009-1024.ix002

- $^1$H NMR spectrum of, with iodine and triazole end groups, 241*f*
- iodine transfer polymerization (ITP), 235
- livingness of polymerization, 237
- Mn increase with conversion, 239*f*
- molecular weight analyses, 236–237, 241–242
- polydispersities, 237–238
- synthesis of end functionalized, 239

Poly(*N*-vinylpyrrolidone) (PVP)
- RAFT-mediated polymerization, 168
- *See also* *N*-Vinylpyrrolidone (NVP)

Propagation, RAFT polymerization, 4

**R**

Radical interchange
- organo-cobalt porphyrin complexes, 118
- vinyl acetate polymerization, 125–128

Radical ring opening (RRO)
- initiation from epoxide RRO, 150
- mechanism of Ti-mediated isoprene polymerization, 152, 153
- *See also* Isoprene polymerization

Radical termination, RAFT polymerization, 4–5

Radius of gyration, equation, 30

RAFT. *See* Reversible addition-fragmentation chain transfer (RAFT) polymerization

RAFT/miniemulsion polymerization of methyl methacrylate (MMA)
- amphiphilic random copolymers of [2-(acryloyloxy)ethyl]trimethylammonium chloride and stearyl methacrylate [poly(AETMAC-*co*-SMA)], 293, 295
- conversion-time profiles for, 299*f*
- de-emulsification of PMMA latex, 296–297
- experimental, 295–297
- $^1$H NMR spectra of poly(AETMAC-*co*-SMA), 298*f*
- kinetics, 299–300
- particle size and particle size distribution of latexes, 300*f*, 301*f*
- poly(AETMAC-*co*-SMA) by free radical polymerization, 297
- polymeric surfactant [poly(AETMAC-*co*-SMA)] synthesis, 296, 297*t*
- typical procedure, 298–299

Rate autoacceleration, kinetic behavior, 185–186

Reduced gel, RAFT polymerization, 5

Reinitiation, RAFT polymerization, 4

Retardation, RAFT polymerization, 4–5

Reverse iodine transfer polymerization (RITP)
- BA (butyl acrylate) by, in *ab initio* emulsion polymerization, 68
- BA in miniemulsion, 74
- block copolymerization, 76, 77*f*
- chain extension, 70
- characterization methods, 70–71
- experimental, 69–71
- iodine concentration for BA RITP, 74–75

Downloaded by 89.163.34.136 on June 25, 2012 | http://pubs.acs.org
Publication Date: August 13, 2009 | doi: 10.1021/bk-2009-1024.ix002

- iodine concentration for methyl methacrylate (MMA) RITP, 72–73
- iodine disproportionation, 68
- iodine regeneration, 68
- kinetics of MMA miniemulsion, 71, 72*f*
- mechanism, 68
- MMA in miniemulsion, 71
- molecular weight distributions (MWD) of PBA, 75*f*
- MWD of PMMA, 74*f*
- new controlled radical polymerization (CRP) method, 67
- procedure for miniemulsion polymerization of BA, 69–70
- procedure for miniemulsion polymerization of MMA, 69
- targeted molecular weight, 67–68

Reversible addition fragmentation chain transfer (RAFT) polymerization
- azobis(isobutyronitrile) (AIBN) consumption during styrene polymerization, 8 *f*
- benzyl dithiobenzoate experiments, 9, 10 *f*
- benzyl dithiobenzoate-thiocarbonyl-$^{13}$C experiments, 11
- byproduct KB from ketenimine K, 8*f,* 9, 14
- $^{13}$C-labeled initiators, 5–6
- $^{13}$C NMR chemical shifts of, agents and macro-RAFT agents with styrene, 14 *f*
- $^{13}$C NMR spectra of styrene, with time, 13*f*
- controlled radical polymerization (CRP), 66, 82
- cyanoisopropyl RAFT agents, 9, 10*f*
- disappearing of RAFT agent, 9, 10*f*
- end functionalization techniques, 248
- experimental, 15–16
- factors influencing kinetics, 4–5
- mechanism, 4
- monomer consumption with time, 12, 13 *f*
- NMR spectrum during styrene, with benzyl dithiobenzoate-thiocarbonyl-$^{13}$C, benzyl dithiobenzoate, and AIBN-α-$^{13}$C, 8 *f*
- peptide-polymer conjugates by, 270–275
- reagents concentrations in styrene, 16 *t*
- real-time $^{1}$H NMR, 5
- retardation, 4
- side reactions of benzyl dithiobenzoate, 11–12
- styrene and efficient initialization, 5
- thermal decomposition of AIBN, 6–7
- well-defined polymers, 182
- *See also* Amphiphilic block copolymers; Copolymerization of methacrylate and dimethacrylate; *N,N*-Dithiocarbamates (DTCs); Peptide-polymer conjugates; RAFT/miniemulsion polymerization of methyl methacrylate (MMA); Soft nanoparticles; Stereospecific radical polymerization; *N*-Vinyl pyrrolidone (NVP); Z-RAFT star polymerization

Reversible addition-fragmentation chain transfer with chain length dependent termination (RAFT-CLD-T)
- change in molecular weight distribution (MWD) vs. conversion in styrene polymerization, 24–25, 27*f*
- conditions for polymerization of styrene, 23, 24*t*

Downloaded by 89.163.34.136 on June 25, 2012 | http://pubs.acs.org
Publication Date: August 13, 2009 | doi: 10.1021/bk-2009-1024.ix002

- conversion, molecular weight and polydispersity index (PDI) at gel onset, 29*t*
- conversion vs. time profiles, 24, 25*f*
- determination of termination rate coefficients ($k_t$), 22–23, 25–26
- differential scanning calorimetry (DSC) RAFT polymerization of styrene, 21
- experimental, 21–23
- gel effect and PDI, 29–32
- kinetic parameters for determining $k_t$, 23*t*
- molecular weight vs. conversion at gel onset, 32*f*
- procedure for, of styrene, 21
- radius of gyration, 30
- size exclusion chromatography (SEC) method, 22
- technique, 20

Reversible termination, methyl acrylate polymerization, 124

Reversible termination (RT), mechanism in living radical polymerization, 116

Rubbery polymers, toughening epoxies, 370

## S

Sedimentation, emulsion destabilization, 349

Selectivity of initialization. *See N*-Vinylpyrrolidone (VP)

Self-assembled aggregate, shell cross-linking, 199

Self-assembled nanostructures, block copolymers, 211–212

SG1 and BlocBuilder® technology
- α-functionalization of polymer chains, 252–258
- α,ω-telechelic polymers, 247, 260
- activated esters binding amines with carboxylic acids, 254
- controlled radical polymerization, 246, 247
- coupling reaction for α-functionalization, 252–256
- di- and tri-block copolymers, 257–258
- 2,2-dimethyl-4-[*N*-*t*-butyl-*N*-(1-diethoxyphosphoryl-2,2-dimethylpropyl)aminoxy]-4-(4-(sodium sulfonate)phenyl) butanoic acid (MAMA-SSNa-SG1), 250
- 2,2-dimethyl-4-[*N*-*t*-butyl-*N*-(1-diethoxyphosphoryl-2,2-dimethylpropyl)aminoxy]-4-(*N*-(2,4,5-trihydroxy-6-(hydroxymethyl)tetrahydro-2H-pyran-3-yl)carbamoyl) butanoic acid (MAMA-NAG-SG1), 251
- end-functionalization technique by CRP, 248
- experimental, 249–252
- functionalization methodology from Blocbuilder®, 248
- grafting of silylated alkoxyamine onto silica nanoparticles, 250
- 1,2-intermolecular radical addition for α-functionalization, 256–258
- liquid chromatography at critical condition of PS–SG1, PS–TEMPO and PS–ketone, 260*f*
- MAMA-NHS (*N*-succinimidyl derivative of BlocBuilder®), 254–255
- MAMA-NHS coupling with (3-amino propyl)triethoxysilane, 255
- 2-methyl-2-[*N*-*t*-butyl-*N*-(1-diethoxyphosphoryl-2,2-dimethylpropyl)aminoxy]-N-(3-triethoxysilylpropyl) propionamide (MAMA-NH-Si), 249–250
- nitroxide SG1, 246, 247

Downloaded by 89.163.34.136 on June 25, 2012 | http://pubs.acs.org
Publication Date: August 13, 2009 | doi: 10.1021/bk-2009-1024.ix002

Downloaded by 89.163.34.136 on June 25, 2012 | http://pubs.acs.org
Publication Date: August 13, 2009 | doi: 10.1021/bk-2009-1024.ix002

  polystyrene–DNPH (PS–DNPH) conjugate, 259, 260*f*
  potential of α-functionalized polymers, 248
  preparation of PS–DNPH conjugate, 252, 259
  radical chain-end functionalization of SG1–based PS, 258, 259
  synthesis of *N*-(2-hydroxyethyl)pivalamide, 249
  synthesis of PEI–diacrylate (poly(etherimide)-diacrylate), 251
  synthesis of PEI–dialkoxyamine, 251
  synthesis of PS–ketone, 252
  synthesis of PS–PEI–PS, 251
  TEMPO nitroxide, 246, 247
  ω-functionalization, 247
  ω-functionalization of polymers, 258–260
  yield of coupling between acids and hydroxy terminated PEO, 253*t*
  *See also* BlocBuilder® technology
Shell cross-linking (SCL)
  drug delivery vehicles, 199
  incorporation of activated esters, 204–207
  in situ nanoparticle formation, 209–212
  interpolyelectrolyte complexation, 199–203
  micellization of triblock copolymer, 208
  transmission electron microscopy (TEM) image of SCL micelles, 208*f*
Shielding effects, Monte Carlo simulations, 223–226
Side chains. *See* Copolymers with covalent bonds in side chains
Soft nanoparticles
  block poly(acrylic acid-*b*-isoprene) P(AA-*b*-I) synthesis, 283
  block poly(ethyl acrylate-*b*-hydroxyethyl acrylate) P(EA-*b*-HEA) synthesis, 282
  block poly(*t*-butyl acrylate-*b*-isoprene) P(tBA-*b*-I) synthesis, 283
  chain extension experiment of P(tBA) with I, 288*f*
  chain extension of P(EA) with HEA, 285*f*
  COOH-functionalized, P(AA-*b*-I), 288–290
  crosslinking of P(AA-*b*-I) micelles, 283
  crosslinking of P(EA-*b*-(HEA-*co*-NAS)) micelles, 282–283
  evolution of Mn and PDI with conversion for P(EA-*b*-HEA), 284*f*
  experimental, 281–283
  FTIR spectra of shell cross-linked micelle, micelle, and crosslinked nanoparticle, 289*f*
  functional amphiphilic block copolymers, 280–281
  GPEC (gradient polymer elution chromatography), 281
  GPEC chromatograms of macroCTAs and P(EA-*b*-HEA) diblock copolymers, 285*f*
  living radical polymerization (LRP), 280
  micellization of P(AA-*b*-I), 283
  micellization of P(EA-*b*-HEA) and P(EA-*b*-(HEA-*co*-*N*-acryloxysuccinimide), 282
  OH-functionalized, P(EA-*b*-HEA), 284–287
  RAFT polymerization, 282, 283
  surface tension vs. concentration for critical micelle concentration (CMC), 287*f*

- TEM images of micelles and shell cross-linked micelles of P(AA-*b*-I), 290*f*
- transmission electron micrograph (TEM) of P(EA-*b*-HEA) micelles, 286*f*

Solvents
- cobalt-mediated radical polymerization (CMRP), 141, 142*f*
- Ti-mediated isoprene polymerizations, 158–159

Stable free-radical polymerization (SFRP)
- cobalt complex, 132
- stable radicals as mediators, 96
- *See also* Nitroxide mediators for controlled polymers

Star-like nanogels
- topology, 326
- *See also* Copolymers with covalent bonds in side chains

Star polymerization. *See* Z-RAFT star polymerization

Star-star coupling, Z-RAFT star polymerization, 226–228

Stereospecific radical polymerization
- conditions for *N,N*-dimethylacrylamide (DMAM), with thiourea derivatives, 52*t,* 54*t*
- conditions for *N*-isopropylacrylamide (NIPAM), with thiourea derivatives, 54*t*
- conventional radical polymerization, 60
- DMAM and NIPAM with thiourea derivatives, 51–55
- experimental, 59–61
- $^1$H NMR spectra of poly(DMAM), 53*f*
- $^1$H NMR spectra of poly(NIPAM), 55*f*
- interaction of thioureas with DMAM monomer and dimer, 55–56
- interactions by Job's method by varying concentrations, 56, 57*f*
- measurements, 61
- method for RAFT polymerization, 61
- 1-phenylethyl phenyldithioacetate (PEPD), 58–59
- polymer properties, 50
- RAFT polymerization of DMAM with thiourea additives, 57–59
- synthesis of DMAM dimer, 60
- synthesis of thioureas, 60
- thiourea-mediated, of acrylamides, 50–51
- thioureas with 3,5-*bis*(trifluoromethyl)phenyl and aromatic substituents, 53, 54*t*
- trithiocarbonate-type RAFT agent (CPETC), 58–59

Stimuli responses
- drug transport, 198–199
- morphological transitions, 197–198
- pH and shell cross-linked micelles, 207, 208
- temperature and shell cross-linked micelles, 205–206
- *See also* Amphiphilic block copolymers

Structural transformation. *See* Copolymers with covalent bonds in side chains

Styrene
- bulk polymerization by water-soluble macroalkoxyamine, 307, 309*t,* 312–313, 314*f*
- controlled synthesis using nitroxide precursors, 101–103
- copolymerization with acrylonitrile (AN), MMA, and *N*-vinylpyrrolidone (VP), 106–108

Downloaded by 89.163.34.136 on June 25, 2012 | http://pubs.acs.org
Publication Date: August 13, 2009 | doi: 10.1021/bk-2009-1024.ix002

Downloaded by 89.163.34.136 on June 25, 2012 | http://pubs.acs.org
Publication Date: August 13, 2009 | doi: 10.1021/bk-2009-1024.ix002

  copolymer with isoprene, 159, 160*f*
  Z-RAFT star polymerization, 220–221
  *See also* Water-soluble macroinitiators; Z-RAFT star polymerization
Styrene polymerization
  azobis(isobutyronitrile) consumption during, 7, 8*f*
  $^{13}$C NMR spectra during, 12, 13*f*
  $^{13}$C NMR spectra of, using dithiobenzoate and trithiocarbonate esters, 10*f*, 11
  conditions using 1,3-*bis*(benzylthiocarbonyl-sulfanyl-2-prop-2-yl)benzene (BTBTPB) RAFT agent, 23, 24*t*
  cumyl or cyanoisopropyl dithiobenzoate, 5
  differential scanning calorimetry (DSC) RAFT, of, 21, 22
  kinetic plot of monomer consumption with time, 12, 13*f*
  living radical polymerization with imidazole-type nitroxides, 97–101
  nuclear magnetic resonance (NMR) spectrum, 8*f*
  radical, with $^{13}$C-labeled AIBN, 5–6
  RAFT of, with methyl acrylate (MA) and *t*-butyl acrylate (tBA), 43*t*
  termination rate coefficients, 25–26, 28*f*
  *See also* *N,N*-Dithiocarbamates (DTCs)
Supercritical carbon dioxide ($scCO_2$)
  alternate solvent, 234
  poly(vinylidene fluoride) (PVDF), 235, 238*t*
Super-swelling, miniemulsion polymerization, 66
Surfactants
  diblock conformation in, film, 355*f*
  interfacial tension, 354*f*
  role of, in emulsions, 353–355
  *See also* Emulsions; RAFT/miniemulsion polymerization of methyl methacrylate (MMA)

**T**

Tacticity
  control in thiourea-mediated polymerization, 57–59
  living radical polymerizations, 50
  *See also* Stereospecific radical polymerization
Telechelic polymers. *See* SG1 and BlocBuilder® technology
Temperature
  cobalt-mediated radical polymerization (CMRP), 135–138
  response of shell cross-linked micelles, 205–206
  responsive self-assembly of block copolymers, 210–211
  Ti-mediated isoprene polymerizations, 158–159
TEMPO (2,2,6,6-tetramethylpiperidinyl-1-oxy) based alkoxyamine, covalent polymers, 320
Termination
  RAFT polymerization, 4
  *See also* Reversible addition-fragmentation chain transfer with chain length dependent termination (RAFT-CLD-T)
Termination rate coefficient ($k_t$)
  determination method, 22–23
  kinetic parameters for determining, 23*t*
  RAFT-CLD-T method for determining, 25–26

Downloaded by 89.163.34.136 on June 25, 2012 | http://pubs.acs.org
Publication Date: August 13, 2009 | doi: 10.1021/bk-2009-1024.ix002

*See also* Reversible addition-fragmentation chain transfer with chain length dependent termination (RAFT-CLD-T)

Terpolymers. *See* Fluoropolymers

Tertiobutyl aminoethyl methacrylate (TBAEMA), application as co-monomer, 366*t*

Thermal decomposition, azobisisobutyronitrile, 6, 7

Thermally exchangeable bonds. *See* Copolymers with covalent bonds in side chains

Thermoplastic elastomers, BlocBuilder® technology, 371

Thermoset additives, BlocBuilder® technology, 369–371

Thiourea derivatives
- acrylamide polymerizations in presence of, 51–55
- 3,5-bis(trifluoromethyl)phenyl group and other aromatic substituents, 53–54
- interaction with *N,N*-dimethylacrylamide (DMAM) monomer and dimer, 55–56
- RAFT polymerization of DMAM, 57–59
- stereospecific radical polymerization of acrylamides, 50–51
- structures, 51
- *See also* Stereospecific radical polymerization

Titanium-mediated polymerizations. *See* Isoprene polymerization

Transition metals. *See* Isoprene polymerization

Triblock copolymers
- micellization of, and formation of shell cross-linked micelles, 207, 208
- PS macroinitiators with methyl methacrylate (MMA) and butyl acrylate (BA) using nitroxides, 111, 112*f*

Triethylborane
- oxidation mechanism, 335
- *See also* Borane-mediated radical polymerization

Trifluoroethylene (TrFE). *See* Fluoropolymers

Trithiocarbonates
- chain transfer agents for bioconjugates, 270, 273
- mono- and multifunctional, for Z-RAFT star polymerization, 218, 219

Trommsdorf effect, RAFT polymerization, 5

**U**

Ultrasonication, miniemulsion polymerization, 66

**V**

Vinyl acetate (VAc)
- block copolymer using poly(methyl acrylate) macroinitiator, 44–45, 46*f*
- controlled/living radical polymerization, 38
- degenerative transfer and associative radical interchange, 125–128
- kinetics of formation of cobalt-organo complexes, 127–128
- living radical polymerization, 120–122
- Mn and polydispersity vs. conversion using cobalt-organo complexes, 122*f*
- molecular weight and polydispersity vs. VAc conversion using RAFT agents, 41, 42*f*
- procedure for RAFT polymerization, 40

Downloaded by 89.163.34.136 on June 25, 2012 | http://pubs.acs.org
Publication Date: August 13, 2009 | doi: 10.1021/bk-2009-1024.ix002

- radical propagation, exchange, and termination after induction, 126
- reactions of cyanoisopropyl radicals with cobalt complex and, during induction, 125–126
- temperature and cobalt-mediated radical polymerization (CMRP), 135–138
- water in CMRP of, 138–139, 140*f*
- *See also* Cobalt-mediated radical polymerization (CMRP); *N,N*-Dithiocarbamates (DTCs)

Vinylidene fluoride (VDF)
- $^1$H and $^{19}$F NMR spectra of poly(VDF), 337*f,* 338
- polymerization by triethylborane/$O_2$, 336*t,* 337
- *See also* Fluoropolymers; Poly(vinylidene fluoride) (PVDF)

*N*-Vinyl pyrrolidone (NVP)
- candidates for RAFT-mediated polymerization, 168
- concentration of S-(4-cyano-4-pentanoic acid) O-ethyl xanthate (X3) in polymerization of, 176*f*
- concentration profiles of S-(1-cyanoethyl) O-ethyl xanthate (X4) and S-(2-propionic acid) O-ethyl xanthate (X6) in polymerization of, 175*f*
- concentration profiles of S-(2-cyano-2-propyl) O-ethyl xanthate (X2) and S-(2-ethyl phenylacetate) O-ethyl xanthate (X7) in polymerization of, 172*f*
- concentration profiles of S-(2-phenylethyl) O-ethyl xanthate (X1) in polymerization of, 173*f*
- concentration profiles of S-(*t*-butyl) O-ethyl xanthate (X5) in polymerization of, 174*f*
- copolymerization with styrene and methyl methacrylate, 106–108
- dithiocarbamates and xanthates, 168
- experimental for RAFT polymerization, 169–171
- initialization and side reactions, 176
- initialization at low RAFT agent concentration, 176–177
- in situ NMR initialization experiments, 170–171
- intermediate selectivity of X4 and X6, 175
- poorly selective initialization of X5, 174–175
- RAFT pre-equilibrium and rate constants of radical reactions, 173
- range of O-ethyl xanthate R groups, 168, 169*f*
- reactivity of, and classification of R groups, 177
- selective initialization with X2 and X7, 171–173
- slow initialization of X1, 173–174
- synthesis of RAFT agents, 169–170
- xanthate structures (X1–X7), 169*f*

**W**

Water, cobalt-mediated radical polymerization, 138–139, 140*f*

Water-soluble macroinitiators
- advantages of including poly(ethylene glycol) (PEG), 304–305
- analytical techniques, 305–306

Downloaded by 89.163.34.136 on June 25, 2012 | http://pubs.acs.org
Publication Date: August 13, 2009 | doi: 10.1021/bk-2009-1024.ix002

- bulk polymerization of styrene by P(MePEGMA-*co*-S)-SG1 macroalkoxyamine, 307
- chain-end analysis and extensions, 310–312
- conversion vs. time, 311*f,* 316*f*
- experimental, 305–309
- experimental for chain extensions of SG1-capped poly(ethylene glycol) methyl ether methacrylate (MePEGMA)-*co*-styrene) [P(MePEGMA-co-S]and P(MePEGMA-*co*-methacrylic acid-*co*-S) [P(MePEGMA-*co*-MAA-S] with styrene, 309*t*
- experimental for SG1-mediated copolymerization of MePEGMA and MAA with S, 308*t*
- number-average molar mass and polydispersity index vs. conversion, 311*f,* 316*f*
- SG1-terminated macroalkoxyamines based on MAA and MePEGMA, 310–313
- size exclusion chromatography evolution with conversion, 313*f,* 317*f*
- styrene polymerization by P(MePEGMA-*co*-MAA-*co*-S)-SG1 macroalkoxyamine, 307, 309*t*
- surfactant-free emulsion copolymerization of MMA and styrene by P(MePEGMA-*co*-MAA-*co*-S)-SG1, 309
- synthesis and use in batch emulsion polymerizations, 304
- synthesis of P(MePEGMA-*co*-MAA-*co*-S)-SG1, 306–307
- synthesis of P(MePEGMA-*co*-S)-SG1, 306
- synthesis of well-defined block copolymer, 312–313, 314*f*
- using MePEGMA-based macroalkoxyamines in surfactant-free emulsion polymerization, 314–316*f,* 317*f*
- well-defined polymethacrylates, 304

**X**

Xanthates
- agents for RAFT polymerization, 168, 178
- classification of R groups and NVP reactivity, 177
- MADIX technology, 348
- range of O-ethyl, 168, 169*f*
- selectivity in initialization, 171–175
- structures, 169*f*
- synthesis of, 169–170
- *See also N*-Vinyl pyrrolidone (NVP)

**Z**

Zinc. *See* Isoprene polymerization
Z-RAFT star polymerization
- chain length dependence of shielding factors, 225
- characterization, 219–221
- equilibrium, 218
- equilibrium between dormant linear polymer and dormant stars, 220
- expanding arm numbers, 228–230
- $^1$H NMR spectrum of star-shaped RAFT agent, 222*f*
- initialization of arm growth, 222–223
- mechanism, 218
- molecular weight data for polystyrene using octa-

functional Z-RAFT agent, 229*f*
molecular weight distributions of PS with linear and tetra-functional RAFT agents, 221*f*
mono- and multifunctional RAFT agents, 218, 219
Monte Carlo simulations of shielding effects, 223–226
MWD of 6-arm Z-RAFT star polymerization of butyl acrylate (BA), 226*f*
non-reacted RAFT groups vs. monomer conversion, 223*f*
octa-functional silsesquioxane-type Z-RAFT agent, 228, 229*f*
reaction pathways leading to star-star couples, 227
shielding factors vs. reduced position for interaction, 224*f*, 225*f*
star-star coupling, 226–228
synthesis of octa-functional Z-RAFT agent, 229–230

Downloaded by 89.163.34.136 on June 25, 2012 | http://pubs.acs.org
Publication Date: August 13, 2009 | doi: 10.1021/bk-2009-1024.ix002